

UNCLASSIFIED

NATIONAL AERONAUTICS AND SPACE ADMINISTRATION
CONTRACT NO. NAS 7-100

Technical Report No. 32-353
The Mariner R Project:
Progress Report
September 1, 1961–August 31, 1962 (U)

Classification Changed to	
UNCLASSIFIED	
Authority	
Executive Order # 11652	
Date	By
7-30-1975	G. Castain

JET PROPULSION LABORATORY
LIBRARY

JAN 22 1963

0634

CALIFORNIA INSTITUTE OF TECHNOLOGY

Copy No. _____

JET PROPULSION LABORATORY
CALIFORNIA INSTITUTE OF TECHNOLOGY
PASADENA, CALIFORNIA

JANUARY 1, 1963

~~UNAUTHORIZED DISSEMINATION OF SECURITY INFORMATION~~

LOG-M01082

191 491

UNCLASSIFIED

UNCLASSIFIED

JPL TECHNICAL REPORT D. 32-353

Copyright © 1963
Jet Propulsion Laboratory
California Institute of Technology

UNCLASSIFIED

Contents

I. Project Objectives and Status	1
II. Project History	3
A. Background	3
B. <i>Mariner R</i> Proposals	3
C. <i>Mariner</i> Chronology	4
III. Project Organization and Management	9
A. Management Organization	9
B. Launch Vehicle Relations	15
C. JPL Activities and Implementation of JPL Activities	15
IV. Spacecraft System	33
A. <i>Mariner R</i> Design	33
B. Spacecraft Description	36
V. Spacecraft Subsystems	39
A. Structure and Thermal Control	39
B. Power	74
C. Central Computer and Sequencer	80
D. Attitude Control	85
E. Telecommunications System	110
F. Science	154
G. Cabling	202
H. Propulsion	210
VI. Spacecraft Assembly and Launch Operations	219
VII. Spacecraft Ground Support Equipment and Facilities	227
A. Introduction	227
B. Facilities	227
C. System Test Complex	232
D. Launch Complex	235
E. Engineering Support Facilities	237
VIII. Quality Control	253
A. Quality Control Requirements	253
B. Environmental Requirements	255

Contents (Cont'd)

IX. The Launch Vehicle	273
A. <i>Atlas-Agena</i> System	273
B. Vehicle Integration	276
X. Trajectories and Systems Analysis	281
A. Introduction	281
B. Trajectories	281
C. Guidance	289
D. Orbit Determination	300
XI. Launch Restraints	305
A. Introduction	305
B. <i>Atlas</i> Booster Vehicle	306
C. <i>Agna B</i> Second Stage	306
D. <i>Mariner R</i> Spacecraft	307
E. Range Safety	319
F. Tracking and Telemetry Coverage	319
G. Space Flight Operations	319
XII. Space Flight Operations	321
A. Purpose and Organization	321
B. Operational Facilities	323
C. Data Flow and Processing	331
D. Preflight Planning and Testing	333
Appendix A. <i>Mariner R</i> Project Policy and Requirements	335
Appendix B. <i>Mariner R</i> Change Freeze Requiring ECR Action	342
Appendix C. <i>Mariner R</i> P List	344
References	345

Abbreviations Used in This Report

A/C	Attitude Control	GBQ	Good, Bad, Questionable
A/D	Analog to Digital	GC	Gyro Control
ADC	Analog-to-Digital Converter	GD/A	General Dynamics/Astronautics
AFSCSSD	Air Force Systems Command, Space Systems Division	GHE	Ground Handling Equipment
AGC	Automatic Gain Control	GIP	Ground Instrumentation Plan
AMR	Atlantic Missile Range	GM	Ground Mode
AOP	Assembly and Operations Plan	GSE	Ground Support Equipment
APC	Automatic Phase Control	GSF	Ground Support Facility
		GSFC	Goddard Space Flight Center
BCD	Binary Coded Decimal	IP	Isolated Pulse
BPF	Band Pass Filter	IRFNA	Inhibited Red Fuming Nitric Acid
BRD	Booster Requirements Document	IS	Isolated Step
CCF	Central Computing Facility	JCLOT	Joint Closed-Loop Operations Test
CC&S	Central Computer and Sequencer	JFACT	Joint Flight-Acceptance Composite Test
CCW	Counterclockwise	JPL	Jet Propulsion Laboratory
CO	Checkout	L	Launch
COE	Corps of Engineers	LC	Inductance-Capacitance
CPU	Central Processing Unit	LCE	Launch Complex Equipment
CR&P	Celestial Relays and Power	LCOS	Launch Checkout Station
CW	Clockwise	LCS	Launch Control Shelter
DCI	Data Condition Indicator	LCTT	Launch Compatibility Test Trailer
DCS	Data Conditioning System	LL	Low Level
D/D	Digital-to-Digital	LOB	Launch Operations Building
DDC	Digital-to-Digital Converter	LOC	Launch Operations Center
DE	Data Encoder	LOD	Launch Operations Directorate (later LOC)
DSIF	Deep Space Instrumentation Facility	LOX	Liquid Oxygen
DVM	Digital Voltmeter	LPB	Launch Pad Building
E	Encounter	LMSC	Lockheed Missiles and Space Company
ECR	Engineering Change Requirement	MF	Main Frame
EF	Emitter-Follower	MGC	Manual Gain Control
EG	Earth Gate	MOIS	Mission Operational Intercom System
ETL	Environmental Testing Laboratory	MRB	Materials Review Board
ESA	Explosive Safe Area	MSD	Most Significant Digit
F-A	Flight-Acceptance (test)	MSFC	Marshall Space Flight Center
FEP	Fluorinated Ethylene Propylene	MTBF	Mean-Time-Between-Failures
F-F	Flip-Flop	MTS	Mobile Tracking Station
FM	Frequency Modulation	NASA	National Aeronautics and Space Administration
FR	Failure Report	N/B	Noise Power/Unit Band Width
FTD	Flight Test Directive		

Abbreviations (Cont'd)

NPN/PNP	<div> <div>NPN—junction transistor with <i>p</i>-type base and <i>n</i>-type collector</div> <div>PNP—junction transistor with <i>n</i>-type base and <i>p</i>-type collector and emitter</div> </div>	SCF	Spacecraft Checkout Facility
NRT	Non-Real Time	SCR	Silicon Control Rectifier
NRZ	Non-Return to Zero	SDAT	Spacecraft Data Analysis Team
OD	Operational Directive	SDS	Spacecraft Design Specification
ODP	Orbit Determination Program	SDT	Scientific Data Translator
OR	Operation Requirements	SFO	Space Flight Operations
PCA	Pyrotechnic Control Assembly	SFOC	Space Flight Operations Complex
PCM-PSK-PM	Phase Code Modulated—Phase Shift Key—Phase Modulated	SFOF	Space Flight Operations Facility
PDP	Project Development Plan	SFOP	Space Flight Operations Plan
PDP	Programmed Data Processor	SG	Sun Gate
PFD	Particle Flux Detector	SNR	Signal-to-Noise Ratio
PHP	Planetary Horizontal Platform	SPDT	Single-Pole, Double-Throw
PLL	Phase-Locked Loop	STC	Systems Test Complex
PMP	Project Management Plan	STL	Space Technology Laboratories
PN	Pseudo Noise	ST/N/B	Signal Energy / Noise Power/Unit Bandwidth
PR	Program Requirements	STO	Systems Test Objectives
PRD	Program Requirements Documentation	SYNC, sync	Synchronization
PSK	Phase-Shift Key	T-A	Type-Approval (tests)
PS&L	Power Switching and Logic	TC	Temperature Control (unit)
PSP	Program Support Plan	TCM	Temperature Control Model
PTM	Proof Test Model	TDEP	Tracking Data Editing Program
QCRR	Quality Control Requirement Report	TFV	Twin Falls Victory (ship)
QL	Quick-Look	TIL	Telecommunications Investigation Laboratory
RC	Resistive-Capacitive	T/M	Telemetry
RFI	Radio Frequency Interference	TMC	Telecommunications Monitor Console
RFT	Radio Frequency Trailer	TMS	Telecommunications Monitor System
REP	Request for Programming	TPS	Telemetry Processing Station
RPI	Relay Position Indicator	T-R	Transformer-Rectifier
RT	Real Time	TRL	Transistor-Resistor-Logic
RTC	Real-Time Commands	TT	Telemetry Trailer
RWV	Read-Write-Verify	TTY	Teletype
SAC	Switching Amplifier Compensation	UDMH	Unsymmetrical Di-Methyl Hydrazine
SAF	Spacecraft Assembly Facility	VBE	Voltage (Beta) Drop
SCAMA	Switching Conferencing and Monitoring Assembly	VCO	Voltage-Controlled Oscillator
		VLF	Vehicle Launch Facility
		VSWR	Voltage Standing Wave Ratio
		VTVM	Vacuum Tube Voltmeter

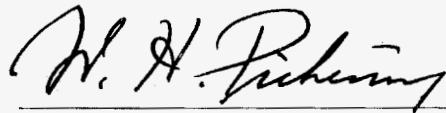
[REDACTED] UNCLASSIFIED

JPL TECHNICAL REPORT NO. 32-353

Preface

This Progress Report covers the *Mariner R* Project for the period August 1961 to September 1962. The chronology begins with the activation of the project as a means for meeting the 1962 Venus launch opportunities. Reported activities include project management, design and development, fabrication, testing, prelaunch checkout, and launch operations.

A report scheduled for publication in Spring 1963 will cover the space flight operations and mission results for *Mariner II*.



W. H. Pickering, Director
Jet Propulsion Laboratory



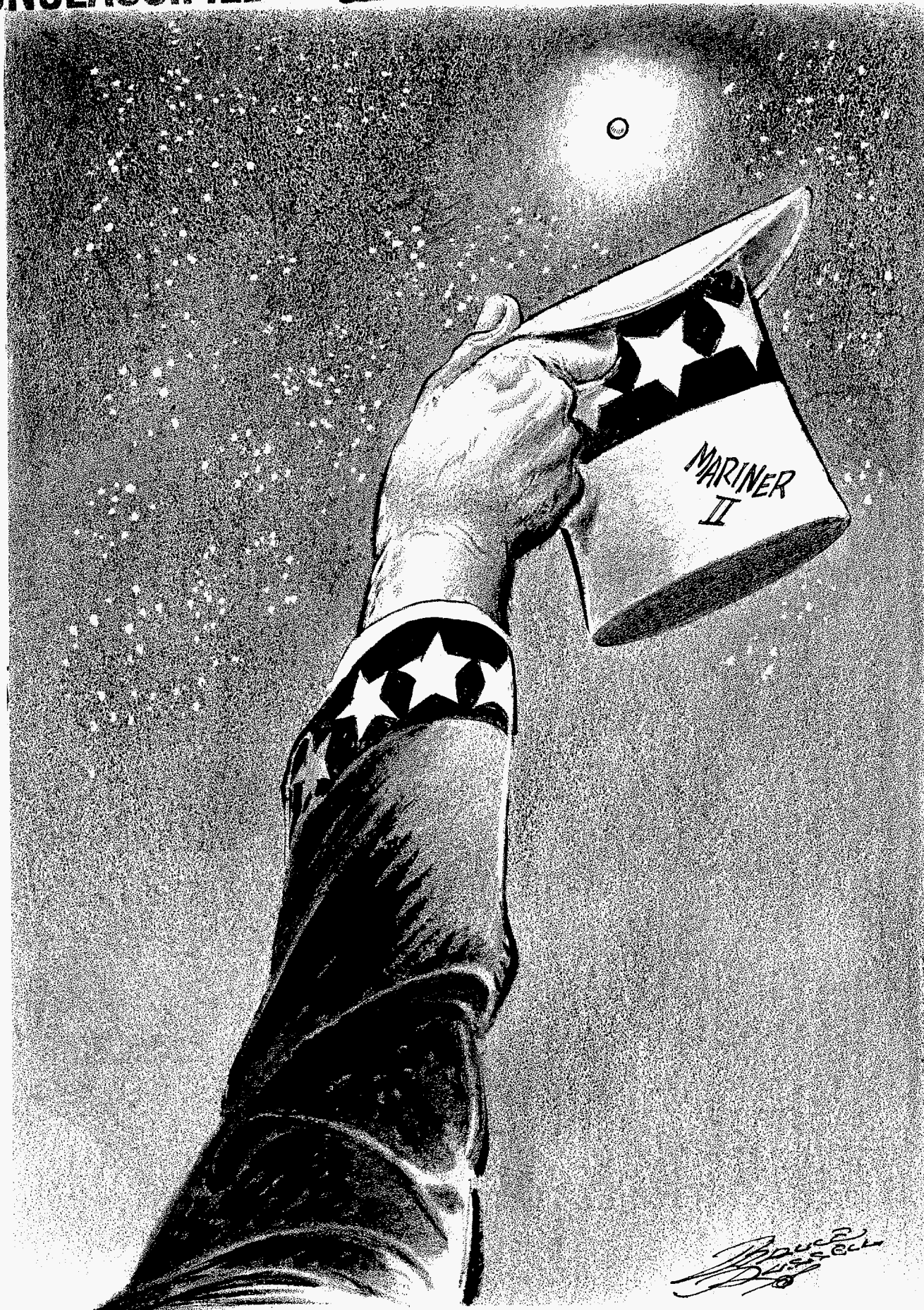
R. J. Parks
Planetary Program Director



J. N. James
Mariner R Project Manager

[REDACTED] UNCLASSIFIED

UNCLASSIFIED



Reprinted through courtesy of Bruce Russell and the Los Angeles Times.

UNCLASSIFIED

I. Project Objectives and Status

The purpose of the *Mariner R* (1962) Project was to perform the National Aeronautics and Space Administration P-37 and P-38 missions to Venus during the third-quarter launch opportunities in 1962. The *Mariner R* was a replacement for the *Mariner A* Project, which was cancelled in September 1961 because of the unavailability of the *Centaur* launch vehicle.

The primary objective of the *Mariner R* (1962) Project was to develop and launch two spacecraft to the near-vicinity of the planet Venus in 1962, to make interplanetary measurements on the way to and in the vicinity of the planet, to receive communications from the spacecraft while in the vicinity of Venus, and to perform a scientific survey of the characteristics of the planet itself.

The launch vehicle used in this project was the *Atlas D-Agena B*, providing a spacecraft weight of approximately 446 lb.

It was planned to launch the two probes sequentially off the same launch pad. All activities were planned to exploit the limited launch period to the maximum extent, based on a nominal launch period of 56 days, from July 18 through September 12, 1962. The minimum separation between the two launches was established as 21 days.

Since the time from the first consideration of a *Mariner R* mission to its launch date was less than one year (mid-August 1961 to mid-July 1962), many aspects of the project assumed the characteristics of a "crash" program. To meet the objectives in the time available, decisions had to be made quickly, a design had to be frozen at the earliest possibility, and all schedule milestones had to be met on time. To save time and to take advantage of experience already gained, use was made of existing *Ranger* committees and procedures wherever possible. The resultant design, with the limitations of time and weight allowance, produced a spacecraft with little or no

UNCLASSIFIED



JPL TECHNICAL REPORT NO. 32-353

redundancy and, consequently, one in which lower reliability was the trade-off for time. Thus, the high-risk nature of the mission was recognized.

Since it was recognized during project planning that there would be insufficient time for a proof test model, none was scheduled. The first spacecraft would be a flight model. Flight-acceptance testing of all assemblies was mandatory. Flight-acceptance test specifications were to be written and reviewed for adequacy. It was assumed that there would be insufficient time for type-approval testing of assemblies; therefore, such testing was encour-

aged but not made mandatory. Quality control inspection of all delivered assemblies was mandatory.

The planning called for two spacecraft and one set of spares, two sets of System Test Complex equipment and one set of spares, and two sets of launch complex equipment in support of the spacecraft.

All major milestones were met on time, including arrival of equipment at Atlantic Missile Range and the subsequent launches on July 21 and August 27, 1962, respectively, for the P-37 and P-38 missions.

UNCLASSIFIED



II. Project History

A. Background

The *Mariner R* Project was developed from the commitment of the Jet Propulsion Laboratory to the unmanned exploration of space for the National Aeronautics and Space Administration. Following the *Vega* program in 1959 and the *Mariner A* and *B* Projects, *Mariner R* was activated in September 1961 in order to take advantage of the 1962 Venus launch opportunities, despite delays in the development of advanced second-stage vehicles.

The *Mariner A* and *B* spacecraft were in the 1250-lb class and were designed to make scientific investigations in interplanetary space and in the vicinity of Venus and Mars, respectively, during the 1962/1964 launch opportunities. Because of funding limitations, no Mars missions were scheduled in 1962. Both spacecraft were to be launched by a vehicle consisting of a modified *Atlas D* first stage, and a *Centaur* liquid-hydrogen/liquid-oxygen, high-energy second stage.

The *Centaur* vehicle, under development by General Dynamics/Astronautics at San Diego, California, had two gimbal-mounted engines, each capable of generating 15,000 lb of thrust. Ten small hydrogen peroxide monopropellant engines were provided for attitude control,

consolidation of main propellants, and final velocity correction.

The *Mariner A* configuration was scheduled to fly the NASA P-37 and P-38 missions to Venus in summer 1962 as a developmental spacecraft on *Centaurs* 7 and 8. However, slippages in the *Centaur* schedule began to compromise the Venus launches and the missions were forced into a rescheduling. In the summer of 1961, Space Technology Laboratories of Los Angeles, California, were proposing an *Able-M* solid-stage, spinning rocket to be launched by an *Atlas-Agena* vehicle to Mars in 1962, with a dual capability to Venus in 1962 as a back-up to *Centaur* slippages. This proposal was considered but not approved by NASA.

B. *Mariner R* Proposals

The situation did not improve and, by the second week of August 1961, it was generally recognized that the *Centaur* would not be available for the 1962 Venus launch

UNCLASSIFIED

JPL TECHNICAL REPORT NO. 32-353

period. Consequently, in mid-August, discussions with NASA explored the possibility of using lightweight, attitude-stabilized spacecraft for the P-37/P-38 missions, since it was considered most important that the United States launch probes to the planets in 1962 if at all possible.

Without adding another stage to the *Atlas-Agena* or modifying the launch vehicle in any way from the configuration used for *Ranger*, it would be impossible to include a midcourse trajectory correction system or to conduct more than one launch. However, NASA and JPL both believed that the inclusion of a midcourse guidance capability and the scheduling of two launches within the 1962 period should be accomplished if at all possible.

On August 28, 1961, in a letter to NASA Headquarters, JPL proposed the feasibility of a 1962 Venus mission, based on an *Atlas-Agena* launch vehicle and the use of a hybrid spacecraft combining features of the *Ranger 3* and *Mariner A* designs. This spacecraft was proposed to carry 25 lb of instruments (later increased to 40 lb). Only one launch could be guaranteed, but two were possible within the July–September 1962 period if the *Agena* weight could be reduced. The project would not require significant changes in the *Ranger* schedule, but would necessitate the transfer of certain launch vehicles.

In addition to the activation of a *Mariner R* Project, JPL would proceed with the design and development of the *Mariner B* spacecraft, scheduled for launch by *Atlas-Centaur* with dual Mars-Venus capability in 1964 and beyond. Coincidentally with the implementation of the *Mariner R* program and the shift of emphasis in *Mariner B*, the *Mariner A* Project was to be cancelled.

Accordingly, NASA authorized cancellation of *Mariner A*, activation of the *Mariner R* Project, and establishment of the dual capability for the *Centaur*-based *Mariner B* in 1964.

With the new *Mariner R* Project approved, an all-out effort was begun to design, develop, procure, assemble, test, and launch two spacecraft within an 11-mo period. In addition, a significant launch vehicle effort involving design modifications and manufacturing changes was undertaken. The many associated efforts encompassing trajectory work, launch and flight operations preparation, design and fabrication of special ground support equipment and handling fixtures, and implementation of range support were pursued on a "crash" basis.

JPL entered the *Mariner R* Project with the objective of performing meaningful scientific experiments in interplanetary space and in the vicinity of Venus in 1962, with primary emphasis on experiments relating to the surface and atmosphere of the planet. The improvised program would also enable the Laboratory to recoup part of the investment in time and money already expended for the *Mariner A* Project.

Making maximum use of *Ranger* and *Mariner A* experience, reprogramming and rescheduling decisions were made. A design team and a project management team were appointed. Initial contacts were made with Marshall Space Flight Center and the Air Force Space Systems Division in September. Two preliminary design freeze dates were established: October 16, 1961, for subsystem interfaces; and December 15, 1961, for the total spacecraft design. Changes were possible after those dates, but only as the result of a thorough project review, and if necessary in order to achieve the basic mission objectives.

It was determined that the total spacecraft weight would be about 460 lb, rather than the some 1050 to 1250 lb planned for *Mariner A* and *B*. An 85-n mi parking orbit was initially selected in order to make 14 lb more payload available; however, this orbit was later changed to 100 n mi. In order to meet the flight schedule, tested flight assemblies and instruments would have to be available in the assembly building at Pasadena on January 15, 1962. Where possible, the estimated 40 lb of instruments would have to be procurable essentially in flight configuration, without benefit of breadboard and engineering-model phases of development. Except for the infrared radiometer, all instruments would have to be reworked *Ranger* or *Mariner A* designs.

C. Mariner Chronology

Although the plan to place two flight-ready *Mariner R* spacecraft on the launch pad in time for the July–September 1962 launch period started at a point 6 wk behind a comparable stage in the *Mariner A* schedule, the spacecraft were designed, assembled, tested, shipped, flight-checked, and launched within the scheduled times.

A chronological listing of the more important milestones in the *Mariner R* operations follows, covering the period from August 1961 through August 1962.

UNCLASSIFIED

Week of July 31, 1961. NASA estimated 9-mo slip in *Centaur 4* and asked JPL to reprogram *Mariner*.

Week of August 7, 1961. Project and Systems Division study effort begun to reprogram *Mariner*.

Week of August 14, 1961. Series of meetings with NASA and JPL groups on reprogramming of *Centaur* and *Mariner*. Feasibility study on *Mariner R* for Venus 1962 under way.

Week of August 21, 1961. Recommendations for planetary reprogramming issued to Director and staff.

Week of August 28, 1961. NASA approved activation of *Mariner R*, cancellation of *Mariner A*, and effort toward dual capability for *Mariner B*. Work started on the Project Development Plan, schedules, and design activity; initial liaison with Lockheed.

Week of September 4, 1961. Initial contact with MSFC and AFSSD; discussion on problems associated with a double shot.

Week of September 11, 1961. Discussions at Lockheed to determine *Agna* capability for *Mariner R*; 460-lb spacecraft indicated.

Week of September 18, 1961. *Mariner R* preliminary design frozen. Scientific package to include infrared and microwave radiometers, magnetometer, plasma, ion chamber, and micrometeorite experiments.

Week of September 25, 1961. Feasibility of two Venus launchings in 1962 confirmed to NASA Headquarters. Interface scheduling meeting held with LMSC.

Week of October 2, 1961. Schedule established to deliver two spacecraft to SAF on January 15 and 29, 1962; spares to follow 2 wk later. Project team concept established and assignments made. *Mariner R* Project Policy and Requirements interoffice memorandum issued to divisions. Control schedule issued to divisions.

Week of October 9, 1961. Discussions with NASA about experiments to be flown. Spacecraft mock-up ready for cabling layout to begin.

Week of October 16, 1961. Assistant *Mariner R* Project Manager added to staff. Equipment list and flow chart requirement issued.

Week of October 23, 1961. Vibration test of spacecraft test model superstructure.

Week of October 30, 1961. Two-day meeting at MSFC to coordinate Project Development Plan. Flow charts on equipment due.

Week of November 6, 1961. Match-mate tests, spacecraft mock-up, *Agna* shroud and adapter. Thermal control model into 6-ft simulator. Systems Division assumed function of preparation and coordination of working schedules and Project meetings.

Week of November 13, 1961. Spacecraft-*Agna* adapter separation tests in process. Meetings with MSFC and LMSC representatives to discuss relationships, schedules, and reports.

Week of November 27, 1961. Parking orbit changed from 85 to 100 n mi; spacecraft weight reduced from 460 to 446 lb.

Week of December 4, 1961. *Mariner R* Project-Wide Status Review.

Week of December 11, 1961. ECR total freeze date deferred until January 8-15. Interface freeze list established December 14. Divisions asked to order complete MR-3 spares and to plan on assembling MR-3 and checking it after launch of MR-1 and MR-2. Experimenter participation invited by NASA letter.

Week of December 18, 1961. Experimenters meeting at JPL. PDP sent to MSFC.

Week of December 26, 1961. Decision made to use MR-3 as test device. Meeting with MSFC to resolve interface schedules.

Week of January 2, 1962. Spaceframe delivered to SAF 1 wk ahead of schedule. JPL requested additional days on launch pad from MSFC; pad schedule meeting held at JPL.

Week of January 8, 1962. MR-1 in assembly; final PDP transmitted to NASA; Assembly and Operations Plan issued; first PDP revision issued.

Week of January 15, 1962. MR-1 assembly 80% complete. Materials Review Board action delayed until inspection at SAF on mechanical items.

Week of January 22, 1962. MR-1 assembly complete; electrical and magnetic field tests started. MR-2 assembly started. First magnetic field test of assembled MR-1 showed fields of 10 to 15 gamma. MR-1 weighed; predicted weight now 446 ± 2 to 3 lb.

Week of January 29, 1962. Project Design Status Review. MR-1 estimated about 1 wk ahead of schedule. LMSC-JPL r-f tests under way at JPL. Range Safety consideration for *Mariner R* approved by Air Force Missile Test Center.

UNCLASSIFIED

JPL TECHNICAL REPORT NO. 32-353

Week of February 5, 1962. Status Review held at LMSC. Meeting at Cape Canaveral to discuss mission objectives, uncover areas needing attention.

February 10, 1962. Initial MR-2 power turn-on.

Week of February 26, 1962. Temperature control model into space simulator; only limited tests possible since no Sun simulation available; MR-1 and MR-2 on schedule, by-passing shortages. Attitude-control gas system and solar panels major trouble areas.

Week of March 5, 1962. TCM into simulator for second test series. MR-1 about half-week behind schedule; MR-2 still ahead. System Test Objectives document signed off. Decision not to impose any mandatory AMR data requirements on MR-2. Meeting to discuss large number of firing tables required for *Mariner R*.

Week of March 12, 1962. System tests begun on both spacecraft. Decision that MR-1 and MR-2 were planned to go into small space simulator, TCM into large facility.

Week of March 19, 1962. Trajectory meeting with LMSC, STL, and other interested agencies; first launch possibility set for July 15. *Atlas*, *Agna*, spacecraft essentially on schedule. Gas valves, infrared radiometer, solar panels principal problems.

Week of March 26, 1962. Match-mate tests on MR-1 and *Agna* shroud and adapter.

Week of April 2, 1962. MR-1 small simulator tests revealed CC&S and power problems. Match-mate on MR-1 and MR-2 complete. Preliminary estimate issued on down-range tracking and telemetry support to be provided by AMR (PAA). Squib test on type-approval solar panel latching pin-puller systems.

Week of April 9, 1962. MR-1 small simulator tests complete; MR-2 dummy run and match-mate conducted; TCM in large simulator. Project-Wide Status Review meeting held. First use of "Problem List" monitoring of daily progress on spacecraft status.

Week of April 16, 1962. MR-2 undergoing vibration tests. Project Manager observed RA-4 operations at AMR.

Week of April 23, 1962. MR-2 in small simulator; MR-1 in vibration tests. AMR Range Safety defined launch sector as 93-110 deg with no destruct receiver on *Agna*.

Week of April 30, 1962. Spacecraft Systems Manager appointed. MR-1 magnetometer-mapped; MR-2 simulator tests completed.

Week of May 7, 1962. MR-1 dummy run completed. JCLOT test conducted with the spacecraft, SFOC, CCF,

and SDAT participating. Interplanetary measurements on way to Venus established by NASA as primary mission objectives, as well as planet-related experiments. Meetings held to discuss incorporation of 960-mc telemetry on Ascension and TFV.

Week of May 14, 1962. Clean-up, microscopic inspection, completion of ECR's on both MR-1 and MR-2. MR-3 assembly begun. First two vans of equipment shipped to AMR.

Week of May 21, 1962. Final system test of MR-1 completed satisfactorily; spacecraft prepared with GSE for shipment. All outstanding ECR's completed. Final system test of MR-2 completed satisfactorily.

Week of May 28, 1962. MR-1, MR-2, MR-3 and all associated GSE shipped to AMR. Spacecraft System Manager status report to Senior Staff. *Atlas* for MR-1 aboard a C-133 at San Diego; all C-133 aircraft grounded.

Week of June 4, 1962. All spacecraft and equipment arrived at AMR. Shipment of *Atlas* for MR-1 delayed until June 9.

Week of June 11, 1962. MR-1 and MR-2 firing dates established. Both spacecraft in ready-to-fly condition. *Atlas* erected at AMR.

Week of June 18, 1962. MR-2 *Atlas* and *Agna* arrived at AMR. MR-3 assembled and in electrical checkout at AMR. Documents published: SFOP revision 1, STO major revision, OR 3300 and 3330, and FTD.

Week of June 25, 1962. MR-3 system-tested satisfactorily.

Week of July 2, 1962. Dummy run and JFACT test on MR-1.

Week of July 9, 1962. MR-1 final flight preparations and system test; final system test on MR-2.

July 22, 1962. MR-1 launched; destroyed by Range Safety at about 292 sec of flight because of erroneous *Atlas* yaw-left maneuver.

Week of July 23, 1962. MR-1 review meeting held at Air Force Space Systems Division; panels formed to investigate GE rate beacon and guidance equations.

Week of July 30, 1962. MR-2 JFACT completed.

Weeks of August 6, 13, 20, 27, 1962. MR-2 tests concluded. MR-2 launch postponed from August 17 to 18 to 20 to 27 because of *Atlas* autopilot troubles.

UNCLASSIFIED

UNCLASSIFIED

JPL TECHNICAL REPORT NO. 32-353

MR-2 was finally launched on August 27, 1962, on an azimuth of 106.8 deg. Telemetry showed that all engineering systems were functioning and that the spacecraft was successfully injected into a Venus transfer trajectory within the capabilities of the midcourse correction system. Following separation and shroud ejection, Sun ac-

quisition was successfully completed. On August 31, 1962, the closest approach (uncorrected) to Venus was estimated to occur on December 13, 1962, at 376,000 km. At 8 a.m. on August 31, the spacecraft was 777,025 st mi from Earth, flying at an Earth-referenced speed of 6,927 mph. A later report will cover the flight operations.

UNCLASSIFIED

UNCLASSIFIED



UNCLASSIFIED

2011-01-01



III. Project Organization and Management

A. Management Organization

1. National Aeronautics and Space Administration

The responsibility for the *Mariner R* Project at National Aeronautics and Space Administration headquarters was assigned to the office of the Director of Lunar and Planetary Programs, under the over-all direction of the Office of Space Sciences. The organization chart shown in Fig. 1 indicates the relationship of these offices.

2. Jet Propulsion Laboratory Organization

The Jet Propulsion Laboratory was assigned project management responsibility for the *Mariner R* Project. JPL was also assigned system management responsibility for the *Mariner R* spacecraft system, including the associated complex for postinjection space flight operations. Figure 2 is an organization chart of the Jet Propulsion Laboratory. A summary of the responsibilities under the project manager structure is shown in Fig. 3.

3. Marshall Space Flight Center

The George C. Marshall Space Flight Center was assigned responsibility for the over-all management and conduct of the launch vehicle portion of the *Mariner R* Project. In particular, this assignment included administrative and technical responsibility from vehicle procurement through launch and tracking to spacecraft injection. Figures 4 through 6 show the organizational structure at MFSC.

Vehicle system responsibility. The Director, MFSC, in order to assume management cognizance of the *Agena B* and *Centaur* Projects, established as his principal agent a Light and Medium Vehicle Office directed by Mr. Hans Hueter. Mr. Hueter has responsibility for assuring proper vehicle support to the several space projects, including *Mariner R*, which utilize these vehicles, along with procurement and proper coordination with Air Force boost vehicles, such as *Atlas*, to be utilized with *Mariner R*. In order to support the *Mariner R* Project, as well as others utilizing the *Agena B* vehicle, an *Agena B* Sys-

tems Manager, Mr. Friedrich Duerr, was appointed within this organization. Mr. Duerr is responsible for the planning and execution of the approved *Agna B* vehicle projects, including procurement; modification; GSE; planning and implementation of launch-to-injection, tracking, and instrumentation; and certification of performance and reliability analysis. The assigned responsibility includes ensuring the integrity and performance of the launch vehicle and spacecraft for proper mating of these systems necessary for the successful injection of the spacecraft. This effort includes facilities and ground support equipment for the various phases of manufacturing, testing, and launch preparation. In view of the contractual arrangements for launch vehicles, the activities of the prime contractors and subcontractors are directed by Mr. Duerr through the Air Force Space Systems Division.

Launch operations responsibility. Within Marshall Space Flight Center, a Launch Operations Directorate was assigned responsibility for NASA launches in accordance with Marshall Manual 2-2-9, dated July 1, 1960. For the project assigned to the Light and Medium Vehicle Office, LOD was to perform the launch operations in response to program requirements and objectives as specified by the *Agna B* Systems Manager. LOD Director, Dr. Debus, designated within LOD Mr. Charles Cope as the NASA *Agna B* Coordinator. The NASA *Agna B* Systems Manager placed requirements with LOD through Mr. Cope. On July 1, 1962, LOD was redesignated as the Launch Operations Center, Dr. Debus, Director. There was no need, however, to renegotiate agreements reached earlier with LOD relating to the *Mariner R* Project.

4. Air Force Space Systems Division

Responsibility for procurement, together with logistic and management support to meet NASA *Agna* launch schedules, was assigned to the USAF. AFSSD was responsible for operational, administrative, and technical support for NASA *Agna* launch vehicles. This assignment included personnel and facilities in support of launch operations. AFSSD acted as agent for MSFC in contract procurement of launch vehicles in accordance with USAF procedures, except as modified by NASA regulations and policy, or by law. The SSD Director for NASA *Agna* Projects (Major J. Albert) was the normal USAF contact for SSD operations associated with the NASA *Agna* Project (Fig. 7).

5. Lockheed Missiles and Space Company

Within LMSC, the NASA *Agna* Project was managed by a Program Office headed by Mr. H. T. Luskin. The

MSFC plant representative's office, Mr. Luskin, and a portion of the LMSC staff active on the project were located together for ease of communication. In 1960, LMSC "projectized" its organization to increase the responsiveness of the various technical groups contributing to the program. Figure 8 shows the LMSC organization supporting the NASA activities, including the *Mariner R* Project.

6. Permanent Project-Wide Bodies

In order to utilize the relationships developed on *Ranger/Agna* to the maximum, the same board and panels as existed in the *Ranger* Project were used for *Mariner R*, serving as technical advisers to the project and system managers.

Agna B Coordination Board. This board was appointed at the beginning of the *Ranger* Project to coordinate the vehicle requirements of the various users of the *Agna B* vehicle and to provide a mechanism for the settlement of interagency problems. The *Agna B* board composition follows:

J. L. Sloop	NASA	Chairman
D. L. Forsythe	NASA	Deputy Chairman
B. Milwitsky	NASA	Lunar Program Director
J. L. Mitchell	NASA	
W. Jakobowski	NASA	
F. Duerr	MSFC	<i>Agna B</i> Systems Manager
J. D. Burke	JPL	<i>Ranger</i> Project Manager
J. N. James	JPL	<i>Mariner R</i> Project Manager
E. A. Rothenberg	GSFC	

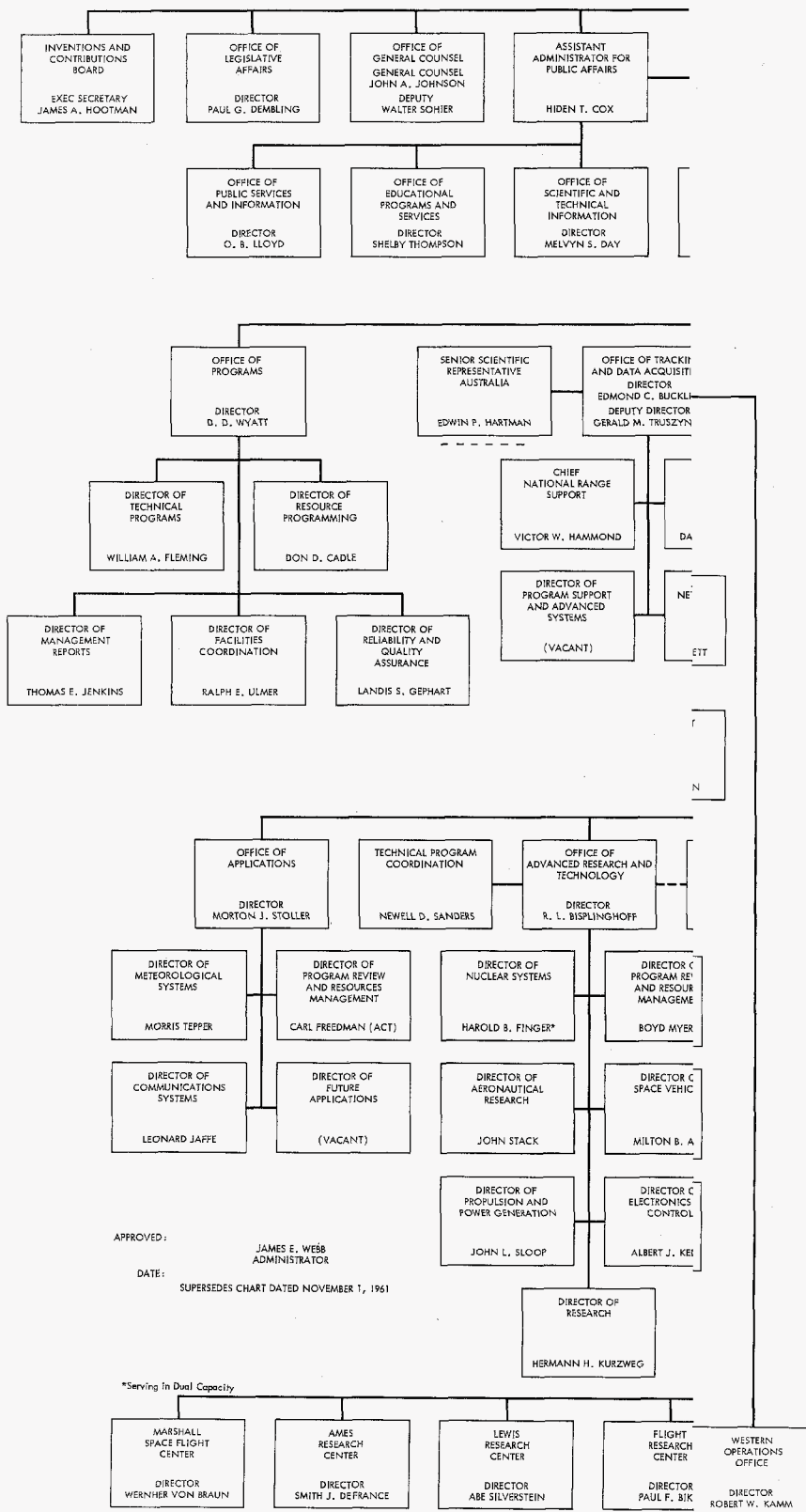
Vehicle Integration Panel (F. Duerr, Chairman). This group continually monitors, compiles, and evaluates the structural, network, and configurational problems as they relate to the interface between the spacecraft and vehicle with shroud. The panel is also responsible for the interface aspects of the launch checkout procedure.

Performance Control, Trajectories, Guidance and Control, and Flight Dynamics Panel (J. L. Stamy, Chairman). This panel continually monitors, compiles, evaluates, and coordinates data relating to performance, trajectories, guidance and control, and flight dynamics as they interact with the vehicle, the shroud, and the spacecraft interface.

Tracking, Communication, In-Flight Measurements and Telemetry Panel (M. S. Johnson, Chairman). This

UNCLASSIFIED

ICAL REPORT NO. 32-353



ministration

UNCLASSIFIED

[REDACTED]



Approved W. H. Fickering
Director
September 10, 1962

[REDACTED]

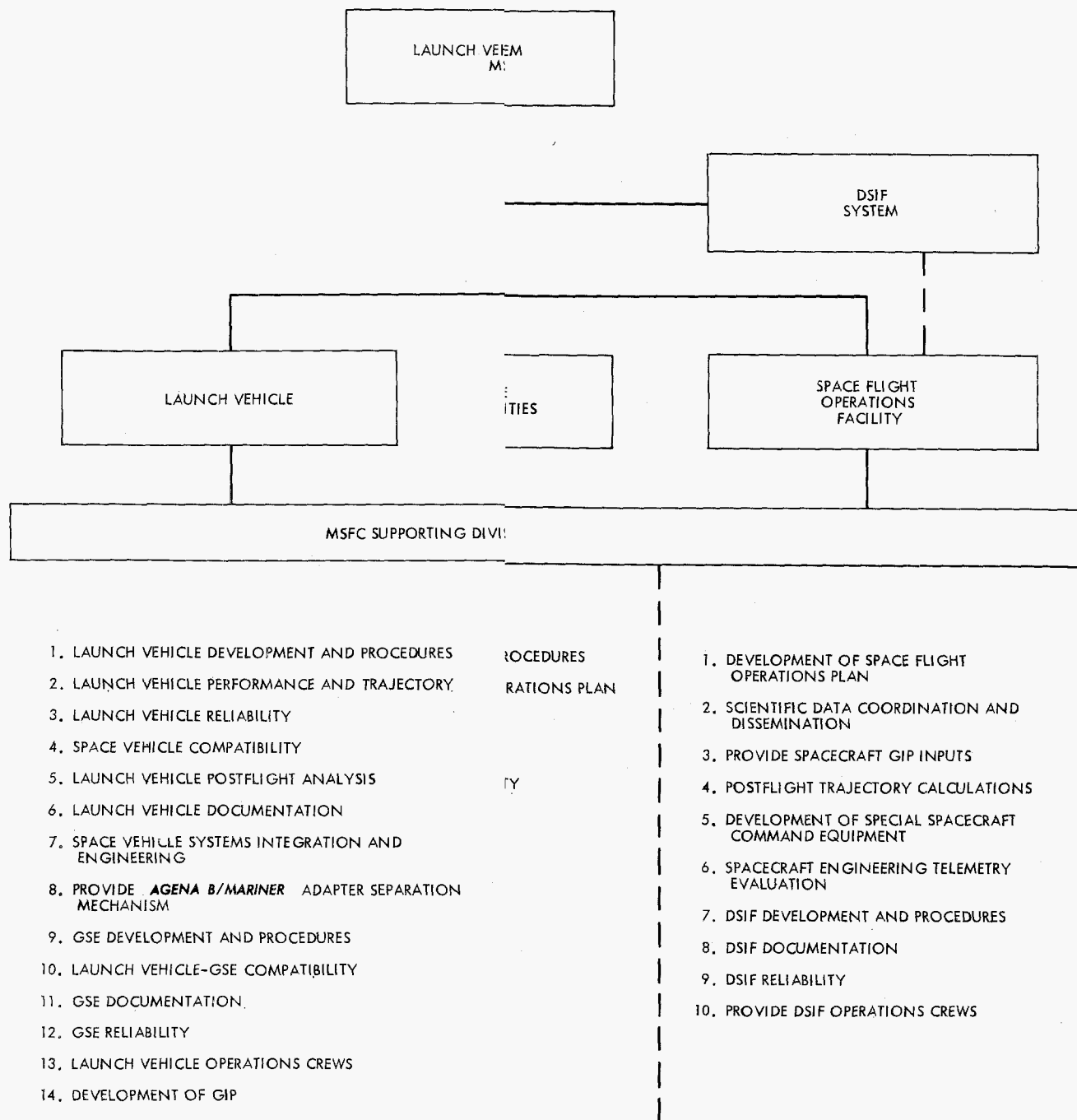


Fig. 3. Responsibilities assignments for Mariner R Project

UNCL A

UNCLASSIFIED

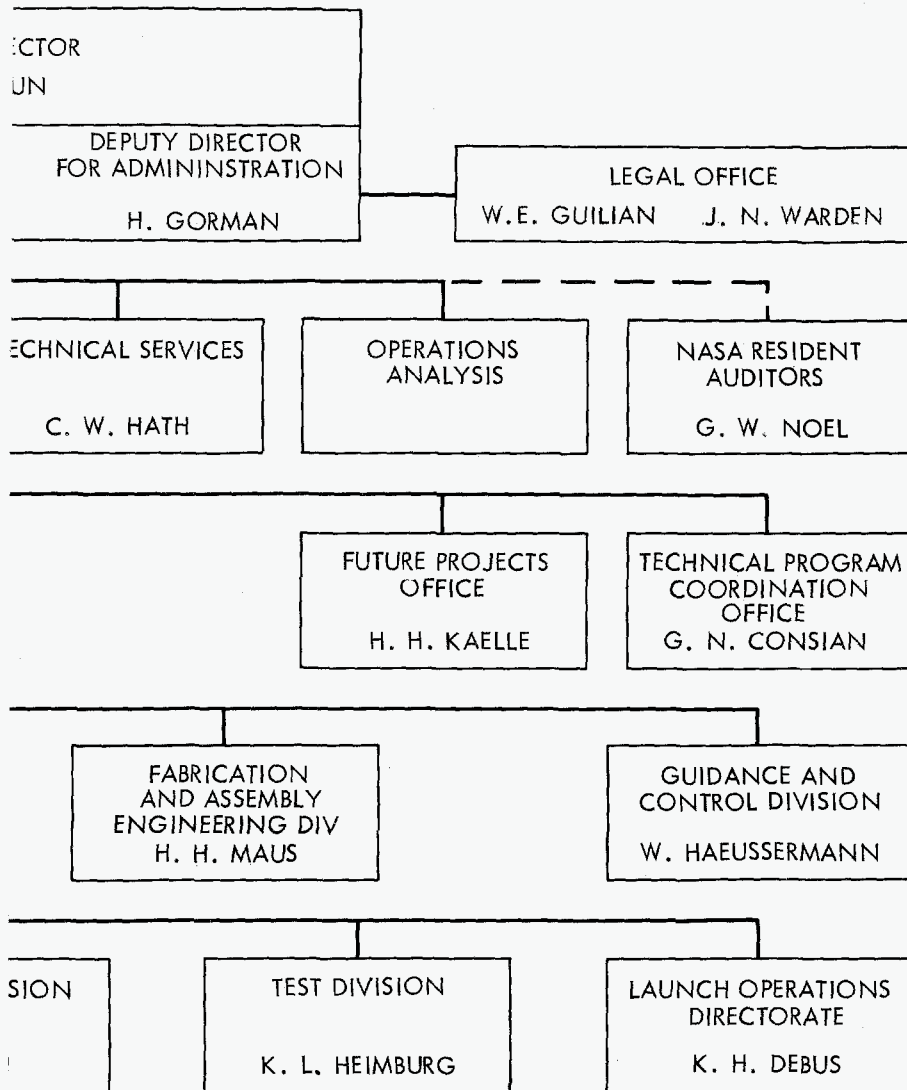


Fig. 4. George C. Marshall Space Flight Center

UNCLASSIFIED

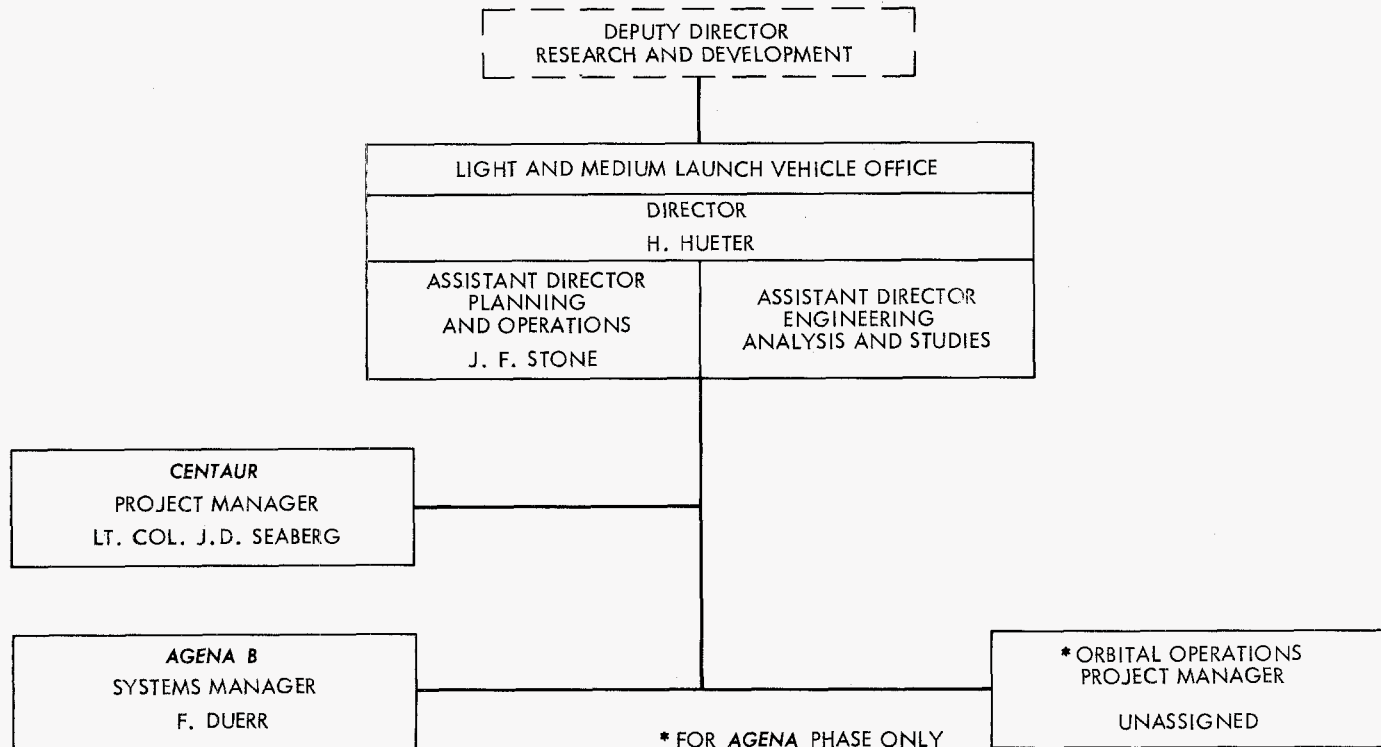


Fig. 5. MSFC Systems Support, Equipment Division, Flight and Medium Launch Vehicle Office

group continually monitors, compiles, evaluates, and coordinates data relating to tracking, communications, in-flight measurements and telemetry as these items interact with the vehicle, the shroud, and the spacecraft.

Atlas/Agena B Flight Test Working Subgroup. This group acts as the prime mechanism for coordinating flight preparations. Members participate in vehicle and range readiness meetings, culminating at T - 1 day, at which time the Launch Operations and Test Director (Dr. Debus) assumes over-all control with AFSSD assistance.

unite the different organizations for achieving the objectives of the *Mariner R* Project, considerable person-to-person contacts were made.

A series of status reviews was held. These meetings were held at Lockheed Missiles and Space Company (Sunnyvale, Calif.); Jet Propulsion Laboratory (Pasadena, Calif.); Atlantic Missile Range (Cape Canaveral, Fla.); and General Dynamics Corporation (San Diego, Calif.). At these reviews, project policies and orientation were presented and all agencies involved in the project were represented. It is believed that the status meetings promoted better understanding of organizational interfaces within the project. It is expected that *Mariner* (1964) will continue to use this technique.

B. Launch Vehicle Relations

A major concern of the *Mariner R* Project management was to control, coordinate, and follow the many activities of the project. As noted in Section I, five separate organizations have areas of prime technical cognizance in the project. To assist in the resolution of problems, to keep channels of communications open, and to inform and

C. JPL Activities and Implementation of JPL Activities

In addition to project management responsibility for the *Mariner R* Project, JPL was responsible for: (1) the

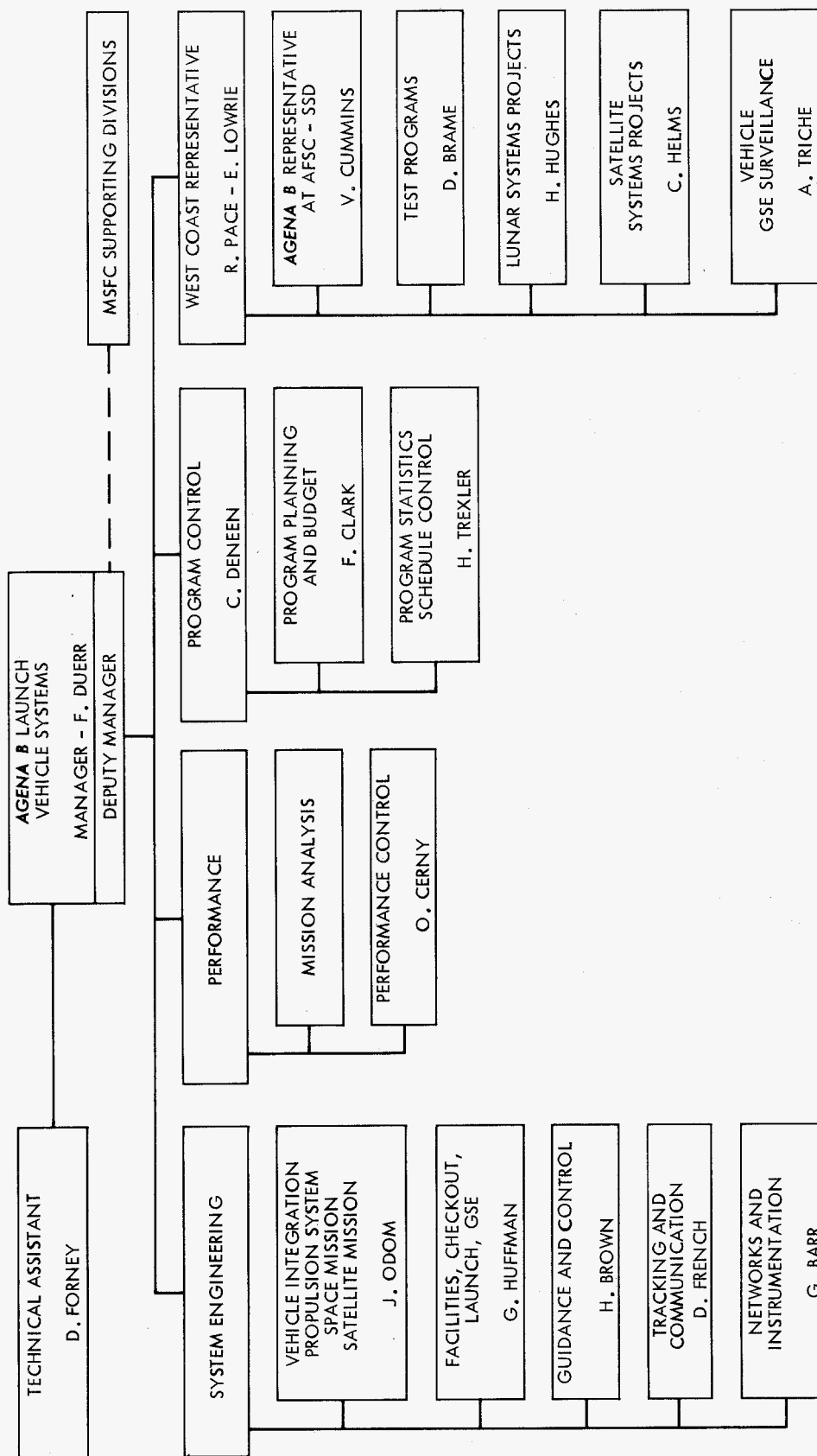


Fig. 6. MSFC Agena B launch vehicle system organization

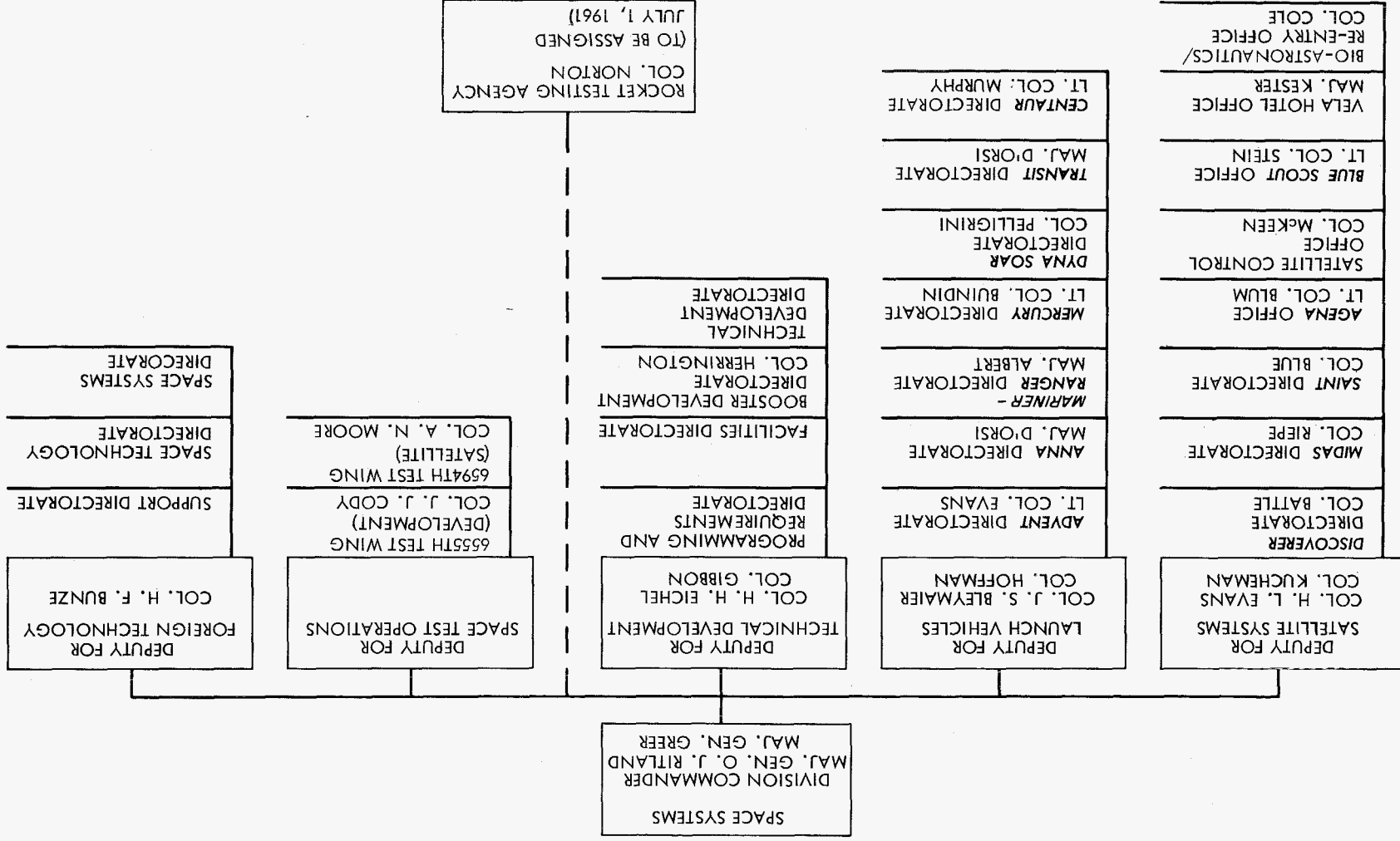


Fig. 7. Air Force Systems Command, Aerospace Systems, Space Systems Division

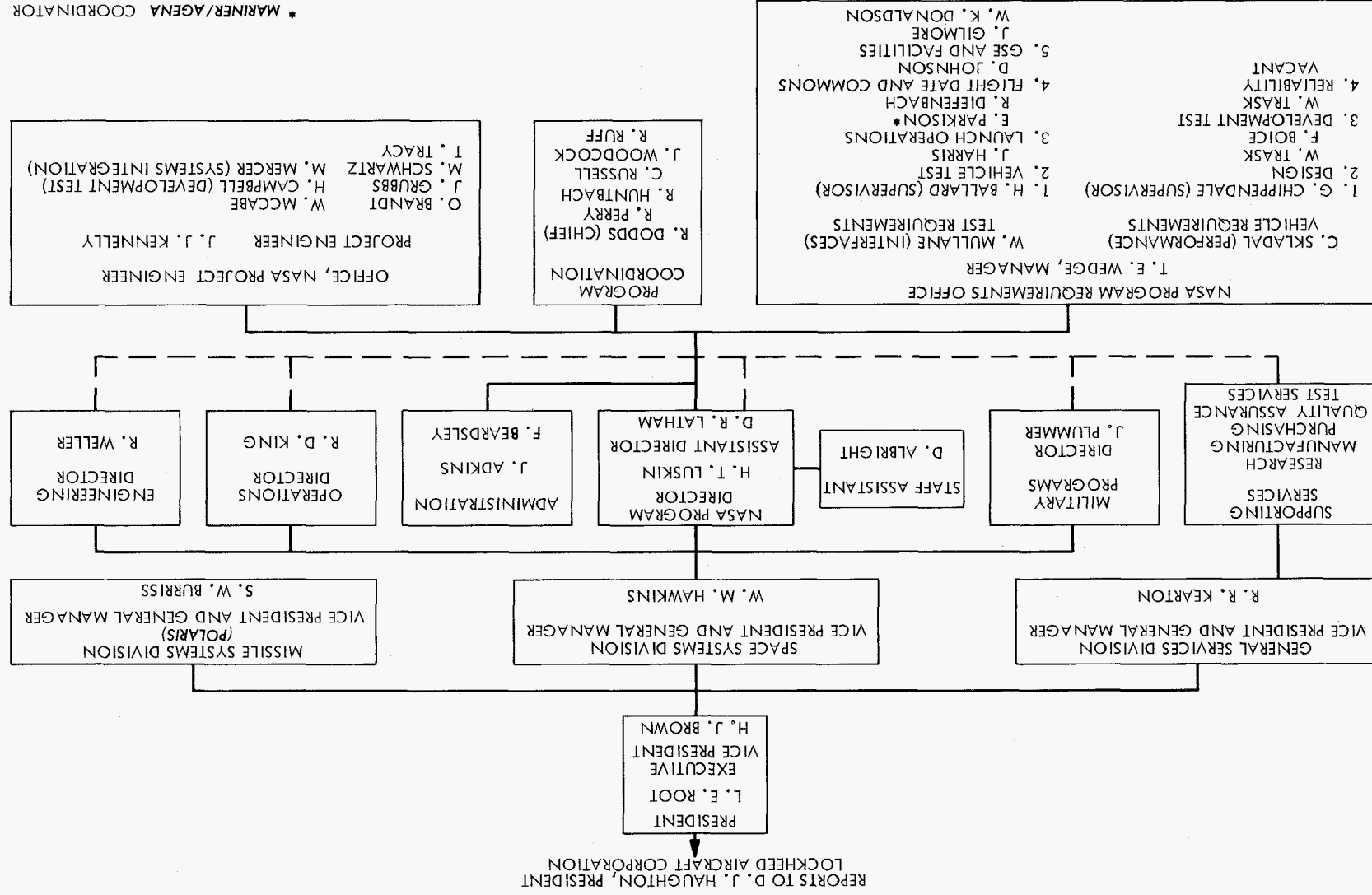


Fig. 8. Lockheed Missiles and Space Company organization supporting Mariner R Project

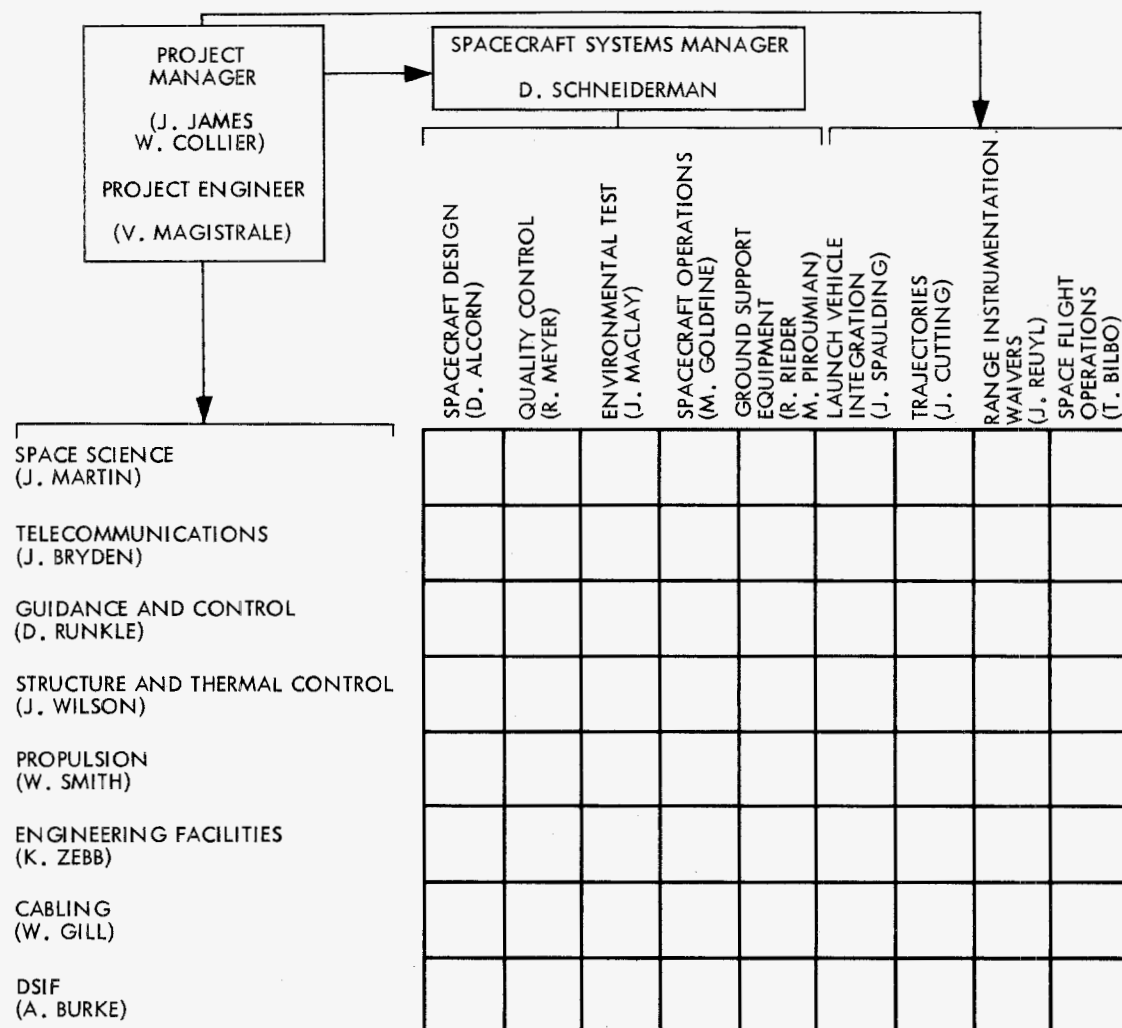


Fig. 9. JPL division project representative organization

design, fabrication, and testing of the spacecraft and its associated ground support equipment; (2) the space flight operations of the spacecraft from injection to planetary encounter; and (3) the Deep Space Instrumentation Facility tracking operations. To implement these responsibilities, the following techniques were developed by the project.

1. Project Policy and Requirements Document

This document specified the project policy and requirements for the *Mariner* (1962) mission. It established the operational procedures for the project in that it stated mission objectives, system requirements, milestones, and an over-all guideline schedule. The document is attached to this Report as Appendix A.

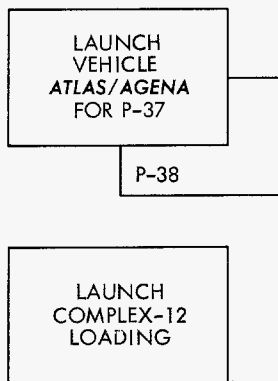
2. Weekly Project Meeting

Weekly project meetings were held with representatives from each of the operating divisions. These meetings established the hard core of individuals who had a continuity with the over-all aspects of the project. These individuals were assigned from each technical area and formed an organizational matrix to aid in the exchange of information, to monitor progress, and to function as the hub of all project action. Minutes of the meetings were published and distributed to all other interested personnel at JPL. The organizational structure is shown in Fig. 9.

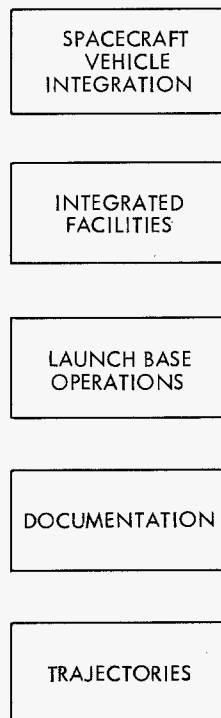
3. Design Freeze

Since *Mariner R* was a crash project, requiring shipping of equipment to AMR 9½ mo after the go-ahead, it was

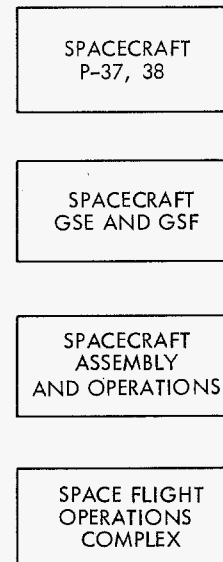
MARSHALL SPACEFLIGHT CENTER SCHEDULES



INTERFACE SCHEDULES



JET PROPULSION LABORATORY SCHEDULES,

Fig. 10. *Mariner R* Project schedule reporting structure

necessary to freeze the design without inhibiting necessary design action. The problem of when and how to freeze the design was complicated by a natural tendency by hardware-producing divisions to set the cut-off date as late as possible, while wishing other areas to freeze as early as possible. In addition, documentation was incomplete for all subsystems.

An initial survey of the subsystems was conducted to determine when to freeze and in what order. Major interfaces were scheduled first. Thereafter, any individuals who desired to freeze their particular subsystems, in whole or in part, could do so by referencing the appropriate control documents on the freeze list. A list—"Mariner R Change Freeze"—was published periodically and any changes to those drawings and specifications listed required an Engineering Change Requirement.

Thus, the *Mariner R* Project was able to institute a continuing freeze concept while maintaining flexibility of operation by scheduling major interface freezes and allowing other areas to be frozen at will for defensive reasons. A complete freeze requiring ECR action was instituted January 15, 1962. Appendix B is a sample of the Change Freeze List as of December 29, 1961.

4. Scheduling

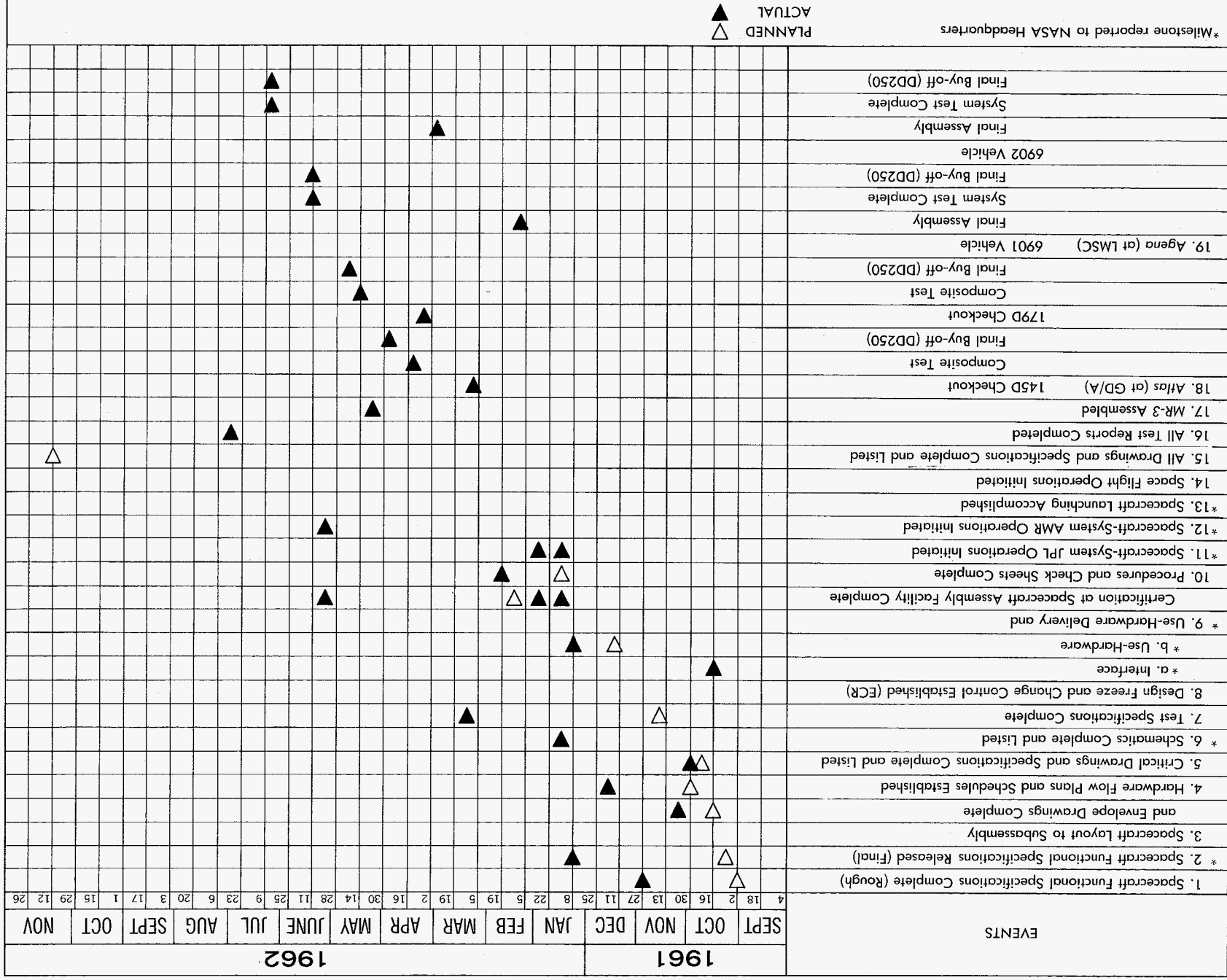
An initial schedule structure for the *Mariner R* Project is shown in Fig. 10. The evolution of schedules continued during the project so that two agencies, JPL and MSFC (via LMSC), were providing the following schedules:

JPL schedules

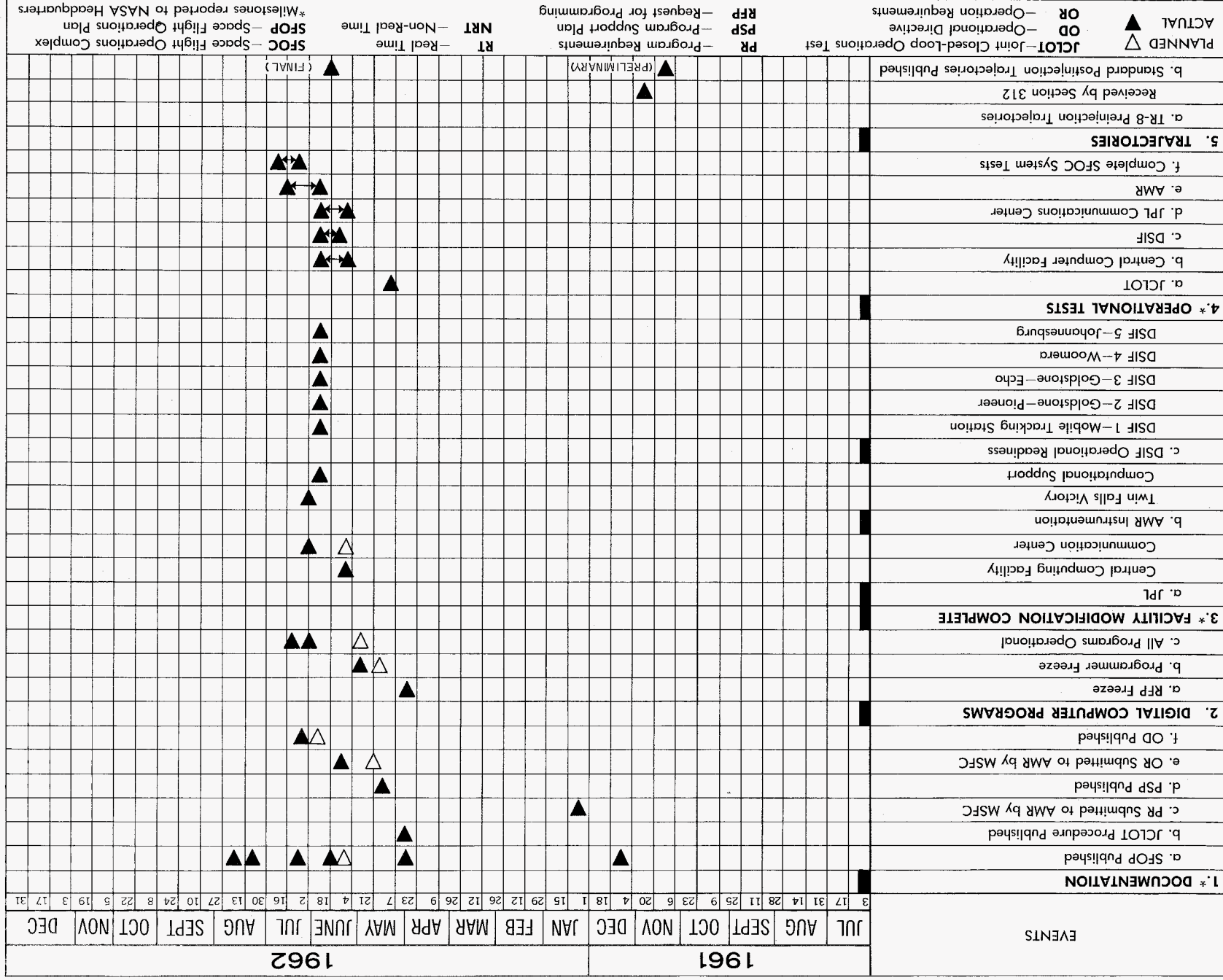
- (1) Spacecraft Schedule, P37, P38 (Fig. 11)
- (2) Space Flight Operations Complex Schedule (Fig. 12)
- (3) Spacecraft GSE and GSF, P-37, P-38 (Fig. 13)
- (4) Documentation, P-37, P-38 (Fig. 14)
- (5) *Mariner R* Trajectory Schedule (Fig. 15)
- (6) Spacecraft Assembly and Operations (Fig. 16)
- (7) AMR Facilities and GSE (Fig. 17)
- (8) Launch Base Operations (Fig. 18 and 19)

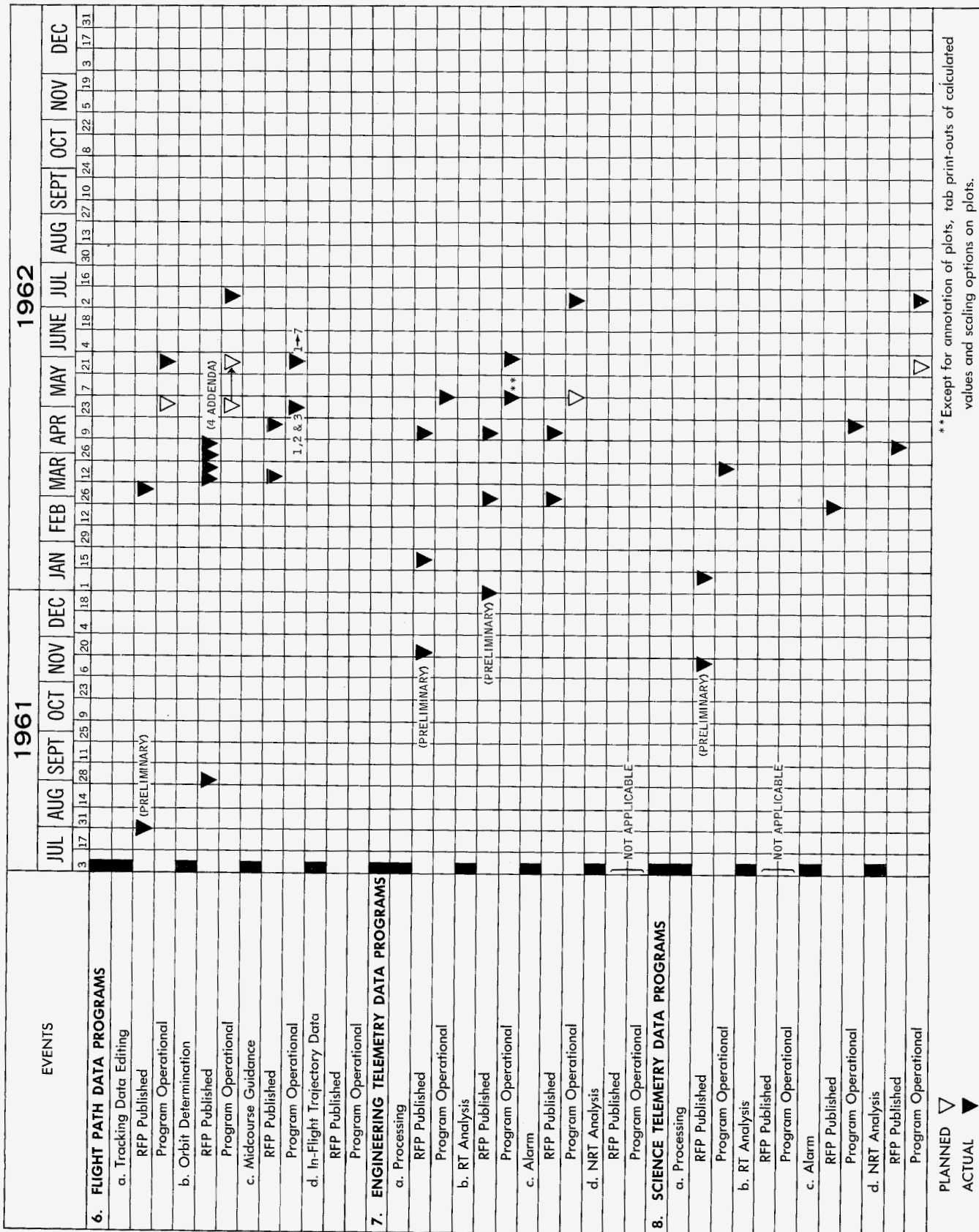
UNCLASSIFIED

JPL TECHNICAL REPORT NO. 32-353



UNCLASSIFIED





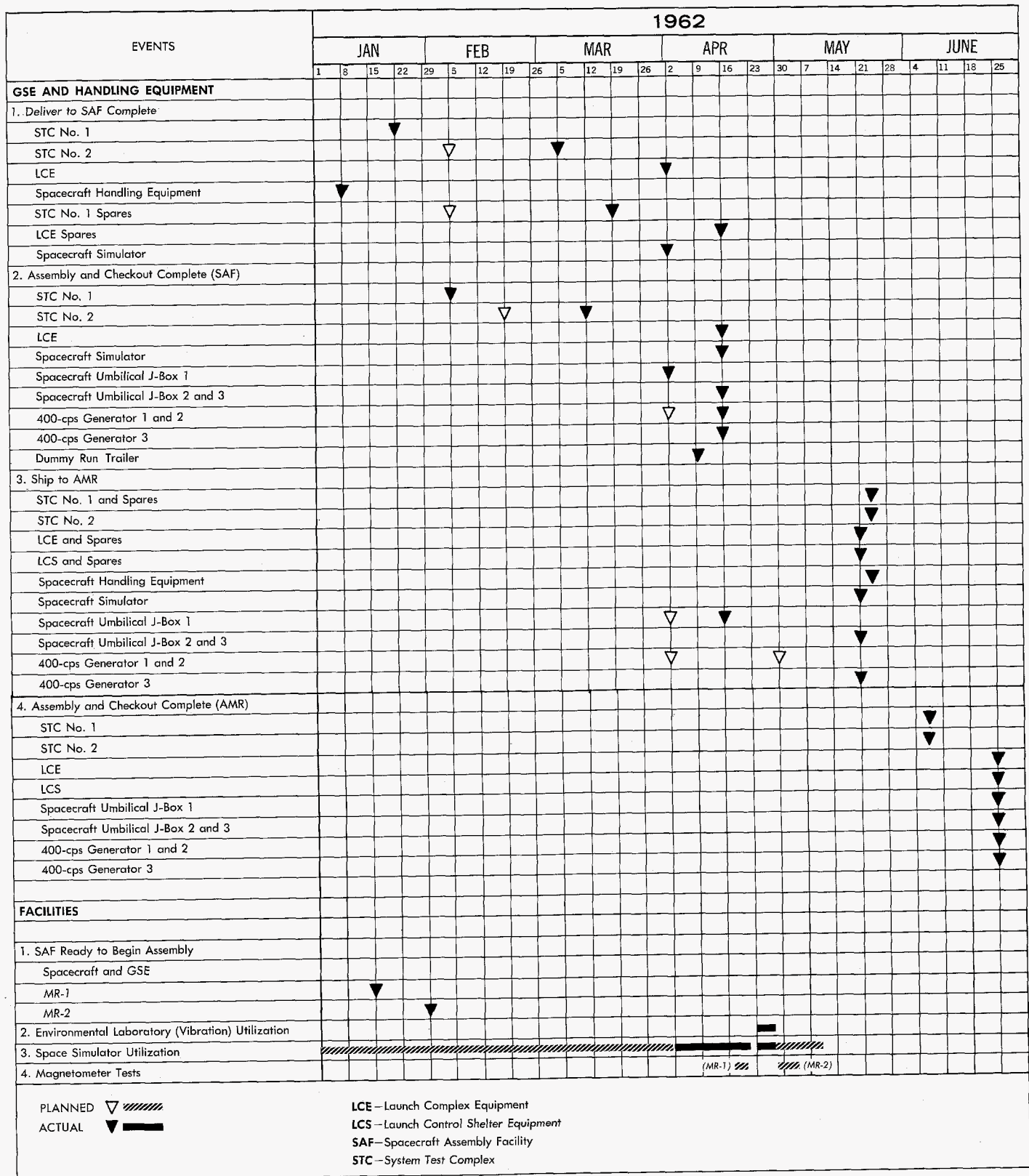


Fig. 13. P-37, P-38 spacecraft GSE and GSF schedule

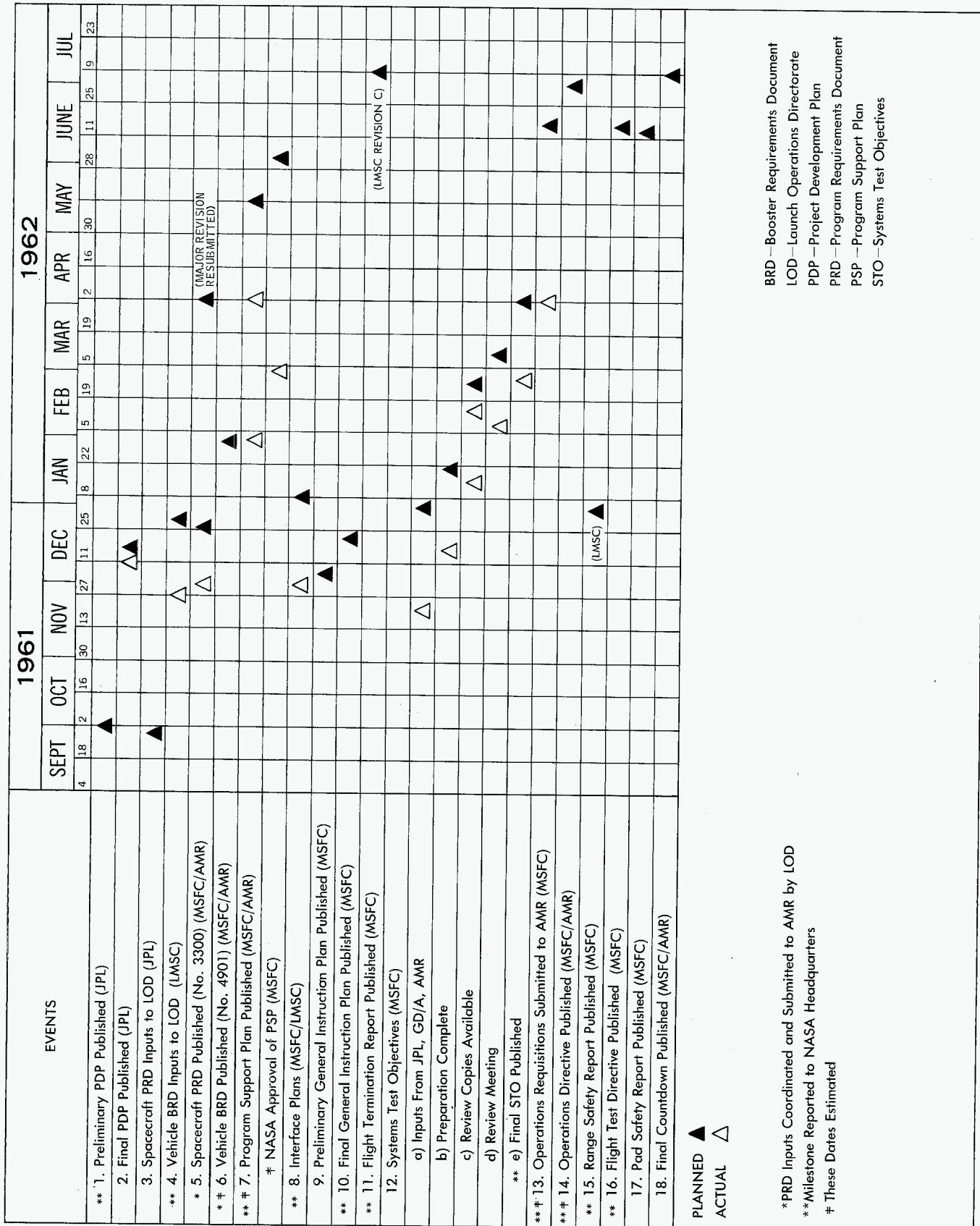


Fig. 14. P-37, P-38 documentation schedule

UNCLASSIFIED

JPL TECHNICAL REPORT NO. 32-353

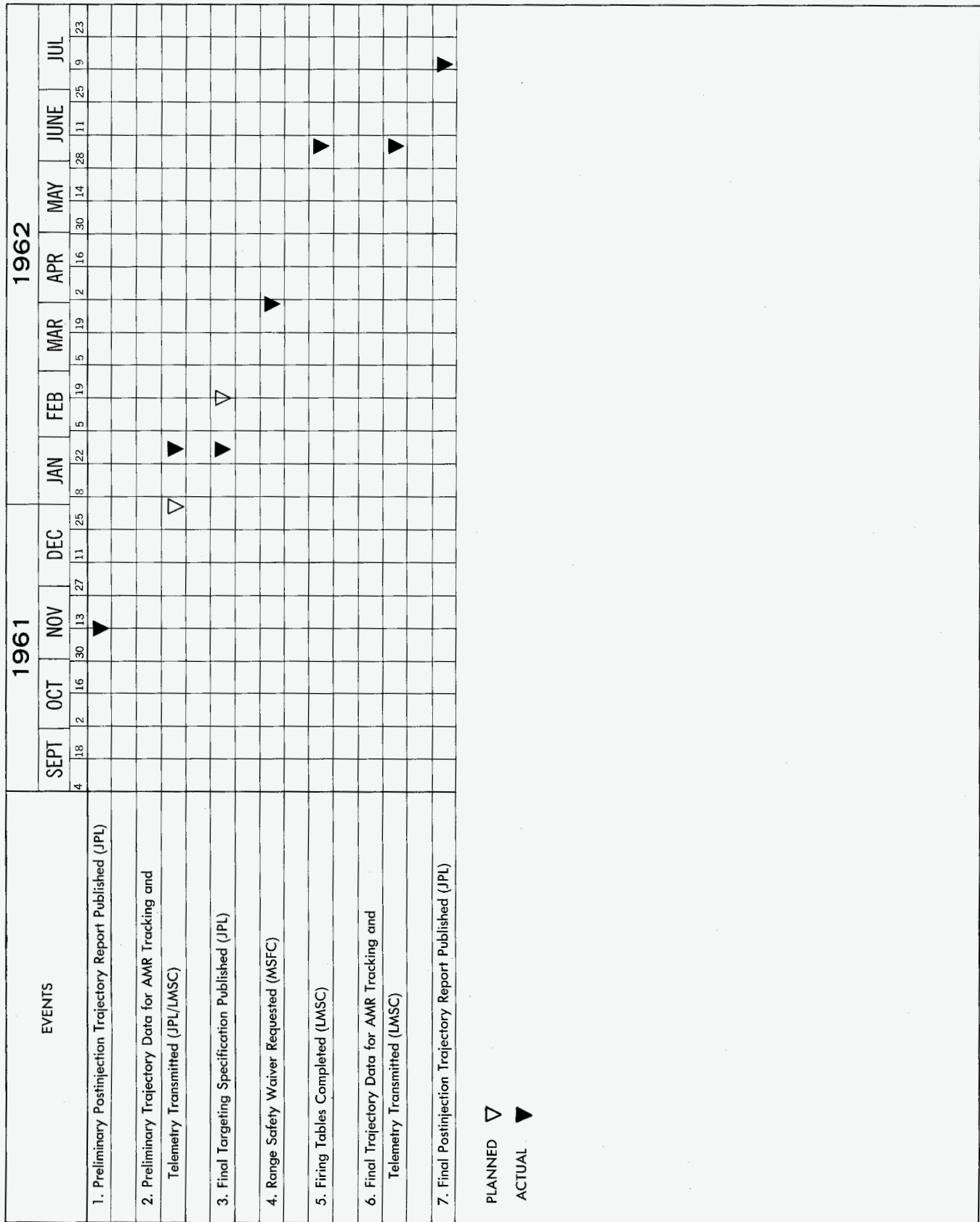


Fig. 15. Mariner R trajectory schedule

UNCLASSIFIED

UNCLASSIFIED

JPL TECHNICAL REPORT NO. 32-353

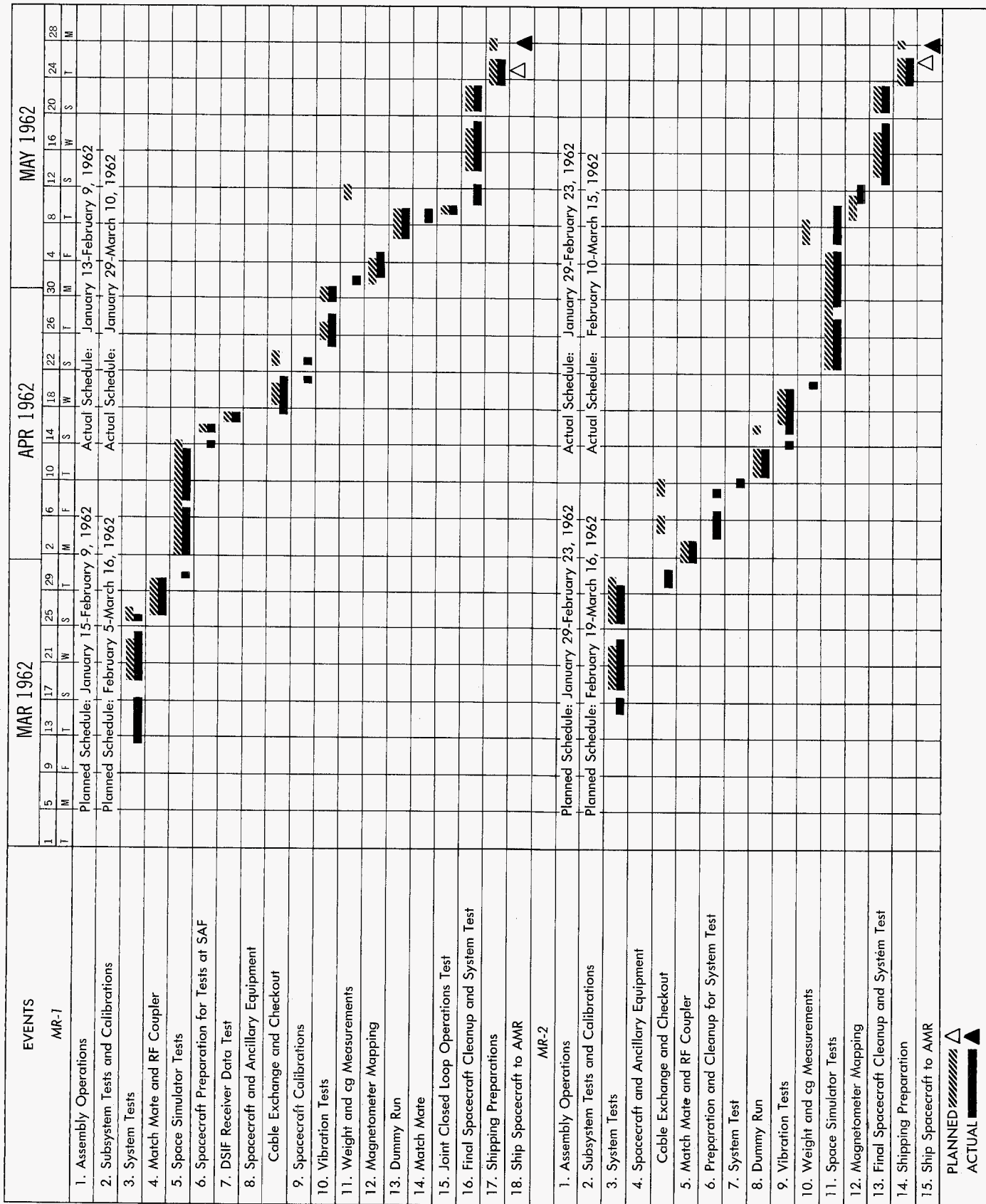
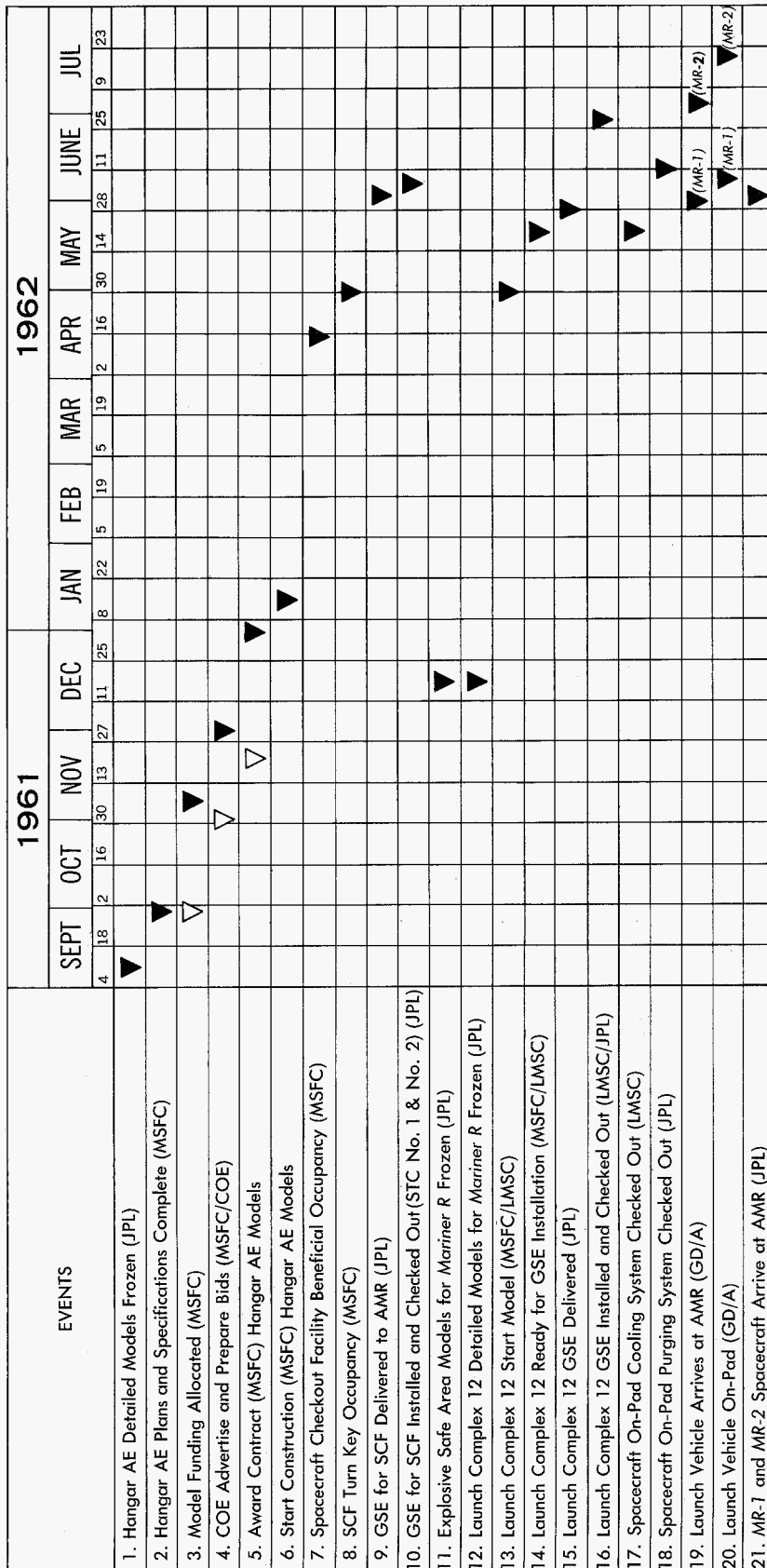


Fig. 16. JPL spacecraft assembly and operations schedule

UNCLASSIFIED



PLANNED ▽
ACTUAL ▼

Fig. 17. AMR facilities and GSE schedule

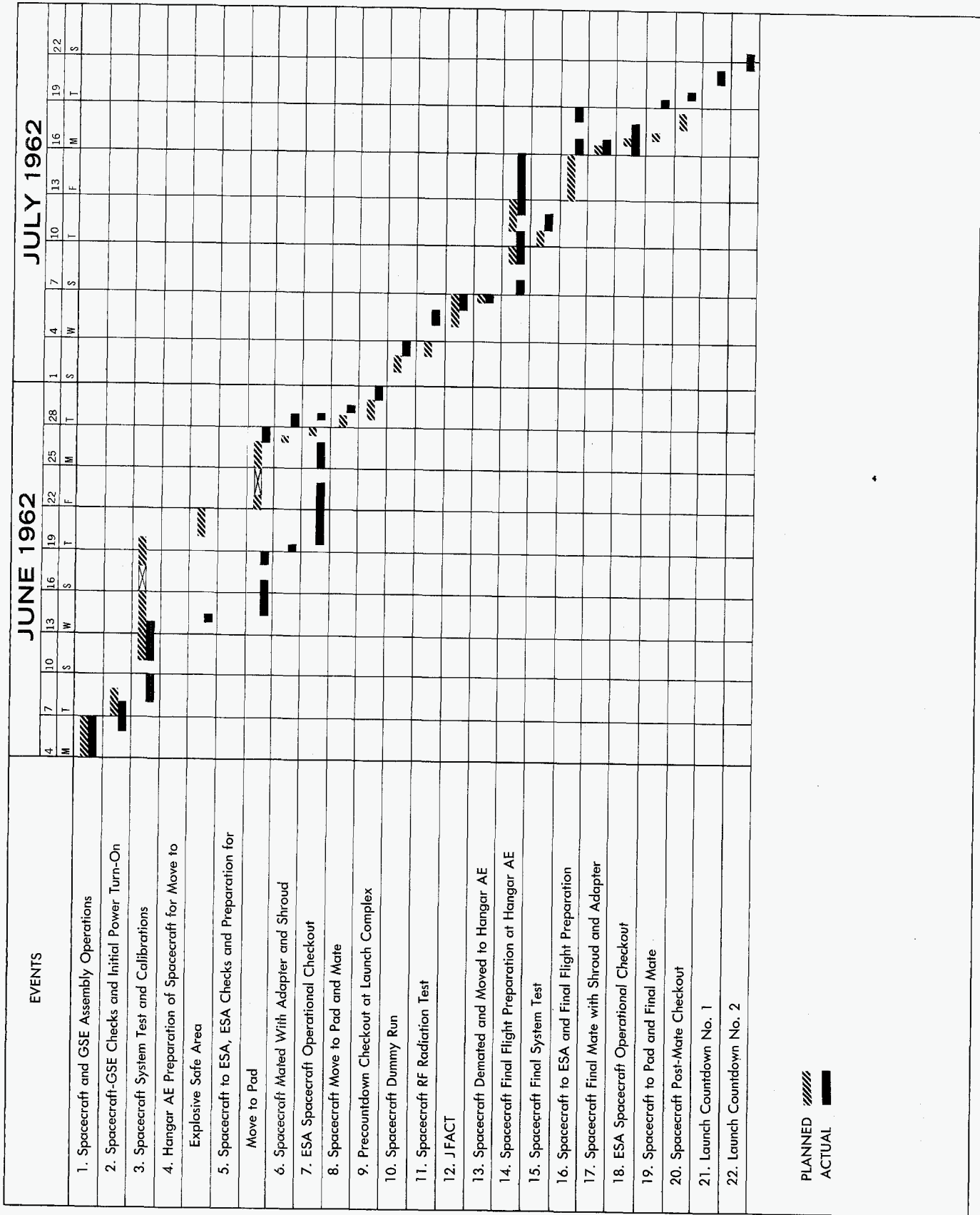
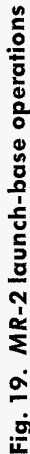


Fig. 18. MR-1 launch-base operations



MSFC (via LMSC) interface planning schedules

- (1) Interface Plan-Agena 6901/6902; MR-1 and MR-2
- (2) *Mariner R* Documentation Schedule, MR-1 and MR-2
- (3) Pad Loading Modification and Checkout
- (4) *Mariner R* Milestone Schedule—Pad 12 Operations

MSFC schedules (2), (3), and (4) and JPL schedules (3), (4), and (7) were, in general, compatible with JPL and project planning, which were reflected in greater detail in the JPL schedules. During the course of the project, by a process of reiteration, these particular JPL and MSFC/LMSC schedules were combined into a single issue.

The responsibility for preparing the various JPL schedules was assumed by cognizant individuals in the Systems Division who were in close contact with detail operations of the project.

It was project policy to accept the schedules as being at all times dynamic in nature and, therefore, subject to change. However, it was also project policy to insist that all phases of the project be scheduled with the best available information, and to use the schedules as a measurement of planning efficiency.

From the schedules, Project Management Plan reports were prepared and reporting of PMP milestones to NASA Headquarters was accomplished.

5. Mariner MR-3

The original plans for the *Mariner* Project stated a requirement for two flight-ready spacecraft and one set of unassembled spares. When the delivery of the three sets of spacecraft parts was complete, it was decided that the incorporation of the set of spares into an assembled and tested spacecraft would be beneficial and useful to the project. Subsequent events showed this decision to be wise. The resulting MR-3 spacecraft was used for problem detection at AMR while MR-2 was in a launch condition. At the present time, the MR-3 is being used to support the space flight operations; it will also be used for design verification tests and life tests for the 1964 spacecraft.

6. P List

In order to focus attention upon and keep cognizant individuals informed of any "problems that are considered to be jeopardizing the *Mariner R* mission," a problem or "P" list was developed. This list was first issued on April 16, 1962. Sixty-one problems were identified on the list from this date until completion of the midcourse maneuver for MR-2. Appendix C is a typical P List.

UNCLASSIFIED



UNCLASSIFIED

REDACTED



IV. Spacecraft System

A. Mariner R Design

Upon cancellation of the *Mariner A* Project in mid-August 1961, a feasibility study was conducted to determine the practicability of flying a Venus mission in 1962 with the *Atlas-Agena B* boost vehicle. Initially, the spacecraft took the form of a Venus fly-by vehicle with no midcourse maneuver to correct for booster error, because of the anticipated weight limitation of 375 lb. Re-evaluation of the *Agena* vehicle capability in view of the Venus 1962 mission objectives showed that certain hardware could be removed without compromising the objectives, resulting in an allowable spacecraft weight of 460 lb.

The *Mariner R* preliminary design was initiated in early September 1961, using this new weight constraint. It was then possible to include the weight of a midcourse propulsion system to increase the probability of approaching near enough to Venus to perform a planet-oriented scientific experiment. The initial weight allocations of the *Mariner R* spacecraft are shown in Table 1.

Certain design characteristics served as guidelines in the preliminary design phase. These included (not in order of priority):

- (1) The capability of two-way communications until the spacecraft passes Venus

- (2) Reasonable assurance of not impacting the planet because the spacecraft would not be sterilized
- (3) The capability of performing planetary and interplanetary experiments
- (4) Performance of a midcourse maneuver to correct for miss components and time of arrival; planet

Table 1. Initial *Mariner R* spacecraft weight allocations

Subsystem	Initial allocation weight, lb	Final weight, lb
Transponder	41.07	39.0
Command	10.00	8.8
Power	108.39	105.3
CC&S	9.96	11.2
Data encoding	15.50	13.6
Attitude control	57.40	53.3
Structure	82.30	77.2
Actuators	3.40	3.3
Pyrotechnics	3.75	4.3
Motion sensors	1.33	1.4
Spacecraft wiring	33.00	37.8
Propulsion	31.18	33.9
Thermal control	17.00	10.1
Science	40.00	49.5
Contingency	5.72	—
TOTAL	460.00	448.7

encounter to occur within view of the Goldstone tracking station

- (5) Maintenance of Sun-Earth lock to enhance the reception of telemetry through the directional antenna and to assist in the environmental control of the spacecraft
- (6) Use of two data rates: a high rate early in the flight to assist the functional relationship with the DSIF, and a second rate at Earth acquisition to permit reception of data at all DSIF stations while in the vicinity of Venus, on the basis of nominal performance
- (7) Derivation of power primarily through use of solar cells
- (8) Transmission of science data in real time

A Spacecraft Design Specification Book was prepared and published to provide a single source of information about the spacecraft; it has served as a design tool and a control document defining the system in general terms. The book is used in the establishment of systems, subsystems, and over-all spacecraft design, and in the dissemination of design changes to all persons concerned with the program. It covers only spacecraft flight systems and associated ground equipment.

The specifications in effect on September 1, 1962 follow:

General specifications

- | | |
|--|-----------|
| (1) Mission Objectives and Design Criteria | MR-2-110A |
| (2) Design Characteristics | MR-3-110 |
| (3) Design Restraints | MR-3-120C |

Functional specifications

- | | |
|---|-----------|
| (1) <i>Mariner R</i> Standard Trajectories | MR-4-110 |
| (2) Spacecraft Design Parameters, Nomenclature, and Locations, <i>Mariner R</i> | MR-4-120D |
| (3) Flight Electrical Harnessing and Ground Cabling | MR-4-130 |
| (4) Vehicle Integration, <i>Mariner R</i> | MR-4-140 |
| (5) Telemetry Criteria | MR-4-150B |

- | | |
|---|---------------------------|
| (6) Scientific Experiments for <i>Mariner R</i> | MR-4-210A |
| (7) <i>Mariner</i> Scientific Power Switching Unit | MR-4-220B |
| (8) Data Conditioning System, Scientific Instruments, <i>Mariner R</i> | MR-4-230B |
| (9) Telecommunications System, <i>Mariner R</i> | MR-4-310 |
| (10) Spacecraft Radio Subsystem | MR-4-320A |
| (11) Spacecraft Telemetry Subsystem | MR-4-321B |
| (12) Spacecraft Command Subsystem | MR-4-322A |
| (13) Attitude Control System, <i>Mariner R</i> | MR-4-410A |
| (14) Midcourse Guidance System, <i>Mariner R</i> | MR-4-420A |
| (15) Midcourse Autopilot, <i>Mariner R</i> | MR-4-430 |
| (16) Central Computer and Sequencer, <i>Mariner R</i> | MR-4-450A |
| (17) Power Supply System, <i>Mariner R</i> | MR-4-460A |
| (18) Temperature Control System, <i>Mariner R</i> | MR-4-510 |
| (19) Structure, <i>Mariner R</i> Spacecraft | MR-4-520 |
| (20) Structural Design Criteria, <i>Mariner R</i> | MR-4-521 |
| (21) Pyrotechnic Subsystem, <i>Mariner R</i> | MR-4-530B |
| (22) <i>Mariner R</i> Control and Determination of Weight, Center of Gravity, Moments of Inertia, and Products of Inertia | MR-4-540 |
| (23) <i>Mariner R</i> Midcourse Propulsion System | MR-4-610 |
| (24) Layout Configuration and Packaging, <i>Mariner R</i> | MR Appendix I, Revision B |

- (25) Flight Sequence, *Mariner R* MR Appendix II,
Revision C
- (26) Environmental Require-
ments, *Mariner R* MR Appendix III
- (27) Ground Checkout Equip-
ment, System Test Complex MR Appendix IV

A series of meeting was held in which the electrical interfaces between the subsystems were defined. As a result, a number of circuit data sheets, one for each signal, were generated. These sheets provided information useful to the cable designers, as well as a record of the circuit characteristics for signals between every source and user. The telemetry channels were assigned as shown in Table 2.

Another series of meetings defined the mechanical configuration, packaging layout, cabling, and thermal-control aspects of the spacecraft. The interface definitions, both mechanical and electrical, were determined so that the subsystem design could proceed.

The *Mariner R* spacecraft flight sequence was defined as follows: At liftoff, the pyrotechnics are safe-armed by the inclusion of a plunger switch at the spacecraft separation plane, in the open position; the switch is in series with the power supply and the pyrotechnical control sub-assembly. This switch closes upon separation of the spacecraft from the adapter. CC&S commands are inhibited until parting of the spacecraft in-flight separation connector occurs. At this time, the transponder power-up function is also performed. This function permits the plate voltage of the r-f power amplifier to be increased from 150 to 250 v, thus increasing the radiated r-f power from 1 to 3 w. The voltage is maintained at the lower level until after the critical arc-over pressure point is passed. Shortly after *Agna*-spacecraft separation, the solar panels are opened.

At 1 hr after liftoff, the attitude control subsystem begins to remove the separation rates imparted to the spacecraft by the *Agna* and then goes into a Sun-acquisition mode. The Earth acquisition commences at 167 hr after liftoff. During the period from Sun acquisition to Earth acquisition, the spacecraft transmits through the omnidirectional antenna. The telemetry data rate is reduced from 33 bps to 8 bps at the initiation of Earth acquisition, or by command when cruise science is turned on. This data rate is used throughout the remainder of the flight. After Earth acquisition, the directional antenna

Table 2. Telemetry channel assignments

Measurement	Parameter
Battery voltage	23 to 40 v
Yaw control gyro	1800 deg/hr
Pitch control gyro	1800 deg/hr
Roll control gyro	1800 deg/hr
Battery current drain	0 to 25 amp
Pitch Sun sensor	± 0.2 deg. arc
Yaw Sun sensor	± 0.2 deg. arc
Roll Sun sensor	± 1.25 deg arc
Spacecraft events	Not applicable
Command detector monitor	Frequency error
Earth brightness	Not defined
Antenna reference hinge angle	0 to 180 deg arc
Antenna hinge position	0 to 180 deg arc
L-band AGC	-70 to -15 dbm
L-band phase error	± 30 deg phase
Propellant tank pressure	0 to 500 psia
Battery charger current	0 to 1 amp
Midcourse motor N ₂ pressure	0 to 4000 psia
Science experiments data	Not applicable
L-band phase error	± 3 deg
L-band direct power	0 to 3 w
Louver position	0 to 90 deg arc
Low reference	Not applicable
Solar panel 4A11 voltage	20 to 60 v dc
L-band omni power	0 to 3 w
Attitude control N ₂ pressure	0 to 3500 psia
Panel 4A11 current	0 to 5 amp
Panel 4A12 voltage	20 to 60 v dc
Panel 4A12 current	0 to 5 amp
High reference	Not applicable
Reference temperature	500 ohm
Booster-regulator temperature	70 to 200°F
Midcourse motor nitrogen tank temperature	0 to 170°F
Propellant tank temperature	-25 to +165°F
Earth-sensor temperature	-40 to +150°F
Battery temperature	20 to 170°F
Attitude control nitrogen temperature	35 to 165°F
Panel 4A11 front temperature	70 to 250°F
Panel 4A12 front temperature	70 to 250°F
Panel 4A11 back temperature	-300 to +300°F
Electronic assembly I temperature	20 to 170°F
Electronic assembly II temperature	20 to 170°F
Electronic assembly III temperature	20 to 170°F
Electronic assembly IV temperature	20 to 170°F
Electronic assembly V temperature	20 to 170°F
Lower thermal shield temperature	-100 to +100°F
Upper thermal shield temperature	10 to 300°F
Plasma electrometer temperature	15 to 160°F
Antenna yoke temperature	-50 to +150°F

is used for r-f transmission, except during the midcourse maneuver or whenever the ground command to switch to the omni-antenna is transmitted.

The midcourse maneuver is performed on the next pass over Goldstone following Earth acquisition. Following the completion of the required pitch and roll turns and the addition of the required velocity increment, the spacecraft reacquires the Sun and Earth. There is capability of only one start of the midcourse motor.

When the spacecraft arrives at the planet, the CC&S or a ground command turns on the planetary radiometer experiments. This command also changes the telemetry mode to sample only science data.

The limited time available to the *Mariner R* Project eliminated the proof test model. The PTM has been a convenient means for identifying and resolving subsystem interfacing problems and also has been the vehicle used for verification of the spacecraft design.

This handicap was partially overcome by paying particular attention to the interface between subsystems and the System Test Complex. This interface was defined in terms of the signal characteristics on either side of the interface, an approach that had not been used previously. Furthermore, intensive preplanning made it possible to achieve a maximum result from the comparatively short period allocated to system and environmental testing.

The design verification tests normally performed on the PTM were performed on the first assembled flight spacecraft, *MR-1*, which served the dual function of a restricted PTM and a flight unit. Required design changes were immediately incorporated into the *MR-2* spacecraft and the spares.

The System Test Complex was the basic equipment used for system design verification of the spacecraft. It has the capability to:

- (1) Operate the entire spacecraft in a manner simulating the countdown and flight sequence.
- (2) Monitor system functions as well as subsystem inputs and outputs for quantitative evaluation of spacecraft performance.
- (3) Exercise all elements of the spacecraft through their entire dynamic range for the purpose of evaluating their performance under influences produced by the presence of the complete spacecraft.

B. Spacecraft Description

The *Mariner R* spacecraft (Fig. 20) employs many of the design principles and techniques developed for the *Ranger* program. This type of design resulted from the basic requirements of providing two-way communications with the spacecraft, performing planetary and interplanetary experiments, performing a midcourse maneuver to correct for miss components and time of arrival, and maintaining a reasonable thermal environment for the spacecraft.

Power for the spacecraft is obtained by converting the solar energy incident on solar cells into electrical energy. About 4900 cells are mounted on each of two 30- × 60-in. solar panels. These panels are removed to a position perpendicular to the roll axis shortly after *Agena*-spacecraft separation. The raw-power capability of the solar panels is about 200 w at Earth and 175 w at Venus. This solar cell performance degradation at Venus is due to a higher stabilized panel temperature and an expected damage by high-energy radiation during the flight.

A rechargeable battery of approximately 100-w/hr capacity is also flown to share the peak power loads with the solar panels and to provide electrical energy for the spacecraft during periods when the spacecraft is not pointed at the Sun. The spacecraft power subsystem supplies 50-v, 2400-cps; 26-v, 400-cps; and 25.8 to 33.3-v d-c power to the various users. The 2400-cps power is the primary supply used; the 400-cps power is used only for the gyros, the antenna hinge actuator, and the radiometer scan actuator. The battery powers such events as relay closures, pyrotechnic device activation, and attitude control gas-jet-valve actuation.

The spacecraft is stabilized in space by the attitude control subsystem. The roll axis is pointed at the Sun to provide stability about the pitch and yaw axes. Roll stability is achieved by keeping the Earth sensor, mounted on the directional antenna, pointing at Earth. Pointing the roll axis at the Sun allows the maximum amount of solar energy to strike the solar panels and aids the thermal control of the spacecraft by maintaining the Sun at a constant known attitude relative to the spacecraft.

The pattern of the high-gain antenna is very directive and, consequently, must be pointed at Earth. This requirement is used to roll-stabilize the spacecraft, thus providing a stabilized platform for the science experiments. The Sun and Earth acquisitions are achieved

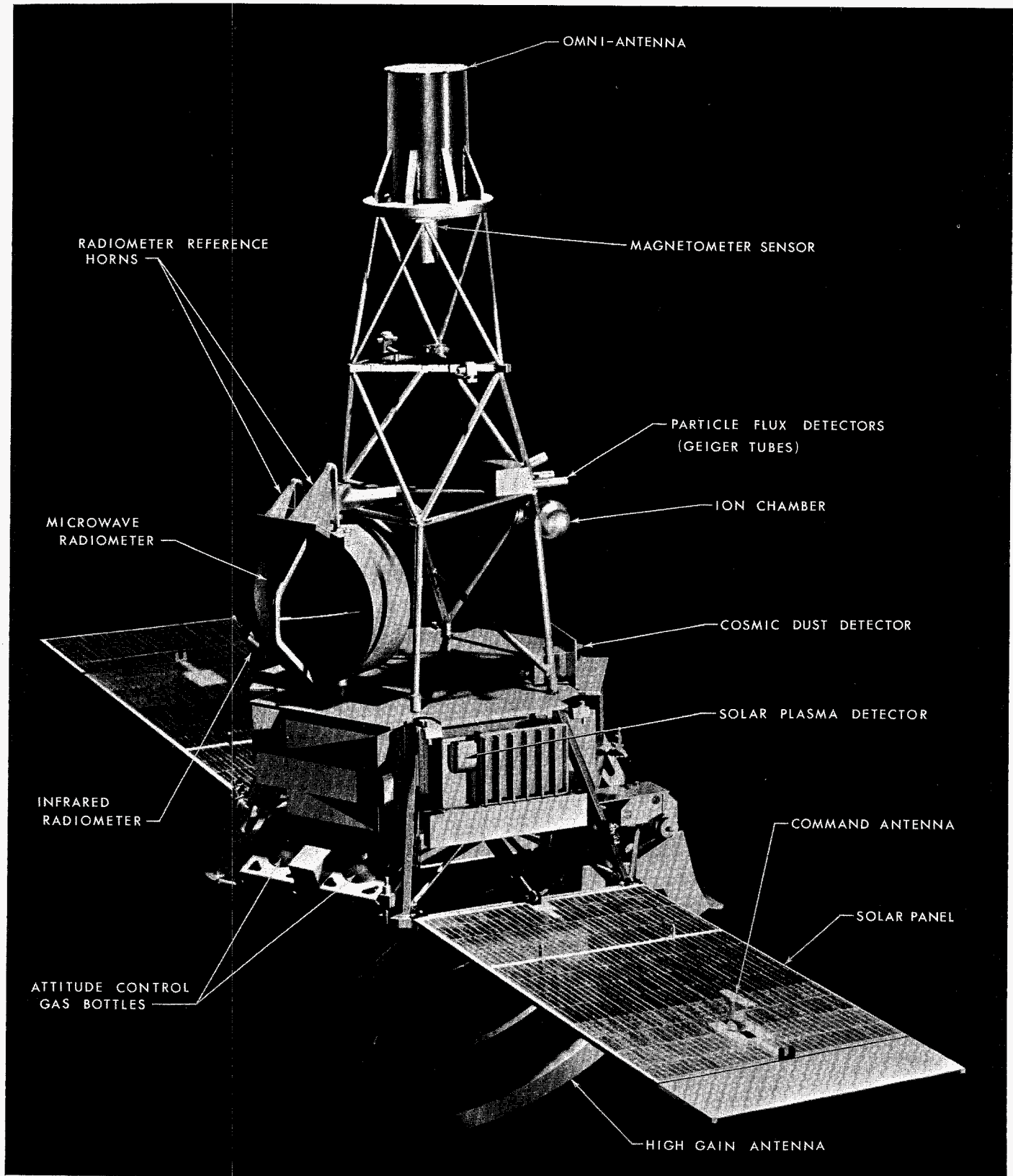


Fig. 20. Mariner R spacecraft

UNCLASSIFIED

JPL TECHNICAL REPORT NO. 32-353

through a series of sensors, gyros, and internal logic circuits which cause actuation of cold-gas valves. Expulsion of gas in preferential directions provides desired rates about the various axes to bring the spacecraft into the desired stable attitude.

Pointing the spacecraft roll axis in a preferred direction for performance of the midcourse propulsion maneuver is another function of the attitude control system. The desired inertial attitude is attained by performing a roll turn and a pitch turn upon commands from the central computer and sequencer. During motor firing, the autopilot portion of the attitude control subsystem maintains the thrust vector pointing through the spacecraft center of gravity.

The CC&S subsystem supplies timing, sequencing, and computational services for other subsystems of the spacecraft. All events of the spacecraft are contained in one of three CC&S sequences: (1) The launch sequence controls events which occur from launch through the cruise mode. (2) The propulsion sequence controls the events necessary to perform the midcourse maneuver. (3) The encounter sequence includes all CC&S commands to be given in the vicinity of Venus.

The launch sequence is always initiated at 3 min prior to liftoff. The propulsion sequence begins when the spacecraft receives a ground-originated activation command. Prior to this command, three other commands will have been sent to the spacecraft to indicate the magnitudes and direction of the required turns, and the velocity increment to be applied during the propulsion sequence. The time for initiation of the encounter sequence is placed into the CC&S by a command through the umbilical during the launch countdown. All CC&S commands are inhibited until after spacecraft separation from the Agena.

Radio commands sent to the spacecraft are in the form of two modulated subcarrier signals. One of the subcarriers is modulated by a pseudo-noise sync code and the other subcarrier is modulated by command bits. The radio receiver recovers these signals and transmits them to the command subsystem. The command detector recovers the sync and command bits and applies them to

the command decoder. The decoder determines which command has been sent and issues an output to the designated spacecraft subsystem.

Use of the real-time commands permits up-dating of the antenna hinge reference, "unlocking" the Earth sensor from some object other than Earth, switching of the r-f signal from either the omni- or directional antenna, initiating the propulsion sequence, turning on or off the planet science, and changing the data rate back to 33 bps should it be lost during the launch. The stored commands are the polarity and magnitudes of the turns to be performed and the velocity increment to be applied in the midcourse maneuver.

The radio subsystem is utilized to transmit an r-f signal modulated with a composite telemetry signal and to receive r-f commands transmitted by the DSIF. The transmitter operates at 960 mc and the receiver at 890 mc. From liftoff to spacecraft separation, the output from the transmitter is about 1 w. At separation, the r-f amplifier plate voltage is increased from 150 to 250 v, thus increasing the output of the transmitter to about 3 w. Until 167 hr after launch, the transmitted r-f signal radiates from the omni-antenna. At this time, the r-f signal is transferred to the high-gain directional antenna. This antenna is used throughout the flight except during the midcourse maneuver, at which time a ground command causes the r-f signal to be switched to the omni-antenna.

The spacecraft is mechanized so that in the cruise mode of operation the gyros and the science instruments will not be in operation at the same time. This mode is required to maintain the spacecraft power requirements within the solar panel output capabilities. The gyros will be on during the midcourse maneuver and during any acquisition periods.

During planet encounter, however, all science instruments will operate despite the status of the gyros. This time is the most critical as far as securing science data is concerned. Should the gyros be on during encounter and the solar panels be unable to supply the necessary power, the battery will furnish the additional capacity needed to operate the spacecraft.

UNCLASSIFIED

V. Spacecraft Subsystems

A. Structure and Thermal Control

1. Introduction

As a result of the program change to adapt the *Mariner* spacecraft to the *Atlas-Agena B* launch vehicle for the 1962 Venus mission, the Engineering Mechanics Division started, in August 1961, to design an essentially new spacecraft. This design relied heavily on hardware and techniques that had been developed for *Ranger* and *Mariner A*. By retaining the established working team and using the experience gained on *Mariner A*, the design of the configuration, the detail design of the spacecraft, and the fabrication of prototype and flight hardware progressed rapidly and with a minimum of problems. The first flight structure was delivered a little over 3 mo from the start of preliminary design.

Several interface and qualification tests were completed, ultimately verifying the adequacy of the design. Some of these were:

- (1) Match-mate tests between the spacecraft and the *Agena* adapter

- (2) Spacecraft separation tests from the adapter
- (3) Temperature control tests
- (4) Structural qualification tests

These and other tests will be discussed in more detail.

The mechanical assembly of all components onto the flight spacecraft progressed smoothly and rapidly, due, at least in part, to the many mechanical compatibility checks performed as part of the development test program. Many interface problems were resolved in this fashion before assembly of the flight spacecraft began.

Handling, shipping, and field operations relied heavily on *Ranger* and *Mariner A* techniques and hardware. A minimum of new problems materialized in these areas.

2. Spacecraft Development

a. Description of spacecraft. The spacecraft configuration is shown in Fig. 21. The basic building block for the *Mariner R* was the RA-3 type basic hexagonal structure, which introduced only minor changes to interfaces with the *Ranger*-developed *Agena* adapter and shroud.

The basic structure was modified to reduce weight and increase the cable access. A trough to support the ring harness cables and connectors was located under the structure and provided clearance for the installation of the modified RA-3 midcourse propulsion system from the bottom.

The Sun sensors and attitude control jets are mounted near the same locations as RA-3. Two *Mariner A* spherical attitude control bottles are mounted together between the battery box and high-gain antenna. The regulator is located between the bottles.

Three fixed thermal shields are provided. One is located under the bottom of the spacecraft in the cable trough motor nozzle area; a second is mounted immediately above the hex structure to shield the hex electronic boxes from the Sun; and the third shields the Earth sensor from the Sun. The cosmic dust experiment mounts on the top thermal shield, and the solar corpuscular detector is mounted in a primary hex box and protrudes from under the shield to see the Sun.

A superstructure mounts through the top thermal shield to the top of the primary hex. The structure consists of three truss sections bolted together, with equipment support frames between each. The RA-1 type omni-antenna mounts on the top and the *Mariner R* fluxgate magnetometer is mounted beneath it. The upper frame contains the top solar panel ties. The lower frame contains the *Mariner R* ion chamber experiment and particle flux detector.

The radiometer and infrared radiometer are mounted above the top thermal shield and below the lower superstructure frame. These experiments are designed to be articulated at planet encounter approximately 120 deg about an axis parallel to the roll axis, by a scan actuator mounted on the lower superstructure bulkhead frame. The radiometer package is restricted from rotating during boost by a pyrotechnic latch.

The high-gain antenna mounts under the basic structure in the same manner as in the *Ranger* series. A 4-ft-diam. *Mariner A* dish structure and a redesigned *Ranger* feed are used. The *Mariner A* long-range Earth sensor is mounted on a new high-gain antenna yoke, and is inclined at an angle with respect to the high-gain antenna "look" direction. A mirror mounted on the yoke allows the sensor to "see" in the antenna pointing direction. A baffled hood minimizes the effects of off-axis stray light reflections into the Earth sensor.

Two articulated solar panels are included. Additional solar cell area was provided by the inclusion of a bolt-on extension to the end of one panel. A sail was installed on the other panel to balance the solar pressure loads. The panels are latched during boost to the structure by three pyrotechnic latches: two at the top of the hex structure and one at the top of the panel. The command omni-antennas mount on the front and back of one of the panels.

b. Design. As mentioned earlier, full use was made of *Mariner A* and *Ranger* design experience. Some of the benefits derived from the *Ranger* program were:

- (1) Basic hex structures were available from *Ranger* test programs for use as temperature control, mock-up, separation test, and structure test models. Only three flight structures had to be fabricated: MR-1, MR-2, and the flight spare.
- (2) The solar panel actuators and hinge geometry were the same as those used on the *Ranger* series.
- (3) The high-gain antenna feed was very close mechanically to that on the early *Ranger* flights.
- (4) The Sun-sensor mounting locations, as well as mechanical alignments, are the same as on *Ranger*.
- (5) The basic ground-handling dollies were identical to the *Ranger* units.

Many of the design and fabrication techniques developed for *Mariner A* were either used directly, or were applied to the new design. Among these items were:

- (1) The high-gain antenna dish was the same as that designed for *Mariner A*.
- (2) The Earth-sensor package, mechanical alignment, and mounting provisions were defined during the *Mariner A* design period.
- (3) The type of construction used on the solar panels was identical to that verified as adequate for *Mariner A*.
- (4) The temperature control louvers used on one of the hex electronic boxes were designed, built, and tested during the *Mariner A* program.
- (5) Much of the electronic packaging and hardware was identical to that built for *Mariner A*.
- (6) The superstructure struss configuration and fabrication techniques evolved directly from *Mariner A* experience.

UNCLASSIFIED

UNCLASSIFIED

UNCLASSIFIED

JPL TECHNICAL REPORT NO. 32-353

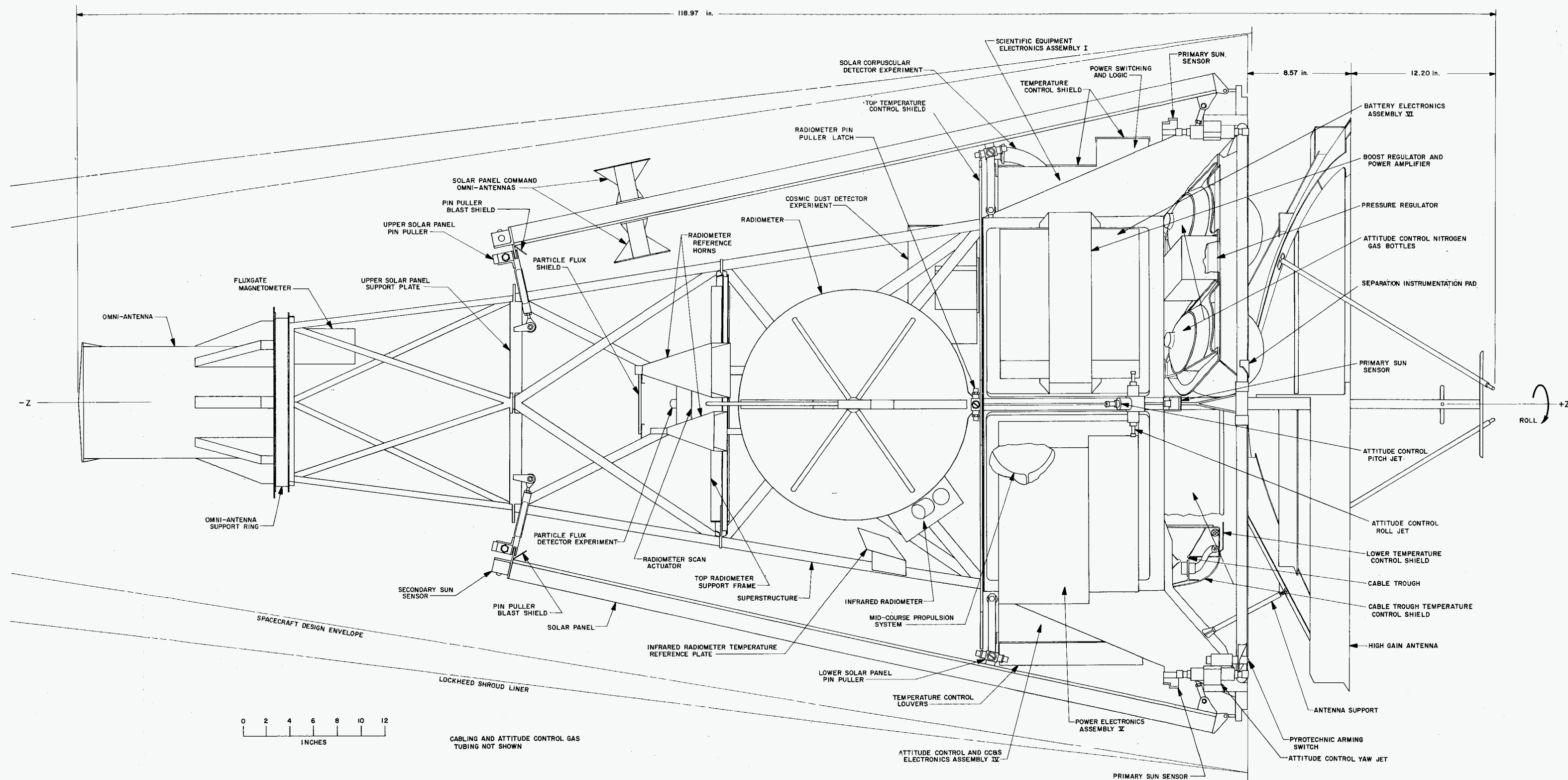
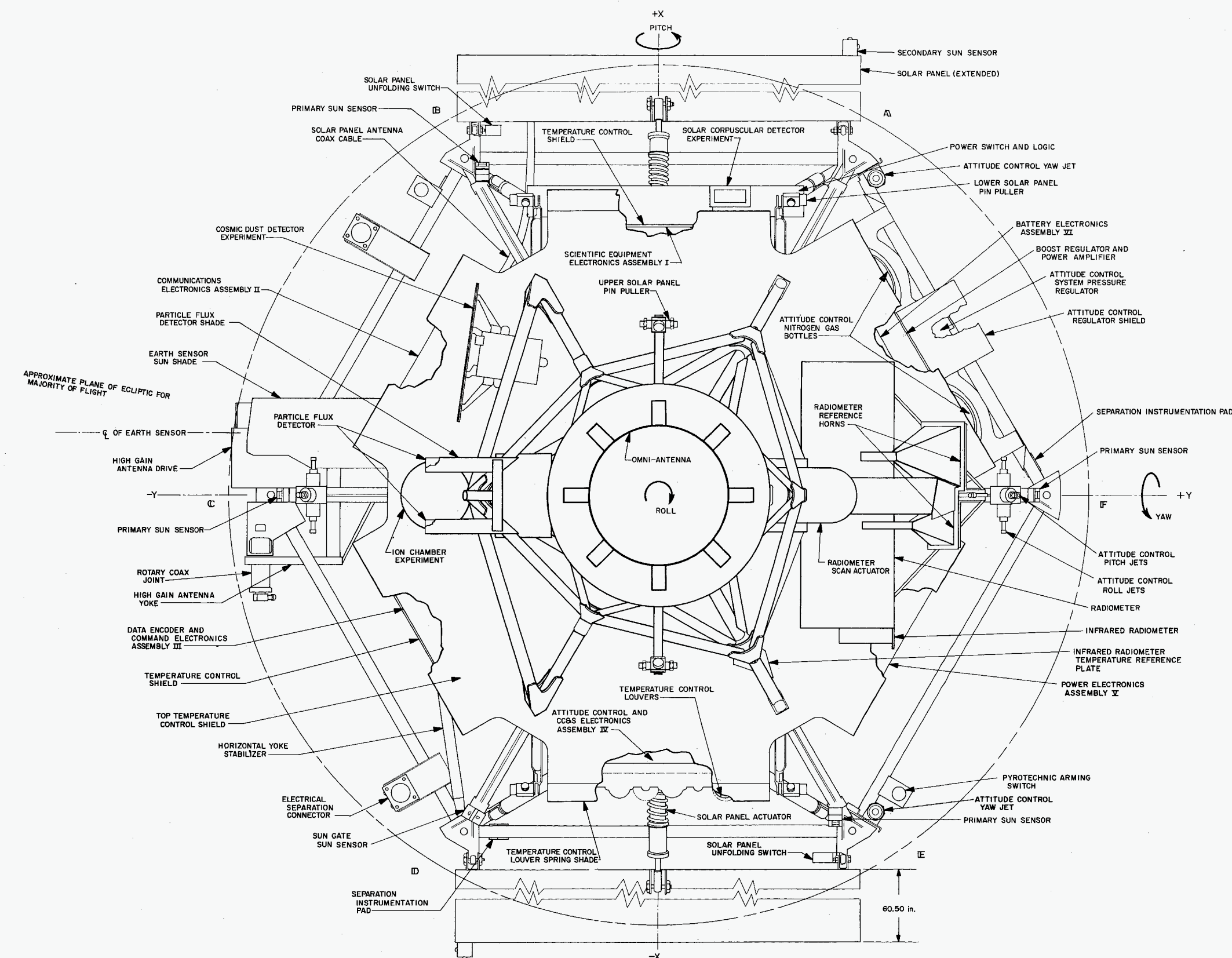


Fig. 21. Mariner R spacecraft configuration

UNCLASSIFIED

UNCLASSIFIED

UNCLASSIFIED

- (7) The integration of the radiometer, including the type and method of articulation, was expedited by the understanding derived during the *Mariner A* design period, in relation to the trajectory passes in the vicinity of Venus.
- (8) The system test stand and shipping technique devised for *Mariner A* were used for *Mariner R*.

Many new items and concepts, yet untried on *Ranger* or *Mariner A*, had to be designed and built. Among the larger new efforts on *Mariner R* were:

- (1) The cable trough was relocated below the hex to facilitate the midcourse motor insertion. The assembly cabling connected directly into connectors hard-mounted to the trough.
- (2) The *Ranger-Agena* adapter structure dictated that the *Mariner A* long-range Earth sensor be mounted on a redesigned high-gain antenna, and be inclined at an angle with respect to the antenna pointing direction. A mirror mounted on the yoke allowed the sensor to "see" the antenna "look" direction.
- (3) After several tests, it was found that stray light reflecting off spacecraft components, such as the high-gain antenna feed, affected the Earth sensor performance. A light baffle box was installed around the mirror assembly to reduce the amount of stray light entering the Earth sensor.

A number of philosophical and detail changes from current approaches were used to advantage in designing new hardware. Some of these are summarized:

- (1) A concentrated effort was made to provide rectangular solar panels. These panels allow a much higher solar cell density since there is little or no waste space (98% of panel area is covered with cells vs 85% for trapezoidal panels). The width of the panel was determined to be one-third of the solar cell module length, allowing series-parallel connections to be made with minimum wiring. Panel length was set to give enough cells connected in parallel to provide proper power capability. To get rectangular panels inside the shroud, they were inclined at a larger angle than the *Ranger* panels, ultimately bringing the panel face very close to the electronic box upper corners. To minimize damage to the panels, the strip adjacent to the box corner was left free of cells so that contact during vibration would not damage cells. Two links on each panel kept panel excu-

sion in this area to a minimum. A third link was placed at the top of the panel, thus restraining it without further interference with cell layout. The edges of the panels were reinforced to act as shroud guide bumpers.

- (2) The links attaching the solar panels to the structure and superstructure were essentially pivots at each end. Thus, solar panel motions relative to the structure or superstructure did not twist or bend the links and thus did not throw unwanted loads into the panel or structure. The links restrained the panel only in its weaker direction. Pin pullers were attached to the solar panel end of the links by a single screw, the pin restraining the panel through a clevis and lug (Fig. 22). This provision allowed rapid attachment of the panels to the structure with minimum probability of damaging the solar cells during the operation. No significant preload was applied, the rattling of the panel due to pin clearances being difficult to analyze, but no damage was apparent during vibration testing.
- (3) A similar technique of isolating the radiometer from structural distortions was used. The radiometer was supported at the base by a ball joint which also served as a pivot. A pyrotechnic retractable pin fitted into a slotted hole, restraining the radiometer only from rotating. The radiometer was restrained at its top by the scan actuator. A universal joint was provided between the two. The structure supporting the actuator was rigid in a lateral plane, but flexible in the axial direction. Thus, no conceivable structural or thermal distortions could throw unwanted loads or restraints into the structure, actuator, or radiometer.
- (4) The superstructure was designed as a determinate truss, thus using a minimum of members. A truncated conical monocoque construction was rejected because it promised to be heavier. The truss proved lighter because a minimum of equipment is mounted to it, its primary function being to support the top of the radiometer, the tops of the solar panels, and the forward omni-antenna. The three scientific instruments were added to the basic structure for negligible bracket weight.
- (5) Continuous attention was paid to reducing weight. Truss fittings were reduced to a minimum. An oversight left most of them fabricated from aluminum, but magnesium was used extensively where practicable. Truss tubes are aluminum, no weight being saved by using magnesium tubes.

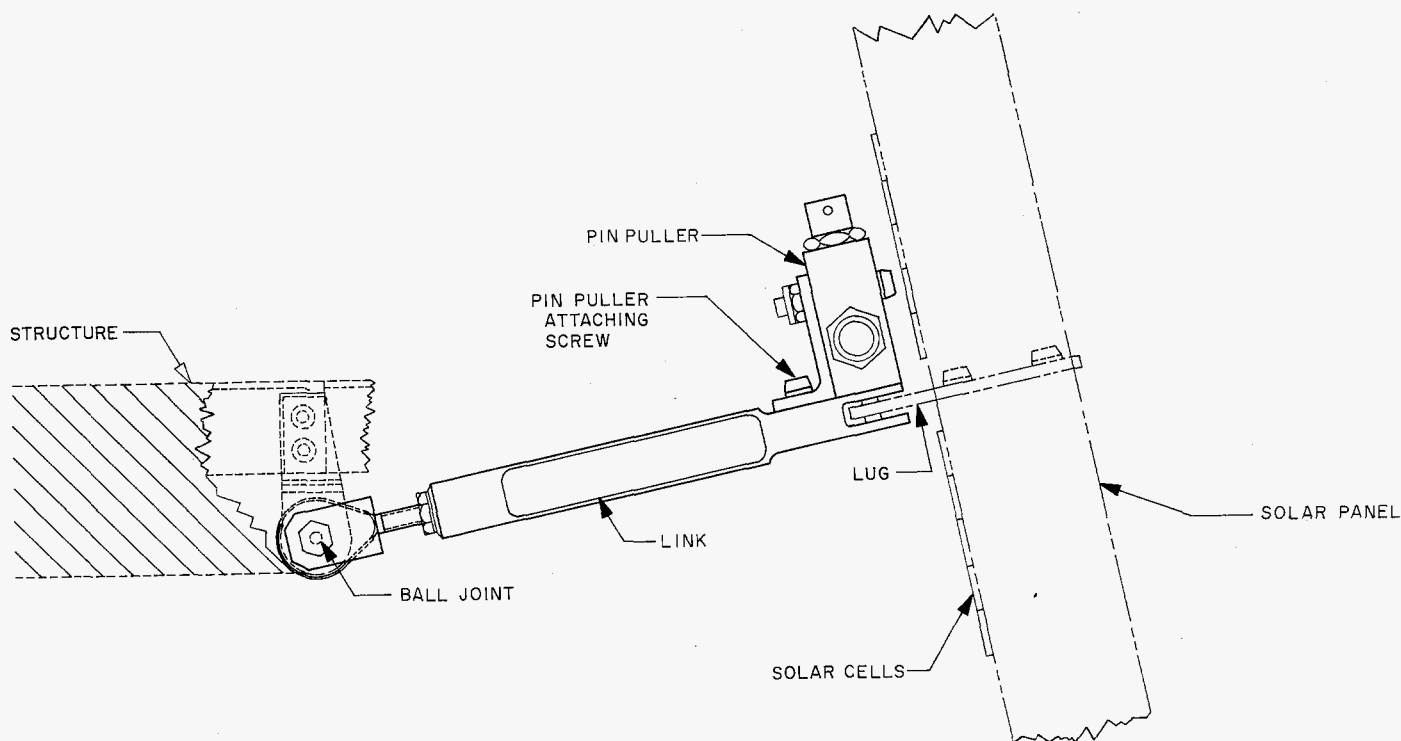


Fig. 22. Upper solar panel latch installation

Parts were redesigned to save 0.1 lb if feasible. Titanium bolts were used throughout. Lightweight nuts were used universally. The net result was a total structural saving of nearly 15 lb from the original estimates, most of which were based on *Ranger* weights.

- (6) Since the attitude control gas system was to be a welded unit, including valves, regulators, and plumbing, a successful effort was made to install it on the spacecraft structure as a unit. The original plan was to build the system on the flight structure before SAF delivery. This approach was changed to build the system on a mock-up and transfer the welded system from the mock-up to the structure. Some minor changes were made to allow the complete system (including bottles and brackets) to be installed as a unit. Thus, the system could be tested as a unit prior to delivery, and could be exchanged for a spare system without appreciably interrupting spacecraft testing.
- (7) The installation of the midcourse propulsion system from the bottom was proposed to minimize disturbances to the rest of the spacecraft, since it was preferable to install the system as the last item. Although clearances for this operation were

minimal, the system could be safely installed in this fashion, provided installation crews had practiced as a team.

- (8) Locating the spacecraft center of mass (cg) near the Z axis proved to be a formidable design problem. The light spacecraft with the high-gain antenna extended to the exit position for midcourse maneuver had the cg well outside the allowable circle. The configuration design was heavily influenced by the need for a reasonable location of the cg. The antenna exit position of 120 deg was the minimum allowable position consistent with clearing the midcourse motor blast cone. Every possible item was located on the opposite side of the spacecraft and placed as far from the Z axis as possible. Although the attitude control gas system has a variable weight and thus should be placed symmetrically about the Z axis, a calculated risk was taken by placing the bottles containing the gas on the light side of the spacecraft. Should gas consumption before midcourse maneuver be significantly greater than anticipated, the cg shift could degrade accuracy. However, it was believed that, in this case, the mission lifetime would be too short, and the accuracy of the maneuver would be less significant.

c. Development and test. Five different types of spacecraft structures were assembled and used during different phases of the program:

Mock-up. While the spacecraft was still in the preliminary design stage, work commenced on building a full-size mock-up. As the mechanical design was firmed up, the mock-up was constantly up-dated. This mock-up was used in a match-mate test with a prototype Lockheed Agena adapter. The early completion of this test allowed the interface incompatibilities to be corrected without a schedule delay. After the match-mate test, the mock-up was delivered to the cabling group for use as a cabling mock-up. When the cabling function had been completed, the mock-up was used by the Telecommunications Division for measuring the spacecraft antenna patterns.

Structural test model. Various vibration tests and modal surveys were performed on prototype and type-approval component parts. Tests were conducted to verify the adequacy of the superstructure and the radiometer structure and their methods of attachment. Type-approval tests verified the adequacy of the solar panel structure and high-gain antenna when subjected to a greater-than-normal vibration environment.

A structural-test prototype spacecraft was fabricated of flightworthy components. This spacecraft was used in a second match-mate test as a final verification of the mechanical interface with a flight-type adapter structure. After match-mate, the structural test model was successfully subjected to modal vibration test and type-approval vibration tests. This structure was used throughout the program for developmental and prototype work. Among the items tested on this structure, to be later added to the flight units, were: (1) the Earth-sensor damper system; (2) the solar panel extension; (3) the solar sail; and (4) the high-gain antenna vibration damper.

Temperature control model. Thermal tests were conducted in the new space simulator chamber with a complete thermal mock-up of the spacecraft, and later on the basic hex structure in the 6-ft vacuum chamber. Electric strip heaters were placed on the exterior of the spacecraft to simulate the solar load. The power dissipation load in the hex boxes was also simulated with heaters. Several different tests were conducted. All of them supplied valuable information as to the proper temperature control surfaces and techniques to be applied to the flight units.

Separation test model. A primary hex structure was ballasted to the proper weight, center of gravity, and

moment of inertia. This structure was taken to Lockheed, where a separation test was conducted, using a test setup similar to that developed for *Ranger*. Specifically, Lockheed checked the effects of:

- (a) The lighter-than-*Ranger* spacecraft on the separation rates
- (b) The location and forces of the pyrotechnic arming switches on the separation
- (c) The Earth-sensor baffle box and the adapter on the separation clearance angles
- (d) The removal of the *Ranger* sterilization diaphragm from the adapter
- (e) The forces applied to the spacecraft as a result of the Earth-sensor damper installation

Flight spacecraft structures. Three complete sets of flight equipment were fabricated: *MR-1*, *MR-2*, and the spare (*MR-3*). The flight spacecraft were assembled with a minimum of difficulty. After the spacecraft were transferred to the Systems Division, the Engineering Mechanics Division assisted in all phases of the testing, shipping, and launching operations.

3. Structures and Dynamics

The spacecraft structure was designed to meet the requirements established in JPL Specification MR-4-521, *Mariner R* Structural Design Criteria. The tests designed to qualify this structure to the above specification are defined by JPL Specification 30254, *Mariner R* Structural Qualification Test Requirements.

Certain major components of the spacecraft have been designed to other detail specifications. However, these detail specifications have been, in turn, derived from MR-4-521 and 30254.

a. Spacecraft structural components. The portions of the spacecraft that received extensive structural and dynamic considerations include: hex structure, superstructure, solar panels, high-gain antenna, midcourse propulsion unit, radiometer, and ground support equipment.

Hex structure. The *Mariner R* was conceived around an RA-3 primary hex structure, to which would be added solar panels, a superstructure, and scientific experiments.

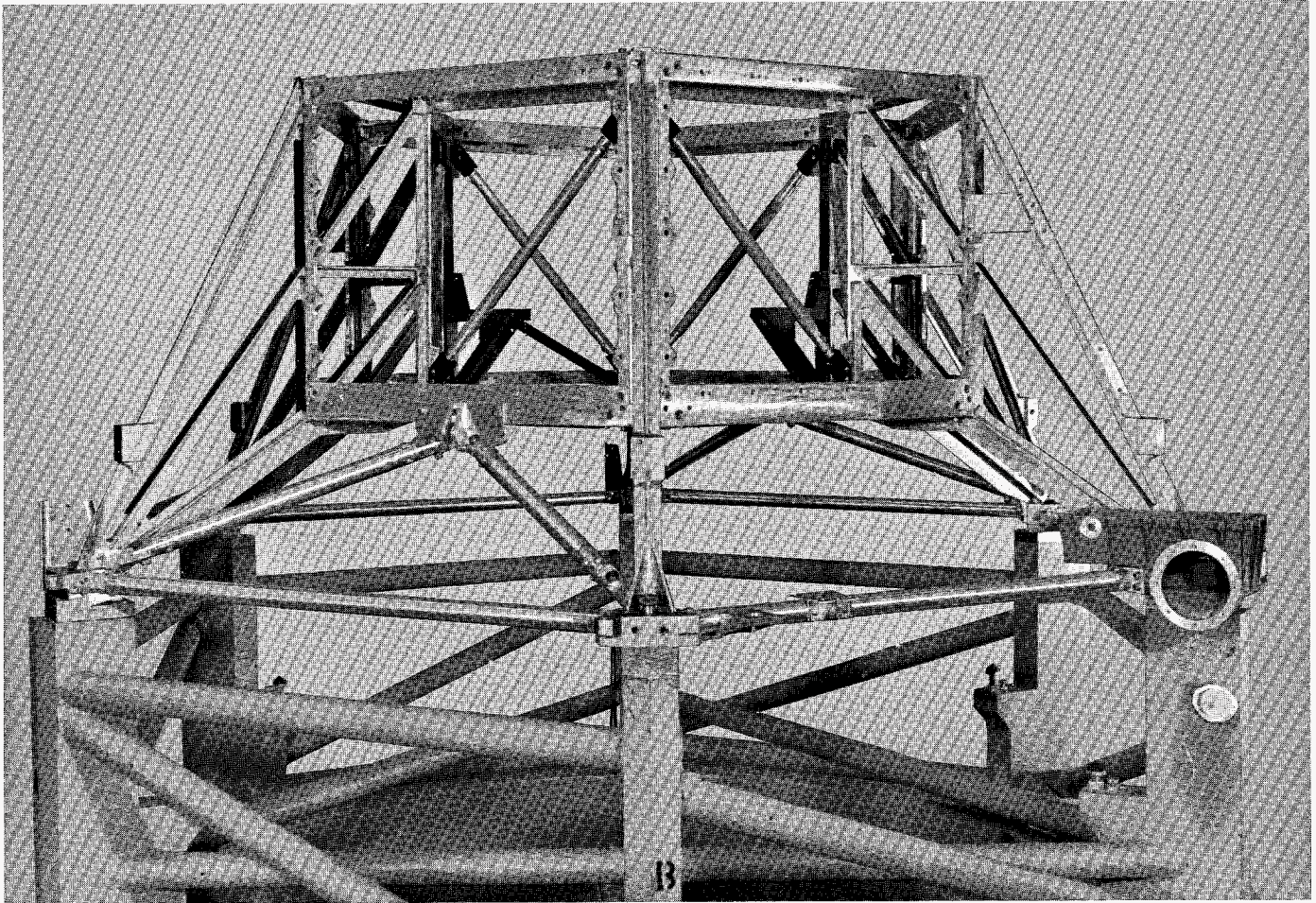


Fig. 23. Spacecraft hexagonal structure

Preliminary investigations indicated that weight could be saved from the *RA-3* hex structure for the *Mariner* mission. *Mariner R* was to weigh approximately one-half as much as *RA-3*; therefore, it seemed logical to assume that the *Ranger* hex had more than enough strength to carry all the essential elements of the mission. While weight reduction was of lesser priority than such items as ease of fabrication and schedule, all weight saved helped increase the firing period so that both spacecraft could be launched on Venus trajectories.

During the detail design period, various inputs and requirements were set forth which formulated the spacecraft configuration, resulting in many necessary modifications to the hex structure (Fig. 23). Among these were:

- (1) The X-shaped back ties on the inside of the hex were changed to single diagonal members. The new members had a smaller projected area, enabling each electronic subassembly to "see" all the

others. This was intended to help decrease the thermal gradients through the primary structure.

- (2) The upper and lower shear panels in the hex-box support bay were also replaced with diagonals. The new members increased the access to the cabling and also reduced the weight.
- (3) The intercostal tubes around the base of the hex structure were changed from magnesium to aluminum. The tubes were changed because: (a) magnesium tubing was not readily available; (b) an additional operation, gold-plating for temperature control, had to be performed; and (c) the analysis showed that the material change did not affect the weight of the components, because for tube buckling loads (the main design criterion), the equivalent stiffness of magnesium tubing can be achieved with aluminum tubing of a thinner wall thickness.

While analyzing the intercostal tube material substitution, it was discovered that the brackets that attach the intercostal tubes to the bus were marginal. These parts were redesigned with no weight change.

The design changes enumerated made necessary a complete new static and dynamic analysis of the bus. Although the design changes were minor, it was believed that the sizing of the new members could radically affect the load distribution and dynamic behavior of the bus. This analysis was performed with the aid of the STIFF-EIG 7090 computer program. In order to more accurately perform this analysis, it was necessary to consider the entire spacecraft in preparing a suitable structural idealization. Therefore, upon completion of this analytical process, the static and dynamic behavior of the entire spacecraft was known.

Superstructure. The superstructure is a truss-type assembly which attaches to the top of the hex and provides support for the solar panels, omnidirectional antenna, and various scientific instruments.

The tight schedule dictated that previous design concepts be utilized wherever possible. The height of the superstructure was determined by the omni-antenna, which was located to match the RA-3 shroud coupler position. Of secondary importance was the desirability of locating the magnetometer as far as possible from the rest of the spacecraft. It mounts on the plate truss at the upper level of the superstructure.

The middle and top truss sections were composed of six members arranged in the best structural orientation. This configuration provides stability for the least number of members and joints, and, consequently, achieves the least weight. The lower truss had to be designed to provide clearance for the radiometer during its scan mode. It was found that a variation of the *Mariner A* superstructure would provide the needed radiometer clearance. Bulkhead structures were mounted between the truss sections. To these sections were attached scientific instruments, the solar panel tops, and the top of the radiometer.

Before preliminary analysis could be started, the loads induced in the superstructure by the solar panels and radiometer had to be determined. All that was available was the approximate radiometer weight, its manner of support, and similar parameters for the solar panels. By estimating the portion of these components supported by

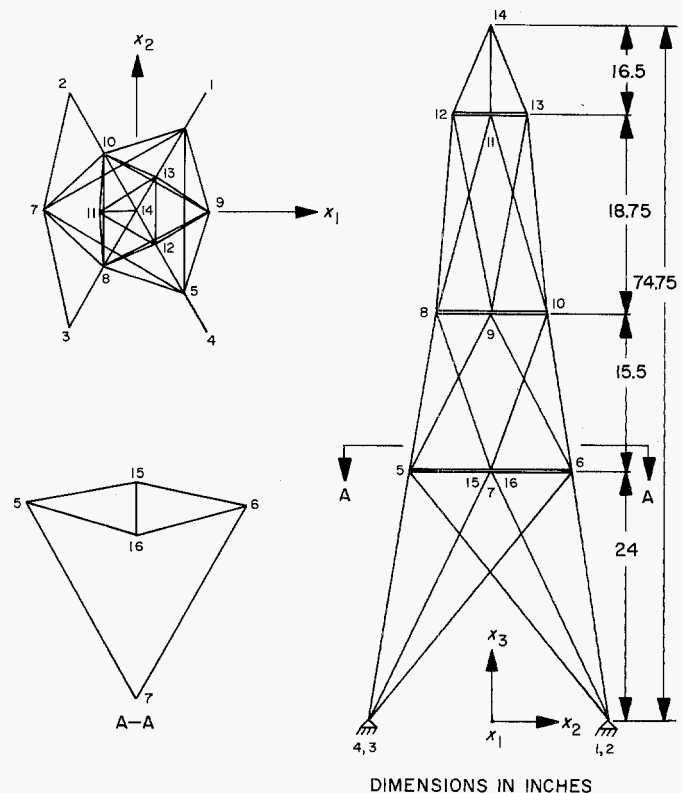


Fig. 24. Superstructure idealization

the superstructure, idealizing the omni-antenna as a three-member truss with a concentrated mass at its center of gravity, and obtaining the approximate weight and location of all instruments sitting on the structure, a preliminary design was conceived and analyzed as a pin-jointed truss through the use of the STIFF-EIG 7090 computer program (Fig. 24). A maximum acceleration of 35 g at resonance was assumed. This was based upon experience with the *Mariner A* superstructure, as related to an assumed damping factor.

With the loads thus obtained, member sizes were determined, and as instruments were moved from one tier to another, and component weights changed during the design period, the 7090 computer faithfully provided loads and frequencies for each new input. Eventually, member sizes reached a point where either: (1) they were on the verge of buckling; (2) they were down to minimum sizes consistent with ease of procurement; or (3) any further decrease would lower the first resonant frequency of the structure to a point where it might tend to couple with the twisting mode of the solar panels.

As the design phase drew to an end, a structural mock-up of the superstructure was built, using welded joints.

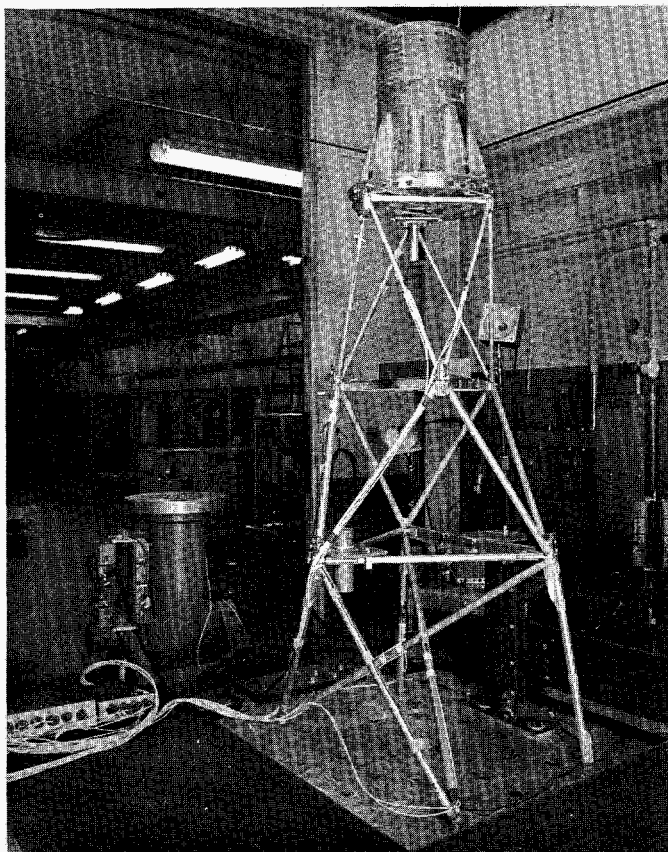


Fig. 25. Superstructure mock-up shake table

This mock-up was subjected to exploratory sinusoidal shakes to determine resonant frequencies. To simulate the radiometer, a heavy I-beam was used. The solar panels and scientific instruments appeared as concentrated weights. Figure 25 shows the structure on the Ling electromagnetic shaker used in the tests.

Solar panels. The *Mariner R* solar panel design was based on structural concepts developed during the *Mariner A* program. The *Mariner A* panels were considered an improvement over the *Ranger* panels, exhibiting less motion at resonance, and lower weight-to-area ratio. In addition, the well-developed fabrication techniques of the solar panel contractor, Ryan Aerospace Division (San Diego, Calif.), led to the belief that the tight schedules associated with *Mariner R* could easily be met.

In order to satisfy power requirements and geometrical constraints, a rectangular panel, 30 in. wide by 60 in. long, was utilized. Geometrical constraints required that the panel be located about $\frac{1}{8}$ in. away from the top of the temperature control louvers. In order to maintain this minimum separation, it was necessary to support the

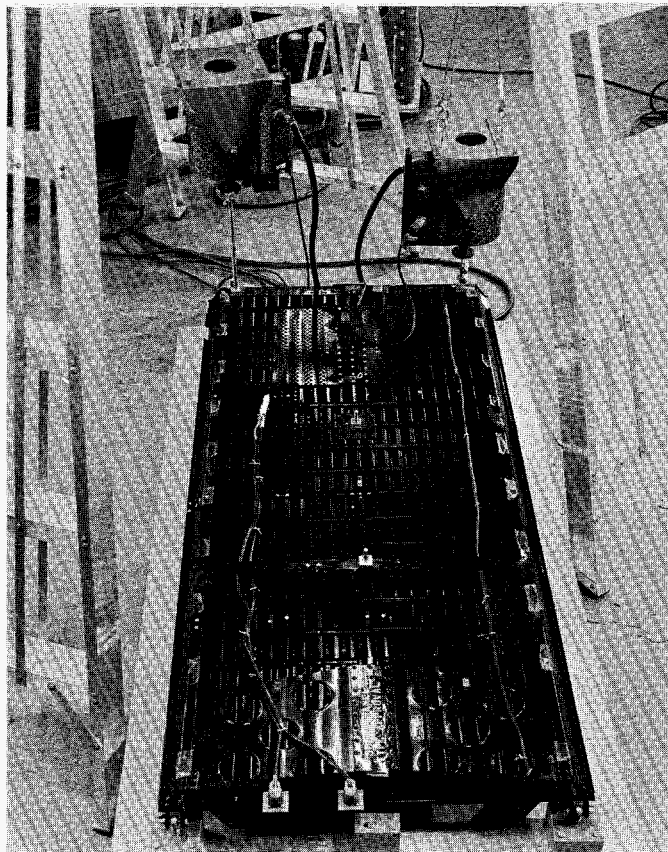


Fig. 26. Solar panel modal survey

panel with two pin-puller ties at this level. It was also necessary to tie the panel at the top to reduce the vibration levels. A preliminary investigation indicated the combination of two supports at the top of the hex, together with one support at the top of the solar panel, would keep frequencies, deflections, and stresses within prescribed limits.

The solar panels were designed to meet the requirements of JPL Specification 30882. The solar panels were tested to the requirements of JPL Specification 30498.

From the preliminary investigation, maximum reactions at the supports were obtained. These loads were used to design the latches between the panel and the hex or superstructure. The bulk of the solar panel support load is in a direction normal to the face of the panels. Because of this, and in order to minimize any nonanalyzable over-constraint of the panel or superstructure, the supports were designed to allow for transverse motion and for rotation.

The hard design and fabrication of the solar panels were performed by Ryan. One of the first panels was

shipped to JPL for structural tests. The weight of this panel, with cell weight simulated by independently attached strips of aluminum, was about 23 lb.

The first test was a modal survey (Fig. 26). This test located the resonant frequencies of the panel as follows:

First torsion: 25 cps

First longitudinal bending: 62.4 cps

A true transverse bending mode never was located.

Logarithmic decrement tests were performed to determine the damping in each mode. The torsional mode exhibited an extremely high damping rate, with values for structural damping varying from 0.1 to 0.2, depending upon the input acceleration. In the first longitudinal bending mode, a value of about 0.032 to 0.036 was obtained for structural damping. This range checks well with amplifications observed during qualification testing.

The panel was then subjected to the tests detailed in JPL Specification 30498, the solar panel test specification. The panel passed these tests with no visible damage, and when once again subjected to a modal survey, produced the same resonant frequencies as previously obtained.

Temperature-cycling tests were performed by Spectrolab¹ who attached the solar cells to the panels. These tests indicated that in some areas of the panel (without cells), bowing occurred between corrugations as the temperature was increased, leading to the fear that either the cells or the connections between cells would be in danger of breaking. These tests were repeated at JPL, the panel being fully instrumented to measure temperature and deflection. The bowing again occurred. Next, a series of tests was performed to determine qualitatively the stiffening effect of the cells themselves on a sheet whose thickness is the same as the face sheet on the panels (Fig. 27). These tests indicated a considerable increase in stiffness due to the cells, leading to the conclusion that any bowing of the skin with cells would be so small it would not affect the solar panel performance.

After the completion of all structural tests, it was found that the existing panel did not provide sufficient power and that additional square feet of solar cells were required. Realizing that this additional panel area needed to be designed, fabricated, and qualified in a period of 3 wk, the decision was made to extend one panel 11 in. An alternative approach of extending each panel 5 in.

¹Division of Textron Electronics, Inc., North Hollywood, Calif.

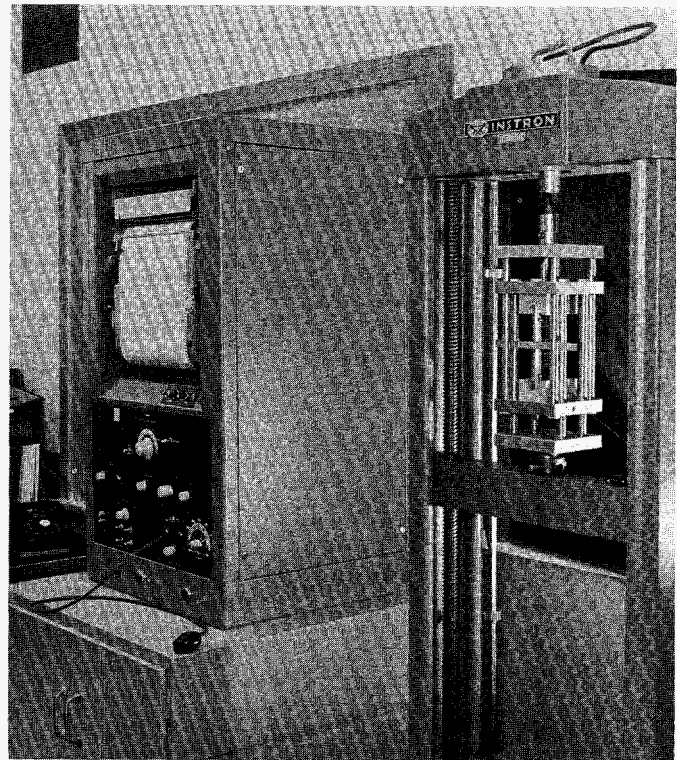


Fig. 27. Solar panel cell stiffness test

would have interfered with the ground plane of the antenna located on one panel, a circumstance that would have required an intolerable amount of antenna requalification.

The panel extension, the same basic structure as the original panel, was supported by two beams cantilevered from the original panel (Fig. 28).

High-gain antenna. The high-gain antenna is a 4-ft-diam. paraboloid of revolution, made of ¼-in. opening wire mesh, with a supporting structure of thin, formed aluminum sections. The feed element protrudes from the apex of the paraboloid, locating the ground plane at the focal point of the antenna (Fig. 29).

The antenna is nested beneath the spacecraft, and is held in place by a series of compression supports coming down from the bus and up from the adapter.

The structural design of the *Mariner R* antenna evolved directly from the earlier *Ranger* and *Mariner A* designs. Specifically, this antenna utilized the *Mariner A* dish, a modified *RA-1* feed, and the *Ranger* truss-type feed support. The pivot arm has a fiberglass end portion attaching to the yoke for thermal insulation purposes. Also, the

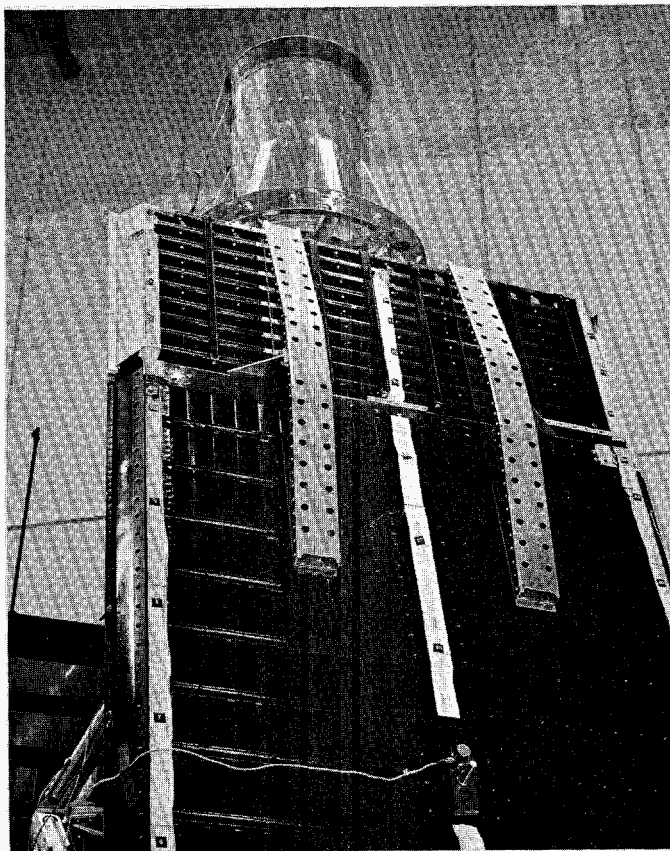


Fig. 28. Solar panel extension

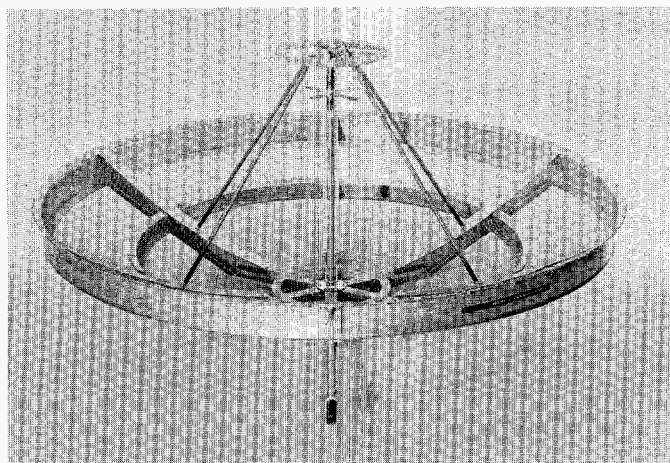


Fig. 29. High-gain antenna

vertical strut from the pivot arm to the radial member below has been modified to better support the long-range Earth sensor, which is mounted to the yoke.

The structural analysis of the antenna was performed with the aid of the STIFF-EIG program on the IBM 7090

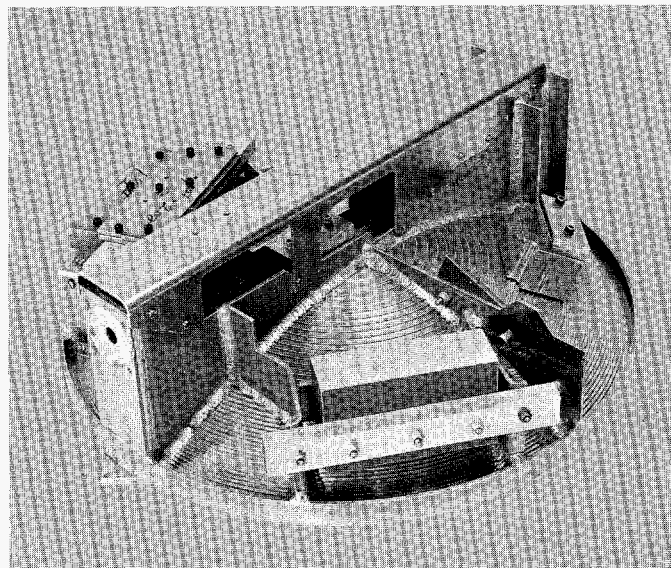


Fig. 30. Radiometer mock-up

digital computer. The dish was idealized as a planar grid, the members of which corresponded to the supporting structure on the antenna.

The antenna was successfully subjected to a complete series of static and dynamic structural tests, and was subsequently found to exhibit no structural or electrical deterioration.

Other major structural components. The midcourse propulsion unit, radiometer, and certain pieces of ground support equipment also were subjected to structural analysis and/or test.

The midcourse propulsion unit used was essentially the same as that used on RA-3. However, certain minor structural modifications were made in the attachments between the hex structure and the unit.

An analysis and a subsequent series of vibration tests emphasize the need for a strengthening of the backbone beam on the radiometer. A structural mock-up radiometer with the strengthened beam is shown in Fig. 30.

The system test stand, handling dollies and slings, and magnetometer test fixture were some of the more significant pieces of ground support equipment which received structural consideration.

b. Spacecraft analyses and tests. As discussed earlier, the primary analysis of the spacecraft as a complete unit

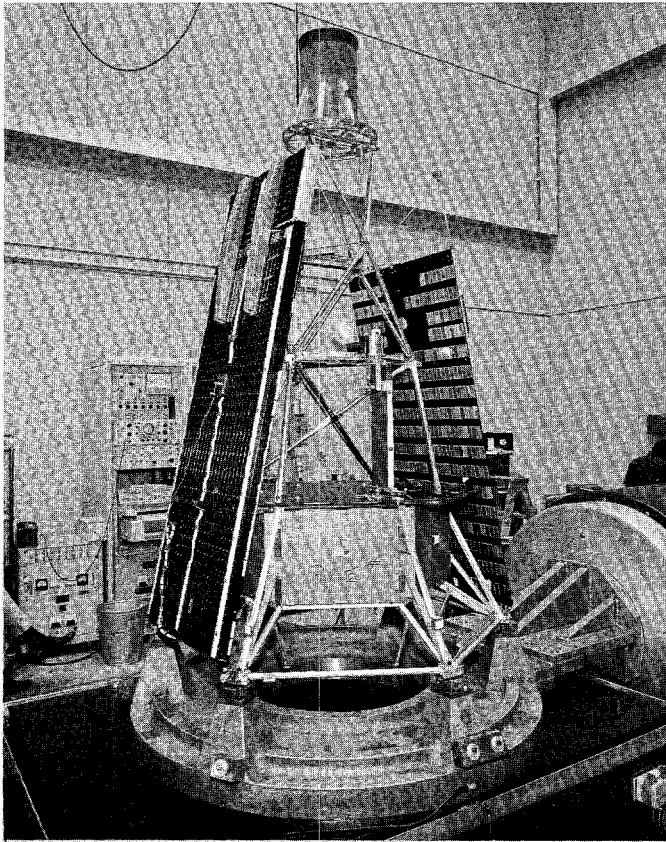


Fig. 31. Spacecraft with panel extension

was conceived as a result of the need for a detailed analysis of the hex structure.

Using a structural prototype model of the spacecraft, a series of tests was performed to qualify the vehicle as a flightworthy structure. From experience gained during the *Ranger* program and the results of analysis, it was determined that a static test of the entire spacecraft would be unnecessary.

A dynamic test program was undertaken to determine whether or not the *Mariner R* spacecraft was structurally capable of withstanding the dynamic loads as defined in JPL Specification 30254. The test program was basically divided into two parts: (1) modal survey testing; and (2) structural type-approval testing.

The primary objective of the modal survey testing was to determine the fundamental natural frequencies, corresponding mode shapes, and structural damping ratios of the *Mariner R* spacecraft by exciting the spacecraft with a series of small shakers. With this information, a modal

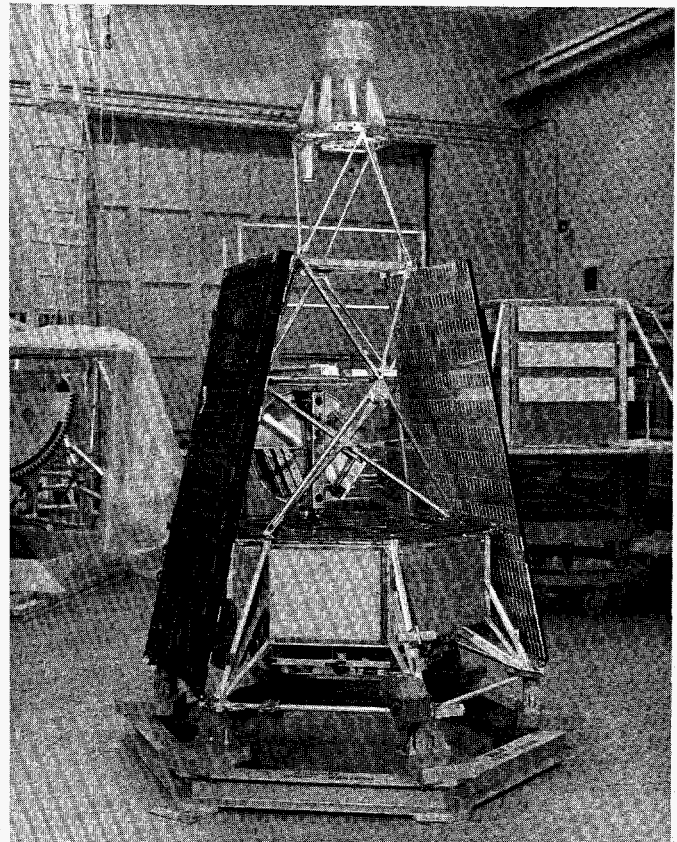


Fig. 32. Spacecraft without panel extension

analysis could then be performed to analytically determine the response of the spacecraft to a forced excitation at its base. The objective of the structural type-approval testing was to simulate the expected in-flight vibration environment by exciting the spacecraft on a shake table to the levels defined in JPL Specification 30254. The results of these two types of tests could then be plotted as amplitude ratio-vs-frequency curves to illustrate the response of various points on the structure to forced excitation at the base of the spacecraft.

When it was decided that the additional solar panel area was to be located on the far end of the panel as an 11-in. extension, a complete requalification test of the spacecraft structure was performed. The purpose of the test was (1) to prove the structural adequacy of the solar panel extension; and (2) to prove that the spacecraft was still structurally and dynamically adequate (Fig. 31 and 32 show the spacecraft with and without the solar panel extension). This testing was performed and, as a result, two groups of data were compiled. Each group was composed of information concerning shake-table testing and modal survey analysis.

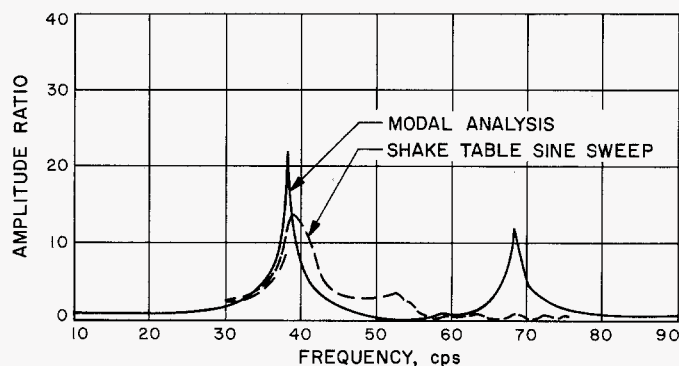


Fig. 33. Plot of x/x_0 vs frequency,
solar panel support plate

To illustrate the behavior of the spacecraft under a forced excitation, the two groups of results were reduced and plotted as amplitude ratio-vs-frequency curves. Two of these response curves are presented in Fig. 33 and 34. Generally, as seen from these curves, the response of the structure at resonance is greater during the modal survey than during the type-approval test. This is to be expected since the damping, which was assumed constant, usually increases with increasing amplitude. The responses generated during these tests generally substantiate other somewhat conservative analysis.

Certain structural failures did occur during these additional tests. Notable were: a failure of the superstructure bulkhead supporting the top of the solar panels, a failure in the base of the omni-antenna, and a failure in the braze joint at the upper end of the attitude control gas bottle bracket. The necessary modifications were made to the flight vehicle.

The high-gain antenna and Earth sensor exhibited high vibration gains during several parts of the test. While this structure successfully survived the test, it was believed that, if electronics had been in the Earth sensor mock-up, they would probably have experienced failure. An extensive program was conducted to provide more stiffness and damping in this area, resulting in changing of the antenna supports in the adapter from rubber to aluminum and the addition of a spring-loaded, concentric-tube viscous damper system between the long-range Earth sensor and the adjacent structure. The resulting system produced responses well within acceptable limits.

A vibration test was performed with the spacecraft supported on the *Agna B* adapter and placed under the *Agna* shroud. The primary objective of this test was to verify clearance between the dynamic envelopes of the

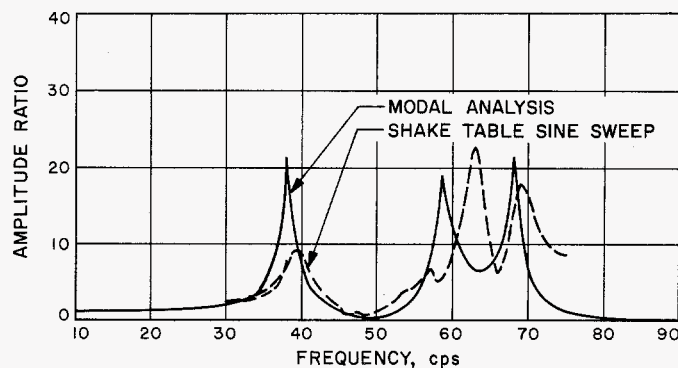


Fig. 34. Plot of x_{77}/x_0 vs frequency
⊙ of + X solar panel

shroud and the spacecraft under the extreme steady-state flight-vibration environment as it is presently known. The dynamic deflections in the critical interface locations were measured and found to remain well within the prescribed dynamic envelope of the spacecraft.

An additional series of modal survey tests was conducted with the spacecraft in its cruise configuration (Fig. 35). While this configuration did not produce critical structural loads, calculations indicated that spacecraft natural frequencies in the range of 2 to 30 cps could destabilize the autopilot during midcourse maneuver, depending on the mass, moment of inertia, location, and damping characteristics of the component resonating. During this series of tests, the midcourse configuration was simulated by placing the spacecraft on the system

Table 3. Summary of primary modes of vibration
(midcourse configuration)

Mode	Frequency cps	Damping ratio c/c_c
Solar panel about hinge axis	2.00	0.0275
High-gain antenna about actuator axis	2.66	0.055
High-gain antenna, combined bending and torsion	3.15	0.0624
High-gain antenna, torsion about pivot arm	5.4	0.0835
Radiometer, torsion about hinge axis	6.2	0.35
Solar panel torsion	14.2	0.0398
High-gain antenna about actuator axis	15.9	0.1005
High-gain antenna breathing	27.3	0.047
Solar panel, bending in-plane of panel	32.0	0.0317
Solar panel about hinge axis	43.5	0.0106

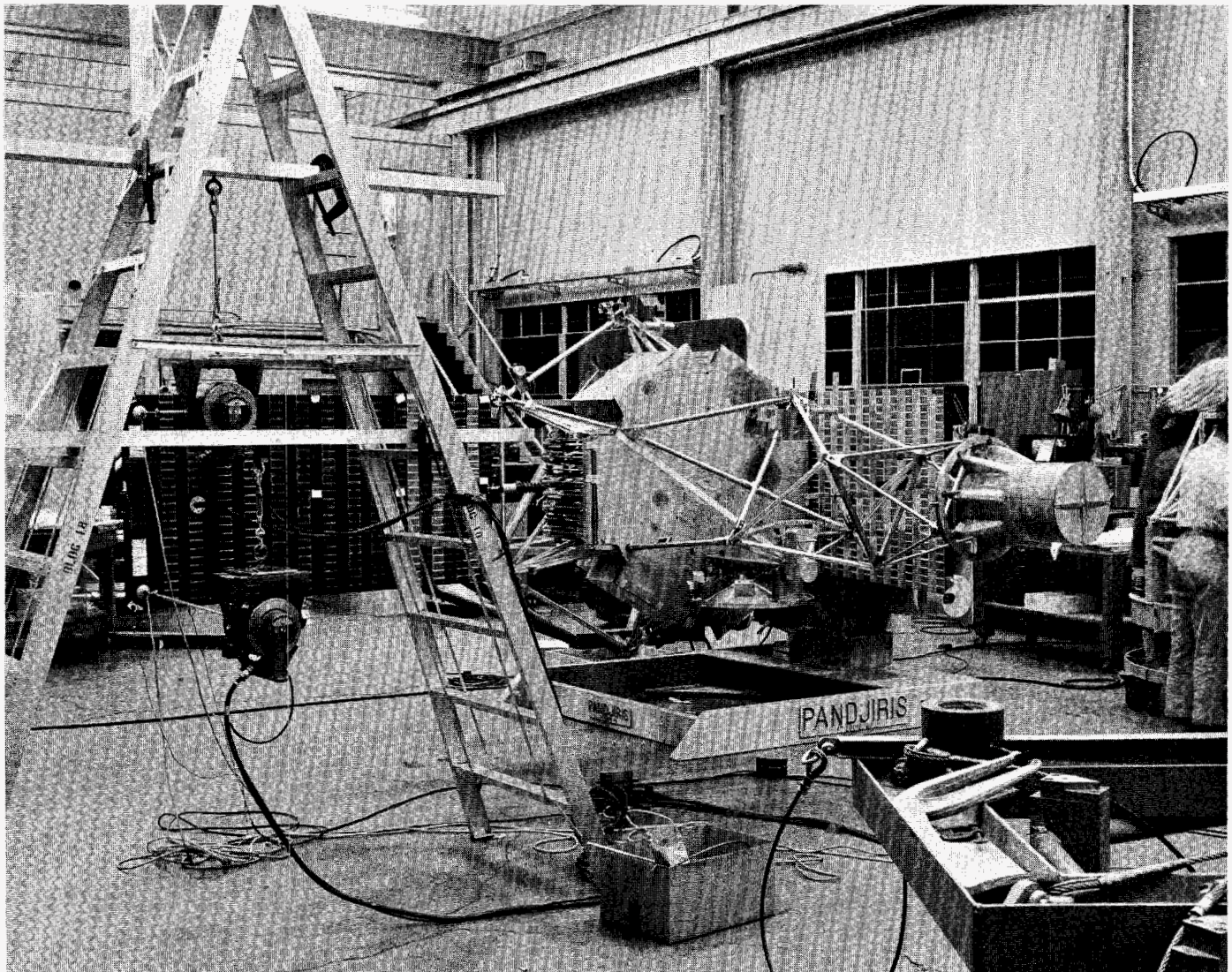


Fig. 35. Spacecraft during cruise configuration modal survey

test stand and extending the solar panels and high-gain antenna, and unlatching the radiometer as necessary.

Because the system test stand stiffens the spacecraft structure, these tests gave higher natural frequencies than would be expected in space. Solar panel resonances were measured with the spacecraft roll axis held at a 12-deg angle from the horizontal, thus simulating the suddenly applied 1/9-g load from the midcourse motor.

The fundamental frequency of the extended solar panel and the fundamental torsion frequency of the extended high-gain antenna were found to fall within the critical range. In order to eliminate these problem areas, the

following modifications were made to the spacecraft. First, the solar panel frequency was reduced from 6.5 cps to 2 cps by replacing the aft monoball joint on the solar panel actuator with a cylindrical rubber bushing. Next, the damping in the high-gain antenna was increased from $c/c_c = 0.0179$ to $c/c_c = 0.0835$ during the torsion mode, through the installation of a concentric tube grease-in-shear damper.

The natural frequencies in or near this critical range, together with their respective damping ratios, are presented in Table 3. The Guidance and Control Division indicated that the spacecraft, with the modified dynamic characteristics, would not destabilize the autopilot.

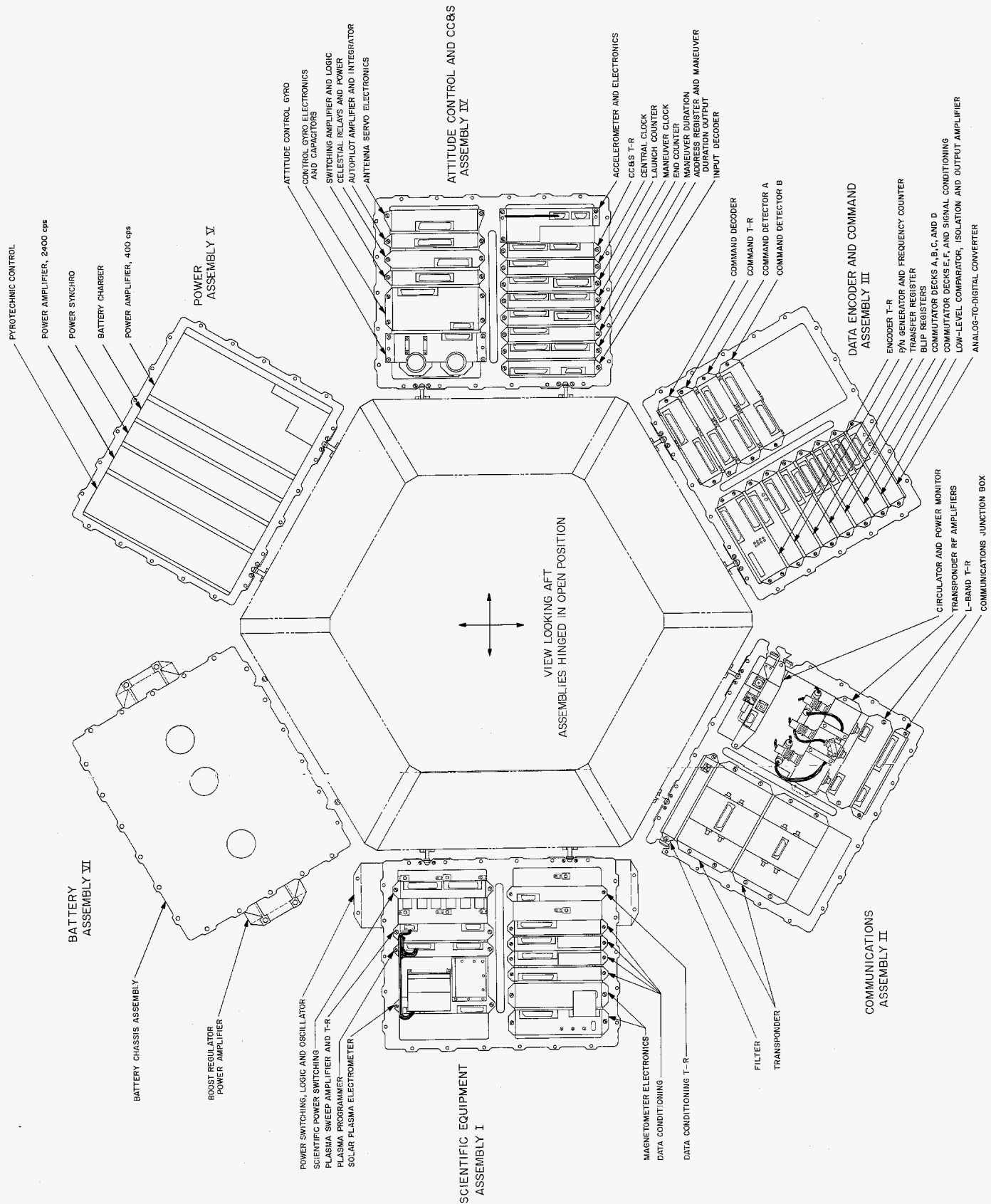


Fig. 36. Mariner R packaging assembly

4. Packaging

a. General. Packaging of the *Mariner R* electronic equipment was basically a return to the *Ranger* configuration (Fig. 36), since *Mariner R* largely utilized *Ranger* techniques. Thus, communications, attitude control, CC&S, data encoder, and the command electronics required only minor packaging changes in those few areas where new circuits were used.

The power subassemblies, which were uniquely packaged in the secondary hex and on the intercostals for the *Mariner A*, had to be adapted to the *Mariner R* vehicle. This was accomplished without any changes to the subassemblies by fabricating a new assembly chassis, which accepted the *Mariner A* subassemblies and yet was compatible with the *Mariner R* vehicle. Also, a new battery chassis was developed.

Several basic magnesium chassis which were fabricated for the *Mariner A* were used for *Mariner R*. Hinges were added to these chassis for more convenient service and checkout. For other vehicles, the assembly chassis have typically been gold-plated for thermal control purposes; however, for *Mariner R*, these chassis have not been gold-plated, but rather had polished aluminum shields located in those areas where low emissivity surfaces were required.

As can be noted on the *Mariner R* packaging assembly (Fig. 36), a rather high degree of subassembly profile standardization has been obtained. With this standardization, better weight and volume efficiency were achieved than in the *RA-I* spacecraft. Only the battery and power subassemblies remained nonstandard to utilize existing *Mariner A* equipment.

b. Assembly description

Assembly I, scientific equipment. Figure 37 shows this assembly on the spacecraft. The power switching and logic subassembly is bolted to the outside surface. The unusual shape of this subassembly is explained by the fact that it was originally designed for the *Mariner A* spacecraft and was to be located on the intercostals. On the *Mariner R* spacecraft, this subassembly is located on the face of Assembly I so that short cables from the power switching and logic subassembly to the battery and solar panels could be used. In addition, this location allowed some 15 w of heat dissipated in the power switching and logic to be utilized to keep the scientific instruments, located inside the hex, warm.

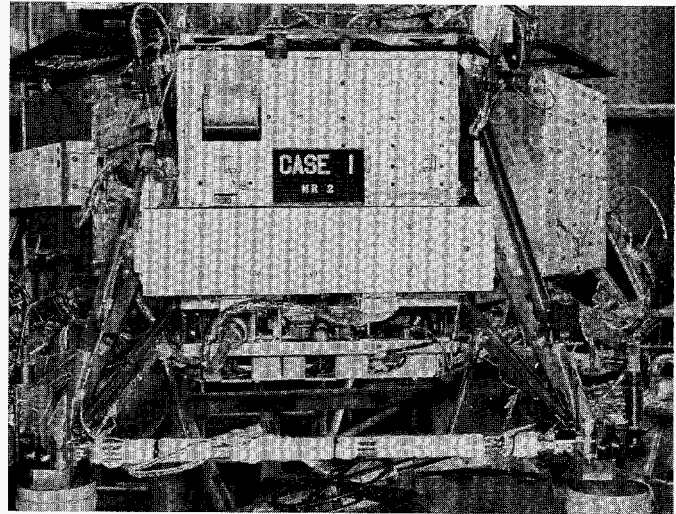


Fig. 37. Assembly I on spacecraft

Deflection plates for the solar plasma instrument are in the upper left corner of the assembly, as shown in Fig. 37. In this location, the requirement for deflector orientation to the Sun was satisfied. The electronics inside the assembly could be packaged on subassemblies of the standard shape; thus, better weight efficiency could be obtained for other electronic subassemblies in the same chassis; i.e., magnetometer electronics, data conditioning, and scientific power switching.

Assembly II, communications. Figure 38 shows the communications assembly in a handling fixture which was provided to protect the thermal coatings, transducers, and louvers on the chassis from damage during electrical assembly and checkout. Such fixtures were provided for all of the electronic assemblies.

A significant packaging improvement in this assembly can be noted in the transponder and r-f amplifier areas. Figure 39 shows an *RA-I* communications assembly. The transponder was packaged in a large, heavy case bolted across the chassis, while the three amplifiers were located on the bottom surface. This type of communications packaging was defined prior to the establishment of modular packaging techniques for *RA-I*. For the *Mariner* spacecraft, more compatible packaging was obtained by mounting the same transponder modules in a standard configuration (Fig. 40). In this form, the transponder subchassis was used as an assembly chassis stiffener, in a manner similar to other standard electronic subassemblies. These transponder subassemblies occupied less than half the volume of the assembly.

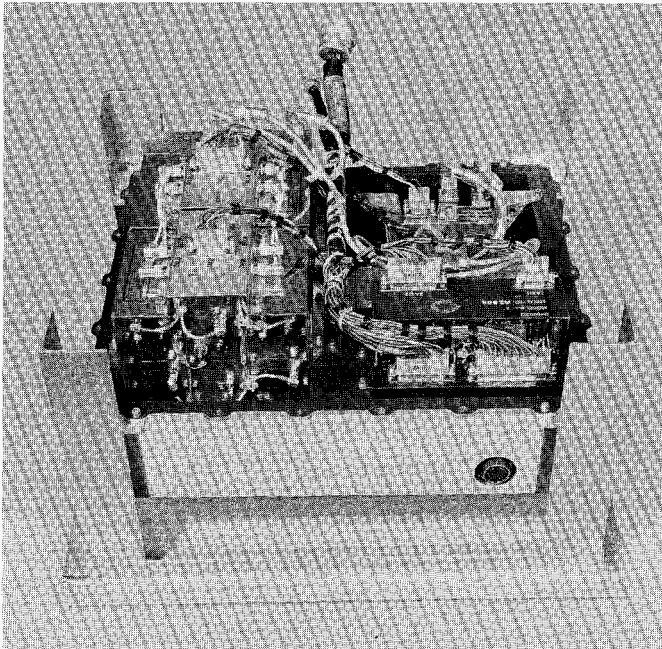


Fig. 38. Assembly II in handling fixture

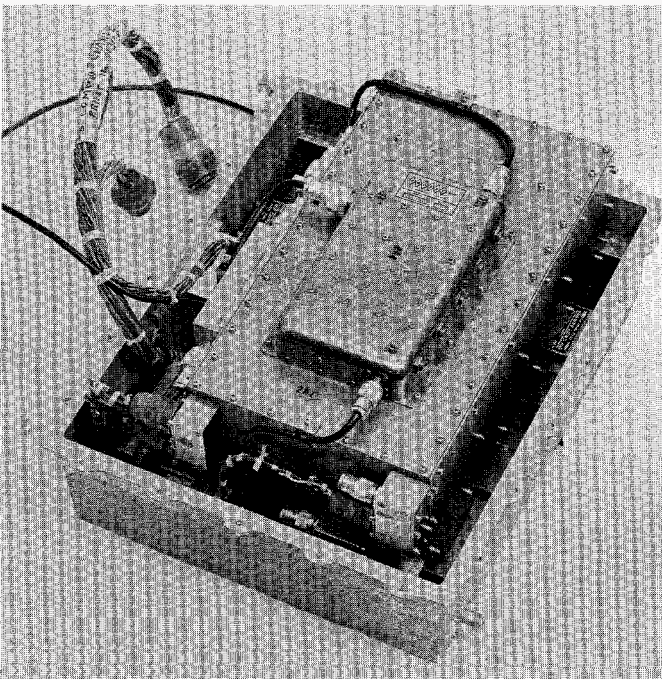


Fig. 39. RA-1 communications assembly

Similarly, the three cavity amplifiers were combined into a single unit (Fig. 41), in a shape compatible with the standard configuration.

Both the transponder and cavity amplifier packages used the same inside parts previously developed for

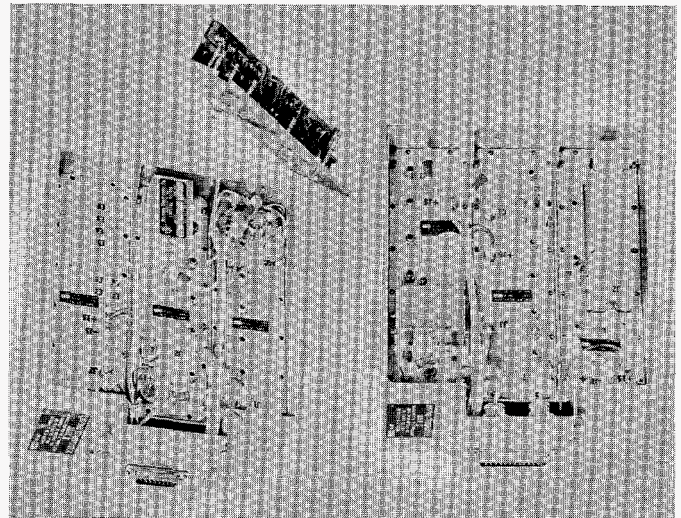


Fig. 40. Transponder

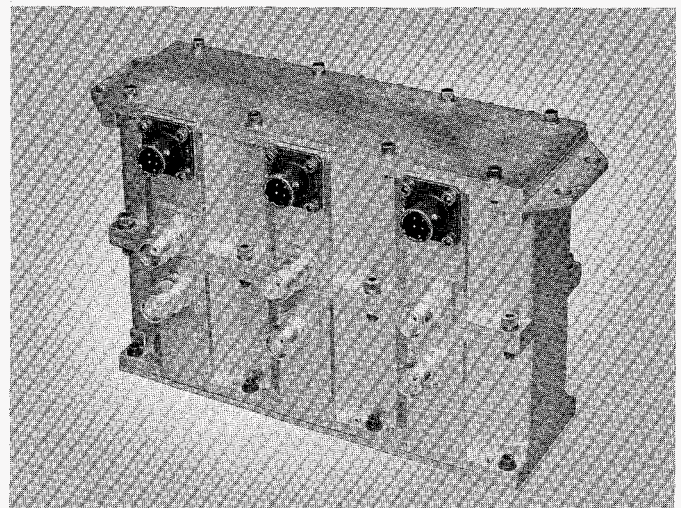


Fig. 41. Cavity amplifiers

Ranger. With this new communications package, an appreciable weight reduction was effected by packaging the complete subsystem in one standard chassis (transponder, transponder amplifiers, filter circulator, power monitor T-R unit, and the junction box).

Assembly III, data encoder and command. This assembly contains densely packaged electronics on standard-shaped subassemblies. The chassis for Assembly III is shown in Fig. 42. This chassis, as well as chassis for Assemblies I, II, and IV was made from a *Mariner A* standard magnesium chassis. Low emissivity surfaces were obtained by riveting 0.016-in.-thick polished aluminum shields to the chassis. Figure 42 shows temperature transducers mounted on the front surface and special hinges

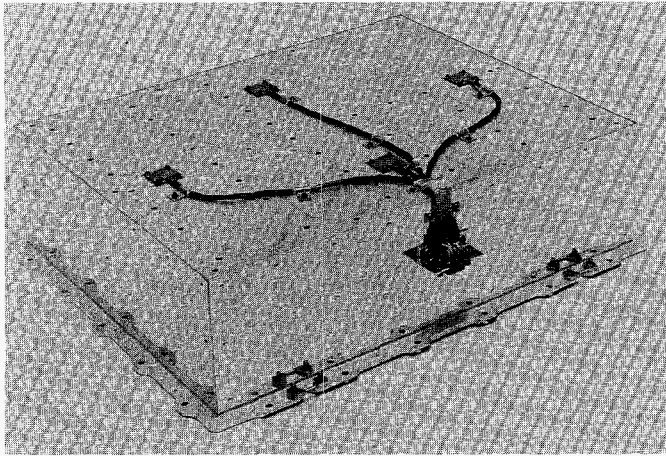


Fig. 42. Assembly III chassis

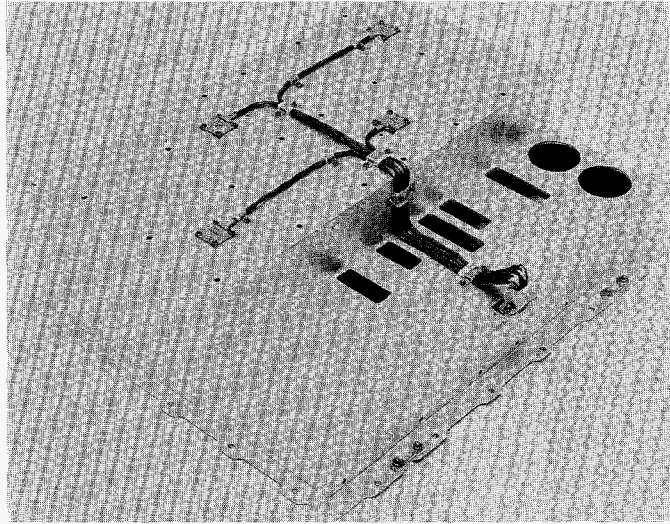


Fig. 44. Assembly V chassis

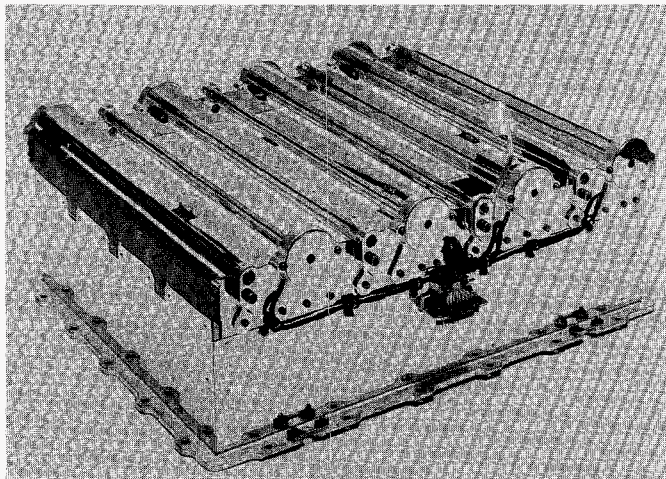


Fig. 43. Assembly IV chassis

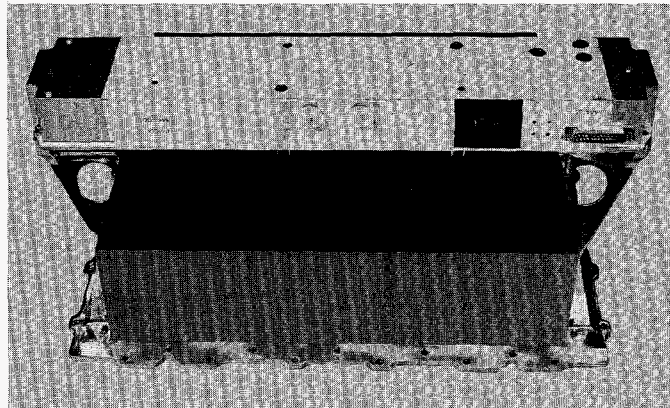


Fig. 45. Assembly VI chassis

which were added to ease service handling problems after the assemblies are attached to the spacecraft.

Assembly IV, attitude control and CC&S. The equipment is packaged in standard-shaped subassemblies. Attitude control electronics were adapted from *Mariner A*, while the CC&S required only one new subassembly. This chassis required temperature control louvers to accommodate large power dissipation changes occurring during spacecraft acquisition and maneuver. Figure 43 shows a standard chassis with louvers attached.

Assembly V, power. This assembly was packaged to contain the *Mariner A* secondary hex power subassemblies which were in an L-shape for *Mariner A* and, therefore, required a new chassis to accommodate them on the *Mariner R* hex. Figure 44 shows the chassis which was

developed to accommodate these subassemblies. The cutouts are for connectors since the power cabling is external.

Assembly VI, battery. Figure 45 shows the battery chassis which utilized *Mariner A* battery cells. Location of this assembly on the hex was primarily governed by cabling requirements and spacecraft cg location.

The power amplifier subassembly is on the outside of the battery assembly developed for *Mariner A*. This location was chosen to provide heat to the battery from the power amplifier.

Radiometer. For *Mariner R*, a new microwave radiometer was packaged, using much of the electronics and r-f components from a three-dish *Mariner A* radiometer

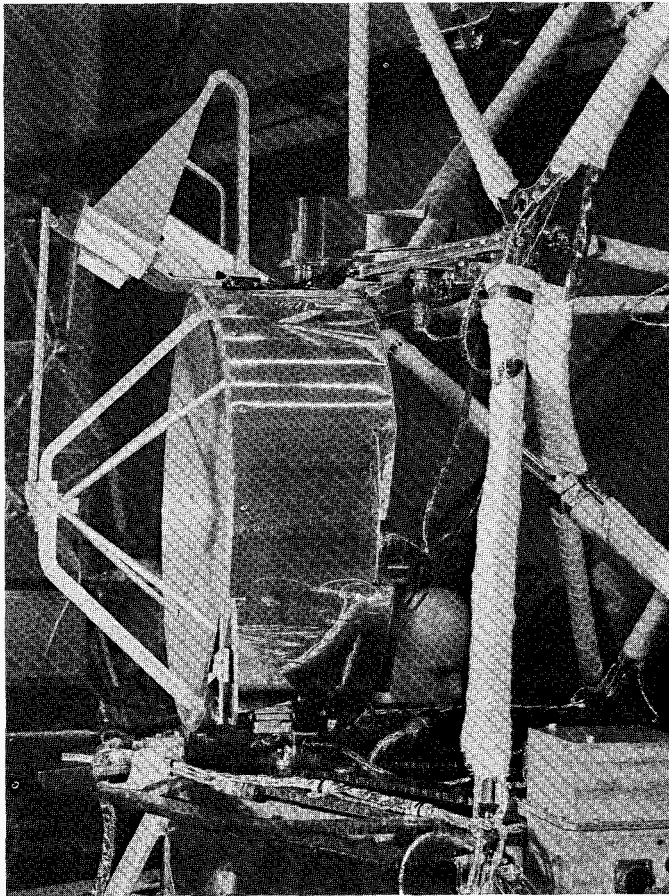


Fig. 46. Radiometer on spacecraft

design. Figure 46 shows the instrument complete with thermal shield as installed on the spacecraft.

The generally parabolic shape of the dish was machined in steps, to avoid focusing solar energy at the feed of the instrument. To conserve weight, the back side of the instrument also utilized stepped machining, which was coordinated with that on the face of the dish (Fig. 47).

Note the one-piece machined chassis; this was done to obtain a more efficient and stiffer configuration by utilizing the structure of the dish while the stiffening ribs were used for mounting electronic components. The center channel, while serving as a stiffener, is also used for attaching the thermal shield over the instrument. The two ribs on the lower right corner are included to provide an attachment for the infrared radiometer.

Particle Flux Detector. Figure 48 shows the instrument with the thermal control cover removed. The chassis is shaped around the power supply beneath and the three

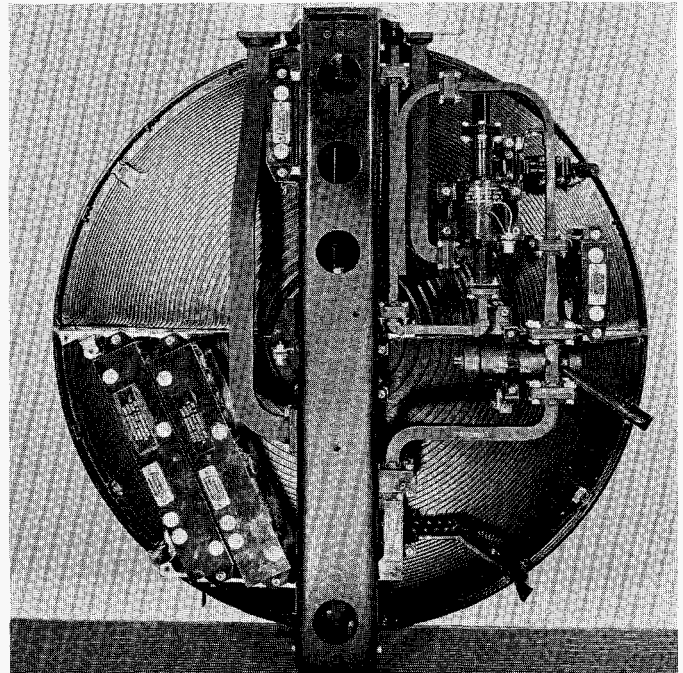


Fig. 47. Radiometer, rear view

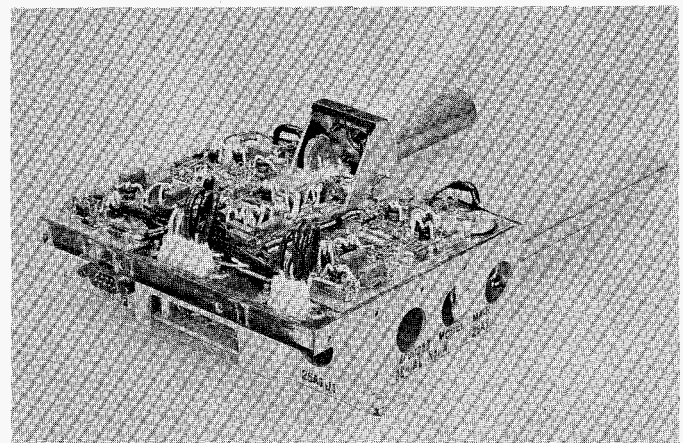


Fig. 48. Particle flux detector electronics

Geiger-Mueller tubes, leaving the top surfaces for the electronics.

5. Mechanisms

a. Radiometer scan actuator. Initially, the infrared radiometer consisted of a 19.25-in.-diam. parabolic dish with electronics components packaged on the back of the dish. As the program advanced, an additional infrared detector was integrated into the original instrument and attached to the periphery of the dish.

In order to obtain a maximum of temperature information, it is desirable to scan the planet. A single, mechanized degree-of-freedom is adequate, since the spacecraft passing the planet provides the second degree-of-freedom required. The mechanized scan is implemented by an actuator which scans about an axis parallel to the Sun-probe line.

Prior to planet encounter, the actuator moves the radiometer through a ± 60 -deg search scan as governed by scan stop switches, at the rate of 1 deg/sec. Upon planet acquisition by the radiometer, the scan rate is decreased to 0.1 deg/sec and the scan amplitude is governed by signals from the radiometer when the horizon of the planet is crossed, thus giving a horizon-to-horizon scan. During the scan operation, the angular position of the radiometer is indicated by the feedback potentiometer.

The scan axis is established by the actuator mounted on the superstructure and a monoball bearing on top of the primary hex structure. During the boost phase, the instrument is constrained from rotating by a pyrotechnic pin puller mounted on the hex structure. In this position, should the actuator or the latch fail to function, there would still be a reasonable probability of seeing Venus.

The requirements for the scan actuator were that it consume no more than 2 w of power, and that it be capable of scanning at two rates (1 deg/sec and 0.1 deg/sec). Taking advantage of RA-1 and -2 experience, the Lyman-alpha size 8 synchronous drive motor and gearhead were chosen to drive the scan actuator. To accomplish the change in scan rate without shifting gears, two motors and a differential were used. Each motor is geared to one side of the differential and the output is taken from the carrier shaft. The input from one motor into its side of the differential is 1/10 the speed of the other and, thus, the speed shift from 1 to 0.1 deg/sec is effected by switching from one motor to the other. Figure 49 shows a flight actuator with its cover removed. The output end of the actuator is in the foreground and the drive motors are at the rear.

A slip clutch is provided at the output to protect the differential and reduction gears from shock loads during boost, or from overloads by improper handling of the radiometer during systems operations.

A universal joint was designed into the actuator output shaft to permit small angular misalignments caused by manufacturing tolerances in the position of the actuator mounting pad and the motion of the superstructure. This

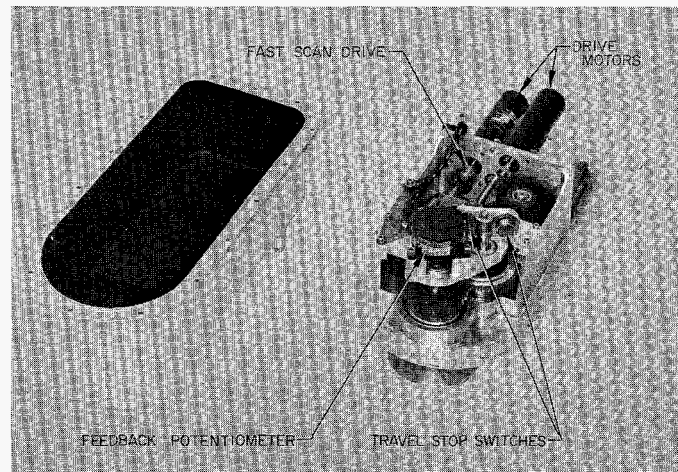


Fig. 49. Radiometer scan actuator with cover removed

provision also isolates the radiometer from superstructure distortions during boost vibration.

The two travel-stop switches, which reverse the fast scan direction by reversing the motor rotation, are operated by a lever which has a cam and spring drive to compensate for over-travel and to avoid damage to the switch. The position potentiometer is coupled directly with the output and provides feedback of actuator position. The actuator enclosure is sealed and pressurized to 4 psig to prevent evaporation of the silicon oil lubricant in space. Over 1 atm pressure is used so that a pressure leak can be detected in preflight tests. Testing of the actuator in a vacuum has verified its ability to function properly should the pressure be lost.

A prototype model of the scan drive unit was mounted on the structural test spacecraft and passed type-approval tests in this configuration. The actuator functioned normally at the conclusion of several type-approval vibration tests.

Flight units were vibration-tested to flight-acceptance levels following an 8-hr run-in period. The purpose of the run-in is to burnish the MoS_2 coating used as a lubricant on the gear teeth and to reveal any defective or contaminated ball bearings in the motors or gear heads. The run-in has proven of value, since faulty parts have been discovered during this period.

b. High-gain antenna yoke. Because of Mariner R geometric considerations and the long-range Earth-sensor alignment requirements, it was not possible to use the Ranger antenna yoke. The yoke designed for Mariner R

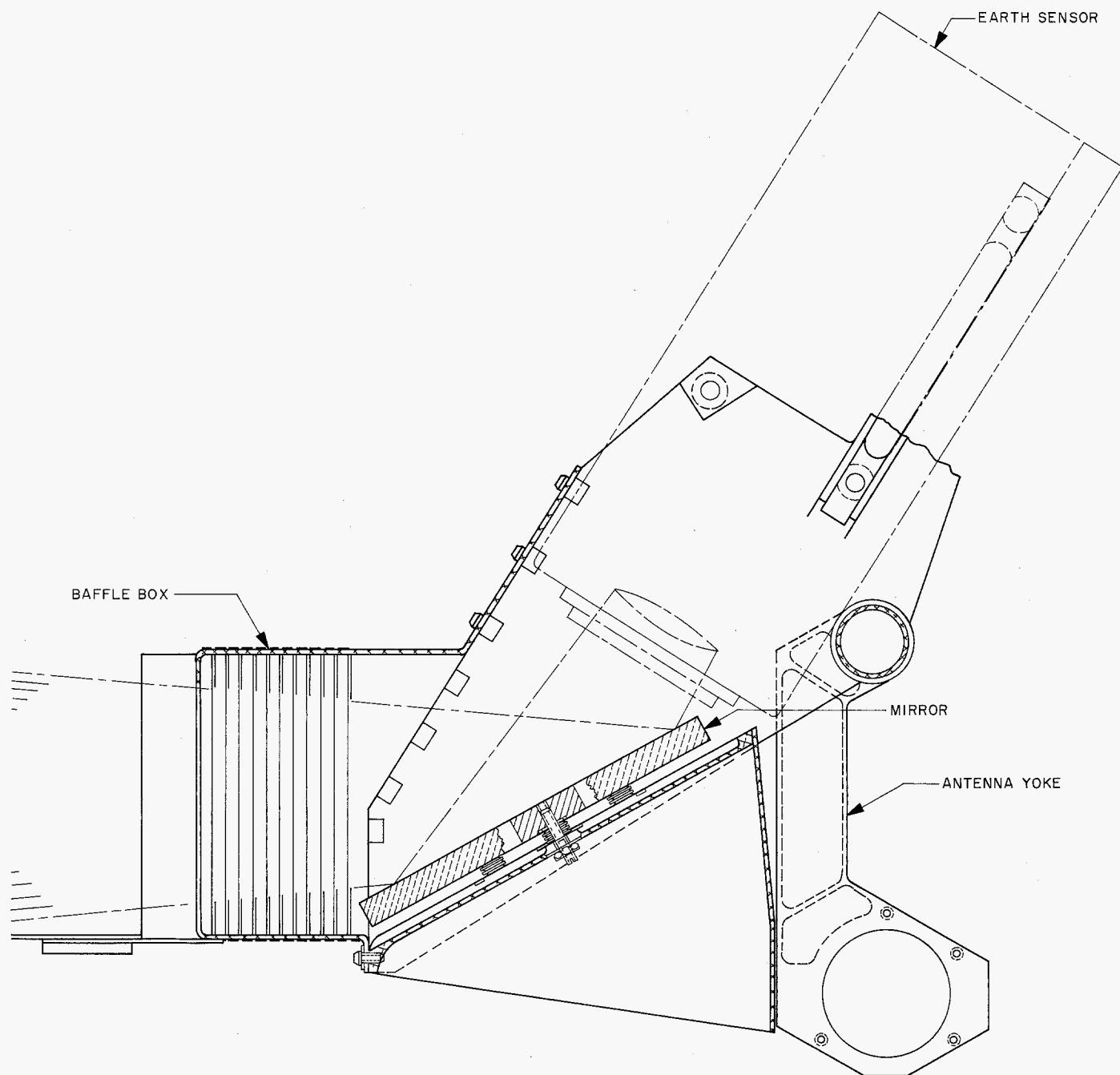


Fig. 50. Earth-sensor mount, mirror and baffle box

makes it possible to mount the sensor axis at an angle with the antenna beam and view the Earth through a front surface quartz mirror.

In the original concept, the antenna yoke provided only basic mounting structure for the Earth sensor and mirror. Later, the sensor was found to be sufficiently sensitive to detect diffuse light from sources outside its field of view. It was necessary to shield reflections from the an-

tenna feed and rim and to provide a Sun shade at that point when the Sun-probe-Earth angle is at minimum. A baffle box, with the baffle elements out of the sensor's view, was designed to absorb light being admitted to oblique angles.

To achieve a black, knife edge on each baffle, a unique method of construction was used. Thin (0.002-in.) strips of black oxidized brass were inserted through slits in the

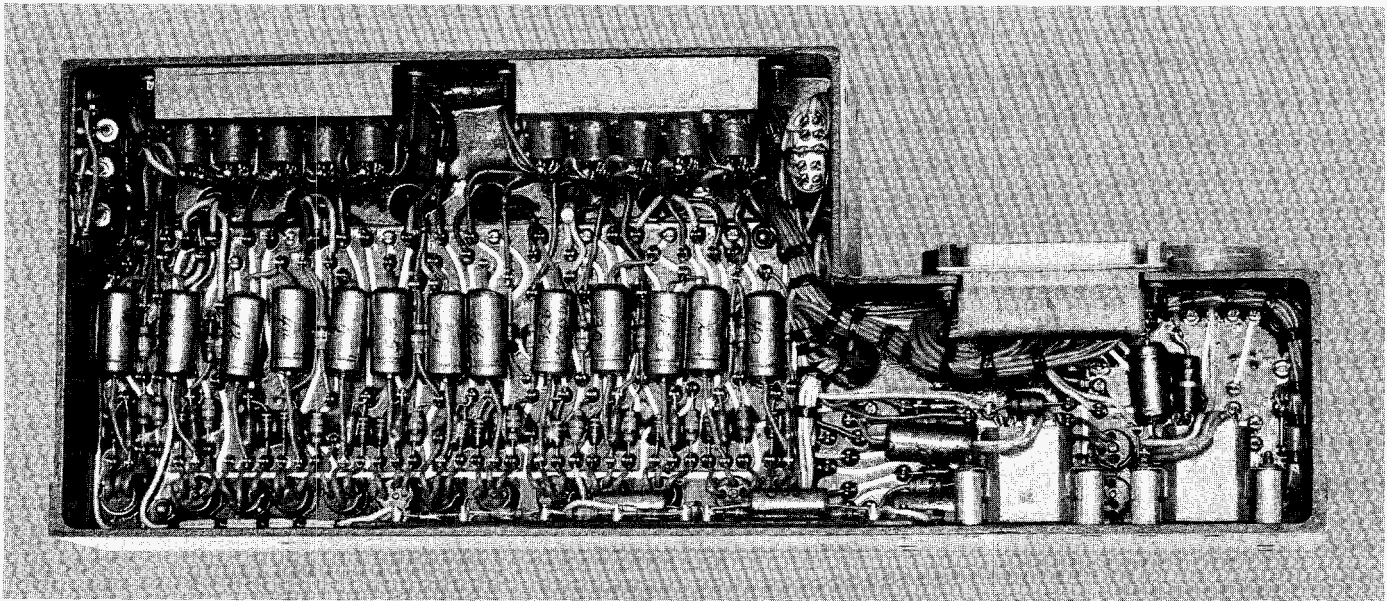


Fig. 51. Pyrotechnic control assembly

box, aligned and bonded in place. The edges of the strips surrounding the sensor's view were rounded with a radius of approximately 0.001 in. The ends of the strips protruding outside the box were then trimmed and aluminum foil was bonded over them to assure a light-tight seal to present a low emissivity surface to space. Tests have indicated the baffle box was effective. Figure 50 shows the details of the Earth-sensor mount, the mirror, and the baffle box.

6. Pyrotechnics

The objective of the *Mariner R* pyrotechnic subsystem design was to produce the most reliable system possible, consistent with the spacecraft development time schedule and weight requirements. Redundancy was to be employed in the switching circuitry to achieve this objective. Each pyrotechnic device was to contain two separate squibs, or, at a minimum, two separate bridgewires with separate electrical firing circuits.

This design of the *Mariner R* pyrotechnic subsystem was based on experience gained from the *Ranger* series. Squibs are identical to those used on *Ranger*, except that powder cans on all squibs are hermetically sealed, and midcourse motor explosive valve squibs contain dual bridgewires. Techniques used to achieve reliability in the pyrotechnic subsystem are: (1) all components used in fabricating the pyrotechnical control assembly undergo rigid preassembly screening tests; (2) redundancy is

maintained throughout the subsystem (all actuated devices are supplied with two independent electrical squib initiation circuits); (3) effects of pyrotechnic subsystem malfunction on the spacecraft power, command, and data acquisition subsystems have been minimized by electrical isolation; (4) arming of the subsystem is accomplished only after *Agena*/spacecraft separation; (5) all flight PCA's undergo defined flight-acceptance environmental tests (one PCA is subjected to defined type-approval tests); and (6) type-approval, reliability, and flight-acceptance tests are performed on all squib lots.

The spacecraft pyrotechnics are initiated by command from the CC&S and are divided into three time-separated events. These are the release of solar panels and radiometer, the initiation of midcourse motor firing, and the termination of midcourse motor firing. Upon command, the PCA switches sufficient electrical energy to initiate the squibs at that event. The PCA package is shown in Fig. 51.

Command and squib initiation power is obtained from the main spacecraft battery. Peak current demand by pyrotechnic firing has been limited to 10 amp at the lowest battery voltage. To prevent depletion of the spacecraft battery because of postfire squib shorts, command and firing circuits are opened 2 sec after pyrotechnic initiation. To minimize the effects of postfire squib shorts, a series resistor is placed in each bridgewire firing circuit, limiting the current and ensuring that other squibs in the same group receive sufficient current to fire. To limit

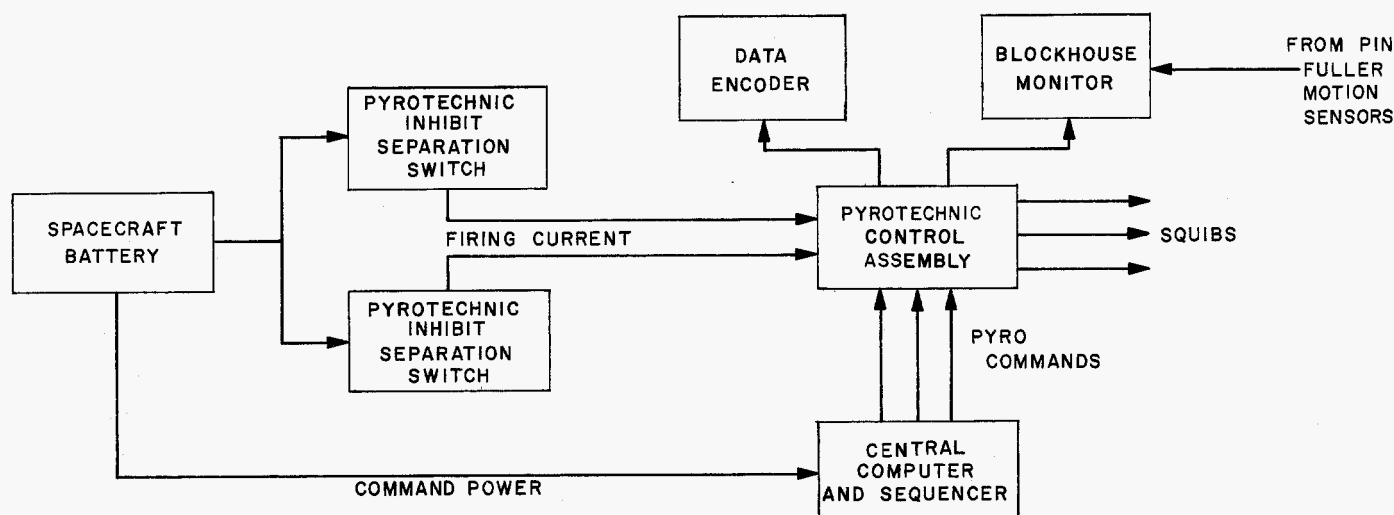


Fig. 52. Pyrotechnic subsystem, block diagram

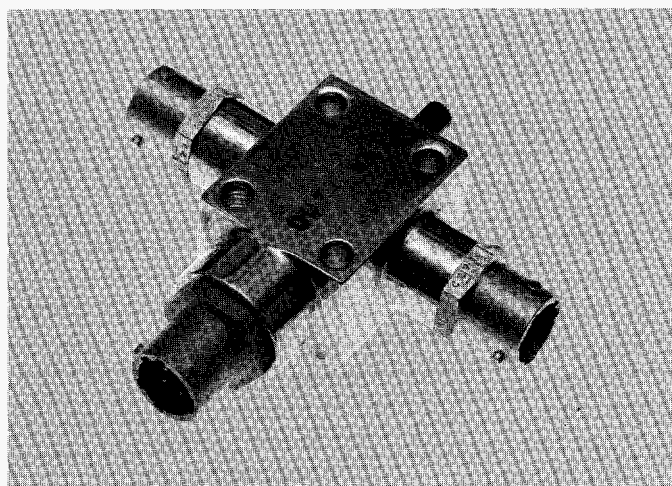


Fig. 53. Pin-puller assembly

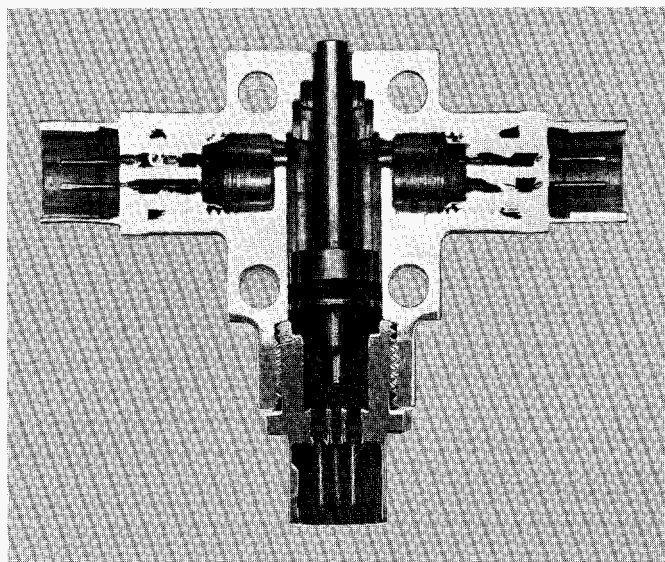


Fig. 54. Pin-puller assembly, cross section view

instantaneous current demands, firing times of squib groups in the first and second pyrotechnic events are subsequenced. Timing within the PCA is controlled by solid-state RC timing circuitry. A block diagram of the pyrotechnic subsystem is shown in Fig. 52.

Pin pullers containing two independent squibs and an integral electrical switch to indicate pin-puller actuation are used to unlatch the solar panels and radiometer. Except for the motion-sensing switch, the pin pullers are identical to those used on *Ranger*, as are the midcourse motor valves. Figures 53 and 54 show a normal and a sectioned pin puller containing squibs and motion sensor switch.

The squibs used in the pin pullers are Ordnance Associates Type OA PT6-2, and the primer chamber assemblies used in midcourse motor valves are Conax Type 1621-055-01. Preproduction lots of 100 squibs of each type were purchased, from which 50 squibs of each lot were subjected to the Bruceton method of sensitivity testing to verify the manufacturers' stated "all fire" and "no fire" currents. Remaining squibs of the two lots were subjected to type-approval tests. Production lots of approximately 550 of each squib type were then purchased and subjected to flight-acceptance tests. Then 300 units of each lot were fired to determine their reliability. Remain-

ing units are utilized in system dummy runs and for flight. Squib simulators containing 0.75-amp glass-tube fuses are used in normal systems tests for PCA checkout.

Monitoring the performance of the PCA during systems tests is accomplished by means of a test console. This console provides: (1) an indication when each firing current pulse is delivered to a simulator; (2) an indication when the firing voltage has been maintained for at least 1.75 sec; (3) outputs of simulator firing current pulses to the central recorder, or other external recorder; (4) circuitry to enable the console operator to determine simulator continuity before, during, or after a test, without having direct access to the simulators on the spacecraft; and (5) self-contained, self-test circuitry. The console also contains a d-c power source to permit operation of the spacecraft pyrotechnic subsystem in the absence of other subsystems.

Pin-puller motion and PCA command relay position are monitored by hard line to the blockhouse. Indications of arming the pyrotechnic subsystem and delivery of firing voltage to primary squibs at each command are routed to the spacecraft telemetry system for flight and postflight analysis.

Six pyrotechnic control assemblies were fabricated, including one prototype, one type-approval unit, two flight units, and two flight spares. Once installed on the spacecraft, neither flight unit was removed. No malfunctions occurred during any preflight test. The reliable performance displayed by the PCA is attributed to the redundancy and simplicity inherent in the circuit design, elaborate screening tests performed on each selected component used in fabrication, and thorough flight-acceptance testing of each unit.

7. Temperature Control

a. Introduction. The *Mariner R* temperature control problem demanded that the spacecraft design be such that each component would remain at an acceptable temperature throughout the mission. Ultimately, the problem resolves to a radiation balance between the energy absorbed from the sunlight and the energy lost to the heat sink of space. In the *Mariner R* spacecraft, a portion of this solar energy is converted to electrical energy and distributed to the various spacecraft assemblies. This distribution changes with the various operating modes of the spacecraft. Some surfaces of the spacecraft will absorb more energy from sunlight than others, either because of their shape or optical properties. With this

nonuniform distribution of energy throughout the spacecraft, the internal conduction and radiation heat exchange must be considered. This Section summarizes the engineering philosophy and the preflight methods used to manipulate the temperatures at which this energy balance will occur.

b. Mariner R design and test philosophy

Design philosophy. The basic elements of the *Mariner R* were made as thermally independent from solar radiation as practical. This provision reduces the large variations in temperature (approximately 90°F) which would otherwise result from the different intensities of the solar radiation between the orbits of Earth and Venus. The attitude control system, which maintains a Sun orientation of the spacecraft, makes this approach practical. During the relatively short periods when the spacecraft is not in a Sun-oriented position, the thermal capacitance of the vehicle is used to limit the temperature variations to an acceptable range. The energy dissipated from each electronic assembly is used to compensate for its heat losses to space. The amount of electrical energy is small when compared to the thermal energy which the surfaces of the spacecraft are capable of radiating, thus dictating an exterior surface which is a relatively poor radiator.

By specifying that most of the internal surfaces of the spacecraft be good radiators, the internal heat exchange is much larger than that between the spacecraft and space, resulting in small temperature differences between the assemblies within the spacecraft. The uncertainties in predicting the steady-state temperature results primarily from variations in the power dissipated by the electronic assemblies and the thermal properties of the radiating and insulating surfaces of the spacecraft. Since the integrated effect of these uncertainties is unpredictable, an active device is included to regulate the amount of energy radiated to space.

The thermal design philosophy for those portions of the spacecraft which are not included in the basic hex enclosure are considered separately. The scientific instruments do not dissipate enough heat within them to account for the unavoidable losses and, for some instruments, shielding from the solar radiation is not desirable from the scientific measurement standpoint. The solar energy absorbed and the heat losses to space are balanced passively by adjusting the surface properties of the radiating surfaces. The temperatures near Earth are near the lowest allowable for the instrument and the temperatures near Venus are near the maximum.

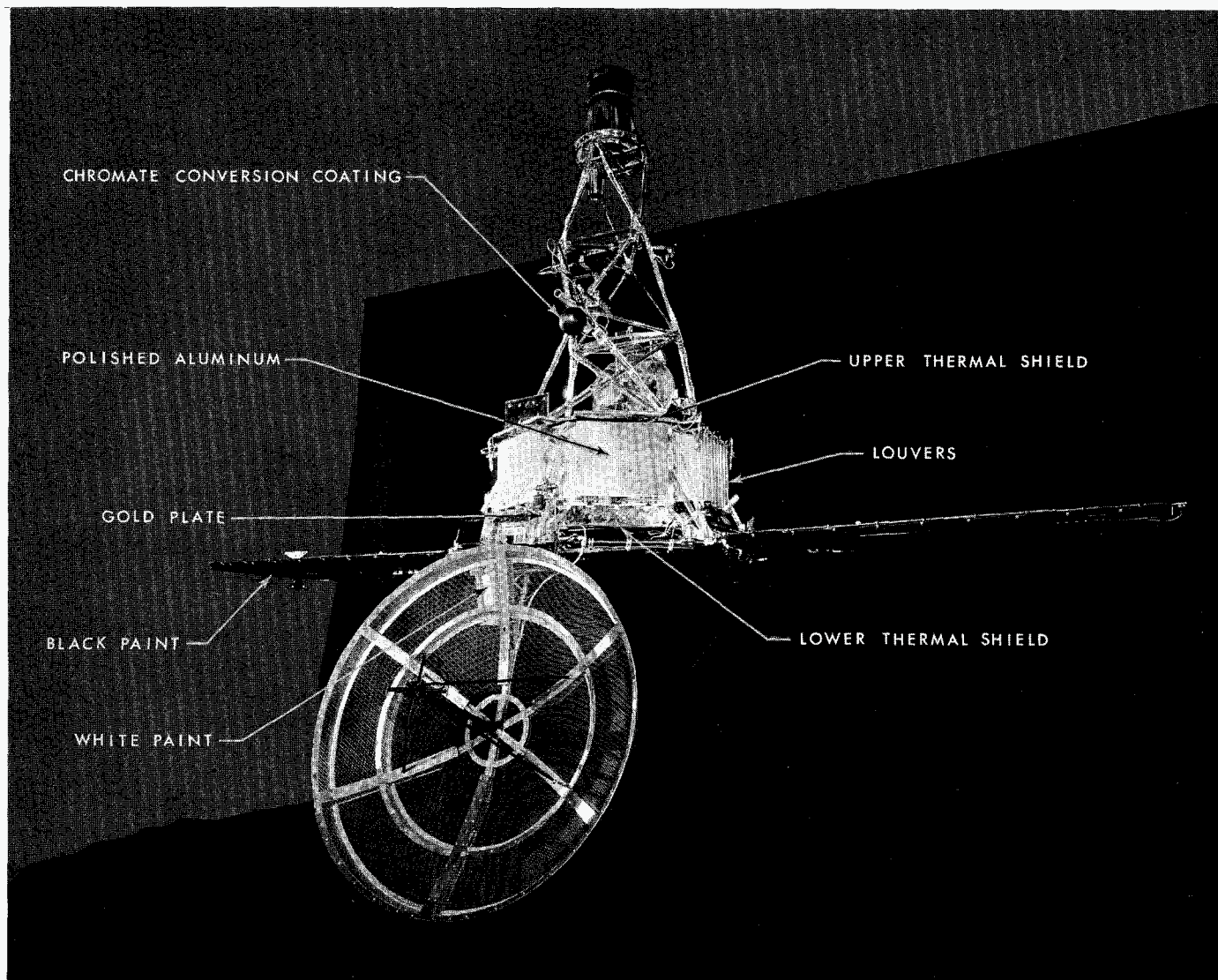


Fig. 55. Mariner R temperature control system

The solar panels are designed to operate at the lowest temperature possible throughout the flight. Ultraviolet filters are used on the solar cells, the temperature drop across the panel is held to a minimum, and the shaded side is made as efficient a radiator as possible.

The Earth-sensor assembly uses an internal heater while it is inoperative for the short period before Earth acquisition to maintain a constant value of internal power. During the major portion of the mission, the sensor is shielded from the Sun and its internal power is sufficient to maintain an acceptable temperature.

The surfaces of all interconnecting cabling and structure have both a low solar absorptance and low thermal

emittance, thus permitting an averaging of the temperature by conduction of those parts in the sunlight with those shaded.

Thermal design. The basic features of the temperature control system are shown in Fig. 55. They are the upper and the lower thermal shields, louvers, and the various coatings and finishes.

The upper thermal shield consists of multiple layers of aluminized mylar supported on a fiberglass honeycomb panel. An aluminized teflon sheet, selected for its optical properties and its immunity to ultraviolet radiation effects, faces the upper surface of the shield. By constructing the upper shield in this way, a rigid, lightweight,

and highly effective thermal barrier results. Less than 2% of the incident solar radiation energy is transmitted to the internal portions of the basic hex.

Due to the low internal power dissipation of the spacecraft, a lower thermal shield has been implemented to minimize heat losses from the lower portions of the hex enclosure. Multiple layers of aluminized mylar are supported on a thin aluminum panel. To prevent destruction of the mylar material from overheating during the firing of the midcourse motor, an aluminum foil facing has been placed on the inboard side of the insulation material. Approximately 5 w of heat leave the spacecraft by means of the lower thermal shield.

The louver assembly on electronics Chassis IV (attitude control and CC&S) fulfills two design requirements. First, it maintains temperature-critical guidance electronics equipment within much closer limits than would otherwise be possible with the widely varying internal power dissipation occurring within this chassis. Second, the louvers provide a variable heat valve, thereby making the temperature of the basic hex less sensitive to variations in internal spacecraft power; to the uncertainties in optical properties of the radiator surface; to changes in surface properties due to cosmic-dust erosion and ultraviolet radiation; to inaccuracies associated with thermal testing of the spacecraft; and to the variation in solar intensity between Earth and Venus.

The louver assembly consists of eight movable, polished aluminum louvers, each individually actuated by a bimetal element. The louvers and actuators are mounted to the electronics chassis by means of a support frame. Should the chassis temperature rise, the bimetal elements will sense this change and rotate the louvers (open), allowing more thermal energy to be radiated to space. Below 60°F, the louvers are completely closed, resulting in a heat loss of less than 3 w. They are fully open at 90°F, permitting 38 w to be radiated. The entire louver assembly weighs less than 2 lb.

In addition to these items of hardware, the temperature control design includes the specification of surface preparation for all articles. Without describing each article in detail, four general categories are discussed which encompass articles treated similarly from a temperature control standpoint.

Items of structure and bracketry external to the basic hex, such as superstructure, intercostals, hex support legs, etc., are either gold-plated if made of magnesium, or

polished if made of aluminum. Treated in this way, these articles are poor thermal radiators, as well as poor solar absorbers, and as such are relatively thermally inert to solar radiation. That is to say, the temperature of these articles is governed primarily by the temperature of the items to which they are conductively coupled. In addition, the temperature of these articles will respond more slowly (longer time constant) to thermal perturbations which occur during Sun acquisition by the spacecraft and during the midcourse maneuver, when the Sun attitude of the spacecraft is not maintained. Cabling, external to the spacecraft, also falls into this category; however, external cables are not gold plated, but are wrapped in aluminized mylar, which makes their thermal behavior similar.

Another category consists of items entirely internal to the basic hex enclosure. The midcourse propulsion system is an example, as are the electronics subassemblies, the internal structure and bracketry, the internal surfaces of the electronics chassis, and the interconnecting cables and connectors. These items are all surfaced with paints or conversion coatings which make them good thermal radiators. Heat is exchanged from warm items to cooler ones easily, thus reducing the deviations of component temperatures from the average temperature of the hex assemblies.

The six basic hex electronics assemblies constitute the third group and are variously treated, depending primarily upon the internal power of each. Assemblies with high internal power are provided with a good radiating surface (ZW 60 white paint); low internal power assemblies are provided with polished aluminum shields to minimize heat loss.

The fourth thermal grouping of articles consists of items external to the hex, excepting structure. Science experiments, Sun sensors, attitude control nitrogen system, are examples of items in this group. Surface treatments have been applied which balance the internal power and the absorbed solar energy with the thermal radiation and conduction losses, resulting in passive temperature control of these items.

Test philosophy. The *Mariner R* design did not lend itself to an extensive analytical analysis. The difficulties in generating a realistic mathematical model, coupled with known variations of surface properties, spacecraft geometry, and electrical power distribution, would have resulted in temperature uncertainties larger than acceptable.

To compensate for this lack of analytical confidence, a number of thermal tests were conducted. To avoid an equivalent uncertainty in the test results, a full-size spacecraft was tested in the most realistic simulation of the space environment available. The spacecraft, referred to as a temperature control model, was structurally identical to the flight model; however, resistors were substituted for the flight-type electronic components. The thermal capacitance of the TCM was reduced, but a number of advantages resulted from this substitution. The principal advantage realized was the flexibility to vary the power dissipated in the various assemblies. This made it convenient to investigate the effect of variations in the power profiles on the assembly temperatures. The use of resistor elements also permitted thermal testing of the TCM very early in the development program, permitting time to correct those portions of the design which were marginal from a thermal standpoint.

Resistance heaters were also used to simulate the energy absorbed from the Sun. It was originally planned to use a radiant solar simulation produced by mercury-zenon compact arc lamps, but this facility was not completed in time for the *Mariner R* development program. While the actual performance of the temperature control system will not be known until flight data is analyzed, it appears that testing errors using electrical heaters are comparable to and possibly less than those introduced by the radiant simulation. All of the tests on the TCM were conducted in a vacuum of at least 10^{-6} mm of Hg, with radiant heat sinks at liquid-nitrogen temperatures.

The test data were interpreted, realizing that the solar simulation did not account for reflected energy. Also, the calculations required to design the heaters simulating the absorbed solar energy required a knowledge of the solar absorptance of the sunlit surfaces. These absorptances were obtained using standard reflectance techniques. Even considering these limitations, the testing was considered more valid than the analysis, and the final design was specified on the basis of these tests. Of particular significance to the validity of this testing philosophy was the design approach selected, which made the temperature of the majority of the spacecraft assemblies independent from solar radiation.

Thermal testing. During the period November 1961 to June 1962, four thermal tests were conducted on the *Mariner R* temperature control model (full scale). Objectives of this test program were: (1) to verify the temperature control design philosophy which had been adopted; (2) to provide information for detail tempera-

ture control design; and (3) to verify the final detail temperature control design.

The configuration of the temperature control model employed in a particular test was dictated by (1) size limitations imposed by the space simulators, and (2) the availability of components. The testing procedure consisted, in general, of subjecting the TCM to a vacuum and "cold-wall" environment; then electrically applying heat to both mocked-up electronic components and to the solar simulation heaters. Thermocouple instrumentation provided the desired information on temperatures and temperature distribution. Deviations from design conditions were corrected by changing the surface optical properties.

Temperature control test I used the basic hex portion of the temperature control model, including the upper and lower shields and the louver assembly. No solar simulation was provided for this test except on the upper thermal shield. This test was conducted in November 1961 in the JPL 6- \times 7-ft space simulator and served to verify the adopted temperature control philosophy and to define acceptable testing techniques.

A more complete TCM was used for test II. Solar simulation heater pads were provided in critical sunlit areas; the long-range Earth sensor was installed; the solar panels were simulated; and instrumentation was improved and expanded. Based on these tests, changes were made in several areas, primarily by the addition of thermal radiation shields on the sides of all basic hex electronics cases to reduce the total heat losses and to raise the average temperature of the hex enclosure.

For test III, which was performed in the JPL 25-ft-diam. space simulator, many components hitherto unavailable were added to the TCM. The TCM included a complete superstructure, improved solar panel simulation, a high-gain antenna, and all of the science experiments. Heater-pad solar simulation was added to essentially all sunlit areas on the spacecraft. Updated values for the internal power dissipation were used. As in the previous two tests, changes were made to the paint patterns and surface treatments, based on temperature information gathered.

Although no additional TCM testing was planned at the conclusion of the third test, it became necessary to conduct an additional test to verify temperature predictions based on unexpected changes in the internal power profiles. It was necessary to remove some portions of

the superstructure, the solar panels, and the high-gain antenna to permit the test to be performed in the 6- × 7-ft space simulator. As a result, only minor changes were made to effect a vernier adjustment in operating temperatures.

8. Materials

a. Introduction. Since the *Mariner R* is largely a modification of the *Ranger* spacecraft, many of the structural materials used on *Ranger* were adapted to *Mariner* with little change. Because of the longer mission time of *Mariner*, there were a number of materials problems that were unique to this spacecraft. Fortunately, much of the work needed to resolve these problems was initiated earlier in connection with the *Mariner A* program.

The materials work applicable to *Mariner R* is presented in the following areas: (1) hardware design and fabrication; (2) friction and lubrication; (3) temperature control materials (including measurement of optical properties); (4) organic polymers; and (5) metals.

b. Hardware design and fabrication. In addition to the routine inputs to design at the check-print stage, the Materials and Methods Group also attempted to influence certain critical designs in as early a stage as possible. Where indicated, some of these items were also fabricated under the direct supervision of the group engineers.

(1) *Propulsion system.* Design and fabrication of the spacecraft propulsion system were supported to ensure that optimum materials and fabrication procedures were used. Because the system is of modular design requiring prepressurization and fueling prior to installation in the spacecraft, some unusual materials problems developed.

Pressure vessels. Highly reliable tankage which can be pressurized in the vicinity of personnel was required. In order to keep weight to a practical minimum, the titanium alloy Ti-6Al-4V in the stabilized annealed condition was selected for the high-pressure nitrogen tank. A design safety factor of 2.2 times the operating pressure was used. The tank was fabricated under stringent requirements as indicated in the manufacturing specification, which was written for applications of this type.

Plumbing. The long-duration storage requirement, which dictates an almost entirely leak-free system, was met in two ways. First, plumbing was kept to a minimum by designing as simple a system as possible, hous-

ing much of the plumbing in complex manifold blocks. Where joints had to be made, welding or brazing were used where possible. Where mechanical joints were necessary, a special crush-type seal was developed. The seal incorporates a soft aluminum gasket, which is crushed between two serrated flanges. Special tests were performed on various hardnesses of 1100 aluminum to determine what heat treatment was required to produce the required soft material. Further tests were conducted to determine what load was necessary to give a suitable crush. Because of the extremely high reliability required on a unit of this type, only proven materials fabricated by conventional techniques were used.

(2) *Attitude control system.* The attitude control gas system must maintain the spacecraft in a Sun-oriented attitude throughout the life of the mission; also, the system must be pressurized during many of the testing and handling operations. As a result, two problems were presented: producing a leak-free system capable of the necessary storage life in flight, and reducing the hazardous working conditions caused by the high-pressure gas.

Pressure vessels. Safety of the high-pressure nitrogen storage vessels was ensured by the same design and manufacturing techniques used in the *Ranger* propulsion system.

Plumbing. A storable, leak-free system was provided by welding all components together into units. The advantage of this technique is that the only mechanical joints in the entire system are the two required to attach the titanium pressure vessels to the high-pressure, stainless-steel lines. These joints were made with the crushed-type seals similar to those used in the propulsion system.

In order to weld all the components together into a single unit, it was necessary to use 300 series stainless steel for both the high- and low-pressure lines. Although this material is much stronger and heavier than is necessary, it was believed that the high reliability thus achieved was worth the weight penalty.

(3) *Turnstile antenna.* A brazing, gold-plating, and soft-soldering assembly procedure was devised for the turnstile antenna located on the solar panels.

(4) *High-gain antenna feed.* The *Ranger* feed assembly and brazing tooling were changed to ensure highest reliability consistent with short fabrication schedules:

- (1) Hardware changes were made to simplify brazing by substituting an all-gold furnace-braze process for a combination gold furnace-braze and silver-induction brazing.
- (2) Pins and self-aligning joints were incorporated. Threaded attachments were eliminated to allow easier removal of brazing mandrel tooling.
- (3) Complex machined fittings were changed to a combination of simple sheet metal components and stock size materials; e.g., dipoles.
- (4) Tolerances of mating surfaces were made compatible with the gold-brazing process.

c. Friction and lubrication. The general philosophy for lubrication on the *Mariner R* spacecraft was to seal and pressurize all components which were of prime importance in achieving the spacecraft mission. In addition, these and other components are lubricated with off-the-shelf lubricants which have been tested and shown to be the most suitable in a simulated space environment.

d. Temperature control materials

(1) *Introduction.* Surfaces used for temperature control by radiant heat exchange may be classed according to their radiating or absorbing characteristics in the infrared (300°K) or solar portions of the spectrum. Following are the four principal types of surfaces:

Type	Examples	Approximate solar absorptance	Approximate emittance
Solar absorber	1 Polished aluminum	0.2	0.05
	Polished gold	0.2	0.05
Solar reflector	1 White paint	0.2	0.9
	Al-coated teflon	0.2	0.8
Flat absorber	1 Black paint	0.9	0.9
	Black anodize on Al	0.9	0.9
Flat reflector	1 Aluminum paint	0.4	0.4

When such materials are used in locations which "see" the Sun, the ratio of solar absorptance/emittance is important. However, in a complicated spacecraft, some surfaces see the Sun continuously, e.g., the heat shield and upper structure of *Mariner R*. Some surfaces, such as the electronic cover boxes on the sides of the hex

structure, see the Sun during the tumbling phase only. Once the spacecraft is Sun-oriented early in the mission, these latter surfaces are in the shade. During the greater portion of the mission, then, only the emittance of such surfaces is important.

By judicious use of the four classes of surfaces, it is possible to achieve temperature control of a spacecraft. Effective values differing from those shown can be achieved by applying patterns of different surfaces. Because it is impossible to predict with certainty at the design stage the exact pattern to be used, it is mandatory that as many of the surfaces as possible be easily applied or removed after partial or complete assembly of the spacecraft. For this reason, the paints are potentially very practical surfaces. Although many commercial paints are not suitable for use on spacecraft, commercial paints have been used whenever possible.

(2) *Aluminum and black paints.* It was found that satisfactory commercial black and aluminum paints are available. Considerable testing under vacuum and/or vacuum-ultraviolet conditions was performed in order to select suitable products. The following types were found to be satisfactory:

Type	Pigment	Vehicle
Aluminum paint	Aluminum flake	Silicone
Black paint	a. Carbon black plus flatteners	Epoxy
	b. Carbon black plus flatteners	Polyurethane
	c. Carbon black plus flatteners	Modified alkyl

(3) *Stable white surfaces.* The *Mariner R* design philosophy and mission posed a serious problem for one class of temperature control materials. The Sun shields for the hex structure and many of the scientific experiments require a white surface; i.e., a surface whose ratio of solar absorptance to infrared emittance is significantly less than unity. Such a surface will run cool in the Sun. The long solar exposure requirement of the *Mariner* mission, approximately 3 mo in an orbit that leads to doubling of the solar constant, is beyond the stability capabilities of the white paints presently being used for *Ranger*. All of the white paints that had been tested prior to the present program "yellow" seriously on exposure to short-wavelength ultraviolet radiation in the 2000 to 4000 Å range. Typical white paints will show solar absorptance increases of 60 to 100% upon exposure

to simulated solar radiation in the 2000 to 4000 Å wavelength region for a period equivalent to 3 mo at the Earth's orbit.

Unfortunately, the yellowing phenomenon is not confined to organic paints. Many inorganic materials are known to yellow under the influence of short-wave length electromagnetic radiation. One of the most widely used white pigments, rutile (TiO_2), is notorious for its instability. This is believed to be caused by phase changes related to the nonstoichiometric composition of commercial rutile pigments.

In an attempt to develop a stable white for the *Mariner R* spacecraft, JPL instituted a program that involved (1) the development of ultraviolet plus vacuum test equipment; (2) the preparation of special specimens of white surfaces to be screened in the test equipment; and (3) investigation into methods of applying a suitable surface.

The test equipment was designed and constructed by Hughes Aircraft Company in Culver City, California, under the sponsorship of JPL.

The test apparatus was so constructed that six test specimens, each 2 in.², can be arranged in individual quartz tubes around a central irradiating source. Anywhere from 10 solar intensities to a single solar intensity may be obtained by manipulating the distance from source to specimen. By placing each specimen in a separate quartz container, any specimen may be removed without disturbing the remaining specimens. Such an arrangement should also prevent interchange of material from one specimen to another.

The intensity of the source is monitored by periodically irradiating a pyrheliometer and converting the reading into equivalence of the original lamp intensity. The readings were then converted into magnitudes of solar intensity and, on this basis, were used to verify the validity of accelerated testing.

Most materials, including several commercial white paints, anodized ultrahigh purity aluminum, high-purity alumina tile, and porcelain enamels on aluminum or iron yellowed severely after 200 hr of equivalent Earth-orbit ultraviolet exposure. Two materials showed superior resistance to yellowing and were tested to equivalent mission time and intensity. Such extended testing confirmed their suitability for use on the *Mariner R* spacecraft. The

materials were: (1) aluminized FEP teflon film; and (2) a zinc sulfide pigmented silicone paint.

The yellowing rate of these two materials was sufficiently low to permit effective use on the *Mariner R*. The aluminized teflon is used with the teflon side facing the Sun as the outer layer of the heat shield. Its principal function is to prevent the aluminized mylar insulation from overheating. The paint is used on several hard surfaces that are exposed to the Sun continuously.

(4) *Polished metal surfaces.* Clean metallic surfaces fall into the solar absorber class because of their extremely low emittance in the infrared region. This characteristic also renders them desirable for use in locations that do not see the Sun, to keep radiation losses low where required.

All aluminum surfaces that require solar-absorbing properties, or low emittance if in the shade, are buffed to a mirror finish. Such a finish provides consistent optical properties and is relatively easy to clean if accidentally soiled.

All polishing is done by buffing with conventional polishing lathes, using sewed or hard flannel buffs. A red-rouge and a chrome green grease are mainly used as polishing compounds. Almost all polishing is done by a single source trained in the special mission requirements. A JPL inspector monitors all operations.

Successful polishing results from a combination of skill and wise selection of buff wheels and polishing speeds. Light passes are employed to prevent heating the components. Special buffs are used to minimize pulling holes or rounding off critical dimensions. Material removal seldom exceeds 0.001 in. per surface and, if the surface is supplied in the 60-rms surface finish range, even less material is removed.

The polisher works against a set of standard samples, which also serve as inspection-acceptance standards. All parts are source-inspected at the polisher, and then packaged for delivery to JPL.

All magnesium surfaces that require solar-absorbing characteristics, or a low emittance if in the shade, are gold-plated. Buffing of magnesium is not satisfactory because of the instability of this reactive metal in the Earth's atmosphere before launch. Electroplating of magnesium is by no means simple or foolproof. Because of

intrinsic difficulties, the plating process is rigidly controlled by a JPL process specification.

The specification stipulates plating of both compositions and coating thicknesses. A typical gold-plated part will consist of a thin zinc coating followed by copper, silver, and gold. The need to call out the plating process in detail arises from the requirement to reasonably control the solar absorptance and emittance on a statistical basis. Periodically, test samples are prepared for measurement of the radiation characteristics. Both the solar absorptance and emittance are measured and compared against previous determinations. Over a period of time, with all surface finishes and processing constant, sufficient data are collected to provide statistic values for design purposes.

Close control over the plating vendor is also needed to consistently produce porosity-free, adherent-plated surfaces. For magnesium, this is an acute problem and is perhaps more difficult to control than the radiation characteristics. Castings have been virtually eliminated because of the impossibility of producing tight-plated coatings. Whenever possible, parts fabricated from magnesium are made from wrought stock. Critical surfaces are also mirror-finished, primarily to seal off any micro-porosity existing in the subcoatings.

The plating vendor is furnished with consulting services on acceptable methods of processing gold-plated parts. A JPL inspector is stationed at the plater's plant to source-inspect all components. Parts are dimensionally inspected, total coating weights are determined, and the gold plate is tested for adherence.

(5) *Miscellaneous surfaces.* Paints and polished surfaces compose the majority of external temperature control surfaces. There are, however, special circumstances in which conversion coatings are used to furnish a solar-absorbing or infrared-emitting surface. The conversion coatings used are usually oxides or chromates. The coatings are formed by immersing the part in a suitable chemical bath, which oxidizes the surface. Frequently, the process involves electrolytic conversion as in anodizing of aluminum.

Absorption of many conversion coatings is not flat across the spectrum of interest (0.3 to approximately 25μ). For this reason, all of the so-called blacks have to be measured to determine if reflection occurs either in the visible or infrared ranges. Many of the visibly black surfaces have been noted to become fairly good reflectors

in the infrared. Thus, high-visible absorptance does not ensure effective infrared emittance. This is true for blackened nickel, copper, and stainless steels. On the other hand, some treatments yield an acceptably high absorptance (or emittance) at all wavelengths; as, for example, Dow 9 on magnesium or a hard-anodize on aluminum.

It has been reported that some of the conversion coatings were subject to bleaching under ultraviolet. Tests at the Hughes facility failed to reveal such an effect under vacuum-ultraviolet conditions for the following surfaces: (1) black copper oxide; (2) black nickel; (3) hard-anodized aluminum; and (4) dyed black anodized aluminum.

In addition, the Dow 7 treatment was used on many of the internal magnesium chassis to improve radiation heat exchange. Such a treatment, if properly applied, is stable under the vacuum-temperature conditions encountered. There is some question regarding the vacuum-ultraviolet stability of Dow 7 surfaces. For this reason, such a treatment was used only as a substrate for painting on surfaces that see the Sun.

(6) *Measurement of optical properties.* Solar absorptances were calculated from reflectances measured on a Perkin-Elmer Model 4000 spectrophotometer. During the year, this unit was fitted with lead sulfide detection cells so that measurements could be made in the ultraviolet, visible, and near-infrared regions. Considerable attention was paid to development of "making" techniques to ensure an adequately thick Mg-O layer on the inside of the integrating spheres. The modifications introduced during the year up-graded the unit to the extent that rapid, accurate measurements could be made.

Emittances were calculated from reflectance data obtained with a Perkin-Elmer Model 13 infrared spectrophotometer. Improvements are being made in the design of the Hohlraum cavity to reduce temperature gradients.

e. Organic Polymers. The effect of the space environment on crystalline materials can be estimated using the Langmuir equation. However, noncrystalline materials are difficult to handle analytically. To gain an insight into the behavior of polymeric materials in the space environment, an interim experimental program was initiated.

Table 4 lists the materials that were selected for testing. Most of these materials are presently being used on

Table 4. Polymer degradation program materials

Material	Description
Eccocoat C-6	Epoxy coating material
Epon VI + curing agents A and DTA	Epoxy adhesive
Eccobond 55 + curing agents 9 and 11	Epoxy adhesive
Eccobond 45LV + curing agent 15	Epoxy adhesive (semi-flexible)
Dow Corning A-4000	Silicone adhesive
EC-826	Nitrile rubber adhesive
Stabond C-111	Neoprene rubber adhesive
Stycast 2850 GT + curing agents 9 and 11	Epoxy potting compound
Stycast 1090 + curing agents 9 and 11	Epoxy potting compound (low density)
Epon 828 + curing agents Z and DTA	Epoxy potting compound (unmod. resins)
PR-905	Epoxy-polysulfide potting comp.
Eccofoam FP + curing agent 12-2	Polyurethane (2 lb/ft)
PR-1527	Polyurethane potting compound
EC-1641 B	Polyurethane potting compound
Teflon (TFE)	
Polyethylene	
Polymethyl methacrylate	
Nylon-101	
Nylatron-GS	MoS-filled nylon
Fiberglass-reinforced epoxy	
Fiberglass-reinforced phenolic	
Cotton-reinforced phenolic	

Mariner R spacecraft. The testing program was divided into three phases:

Phase	Test Condition	Objectives
I	75°F, 10 ⁻⁶ mm Hg 1, 4, and 7 days	Weight change and visual observations
II	150°F, 10 ⁻⁶ mm Hg 1, 4, and 7 days	Weight change and visual observations
III	300°F, 10 ⁻⁶ mm Hg 1, 4, and 7 days	Weight change and visual observations

Phases I, II, and III have been completed. A more extensive polymer degradation program, including radiation effects, physical and mechanical property changes, and analysis of the degradation products, has been initiated at the Stanford Research Institute. The results, thus far, have been encouraging. Within the limitations of the tests performed to date, the following general conclusions can be drawn:

- (1) The polymeric materials specified for the *Ranger* and *Mariner R* spacecraft will perform satisfactorily in the space environment.
- (2) In general, the relative thermal stability of polymeric materials in the Earth environment reflect their stability in the space environment.

f. Metals. There has been considerable concern about the use of magnesium in the spacecraft because of possible sublimation of this moderately high vapor-pressure material. The Langmuir equation, which is generally considered valid for predicting the sublimation of pure metals, indicates that there should be no great concern for the structural characteristics, as it predicts a loss of about 0.0001 in. in about 9 yr at 135°C (the maximum temperature expected to be reached by any portion of the spacecraft). However, there has been genuine concern regarding the possibility of sublimation from magnesium electronics chassis and subchassis, along with possible deposition as conducting films on cooler parts of the circuitry. In this case, the rates predicted by the Langmuir equation might be significant for long-lived spacecraft such as *Mariner*.

Original plans called for application of low vapor-pressure material electroplated, such as nickel, to all *Mariner* subchassis to inhibit sublimation. Recently, new temperature control analyses indicated the desirability of having a reasonably high-emittance (0.7 or greater) surface on the chassis. The simplicity of applying a chromate conversion coating, such as Dow 7, to the magnesium made this approach appear attractive, if adequate inhibition of evaporation of the magnesium would be provided. There was also the possibility that the coating itself might decompose, causing difficulty.

Accordingly, the Material and Process Department of the Hughes Aircraft Company was asked to run tests of both bare and Dow 7-coated Mg-3 Al-1 Z (AZ31) under the sponsorship of JPL.

The coated magnesium alloy was exposed to an indicated vacuum lower than 10⁻⁷ mm Hg for 130 hr at an indicated temperature of 400°F. The coating darkened considerably during heating, but there was no other apparent change in characteristics. Weight loss of the specimen was less than 0.0001 g.

Somewhat surprising results were obtained on the bare specimen. It was exposed to a vacuum of 10⁻⁶ to 10⁻⁷ mm Hg for about 90 hr at 450°F. There were no weight

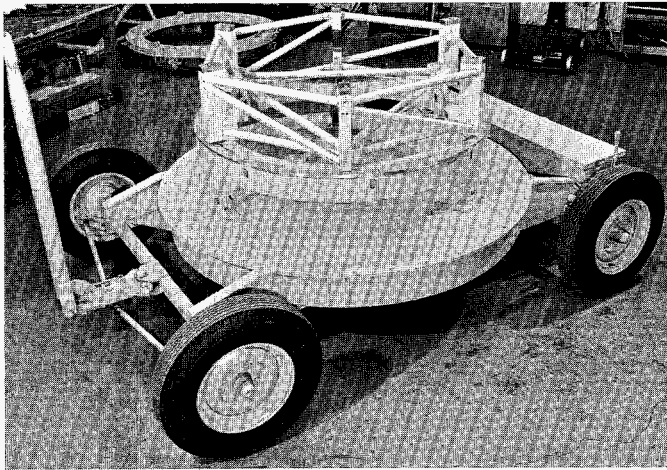


Fig. 56. Adapter and ring support on transport dolly

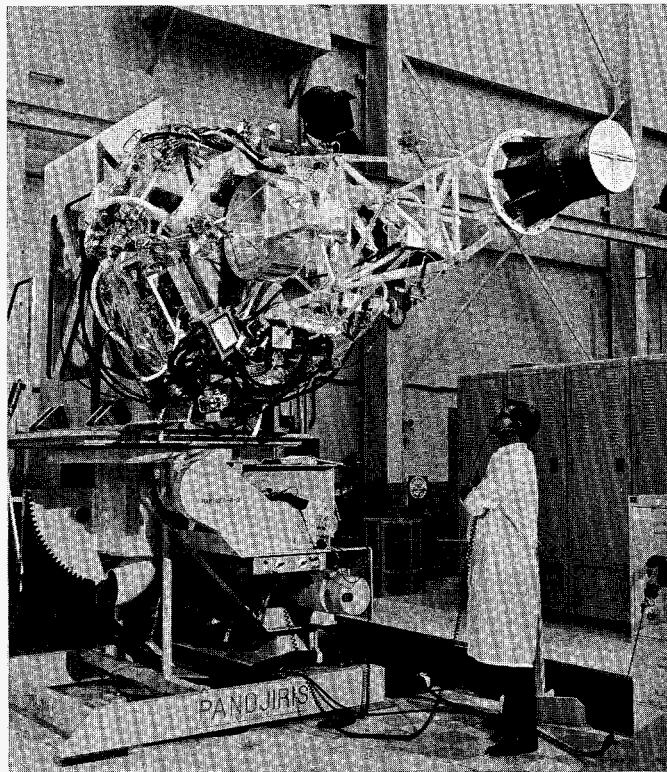


Fig. 57. System test stand with MR-2 mounted

changes to an accuracy of ± 0.0001 g and no sign of metallic deposit anywhere in the all-glass system. The Langmuir equation predicts a loss of about 0.1 g for these conditions for pure magnesium. The experiment was repeated with a metallographically polished specimen. No change in surface was noted, or any detectable weight change. This finding would tend to rule out the possibility that an oxide film was inhibiting evaporation

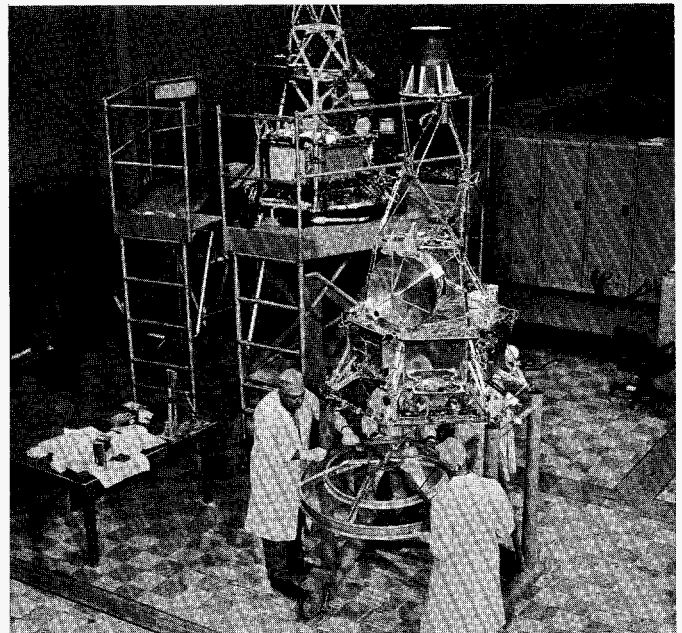


Fig. 58. Spacecraft on motor loading stand

or that the small chamber was bouncing the atoms back to the surface.

At this time, there appears to be no satisfactory explanation for this large deviation from Langmuir behavior. On the basis of this preliminary work, it was decided to use Dow 7-treated AZ31 magnesium alloy subchassis for *Mariner R*. Further work will be done at Hughes in an attempt to explore this subject more fully.

9. Ground Handling Equipment

In general, the ground handling equipment for the *Mariner R* spacecraft is similar to *Ranger* and *Mariner A* equipment.

a. Hoisting gear. The hoisting assembly consists of an upper sling, spreader frame, lower sling, and lifting bars. This equipment is the same as that used for the *Mariner A* spacecraft. All lifting of the spacecraft by overhead cranes is performed with this equipment.

b. Support and JPL adapter. These two assemblies are used with either the shop dolly or the transport trailer for assembly and local transport of the spacecraft (Fig. 56). The upper portion of this assembly also serves to position the high-gain antenna dish for installation and alignment. The lower part provides a mount for the *Agenda* adapter. The height of the two-part assembly is

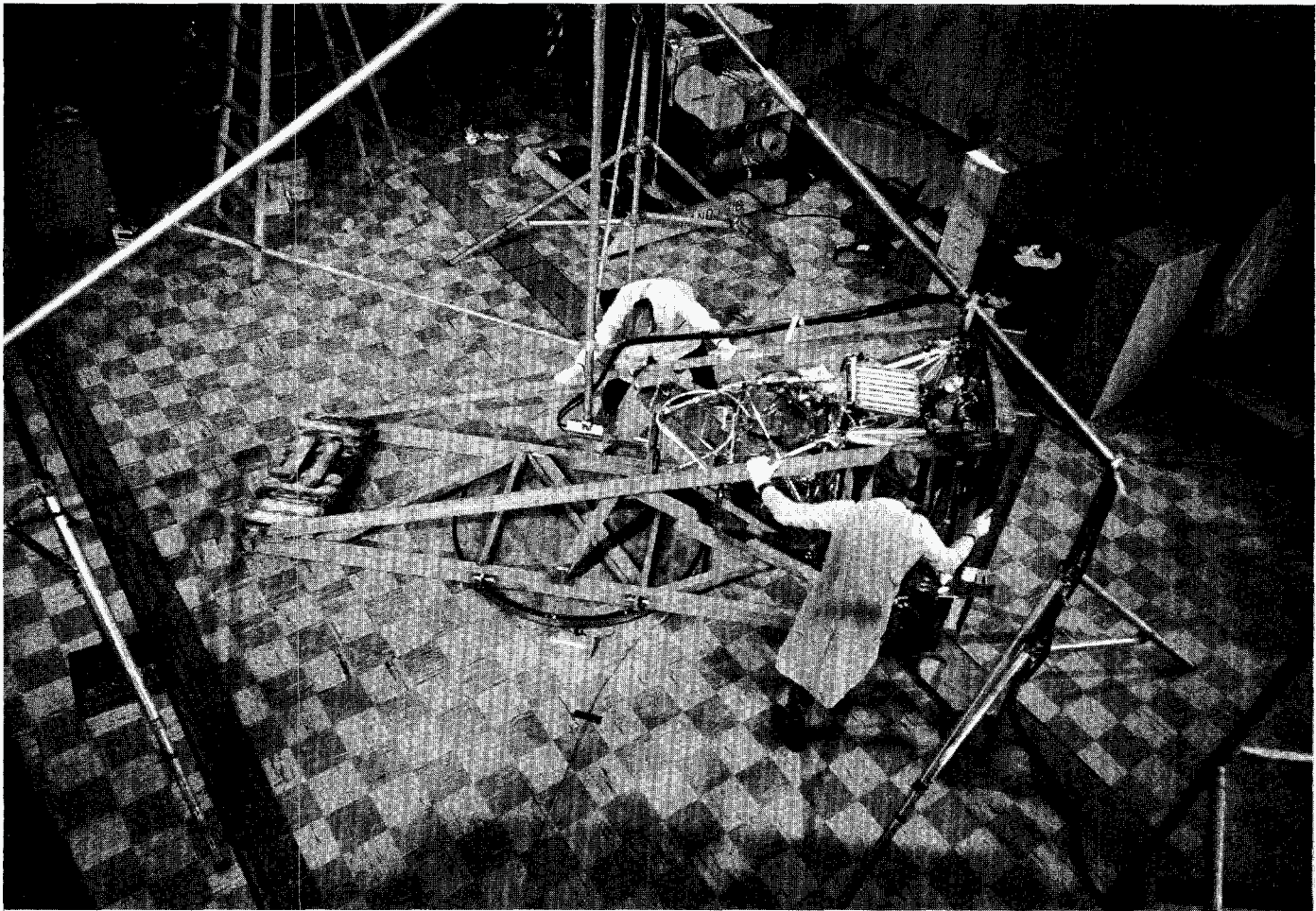


Fig. 59. Magnetometer-mapping stand

designed to protect the antenna feed from damage. Thus, the JPL adapter and support are never separated during normal use.

c. Dolly. This equipment is used with the support and adapter for convenience during assembly of the spacecraft and operations within the shop.

d. System test stand. This assembly is the same as that designed for *Mariner A*. The test stand is capable of holding the spacecraft in an upright position, then swinging it 90 deg to a horizontal position so that the hinge axis of the high-gain antenna is vertical for operation of the antenna through its entire range of travel (Fig. 57). The stand can then rotate the spacecraft to place the hinge axis of the solar panels in a vertical position for the operation of their actuation system. The stand consists of two principal assemblies: (1) a commercial welding positioner, and (2) a fixture to adapt the spacecraft to the welding positioner.

e. Support for motor loading. A stand is required to hold the spacecraft in the vertical position approximately 5 ft from the floor to allow the high-gain antenna to swing down for installation of the midcourse motor. The stand can also be used for general assembly work when it is necessary to have access beneath the spacecraft. Figure 58 shows the motor loading stand, with the system test stand in the background.

f. Magnetometer-mapping stand. Two aluminum magnetometer-mapping fixtures are used to rotate the spacecraft about the magnetometer's *X* and *Z* axis. For 360-deg mapping about the magnetometer *Z* axis, the spacecraft is attached to the vertical support fixture and mounted on an oil table. Using the system test stand, the spacecraft is then mounted on the *X* axis mapping fixture and magnetometer calibrations are performed by rotating the spacecraft 360 deg about the magnetometer's *X* axis (Fig. 59).



Fig. 60. *Mariner R* spacecraft being transported at AMR

g. Packaging and shipping. The spacecraft was shipped by truck, both locally and to AMR. The spacecraft was complete except for the solar panels, midcourse propulsion system, top superstructure tier, and high-gain antenna. A plastic bag and light support frame were placed over the spacecraft and the bag was sealed around the base. Figure 60 shows the assembled *Mariner R* at AMR being transported from Hangar AE to the explosive safe area.

B. Power

1. General

The *Mariner R* power system is a simplified version of the system designed for *Mariner A*, which represented a departure from the concept used in the *Ranger* spacecraft. In *Ranger*, the d-c voltage levels required by the users

were generated in a central power supply and distributed to the various spacecraft subsystems. The *Mariner R* system provides the following voltages: 28-v d-c, 50-v rms, 2400-cps square-wave; and 26-v, 400-cps, sine-wave, three-phase power. Users either accepted these voltages or provided transformer-rectifier circuits operating off the 2400-cps supply to produce the d-c voltages desired.

Experience accumulated during the design of the *Ranger* spacecraft led to the belief that a cleaner interface between user and power source could be made if the power was distributed at a fixed a-c voltage. Many different considerations contributed to this conclusion.

In the usual spacecraft program, users of power begin the development of their equipment at the same time the power subsystem is developed. Thus, it is apparent that the power system cannot be developed properly until the load profile and voltage requirements are firmly known. This is true if the power source produces the variety of voltages required by the user. By supplying a fixed a-c voltage to the user, the principal variable in power supply design is load uncertainty, and the voltage problem is transferred across the interface to the user, who must develop his own transformer-rectifier system. This, then, permits power supply development to proceed on a more realistic schedule, and requires much less communication and iteration.

In addition to this contribution to expediency, it has been indicated that, although less efficient, the weight per watt of useful power is lower for *Mariner* than for the *Ranger* system. On the other hand, it may be argued that the care in cabling required because of the existence of a 2.4-kc square-wave bus exceeds that required in distributing numerous d-c voltages about the spacecraft.

2. Subsystem Configuration

The configuration for the *Mariner R* power subsystem took the form shown in Fig. 61. The system has two main outputs, as shown: (1) a 2400-cps square-wave output supplies power to all T-R units; (2) a 400-cps, 3-phase, sine-wave output supplies power to the attitude control gyros, and single-phase power for antenna servos and scientific equipment motors. The battery furnishes power directly to the various short-term or high-power loads, such as valves, relays, stepping motors, and squibs.

The input power during cruise mode is obtained from two solar panels, with a minimum raw-power capability of approximately 200 w at the Earth, and approximately

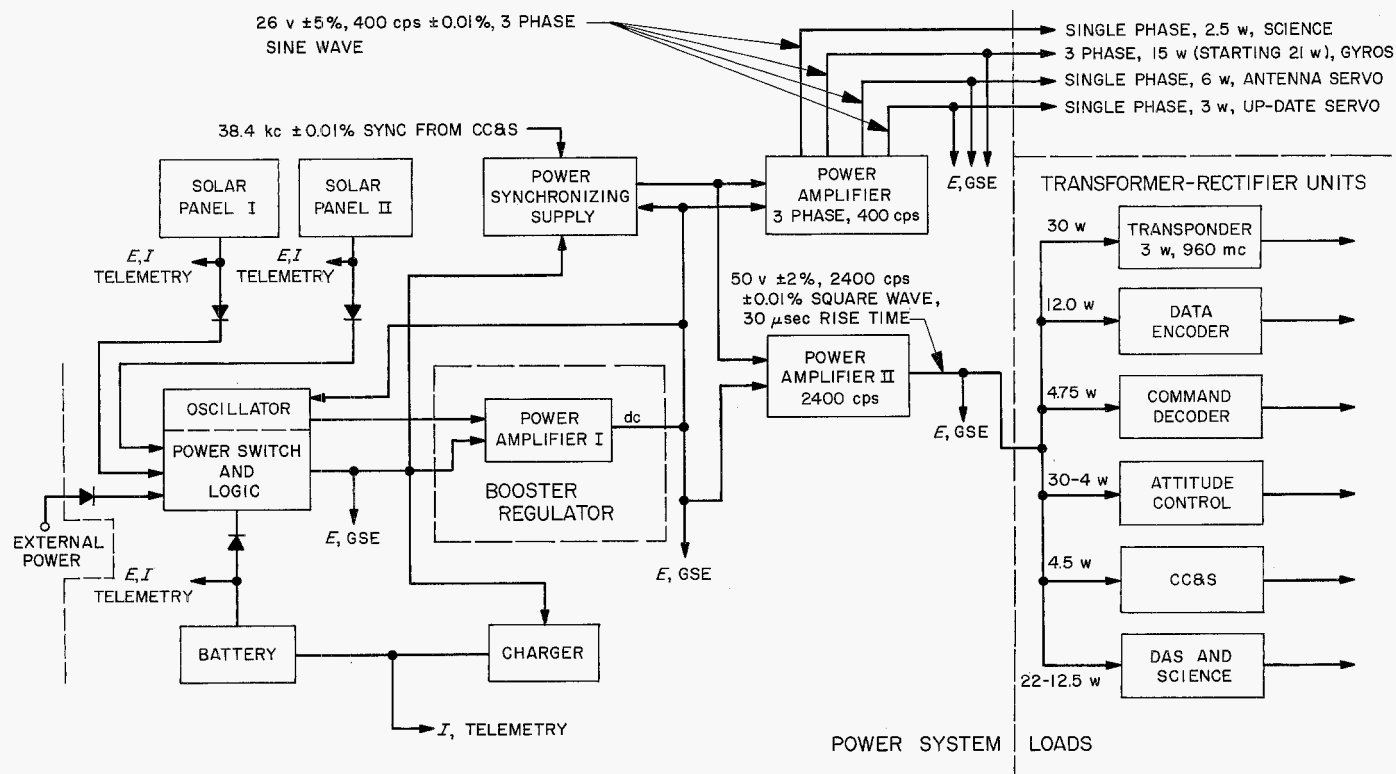


Fig. 61. Power subsystem, functional block diagram

175 w at Venus. A rechargeable battery provides power for the initial acquisition and for the periods of zero solar power, as shown in Fig. 62. A charger is provided to recharge the battery whenever solar power is available.

The power profile (Fig. 62) shows the raw power required by the 2400- and 400-cps systems, and the battery load requirements. Figure 62 also shows raw power available from the solar panels between Earth and Venus. From minimum solar power characteristics, it appears that the battery will be sharing the load with the solar panels during Periods 5, 7, and 12. The battery is expected to be completely charged during Period 4, and to have sufficient capacity to handle the periods of load sharing.

One of the problem areas noted in the *Mariner A* design was an incompatibility between the peak power capability of the 2.4-kc amplifiers and the high instantaneous-current demand of the capacitor input filters in several of the user T-R units. This problem was solved in the *Mariner R* design by the incorporation of choke-input filters in those T-R units which are the major users of power. Most of the smaller T-R units, particularly those involved with high-voltage, low-current outputs, do not require the use of a choke-input filter.

A second *Mariner A* problem was the lower-than-expected efficiencies exhibited by the user T-R units and regulators. In establishing the design criteria for *Mariner R*, a somewhat different and more logical approach was used for allocating the power output to the users. The input power to the T-R units, rather than the output power, was used as the controlled quantity, which resulted in more careful evaluation of the T-R unit characteristics (particularly efficiency) by the users. As a result, some of the regulators were eliminated in order to increase efficiency.

3. Electrical Inverter

The design and development of the electrical inverters and associated subassemblies were performed at JPL. The *Mariner R* design was originated from *Mariner A*, modified and reduced to accommodate the applicable power requirement. A brief description of each subassembly, including the circuit design concept, follows:

a. Inverter. The electrical inverter power system requirements were to provide 50 v $\pm 2\%$ rms, 2400 cps $\pm 1\%$ to transformer-rectifier units, and 26 v $\pm 5\%$, 3-phase, 400-cps, $\pm 0.01\%$, sine-wave to motor and gyro

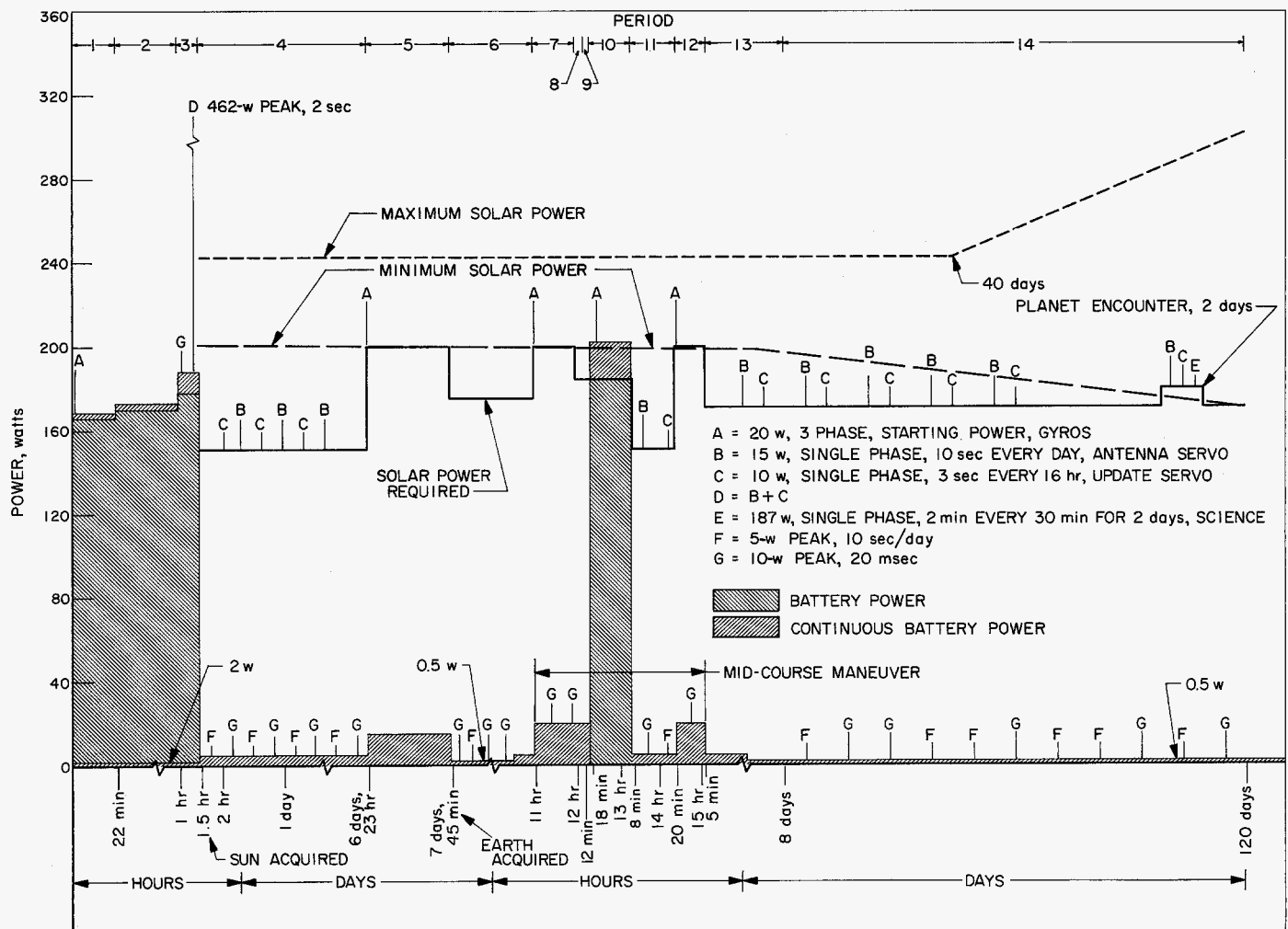


Fig. 62. Mariner R load profile

loads. To accomplish these requirements, the power system employs a booster regulator module which maintains constant power voltage, and a synchronizer module which provides controlled frequency to the 2400-cps power amplifier and to the 400-cps power amplifier.

b. Booster regulator. The booster regulator accomplishes the power voltage regulation over the expected input voltage variation from the solar power source and battery power. The pulse-width modulation technique is utilized, which boosts the available voltage from either power source to the required regulated power voltage. A block diagram of the booster regulator is shown in Fig. 63.

c. Pulse-width modulator. A 3-kc square-wave signal, frequency-controlled to $\pm 1\%$, is fed to the pulse-width modulator. The modulator, a magnetic amplifier, con-

trols the width of the square wave, which is the base drive to the power amplifier. Depending on the signal received from the regulator, the square-wave drive can vary from 160 deg to 0 deg width. The pulsed square-waveform amplified and rectified is added to the d-c input voltage and then filtered. The regulator compares the output of the booster to a reference and provides the error signal to the pulse-width modulator to close the loop for power voltage regulation.

d. Synchronizer. The synchronizer consists of count-down circuits which provide frequency-controlled drive to the 2400-cps and 400-cps 3-phase power amplifiers. The frequency of the drive is controlled to $\pm 0.01\%$ by a signal generated in the central control computer system.

e. Power amplifiers. The 2400-cps power amplifier is a simple Class B power amplifier which provides the 50 v

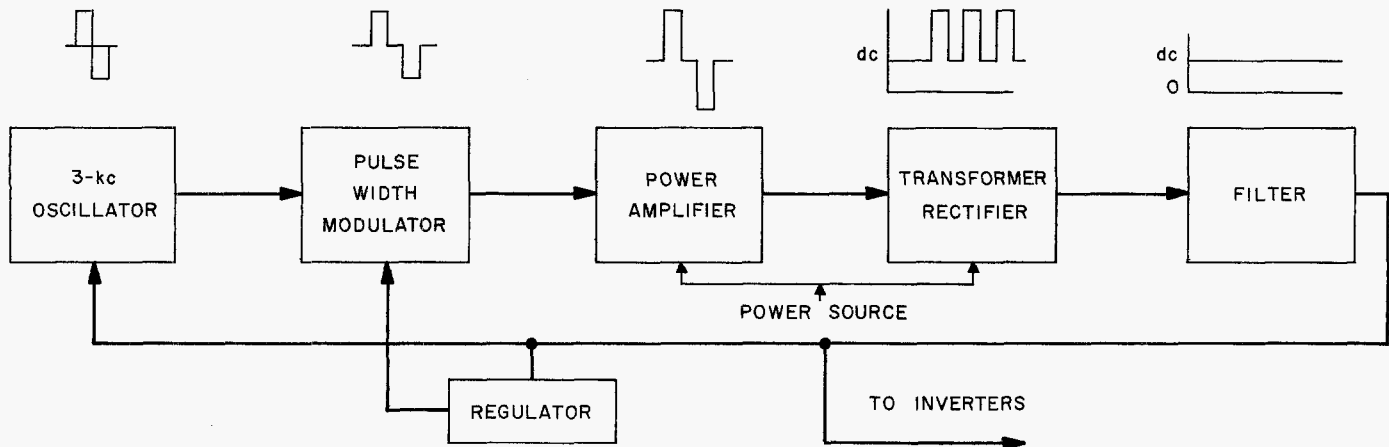


Fig. 63. Booster regulator block diagram

rms to the transformer-rectifiers. The 400-cps power amplifier utilizes three power-amplifier stages, from which outputs (filtered with series and shunt filters) are connected to Y-connected transformers. The shunt filters are connected in delta configuration to provide 26 v rms to the gyro loads, and to single-phase servo loads. The power amplifier switches to single-phase configuration by disconnecting the other two phases when a command is received from the switching amplifier of the attitude control system.

f. Power switch and logic module. The central subassembly of the power subsystem is the power switch and logic module. The function of this module is to receive power from either the two solar panels, the battery, or ground supply and distribute it to the booster regulator, synchronizer, battery charger, and intermittent loads. The power switch and logic module also houses the telemetry measurement circuits for current and voltage of the solar panels, battery, and battery charger.

g. Battery charger. The battery charger subassembly provides charge to the battery, within the capability of the solar power source, and cuts off the charge when the battery reaches full capacity, within $\pm 0.1\%$ of the battery voltage.

4. Solar Panels

The *Mariner R* solar panels were designed with the benefit of only a small amount of experience with the *Ranger* panels, plus additional laboratory experimentation, which resulted in the selection of the filter cement, the cell adhesive, the insulation material, and the method of cell mounting.

The panels were approximately 60 in. long by 30 in. wide. The average electrical output of each cell was to be 22.9 mv at the maximum power point under tungsten light of 100 mw/cm² at 28°C cell temperature. The panel circuit called for a total of 4896 cells with 102 in series and 48 strings in parallel. This configuration was to be capable of producing 110 w per panel in Earth space, and 85 w per panel near Venus, with a maximum power voltage ranging from 47 v at Earth to no less than 25 v at Venus. The power degradation from Earth to Venus is caused by the higher stabilized temperature, and an expected loss due to high-energy radiation.

5. Battery

The *Mariner R* battery design was also an outgrowth of the *Mariner A* prototype. Revisions in the load profile caused changes in capacity only. Temperature and voltage requirements remained the same. The battery used sealed silver-zinc cells and is rechargeable in flight. The 18-cell unit weighs 33 lb and has a capacity of 1100 w-hr. The energy-to-weight ratio is approximately 35 w-hr/lb.

6. System Description

As shown in the functional block diagram (Fig. 61), power is derived from two solar panels and a rechargeable battery. These sources feed a power switching and logic circuit, which in turn drives a booster regulator. The booster provides the power to operate the 2.4-kc and 400-cps power amplifiers, which are driven by the power synchronizer. The power switching and logic unit also feeds a battery charger, thus providing the means for recharging the battery during periods of adequate solar

power. Power to operate pyrotechnic devices, and other 28-v d-c loads is supplied directly from the battery.

The operation of the power subsystem is sensitive to the orientation of the spacecraft and to the electrical loads. During the launch phase, the battery must supply the power, since the spacecraft solar panels are not oriented toward the Sun. When the spacecraft becomes Sun-oriented, the solar panels assume the load and recharge the battery. For the remainder of the mission, the modes of operation are obvious: when the spacecraft is Sun-oriented, the panels are the prime source of electrical energy; at other times, when the panels are not directed toward the Sun, the battery is the primary power source.

When the load exceeds the maximum power capability of the solar panels, or when the output from the solar panels is decreased because of spacecraft orientation, the solar panels and the battery share the load. In either case, sustained operation will deplete the store of energy in the battery and result eventually in spacecraft failure. It is anticipated that normally the sharing mode will be ended either by Sun reacquisition or reduction of load.

The mechanism of the sharing mode is of considerable interest. Solar panel characteristics are conveniently described in terms of power vs voltage, as shown in Fig. 64. Analysis of the power system reveals that, for stable operation, the slope of the power-voltage characteristic must be negative. Clearly, then, the region to the right of the maximum power point on the solar panel characteristic is stable, whereas the region to the left is unstable. In the *Mariner R* system, operation to the left of the maximum power point of the solar panel characteristics is stabilized by setting the maximum power point above the battery voltage.

The effect of combining battery and solar panel characteristics is illustrated in Fig. 65, in which the composite

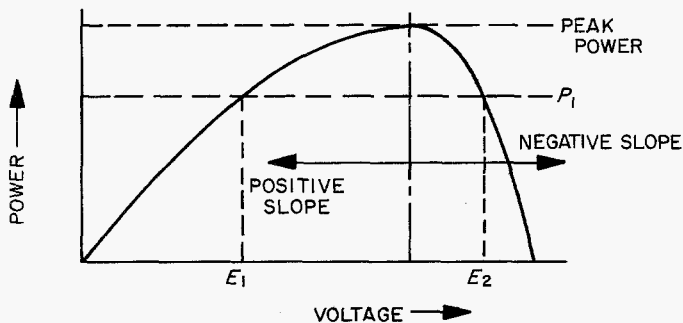


Fig. 64. Solar panel power vs voltage

power is plotted as a function of voltage. The circuit logic which results in this characteristic is shown in Fig. 66. Note that the solar panel characteristic is modified by the shunt zener diode, which reduces the voltage swing which must be handled by the booster regulator, but does not affect the stability of the system. The composite characteristic is shown as a solid line in Fig. 65 and the solar panel characteristic appears dotted. Stable regions of operation are labeled I and III. Region II is unstable. The actual shape and size of the solar panel portion of the characteristic curve is determined by the temperature of the panel, the incident solar intensity, and the degradation sustained because of radiation damage; hence, there is considerable uncertainty in the location of critical points on the curve.

For a given set of conditions (i.e., a fixed composite characteristic), it is enlightening to examine the opera-

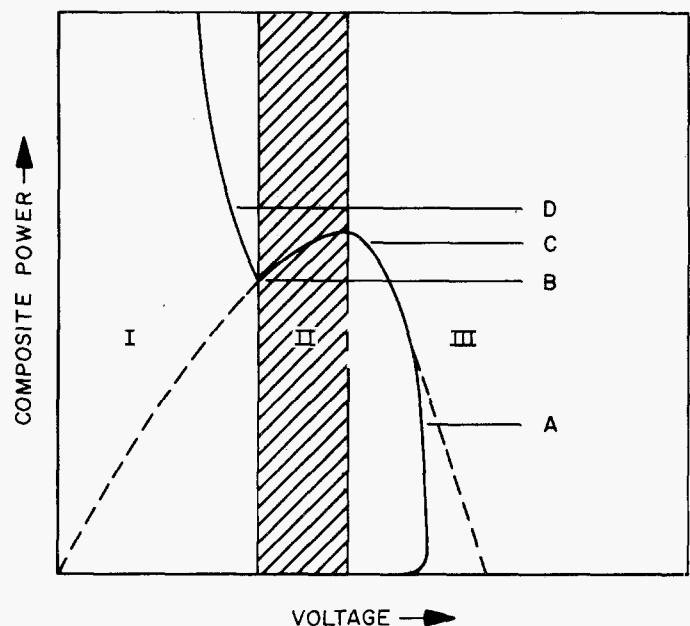


Fig. 65. Composite power vs voltage

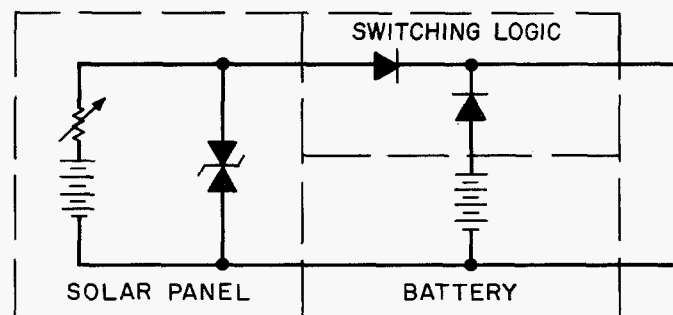


Fig. 66. Circuit logic

tion. If the power required is represented by level A in Fig. 65, the operating point is at the intersection of A and the characteristic curve and is seen to lie in a stable region (III). If the load is increased from A to C, the operating point will still remain in region III, and upon further increase in load to level D, the operating point will jump into region I. Between levels B and C, the voltage is multivalued; however, the operating point will be in stable regions only. If the load is reduced from a value such as D, the curve is followed down to point B, whence the voltage jumps, upon further reduction of load, to a stable point in region III. Note that in region I, the battery and the solar panel are sharing the load, whereas, in region III, the solar panel carries the load alone.

In the sharing condition, the input voltage to the battery charger is the battery voltage; thus, no changing can occur. Generally speaking, sharing is an undesirable condition which, if continued, will lead to depletion of the battery and failure of the power system. The only way to escape the sharing mode is to reduce the load (power demand) below point B in Fig. 65.

In *Mariner R*, the solar panel source has been designed to provide sufficient power in the battery-sharing voltage so that the system will drop out of sharing when the spacecraft load is reduced from the peak demand to cruise mode operation. In addition, a capability of switching off a load (science) is incorporated to assure the drop-out from sharing if the panel characteristics deteriorate beyond the predicted values.

7. Power System Performance

The power system was installed in the spacecraft and was subjected to system tests at the spacecraft assembly facility. System, flight-acceptance and type-approval testing presented two major problems requiring rework of flight hardware. During evaluation test of the *MR-1* spacecraft, the 400-cps, 3-phase supply appeared to develop abnormal voltages when the unit was switched from single-phase to 3-phase operation. The problem was traced to high-current arcing of approximately 20 amp through a relay contact. To correct the arcing condition, a high-power relay, which is capable of switching 10 amp per contact, was selected. Parallel contacts have been utilized, with a total capability of 20 amp. In addition, a current-limiting resistor has been introduced to limit the maximum current discharge to approximately 5 amp. All 400-cps amplifiers have been modified to incorporate the new relay.

The second problem occurred in the booster regulator of *MR-2*, when the module showed abnormal oscillations during a high-load condition and input voltage of around 35 v. The problem was traced to unmatched power switch and logic oscillator-regulator circuit and booster power amplifier. Because of packaging requirements, it was decided to separate the oscillator and the regulator circuits of the booster regulator and house them in the power switch and logic module. The units, therefore, required matching to perform properly over the range of load and voltage regulation. The problem was corrected by publishing the matched serial number of the booster regulator modules and the power switch and logic modules.

Analysis of the power system performance from launch to encounter revealed that a *potential* shortage of power was anticipated, based on a review of the *Ranger 3* flight data. *Ranger 3* solar panels operated at approximately 60°C, which was 15°C higher than expected. Consequently, the voltage, and hence the power, was approximately 8% low. This situation did not present a problem on *Ranger*, since there is adequate contingency for this magnitude of a decrease. The implication of the *Ranger* temperature data, however, when applied to the *Mariner R* solar panels, indicates that there would be a 13% power shortage.

This power deficiency was corrected by increasing the area of the solar array to permit the addition of 918 solar cells, increasing the total number of 1- × 2-cm cells from 9792 to 10,710 (approximately 9%), and thereby enlarging the solar panel capability by 15 w at the maximum power point and 12 w at the battery sharing point. The battery-sharing point power increase is of primary importance since the power system depends on the amount of solar power available at the battery voltage level to assure drop-out from the sharing mode when the peak load demand is reduced to the normal cruise mode load.

In addition, modifications in the spacecraft operation were introduced by providing a radio command capability over the cruise science electrical load, which ensures adequate margin for the power system to shift out of the sharing mode during the cruise periods.

Data of the leakage current of the solar panel cells revealed that the series-connected blocking diodes in the power switch and logic modules could be removed. The elimination of these diodes reduced the power requirement by approximately 5 w, thereby adding to the safety

margin of solar panel power operation during cruise condition.

C. Central Computer and Sequencer

1. Functions

The *Mariner R* central computer and sequencer is responsible for all spacecraft time-sequenced events (excluding the science experiment sequence). In performing these functions, the CC&S must generate spacecraft time after launch, and execute commands at predetermined times during the *Mariner R* mission.

Briefly, the CC&S performs the following functions:

- (1) Provides a 38.4-kc sync frequency used as a spacecraft time reference.
- (2) Provides commands, shortly after launch, to extend solar panels and turn on attitude control power.
- (3) Provides an Earth-acquire command 7 days after launch.
- (4) Provides decoding and duration-storage capability for the three midcourse maneuvers: roll, pitch, and velocity correction.
- (5) Provides sequenced commands to the attitude control system for spacecraft positioning, and start and stop commands to the pyrotechnics for motor burn during the midcourse maneuver.
- (6) Provides on-pad adjustment of the planetary encounter start and stop commands normally sent to the science subsystem in the vicinity of the planet.
- (7) Provides a continuous 16.7-hr periodic command to the attitude control system to up-date the reference position of the high-gain antenna during flight.

The *Mariner R* CC&S block diagram is presented in Fig. 67.

The 38.4-kc sync signal is a square wave obtained by frequency division from the central 307.2-kc oscillator in the CC&S. This oscillator is crystal-controlled with a frequency stability of $\pm 0.01\%$ over the temperature range

of 0°C to 65°C . This 38.4-kc signal is used by the power subsystem as a stable frequency sync for the spacecraft primary 2.4-kc a-c power.

Further frequency division of the crystal-oscillator-derived output yields frequencies of one pulse per sec (1 pps), one pulse per min (1 ppm), one pulse every 3.3 hr, and one pulse every 16.7 hr. The 1-pps signal is used as the time reference during countdown of the roll and pitch midcourse maneuvers. The 1-ppm signal serves as the basic count frequency for the launch events: solar panel extension at $L + 44$ min and attitude control power on at $L + 60$ min. The 1-ppm signal is also used as the basic count input to the midcourse counter during the midcourse maneuver to provide roll, pitch, and velocity correction start commands at 60, 72, and 94 min, respectively, after the start of midcourse. The 3.3-hr pulses (50) are counted to obtain the acquire-Earth command at 167 hr after launch. The 3.3-hr pulses are also used as the basic input to the pulse counter associated with the planetary encounter start and stop commands. The 16.7-hr signal is used to command the high-gain antenna position reference up-date directly.

In addition to the basic 3.3-hr input, the encounter pulse counter mentioned above can be advanced by up-date pulses from the CC&S blockhouse panel prior to launch. These up-date pulses are used to adjust the time after launch at which the encounter start command is given. With this blockhouse signal, the encounter-start command can be adjusted to occur at any 3.3-hr increment between $L + 3.3$ hr and $L + 277$ days. The encounter-stop command is actuated a fixed 66.7 hr after encounter start.

Since all commands are referenced to launch, or a short time before, the CC&S must be inhibited until the proper time is reached in the countdown. The *Mariner R* CC&S is normally inhibited before spacecraft power is turned on, and is released at $L - 3$ min. The inhibit is located at the 1-pps point in the counter chain and thus prevents all frequencies or repetition rates beyond 1 pps from functioning.

In addition to the blockhouse inhibit and up-date functions, there is also a clear command to enable the CC&S counters to be cleared to zero before the inhibit is released. The relay-hold function, which is initiated prior to spacecraft power on, commands all relays to the reset position and holds them there until it is released. This prevents any command relay from being actuated erroneously on the launch pad prior to launch. If any

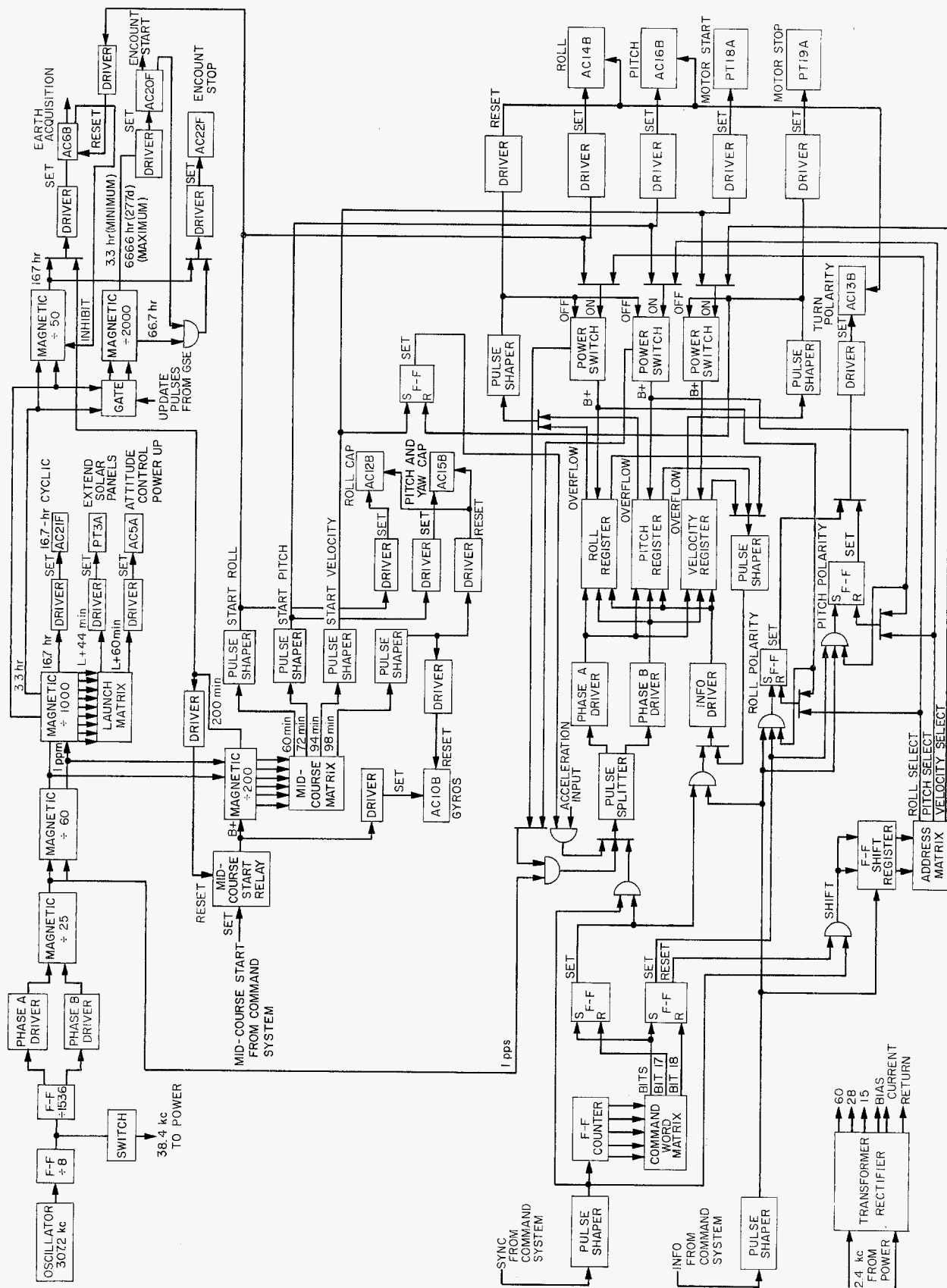


Fig. 67. Mariner R central computer and sequencer, block diagram

relay is not in the reset condition, the relay position indicator lamp will glow red.

After the inhibit is released at $L - 3$ min, the CC&S will begin counting, and after 2 min will send a "clear release" command to the blockhouse to extinguish a lamp on the panel. At the time the inhibit is released, a 2-min timer in the blockhouse panel is started and, if the clear release coincided with the 2-min timer, the *go-no-go* lamp on the panel will remain white (*go*). If the two signals do not coincide, the lamp will glow red (*no-go*). This provides a cursory check of the ability of the CC&S to count correctly.

All CC&S commands, with the exception of the 38.4-kc sync and the event blip output, are relay contact closures which either apply or remove spacecraft battery power on the signal lines from the CC&S to the other spacecraft subsystems affected. Each command relay, upon actuation, generates an event blip which is sent to the data encoder for subsequent transmission to the Earth. The 38.4-kc sync signal and the event blip output are transformer-coupled to the user.

2. Subsystems

The CC&S subsystems consist of eight $6 \times 6 \times 1$ -in. modules which weigh 12 lb and occupy approximately 330 in.³ They are located in spacecraft Case IV along with the attitude control subsystem. Figure 68 shows an assembled CC&S before encapsulation. The CC&S subsystem dissipates approximately 4.75 to 7.0 w of 2.4-kc power.

A brief description of each module follows:

a. Central clock. The central clock contains the stable, transistorized 307.2-kc crystal-controlled oscillator from which all CC&S basic frequencies or repetition rates are obtained. The 38.4-kc sync signal is an output of this module, obtained from a transistorized flip-flop, divide-by-8 frequency divider chain from the 307.2-kc oscillator. The 38.4-kc signal is further flip-flop divided to obtain a 25-cps square wave. This signal is converted from a low-level square wave to a high current level pulse train of the same frequency (repetition rate). This high-current pulse train is fed as an input to a two-core-per-bit magnetic divider chain, which has an output of 1 pps. This pulse train, although high current, has a short pulse duration (2 to 3 μ sec) and, therefore, low average power for repetition rates of 25 pps or less. The low average power

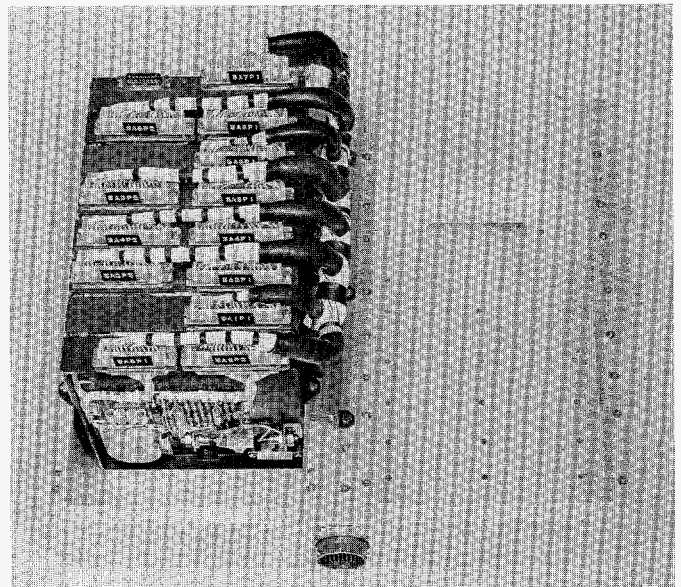


Fig. 68. Mariner R central computer and sequencer before encapsulation

magnetic-core divider principle is used to obtain all basic repetition rates from this point on in the CC&S.

b. Launch counter. The launch counter receives the 1-pps output from the central clock and converts it, through a magnetic divide-by-60, to the 1-ppm repetition rate used as a basic frequency input for the maneuver counter as well as the remainder of the launch counter. The launch counter is used to provide, from a diode matrix, any duration from 1 min to 999 min. Matrixed outputs furnish the 44-min and 60-min commands for solar panel extension and attitude control power-on, respectively. The overflow of this counter yields one pulse every 1000 min (16.7 hr), which is used to command the high-gain antenna up-date.

The 2-min interval which tests the CC&S timing in the blockhouse is also obtained from this counter/matrix. This signal is designed to extinguish the clear light prior to the normal 2-min time after inhibit removal, if the counter has not been completely cleared.

This subassembly also contains the transistorized relay drivers and the relays associated with the clear test, solar panel extension, attitude control power-on, antenna up-date, and end counter up-date verify signals to the blockhouse (see discussion of the end counter which follows). An additional output, obtained from within the launch counter, is the basic 3.3-hr signal used for Earth acquisition and encounter-start and -stop commands.

c. End counter. This module is similar to the launch counter in that it contains magnetic counters, relay drivers, and relays. Two magnetic counter chains are driven in parallel by the 3.3-hr input from the launch counter. One counter divides by 50 to obtain the 167-hr Earth-acquisition command. The other is the up-dateable counter, mentioned in the preceding discussion, which is used for the encounter commands.

Because the time of flight between Earth and planetary encounter will vary from launch date to launch date, the contents of the counter associated with the encounter commands must be variable. This variability is obtained with a counter whose normal overflow is greater than the longest flight time expected, but which can be shortened for any particular flight time anticipated by presetting it with an appropriate number of counts from the blockhouse. The variability of this counter is between $L + 3.3$ hr and $L + 6600$ hr (277 days), in 3.3-hr increments. The encounter-stop command is obtained from a point within this counter which yields a pulse every 66.7 hr. This pulse is normally inhibited from actuating the encounter-stop relay until after the encounter-start command has been delivered.

In the process of accepting the normal 3.3-hr input or the up-date pulses from the blockhouse, the count-by-20 point in the counter will be activated once for every 20 pulses received at the counter input. This once-every-20 pulse is sent to the blockhouse equipment by way of the driver and relay in the launch counter (discussed in Section 2b) and serves as a verify signal for the encounter up-date command.

In addition to the drivers and relays associated with Earth acquisition and the encounter commands, three of the drivers and relays associated with the midcourse maneuver are located in this subassembly to utilize the existing space.

d. Input decoder. The input decoder receives the radio-transmitted command words from the command subsystem, separates the information bits from the address bits, and routes this information to the appropriate storage register in the maneuver duration module. To perform this operation, the input decoder contains a 5-bit, transistorized flip-flop counter with a matrix output to provide signals at the end of the 5th bit (end of address), the end of the 17th bit (end of command information), and the end of the 18th bit (end of word). This binary counter counts sync pulses received from the command subsystem in order to perform its function.

Because logic levels are needed, two logic flip-flops are used to convert the pulses from the matrix into voltage levels. These levels gate the information associated with the first 5 bits into the address register, the next 12 bits into the appropriate storage register, and the last bit into the appropriate polarity storage flip-flop.

e. Address register and maneuver duration output.

Part of this module contains the two-bit flip-flop address shift register which decodes, by diode matrix, the last two bits of the five-bit address. The input decoder provides shift pulses and the address information bits, derived from the command subsystem outputs, to the flip-flop register. The address contains the binary information to select a particular storage register (roll, pitch, or velocity) in the maneuver duration subassembly (to be discussed later). The polarity storage flip-flops, for roll and pitch, are also located in this subassembly. The rest of this unit contains the midcourse maneuver command relays not located in the end counter.

f. Maneuver clock. The maneuver clock contains a magnetic divider and diode matrix similar to the launch counter. It receives the 1-ppm signal from the launch counter as its basic frequency input. This counter is normally gated-off until the midcourse-start command is received from the command system. At receipt of this command, the counter begins counting and a command signal is sent to the driver and relay associated with turning on the gyros and accelerometer. During the operation of the midcourse counter, the diode matrix provides outputs at 60, 72, 94, and 98 min after start, which correspond to the roll, pitch, velocity correction start, and gyros and accelerometer-off commands, respectively. The overflow of the midcourse counter occurs 199 min after start and is used to re-command Earth acquisition.

g. Maneuver duration. The maneuver duration module contains the storage-shift registers which are used to store the midcourse turn durations transmitted by radio prior to the actual maneuver. At the start of each maneuver, commanded by the maneuver clock, the shift register associated with a particular maneuver is turned on and shifted to "overflow" to obtain the stop command for that maneuver.

Each register consists of an 11-bit magnetic-core shift register with "exclusive or" feedback which enables a particular "all ones" condition to exist once every 2047 shift pulses (if shift pulses are applied continuously). Because definite patterns of ones and zeroes are produced

in shifting from 1 to 2047, it is therefore possible to "preset" the shift register to some predetermined count in order to have the overflow (all ones) occur sooner than 2047. Thus, the radio-transmitted midcourse data supplies the "preset" ones and zeroes to allow each register to count to overflow in the desired length of time.

The roll and pitch maneuver registers are counted to overflow by the 1-pps signal from the central clock. The velocity register is driven directly by the output of the accelerometer.

h. Transformer-rectifier. The transformer-rectifier provides all d-c voltages used by the CC&S. The input to this module is the 100-v peak-to-peak, 2.4-kc square wave generated as primary power by the power subsystem. Rectified d-c voltages available as outputs are -3, +15, +28, and +60 v. The +15- and +28-v outputs are zener-regulated to maintain a more constant voltage for the transistor circuitry they service.

3. Design and Fabrication

a. Design. The design effort on the *Mariner R* CC&S began in September 1961, when it became evident that the *Centaur* booster, needed for the heavier *Mariner A* spacecraft, would not be available for the 1962 Venus launch window. Use of the *Atlas-Agena B* booster was mandatory if a spacecraft were to be launched to Venus in 1962. Because of the lower weight restrictions of the *Atlas-Agena B* combination, the *Mariner* spacecraft concept required modification, which resulted in a reduction in the over-all capabilities of the spacecraft. This simplification reduced CC&S requirements as well.

The original *Mariner A* CC&S subsystem was required to continuously control several scientific experiments, both interplanetary and planetary, as well as to perform the initial postinjection sequencing and the two midcourse maneuvers. The mechanization adapted for these requirements was a multiple magnetic-core memory array which would contain all the information necessary for the scientific experiment sequencing and a frequency-dividing counter (*Ranger* type), which would handle the postinjection and midcourse requirements. This design required thirteen 6- × 6- × 1-in. subassemblies weighing approximately 22 lb (including harness) and consuming approximately 15 w of power.

The reduced *Mariner R* design required only the following CC&S functions:

- (1) A frequency synchronization signal for the power subsystem
- (2) Postinjection commands (three)
- (3) A periodic command to up-date the high-gain antenna position
- (4) Sequencing for one midcourse maneuver
- (5) A start and a stop command to the science subsystem to control the encounter scientific experiments

These reduced requirements removed the need for the core memory and its associated circuitry, since a *Ranger*-type frequency dividing counter could be used to provide the simple sequencing necessary. This simplification resulted in eight 6- × 6- × 1-in. subassemblies weighing approximately 12 lb (including harness) and consuming approximately 7 w of power—roughly half the weight and power requirements of the *Mariner A* design.

The counter and sequencer designed for *Mariner A* was used almost intact to take advantage of the high-reliability components used. Almost all components used in this design are covered by a *Minuteman* or JPL-equivalent specification.

b. Fabrication. Fabrication of the *Mariner R* CC&S began in October 1961, with the delivery date to SAF tentatively set for January 1, 1962. Because of the short schedule, the fabrication was performed at JPL on all three required CC&S subsystems (two flight, one spare). Later, the delivery date was changed to January 15, 1962, and all schedules were adjusted to conform to this date. The first subsystem was completed and assembled about November 20, 1961. Functional and temperature tests, subassembly inspection, and potting followed.

Flight-acceptance tests started on December 26, 1961, and were concluded successfully on December 28, 1961, after which the CC&S subsystem was installed in the flight case and delivered for installation of the attitude control subsystem. The completed guidance and control case was delivered to SAF on schedule. Similarly, the two following subsystems were assembled, tested, and delivered to SAF on schedule on January 29 and February 12, 1962.

Initial power turn-on at SAF in the complete GSE/spacecraft configuration revealed several CC&S/GSE interface problems, primarily due to the long electrical

cabling between the two. Other CC&S anomalies were found as follows:

- (1) Two diodes appeared to have their cases shorted together, causing the event pulse associated with a particular relay to be erratic on *MR-1*.
- (2) Relay bounce from the CC&S relays, when actuated, caused multiple event pulses to occur. Increasing the size of a filter capacitor solved this problem.
- (3) A diode was found reversed in one subassembly on *MR-2*, causing the event pulse circuitry to be oversensitive and produce multiple event pulses.
- (4) During an *MR-1* test in the space simulator, all antenna-up-date commands, after the first one, occurred sooner than expected. A wire was found missing in one of the magnetic counter circuits.

After these problems were corrected, the CC&S subsystems operated properly, with only minor GSE interface problems, throughout the remainder of the SAF prelaunch tests. After shipment to AMR, testing was resumed. Two CC&S malfunctions were traced to GSE-induced shorts on one of the CC&S d-c voltages. In both cases, components in the CC&S were replaced as a precautionary measure.

CC&S serial No. 001 was launched on July 22, 1962, as part of the *MR-1* spacecraft. The CC&S performed normally for 5 min after launch, at which time the vehicle was destroyed by the Range Safety officer.

CC&S serial No. 002 was launched on August 27, 1962, as part of the *MR-2* spacecraft. As of August 31, 1962, all telemetered indications were that the CC&S subsystem was functioning normally.

D. Attitude Control

1. Attitude Control System Design

The *Mariner R* coasting attitude control system, like *Ranger*, uses a Sun-Earth system for directional references. In the normal attitude, the roll axis and solar panels point toward the Sun, requiring control about the pitch and yaw axes with reference to the Sun. Roll control is referred to the Earth. Roll attitude is constant

with respect to the Sun-probe-Earth plane. Optical sensors provide error signals in two perpendicular directions each, with respect to the Sun and Earth.

The Sun-sensor errors control spacecraft pitch and yaw. The Earth-sensor errors control spacecraft roll and antenna hinge angles. The Earth sensor is mounted collinearly with the antenna so that the Earth sensor provides control about the roll axis and tracks the Earth along the roll axis (about the hinge axis) to always maintain the antenna pointing at the Earth.

Control torques are provided as required during coasting intervals of flight by a cold-gas, mass-expulsion technique. On-off valve assemblies and gas nozzles mounted about the three spacecraft axes, coupled with switching-amplifier compensation provide the required damping and control.

The requirements for the coasting attitude control system are:

- (1) Establishment of reference directions to the Sun and Earth to an accuracy of ± 17.0 mrad.
- (2) Orientation of the spacecraft reference directions in an arbitrary position with a $3\text{-}\sigma$ pointing error of not more than 23 mrad and a drift rate of not more than 10.3×10^{-3} mrad/sec.
- (3) Re-establishment of spacecraft directions following a noncatastrophic disturbance of normal spacecraft orientation.
- (4) Lifetime extending a minimum of 4000 hr from launch.
- (5) The limit cycle size of the control system in pitch and yaw is ± 2.0 mrad in angle and ± 2 μ rad/sec in velocity, during cruise, while the roll channel is ± 4.0 mrad in angle and ± 2 μ rad/sec in velocity.

The design of the coasting attitude control provides automatic acquisition both during normal acquisition sequences and during any unexpected loss of acquisition (e.g., noncatastrophic meteoric impact). This method appears superior to acquisition based upon timed sequences, wherein a sequence may be stopped before its function is accomplished or be delayed beyond the completion of a previous function. Automatic acquisition is required for any outside disturbance to the spacecraft that involves loss of communications.

In order to meet the lifetime requirements of the mission, the gyros are only used during acquisition and maneuvers. During the cruise phase, the gyros are shut down and damping is provided by passive compensation of the control loop.

a. Sun sensors. The Sun sensors have a completely unobstructed field of view with a single stable null in the pitch and yaw channels in order to point the roll axis at the Sun. There are two types of Sun sensors to provide a 360-deg field of view about the pitch and yaw axes. Primary Sun sensors detect the Sun within a nominal range of 45 deg of the roll axis. Secondary Sun sensors provide the rest of the field of view, for purposes of Sun acquisition.

There is an additional simple auxiliary Sun sensor to detect when the Sun is within $2\frac{1}{2}$ deg of the roll axis to provide logic switching in the control system.

b. Earth sensor. The Earth sensor provides signals to both the roll control and hinge servo. The Earth sensor has a nominal field of view of ± 5 deg about the hinge axis and ± 2 deg about the roll axis. A fixed threshold is provided on the Earth sensor to be used in the logic switching in the control system.

c. Gyros. The spacecraft carries three single-degree-of-freedom gyros, which are body-fixed along the three mutually perpendicular axes (pitch, yaw, and roll). Pitch and roll gyros are independently capable of operation as rate or position-sensing devices. The yaw gyro is always maintained in the same mode as the pitch gyro.

The control-system mechanization is shown in Fig. 69. In this system, several sequences of operation take place: initial acquisition, commanded turn, reacquisition after a commanded turn, and the roll override sequences.

Conditions prior to initial acquisition (Fig. 69) are that the gyros have been on since launch and hinge up-date reference is set to the expected acquisition angle. The CC&S applies power to the Sun sensors, Sun gate, and control system to start Sun acquisition. Upon acquisition, the Sun gate activates the Earth sensor, initiates a roll search, and removes power from the secondary Sun sensors. With Earth acquisition, the Earth gate switches the roll and hinge channels to Earth-sensor control and deactivates the gyro loop.

Prior to midcourse turn, the spacecraft is controlled by the Sun and Earth sensors. The CC&S begins the turn

sequence by activating the gyro loop, in the integrating mode, slewing the antenna to the exit position, and disabling the Earth sensor. The turn is initiated by applying the turn command signal to the roll gyro. At the completion of a roll turn, a CC&S command disables the Sun sensor and switches the turn command signal to the pitch gyro, which performs the pitch turn.

Reacquisition after midcourse maneuver is accomplished by reactivating the gyros, supplying power to Earth and Sun sensors, and transferring the hinge angle program to the acquisition position. Reacquisition then proceeds as in initial acquisition.

In the event of a noncatastrophic disturbance, the loss of Earth gate, Sun gate, or both, initiates reacquisition as in initial acquisition, with the exception that the antenna remains at its last acquired position.

If the Earth sensor acquires some object other than the Earth, a new search can be initiated by ground command. A roll override command is transmitted, which energizes the search command and gyros, and thereby overrides the Earth-sensor roll signal. With loss of the Earth gate, acquisition proceeds as in initial acquisition.

d. Control gyros. Gyro requirements for the attitude control system in *Mariner R* are modified over the earlier *Ranger* configuration. The angular rate information will be derived from another part of the attitude control system during the cruise mode. This eliminates the need for the rate signals during this period as provided from gyros in the earlier system. However, gyros are required to provide the angular and rate measurements of maneuvers which will be accomplished in the same manner as in *Ranger*.

The gyros are miniature, single-axis, floated units, with a change proposed to further improve their accuracy over the *Ranger* instruments. A permanent-magnet torquer is incorporated, thus eliminating the need for a separate d-c current supply while providing the better linearity and torquing range inherent in the permanent-magnet torquers.

2. Attitude Control System Functional Mechanization

The functional mechanization of the *Mariner R* attitude control system is shown in Fig. 70. The following

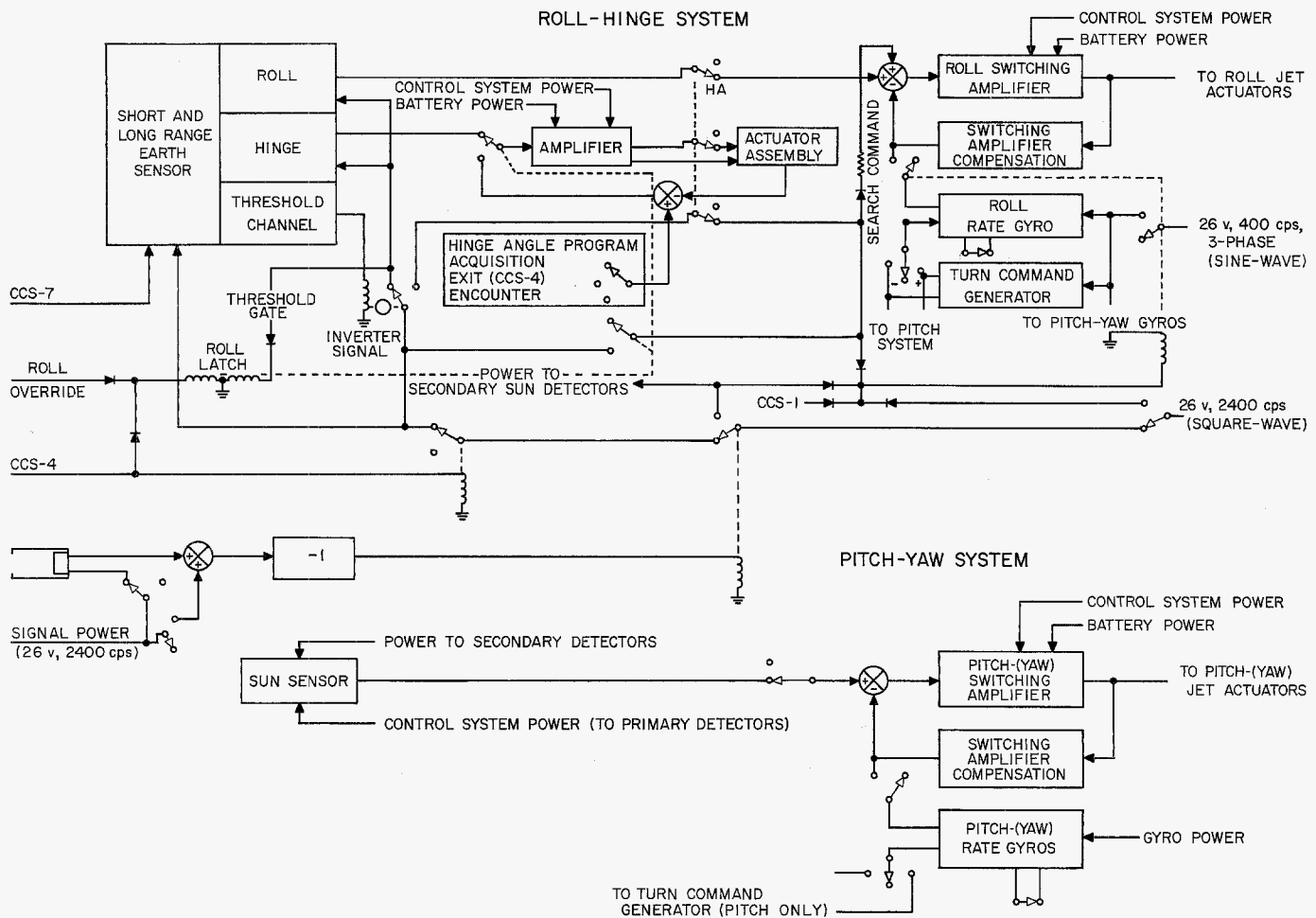


Fig. 69. Mariner R attitude control system

discussion describes the sequence of operations and the functions of the various commands during the flight.

a. Functions of commands

(1) **CCS-1.** This is the main power signal which energizes the attitude control system after separation. Once power is applied to the system, it remains on throughout the remainder of the mission. This is a timed command in the CC&S sequence. Prior to separation, power is applied to the gyros through this relay; hence, the gyros are on from launch.

(2) **CCS-2.** CCS-2 inhibits initial Earth acquisition until a prescribed time after launch to prevent acquisition during a period of time when the Earth-probe-Sun angle is changing rapidly, and the Earth light intensity is greater than 10^{-6} w/cm².

(3) **CCS-3.** The CCS-3 command is given approximately 1 hr prior to the first midcourse turn command to permit gyro warm-up and stabilization time and remains activated throughout the entire maneuver period. It actuates the GC relay and thereby applies gyro loop power.

(4) **CCS-4.** CCS-4 is the roll maneuver command signal which is derived from the CC&S and is applied throughout the entire maneuver period. On application of this command, the Earth sensor and search command generator are disabled. This command also places the roll gyro in the integrating mode prior to application of the turn command, and commands the antenna to the exit angle.

(5) **CCS-5.** The function of CCS-5 in the pitch and yaw systems is similar to that of CCS-4 in the roll system. It disables the pitch and yaw Sun sensors and places the

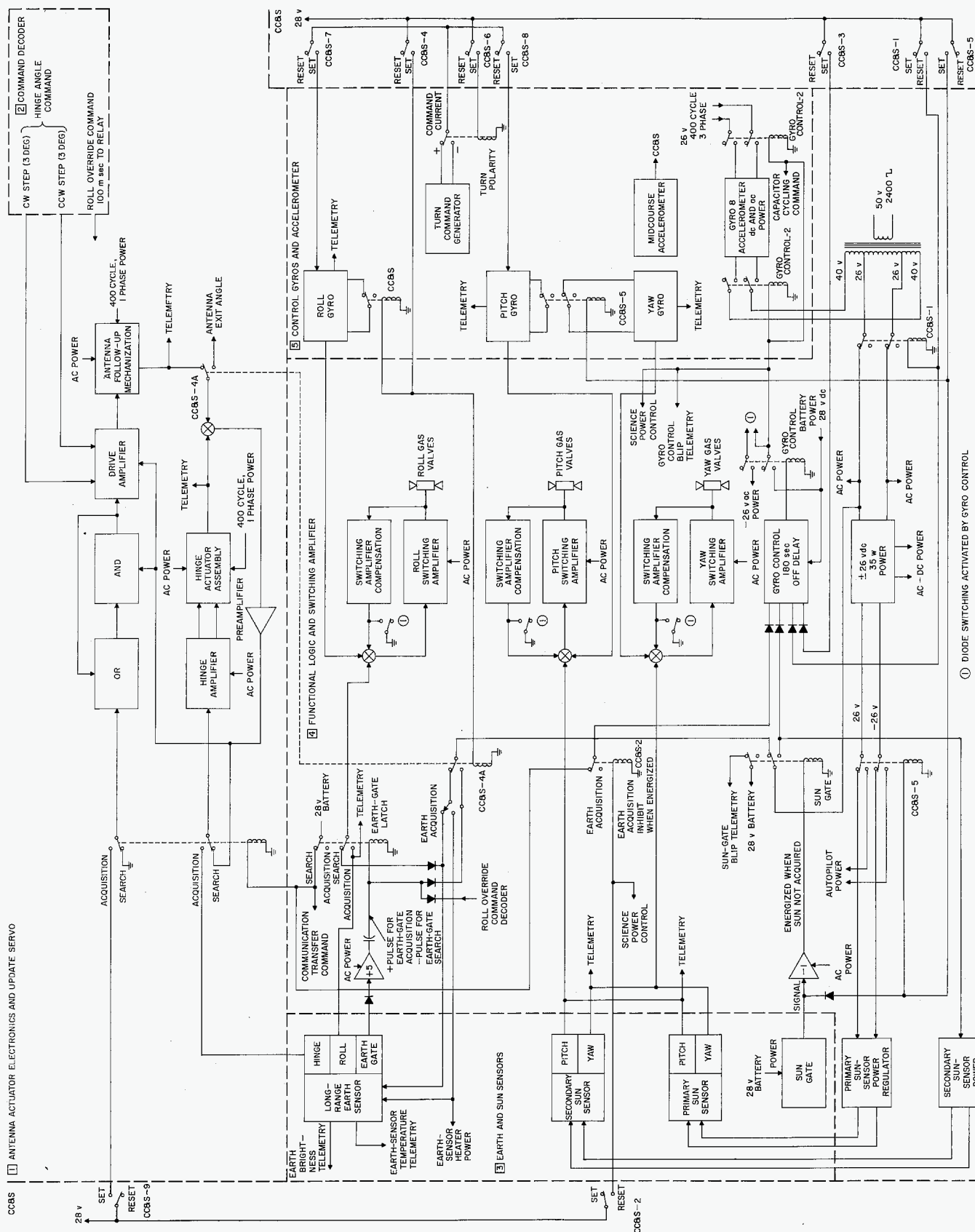


Fig. 70. Attitude control system mechanization, block diagram

pitch and yaw gyros in the integrating mode after completion of the roll maneuver.

(6) *CCS-6.* CCS-6 sets the polarity of the command to be executed by CCS-7 and -8.

(7) *CCS-7 and -8.* These command signals apply torquing current to the gyros during maneuver turning periods and determine the length of time the command is applied. These command polarities and times are computed on the ground, based on trajectory observations, transmitted to the spacecraft, and stored in the CC&S prior to execution of the command.

(8) *CCS-9.* CCS-9 up-dates the antenna reference angle continually during flight, provided the hinge system is under Earth-sensor control.

b. Function of relays

(1) *Gyro control.* This relay switches power to the gyros and grounds the input to the switching amplifier compensation networks. It is actuated by CCS-1, CCS-3, Sun gate, and Earth gate through diode logic.

(2) *Earth gate.* The Earth-gate relay is a latching-type relay which is actuated through diode logic by CCS-4, roll override, and Earth-gate signals. The EG relay is reset when attitude control power is turned on. The Earth-gate channel applies a positive pulse through the inversion amplifier to the EG relay when the Earth sensor has acquired the Earth. On loss of Earth acquisition, a negative pulse is applied to the EG relay through the inversion amplifier, which transfers the roll input of the switching amplifier from the Earth-sensor roll error signal to the search command signal. Also, the EG relay transfers the antenna hinge control from the Earth-sensor hinge outputs to the follow-up servo or up-dated reference angle. The roll override and CCS-4 signals are capable of overriding the Earth-gate acquisition signal. These commands only transfer the EG relay from the acquired state to the unacquired state.

(3) *Sun gate.* The Sun-gate sensor, inversion amplifier, and relay are provided for actuation of the GC relay, disabling the Earth sensor and the roll search command until Sun acquisition.

c. Sequence of operations. Several sequences of operation take place in the control system. These may be summarized as follows:

- (1) Initial Sun acquisition
- (2) Initial Earth acquisition
- (3) Midcourse-command turn
- (4) Reacquisition after midcourse maneuver
- (5) Reacquisition in the event of a noncatastrophic disturbance
- (6) Roll override sequence
- (7) Hinge override sequence

In detail, these sequences take place in the following manner:

(1) Initial Sun acquisition

Initial conditions

- (a) Rate feedback from gyros (GC actuated by CCS-3 at launch)
- (b) Sun sensor switched in (CCS-5)
- (c) Hinge and roll sensor switched out (EG)
- (d) Hinge angle program to up-date and preset
- (e) CCS-4 not actuated (NC position)
- (f) CCS-2 to Earth acquisition inhibit position

Sun acquisition sequence

- (a) CCS-1 turns on power to control system. Sun sensors start pitch and yaw control. Antenna moves to acquisition angle. CCS-1 remains in throughout flight.
- (b) Sun gate switches power to Earth-sensor line and removes power from secondary Sun sensors. Earth acquisition is inhibited by CCS-2. Therefore, when Sun acquisition is complete, gyros shut off.

(2) Initial Earth acquisition

Initial conditions

- (a) Gyros are off
- (b) Derived rate stabilization in pitch and yaw
- (c) CCS-2 inhibiting Earth acquisition in set position
- (d) CCS-4 in reset position
- (e) CCS-5 in reset position

UNCLASSIFIED

JPL TECHNICAL REPORT NO. 32-353

Earth acquisition sequence

- (a) CCS-2 removes the inhibit on Earth acquisition and applies power to the Earth sensor. Gyros are now turned on again since EG relay is in search position, and roll search begins.
- (b) Earth falls into field of view of the Earth sensor, activates Earth gate, which switches in hinge and roll error signals from Earth sensor. The Earth gate also switches out search command and deactivates the GC, which transfers system to derived rate control.

(3) Midcourse-command turns

Initial conditions

- (a) Sun sensor and Earth sensor controlling spacecraft attitude and hinge angle
- (b) Control system in derived rate mode

Command turn sequence

- (a) CCS-3 activates GC, turning on gyros and gyro rate feedback, and removes derived rate.
- (b) CCS-4 and CCS-2 switch out Earth-sensor power, search command power and roll gyro to integrate mode and transfer the EG relay to search position. Hinge angle program to exit position.
- (c) CCS-6 and -7 switch in command roll turn
- (d) CCS-5 switches out Sun sensors. Pitch and yaw gyros to integrate mode.
- (e) CCS-6 and -8 switch in command pitch turn

(4) Reacquisition after midcourse maneuver

Initial conditions

- (a) Sun and Earth sensors switched out (CCS-4, -5, and -2)
- (b) Gyros in integrating mode (CCS-4 and -5)
- (c) Sun gate has turned on secondary Sun sensors, opened Sun-gate link of search command chain and applied holding power to GC.

Reacquisition

- (a) CCS-1 is opened.
- (b) Hinge angle program to acquisition angle

- (c) CCS-4 and -5 relays to R position, applying power to Sun sensor and closing Earth-sensor link. To Earth acquisition inhibit relay.

(5) Reacquisition in the event of a noncatastrophic disturbance

Condition prior to loss of acquisition

- (a) Sun sensors and Earth sensor controlling system
- (b) Control system in switching amplifier compensation mode

Sequence assuming simultaneous loss of pitch, yaw, and roll control

- (a) Loss of pitch and/or yaw control activates Sun-gate switch which activates secondary Sun sensor, turns on gyros, and removes SAC through GC, switches out Earth sensor and search command.
- (b) Reacquisition proceeds as above.

(6) Roll override sequence

Mode of control

- (a) Sun and Earth sensors controlling spacecraft
- (b) Hinge angle program in acquisition position
- (c) Earth sensor has acquired and is tracking the wrong object.

Reacquisition sequence

- (a) Roll override command switches EG to search position, which introduces search command.
- (b) Gyros are turned on and search continues for new object.
- (c) On acquisition of Earth, the system proceeds as above.

(7) *Hinge override sequence.* In the event of a non-standard trajectory, and due to the limited Earth-sensor field of view, the reference antenna angle may be commanded incrementally to any arbitrary value by using the hinge override command channel. This command provides ground control for setting a new antenna reference angle for acquiring the Earth.

UNCLASSIFIED

3. Determination of System Parameters

a. Sun sensors. The Sun sensors used for control about the pitch and yaw axes are the same as those used on RA-1 and -2. These were selected because the pointing requirements for *Mariner* were similar to those for *Ranger*. The principal characteristics of the pitch and yaw Sun sensors are as follows:

Field of view:	4π steradians
Scale factor:	$9.7 \text{ v/deg} \begin{smallmatrix} +7 \\ -53 \end{smallmatrix} \%$
Saturation level:	$14.95 \text{ v} \pm 7\%$
Noise level:	$50 \text{ } \mu\text{rad}$ peak-to peak max.
Null offset, mechanical and electrical:	$\pm 5.25 \text{ mrad } 3\sigma$

b. Pitch and yaw gyro mix ratio (rate to position gain). The chief constraint on picking the gyro mix ratio τ is the saturation level of the gyro rate measurement. When the Sun is in the saturated region of the sensor, the spacecraft turning rate will stabilize to a constant rate, determined primarily by the saturation level of the sensor and the gyro mix ratio. Tolerances are applied to the parameters in a manner to provide an absolute worst case condition, and the gyro mix ratio τ is determined to be the value that provides the greatest rate without saturating the gyros. In this case, for pitch and yaw,

$$\tau = 5.3 \text{ sec} \pm 20\%$$

c. Pitch and yaw dead-band (switching amplifier setting). Due to the pointing accuracy requirement of 1 deg for the pitch and yaw axes, and since the sensor null offset is only $\pm 5.25 \text{ mrad } 3\sigma$, the size of the dead-band is not critical. It was decided that it was practical to keep it as small as $\pm 2 \text{ mrad}$, which is well within the pointing accuracy requirements.

d. Pitch, yaw, and roll control torque acceleration. The control torque acceleration that was selected is determined for cruise primarily by the minimum impulse capability of the gas valves, in order to minimize gas consumption during the cruise-limit cycle operation. The second constraint on the acceleration constant is the commanded turn sequence which has a minimum α to prevent gyro saturation. Therefore:

$$\alpha = \pm 0.225 \text{ mrad/sec}^2 \pm 20\%$$

e. Pitch and yaw derived-rate parameters. The derived-rate parameters for cruise-limit cycle operation are selected on the basis of three criteria:

- (1) The ability to reacquire from a small disturbance; that is, a disturbance not large enough to activate the gyros for automatic acquisition.
- (2) The derived-rate signal must be large enough that a noise pulse will not cause an extra rate increment in the limit cycle.
- (3) The rate of decay of the derived-rate signal must be long enough that a noise pulse will not cause an extra rate increment until the position signal is far enough inside the switching dead-band to prevent it.

The following derived-rate parameters were selected:

Derived-rate gain $40 \text{ mrad} \pm 10\%$

Derived-rate time constant: $27 \text{ sec} \pm 10\%$

f. Earth sensor. Most of the Earth-sensor parameters are predetermined due to difficulty of mechanization. These characteristics are as follows:

Field of view in roll:	$\pm 2 \text{ deg} \pm 5\%$
Field of view in hinge	$\pm 5 \text{ deg} \pm 5\%$
Scale factor in roll:	8 v/deg
Scale factor in hinge:	2 v/deg
Noise:	
Null offset:	$\pm 10.5 \text{ mrad } 3\sigma$
Dynamic response:	Time constant = 2.0 sec max.

The chief constraint that determines the rest of the Earth-sensor parameters is the limited roll field capable of reducing the roll rate to zero before the Earth is out of the field of view of the sensor. A combination of factors determines whether or not this condition is met:

- (1) Sensor saturation level
- (2) Control torque acceleration
- (3) Gyro mix ratio (rate-to-position gain)
- (4) Sensor dynamics
- (5) Roll search rate
- (6) Switching dead-band

The sensor saturation level was picked so that the roll rate in the saturated region of the sensor is close to the roll search rate. Trade-offs were made between dead-band and search rate so as to arrive at a compromise for

each. The gyro mix ratio was determined by the maximum acquisition rate that could be tolerated. Tolerances were added in an absolute worst-case manner, and then the parameters were selected such that acquisition was still possible. On this basis, the following parameters were selected:

Sensor saturation: $3.67 \text{ v} \pm 12\%$
 Gyro mix ratio: $6.45 \text{ sec} \pm 20\%$
 Roll search rate: $2.88 \text{ mrad/sec} \pm 10\%$
 Switching amplifier
 dead-band: $\pm 4.0 \text{ mrad} \pm 10\%$

g. Roll control torque acceleration. This value is the same as the pitch and yaw.

h. Roll derived-rate parameters. These parameters are picked on the same basis as the pitch and yaw parameters, but since the noise level and dead-band are different for roll, the parameters are different:

Derived-rate gain: $122 \text{ mrad} \pm 10\%$
 Derived-rate time constant: $36 \text{ sec} \pm 10\%$

i. Hinge servo. The criteria used to determine the hinge servo parameters were:

- (1) Under the worst-case tolerances, the Earth sensor must be capable of supplying a sufficient error signal to operate the hinge-actuator amplifier.
- (2) Under the worst-case tolerance situation, the total overshoot from the maximum slewing rate, including the effects of the filter time constants in the Earth sensor, must not cause the minimum hinge-actuator amplifier dead zone to be entirely consumed and the antenna to reverse direction.
- (3) The tolerance of setting the acquisition antenna angle shall result in a net field of view at the time of Earth acquisition of not less than $\pm 2 \text{ deg}$ in hinge.
- (4) At the minimum slewing rate, the antenna must arrive at the exit angle 2 min before motor ignition.
- (5) Earth acquisition by the use of overrides must be possible in all geometry situations.

Hinge servo:

Hinge servo dead zone: $12.5 \text{ mrad} \pm 15\%$
 Hinge servo slewing
 rate: $0.1 \text{ to } 0.16 \text{ deg/sec}$

Hinge servo backlash: 3 deg max
 Antenna exit angle: $60 \text{ deg} \pm 2 \text{ deg}$

Up-date reference servo:

Magnitude of stepping
 increment $3 \text{ deg} \begin{matrix} +0 \text{ deg} \\ -2 \text{ deg} \end{matrix}$

Over-all initial
 acquisition hinge
 angle error $0 \text{ deg} \pm 17.5\%/\text{deg}$

- (6) The roll search direction of CCW (-) roll rotation is also determined by a hinge servo constraint. The constraint occurs when the Earth and the Moon are in the field of view of the Earth sensor at Earth acquisition, using a CCW roll search, causing the absolute assurance of seeing the Earth first and avoiding the Earth-Moon ambiguity problem.

j. Gas consumption. The gas consumption consists of estimating the gas consumed during the three basic phases of flight:

- (1) Sun and Earth acquisition (reacquisition)
- (2) Midcourse maneuver and encounter
- (3) Cruise

Due to the extended mission time of *Mariner R*, the primary source of gas consumption is the long cruise phase of flight. The preflight gas consumption estimate was 1.82 lb, and 4.32 lb was carried at launch.

4. Switching Amplifier and Logic Subassembly

The switching amplifier and logic subassembly contains the amplifiers for the spacecraft attitude sensors. The three amplifiers in the subassembly — pitch, roll, and yaw — activate the pitch, roll, and yaw gas jets. The secondary and primary Sun sensors, the Earth sensor, and the pitch, roll, and yaw gyros all provide inputs to the switching amplifiers. Also, included in the subassembly is the logic circuitry: the Earth gate, the Sun gate, and the gyro control switch.

The *Mariner R* switching amplifier is a "minimum-on-time" amplifier with derived-rate feedback. It is termed minimum-on-time because once the input signal has caused the output to turn on, the output is maintained on for a minimum length of time, regardless of subsequent input variations. As mechanized, the amplifier turn-on energizes a pulse circuit which turns the ampli-

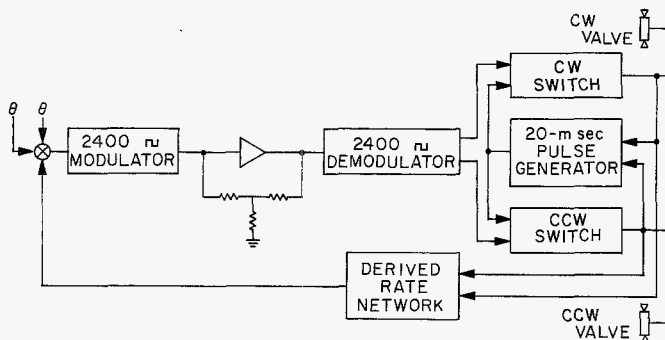


Fig. 71. Switching amplifier, block diagram

fier off at the end of a 20-msec period. Thus, after the minimum on-time of 20 msec, the output can again be controlled by the input. This mechanization scheme eliminates the effects of noise during the actuation period and produces a predictable velocity increment each time a switching command is given. Multiple switchings are inhibited by the use of a derived-rate signal. The derived-rate parameters are selected so that the derived-rate feedback signal is greater than the peak-to-peak noise level and the discharge rate of the derived-rate signal is less than the (average) rate of change of the sensor signal. The switching amplifier block diagram is shown in Fig. 71.

The internal logic is composed of a Sun-gate switch, an Earth-gate switch, and a gyro control switch with a 180-sec delay on shut off. The Sun-gate switch uses the Sun-gate sensors in a voltage divider arrangement in which the switch turns off when the sensor resistance decreases to 5000 ohms. The Earth-gate switch is controlled by the Earth acquisition channel of the Earth sensor. The switch transfers to the on-state with an input signal of 7.0 v dc, applying a positive pulse to the Earth-gate relay and transferring the relay to the acquired position. The Earth-gate relay is transferred to the search position by a negative pulse from roll override or from the roll maneuver command. The gyro control switch is activated by 28 v dc from the CC&S, the Earth-gate switch, or from the Sun-gate switch. Thus, gyro power is turned on by CC&S command or loss of either Earth or Sun acquisition. The switch has a 180-sec off delay, maintaining the gyros on 180 sec after Sun and Earth acquisition.

The switching amplifier and logic specifications and requirements follow:

Weight: 1.10 lb

Size: 6 in. × 6 in. × 1 in.

Power:

+26 v dc ± 1 v, 1 w
 -26 v dc ± 1 v, 0.9 w
 +28 v dc $\pm 10\%$, 1 w
 2400 cps, 26 v ± 1 , 0.1 w

Roll amplifier

Earth-sensor input:

Voltage switch point: ± 1.84 v $\pm 10\%$
 Input impedance: 600,000 ohms $\pm 1\%$

Roll gyro input

Voltage switch point: 2.14 v $\pm 10\%$
 Input impedance: 690,000 ohms $\pm 1\%$

Earth sensor, T/M

Output impedance: 51,000 ohms

Pitch and yaw amplifiers

Sun-sensor input:

Voltage switch point: 1.1 v $\pm 10\%$
 Input impedance: 180,000 ohms $\pm 1\%$

Gyro input

Voltage switch point: ± 0.47 v $\pm 10\%$
 Input impedance: 78,000 ohms

Fine Sun-sensors, T/M

Output impedance: 51,000 ohms

Sun gate

Sun-gate resistance for switch activation:
 5,000 ohm

Earth gate

Input switch voltage: 7 v dc
 Input impedance: 3000 ohms

Gyro control delay

180-sec off delay
 Input-on voltage: +25 v dc
 Input impedance: 20,000 ohms

5. Celestial Relays and Power Subassembly

The celestial relays and power subassembly contains the main transformer-rectifier power supplies in the atti-

tude control system. It transforms a 2400-cps square wave from the spacecraft power supply to voltages needed throughout the attitude control system. Also included in the CR&P subassembly are relays to switch the needed voltages to various attitude control subassemblies.

The subassembly consists of three 2400-cps transformers, two transformer-rectifier power supplies, two d-c voltage regulators, and six relays.

General specifications

Weight: 1.02 lb

Size: 6.0 in. \times 4.25 in. \times 1.2 in.

Power dissipation:

(1) 2400-cps power

Launch: 1.5 w

Cruise: 0.8 w

Maneuver: 2.4 w

(2) 28-v d-c power

Launch: 4.4 w

Sun cruise: 1.1 w

Earth cruise: 0.0 w

Maneuver: 3.3 w

Transformers

a. Gyro power

(1) Primary: 50 v rms square wave, 16 w

(2) Secondary: 80 v rms square wave, center-tapped, 2% regulation from 8 to 16 w

b. Attitude control 2400-cps power

(1) Primary: 50 v rms square wave

(2) Secondary: Phase A, 26 v rms square wave, 14 w, 5% regulation from 2.5 to 10 w
Phase B, 26 v rms square wave, 5 w, 5% regulation from 1.25 to 5 w

c. Attitude control d-c power

(1) Primary: 50 v rms square wave

(2) Secondary: 54 v rms square wave, center-tapped, 5% regulation from 10 to 40 w

Direct-current supplies

a. Attitude control d-c power

(1) Input: 54 v rms square wave, center-tapped, 5% regulation

(2) Output: ± 26 v dc, 5% regulation, less than 75 mv peak-to-peak ripple when loaded from 1 to 16 w

b. Secondary Sun-sensor power

(1) Input: 27 v rms square wave

(2) Output: ± 16.2 v dc, 5% regulation

c. Primary Sun-sensor power

(1) Input: ± 26 v dc

(2) Output: ± 16.2 v dc $\pm 1.0\%$, balanced to 0.02 v

Relay functions

a. Sun-gate relay

(1) *Sun-gate energized.* The Sun-gate relay, when energized, supplies ± 16.2 v to the Sun-sensor secondary and 28 v dc to the gyro control.

(2) *Sun-gate de-energized.* The Sun-gate relay, when de-energized, supplies 26-v 2400-cps square-wave power to the roll maneuver relay.

b. Roll maneuver relay

(1) *Roll maneuver energized.* The roll maneuver relay, when energized, supplies 26-v 2400-cps square-wave power to the Earth gate (CCS-4 command to Earth gate, Sun-gate relay de-energized). It also supplies antenna exit angle to antenna preamplifier input.

(2) *Roll maneuver de-energized.* The roll maneuver relay, when de-energized, supplies the antenna stored angle to the antenna preamplifier input and also supplies 26-v 2400-cps square-wave power to the Earth acquisition inhibit relay (Sun-gate relay de-energized).

c. Earth acquisition inhibit relay

(1) *Earth acquisition inhibit energized.* The Earth acquisition inhibit relay, when energized, supplies 26-v 2400-cps square-wave power to the Earth-sensor heater. (Roll maneuver relay and Sun-gate relay both de-energized).

- (2) *Earth acquisition inhibit de-energized.* The Earth acquisition inhibit relay, when de-energized, supplies 26-v 2400-cps square-wave power for the Earth sensor and 8-v 2400-cps square-wave for roll search command. Roll maneuver relay and Sun-gate relay are both de-energized. The relay also supplies Earth-gate command through the relay contact to gyro control.

d. Attitude control power control relay

- (1) *Attitude control power control energized.* The attitude control power control relay, when energized, interrupts the ± 26 -v d-c power to the attitude control system.
- (2) *Attitude control power control de-energized.* The attitude control power control relay, when de-energized, supplies ± 26 -v d-c power to the attitude control system.

e. 2400-cps square-wave power relay

- (1) *2400-cps square-wave power energized.* The 2400-cps square-wave power relay, when energized, interrupts the 26-v rms 2400-cps, square-wave power to the attitude control system.
- (2) *2400-cps square-wave power de-energized.* The 2400-cps square-wave power relay, when de-energized, supplies 26-v 2400-cps, square-wave power to the attitude control system.

f. Pitch maneuver relay

- (1) *Pitch maneuver energized.* The pitch maneuver relay, when energized, supplies ± 26 v dc to the autopilot.
- (2) *Pitch maneuver de-energized.* The pitch maneuver relay, when de-energized, supplies ± 16.2 v to the primary Sun sensors.

6. Mariner R Antenna Electronics

The antenna electronics module contains all the electronics associated with the antenna servo loop except for the Earth sensor, the power supplies, and the feedback potentiometer in the actuator. The narrow-beamwidth, high-gain antenna is the deep-space telemetry link between the Earth and the spacecraft. The antenna is rotated with respect to the spacecraft about a hinge axis which is perpendicular to the roll axis and parallel to the pitch axis.

The change from *Mariner A* to *Mariner R* required extensive circuit modifications to the module because of the removal of the planetary horizontal platform control circuitry, the substitution of an *RA-1* actuator to drive the antenna, the elimination of the short-range Earth sensor, and the addition of extra control modes for the up-date servo. The removal of the PHP electronics made available the necessary space for the additional circuitry.

The drive amplifier circuitry required extensive modification in order to utilize the *RA-1* antenna actuator, which consists of a high-speed 400-cps servo-motor driving several stages of speed-reducing gears. In order to achieve the required antenna rates, the motor must operate at maximum speed during the commanded period. The motor will not operate from either a square-wave or half sine-wave source because of its unique design, which was required to minimize power consumption.

The drive amplifier accepts either a d-c or suppressed-carrier analog input signal and supplies drive power to the actuator motor. The transfer characteristic of the amplifier is a fixed dead-band, on-off switch. The drive amplifier (Fig. 72) can be divided into two sections: the input chopper and the output switches. The input circuit is a half-wave chopper which accepts either a d-c signal from the Earth sensor or a square-wave, suppressed-carrier signal from the command channel amplifier. The chopper output signal at the input to the gate of the semiconductor switches is a 2400-cps zero-reference pulse train whose polarity depends on the input signal polarity and whose magnitude is proportional to the peak input signal.

The output of the chopper is clamped in order to maintain a zero-referenced signal and to prevent transformer voltage backswing from false-triggering the semiconductor switch. Signal current drawn at the firing point is approximately 100 μ amp.

In order to obtain satisfactory system performance with the actuator's long-coast-down characteristic, the dead-zone of the drive amplifier was widened and the temperature stabilization was improved by adding a thermistor network that inversely tracks the temperature characteristic of the input SCR's. The output stage was redesigned in order to provide a full-wave sine-wave drive.

The antenna up-date servo (contained in the electronic module) is an electromechanical device which stores as a potentiometer ratio the desired reference angle of the

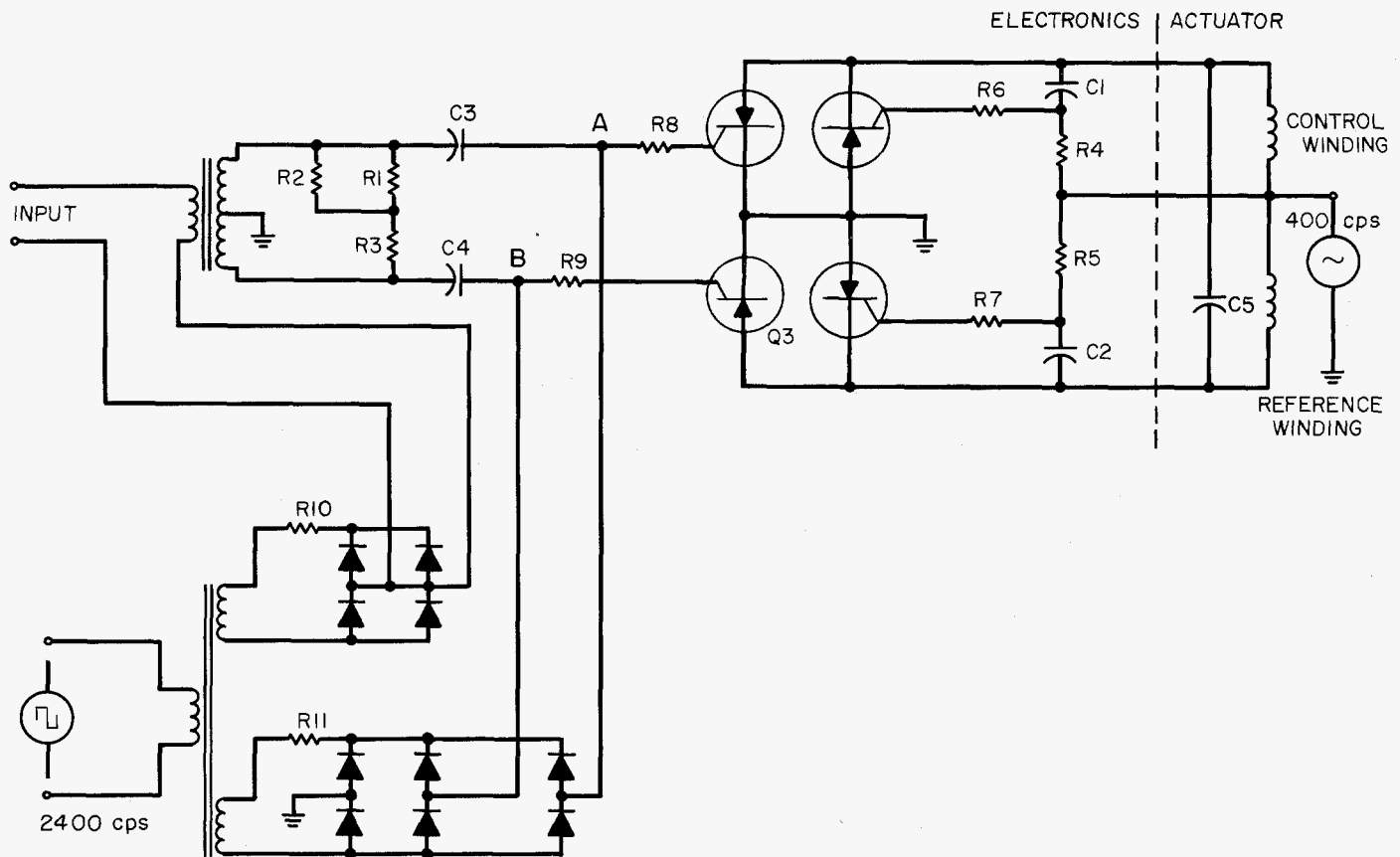


Fig. 72. Antenna drive amplifier

antenna. In the basic mode, the up-date potentiometer periodically stores the current Sun-probe-Earth angle for use as a reference in case the Earth sensor loses its target. The up-date is inhibited if the Earth sensor is off-target.

The up-date servo was modified to add two modes of operation. Due to the elimination of the short-range Earth sensor, the initial setting of the up-date angle, the acquisition angle, is very critical and new settings are required several times during one firing window. The adjustment must be made from the Control Center while the spacecraft is in position on the launcher and with only raw battery power and 400-cps sine-wave power available.

7. Mariner R Autopilot

The autopilot maintains vehicle dynamic stability during the interval of midcourse propulsion. Stability is maintained by the use of movable jet vanes mounted in the exhaust of the midcourse propulsion motor. Deflec-

tion of the jet vanes aligns the direction of the motor thrust with the center of gravity of the spacecraft and thus maintains stability.

Vehicle rate and position are sensed by body-fixed integrating rate gyroscopes. The electrical outputs of the gyros control the positions of the respective jet vanes, as shown in the mechanization block diagram of Fig. 73. The position of each of the four jet vanes is controlled by a position servo consisting of an actuator amplifier, actuator torque motor, and an output-coupled potentiometer for position feedback.

Pitch and yaw corrections require equal deflection of the respective pitch and yaw jet vanes. A roll correction requires a differential deflection on the pitch jet vanes and also on the yaw jet vanes. A positive roll input must then produce equal and opposite voltages at the inputs of the +X, +Y, and -X, -Y actuator amplifiers. This signal inversion is obtained in the roll inversion amplifier. The schematic diagram of the actuator amplifier is shown in Fig. 74.

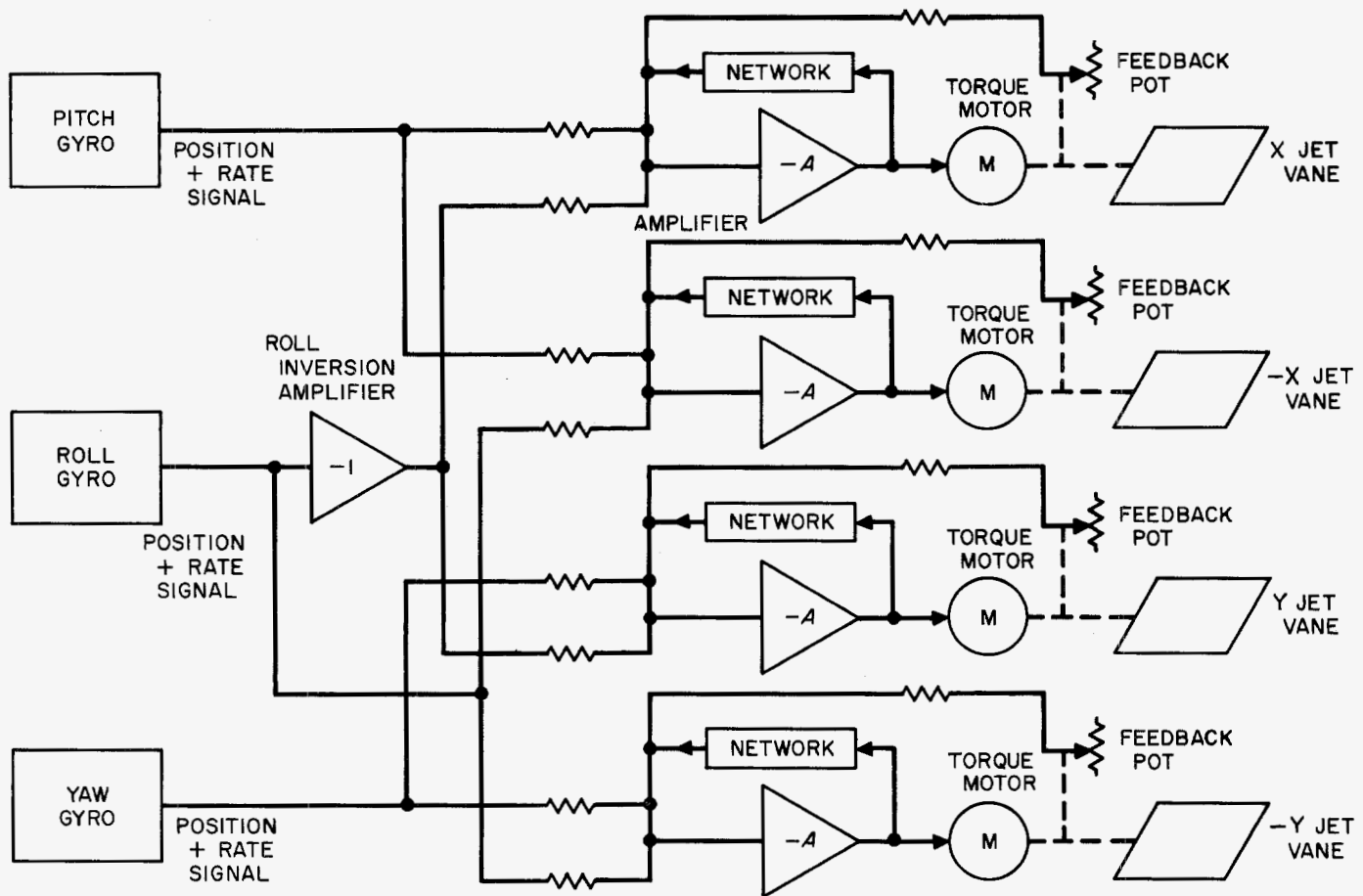


Fig. 73. Autopilot system

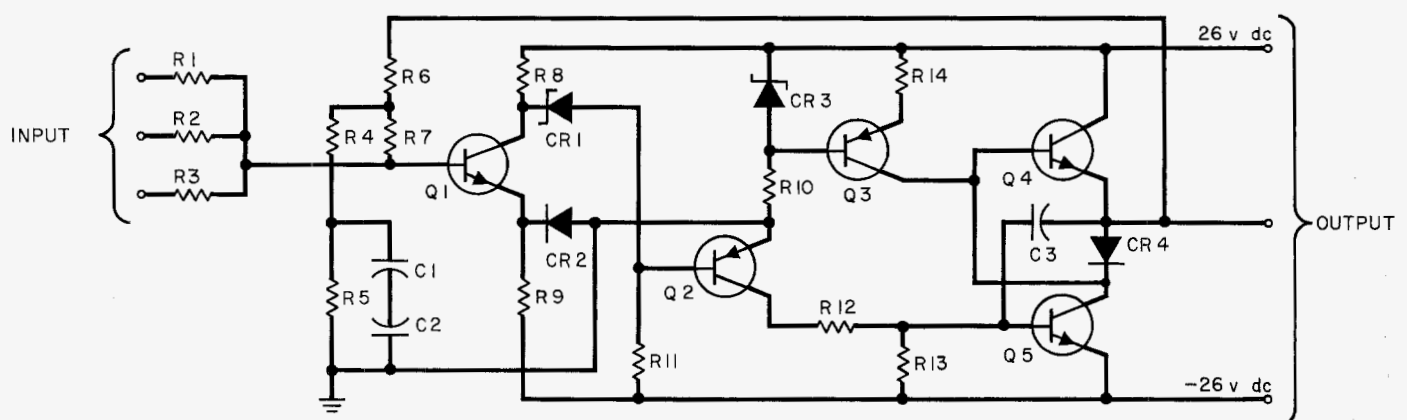


Fig. 74. Actuator amplifier

The amplifier has a d-c current gain of 6500 and a maximum phase lead of 50 deg at 12.5 cps. The maximum power output is 2.7 w with a 150-ohm load. The maximum offset is less than 0.5 v, referred to the 75-k ohm input.

8. Inertial Sensors

The gyro control electronics module and the gyro module comprise the inertial reference system. These two modules are integrated to:

- (1) Supply rate information (i.e., control system damping during the acquisition phase).
- (2) Supply both rate and position information during the commanded turn and midcourse correction autopilot modes.
- (3) Rotate the gyros (and the spacecraft) through precise angles during the command turn mode.

As a consequence of the spacecraft lifetime requirements, the gyros are turned off after acquisition and the spacecraft operates under derived-rate control during the extended cruise periods. This is a departure from the *Ranger* concept and is primarily the result of the limitations existing on the gyro spin-motor bearings.

a. Gyro control electronics module. The gyro control electronics module contains the majority of the circuits for the inertial system. This includes the circuits to provide the gyros with the electronic damping and spring-restraining torque necessary to convert the gyro from a position sensor to an angular rate sensor. To fulfill the system requirements, the control electronics sets the gyro rise time to 100 msec or less. In addition, the control electronics produces the precision command current used to command the spacecraft during the commanded turn mode.

To fulfill the system and gyro requirements, the gyro control electronics module contains the following devices:

- (1) Three electronic capture loops, each consisting of an a-c preamplifier, a double-ring diode demodulator, and a d-c compensation and power amplifier
- (2) A precision command current regulator with a polarity reversing relay
- (3) Twelve 1020- μ f differentiating capacitors to generate the angular position information
- (4) A 10-sec one-shot multivibrator for cycling the above capacitors
- (5) The scale factor resistors for establishing the rate scale factors for the switching amplifier and the autopilot
- (6) A ± 35 -v regulated power supply
- (7) Seven relays for mode switching

All these devices were present in the RA-3 to -5 inertial system, with the exception of the power supplies, which have been added consistent with the *Mariner R* power distribution concept. The pattern field regulator, present in the *Ranger* systems, is not required in *Mariner R* since the Kearfott 2519 gyros employ a permanent-magnet torquer.

Fig. 75 illustrates the electronic block diagram of a single channel of the gyro system. The high-gain pre-amplifier in the electronic capture loop amplifies the 2400-cps suppressed-carrier signal, which is proportional

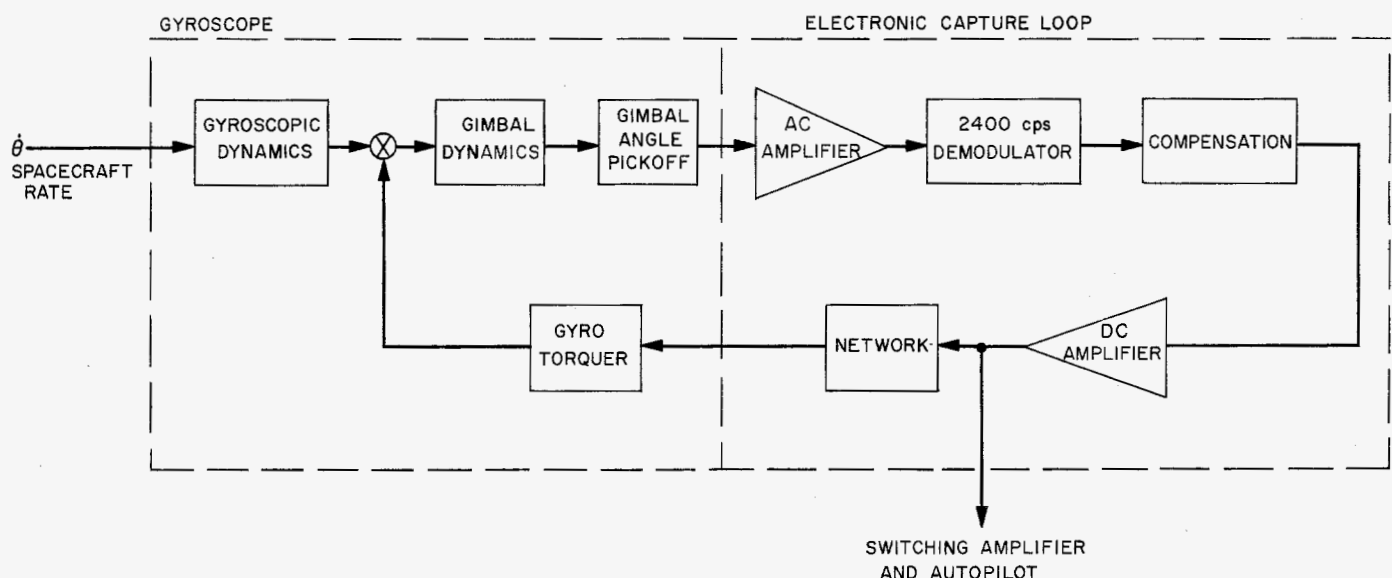


Fig. 75. Gyro loop block diagram

to the gyro output axis angle. The signal is then phase-detected in the demodulator and then power-amplified and compensated in the d-c amplifiers. The resulting signal is fed to the gyro torquers through either the rate or rate plus position scaling networks, and provides the angular rate and position information for the switching amplifier and autopilot as required. Since the current in the gyro torquer control field is proportional to angular rate, only resistors are required in the acquisition and cruise modes to establish the correct voltage-to-rate scaling. In the commanded turn and autopilot modes where position information is required, capacitance and resistance are inserted in series with the gyro torquer to provide a signal proportional to angular rate plus position.

An apparent high-leakage difficulty was initially encountered in the *Ranger* program with the large 1020- μ f tantalum capacitors. This effect was attributed to the fact that nonpolar tantalum capacitors are not expressible as a pure capacitance until an internal charge has been established in the capacitor. If this internal charge is not supplied prior to its use, the capacitor will extract sufficient energy from the applied signal to satisfy its needs, resulting in an apparent leakage current. It was noted that shorting the device does not remove the internal charge. Laboratory tests have demonstrated that the time constant involved in the decay of the internal charge is of the order of 1 day. The one-shot multivibrator, located in the gyro electronics module, provides the timing for the injection of the internal charge into the capacitors. This operation is referred to as "cycling" and is performed 1 hr prior to the roll commanded turn.

The command current regulator supplies a precise torquer current to the appropriate gyro, when commanded. This current is stable to 0.05%. The length of time and the polarity of the current are dependent on the desired direction of the midcourse maneuver and are determined by ground computation.

The gyro control electronics module was designed at JPL and was packaged, fabricated, and environmentally tested at Nortronics, Division of Northrup Corporation. Figures 76 and 77 illustrate a typical gyro control electronics flight module.

b. Gyro module. The most significant feature of the gyro module is the use of the Kearfott D4 or 2519 gyro. This gyro was used in place of the Minneapolis-Honeywell GG-49E12 unit, which is presently used in *Ranger*. The 2519 gyro, which is slightly larger than the MIG

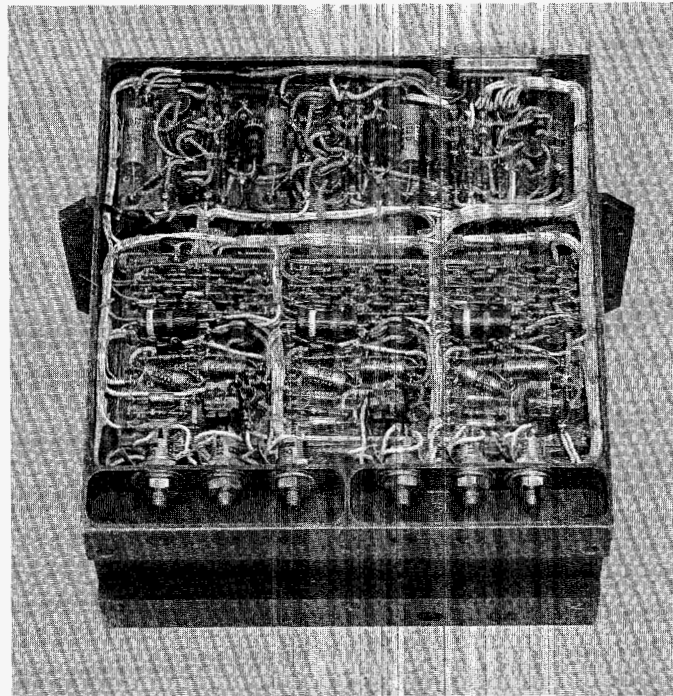


Fig. 76. Gyro control electronics flight module, top view

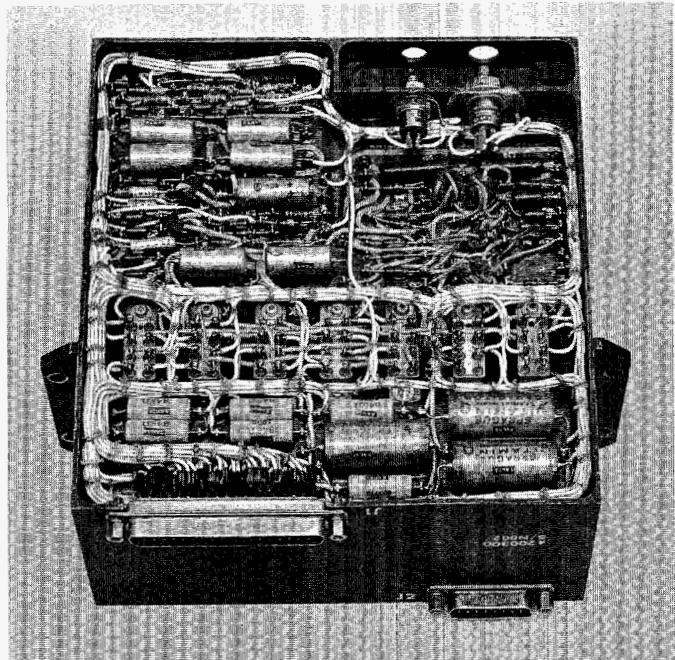


Fig. 77. Gyro control electronics flight module, bottom view

GG-49E12 gyro and has a higher angular momentum, offers a significant increase in performance. As in the case of the GG-49 gyro, the 2519 unit was modified to

reduce the amount of gimbal damping by reduction of the fluid viscosity. The gyro operating temperature was reduced and the instrument operates without the use of gyro heaters. Consistent with the lower operating temperature, the preload on the spin motor bearings was reduced to assure that the performance life is maintained at a 2000-hr minimum. The following indicates the improvement achieved by use of the 2519 versus the GG49E12 gyro:

Performance value	GG-49E12 gyro (Maximum allowable values)	2519 gyro
Mass unbalance drift stability	3.0 deg/hr/g	0.9 deg/hr/g
Mass unbalance drift	2.0 deg/hr/g	0.2 deg/hr/g
Reaction torque drift	2.0 deg/hr	0.5 deg/hr
Reaction drift stability	0.75 deg/hr	0.2 deg/hr
Random drift	0.2 deg/hr	0.2 deg/hr

In designing the gyro module, the gyros were located within the subchassis in a configuration that provides the optimum heat transfer flow paths for each gyro. Inasmuch as the gyro is mounted with end-bell mounting surfaces at each end, the design of the subchassis differs considerably from the earlier *Ranger* gyro module designs. The end-bell mounting method allows all gyros to be installed from one side of the subchassis, leaving the back of the subchassis for the associated electrical components and the connector. Figures 78 and 79 illustrate the *Mariner R* gyro module. As a continuation of the high-reliability component program, all components in the gyro module were screened to JPL specifications.

9. Accelerometer and Electronics

The magnitude of the velocity increment to be added during the corrective midcourse maneuver of the spacecraft is measured by means of a linear accelerometer and integrator combination. Since a digital computer is carried in the CC&S unit and the magnitude of the corrective velocity increment is transmitted digitally from Earth, a digital accelerometer system is required. This system was developed at JPL and is used in combination with the digital computer for midcourse motor shutoff.

This digital accelerometer system consists of a force-balance accelerometer with a pulse-torqued rebalance loop to provide capture current to the proof mass. In this method of operation, the pulsing rate is directly proportional to the applied acceleration and each pulse

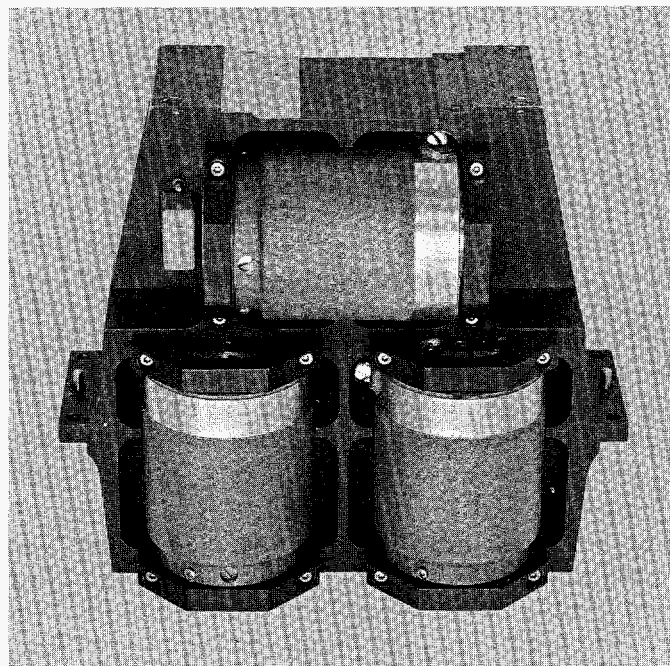


Fig. 78. *Mariner R* gyro module, top view

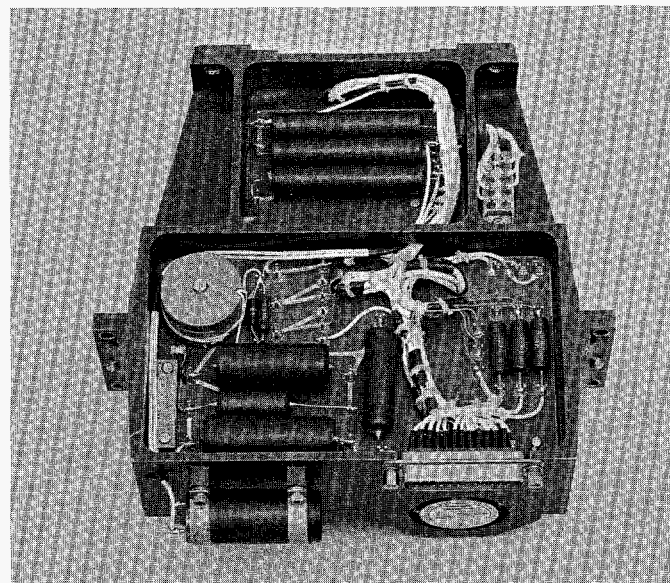


Fig. 79. *Mariner R* gyro module, bottom view

produced represents a constant value of velocity increase (or decrease, depending on the direction of the acceleration). In the *Mariner R* application, this value, or scale factor, will be 0.03 m/sec of velocity increase per pulse.

The accuracy in this type of system is determined to a large extent by how accurately the current pulses to

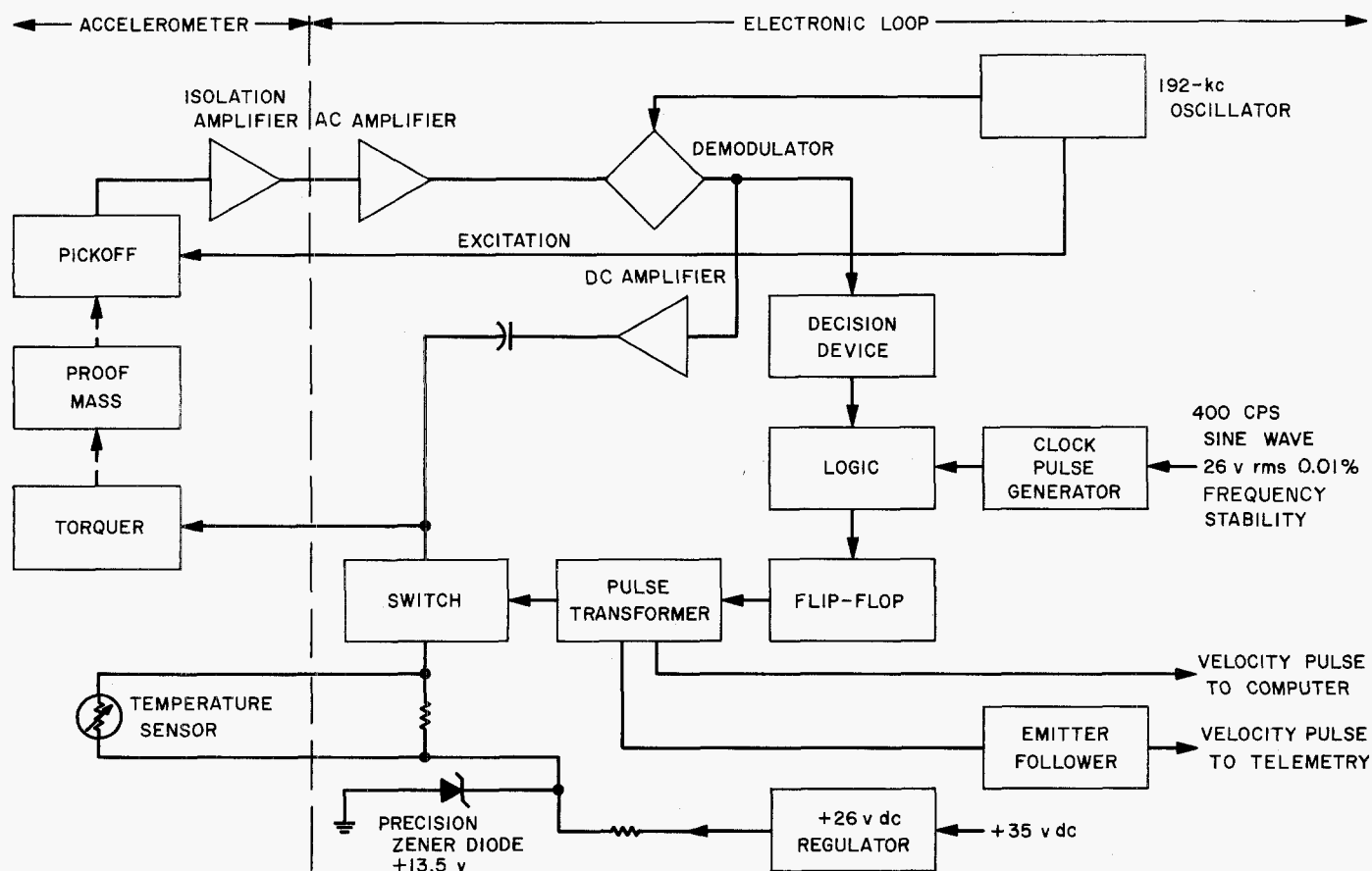


Fig. 80. Accelerometer and electronics, block diagram

the torquer can be generated. The method for developing this pulse in the *Mariner R* system is referred to as the "open loop" system. Basically, this system uses an accurate frequency (from the computer clock) to control the pulse width and an accurate voltage, controlled from a precision zener diode to determine the pulse height. A block diagram of the electronics is shown in Fig. 80.

The accelerometer pickoff is a capacitive type which is excited with 192 kc from an oscillator in the electronics package. This pickoff produces an error signal to the a-c amplifier, which has a gain of 600. The output of the a-c amplifier is coupled through a one-to-one transformer to a double bridge or ring demodulator. The demodulator reference signal is obtained from the same 192-kc oscillator as the accelerometer excitation.

The demodulated error signal is applied to a Schmitt trigger-circuit decision device. This circuit will detect displacement of the proof mass, which, for a predetermined amount of acceleration, will develop a rebalance pulse. When the Schmitt circuit changes state, the

logic circuit will then allow the precision clock pulses to pass through the circuit to the flip-flop. In this circuit, the flip-flop is actually a trigistor. The first positive clock pulse will cause the trigistor to conduct. At 1250 μ sec later, a negative clock pulse returns the trigistor to the non-conduction stage. This on-off action of the trigistor is transformer-coupled to a low-leakage, high-speed transistor switch, which is supplied with a 13.5 v excitation from a precision zener diode. This diode voltage is stable to $\pm 0.01\%$ over a 100°F temperature range.

A current-limiting resistor is placed in series with the switch and zener diode. The value of this resistor is varied as a function of the accelerometer temperature to compensate for the change in accelerometer permanent-magnet torquer characteristics. This torquer has a gain function which changes rapidly with temperature.

Note from the block diagram (Fig. 80) that pulses of only one polarity can be generated. This provides capture in only one direction since the spacecraft can only accelerate in one direction.

The accelerometer has a built-in eddy-current damper associated with the proof mass. Internal damping is not sufficient for restraining the pendulum against vibration, so an additional rate-feedback loop is applied around the accelerometer. This loop uses the same demodulated signal as the decision device. The d-c error signal is amplified by a low-gain, a-c current driver amplifier. Output from this amplifier is capacitor-coupled back to the torquer to produce a current which is proportional to the proof-mass rate of motion. The rate amplifier provides a damping increase of five.

Laboratory testing under constant temperature, no-vibration conditions has shown that the accelerometer system is stable to a 3σ accuracy of 0.03% of applied acceleration. The system can retain capture up to 1 g of acceleration while the expected acceleration of the mid-course maneuver is 0.05 g.

The *Mariner R* accelerometer parameters follow:

Volume: 64 in.³

Weight: 2.4 lb

Power inputs: +35 v dc at 32 ma $\pm 5\%$ regulation
 -35 v dc at 10 ma $\pm 5\%$ regulation
 26 v rms 400-cps, single-phase, 6 ma
 -0.01% frequency stability -5 \pm % voltage stability

Signal inputs: none

Signal outputs: CC&S transistor switch closure for 1250 msec for each ΔV pulse
 Telemetry 5-v d-c level dropping to 0 v dc for 1250 msec for each ΔV pulse. Emitter-follower output at 1.8 kohm output Z. Laboratory test point: accelerometer pendulum position signal

Accuracy: Scale factor = 0.03 m/sec of velocity increase per pulse

One σ : $\pm 0.25\%$ of applied at 0.05 g $\pm 20\%$

Three σ : $\pm 0.75\%$ of applied at 0.05 g $\pm 20\%$

Null offset = $\pm 1 \times 10^{-4}$ z_g 1 σ

Sensitive axis alignment = ± 30 arc-sec to locating pins on accelerometer module

Environmental limitations:

Temperature: Operating, 0 to 70°C
 Non-operating, -55 to 125°C

Vibration: Operating 2 g rms noise

Static acceleration: Operating to above accuracy ± 0.05 g $\pm 20\%$

Operating to maximum capture limit +1.0 g

Nonoperating ± 15 g any axis

10. Long-Range Earth Sensor

The *Mariner R* long-range Earth sensor uses a single photomultiplier tube together with a lens, a fixed aperture, and a modulating mask. The modulating mask is attached to a vibrating reed with a frequency of approximately 22 cps. The electronics associated with the reed and the reed itself operate closed-loop with a position pickoff device such that the reed oscillates at a constant amplitude. The frequency of oscillation is determined by the mechanical resonance of the reed only.

The shape of the reed is shown in Fig. 81. Figure 82 shows the relative position of the optical elements.

The knife edges on the modulating mask are in the focal plane of the optical system. The photomultiplier tube serves only as a light detector and has no position discrimination by itself.

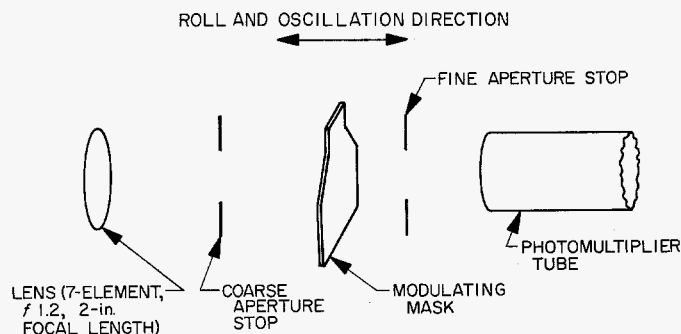


Fig. 81. Relative position of long-range Earth-sensor optical elements, side view

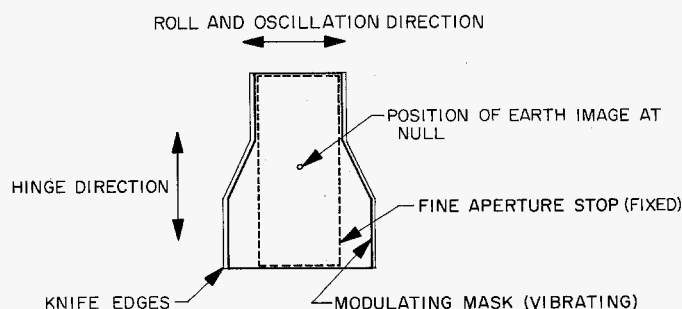


Fig. 82. Relative position of long-range Earth-sensor optical elements, end view

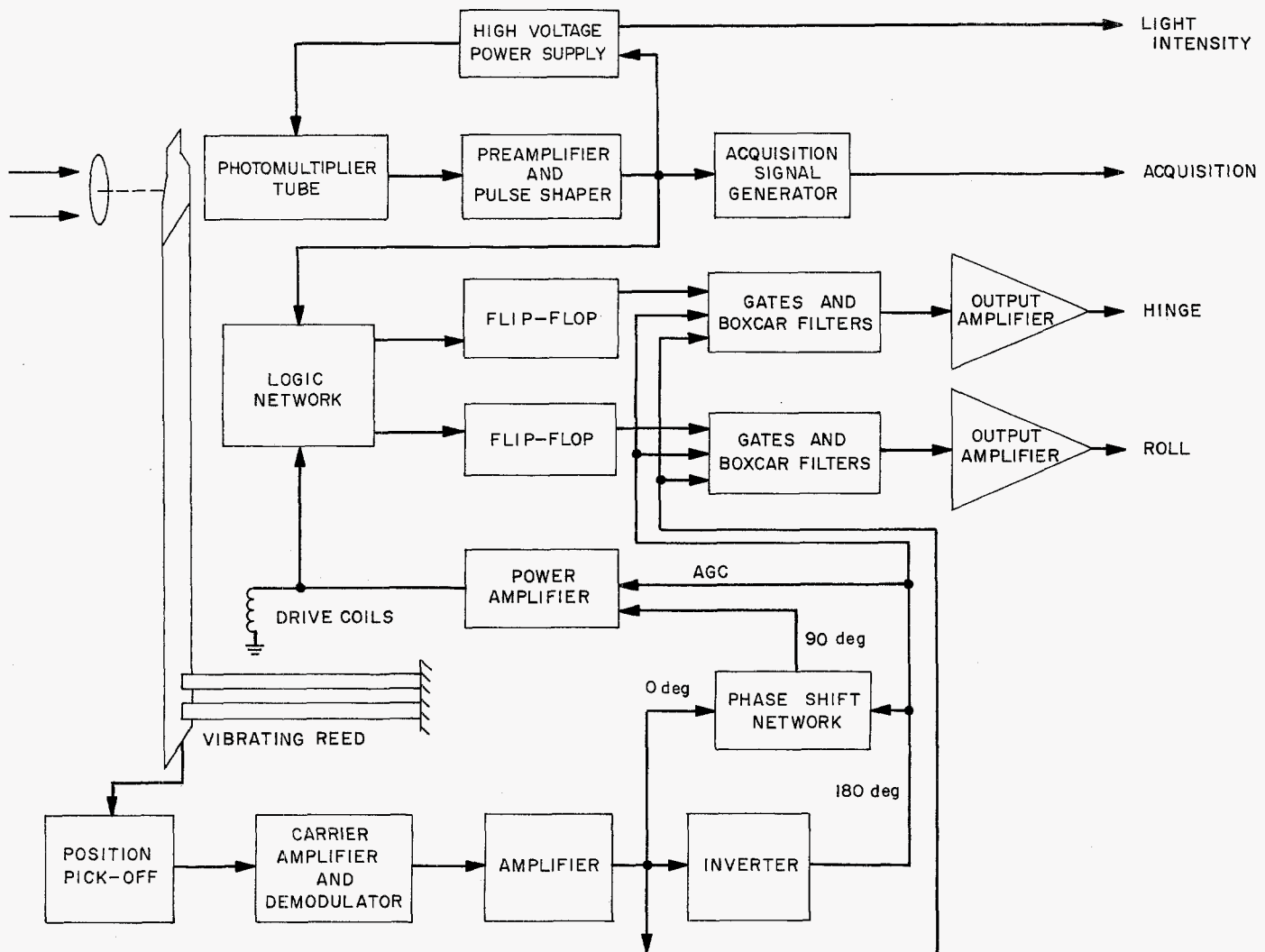


Fig. 83. Long-range Earth-sensor circuit, block diagram

The vibrating reed moves through a sufficient arc to completely uncover the fixed aperture at the extremes of motion. The output, therefore, is a series of pulses. As can be seen in Fig. 82, a shift in the position of the Earth image in hinge causes a variation in the output pulse width. Similarly, a shift in roll causes a variation in the phase (or time) of the output relative to the reed motion. The electronics senses these properties in the pulse chain and at the output produces a d-c voltage proportional to this error. Also present at the output are signals which indicate that an object is being tracked by the sensor and the amount of light being sensed.

The threshold of the unit is approximately 5×10^{-11} w/cm² (bolometric at a color temperature of 6000°K).

The maximum intensity is a function of photomultiplier tube life and has been defined as 5×10^{-7} w/cm². Intensities much higher than this will not affect the tube for short periods of time. With power off, the sensor may be pointed directly at the Sun for extended periods.

The accuracy of the long-range Earth sensor is ± 0.1 deg in roll and ± 0.25 deg in hinge over the range of 0 to 100°F. Expected inflight stability is approximately ± 0.02 deg in roll and ± 0.05 deg in hinge.

Figure 83 is a block diagram of the sensor and Fig. 84 is the schematic. Power dissipation is approximately 6.5 w and total assembled weight is 6.2 lb.

The Earth-sensor parameters follow:

Field of view:	± 2 deg roll, ± 5 deg hinge
Radiant input range:	5×10^{-11} w/cm ² to 5×10^{-7} w/cm ² (bolometric at 6000°K)
Power dissipation:	6.5 w
Weight:	6.2 lb
Null stability (absolute):	0.1 deg 3σ roll
(with reference to external mounting pads)	0.25 deg 3σ hinge
Null drift:	± 0.2 deg roll, ± 0.05 deg hinge
Roll scale factor:	4 v/deg $\pm 10\%$
Hinge scale factor:	2 v/deg $\pm 10\%$
Roll saturation:	4 v $\pm 10\%$
Hinge saturation:	4 v $\pm 10\%$
Acquisition signal:	7 v dc ± 1 v
Light intensity T/M:	0 to -3 v dc
Collecting optics:	7 element f/1.2 2-in. focal length

11. Sun Sensors

a. *Acquisition primary Sun sensors.* The *Mariner R* Sun sensors are identical to the *RA-1* and *-2* types. The Sun-sensor parameters are:

Detector numbers G, L, A and F
Slope through null (scale factor): 9.7 v/deg
Resistance and power dissipation of detector at null:
Chilao: 7000 ± 200 ohms, 0.037 w
Space: 6000 ± 200 ohms, 0.041 to 0.044 w
Venus: 4.2 to 4.4 k ohms, 0.058 to 0.061 w
Mars: 8.8 to 9.4 k ohms, 0.027 to 0.029 w
Field of view: 45 deg
Width of sensitive strip: 0.050 ± 0.002 in.
Length of lever arm: 11/16 in.
Weight: 29.8 g

b. *Sun gate.* The Sun-gate parameters follow:

Detector numbers S and T
Scale factor: approximately 3 k ohm/deg at 0.5-deg points
Resistance and power dissipation of gate at null:
Chilao: 3.4 k ohms, 0.0092 w
Space: 3.0 k ohms, 0.010 w
Venus: 2.2 k ohms, 0.007 w
Resistance of gate at ± 2.5 deg points:
Chilao: 6.4 k ohms
Space: 5.5 k ohms

Venus: 4.0 k ohms

Mars: 8.5 k ohms

Field of view: 2.5 deg

Weight: 48 g/unit

Sun-gate characteristics are shown in Fig. 85.

12. Gas System

The *Mariner R* gas system incorporates many basic changes when compared to early *Ranger* systems, which were integral with the spacecraft bus and presented many problems when rework was necessary. Cleanliness, which is paramount to the gas systems, was difficult to achieve and maintenance was difficult to provide on the integral system. Also, the numerous mechanical joints in the *Ranger* gas system plumbing were not conducive to an optimally leak-tight system. The *Mariner* design approach, therefore, was to package the gas system as a strap-system and to reduce the number of mechanical seals.

The *Mariner R* gas system is a unitized, all-metal assembly with all but two welded joints. Two 8-in. pressure vessels capable of storing 4.34 lb of gaseous nitrogen feed a single-stage pneumatic regulator, which supplies low-pressure gas to 10 attitude control jets. The pressure vessels are made from 6 AL 4V titanium alloy and feature lightweight construction. Each vessel is sealed to its mated fitting by virtue of a metal crush gasket. The regulator reduces the vessel pressure, 3300 psi initially, to a range of 15 ± 0.8 psi for use by the control jets. The regulator also includes a safety relief valve which opens at 20 psi. The control jets, which are the metal ball-poppet type, are clustered into two 3-valve assemblies for pitch and roll control, and two 2-valve assemblies for yaw control.

The two pitch valves provide single-torque control and, because they are mounted on opposite sides of the spacecraft and point toward the Sun, they give a small translational component to the trajectory. The control jets provide a nominal acceleration of 0.225 mrad/sec² about each axis. The mass flow rate during jet on-time is nominally 2×10^{-4} lb/sec, providing thrust levels of between 3 to 5 g. The opening time response requirement for all valves was 10 ± 1 msec and the closing time requirement for all valves with a suppression diode across the valve was 20 ± 2 msec. When the valve is pulsed with a 20-msec excitation signal, the output pulse is equivalent to approximately 30 msec of steady state on time.

000000000000

UNCLASSIFIED

UNCLASSIFIED

000000000000

UNCLASSIFIED

000000000000

UNCLASSIFIED

UNCLASSIFIED

UNCLASSIFIED

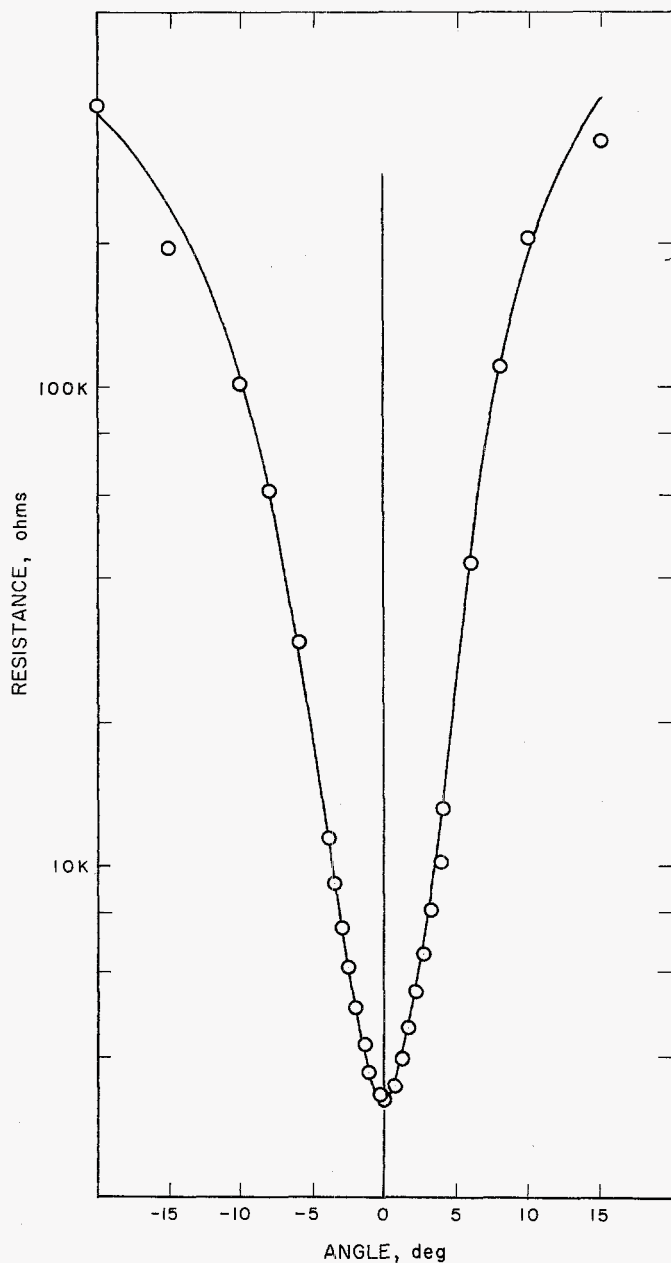


Fig. 85. Characteristics of Sun gate

The cleanliness level achieved on the *Mariner R* gas system is thought to be below the $5\text{-}\mu$ particle level. Heliarc welding of the component parts is accomplished under ultraclean conditions, with the argon purging and arc shield media being taken directly from a liquid supply and filtered to $2\text{ }\mu$ nominal. After final system checkout and up to the time of final system pressurization before flight, the gas system is charged through a series 5 to $2X\text{ }\mu$ filter.

13. Attitude Control System Problems

a. Gyro module relay failure. During system verification of MR-1 and -2 at AMR, the 3-phase power switching relay in each gyro module failed in both spacecraft. The best information available after considerable test on the MR-3 spacecraft indicated that the Clare relay used in this application had a greatly reduced lifetime, but would be adequate for flight.

The tests run on MR-3 did not indicate any single condition which could cause a discrete failure. However, these tests did show that deterioration could result, and therefore, degrade the usable lifetime of this component. As a consequence of these failures, current-limiting resistors were added to alleviate the deterioration experienced in this application. In addition, all information on the environment experienced by this relay was sent to Clare for evaluation. The test results are incomplete; however, the lifetime of this relay in this application is less than 10,000 operations. To ensure flight reliability, using the information at hand, a new relay was obtained for the MR-1 gyro module, using X-ray photographs.

b. Gyro pivot and jewel clearance problem. Comparisons of laboratory tests of the Kearfott 2519 gyro, in both open-loop and closed-loop conditions, with results predicted from the assumed dynamic model, indicated considerable differences in empirical and analytical performance. These differences were displayed as:

- (1) Apparent nonlinearities evidenced by the nature of the transient response to torquer current steps during closed-loop operations.
- (2) Differences in the transient response of the gyro to torquer current steps between spin motor on and off conditions.
- (3) Variations in the nature of the transients as a function of gyro orientation during closed-loop tests.
- (4) Variations in both gyro gain and gyro dynamics under open- and closed-loop conditions.

Subsequent examination of a dynamic model of the gyro, which included consideration of the Kearfott 2519 pivot and jewel clearance, illustrated this to be the problem area and permitted the above effects to be explained. When the pivot and jewel are not in contact—i.e., when the pivot moves under precessional torques from one

UNCLASSIFIED

side of the jewel through the gap to another point of contact—the unit operates as a free, rather than a single-axis gyro. As a result, it displays major dynamic differences.

An analog computer simulation of the gyro and loop was prepared. This representation demonstrated good correlation with the 2519 gyros then at JPL and was used to establish recommendations to Kearfott on pivot and jewel clearances for the *Mariner R* gyros. As a result, a jewel and pivot clearance of 25 to 50 μ in. was determined to be an optimum value. Since previous jewel and pivot tolerances provided for a clearance of 300 to 500 μ in., the proposed change uncovered certain deficiencies in both manufacturing and measuring techniques. Initial units were kept reasonably close to delivery schedule by matching pivots and jewels using a special test fixture developed by Kearfott. As a consequence of this program, the first three 2519 units delivered to JPL had a greatly improved response characteristic.

c. Autopilot solar panel interaction problem. Investigation with the six-dimensional autopilot simulation disclosed a saturation of the yaw gyro during midcourse maneuver. A series of parameter variation studies was undertaken to define the nature and extent of the problem.

The basic cause of the problem was determined to be the unbalanced mass and mass distribution of the two solar panels, which are hinged parallel to the yaw axis. *Mariner R* has an extra 5 lb of solar cells added to one panel. The panel mass is increased from 22 to 27 lb, but the placement of this additional mass as an extension of the normal panel increases the moment of inertia about the hinge axis by a factor of two. With equal mounting and actuator stiffness, this reduces the cantilevered natural frequency of the larger panel to 71% of the other panel, giving nominal frequencies of 1.4 and 2.0 cps. The spacecraft has a free-body resonance in yaw between these two frequencies; therefore, the closed-loop resonance with the autopilot acting is only slightly higher in frequency, and measured 1.8 cps in the simulation.

A further consequence of the unbalanced masses of the solar panels is that the total system center of mass is shifted in the X-direction from the center of mass of the spacecraft without solar panels. The midcourse motor is mounted under the X-center of mass of the total system. When the motor first fires, the panel hinges cannot transmit torque about their axes, and as a result, the effective mass of the solar panels is reduced. With the reduced effective mass of the panels, the effective center of mass

of the system shifts toward the center of mass of the spacecraft without solar panels. Thus, the motor thrust initially has a moment arm about the effective center of mass.

The mechanism of the yaw gyro saturation involves these spacecraft properties in the following sequence:

- (1) The midcourse motor fires. The initial moment arm about the effective X-center of mass causes the central body of the spacecraft to rotate about the yaw axis. The spacecraft central body accelerates in the Z-direction.
- (2) Reaction torques are transmitted through the hinges as the angles of the solar panels relative to the central body increase. The angle of both panels increases due to the Z-acceleration of the spacecraft central body. The central body rotation from the first step above causes the angle of the heavier panel to increase faster than the angle of the lighter panel.
- (3) The panel angles, and consequently the reaction torques, increase to a maximum as the panels swing back. The reaction torques of the two panels are in opposite directions, but due to the unbalanced masses and different cantilevered frequencies, there remains a large net peak torque.
- (4) This large transient of reaction torque excites the free-body resonances of the yaw axis. The initial oscillations of the panels at their cantilevered frequencies quickly became 180 deg out-of-phase, with the result that their reaction torques were in-phase. This produced another source of large net torques on the central body, and further excited the free-body resonance.
- (5) The free-body oscillations in yaw produce peak angular rates of over 20 mrad/sec. The gyro, however, can take less than 9 mrad/sec before saturating the gyro amplifier. Once the amplifier is saturated, control of the gyro gimbal angle is lost, which results in swinging the gimbal over to hit its mechanical limit. As the rate due to the oscillation peaks and returns below the saturation level, the gyro gimbal loop recaptures and again operates linearly. The gyro output to the autopilot is a clipped sine wave, with some transient effects when the amplifier comes out of saturation.

UNCLASSIFIED

Conclusions as to the effects of gyro saturation based on the above simulation, were:

- (1) The gyro saturation does not appreciably degrade autopilot stability. The autopilot would have been better able to damp the oscillations if the gyro did not saturate, but it still provided damping and remained quite stable.
- (2) The simulated gyro saturation did not degrade autopilot accuracy.
- (3) The gyro itself was not damaged by the saturations.

In view of these conclusions, it was decided to fly MR-2 with unbalanced solar panels, since the spacecraft was already assembled in flight configuration.

The parameter variation studies indicated that equalizing cantilevered natural frequencies of unequal solar panels would reduce the severity of the problem. This would be done by adjusting the stiffness of constraint about the hinge. However, a large transient of torque was still generated by unbalanced mass moments.

Gyro saturation is not a desirable situation, and conclusions of necessary actions to avoid this problem on future spacecraft are, whenever possible, to:

- (1) Place flexibly attached members symmetrically with respect to the central body.
- (2) Make their mass moments about the center of mass equal.
- (3) Make their cantilevered natural frequencies equal.

d. Attitude control power switching transient. As a consequence of system verification tests on the spacecraft, a transient in the data encoder subsystem was noted when attitude control power turn-on was initiated. This attitude control subsystem transient caused the data encoder subsystem to drop data system lock. The transient was the result of switching the attitude control power supply before the rectifiers and introducing a surge on the primary 2400-cps spacecraft power supply. This switching resulted in the charging of two 150- μ f filter capacitors which caused the 2400-cps spacecraft primary voltage to drop from 52 v rms to approximately 5 v rms over a 100- μ sec time interval.

To eliminate this power supply transient, the power switching of the attitude control subsystem was changed. The switching at the initiation of A/C-5A is now done on the load side of the attitude control T-R unit. The transient has now effectively been shifted in time to the initial spacecraft power turn-on event, in place of the A/C-5A event.

e. Gas system

(1) *Leakage.* Three gas system assemblies for attitude control were fabricated; the fourth and last system is not complete. Before shipping the spacecraft to AMR, a 48-hr quantitative leak test was conducted on each gas system at the Pasadena facility. Each system, together with a leak-test console, was pressurized to 3500 psi during the test. The leak rates of gas systems designated No. 2 and No. 3 were within the maximum permissible leak rate specification of 30 standard cc/hr and had rates of approximately 22 and 4 cc/hr, respectively. However, system No. 1 indicated a gross leak rate of several hundred cc/hr. Investigation revealed gross internal leakage from a pitch control valve. To investigate the possibility of contamination particles holding the poppet of the valve from fully engaging its seat, the valve was actuated several times with the system pressurized in an effort to blow the valve clear. The leakage rate diminished to approximately 22 cc/hr after repeated actuations, confirming contamination and lack of mechanical damage or wear. Subsequently, this valve unit was changed.

(2) *Contamination disclosure.* Each gas system is supplied with a series 5- and 2- μ inlet filter assembly. These filters have absolute ratings of 17 and 8 μ , respectively. The filter assemblies are not flight hardware, but provide a safety feature to reduce contamination potential during charging and operation assembly.

During spacecraft system tests and evaluations, the filter assembly is at times removed (i.e., vibration environmental tests, cg and inertial testing) from the system. Possible mishandling of the filter assemblies, while they were removed, on gas systems 1 and 2 resulted in questionable reliability of these two systems. This possibility arose at the time when the systems were in preparation for shipment to AMR. Investigation of system 1 was initiated by removing the pressure vessels and running filtration samples on the vessels and the high-pressure circuit. The vessels were found to contain a number of foreign particles in the 100- to 500- μ size. Filter samples taken at each bottle fitting, by flowing gas from the

UNCLASSIFIED

JPL TECHNICAL REPORT NO. 32-353

charging port to the fittings, revealed less contamination with low particle counts in the 10- to 50- μ size. After gas flushing, the high-pressure circuit filtration samples indicated particle size below 5 μ .

The system was broken down further by cutting out each of the four jet valve assemblies from the system. Each jet valve assembly has a 10- μ inlet filter which was checked for contaminants. Three of the filters were found to be relatively clean, with particles measuring 10 μ or less. The fourth filter had entrapped contaminants up to 60 μ in size and, in addition, a small piece of black string. After the low-pressure system was flushed with nitrogen gas, the system plumbing exhibited particle contamination below 5 μ .

Following this segment of the investigation, the pressure vessels were explored further to determine whether the contamination found in the vessels had been self-generated or introduced externally. The pressure vessels used on the *Mariner R* program are of the unweld type, with an internal back-up ring at the weld joint. The coupling to the vessel is accomplished with a special fitting and a crush metal seal. The inlet hole diameter is 0.152 in., making the cleaning operation of the vessels difficult. A syringe is used to inject cleaning solvent into the vessel and then a vacuum is used to withdraw the solvent from the vessel through a millipore filter. Repeated flushes and filter examinations are conducted until the cleanliness level of the vessel is 5 μ or less, with attempts continuing to eliminate *all* contamination. If the vessels contained residual contaminants after cleaning, subsequent pressurization and possibly vibration would loosen these contaminants and allow them to enter critical areas.

After cleaning the two vessels which were found to contain contaminants, the vessels were prepared for a shake test. One-half pint of cleaning solvent was placed in the vessels and each vessel was pressurized to 3000 psi during the test. One vessel was subjected to 6.2 g and the second vessel to 10 g through the frequency range of 50 to 1000 cps along the vessel axis. Following the shake test, the cleaning solvent from each vessel was examined and found to contain no contamination above the 5- μ level. This revelation substantiated the theory that the contamination was externally introduced and not self-generated. This result further establishes the conclusion that the cleaning process used on these vessels, while in no way sophisticated, ensures retention of cleanliness levels after the vibration environment.

E. Telecommunications System

1. Introduction

The telecommunications system was designed to provide two-way doppler, automatic angle tracking, command, and scientific and engineering data transmission. This Section discusses the flight telemetry equipment for the *Mariner R* spacecraft, and also the associated ground support equipment. Since the Read-Write-Verify command subsystem is used to send commands in the launch configuration, it is also discussed in this Section.

2. General System Requirements

The telecommunications subsystem must accommodate scientific data and the engineering measurements required for system evaluation in a reliable yet flexible manner. The limited bandwidth available on an interplanetary mission implied the capability of adding or deleting measurements as a function of specific flight phases, thus transmitting some data only when they are needed.

In addition to telemetry, the telecommunications subsystem had to provide an Earth-to-spacecraft command link for the initiation and modification of various spacecraft functions. The subsystem had to also provide two-way doppler information for accurate trajectory determination, and allow automatic angle-tracking of the spacecraft at the receiving sites.

A study of the possible Earth-Venus trajectories revealed that the telecommunications subsystem had to be capable of operating over a distance of 6×10^7 km. A prediction of the maximum available communications system capacity at this distance showed that a telemetry system with variable data transmission rate was required.

At launch and until such time as attitude control was achieved, communications could not depend on the high-gain directional antenna; so it was necessary to provide an omnidirectional antenna system, which was also required to receive information on spacecraft performance during the midcourse maneuver.

A further telecommunications subsystem requirement was that it had to be compatible with, and utilize to the fullest extent possible, the existing Deep Space Instrumentation Facility. Compatibility with the DSIF requires

UNCLASSIFIED

that the R-F carrier be phase-modulated, that the modulation spectrum be confined within certain limits, and that the modulation not completely suppress the carrier. The latter requirement was necessary to ensure automatic angle-tracking and receipt of the required two-way doppler.

In order to utilize the most efficient digital modulation technique, phase-shift key was chosen. It has been conclusively proved that the so-called binary-symmetric channel, or the conveyance of information in the state of one of two possible orthogonal conditions, is the most efficient digital means of communication. It has also been shown that biphase modulation is the simplest and perhaps the best mechanization of such an orthogonal system.

Demodulation was performed by a coherent system using matched-filter detection. Both systems may be described as PCM/PSK/PM, since the binary data waveform phase-shift keys or biphase modulates the subcarrier, which in turn phase-modulates the R-F carrier. The use of subcarrier techniques was necessary to keep the telemetry system compatible with the DSIF receiving systems and the command system compatible with the spacecraft transponder receiver.

Tables 5 and 6 indicate the estimated communication and telemetry performance for the MR-2 spacecraft at encounter over Goldstone. The established criterion for acceptable predicted performance of a communications or telemetry channel is that the nominal performance margin equals or exceeds the sum of the adverse tolerances. Using this criterion and assuming that the system is performing within tolerance, it can be said that the probability is unity that the system will perform to specification. Further loss of performance margin results in the probability of adequate system performance decreasing as a function of the probability distribution that can be applied to the tolerances.

Inspection of the design control table for the spacecraft-to-Earth channel (Table 5) reveals a more than adequate performance margin under the previously mentioned criterion. However, upon inspection of the table for the Earth-to-spacecraft channel (Table 6), it is obvious that this criterion is not met. The fact that the criterion for command capability at encounter would not be met was known before the flight and, therefore, the requirement for command capability at encounter was removed.

However, further investigation of the criterion invoked to define command-channel performance reveals that

the situation is not as bad as it might appear. The definition of acceptable system performance includes the requirement that the maximum bit error rate not exceed 1 part in 10^5 , as well as the requirement that, given a command was sent, the probability will exceed 0.999 that the command will not be inhibited by the quadrature channel in the command detector.

The command detector mechanization is set to inhibit the receipt of a command when the signal-to-noise is low enough to cause the detector to lose synchronism. System tests show that, as a result of the inhibit action, operation at signal-to-noise ratios as much as 3 db below the defined threshold result in only a reduced probability that the command will be admitted rather than an increase in error rate over the 1 in 10^5 bits. Thus, at this point, a given command could be executed by sending it a sufficient number of times.

Therefore, if the system tolerances break reasonably symmetrically, command capability would exist at encounter under a relaxed definition of acceptable performance.

3. System Implementation

a. System Description

Within the bounds of the foregoing requirements, a telecommunications system has been implemented. The flight system consisted of a data encoder, a transponder, a command assembly, antennas, and transducers. Associated with the flight system is the ground support equipment used to verify proper operation of flight components. Figure 86 shows the functional block diagram of the spacecraft telecommunications subsystem and the associated ground support equipment.

The encoder multiplexes engineering and scientific data. It has three operational modes and two data rates. During Mode I (launch), only engineering data are sampled. In Mode II (cruise), engineering and scientific data are processed, while in Mode III (planetary encounter), only scientific data are processed. The engineering data are in two forms: analog signals which are digitized to 7-bit accuracy, and parallel-shifted digital command data.

The scientific data are in serial digital form. Each of these signals, when sampled, is used to biphase-modulate a carrier generated in the encoder.

Table 5. Telecommunication design control MR-2 spacecraft-to-Earth channel Goldstone (Pioneer); maser-Cassegrain listen — undiplexed at encounter

No.	Parameter	Value ^a	Tolerance	No.	Parameter	Value ^a	Tolerance
1	Total transmitter power	+ 34.58 dbm	+0.00 -2.00 db		Carrier performance—tracking (two-way)		
2	Transmitting circuit loss	- 0.25 db	±0.05 db	19	Threshold SNR in $2B_{LO}$	+ 2.00 db	—
3	Transmitting antenna gain	+ 19.60 db	±0.60 db	20	Threshold carrier power	-167.42 dbm	+1.46 -1.77 db
4	Transmitting antenna pointing loss	- 0.33 db	+0.33 -0.10 db	21	Performance margin	+ 16.61 db	+3.67 -5.13 db
5	Space loss @ 960 mc, $R = 5.78 \times 10^7$ km	-247.33 db	—		Carrier performance—telemetry		
6	Polarization loss	- 0.00 db	+0.00 -0.08 db	22	Threshold SNR in $2B_{LO}$	+ 4.00 db	—
7	Receiving antenna gain	+ 45.50 db	±0.50 db	23	Threshold carrier power	-165.42 dbm	+1.46 -1.77 db
8	Receiving antenna pointing loss	—	—	24	Performance margin	+ 14.61 db	+3.67 -5.13 db
9	Receiving circuit loss	- 0.10 db	Maximum		Data channel		
10	Net circuit loss	-182.91 db	+1.48 -1.33 db	25	Modulation loss	- 4.30 db	+0.47 -0.40 db
11	Total received power	-148.33 dbm	+1.48 -3.33 db	26	Received data subcarrier power	-152.63 dbm	+1.95 -3.73 db
12	Receiver noise spectral density (N/B) $T_{system} = 41.37^\circ K$	-182.43 $\frac{dbm}{cps}$	+0.67 -0.80 db	27	Bit rate (1/t)	+ 9.21 db·bps	±0.00 db
13	Carrier modulation loss	- 2.48 db	+0.42 -0.34 db	28	Required ST/N/B	+ 8.40 db· cps/bps	±1.20 db
14	Received carrier power	-150.81 dbm	+1.90 -3.67 db	29	Threshold subcarrier power	-164.82 dbm	+1.87 -2.00 db
15	Carrier APC noise $BW (2B_{LO} = 20.0 \text{ cps})$	+ 13.01 db·cps	+0.79 -0.97 db	30	Performance margin	+ 12.19 db	+3.95 -5.60 db
	Carrier performance—tracking (one-way)				SYNC channel		
16	Threshold SNR in $2B_{LO}$	+ 0.00 db	—	31	Modulation loss	- 16.34 db	+0.25 -0.38 db
17	Threshold carrier power	-169.42 dbm	+1.46 -1.77 db	32	Receiver SYNC subcarrier power	-164.67 dbm	+1.73 -3.71 db
18	Performance margin	+ 18.61 db	+3.67 -5.13 db	33	SYNC APC noise $BW (2B_{LO} = 0.5 \text{ cps})$	- 3.01 db·cps	±0.40 db
				34	Threshold SNR in $2B_{LO}$	+ 8.00 db	±1.00 db
				35	Threshold subcarrier power	-177.44 dbm	+2.07 -2.20 db
				36	Performance margin	+ 12.77 db	+3.93 -5.78 db

^aValues carried to two decimal places to retain computational accuracy when taking anti-logarithms.

In addition to multiplexing and conditioning data, the encoder generates a pseudo-random code and a subcarrier frequency. The data biphase-modulates the carrier, and the synchronizing signal is linearly added to the phase-modulated signal. The composite signal is used to modulate the transmitter.

The encoder GSE has four main functions that are used to checkout the data encoder. It provides power, monitors outputs, generates mode and rate change commands, and simulates data inputs. There are three possible connections to the data encoder: (1) the encoder may be mounted on the pull-out drawer of the GSE; (2) the

Table 6. Telecommunication design control MR-2 Earth-to-spacecraft channel
Goldstone (Echo); 10-kw horn — undiplexed at encounter

No.	Parameter	Value	Tolerance	No.	Parameter	Value	Tolerance
1	Total transmitter power	+ 70.00 dbm	±0.08 db		Carrier performance—tracking (two-way)		
2	Transmitting circuit loss	— 0.60 db	±0.20 db	19	Threshold SNR in $2B_{LO}$	+ 4.60 db	—
3	Transmitting antenna gain	● 45.20 db	±0.90 db	20	Threshold carrier power	—141.4 dbm	+2.00 —1.00 db
4	Transmitting antenna pointing loss	—	—	21	Performance margin	+ 5.06 db	+5.48 —6.43 db
5	Space loss @ 890 mc, $R = 5.78 \times 10^7$ km	—246.68 db	—		Carrier performance—command		
6	Polarization loss	— 0.00 db	+0.30 —0.28 db	22	Threshold SNR in $2B_{LO}$	+ 10.00 db	±1.00 db
7	Receiving antenna gain	+ 5.50 db	±1.00 db	23	Threshold carrier power	—136.00 dbm	+3.00 —2.00 db
8	Receiving antenna pointing loss	— 6.00 db	±1.50 db	24	Performance margin	— 0.34 db	+6.48 —7.43 db
9	Receiving circuit loss	— 0.55 db	±0.10 db		Data channel		
10	Net circuit loss	—203.13 db	—3.98 +4.00 db	25	Modulation loss	— 8.48 db	+0.28 —0.25 db
11	Total received power	—133.13 dbm	+4.08 —4.06 db	26	Received data subcarrier power	—141.61 dbm	+4.36 —4.31 db
12	Receiver noise spectral density (N/B)	—159.01 $\frac{\text{dbm}}{\text{cps}}$	+2.00 —1.00 db	27	Bit rate (1/t)	+ 0.00 db·cps	±0.00 db
	$T_{\text{system}} = 9130^\circ \text{K}$			28	Required ST/N/B	+ 17.70 db· cps/bps	±1.00 db
13	Carrier modulation loss	— 3.21 db	+0.40 —0.37 db	29	Threshold subcarrier power	—141.31 dbm	+3.0 —2.0 db
14	Received carrier power	—136.34 dbm	+4.48 —4.43 db	30	Performance margin	— 0.30 db	+6.36 —7.31 db
15	Carrier APC noise BW ($2B_{LO} = 20.0$ cps)	+ 13.01 db·cps	Included in No. 12		SYNC channel		
	Carrier performance—tracking (one-way)			31	Modulation loss	— 5.41 db	+0.29 —0.41 db
16	Threshold SNR in $2B_{LO}$	+ 0.00 db	—	32	Receiver SYNC subcarrier power	—138.54 dbm	+4.37 —4.47 db
17	Threshold carrier power	—146.00 dbm	+2.00 —1.00 db	33	SYNC APC noise BW ($2B_{LO} = 2.0$ cps)	+ 3.01 db·cps	±0.2 db
18	Performance margin	+ 9.66 db	+5.48 —6.43 db	34	Threshold SNR in $2B_{LO}$	+ 17.70 db	±1.0 db
				35	Threshold subcarrier power	—138.30 dbm	+3.2 —2.2 db
				36	Performance margin	— 0.24 db	+6.57 —7.67 db

encoder may be mounted to the spacecraft and connected through the direct-access connector; or (3) the encoder may be in the launch position and be connected only through the umbilical connector. When the encoder is mounted on the spacecraft, the GSE no longer simulates inputs but may still generate mode and rate commands and monitor the data output. When the spacecraft is in

the launch position, only limited commands may be sent by the GSE and it retains its data monitoring function.

The flight command assembly is divided into three functional units: (1) the command detector, which filters and demodulates the PSK subcarrier and extracts the bit timing pulses; (2) the command decoder, which decodes

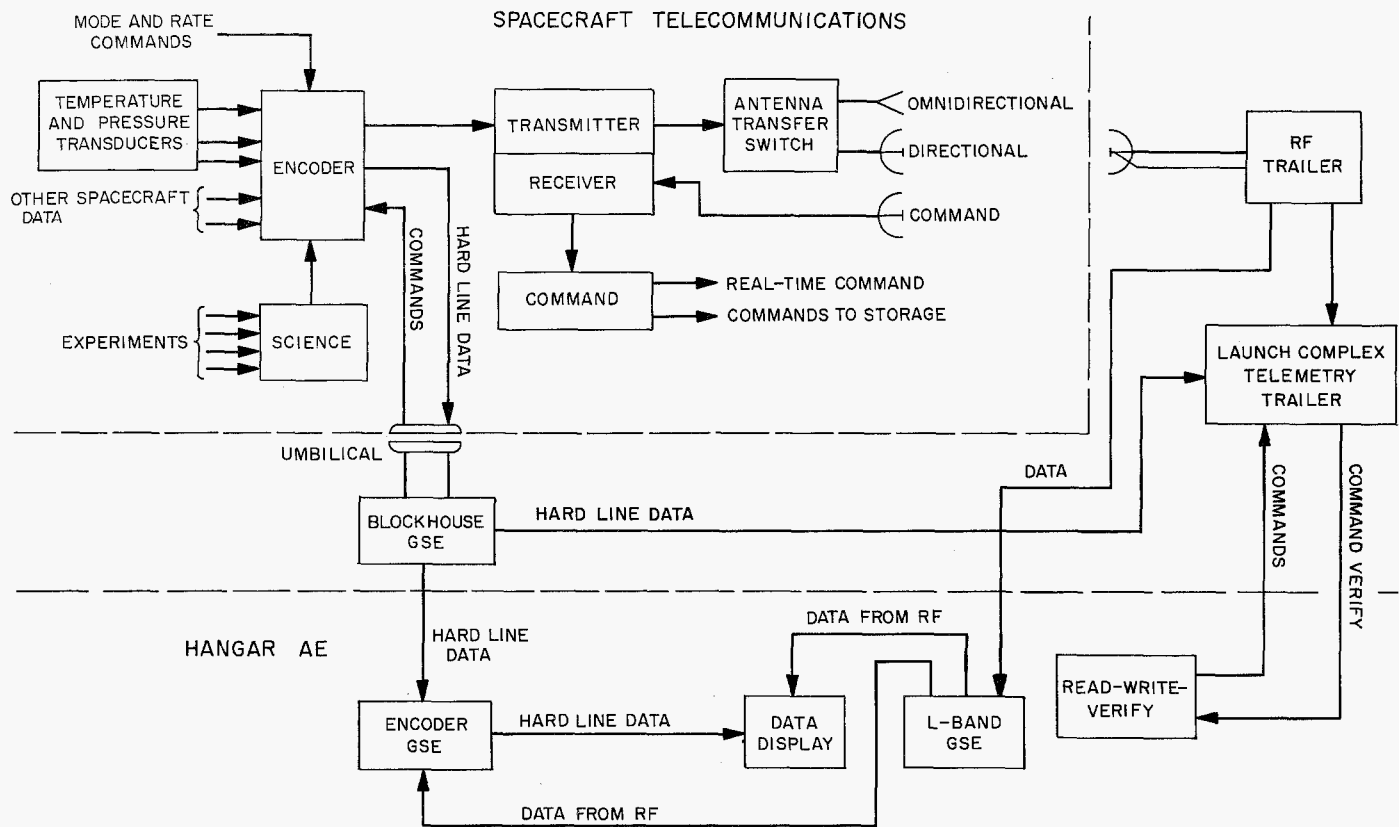


Fig. 86. Telecommunications system launch configuration

the commands and supplies both the commands and appropriate timing pulses to the command users; and (3) the transformer-rectifier.

The command information is transmitted via a coherent PSK subcarrier frequency with the reference signal transmitted in the form of a PN code. The command detector separates the command and reference signals. The filtered reference is used to demodulate the command information coherently and the command bits are detected in a matched filter. The detected binary pulse train is routed along with bit timing pulses to the command decoder.

The command decoder inputs are bit sync, delayed sync, out-of-lock, and command word. The decoder outputs are thus isolated-step or isolated-pulse switches, as required. The command decoder changes the serial, digital information from the command detector into pulse output signals from 12 real-time command users, and a serial binary output for the CC&S subsystem.

The command GSE provides the capability for manual and semiautomatic bench checkout of the flight com-

mand subsystem. The GSE console: (1) generates all the signals and programmable commands required to evaluate the command subsystem; (2) performs certain automatic test functions; (3) checks and displays all command subsystem and subassembly outputs; (4) provides continuous monitoring and display capabilities for all command subsystem output signals; and (5) provides manual selection of interface and key internal subsystem signals.

Read-Write-Verify equipment. The Read-Write-Verify equipment provides the link between the spacecraft and the computer through punched paper tape, and the audio spectrum generator required to modulate the R-F transmitter. RWV is basically DSIF equipment, and as such is part of the over-all ground spacecraft system. The RWV system provides positive verification of actual transmissions and checkout of the communications link between the computer and the transmitter. Although the RWV is basically a piece of DSIF equipment, it is used to check out the command link during prelaunch tests and during actual launch. When used for this purpose, it is part of the launch complex equipment.

R-F system. The *Mariner R* R-F system consists of an airborne transponder and an Earth-based DSIF transmitter/receiver phase-locked together at L-band.

The airborne transponder consists of a receiver operating at 890 mc and a phase-coherent transmitter operating at 960 mc. The local oscillator of the receiver also serves as the master oscillator for the transmitter; thus, the transmitted signal is 96/89 of the received frequency.

The Earth-based DSIF receiver is phase-locked to its own transmitter through the airborne transponder, which is responsible for telemetering to Earth all scientific data, as well as its own electrical behavior. The transponder is also responsible for the reception of DSIF-directed in-flight commands.

The difference between the prelaunch and postlaunch received frequency from the transponder is taken as the basis for in-flight velocity measurements.

The ground support equipment for the airborne transponder performs the prelaunch functions of a simplified DSIF station (with the exception of the velocity measurement). It may be directly coupled (hard-lined) to the transponder during all prelaunch pad activities for a detailed checkout of spacecraft functions and its own electrical behavior. It may also be air-linked to the transponder to provide a somewhat less comprehensive checkout by means of telemetry. The ground support equipment also initiates simulated in-flight commands in order to evaluate various mechanical, electrical, and pyrotechnic functions before flight.

Spacecraft antennas. The R-F system employs four antennas for the various in-flight communications requirements. Reception of DSIF-transmitted signals is through a dipole antenna and a turnstile antenna mounted above and below the outboard end of a solar panel. Both antennas feed received 890-mc energy to the communications transponder through a flexible coaxial cable.

Prior to spacecraft midcourse maneuver, R-F power is radiated to DSIF stations by an omnidirectional antenna located at the apex of the spacecraft structure. The antenna is driven by a separate L-band cavity amplifier.

Following midcourse maneuver and after the attitude of the spacecraft has been corrected, the R-F power is radiated by a high-gain directive antenna located at the base of the spacecraft hex structure. This antenna is also

driven by a separate cavity amplifier. The high-gain antenna is nested at the base of the spacecraft structure until midcourse maneuver, when it swings into position and faces the Earth. R-F power is fed from the cavity amplifier to the high-gain antenna through flexible coaxial cables and a rotary joint. The cavity amplifiers are switched to provide either an omnidirectional pattern or an Earth-directed lobe.

No special ground support equipment is required for the antenna systems. Their individual performances are checked prior to their integration into the spacecraft. After that, they become part of the total communications system and are checked at JPL (match-mate) and at AMR prior to launch. The same ground support equipment that checks the transponder is used to check the over-all communications system at Pasadena and AMR. A special R-F system checkout station is used to check the entire communications system at AMR when the entire vehicle (including the spacecraft) is on the launch pad.

b. Subsystems

Data encoder

(1) **Program background.** On January 26, 1961, a contract was awarded to Texas Instruments, Inc., Dallas, for the production of the *Mariner A* telemetry data encoder. The original contract was for one flight data encoder and one set of ground support equipment.

The first encoder and GSE were delivered on schedule on June 16, 1961. This unit was used as a type-approval model and subjected to all tests indicated in JPL Specification 30218-C. Design changes resulting from this testing were later incorporated in the *Mariner R* program.

The second data encoder, a prototype unit, was purchased and delivered to JPL on August 28, 1961. This unit was used in all system integration work. Loop tests involving the encoder, transponder, test receiver, and data display (demodulator) were run in November 1961 and the effects of phase distortion on the loop were evaluated. Other spacecraft interfaces, i.e., science, power, and command, were evaluated and all data were used in the *Mariner R* redesign effort.

The third unit, a life-test model, was purchased and delivered to JPL on October 25, 1961. After checkout and calibration, the unit was placed on life test and operated for 2660 hr without failures of any kind. This test was

terminated in May 1962 in order to provide ground support equipment for special Goldstone Tracking Station loop checks.

In fall 1961, the *Mariner A* booster vehicle was changed and it became necessary to redesign the spacecraft to adapt it to the *Ranger* bus configuration. The encoder redesign consisted of:

- (1) Reduction of commutator size from 100 channels to 60 channels to save weight and power.
- (2) Elimination of the relay commutator decks (slow rate) and their replacement with a solid-state commutator to reduce weight.
- (3) Redesign of all encoder logic to optimize weak areas revealed by *Mariner A* testing and to incorporate *Minuteman* high-reliability components.
- (4) Reduction of mode capability from 6 to 3 modes and rates from 6 to 2 in order to conserve weight and power.
- (5) Relayout of package, reducing number of modules from 14 to 8.

The first *Mariner R* data encoder was delivered on December 4, 1961, with the second and third units arriving on January 8 and January 15, 1962, respectively.

The *MR-1*, *MR-2* and spare encoders were flight-accepted as provided in JPL Environmental Specification 30251. No problems were experienced and no modifications were made during the testing. All three units were delivered to the JPL Systems Division in the first two weeks of February 1962.

(2) *Design considerations of the data encoding system.* For data transmission at Venus distance, conventional analog techniques, as used in the *Ranger* program, would not be entirely satisfactory because of the limited power and stringent signal-to-noise requirement. With the power limitation, digital techniques were found to yield a considerable improvement over comparable analog techniques. Of the digital systems considered, coherent phase-shift keyed modulation techniques appeared to be optimum.

Matched filter techniques seemed to provide near-optimum detection for a PSK system. A matched filter consists of an integration and dump circuit requiring a binary non-return-to-zero code sequence for its operation. Its characteristics are such that it tends to max-

imize the signal-to-noise ratio at its output. A decision circuit connected to the output of the matched filter discriminates between the two possible outputs which represent the binary digits.

Consequently, for data transmission from the vicinity of Venus, a PSK telemetering system using matched-filter detection is used. Assuming an available transmission rate at Venus distance of 8 bps, the transmission bandwidth would be limited. Using PSK modulation techniques, it can be shown from the sideband spectrum distribution that a bandwidth of six times the modulating frequency should be provided. For the worst possible case of modulation, i.e., a square wave indicating alternating ones and zeroes, the modulating frequency would be one-half the bit rate since there are two bits per cycle. Hence, the required bandwidth at Venus distance for a maximum bit rate of 8 bps would be equal to 24 cycles.

In view of this relatively small bandwidth requirement, a single subcarrier channel is used at Venus distance in lieu of a number of parallel channels. The required subcarrier power was thus kept to a minimum.

Using coherent PSK techniques for all measurements throughout the flight results in three practical approaches to the telemetering system design:

Approach No. 1. Prior to and including midcourse maneuver, the telemetering system would include N parallel PSK subcarrier data channels, each transmitting information in a bit serial-word serial mode of operation. Each subcarrier would be independently connected to an analog-to-digital converter. Following midcourse maneuver, the subcarrier channels would be systematically switched out with increasing distance from the Earth so that only one subcarrier channel would remain in the system in the vicinity of Venus.

Approach No. 2. Prior to and including midcourse maneuver, the telemetering system would include N parallel PSK subcarrier data channels, which would be collectively transmitting information in a bit parallel-word serial mode of operation. The subcarrier would be connected to one common analog-to-digital converter. Following midcourse maneuver, or when the transmission restrictions dictated, $N - 1$ channels would be switched out and the system transferred to a bit serial-word serial mode of operation using one subcarrier data channel.

UNCLASSIFIED

JPL TECHNICAL REPORT NO. 32-353

Approach No. 3. Throughout the entire flight, the telemetering system would include only one PSK subcarrier channel. This would be a wide-band channel which could accommodate a bit rate comparable to the total of the N parallel channels described in design approach No. 1. It would be connected to one analog-to-digital converter. Following midcourse maneuver, the data sampling rates would be systematically lowered with increasing distance from the Earth.

Design approach No. 1 has an advantage of reliability in that if one subcarrier channel is lost, all of the data will not be lost. However, it suffers from a serious disadvantage in that a separate analog-to-digital converter would be required for each channel. Although it might be possible to time-share one analog-to-digital converter, this would require a buffer stage and an impractical degree of complexity.

Design approach No. 2 eliminates the requirement for a separate analog-to-digital converter for each channel. However, it would require a different frequency. Since only one clock frequency will be available from the CC&S, deriving seven different frequencies for each data rate would result in considerable circuit complexity. Also, the analog-to-digital converter design would be required to accommodate both bit parallel-word serial and bit serial-word serial modes of operation.

Design approach No. 3 overcomes the disadvantages of both of the other two methods. Using only one subcarrier channel, it considerably simplifies the circuit requirements, and thereby increases reliability. Although it requires N times the bandwidth of N parallel channels to achieve the same bit rate capacity, the bandwidth of the Goldstone receiver is more than adequate for the bit rates required for *Mariner R*. In addition, the analog-to-digital converter design is simplified due to the need for only a single serial output.

Since design approach No. 3 alleviates the analog-to-digital converter requirements present in approaches 1 and 2, reduces the circuit complications and inflexibility, and suffers from no serious disadvantages, it was selected as the optimum design approach for the *Mariner R* telemetering system.

(3) Design considerations of the data synchronization system. As noted previously, the *Mariner R* telemetry data encoding system employs a complex multiplexing system for the engineering measurements. The analog engineering data sampled by this multiplexing system are

converted to digital form and used to biphase-modulate a subcarrier frequency. In addition, digital scientific data will be obtained from a data conditioning system and used to biphase-modulate the same subcarrier channel. The data bit rates for the engineering measurements will be changed during the flight to adjust to the changing transmission capabilities with increased distance from the Earth.

In order to provide bit and word detection for demodulation purposes, a satisfactory method of synchronization of the encoded data must be provided between the spacecraft and ground. Although a sync signal could be developed from the spacecraft clock by dividing the frequency and transmitting a pulse using PSK matched-filter techniques, this method would not be optimum. For each example, it would entail transmission of a sync pulse which would require reproduction on the ground so that triggering could be accomplished from its leading edge. However, under adverse noise conditions, large timing errors would exist, introducing considerable error. In addition, considerable power would be required to achieve an adequate signal-to-noise ratio.

The best available approach was found to be based upon the use of pseudo-noise techniques. In this case, rather than direct transmission of the sync pulse, a coded PN sequence approximating noise in its characteristics is transmitted. By employing a separate PN generator on the ground to develop the same PN sequence, phase comparison of the transmitted code and the ground-generated code would allow the PN generator on the ground to be slaved to the spacecraft PN generator through use of a phase-locked loop. The advantage of this technique is derived from the fact that an extremely small signal-to-noise ratio is required as the pseudo-noise sequence only has to have sufficient signal-to-noise so that its phase can be recognized. This results in an extremely low power requirement.

(4) Problems and solutions. During the assembly and systems checkout of the spacecraft, one basic problem area was uncovered which affected the data encoder. This problem area was the spacecraft ambient noise level during the flight sequences. Noise as used here is defined as any spurious signal in a circuit, either transient or repetitive. This problem affected three general areas.

The first problem area involved noise directly coupled into the encoder from the 2400-cps main power bus. During the flight sequence, several heavy intermittent loads are placed on the 2400-cps power amplifier. These loads

UNCLASSIFIED

produced severe amplitude and phase distortion on the 2400-cps input power. The data encoder uses the 2400-cps power frequency as its primary clock. All timing pulses and subcarriers are derived from this frequency. As a result of the power transients, the commutator would misstep and subcarrier frequencies were distorted. The latter resulted in loss of telemetry lock by data display since the phase-lock loop could not follow the transient phase shifts in the subcarriers. Data display decommutator lock was also lost as a result of the false steps in the commutator. The high peak loads on the 2400-cps amplifier were caused, for the most part, by the attitude control and science transformer-rectifiers. The problem was alleviated somewhat by placing current-limiting provisions in the transformer-rectifiers.

The second problem area involved noise capacitively coupled into the data encoder on signal lines. On the analog input signals, this noise can be tolerated because the ADC has a narrow bandwidth and a very short sampling time. However, on the digital inputs, channels B0 and B1, steps had to be taken to suppress the noise to ensure proper operation. On channel B0, extra events were being received from almost any attitude control or pyrotechnic system function. Pyrotechnic events were changed from current step inputs to relay closures in the pyrotechnic assembly and heavy filtering was added at the encoder input. The CC&S event input was filtered at the CC&S package.

On channel B1, the command detector monitor, the 2400-cps main power frequency was coupling in on the command interrogate pulse. This pulse is used to parallel-gate the contents of a six-bin register in the command system into the data encoder transfer register. The 2400-cps noise on the interrogate line interfered with the logic of both the command and encoder systems. Filtering was added in the encoder and the noise was suppressed.

The third noise problem area involved noise on the spacecraft primary power, the 28-v battery, which is used to power all high-peak intermittent loads. This created a low-impedance noise source which was coupled into the event registers, channel B0, on the Sun-gate actuate and gyro control on event lines. These lines used relay-gated 28 v as an event signal. The signals proved impossible to filter because of their low impedance and were eliminated.

(5) *Subsystem functional description.* The data encoder samples, encodes, and prepares data originated in the

Mariner R spacecraft for transmission. Data processed include engineering information and measurements, spacecraft functions and events, and certain scientific data and measurements, either in analog or digital form. The engineering measurements are in analog form and are ready as variable d-c voltages. Spacecraft events and scientific data are received in digital form. Figure 87 presents the data encoder signal flow in logic form. The data encoder has three modes of operation: the launch mode (Mode I), the cruise mode (Mode II), and the planetary encounter mode (Mode III). All signal switching and sequencing is accomplished with solid-state circuits; two relays in the master counter are used to accomplish mode switching; one relay is used to obtain the $4F_s$ and $2F_s$ from the frequency divider chain; and one relay is used when the GSE is controlling the encoder in the homing mode of operation.

(a) *Mode and rate commands.* Mode and rate commands can be received from any one of three sources: (1) the central computer and sequencer; (2) the command system; and (3) the data encoder test console (GSE).

(b) *Scientific data.* Scientific data are fed into the data encoder during Mode II and Mode III operation. This input is binary information that bypasses the encoder analog-to-digital converter and goes directly to the bi-phase modulator. The data encoder generates bit sync, word sync, pseudo-noise, and modulates a carrier with digital data. The 2.4-kc clock signal received from the spacecraft is divided and filtered to provide the $4F_o$ sine-wave subcarrier, which is biphase-modulated by the digital data and is mixed with the pseudo-noise sync signal. This mixed signal is fed to the transponder.

(c) *Switch timing sequence.* The data encoder has six solid-state commutator decks (A, B, C, D, E, and F). The solid-state switches are operated by flip-flops in a predetermined sequence. The high-speed decks (A, B, C) are programmed by the master counter, and the low-speed decks (D, E, F) are programmed by the low-deck programmer.

Decks E and F have low-level inputs and use low-level switches. The ADC will give a digital output for any analog input between 0 and 3 v. For maximum signal sensitivity, each input must be conditioned so that the minimum input is equal to zero and the maximum input is equal to 3 v. The low-level signals on Decks E and F (and Deck C positions C4, C5, and C6) are amplified in

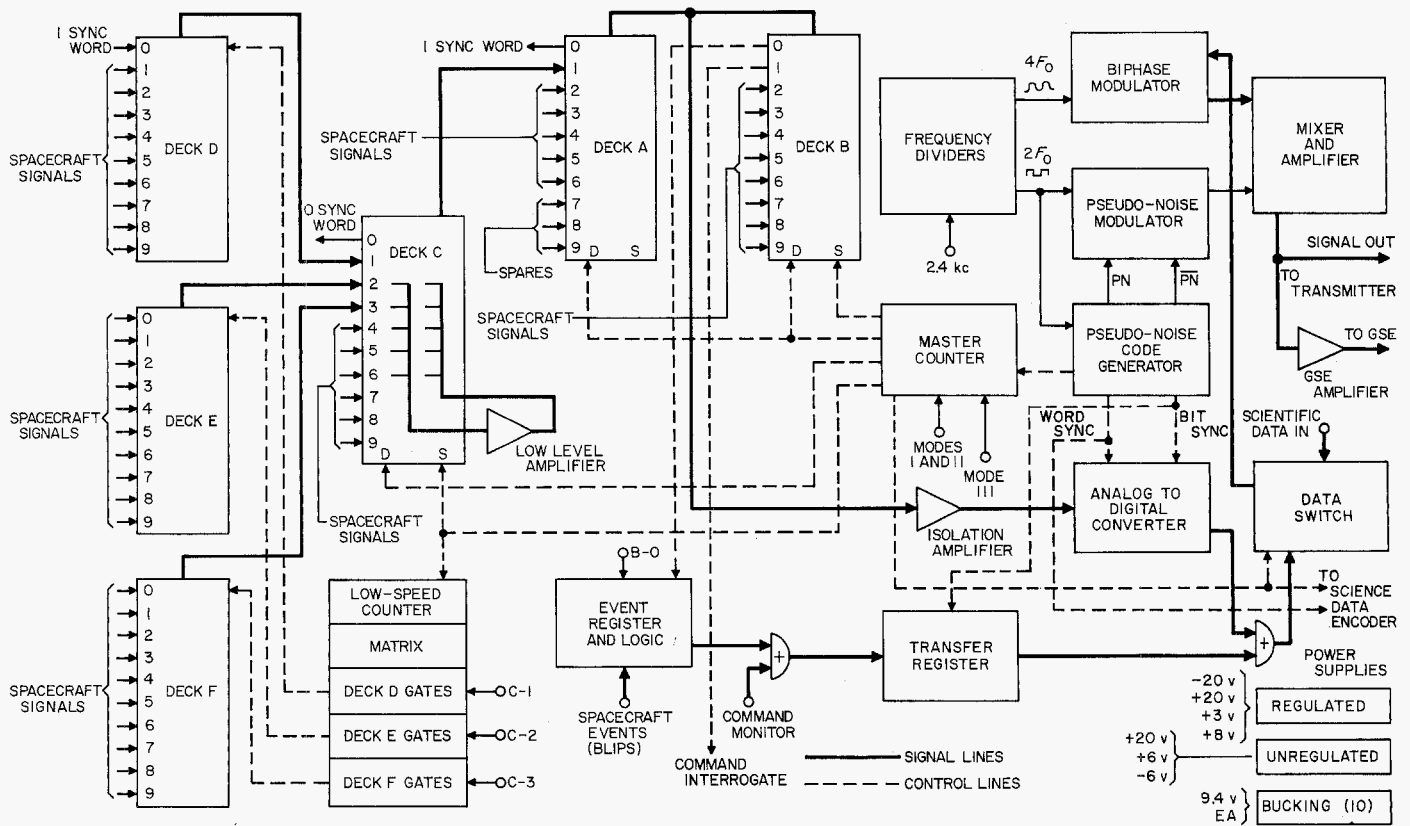


Fig. 87. Data encoder signal flow diagram

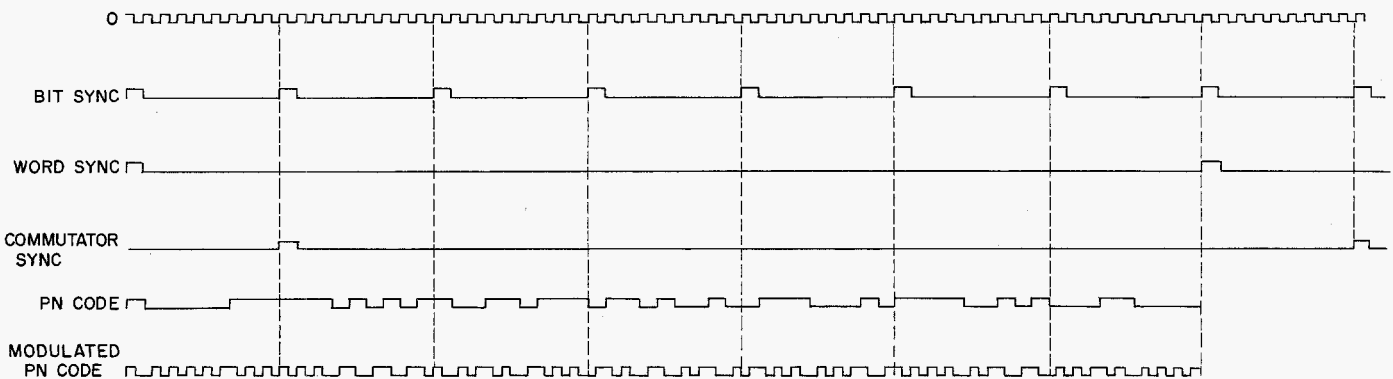


Fig. 88. Pseudo-noise and modulated pseudo-noise waveforms

the low-level amplifier so that an input of 0 to 100 mv gives an output of 0 to 3 v.

(d) *Pseudo-noise generator.* The pseudo-noise generator is used to generate a unique pattern of pulses during each word period (Fig. 88). It also generates word and bit sync. Word sync is sent to the ADC and the scientific data system, and word sync delayed one bit is used to sequence the master counter. Pseudo-noise is sent to the

biphase modulator, where it is combined with $2F_0$ to provide a coded phase-reference for the data subcarrier.

(e) *Master counter.* The master counter generates set and drive pulses for commutator decks A, B, and C, a drive pulse for the low-speed counter, and a 24-word one in Mode II (for scientific data transmission only). There are two inputs to the master counter: one input is the commutator sync from the pseudo-noise generator and

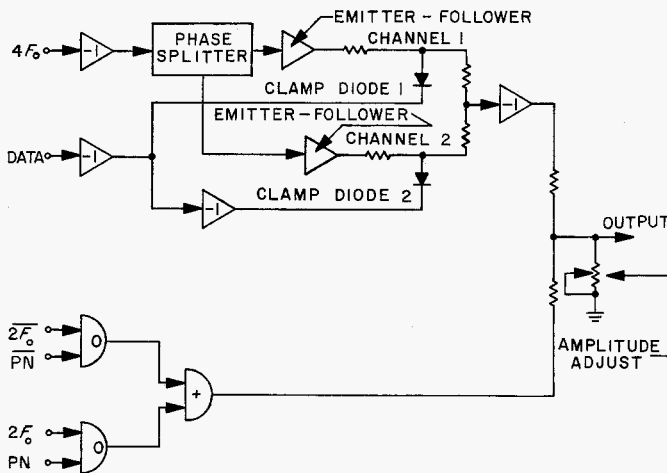


Fig. 89. Biphase modulator, block diagram

the other input is from the GSE. The GSE input is for commutator speed-up (used in GSE homing mode) and operates at 500 cps.

(f) *Biphase modulator.* The biphase modulator has two channels: the data modulator and the PN modulator (Fig. 89). The data are used to modulate the $4F_0$ sine wave. The PN modulator channel modulates the PN code signal with $2F_0$. If the signals are in phase, the modulator output is high, and if the signals are opposite in polarity, the output is low. The outputs of the data modulator and of the PN modulator are resistively added, and the combined signal becomes the output of the biphase modulator.

(g) *Comparator isolation amplifier.* The comparator isolation amplifier is a unity-gain amplifier of approximately 3-megohm input impedance. All input signals to the ADC are fed through this amplifier to prevent overloading of the transducers. The output of the amplifier is fed to the comparator, where the analog voltage is digitized. A direct-coupled amplifier is used for gain stability and to provide a high-input impedance. The operation of this amplifier is shown in block diagram form in Fig. 90. The signal voltage is compared to the voltage of an internal voltage generator, and the error sensor compares these voltages and corrects for any unbalance. The signal is used as the standard voltage in this circuit, and the output of the voltage generator is varied by the error sensor to be equal to the signal input voltage. The voltage output of the voltage generator is the amplifier output.

(h) *Analog-to-digital converter.* The analog-to-digital converter consists of the following basic elements:

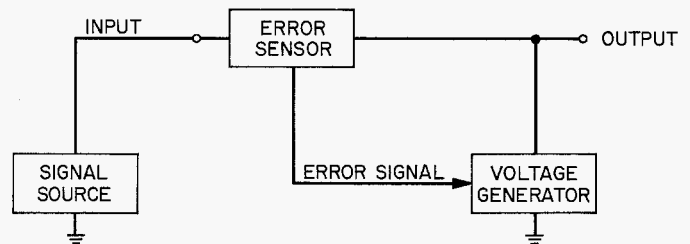


Fig. 90. Comparator isolation amplifier, block diagram

decoder, comparator-integrator, and digitizing pulse generator. As each analog signal is switched into the comparator-integrator, it is analyzed digitally at a rate set by the digitizing pulse generator and is converted in the decoder to a 7-bit digital word. The following paragraphs discuss each of the three circuits and their combined operation (Fig. 91).

The decoder consists of a 7-bit shift register, each stage of which drives a complementary switch. These switches are connected to the resistors in a ladder network. The ladder network output is the sum of the contributions of each stage. As the switches are energized, they select either 3-v reference or 0 v to be switched into the ladder network. If all switches are on, the output is 127/128 of the 3-v reference. If only the most significant digit is switched in, the output is one-half of the reference voltage. The ladder network output is compared to the analog input and switches are set in the OFF or ON position until the ladder output equals the analog signal into the comparator.

The digitizing pulse generator is a 7-bit shift register clocked by a two-stage delay-line oscillator initiated by a blocking oscillator. When a word pulse is received, two inverters improve the rise time and remove base-line noise so that reliable triggering of the blocking oscillator is achieved. The blocking oscillator pulse resets all states of the register except the first, in which it sets a 1 on the Q side, and pulses the delay-line oscillator. The blocking oscillator pulse passes through an inverter and into a delay line. It is again inverted, and the delayed pulse is fed back. Thus, the oscillations continue.

The comparator and integrator in a successive-approximation encoder must condition the input and generate an error signal at any time the internally generated trail voltage is greater than the analog voltage input. The two important parameters of a comparator circuit are resolution of comparison and trigger stability.

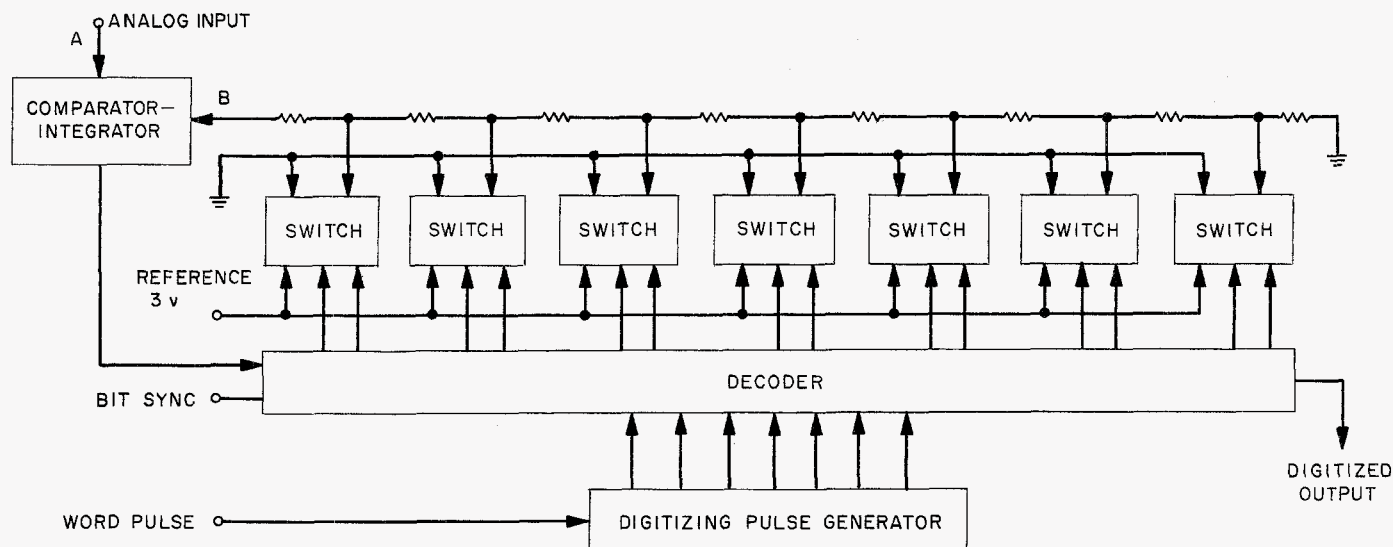


Fig. 91. Analog-to-digital converter, block diagram

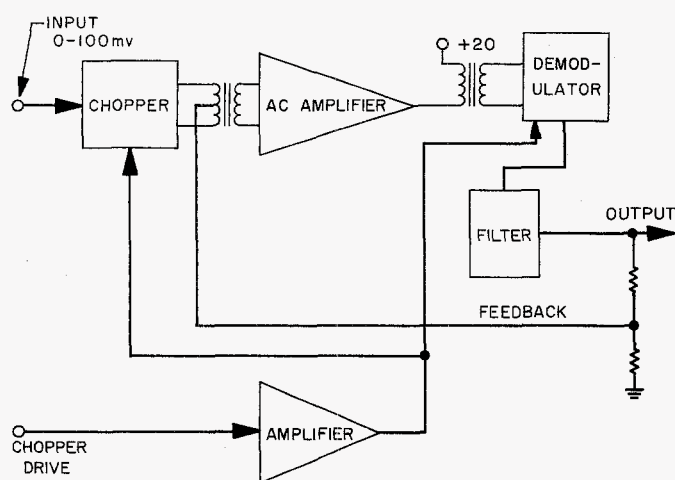


Fig. 92. Low-level amplifier, block diagram

The integrator is a low-pass filter which is dumped at the end of each word. The comparator compares the ladder output to the analog input.

(i) *Blip registers.* The blip registers consist of five major units: four event counters of 4-bit capacity, and a two-stage counter which not only selects the event counter to be read out, but also provides 2-bit address information unique to the event counter interrogated.

(j) *Low-level amplifier.* The low-level amplifier is used to amplify all of the low-level, 0- to 100-mv signals received by the encoder. Since the ADC digitizes only in-

puts varying between 0 and 3 v, all signals must be conditioned to vary over this range. This amplifier (Fig. 92) has a gain of 30, which amplifies the 0- to 100-mv input to the standard 0 to 3 v.

(k) *Bucking supplies.* The bucking supplies operate from ground-isolated 14-v dc obtained from full-wave rectifiers. This voltage is zener-regulated at 9.4 v by a 1N2170 diode and associated series resistor. The regulated voltage is then divided to produce the required output voltages.

(l) *Isolation amplifiers.* The isolation amplifiers are NPN/PNP emitter-follower amplifiers. These transistors are matched for VBE drop to prevent ADC offset through the amplifier.

(6) *Ground support equipment.* The ground support equipment has four main functions (Fig. 93 is a block diagram of the equipment). It provides power, monitors outputs, gives commands, and simulates inputs for the encoder. There are three possible connections to the data encoder: (1) the encoder package may be removed from the spacecraft and mounted on the pull-out drawer of the GSE; (2) the encoder may be installed in the spacecraft, the spacecraft cables terminated to the GSE, and the encoder connected to the GSE through the test jack and interface connections; and (3) the connection may be through the umbilical connector, through which a limited number of commands may be given.

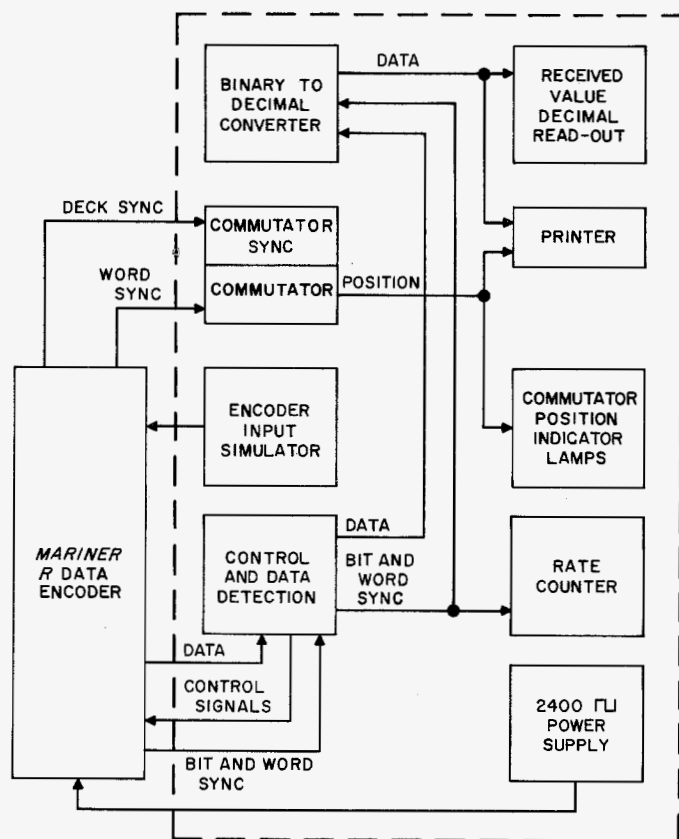


Fig. 93. Ground support equipment, block diagram

(a) *Commands.* The commands possible for each connection are listed below. These commands are generated in the control drawer.

Command	Mounted on GSE	Test jack only connected	Umbilical connection
Channel homing	yes	yes	yes
Mode change	I, II, III	I, II, III	I only
Rate change	33, 8.25	33, 8.25	no
Event counter reset	yes	yes	yes

(b) *Monitoring.* The mixed signal output and the deck sync signals are monitored in each connection. The data output is in digital form so the GSE detects these data and converts them to the decimal equivalent of the binary number. The received value read-out unit displays this decimal equivalent of the binary output from the encoder. Binary-to-decimal conversion is accomplished in the binary-to-decimal converter drawer. These converted data are also printed out by the printer.

(c) *Simulated inputs.* The encoder has several types of inputs. The GSE supplies simulated inputs for each channel. The list below gives the functions to be simulated and the signal supplied for that function.

Function	Simulated signal
Temperature	Variable resistance
Low-level signals	Variable voltage (0 to 100 mv)
High-level signals	Variable voltage: 0 to 3 v, ± 1.5 v ± 30 v, 0 to -3 v ± 16 v, 0 to -20 v -1 to $+5$ v
Events	Pulses and switch closures
Scientific data	String of pulses
Command monitor	Programmed pulses

(d) *Power.* The main power for the encoder is 2.4-kc square wave at 100 v peak-to-peak. This power and 28 v to drive relays are furnished by the GSE when the encoder is out of the spacecraft. Only voltages for commands are furnished by the GSE when the encoder is connected to the spacecraft.

(e) *GSE commutator.* The GSE has two modes of operation — the automatic mode and the homing mode. In the automatic mode, data are being received and recorded continuously as the encoder commutator steps through each channel. The GSE commutator (Fig. 94) must follow the encoder commutator and furnish the address of the data, along with its value. The data output of the GSE lags the encoder data input by two word times, since one word time is lost in the encoding process and one in the decoding process.

(f) *Rate commands.* Mode and rate commands are generated in the GSE. The RATE switch selects the rate to be commanded, and the SET switch pulses the selected one-shot. To maintain ground isolation between the encoder and the GSE, the one-shot output is transformer-coupled to an emitter-follower output stage. There are separate outputs for the 8.3-bps and the 33-bps rates. The commutator control drive is also transformer-coupled to the output. The mode command channels are identical and each has a switch, a 100-msec one-shot transformer-coupling, and an emitter-follower output stage.

Radio system

(1) *Program background.* The Mark II transponder is the outgrowth of certain design modifications of the

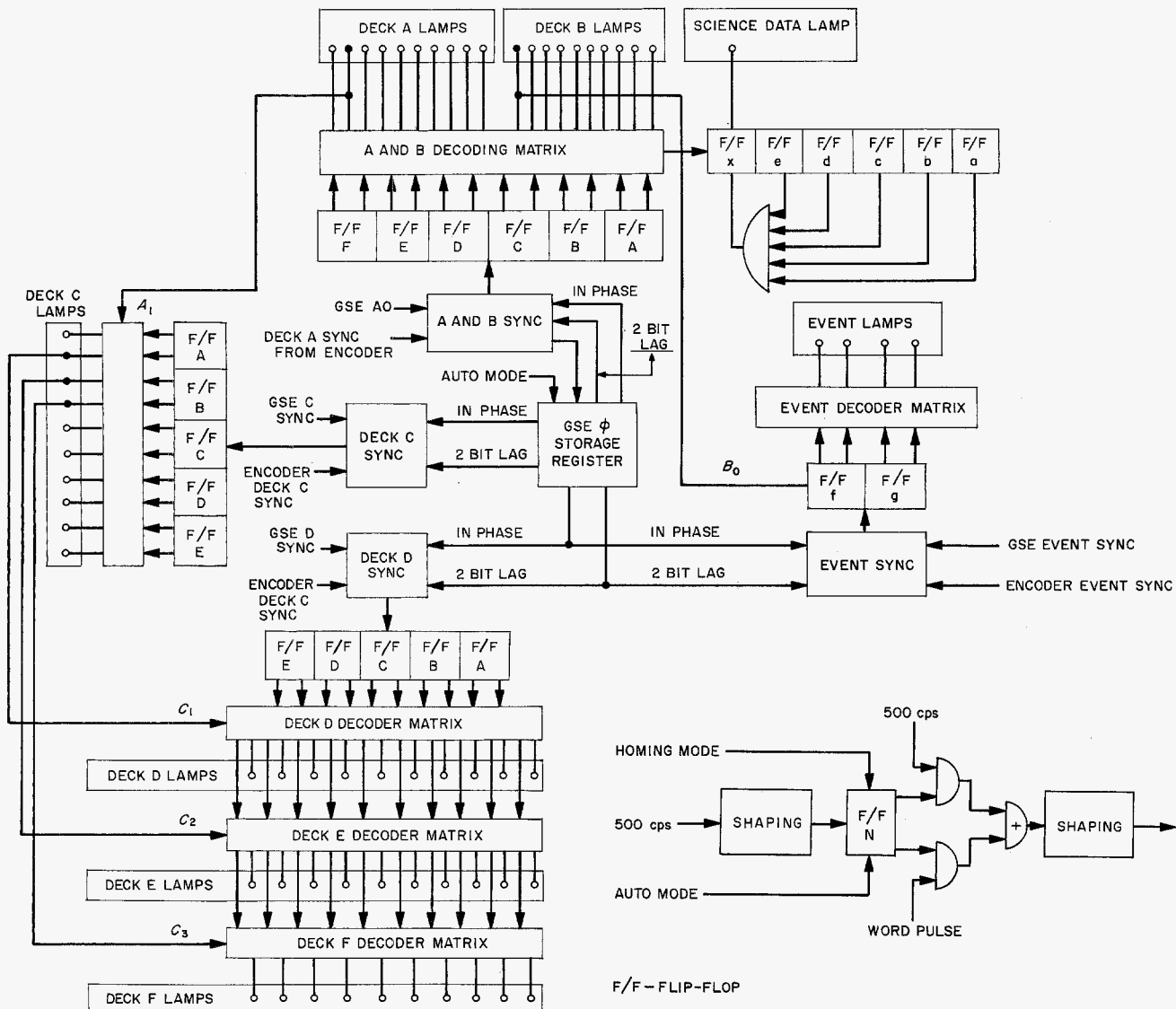


Fig. 94. Commutator, commutator sync, and position indicator lights, block diagram

Mark I model used on *Rangers 1* to 5, which were required to make the transponder capability compatible with planetary mission requirements. These modifications consisted of:

- (1) Reduction of the loop noise bandwidth ($2B_L$) from 100 to 20 cps to improve the sensitivity of the receiver
- (2) Improvement of the circuit design in areas previously found to be critical

With the loop noise bandwidth reduced to 20 cps, a threshold of -146 dbm was achieved. To accommodate the loop noise bandwidth change, it was necessary to extend the linearity of the final I-F stage and AGC de-

tector to handle the increased predetection noise power due to a greater noise-to-signal ratio in the AGC loop. This problem was alleviated by reducing the I-F bandwidth from 6 kc (Mod I) to 3 kc. To meet the additional stability requirements of the narrow-band system, the 20-mc voltage-controlled oscillator sensitivity was reduced from 600 to 120 cycles per volt.

Over-all transponder power consumption has been reduced from 10 to 7.5 w by operating the transistorized modules at 15 v instead of 20 v (as in Mark I), and maintaining the same current drains. The Mark II modules have been repackaged; the resulting configuration reduced the transponder from 17.5 lb (Mark I) to 10 lb (Mark II).

(2) *Design considerations.* The radio communications system was designed to provide reliable communications for a maximum range of 60×10^6 km, under environmental conditions found from launch through planetary encounter. The transponder design included the capability of (1) receiving Earth-transmitted commands, and transmitting to Earth confirmation of such received commands, (2) transmitting scientific data gathered during the flight to and past the planet Venus, and (3) transmitting to the Earth information regarding the progress and behavior of the spacecraft during its flight.

A phase-locked communications system was chosen because of its inherent advantages under high noise-to-signal conditions. The communications package consists of a phase-coherent transmitter/receiver, wherein the transmitted signal is 96/89 of the received signal. The receiver is an extremely stable, double conversion, phase-locked superheterodyne, having a noise bandwidth of 20 cps. The transmitter 3-w output capability provides reliable spacecraft-to-Earth communication.

Reception of the Earth-transmitted signal is through command antennas; one, a turnstile, is mounted on the shaded side of a solar panel. The second antenna, a dipole, is mounted on the Sun side of the same solar panel. The spacecraft signal is transmitted through an omnidirectional antenna prior to midcourse maneuver, and through a parabolic directional antenna thereafter.

Phase modulation of the airborne transmitter by encoded data from position sensors and scientific instruments takes place in the VHF frequency range, and, due to frequency multiplication, results in a total phase-modulation capability of 4 rad at L-band. The data rate of the communications system prior to Earth acquisition is 33.3 bps, and is reduced to 8.3 bits from Earth acquisition to flight termination.

(3) *Problems and solutions.* Flight-acceptance testing started on January 5, 1962. No problems were encountered in the vacuum temperature or vibration tests. Prior to SAF delivery, it was discovered that, due to an error in signal characteristics sheets, the encoder modulation signal level and the transponder modulation sensitivity were incompatible. The problem was solved by changing the transponder modulation sensitivity from 2 rad/v to $\frac{1}{2}$ rad/v. This was accomplished by adjusting R-21 on the auxiliary oscillator module. Pressure relief holes were added to all MR-1 cavities. This allowed air to escape from the cavities so that critical pressures during the

launch phase would not occur prior to cavity "power up" (150 to 250 v).

Systems testing started on February 7, 1962. The command modulation output circuit of the transponder was not compatible with the command decoder input circuit. The problem was lack of d-c isolation. A resistor was removed from the transponder loop filter module and a capacitor in the same module was replaced by a higher-voltage-rated, polarized capacitor.

At AMR, MR-1 tests were good. The directional power telemetry indication, with and without shroud, varied from 58 to 66 or about 0.4 db. The omni-antenna indication varied from 66 to 74, or a variation of 0.9 db.

(4) *Subsystem functional description.* The Mariner R radio communications system consists of the following items: (1) Communications Case II electronics assembly, (2) receiving or command antenna system; and (3) transmitting antenna system composed of an omnidirectional antenna and a directional parabolic disc antenna. Only the Communications Case II assembly will be discussed in this Section.

The Communications Case II assembly (Fig. 95) is mounted to the hexagonal structure of the spacecraft and houses the transponder L-band filter, tricavity amplifier, transformer-rectifier unit (power supply), circulator and power monitors, and the junction box. The modules are interconnected by a subsystem cable harness which has two connectors mating to the spacecraft ring harness. All circuitry, except the cavity amplifiers, is solid state. The tricavity amplifiers contain three planar triodes as the active elements.

System characteristics are as follows:

Receiver threshold: -146 dbm nominal

Antenna: 960-mc input power, 3 w

Power input: 50 v rms, 2400 cps, square wave, 30 va

Total weight, excluding mounting hardware: 26 lb

Telemetry outputs: receiver AGC voltage, receiver static phase error

(a) *Transponder.* The 890/960-mc transponder consists of an extremely narrow-band, double superheterodyne, automatic phase-tracking receiver operating at 890 mc, and an integrally related transmitter operating at 960 mc. The transponder is completely transistorized

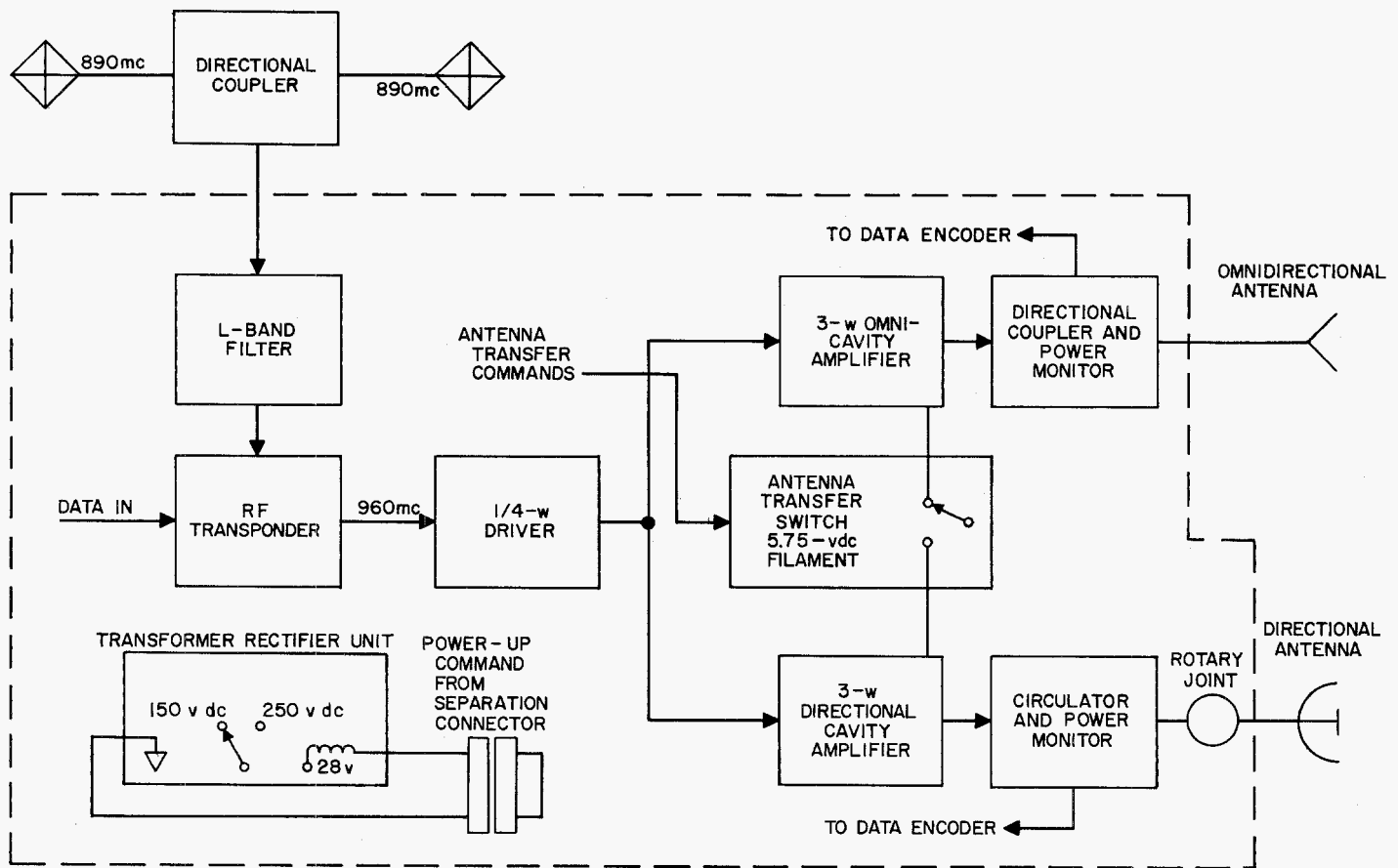


Fig. 95. Communications Case II assembly, block diagram

and is constructed to provide the maximum long-term reliability, minimum power consumption, and minimum weight consistent with the electrical performance required. Figure 96 is a block diagram of the transponder.

The characteristics of the transponder are listed below:

Predetection bandwidth:	3 kc
Threshold noise bandwidth:	20 cps
Strong signal noise bandwidth:	191 cps
Noise figure:	14 db
Threshold sensitivity (carrier):	-147 dbm
Frequency (VCO crystal):	20.001040 mc
Frequency (received):	890.046 mc
Frequency (transmitted):	960.05 mc
Transmitter power:	7 mw nominal
Transmitter modulation:	phase-modulated dc to 1.5 mc
Phase detector K_d :	0.148 v/deg
VCO K_v :	120 cps/v

Phase multiplication M :	44.5
Loop filter time constant T_1 :	51 sec
Loop filter time constant T_2 :	0.075 sec
AGC time constant:	22.5 sec
Tracking range:	± 31.5 kc
Input power:	+15 v/350 ma -15 v/100 ma
Weight:	10 lb
Operating temperature:	0 to 55°C
Storage temperature:	-65 to +125°C

(b) Reception

Automatic phase-tracking loop. The transmitted signal from the transponder is phase-coherent with the signal received by the transponder and is related by the ratio of 960 to 890. Phase coherence is accomplished by an automatic phase-tracking loop. The transfer function of the tracking filter in the tracking loop is designed to be

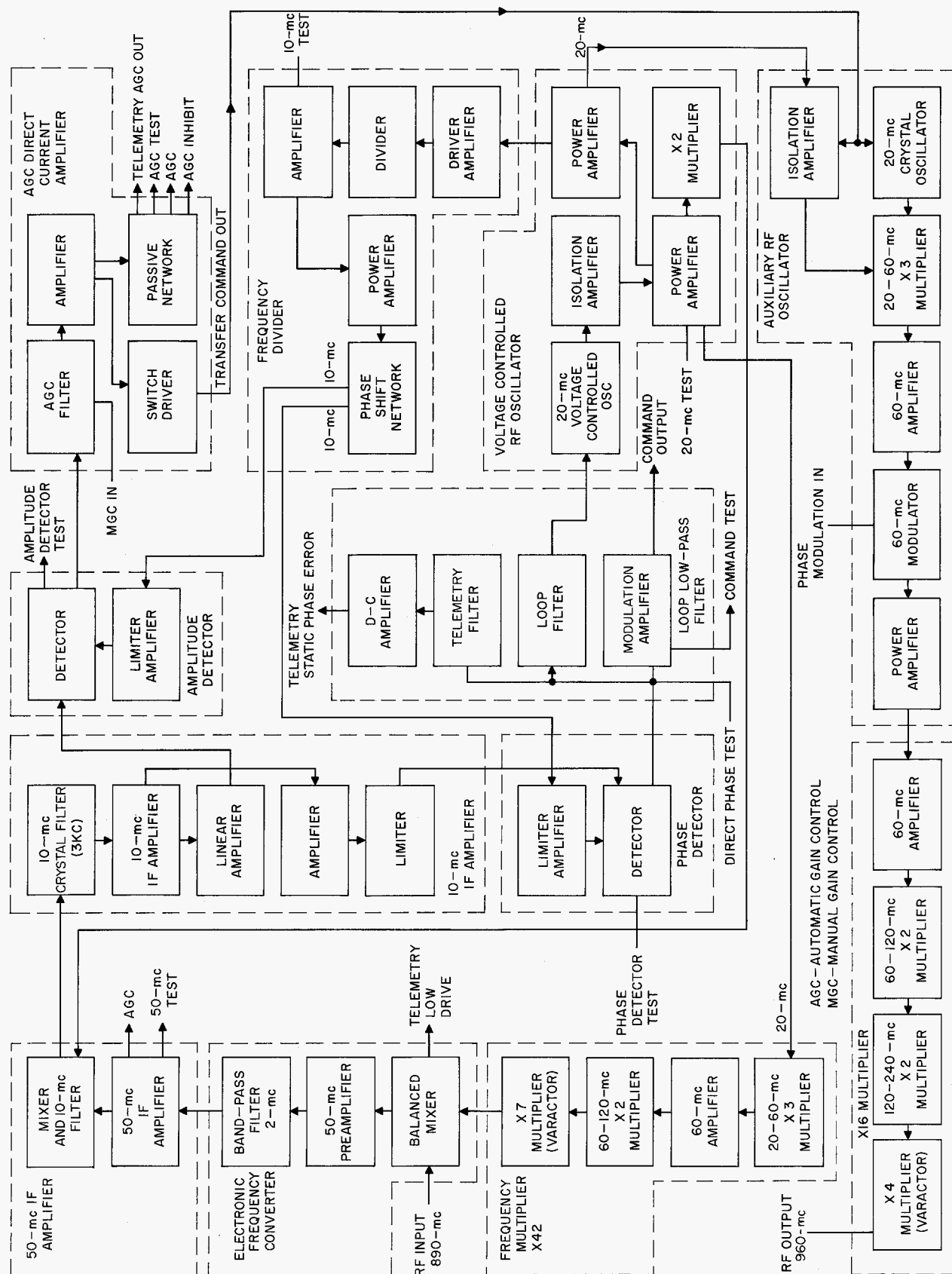


Fig. 96. Mark II 890/960-mc transponder, system block diagram

approximately equivalent to the low-frequency filter form of and if

$$H_{\text{design}} = \frac{1 + \frac{3}{4B_L}S}{1 + \frac{3}{4B_L}S + \frac{9}{32(B_L)^2}S^2}$$

where $2B_L$ = the two-sided loop noise bandwidth.

This provides a second-order filter system with maximally flat damping. The filter form is mechanized as shown in Fig. 97. The transfer function of the assembly is

$$H_{\text{mech}} = \frac{1 + T_2S}{1 + \left[T_2 + \frac{1}{K_d K_v M} \right] S + \frac{T_1}{K_d K_v M} S^2}$$

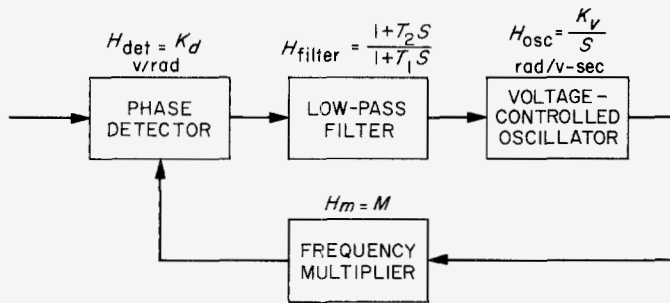


Fig. 97. Filter form assembly, block diagram

The mechanized and the design filter forms are identical if

$$T_2 = \frac{3}{4B_L}$$

and

$$\frac{T_1}{K_d K_v M} = \frac{9}{32 B_L^2}$$

The parameters T_1 , T_2 , K_d , K_v , and M are determined by the desired ratio between the frequencies of reception and transmission and by the physical limitations upon the components. The transponder multiplication system is actually constructed as shown in Fig. 98. From Fig. 98, receiver multiplication M equals $44\frac{1}{2}$ or $(\frac{1}{2} + 2 + 42)$, transmitter multiplication equals 48, and the ratio between the received and transmitted frequencies is $44\frac{1}{2}/48 = 890/960$. The two local oscillator signals for double superheterodyne operations are also provided for in the multiplication system.

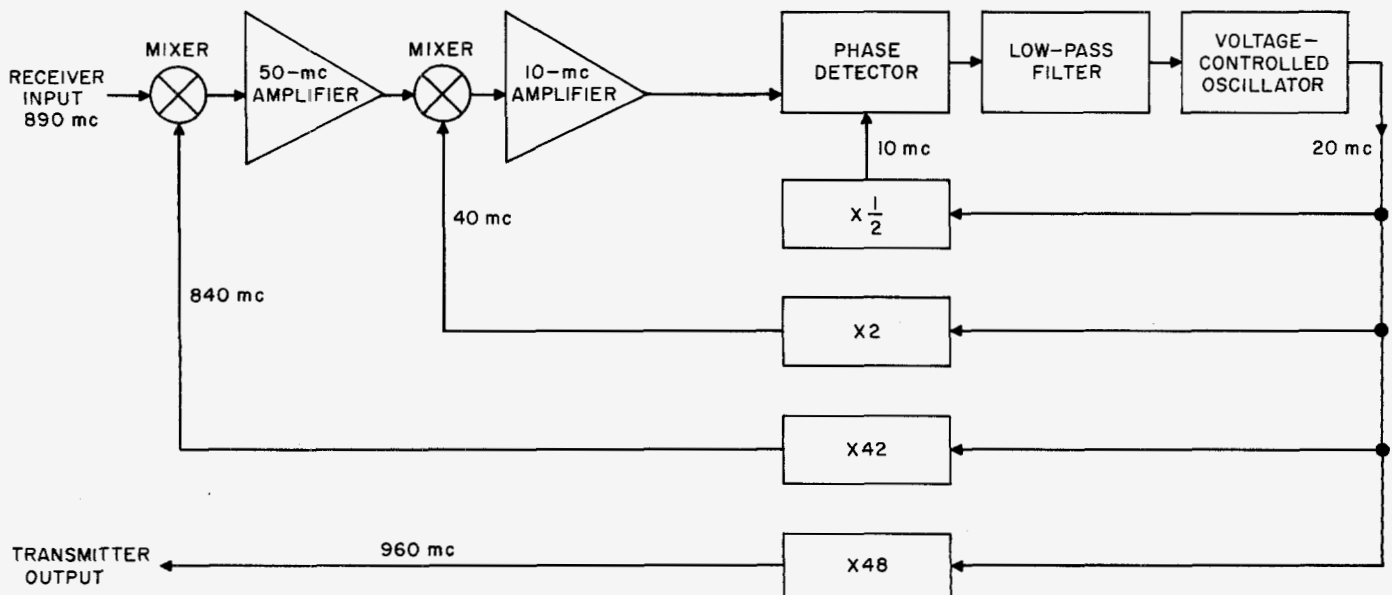


Fig. 98. Transponder multiplication system

Receiver response. The receiving section of the transponder is designed with an input noise bandwidth $2B_L$ of 20 cps at the receiver threshold. As the signal level increases, the noise bandwidth automatically increases up to a limit of 191 cps. This results from the change in the gain of the phase detector caused by the action of the hard voltage limiter preceding the loop signal input.

The receiver loop noise bandwidth can then be shown to be

$$2B_L = 2B_L(\text{threshold}) \frac{1}{3} \left(1 + 2 \frac{K_d}{K_{d \text{ threshold}}} \right)$$

The phase detector gain K_d , a function of the noise-to-signal ratio at the limiter input, is given by

$$K_d = K_{d \text{ threshold}} \left[\frac{1 + \frac{4}{\pi} \left(\frac{N}{S} \right)_i \text{ threshold}}{1 + \frac{4}{\pi} \left(\frac{N}{S} \right)_i} \right]^{\frac{1}{2}}$$

Threshold is defined as unity noise-to-signal ratio in the effective threshold loop noise bandwidth $2B_{L_0}$ of 20 cps. Since the predetection noise bandwidth is set at 3 keps by a crystal filter in the second I-F amplifier, the threshold noise-to-signal ratio at the limiter input is $3000/20 = 150$. The ratio of strong signal

$$\left[\frac{4}{\pi} \left(\frac{N}{S} \right)_i \ll 1 \right]$$

phase detector gain K_d to $K_{d \text{ threshold}}$ is then

$$\left[1 + \frac{4}{\pi} (150) \right]^{\frac{1}{2}} = 13.8$$

The receiving portion of the transponder is designed to track an input signal excursion of 57 cps/deg at the threshold and 785 cps/deg at strong signal conditions. This tracking gain is established by setting the gains of the voltage-controlled oscillator, phase detector, and frequency multiplication ratios to

$$K_d = 0.148 \text{ v/deg (strong signal)}$$

$$K_v = 120 \text{ cps/v}$$

$$M = 44.5$$

The resultant receiver response is shown in Fig. 99.

Modulation response. The phase modulation is extracted from the phase-tracking loop as the untracked output of the loop phase detector. Thus, if the receiver

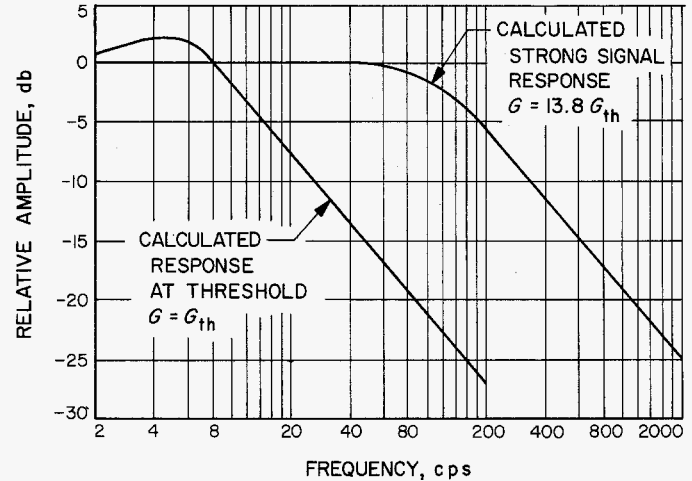


Fig. 99. Resultant receiver response

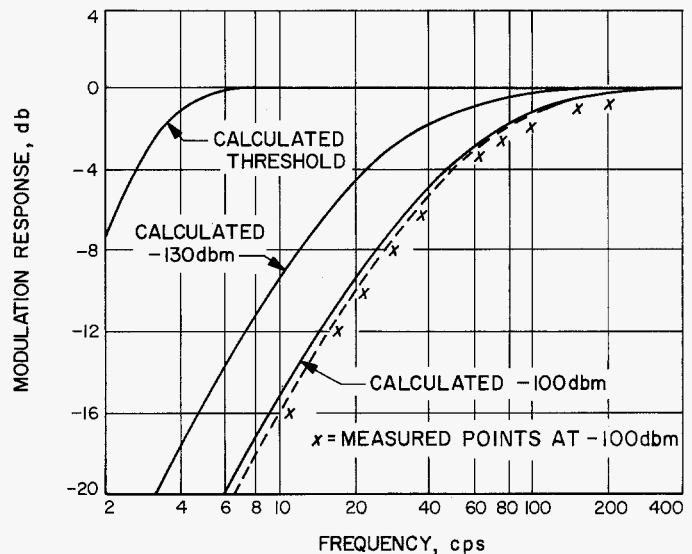


Fig. 100. Calculated vs measured modulation response of receiver

response is H , the modulation response is $(1-H)$. The high-frequency characteristics of the measured response are restricted by the bandwidth of the I-F amplifiers and by the frequency response of the phase detector. Figure 100 shows the calculated and measured modulation response of the receiver.

Receiver threshold. The threshold signal level under which the transponder maintains reliable phase coherence between the input signal and the transmitted output is defined to be that level at which the rms phase error is equal to 1 rad. This level corresponds to unity signal-to-noise ratio in the phase-controlled loop. The nominal

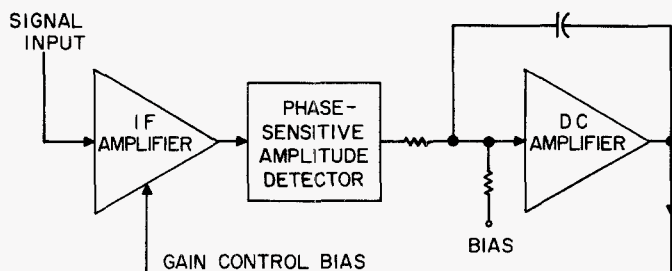


Fig. 101. AGC loop, block diagram

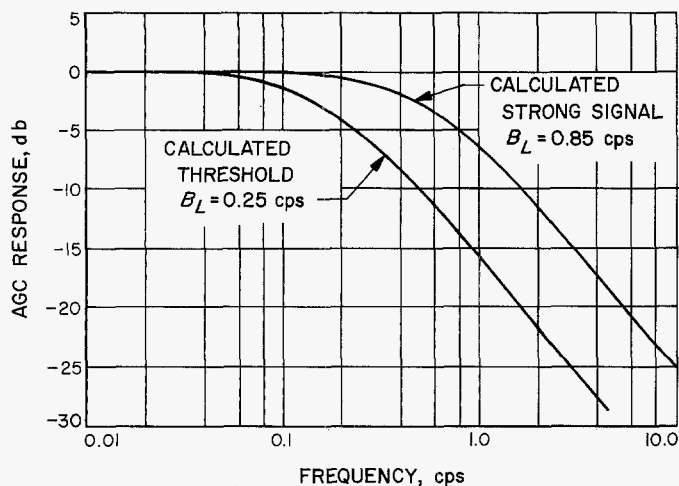


Fig. 102. AGC response of receiver

signal level at which it occurs is found from the loop noise bandwidth and the receiver noise figure to be -147 dbm.

Signal amplification. A total forward signal gain of about 160 db has been designed into the receiver to ensure limiting at the phase detector under threshold conditions and to compensate for the effects of aging, temperature, radiation, and detuning. A tight automatic gain control system controls the gain of the amplifiers to maintain a level of -6 dbm ± 1 db into the phase-detector limiter. The forward gain is provided by a 50 -mc preamplifier with a nominal gain of $+35$ db, including the first mixer loss, a gain-controlled 50 -mc I-F amplifier with a controllable gain of -40 to $+65$ db, and a 10 -mc I-F amplifier with $+62$ -db gain.

Automatic gain control system. The automatic gain control loop is shown in Fig. 101. The automatic gain control system is primarily intended to provide an accurate analog of the receiver input signal strength. In addition, it provides a constant signal level into the phase detector and supplies a method of extracting amplitude modulation from the input signal. The AGC loop is de-

signed to have a noise bandwidth of 0.50 to 1.70 cps over the range of input signal levels from -50 to -147 dbm.

AGC response. The I-F amplifiers are designed to have a gain control sensitivity of 15 to 50 db/v of gain control voltage over the range of levels. The amplitude detector gain at the controlled input level is about 0.15 v/db of input level change, and the d-c amplifier nominal gain is 10 v/v. The loop gain is then 22.5 to 75 , with the lower value occurring near the receiver threshold. The time constant in the loop is provided by feedback around the d-c amplifier and is set to be 22.5 sec. The loop response is then

$$\begin{aligned}
 H &= \frac{1}{1 + \frac{T}{G}S} \\
 &= \frac{1}{1 + \frac{22.5}{22.5}S} = \frac{1}{1 + 1.0S_{\text{threshold}}} \\
 &= \frac{1}{1 + \frac{22.5}{75}S} = \frac{1}{1 + 0.30S_{\text{strong signal}}}
 \end{aligned}$$

AGC response is plotted in Fig. 102.

AGC control characteristics. One major problem in the design of a coherent automatic gain control loop is associated with the large noise-to-signal ratios present prior to detection. In this case, the receiver noise bandwidth of 20 cps and the 3 -kc bandwidth of the I-F amplifiers result in a $150:1$ noise-to-signal ratio at the receiver threshold. Although the receiver loop deliberately introduces a limiter at this point to provide automatic bandwidth suppression, the gain control loop is ideally linear. This arrangement leads to a choice of restricting the signal component to a lower value, or of providing large power handling capability in the amplifiers. The $890/960$ transponder uses a compromise design that restricts the signal power to 0.25 mw at the I-F amplifier output, and provides nearly linear operation over a range that exceeds the expected rms noise level (0 - 40 mw). AGC delay is provided to reduce the effects of detector unbalance, temperature effects, and discriminator action.

The design of the static characteristics of the gain control loop is outlined in Fig. 103 and 104. The predicted performance is compared with measured values in Fig. 105.

(c) **Transmission.** Under normal operating conditions, the transmitted signal is derived from the receiver phase-locked filter signal by frequency multiplication of the

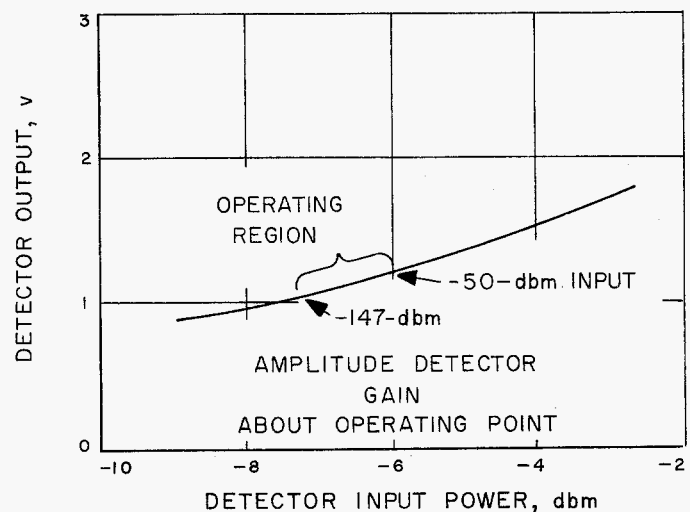
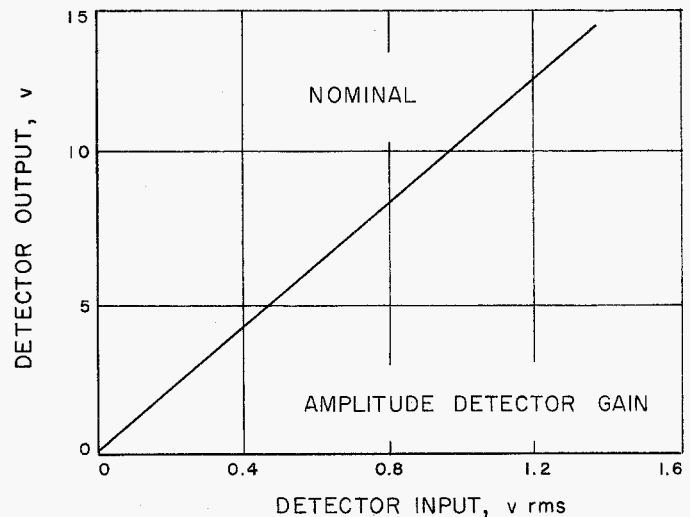
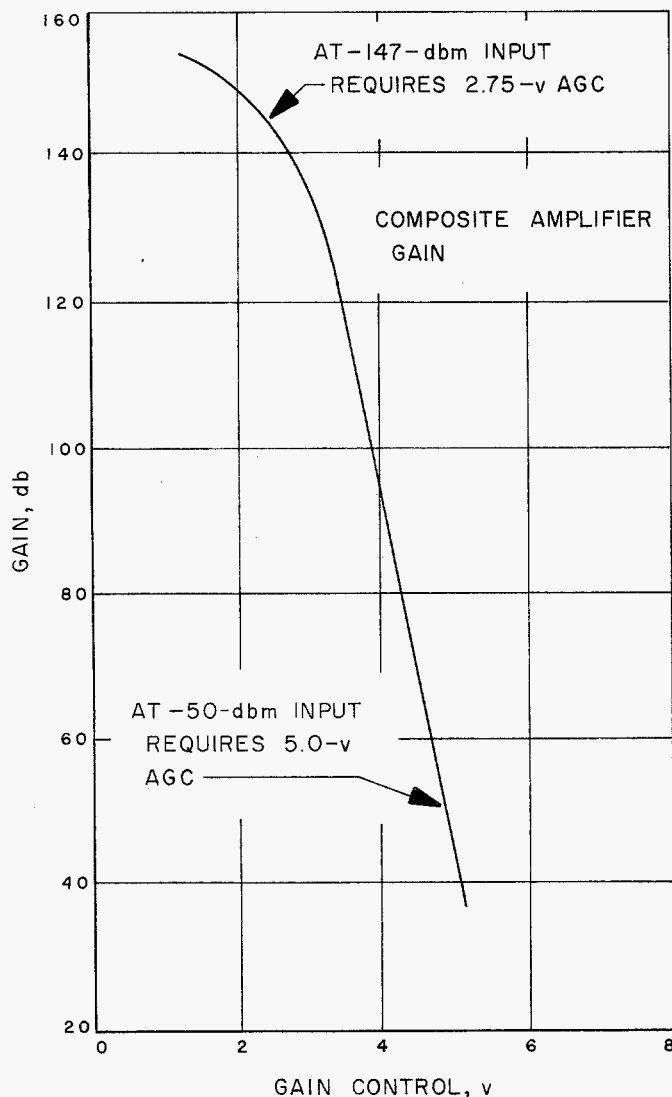


Fig. 103. Characteristics of gain control loop

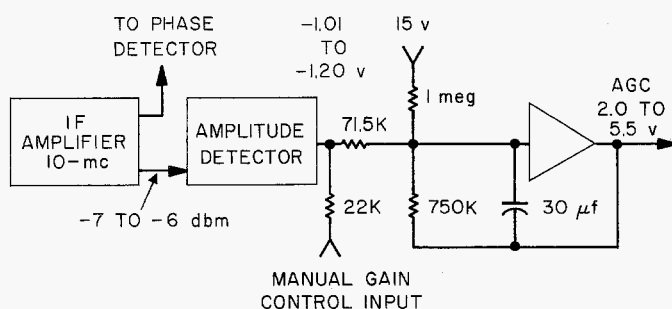


Fig. 104. AGC control characteristics with delay bias, block diagram

voltage-controlled oscillator output. The multiplication ratio of 48:1 is accomplished in the sequence of $\times 3$, $\times 2$,

$\times 2$, $\times 4$ multipliers, where the final quadrupling is completed in a variable reactance multiplier cavity coupled to the transmitter output terminal. The nominal transmitter output power is 7 mw.

Modulation signals are impressed upon the transmitted signal in a phase modulator separating the triplexer and the first frequency doubler. This results in 16 to 1 multiplication of the index of modulation. The modulator is designed to provide ± 4 rad of phase modulation at the transmitter output frequency.

When the receiving portion of the transponder is non-operative due to either the lack of an incident signal or to a disabling command, the transmitter multiplier chain is automatically switched to an auxiliary oscillator source.

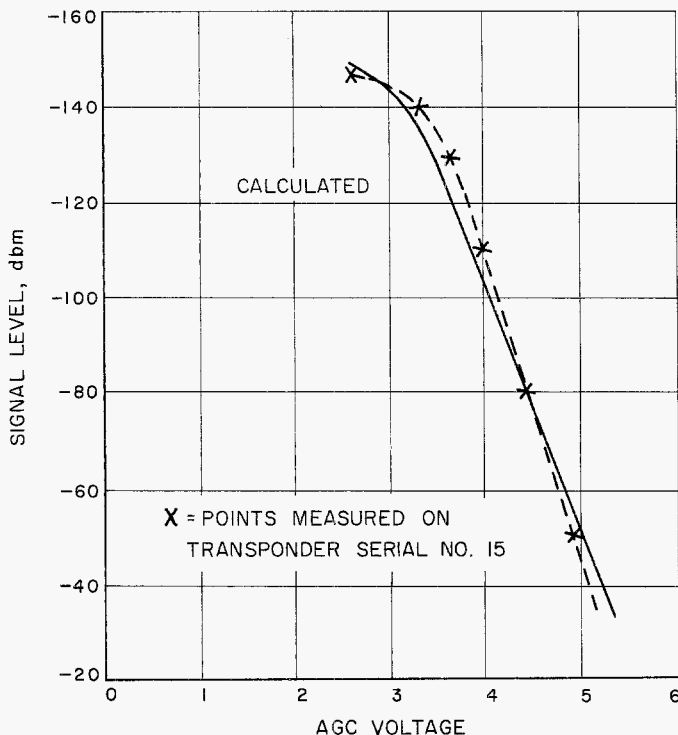


Fig. 105. Calculated vs actual performance of AGC loop

This oscillator operates at the same frequency and power level as the voltage-controlled oscillator in the receiver, but is not linked to the receiver input. The multiplication and modulation system used is the same in either normal or auxiliary operation.

The transmitter frequency of *MR-1* was 960.1 mc; for *MR-2* it was 960.05 mc. This difference in frequency was necessary to eliminate interference during tracking.

The transponder transmitter has two modes of operation. In one mode, the transmitter multiplier chain is excited by a 20-mc voltage-controlled oscillator in the receiver. The resulting 960-mc output is phase-coherent with the 890-mc received signal.

In the other mode, the receiver is not in lock with the ground transmitter. In this mode, the transmitter multiplier is excited by a crystal-controlled oscillator. An electronic switching circuit allows the use of the crystal-controlled oscillator instead of the noisy "out-of-lock" receiver VCO. The crystal-controlled oscillator operates at the nominal VCO frequency.

The telemetry modulation is impressed after the first multiplier stage ($\times 3$) in the transmitter. If for any reason

the receiver fails or the signal strength is low, the transmitter multiplier is excited by the free-running (crystal-controlled) oscillator and telemetry data will still be transmitted. The transponder 960-mc output is nominally 7 mw. This output drives a $\frac{1}{4}$ -w cavity amplifier. The $\frac{1}{4}$ -w cavity drives either of two 3-w R-F output cavity amplifiers. Only one cavity (omni- or high-gain) is operating at a particular time, and switching is accomplished in the cavity filament circuits. It is believed that switching the filaments is more reliable and provides more isolation than a coaxial relay or switch. There are two cavity power modes. At launch, the cavity plate voltage is 150 v dc. At *Agena* separation, an interlock raises the voltage to 250 v dc. The lower plate voltage during the initial portion of the flight eliminates the possibility of voltage breakdown through the critical pressure zone in the cavity. The R-F power output at the reduced plate voltage is about 3 db below the nominal 3-w output.

One cavity drives the omni-antenna and is designated omni-cavity. The power output is monitored by telemetry by means of a directional coupler and crystal detector.

The other cavity drives the directional antenna and is designated directional cavity. The cavity feeds the directional antenna through a circulator which isolates the cavity from the antenna. It was discovered on *Rangers I* and *II* that, in the launch configuration, the directional antenna facing the *Agena* adapter was a mismatched load and the diode probe power monitor readings were very inaccurate under these high VSWR conditions. The circulator was provided in *Mariner* to eliminate these effects and adds 20 db of reverse isolation between the cavity and the high-gain antenna.

Antenna operation is such that the omni-antenna is used at all times the spacecraft is not Earth-acquired, such as initial flight and midcourse correction. The directional antenna is used at all other times. During normal spacecraft operation, cavity, and hence antenna, switching may be accomplished with the umbilical connection prior to launch. In addition, there are two real-time commands for switching antennas during flight and test. A third mode of antenna switching, involving the attitude control system, is also used. In this mode, the directional antenna is pointed by the Earth sensor. One function of the attitude control system is to obtain Earth acquisition. When acquisition is obtained, a command to switch to the directional antenna can be given by the attitude control system. The directional antenna can also be given various angular displacements from the spacecraft perpendicular by the command system.

UNCLASSIFIED

The transformer-rectifier supplies all of the voltages used in the communications pan. Its input is 100 v peak-to-peak, 2400 cps, square wave, regulated to $\pm 1.5\%$. Power allotment to Communications Case II was 30 va, requiring the maximum in T-R efficiency. As a result, only voltages that absolutely required regulation were regulated. The voltages and currents supplied are as follows:

- +5.75 v dc at 1.2 a, filament regulated
- Regulated -15 v dc at 100 ma, transponder
- Regulated +15 v dc at 350 ma, transponder
- +28 v dc holding relay for power-up after separation, no-load unregulated
- Unregulated +100 v dc at 8 ma, driver cavity B+.

Transformer-rectifier efficiency is 75% minimum.

Command

(1) *Program background.* The development of the command subsystem covered both *Mariner A* and *R* vehicles. The initial contract was awarded May 15, 1961, for the development of one *Mariner A* prototype flight system and one test console. JPL had system responsibility in that a functional block diagram was specified and Motorola had the technical responsibility for the design and manufacturing of the system.

Delivery of the first flight system and test console was made on October 18, 1961. During the course of the program, several major changes occurred:

- (1) Change from *Mariner A* to *Mariner R* configuration. This change caused a complete redesign of the decoder portion of the flight system and major changes to the test console. The purpose of the change was to reduce the decoder from a 149-module design to a 60-module design.
- (2) Change in the detector portion of the flight system from a $4F_s$ coherent-reference frequency to a $2F_s$ frequency. This change was a system type to reduce the probability of bit error for a given transmitted power.
- (3) Incorporation of a high reliability program. The selected program made extensive use of *Minute-man*-type components and required redesign of all circuits used in the flight equipment to accommodate these parts.

These changes were being studied in August and became contractual requirements in October 1961. The *Mariner R* configuration consisted of a $2F_s$ detector-decoder utilizing redesign circuitry manufactured in a high reliability type program. A prototype *Mariner R* command subsystem was delivered on December 19, 1961. The three flight subsystems were delivered during January 1962.

(2) *Design considerations.* The design considerations of the command subsystem are discussed under data encoder synchronization in 3b of this Section.

(3) *Problems and solutions.* The problems associated with this project were relatively minor considering the complexity of the system and the extremely short delivery schedule. However, certain significant problems need to be highlighted to emphasize the areas where improvements in the performance of future systems can be made.

(a) *Command detector.* The major problem areas associated with the command detector are: (1) false lock, (2) transponder phase characteristic, and (3) high threshold.

False lock. The command subcarrier was changed from $4F_s$ to $2F_s$ in order to decrease the phase jitter in the filtered reference for a given signal-to-noise ratio in the sync channel. This modification achieved the result, but interference between the information subcarrier and the sync code spectrum caused false lock points in the sync correlation curve at high signal-to-noise ratios. Since the flight units were either fabricated or nearing the final stages of fabrication, it was determined that reduction of command signal power during sync acquisition at high signal-to-noise ratios would satisfactorily overcome this problem. For future command detectors of this type, it is planned to eliminate this problem by rotating the command subcarrier 90 deg.

Transponder interface. The spectrum of the synchronizing signal is relatively broad and has significant components in the lower audio range. During SAF tests at JPL, the command detector would not lock reliably on a signal transmitted through the transponder. This deficiency was traced to low-frequency phase distortion in the transponder detector at high signal levels. The addition of phase equalization was required to allow normal operation of the command detector at high R-F signal levels.

UNCLASSIFIED

High detector threshold. The transmission of the reference frequency by means of a PN-coded signal allows the bit timing to be transmitted without the generation of very low-frequency components near the carrier. The technique does, however, require that the PLL lock in one cycle and sets the practical minimum loop noise bandwidth to approximately 2 cps. Since the loop noise bandwidth is twice the matched filter bandwidth, twice the power is placed in the sync signal and the total signal-to-power must be increased to achieve the required bit error probability of 1×10^{-5} .

(b) *Transformer-rectifier.* The efficiency of the transformer-rectifier was lower than expected. One major contributing factor was a low transformer efficiency due to the form factor necessitated by the packaging constraint. For future models, a more cubical transformer will be utilized.

(c) *Decoder outputs occurring during power turn-on.* It is desirable to prevent the decoder output switches from issuing an output created by power turn-on. Tests showed that a false output does occur from the IP switches approximately 600 μ sec after power turn-on with a 100- to 300- μ sec duration.

In subjecting the decoder to further analysis, the only failure mode that appeared possible was the one in which the AND-invert gate driving the switch input was partially turned on during the switching transient. This possibility could occur if its inputs were partially on (linear operating range) or if the -6-v d-c bias supply was rising at a much lower rate than the +6-v dc. The false outputs were shown to be caused by the drive circuits to the output switches. A power supply modification was tested that would slow the +6-v d-c turn-on time and correspondingly speed up the -6-v d-c power turn-on. Power turn-on tests with the modified power supply indicated that the false outputs had been eliminated.

(d) *Problems revealed in testing*

(1) During the first system testing of *MR-1*, it was found that the command detector was not functioning properly. The detector would lock but initiation of a 1 to start a command would cause the detector to go out of lock. Investigation showed no d-c indication between the transponder command tones output and the command detector input. The addition of a capacitor on this line in the transponder package restored the command detector to normal operation.

(2) Command-data encoder interface tests at SAF revealed improper connection by the encoder to the command switch outputs and improper interrogation connections. These conditions were remedied by encoder circuitry wiring changes and one wiring change in the command case harness.

During post-environmental tests, it was found that channel 11 telemetry readings were erratic at the 8-bps rate. That is, the frequency reading was correct but the lock indication was unstable. Investigation of Case III (data encoder and command subsystems) at the subsystem level revealed the presence of 2.4-kc noise spikes on the interrogate pulse. At the 8-bps rate, the fall time of the interrogate pulse from the data encoder is 30 μ sec. This fall time is too slow to reset the lock flip-flop. Furthermore, during the slow fall time, the drivers in the command telemetry package tend to amplify the slow fall time and to amplify the noise spikes at the trailing edge of the pulse and cause the IP switches to refire, which looks like switch bounce on the output. These amplified noise spikes also reset the lock flip-flop. Capacitors were added in the data encoder on the command detector monitor lines which have bypassed the sharp rise time pulses and restored normal operation to channel 11 telemetry.

(3) When the command subsystem was first connected with the transponder, a peculiar type of false lock was experienced which has been called the "yo-yo" effect. This effect consists of detector bit sync nearing coincidence with ground sync and then abruptly bounding back to approximately 18-msec difference, returning to 6 msec, and then settling at 8-msec difference. Tests performed using *MR-2* revealed a phase-shift problem in the spacecraft transponder receiver at high signal levels. This problem was overcome by passing the composite command signal through a two-phase equalization circuit prior to transmission.

(4) Because of *RA-4* CC&S failure after launch, the RTC assignments of *Mariner* spacecraft were altered to allow direct commands to unfold solar panels and acquire the Sun, acquire the Earth, and command cruise science off.

(5) During the final system test at AMR on *MR-1*, it was found that channel 11 telemetry would give incorrect readings. Investigation proved this to be a digital race problem in the frequency counting circuitry. The problem was corrected in *MR-2* and *MR-3* but not in *MR-1*.

(6) During system tests, it was noted that the first address issued from the GSE after the detector came into lock was erroneous. Tests showed that under these conditions, the GSE issued a false start bit upon initiation of the address. A GSE modification eliminated the problem.

(7) During spacecraft temperature-vacuum tests, the detector VCO's of both MR-1 and -2 increased in frequency by 1 to 2 cps. When ambient temperature and pressure were restored, the VCO's drifted back to their original setting. Assuming this phenomenon to be due to vacuum, all command VCO's were adjusted to $2F_s$ from their previous setting of $2F_s + 1.5$ cps. Subsequent tests on similar VCO's have shown that, after a number of hours of operation, these units assume a new frequency and remain at that frequency.

(4) *Subsystems functional description.* The flight command subsystem digital command information from the transponder, in the form of a phase-shift keyed subcarrier and a coded-reference frequency, detects the serial binary bits, recovers the bit timing pulses, and decodes the commands. These commands are then presented to the appropriate subsystem by means of isolated solid-state switch closures. All d-c voltages required by the command subsystem are derived from a transformer-rectifier that is powered from the central spacecraft power unit.

The flight command subsystem is divided functionally into three units: (1) a command detector, which filters and demodulates the PSK subcarrier and extracts the bit timing pulses; (2) a command decoder, which decodes the commands and supplies both the commands and appropriate timing pulses to the command users; and (3) a transformer-rectifier. The command detector also houses the command telemetry circuit that conditions the detector parameters to be telemetered to Earth.

(a) *Modulator/detector.* The command information is transmitted by a coherent phase-shift keyed subcarrier frequency, with the reference frequency transmitted in the form of a pseudo-random code. The composite subcarrier spectrum is essentially between 20 and 1500 cps. The command detector separates the command and reference signals. The filtered reference is used to demodulate the command information coherently and the command bits are detected in a matched filter. The detected binary pulse train is presented along with bit timing pulses to the command decoder.

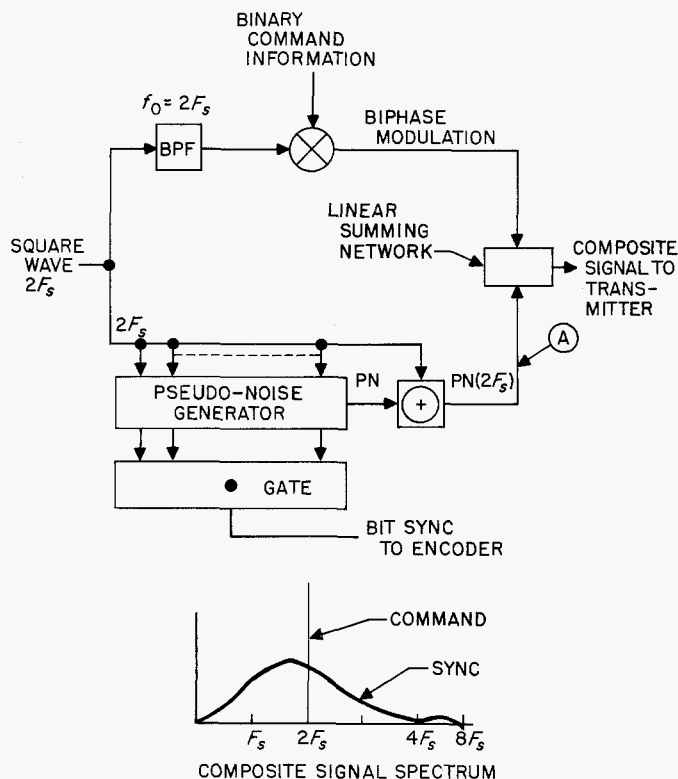


Fig. 106. Command modulator, functional block diagram

(b) *Command modulator.* The command subcarrier modulation is provided by a command modulator located either in the RWV ground system or in the command subsystem ground support equipment. The command modulator performs two major functions. It encodes the command reference signal and bit timing in a pseudo-random signal and biphase-modulates the $2F_s$ subcarrier according to the value of the command bits. A functional block diagram is presented in Fig. 106. The period of the PN generator is equal to the bits with a unique code time.

The reference frequency $2F_s$ is filtered to select only the fundamental. This signal is biphase-modulated with zero phase shift corresponding to a binary one, and 180-deg phase shift corresponding to a binary zero. This signal is linearly summed with the synchronizing signal, and the composite signal is presented to the R-F transmitter.

(c) *Command detector.* The command detector receives the composite subcarrier spectrum and recovers both the digital pulse train and the bit timing pulses. The command detector can be divided into two func-

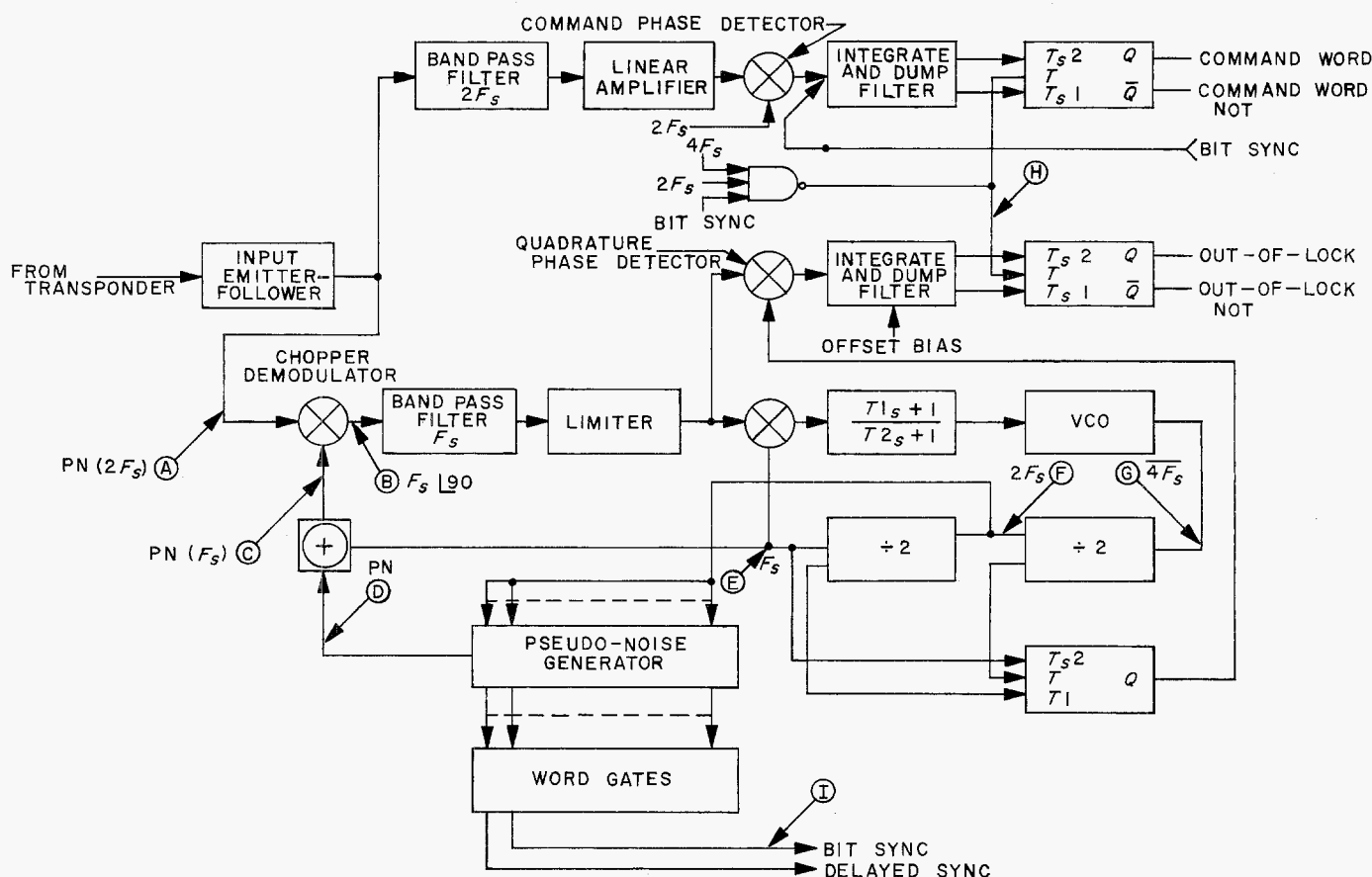


Fig. 107. Command detector, functional block diagram

tional parts—the synchronization channel and the command channel. The functional block diagram of the command detector is presented in Fig. 107.

The *Mariner R* command detector differed significantly from the *Mariner A* command detector as follows:

- (1) The biphasic command subcarrier was changed from $4F_s$ to $2F_s$.
- (2) The limiter in the command channel was replaced by a linear amplifier.
- (3) The command phase detector was replaced with the high-gain, loop phase detector.

These changes were initiated after tests on the JPL breadboard indicated the threshold of the $4F_s$ configuration was too high. The remainder of the *Mariner R* command detector design was essentially the same as the *Mariner A*.

(d) *Synchronization channel.* The synchronization channel is comprised of the chopper-demodulator, the F_s bandpass filter, limiter, phase-locked loop, PN generator, and the out-of-lock circuit.

The subcarrier synchronization signal is the product $\text{PN} \times 2F_s$. This signal is multiplied in the chopper demodulator by the locally generated $\text{PN} \times F_s$. When the two PN sequences are in time coincidence, the output of the chopper demodulator is a square wave with a frequency of F_s and a phase angle of 90 deg with respect to the detector F_s . This signal is filtered and passed through the amplitude limiter to decrease the dynamic range requirement of the phase-locked loop, which follows. The signal has the required phase relationship with the detector F_s for a stable locked condition. Since the shift pulses $2F_s$ for the detector PN generator are derived from the PLL, once the modulator and detector PN codes are in time coincidence, the PLL maintains the synchronism. Should the two PN codes not be in time coincidence, the output of the chopper demodulator is

then random and the offset frequency of the VCO drives the detector PN code past the modulator PN code at a slow rate until frequency and code lock are achieved. The plot of the ideal loop error voltage vs relative code time is presented in Fig. 108.

The $2F_s$ signal is also used as the reference frequency for the coherent detector in the command channel. The out-of-lock signal is generated by multiplying the sync channel output with the detector quadrature F_s signal (i.e., 90 deg with respect to F_s) and integrating the output in a matched filter. A bias voltage is introduced in the threshold detector such that an out-of-lock signal is

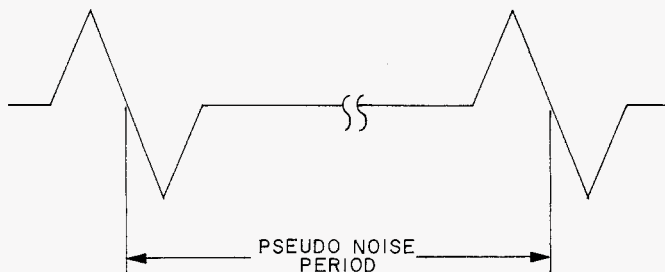


Fig. 108. Ideal loop error voltage vs relative code time

presented until the PLL achieves code and frequency lock.

(e) *Command channel.* The command channel is comprised of a $2F_s$ bandpass filter, linear amplifier, coherent phase detector, and a matched filter. The biphasic command information is filtered and amplified before demodulation in the coherent phase detector. The binary information is detected by an "integrate-and-dump" matched filter.

The integrate-and-dump circuit is comprised of an RC integrator, a shorting switch to dump the integrator at the end of the bit, a pulse amplifier to amplify the transient generated by dumping the integrator, and a storage flip-flop to store the bit decision. The integrating capacitor is shorted by the leading edge of the bit sync pulse. After a delay of 500 μsec to allow the pulse transient to charge the steering inputs of the decision flip-flop, a pulse is generated and applied to the toggle input of the flip-flop. This delay pulse is generated by inverting the logical junction of bit sync, $2F_s$ and $4F_s$. The output of the decision flip-flop is presented to the decoder along with bit timing pulses and the out-of-lock signal.

(f) *Command telemetry.* The command telemetry unit conditions the detector VCO frequency and the out-of-

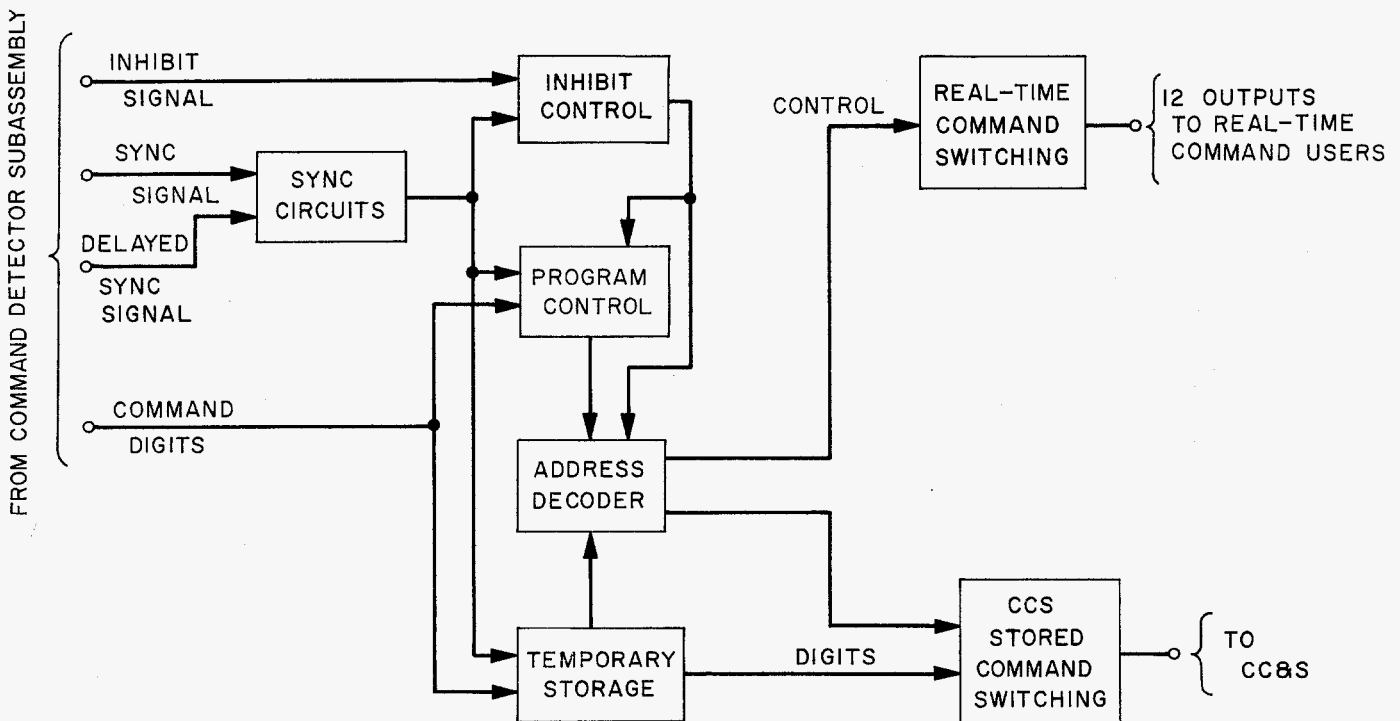


Fig. 109. Command decoder subassembly, simplified block diagram

lock signal prior to transferring the information to the data encoder.

(g) *Command decoder subassembly*

General. The function of the command decoder subassembly is to process the serial, digital information from the command detector subassembly into pulsed output signals suitable for 12 real-time command users and a serial binary data output for the CC&S subsystem. A simplified block diagram of the command decoder subassembly is shown in Fig. 109.

Operation of the command decoder subassembly. Operation of the command decoder subassembly will be explained with reference to the simplified block diagram in Fig. 109. The sync information from the command detector subassembly is processed for use as timing information to control the nonlocked command decoder circuits as well as to provide for correct sequencing of the output switch timing. The program controller circuit is used to start the command decoder when a word bit is received from the command channel; to provide an output upon the receipt of the eighth bit and the internal P2 signal to control the event counter; to sample the address matrix; and to provide end-of-message shutdown after the complete word has been received.

The inhibit control circuit is used to stop decoding operations should the command detector circuits lose phase lock. Additional protection is required to assure that the command decoder will not start in the middle of a command when the command detector recaptures the signal. The inhibit function requires the use of a counter that has a capacity at least equal to the message length to preclude the beginning of a program in the middle of a word after an inhibit period.

The temporary storage register consists of a six-stage shift register used to store the command address for a parallel read-out when sampled during the eighth bit at P2 time by the program controller. To obtain correct timing for the control computer and sequencer quantitative commands (CCS), the first stage of the temporary register is gated to the appropriate output switch. The address decoding circuits are required to direct the command address stored in the temporary register to the proper output circuits. Single pulses (2 to 100 msec) are supplied to 12 real-time command users through isolated output switches. One additional command address is required in the command decoder for this CCS subsystem. The CCS commands are quantitative words of a standard message length. In addition to the CCS commands, sync

clock signals and alert signals are provided to the CCS subsystem.

Command decoder subassembly operational modes. The functions of the command decoder subassembly can be described by three modes of operation:

- (1) Real-time commands
- (2) CCS commands
- (3) Out-of-lock operation.

The command decoder subassembly also contains timing circuits that are used, in general, for these three modes of operation.

(h) *Ground support equipment.* The command test console is the ground support equipment for the command flight subsystem. The command test console provides the capability for manual and semiautomatic bench performance testing for the flight subsystem and the following three command subassemblies:

- (1) Command detector
- (2) Command decoder
- (3) Command transformer-rectifier.

The test console (1) generates all the signals and programmable commands required to evaluate the command subsystem and the individual subassemblies, (2) performs certain automatic test functions, (3) checks and displays all command subsystem and subassembly output signals, (4) provides continuous monitoring and display capabilities for all command subsystem and subassembly output signals, and (5) provides manual selection of interface and key internal subsystem signals.

The test console also permits limited monitoring of key test-point signals when the command subsystem is operating within the spacecraft configuration. Additional test capabilities are also provided with respect to the command test console control over the spacecraft base transmitter, direct interface control of the command decoder subassemblies when these subassemblies are operating within the spacecraft, and means for facilitating environmental test chamber testing of the command subsystem.

The logic and control circuits in the command test console were designed to facilitate fabrication, testing, incorporation of contractual design changes, and field maintenance. This flexibility was obtained by subdivision of subassemblies according to function. All subassembly

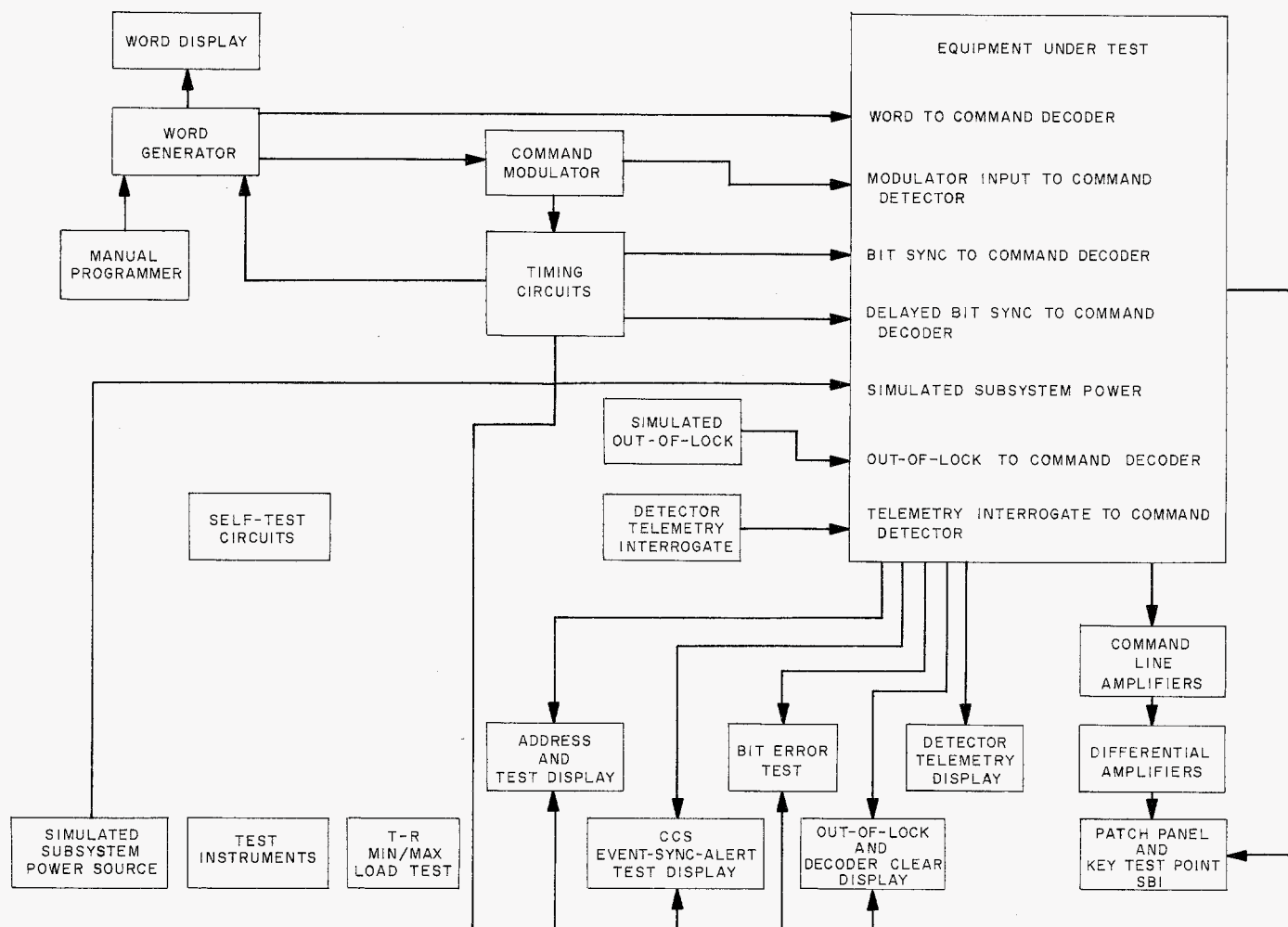


Fig. 110. Command test console, simplified block diagram

interfaces utilize removable connectors which terminate at a centrally located junction panel. The digital circuits use a transistor-resistor-logic family. In addition to the TRL family, other facilitative circuits are employed as required. The control circuits consist of switches and relays which route and provide hard commands to the logic circuits.

Figure 110, a simplified block diagram, reflects the basic design of the test console. As this block diagram shows, the test console timing circuits provide for the correct word generation to the equipment under test and also provide the means for checking the signals received from the equipment under test. The test console timing originates in the command modulator, which contains a free-running tuning-fork oscillator. This oscillator generates the bit sync and the delayed bit sync signals. The timing circuits of the command test console receive the free-running bit sync and delayed bit sync signals, and

upon receipt of a start signal, synchronize the command test console in relation to the command modulator timing signals to provide a bit sync and a delayed bit sync that are in phase with the command modulator timing signals, and always present a full pulse width for each of the two signals.

The equipment under test provides two forms of outputs to the command test console. A direct input is provided for bench test operation; an isolated input is also available for SAF testing. In addition to providing all input stimuli to the equipment under test, the command test console furnishes continuous monitoring of all output signals from the command subsystem. Certain outputs are logically examined to check for the proper timing of events. An entirely self-contained test for the command transformer-rectifier subassembly is available. This test provides for a minimum and maximum load test. Self-test circuits are provided within the command test con-

sole to assure the operator of the command test console's integrity of performance.

Test instruments within the command test console permit the operator to isolate a trouble to the lowest replaceable unit level.

Ground telecommunications equipment

(1) *Program background.* The original *Mariner A* program requirements for ground telemetry equipment were threefold:

- (1) To monitor the output of the spacecraft telemetry system in the same manner as would be done during flight. This included demodulation of the telemetry subcarriers, basic decommutation, a digital printout of all engineering telemetry data, and a magnetic tape recording of all system tests, environmental laboratory tests, and AMR launch operations. The recording at JPL was to be accomplished by equipment located in the Data Reduction Laboratory, which was remote from all test areas. During AMR launch operations, recording was to be performed by the existing Launch Compatibility Test trailer.
- (2) To supply to the DSIF any equipment peculiar to specific telemetry system designs where spacecraft telemetry systems were sufficiently different to require special ground equipment design. All units supplied were to be guaranteed compatible with the spacecraft. This compatibility has been ensured by performing all system tests with units which are exact facsimiles of those supplied to the tracking stations.
- (3) To perform data reduction similar to that now being done by the Central Computing Facility. This included conversion of all data to engineering units, the production of time-tagged tabular records, and the production of analog plots of any data on request.

In the fall and winter of 1960, the original work was done on this basis on the ground telemetry equipment at JPL. In the summer of 1961, it became apparent to many that requirement No. 3 could not be fulfilled by an organization of the size of the Ground Telemetry Group. In this period, by executive directive, the responsibility for *Mariner* data processing and all future data processing was transferred to the Central Computing Facility.

Again in the summer and fall of 1961, three modifications were made to requirement No. 1, above:

- (a) To change the tape recording and reproducing capability from its remote area to a facility in the system checkout circles. Also, appropriate time generation was included to permit immediate and local playback of any system test signals during the spacecraft system tests, environmental tests, and launch operations, for evaluation of the test results by the test team.
- (b) To provide separate telemetry data printouts to the individual subsystem test consoles to speed dissemination of telemetry information during system tests. Individual printers were made program-mable to give only those telemetry measurements applicable to the particular subsystem console at which they were printed out.
- (c) To provide in the spacecraft systems checkout circle a test procedure step number subsystem integrated into the timing generator. This equipment was to give to the test director at any time the ability to display and also record both on magnetic tape and on the teletype paper tape read-out, the number of the test procedure step that was in process, either in real time, or from the tape play-backs.

(2) *Mariner R.* Concurrent with the last of these additions, in fall 1961, the *Mariner A* effort was reoriented toward the *Mariner R* configuration. This involved no gross change in the telecommunications ground equipment requirements, but definitely changed the detailed design of several units within the various systems. Since the initiation of *Mariner R*, there have been two additional changes to the program requirements. The first change (in early 1962) affected requirement No. 3 above, and was a reorientation of the telecommunications laboratory activities. The purpose of the Data Reduction Laboratory became one of telecommunications investigations, which involves research of telemetry methods and analysis, including clean-up of data which is badly distorted or noise-corrupted due to a specific failure in the flight telemetry system. The purpose of this function is the determination of methods of handling and/or resolving such data problems, not the output of data. (Another similar function, data rework, has been defined as the redemodulation and re-recording of data from non-real-time data tapes which were initially improperly demodulated. This work is to be done by the DSIF at one of its Goldstone tracking stations.)

Another requirement in this area is a new activity to be included in the proposed Space Flight Operations Facility. This activity is to be called the Telecommunications Monitor System. Its function will be to monitor, in real time, the quality of all the spacecraft data inputs to the central data processing equipment, which is part of the SFOF, and to report this quality status to the appropriate test and DSIF directors to prevent the possible reduction of inappropriate input data, and to alert the facility to imminence of the loss of adequate signal quality. This system, along with the TIL, will be designed to handle any of the "in-house" JPL programs.

(3) *Design considerations and system histories.* For *Ranger* and *Mariner R*, most of the ground telemetry system design integration work was done by JPL. Each of the major functional units was designed and usually built by a different contractor. These functional units were: (1) telemetry simulators and pole beacon modulators, (2) telemetry data demodulators, and (3) telemetry data decommutators. Table 7 shows how these units were utilized quantitatively in the various subsystems; functional descriptions appear elsewhere in this report. A brief design and contractual history of each unit follows.

(a) *Telemetry simulators and pole beacon modulators.* The basic design was patterned after the *Mariner A* data encoder. It generates an output signal electrically equivalent to the output of the data encoder, including data and sync subcarriers at all six data rates with all the necessary frame synchronization data words. Thus, it could be used in lieu of the data encoder for checkout of all the remaining ground telecommunications equipment; and as a pole beacon modulator it could be used to modulate a test transponder for the DSIF tracking station alignment and checkout. The purchase order was awarded to Epsco-West, Inc., in May 1961. In July 1961, the prototype was received and, with a few minor design changes, accepted by JPL. The remaining units were shipped to JPL in the following two months.

The design change to *Mariner R* was implemented by merely changing the commutator format. This was all that was necessary because the flight data encoder basic design was the same as *Mariner A*. The new format was reflected in JPL Specification 30567-B and the 11 units were shipped back to Epsco-West for the necessary modifications in September 1961. All units were returned to JPL by February 1962. There have been no major failures in these units to date.

(b) *Telemetry data demodulators.* The principal function of this unit is to demodulate with near-optimum

detection means the *Mariner* telemetry subcarriers. This required, at design threshold, a bit error rate accuracy of no worse than 1 bit error in every 1000 bits received.

A certain amount of research and development work at JPL was done to determine the feasibility and practicability of performing telemetry demodulation by the means proposed for the *Mariner A* telemetry system. This work was started in late 1960 and continued in parallel with the production of the demodulators themselves until late 1961. Due to some success apparent at the breadboard level and to program requirements, the purchase order for a prototype unit and one production unit was let in April 1961. The units were built by Texas Instruments, Inc., Dallas, to JPL Specification 30559-A. The procurement of the additional production units was also from Texas Instruments.

In July 1961, concurrent with the procurement of the remaining production units, a problem was discovered in the original design concept when detailed bit error-rate tests were being made using the prototype data demodulator. The addition of a phase-lock loop on the information subcarrier, together with several other circuit changes to each demodulator, solved the problem.

Because there were no differences in the telemetry signal from the *Mariner A* and *Mariner R* data encoders, no additional design changes were necessary in this respect.

The prototype of the final design configuration was delivered to JPL in February 1962. The remaining 11 units were received at JPL at the rate of approximately three per month thereafter. All of these units, without exception, operated within 0.6 db of the theoretical signal-to-noise performance specified. There have been only a few component failures of a minor nature since the units were delivered. Most of these have been due to the operator inadvertently shorting internal signals to ground during alignment procedures and circuit testing.

(c) *Telemetry data decommutators.* The basic function of the data decommutators is to accept the commutated, serial, binary data and associated bit and word synchronization pulses as inputs and convert them to parallel output BCD data with the associated commutator address. In June 1961, a purchase order was awarded to Applied Development Corporation, Monterey Park, Calif., for 11 of these units, built to JPL Specification 30557-A. Some slight modifications were necessary after the delivery of the prototype unit. All units were delivered on

UNCLASSIFIED

JPL TECHNICAL REPORT NO. 32-353

Table 7. Ground telecommunications equipment utilization

Unit No.	Unit title	Selected vendor	Design purpose	Quantity procured	Utilization					
					Proto-type	TIL	TMC	LCTT	DSIF	Spacecraft data record
1.	Pole beacon modulators and telemetry simulators	Epsco-West (now Astrodata), Anaheim, Calif.	Spacecraft telemetry signal simulation	11	1	1	3	1	5	
2.	Telemetry data demodulators	Texas Instruments, Inc., Apparatus Division, Dallas	Telemetry subcarrier demodulation to binary data, bit sync, and word sync	12	1	2	3	1	5	
3.	Telemetry data decommutators	Applied Development Corporation, Monterey Park, Calif.	Using output of demodulator to decommutate telemetry data for use by appropriate display and print-out devices	11		2	3	1	5	
4.	Telemetry data print-out subsystem	Applied Development Corporation	Print-out of all engineering telemetry at TMC and selected data at up to 5 remote printer locations	3			3			
5.	Magnetic tape recorder and time generation console	Astrodata, Inc.	Record and reproduce facility for use in evaluating spacecraft system test	1						1
6.	Telemetry bit error rate checkers	Astrodata, Inc.	Generate a random binary sequence as input to telemetry simulator. Then compare this with binary data received back from demodulator to determine by test the system bit error rate	7		3			4	
7.	Telecommunications monitor consoles (heretofore called data display consoles)	Ransom Research, San Pedro, Calif.	Telemetry data monitor and DSIF compatibility check	3			3			
8.	Systems test step number subsystems	Astrodata, Inc.	Display and record (time-tagged) of systems test step number	2			2			

schedule by September 1961. In October 1961, the modification to allow the decommutation of the new *Mariner R* data encoder commutator format was purchased from Applied Development Corporation. Due primarily to JPL design oversights, two additional modifications were re-

quired to make the decommutator function correctly in every subsystem configuration. Because of the method of cycling the decommutators through the reworking process, there was no loss of spacecraft checkout time in performing these modifications.

UNCLASSIFIED

(d) *Telemetry data print-out subsystem.* This major subsystem is used in the spacecraft test complex. By means of a simple patchboard programming scheme, this system made possible an easy solution to the second addition to requirement No. 1 described above. This provided separate telemetry data print-outs to the individual subsystem test consoles to speed dissemination of telemetry information during system tests. The subsystem was built to JPL Specification 30577-A by Applied Development Corporation. The purchase order was let in December 1961. In spite of this very late purchase date, all units in the subsystem were delivered to JPL within three weeks of JPL's delivery requirement. All units, with the exception of a recurrent malfunction in the Hewlett-Packard printer mechanism, have functioned well with few component failures.

Four other items which do not have as important functional roles but which nevertheless constitute a substantial investment and group effort, are added to Table 7, which indicates the utilization of the ground telecommunications equipment for *Mariner R*.

The first of the telecommunications monitor consoles was completed and checked out for the *Mariner 1* spacecraft systems test complex on January 8, 1961. However, because of a last-minute decision to provide 100% signal isolation from other consoles and from spacecraft systems ground, this console was replaced in the *MR-1* complex two weeks later by the second console. Complete integration with all connecting subsystems was accomplished by the end of February 1962 with both consoles. The third, or spare, TM console was completed and checked out by May 1, 1962. This unit was used primarily during final spacecraft checkout operations on *MR-3*. It was also used as a back-up system during the actual launch of *MR-1* and -2.

(4) Problems and solutions

(a) *Telemetry demodulator.* Tests in the fall of 1961 indicated that the single phase-lock loop demodulation scheme was not sufficient. In fact, degradations in the order of 10 to 15 db in bit error rate performance could be expected. This resulted from using a phase-lock loop at a frequency F_s , multiplying this to $4F_s$, and then using this $4F_s$ as a phase-coherent reference signal for data demodulation. The 30-deg rms phase jitter seen on the signal F_s at design signal-noise threshold was 120-deg rms phase jitter at $4F_s$ and, therefore, an extremely poor reference signal.

A solution was the addition of a second phase-lock loop which locks on the squared telemetry data subcarrier itself. Since almost 13 db more power is allocated to the data than to the sync subcarrier, this provides an almost noise-free reference for data demodulation.

(b) *Telemetry decommutator.* When the decommutator uses input data from a tape recorder, tape skew, gap scatter, etc., cause an effective time jitter between signals on two separate tracks. This jitter between bit and word sync at a typical *Mariner R* recording speed of 3.75 ips is approximately 50 μ sec. The decommutator was originally designed to accommodate a maximum of $\pm 5 \mu$ sec relative jitter.

An effective logical OR of every seventh bit sync and word sync completely solved this problem.

(5) *Subsystems functional descriptions.* The *Mariner R* ground telecommunications equipment has the following basic functions:

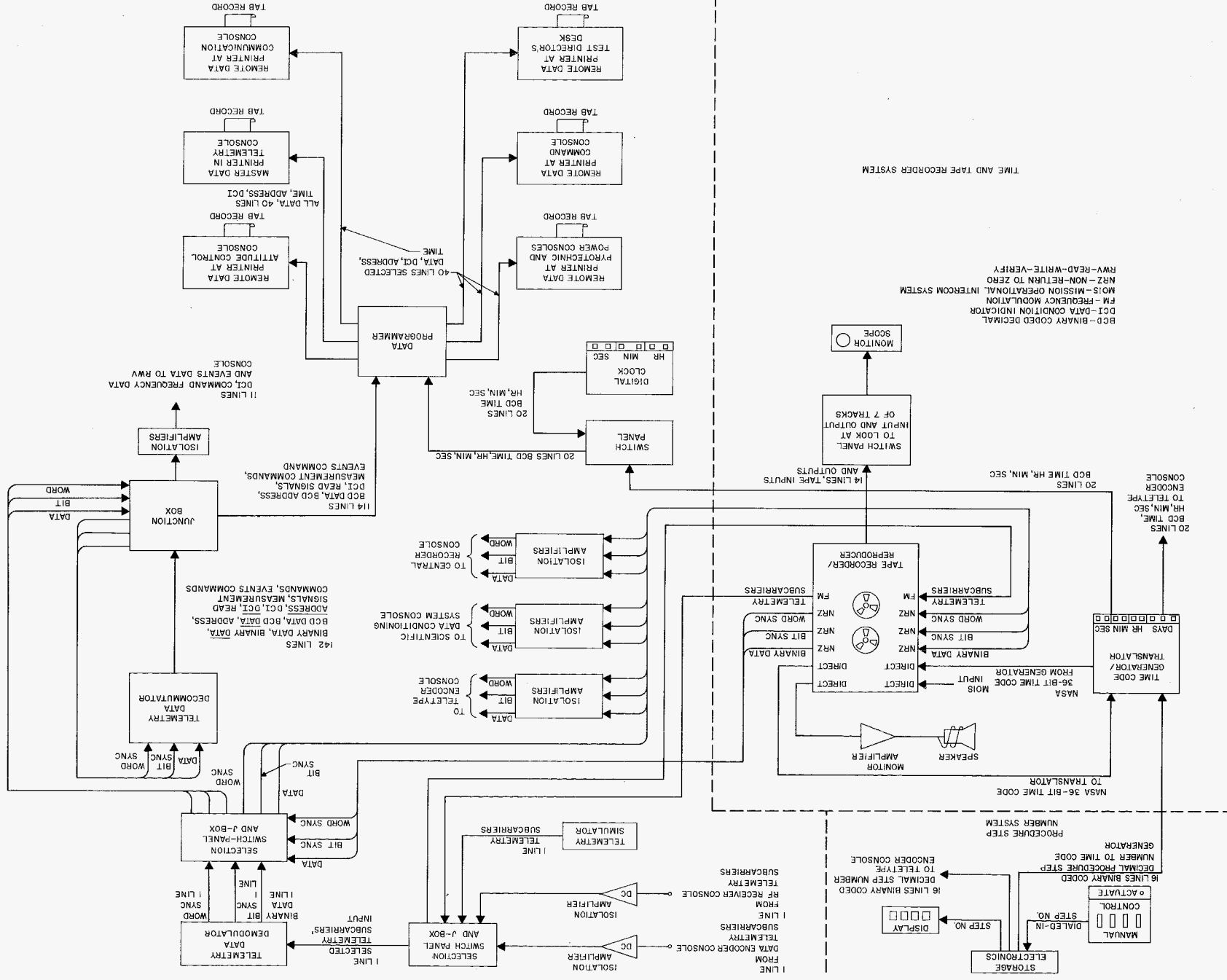
- (1) Ground checkout of the spacecraft telemetry subsystem in spacecraft system tests, dummy runs, and launch operations, a function which is performed by the telecommunications monitor consoles.
- (2) Near-optimum real-time detection of the spacecraft telemetry subcarriers during spacecraft flight at the DSIF tracking stations. This function is performed by demodulators, decommutators, and other equipment supplied to the DSIF for each mission.

(a) *Telecommunications monitor console.* Ground checkout of the spacecraft telemetry subsystem is partially performed through the use of the telecommunications monitor console described in Fig. 111. The right half of Fig. 111 describes the demodulation, decommutation, and printer system portions. The lower left corner shows the tape recorder portion, and the upper left corner the procedure test step number system.

The telemetry subcarriers, data (a linear addition of lines D and K in the timing diagram, Fig. 112) and sync are the primary inputs to the telecommunications monitor console. This signal can originate from several sources, the spacecraft data encoder itself, the output of the R-F receiver in the communications console, a telemetering simulator, or the output of a tape recorder in the playback mode.

[REDACTED]

Fig. 111. Telecommunications monitor console



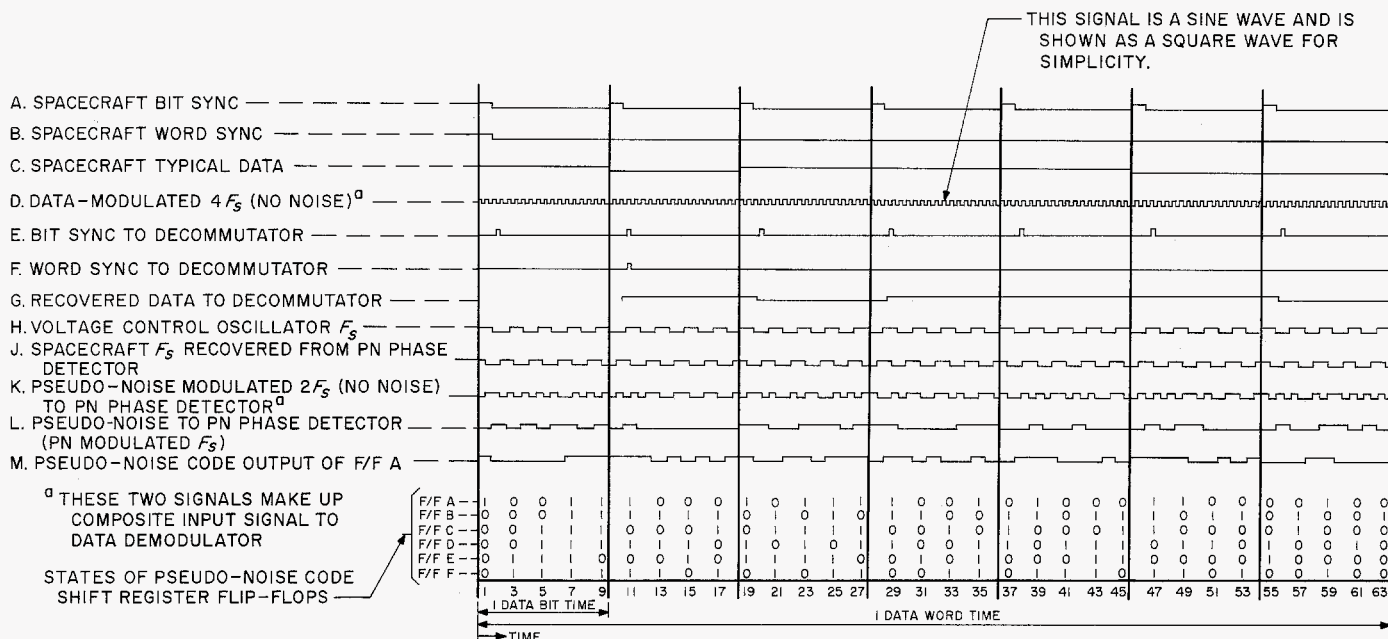


Fig. 112. Telemetry data demodulator timing diagram

One of these signals can then be selected and sent to the telemetry data demodulator. This unit then demodulates the data and sync subcarriers and has a resultant binary output, data, bit sync, and word sync. These signals have the timing relationship shown in Fig. 112, lines G, E, and F.

The binary data, bit sync, and word sync are sent to several places. They are first sent to the data demultiplexer. They are also sent to the tape recorder, the Central Recorder System, the telemetry-to-teletype encoder, and to the scientific Data Conditioning System. The first two simply record the signals. The TTY encoder encodes the data into teletype format and punches a paper tape which is then played back to the Central Computing Facility. The scientific Data Conditioning System decodes and demultiplexes the science portion of the data when the spacecraft is in the SCIENCE + ENGINEERING or the SCIENCE ONLY mode.

The data decommutator uses the binary data, bit sync, and word sync to acquire frame synchronization with the spacecraft data encoder commutator. The data are then converted to decimal, commutator-address tagged, data-sync condition tagged, and sent to the data programmer. A secondary data output from the decommutator is the command events and command frequency data which is sent to the Read-Write-Verify system for

use in monitoring the status of the spacecraft command decoder.

The data programmer has two primary functions. The first is to buffer the data from the decommutator and feed it to all six data printers (one master printer and five remote printers). The second function is to select any group of 20 of the 54 spacecraft telemetry measurements available for each of the five remote printers. Thus, the remote printer located at the attitude control console receives only the measurements telemetered from the spacecraft attitude control system. Also, the remote printer at the communications console receives only those measurements which pertain to the spacecraft transponder (typically static phase error, omni-antenna power, etc.).

The data programmer also accepts binary-coded decimal time from either the digital clock or the time-code generator/translator. These time data are sent out to the data printers synchronous with the spacecraft data.

The data printers perform a simple print function, using the data sent to them from the data programmer. A typical data printer tab paper print-out is shown in Fig. 113.

The tape recorder system provides a magnetic tape recording of all the telemetry data during spacecraft

tests. The magnetic tape track assignment with the particular recording modes for each track is shown in Fig. 114.

The procedure test step number system accepts the dialed-in test step number data from the test director upon his pushing the ACTUATE button. These data are then sent to the TTY encoder for inclusion in its data

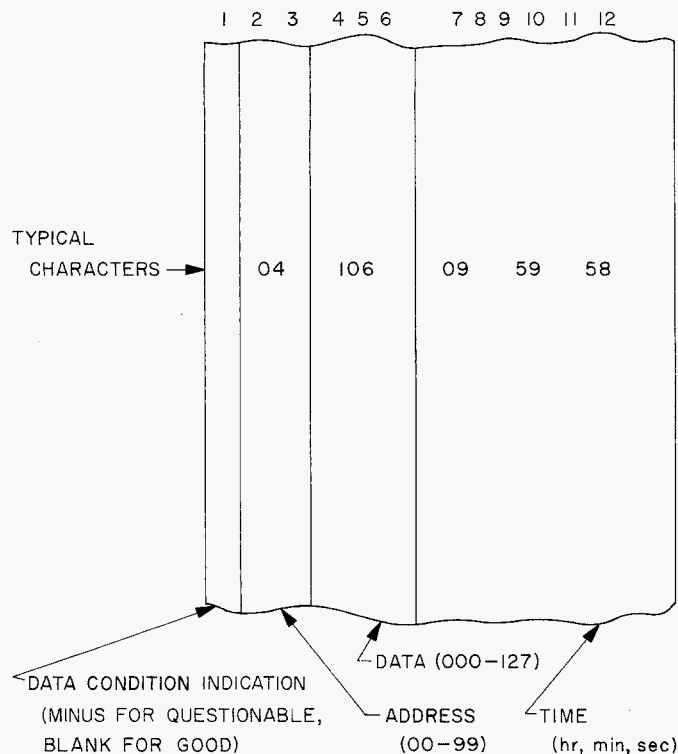


Fig. 113. Data printer tab print-out

transmission, and to the time code generator/translator, where they are encoded within the NASA 36-bit time code and then recorded by the tape recorder.

(b) *DSIF telemetry detection equipment.* A typical DSIF tracking station flow diagram from the output of the R-F receiver is shown in Fig. 115. The output of the receiver (spacecraft telemetry subcarriers plus noise) goes to the telemetry demodulator and to magnetic tape recorders simultaneously. The outputs from the demodulator (data, bit sync, and word sync, as above) are sent to the tape recorder, to the TTY encoder, and to the data decommutator.

The TTY encoder sends the data via teletype lines to the Central Computing Facility for near real-time telemetry data processing. The data decommutator outputs are then sent to a programmable display, which can select any one telemetry measurement and display its value continuously for use in analyzing spacecraft performance.

(c) *Telecommunications investigation laboratory equipment.* Figure 116 shows the telecommunications investigations laboratory diagram. This laboratory has many modes of operation since its primary function is research and development of methods and means for better telemetry demodulation. The facilities shown in the laboratory are designed and aligned to perform optimum detection on whatever data are transmitted to it. It can, if necessary, be used to unscramble and re-record that data which could not be demodulated at the DSIF Data Rework Facility.

TRACK NO.	SIGNAL	RECORDING MODE
TRACK 1	GROUND INSTRUMENTATION	DIRECT
TRACK 2	BINARY DATA	NON-RETURN TO ZERO DIGITAL
TRACK 3	TELEMETRY SUBCARRIERS	FREQUENCY MODULATION
TRACK 4	BINARY BIT SYNC	NON-RETURN TO ZERO DIGITAL
TRACK 5	TIME CODE (NASA 36-BIT) WITH 6.25-kc WOW AND FLUTTER TONE	DIRECT
TRACK 6	BINARY WORD SYNC	NON-RETURN TO ZERO DIGITAL
TRACK 7	VOICE LABEL	DIRECT

Fig. 114. Magnetic tape track assignments

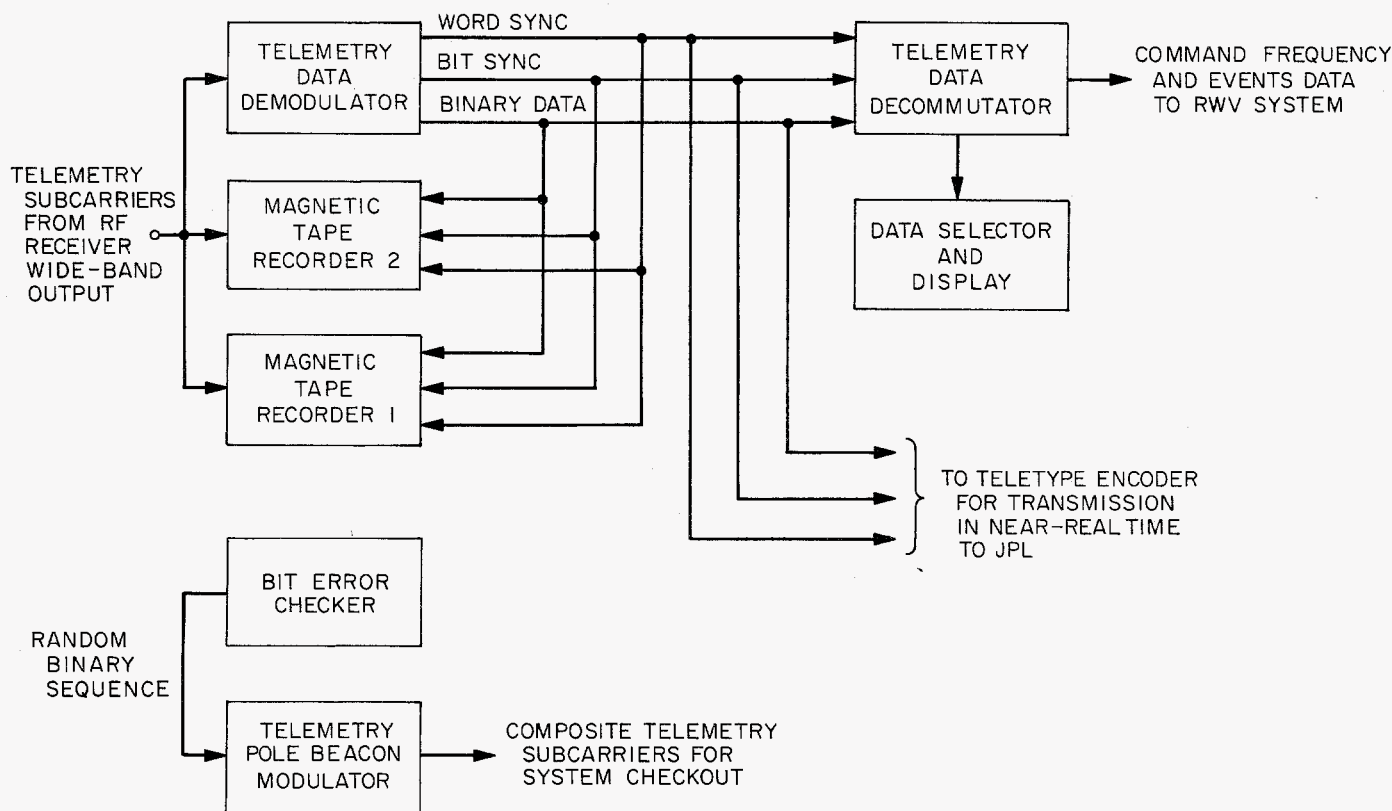


Fig. 115. DSIF tracking station telemetry flow diagram (typical)

Read-Write-Verify ground command subsystem

(1) *Program background.* The RWV ground command subsystem for *Mariner R* is essentially the same as the RWV equipment designed for the *Mariner A* program. The only change was the addition of a switch to permit operation using 8-bit command words instead of 26-bit command words. This feature was not used, however.

The initial contract was awarded in June 1961 for the *Mariner A* equipment and it was later changed to *Mariner R*. Delivery of the initial equipment was made in November 1961 and the last units were delivered in May 1962.

(2) *Design considerations.* The design of the RWV was initiated during the *Ranger* program. Details of design considerations are covered in the *Ranger* program documentation.

(3) Problem areas and solutions

(a) *RWV to data display interface.* Because of a misunderstanding, the logic in RWV was originally designed

to accept d-c signals from the recommutator for display; whereas, the signals were actually clocked-pulse type. A redesign was accomplished prior to the delivery of the last three units. The prototype was modified at JPL. The signals involved were the command events register with its Good, Bad, and Questionable indicator, and the spacecraft VCO frequency (command period), also with its associated GBQ indicator.

It was also found that, although the numerical weighting of the seven lines representing the seven bits of the telemetry word agreed with the weighting used on the spacecraft in the signal out of the command subsystem, due to an inadvertent reversal of this weighting to spacecraft telemetry, it became necessary to compensate at RWV by reversing the order of the seven bits of the telemetry word.

(b) *Yo-yo and false-lock problems.* A description of these two distinct problems is given elsewhere in this report. The appropriate circuitry was added as a modification to all four RWV units in time for intended usage, and adequate operation information was forwarded at the same time.

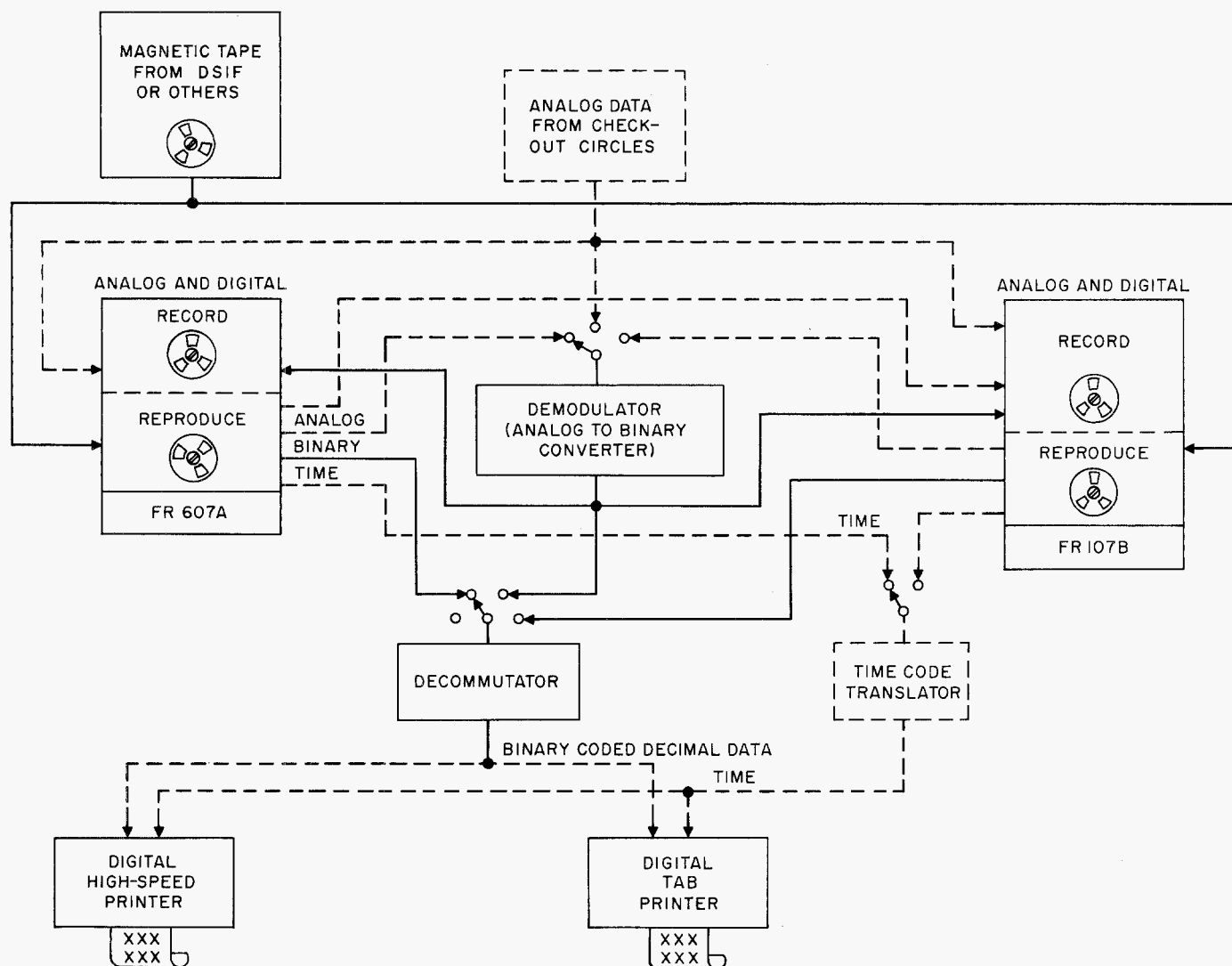


Fig. 116. Telecommunications investigation laboratory, simplified flow diagram

(c) *Inverted transmission line phase.* A unique situation exists at AMR in that RWV is used not only with the test transmitter of the checkout circle during system tests, but also with the remotely located R-F transmitter during ESA, pre-countdown, and launch operations. As a result, two transmission lines are used between AMR Hanger AE and the remote trailer location. Initial test use of the transmission lines showed satisfactory performance: that is, command modulation was sent to the R-F transmitter, broadcast, received by the probe in the antenna, detected by the 890-mc receiver, delivered back to Hanger AE via transmission line, and successfully verified. However, when the time came to broadcast command information to the spacecraft during ESA operations, it was found that, although spacecraft command detector lock was achieved, the information went unrec-

ognized. Because isolation transformers are used in the transmission line, it was at first thought that a double phase reversal had inadvertently occurred in the connections to the transformers, and so an immediate "fix" was accomplished using empirical transformer connections. Subsequent detailed investigation carried out at DSIF stations 3 and 5, and also at AMR, established conclusively that a phase reversal did in fact exist at the trailer-housed AMR transmitter. This was later verified by R-F trailer personnel. The reversal does not exist at DSIF 3 or 5, or in the checkout circle test transmitters. On the basis of the findings, permanent wiring changes were made to the transmission line isolation.

Transformer hookup and the change were reflected in the documentation. The back-up command modulator

located in the R-F trailer was modified to provide an inverted signal.

(4) *Subsystem functional description.* The RWV system is a self-checking modulator of the 10-kw ground transmitter. It also provides an effective check of the communications link between computer and transmitter. Finally, it samples R-F energy to provide real-time verification of command transmissions to the spacecraft. During launch, it modulates the R-F transmitter in the R-F trailer. After launch, the RWV modulates the 10-kw ground transmitter at Goldstone. Actually, the RWV ground command subsystem is part of DSIF but it is also used during launch; it is discussed here because of its latter applications.

Command decisions for the spacecraft are made at the Central Computer Facility in Pasadena. These decisions must ultimately be converted into R-F energy which commands the spacecraft itself.

A given command is forwarded from CCF to Goldstone via teletype. To check validity of the TTY transmission, the identical command is sent three successive times from Pasadena. This information is received by Goldstone at the Kleinschmidt TTY termination in punched paper-tape format. This tape is placed in the RWV tape reader. The mode selector is then set to MODE I. Upon release of the initiate button, the tape is read three successive times and is displayed in octal form on Storages A, B, and C, respectively. Since the three command words were transmitted identically, each of the three displays must concur exactly. A red error light indicates any discrepancy in these identical transmissions. Should such an error occur, the TTY transmission must be repeated.

Before actually modulating the command transmitter, it is desirable to demonstrate normal and proper operation of the ground modulator. RWV MODE II serves this purpose. With the VERIFY/TRANSMIT selector in the VERIFY position, an internal loop check is performed to confirm proper modulator operation (Fig. 117). Operation of the initiate button permits command word entry from the tape reader into the RWV Storage A memory. This stored command is then serially read out of the memory into a frequency-shift keyed modulator. The modulator subcarrier output drives a ground command detector identical to that found in the spacecraft. The reconstructed command output of this detector is then compared serially, bit by bit, with the Storage A memory. At the conclusion of the serial readout, the reconstructed command word appears in Storage B. A parallel

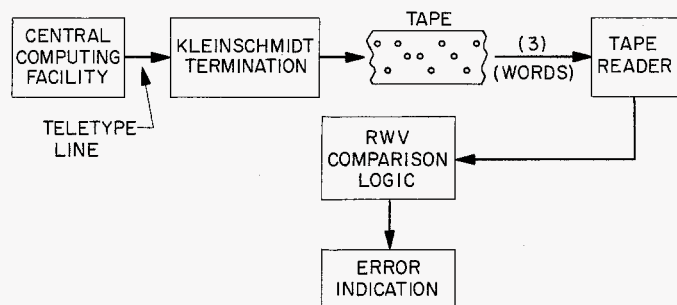


Fig. 117. RWV teletype verification flow diagram

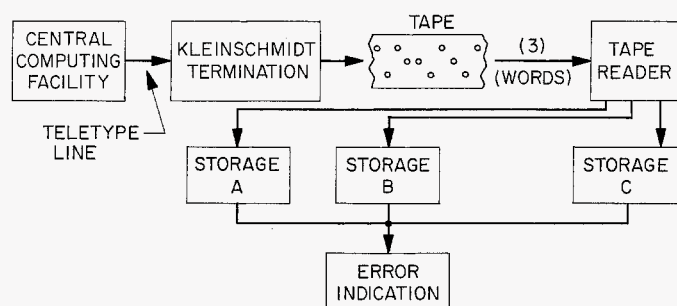


Fig. 118. Logic flow diagram

verification is performed and the process is complete. If any discrepancy exists, an error indication is provided. This loop check establishes spacecraft detector capability to accept command modulation originating from the RWV modulator.

The system is now ready for actual modulation of the R-F carrier. The VERIFY/TRANSMIT selector is set to TRANSMIT (Fig. 118). Upon initiation, the RWV system recycles through the internal modulator/detector loop check. After serial and parallel verification, the command word is again clocked out of the ground modulator. The modulator subcarrier output is buffered and supplied to the R-F command modulation input of the 10-kw transmitter.

R-F energy sensed at an antenna probe drives a ground receiver which strips the subcarrier and feeds the RWV ground detector. This detector output is compared both serially and in parallel with the clocked and stored information, and is then displayed on Storage C. The tape perforator punches out the transmitted command. Any discrepancy during the transmission provides an error indication and simultaneously inhibits. This inhibition may be intentionally by-passed by operation of the TRANSMIT INHIBIT OVERRIDE button. This condition is indicated by the red override light.

Since multiple command sequences are usually required, a word counter is built into the logic circuitry which may be preset on the WORD STOP thumbwheel, up to a seven-word maximum. Both ground and space-craft command detector logic and storage circuitry can accept a maximum command rate of one word/min, while internal loop check and actual transmission cycles require 38 sec for completion. A minimum INTERWORD TIME DELAY of 22 sec must, therefore, be preset on the thumbwheel.

(a) *Command decoder and readout.* The command decoder and readout logic function is to decode and display nine bits of binary data representing a period of event measurement. The data are decoded by the logic and are displayed both in quality and quantity on front-panel indicators and displays. One bit of vehicle sync information is also fed into the logic. The data are amplified and inverted to provide both the true and false input. Since the logic varies between the type of data (command period and/or command events) and manner in which they are displayed, the test will correspond.

(b) *Command period.* After amplification, the command period inputs are fed and stored whenever the set line signal PC MCP is at a 1 level. The storage flip-flops are then integrated with the logic in such a manner that the input magnitude is displayed with a given sign designation of + (plus) or - (minus) according to the chart (Table 8) given below. The quality or condition of data is determined by the signals DC1 and R1. The data condition is displayed on lamp indicators located on the front panel. The condition or logic levels of the flip-flop MP1 and MP2 outputs is shown in Table 9. Bit 32 is used to inform the instrument whether the vehicle is in sync or out of sync. If the signal VEH SYNC is at a 0 level, the indicator on Drawer A will light, indicating that the vehicle is in sync; if the signal is at a 1 level, the XMIT INH circuit will light the TRANSMIT INHIBIT indicator, thus inhibiting the transmission of data.

(c) *Command events.* After amplification, the command events inputs are fed and stored whenever the set line PC-MCE is at a 1 level. After the storage of data, the flip-flop outputs are connected to lamp drivers which, when energized, display the data on binary indicators located on the front panel. The condition of the event data is displayed in the same manner as for command period and Table 9 shows the flip-flop (ME1 and ME2) conditions for the various indicators to light.

(d) *Temperature transducers.* Based on the unsatisfactory mechanical and electrical performance of the platinum film temperature transducers used on *Rangers I*

Table 8. Command period magnitude

Inputs	Displays
0	+ 6
1	+ 7
2	+ 8
3	+ 9
4	+10
5	+11
6	+12
7	+13
8	+14
9	+15
10	-16
11	-15
12	-14
13	-13
14	-12
15	-11
16	-10
17	- 9
18	- 8
19	- 7
20	- 6
21	- 5
22	- 4
23	- 3
24	- 2
25	- 1
26	+ 0
27	+ 1
28	+ 2
29	+ 3
30	+ 4
31	+ 5

+ = greater than
- = less than

Table 9. Data condition

MP1, ME1	MP2, ME2	Condition
0	0	G
1	0	Q
1	1	B

and II, several alternate sources were surveyed for the *Mariner* program.

With high reliability and measurement accuracy the main considerations, platinum wire transducers, with larger case size (20%) and greater sensitivity (40%) the side effects, appeared most promising.

As with *Ranger*, each temperature measurement consists of a 500-ohm transducer switched into a common

bridge with series and parallel resistors adjusted to give equal bridge output for the various ranges required. Four series 125-ohm transducers are mounted so as to give average readings for the case measurements.

The transducers as delivered by Trans-Sonic, Inc., Burlington, Mass., performed well during the T-A and F-A testing. However, after weeks of storage and with non-standard mounting techniques, several transducer elements shorted to their steel base plates. With all transducers in a common bridge, a short of this type (involving spacecraft ground) saturates all other temperature measurements. The first indication of failure was that the mylar tape used as insulation between element and base plate had cold-flowed. Approximately 7% of the 300 transducers tested exhibited this problem. Further investigation showed evidence of poor assembly techniques.

All available transducers were returned to the contractor with a resident JPL inspector for rework and/or replacement. The steel base plates on the transducers were replaced with epoxy glass plates, and better quality control procedures were utilized in the assembly operation.

As the new transducers were returned to JPL, a program of spacecraft transducer replacement was initiated. All flight units were replaced with the exception of the Earth sensor transducer, when the transducer was isolated from spacecraft ground, and the midcourse motor transducers, which were difficult to change without damage to the motor. These transducers were hi-pot tested at 500 v on the spacecraft while all new units were tested before mounting. Of the approximately 100 transducers consigned to flight, there have been no further failures of any kind.

Antennas

(1) *Introduction.* The *Mariner R* antenna system design criteria required the performance of three functions:

- (1) Transmission of flight telemetry until after the midcourse correction, regardless of the spacecraft attitude with respect to Earth
- (2) Reception of ground commands during the early portion of the flight, regardless of the spacecraft attitude
- (3) Directional transmission of telemetry data from midcourse maneuver to Venus encounter

In order to fulfill these functions, three separate antenna systems were used. These systems borrowed heav-

ily from other programs because development time was short. The omni-antenna, for early flight telemetry, was RA-1 type discone antenna. The circularly polarized command antenna subsystem was modified from the *Mariner A* design. The directional high-gain antenna used a RA-1 feed modified for circular polarization and a modified *Mariner A* parabolic reflector. Radio frequency continuity between the high-gain antenna and the communications pan during relative motion of the antenna and bus was provided by a RA-1 type coaxial rotary joint and associated cabling.

(2) *Command antenna system.* The command antenna subsystem consists of a turnstile antenna mounted on the back side of the solar panel and a dipole antenna mounted on the forward side of the solar panel. To split the power between the two antennas, a directional coupler is used with the dipole being driven 6 db below that of the turnstile. A pattern of the antenna system taken about the long axis of the solar panels is shown in Fig. 119. It should be noted that 0 deg is directed toward the rear of the spacecraft.

The type-approval directional coupler failed during the 200-g shock test. Indication of failure was erratic VSWR of the unit; the cause of the erratic behavior was a cracked ceramic load used to terminate the unused fourth arm of the directional coupler. Investigation of the record of the accelerometer on the shock tester revealed that the duration of the shock was 2 msec, whereas the specification calls for $\frac{1}{2}$ to $1\frac{1}{2}$ msec. The longer shock pulse contains more low-frequency energy than the unit is required to withstand. The coupler was repaired and the test repeated, holding the duration of the pulse to $\frac{1}{2}$ msec. The coupler passed the second test. However, since it seems that the coupler was somewhat marginal regarding shock capability, the termination was modified with a more rugged design.

(3) *Omnidirectional antenna.* The omnidirectional antenna, being taken directly from the *Ranger* configuration, required no design work, but some modification was necessary. It was thought early in the program that the RA-1 omnidirectional antenna might have to withstand aerodynamic heating caused by an 85-n-mi parking orbit. A heat shield was designed to alleviate this problem. However, a higher altitude was chosen, which eliminated this requirement. As a result of the requirement for increased solar power on the spacecraft, the solar panels were increased in size. During a routine spacecraft type-approval vibration test which was run with the new solar panels, considerably higher accelerations than expected were noted on the structure supporting

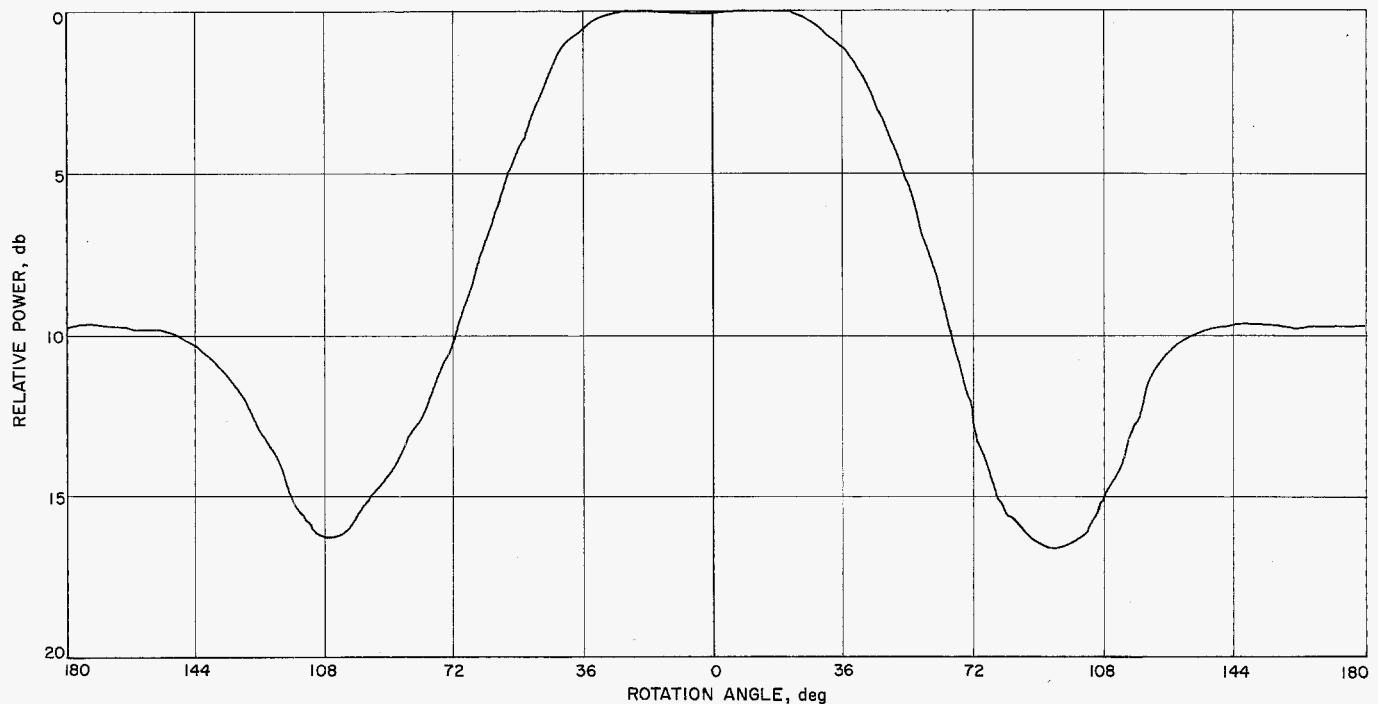


Fig. 119. Radiation pattern, command antenna system

the omnidirectional antenna and the ends of the solar panels. As a result, the omnidirectional antenna was subjected to loads in excess of 50 g and it suffered a series of failures. The first failure resulted when the feet of the supporting buttresses broke. The feet were then strengthened and the tests were repeated. The second failure resulted when one of the buttresses was torn away from the antenna support cylinder. The feet and buttresses were both strengthened on another antenna and the test was repeated. The antenna survived the tests successfully. The modifications required are minor and were performed on all flight antennas.

(4) **High-gain antenna.** The basic program criteria for the *Mariner R* high-gain antenna design are the following: (1) the existing *Mariner A* paraboloidal reflector must be used with a minimum of modification; (2) the design must provide an efficient circularly polarized feed at 960 mc; and (3) the feed structure must be compatible with the adapter diaphragm of the *Ranger-Agena B* vehicle.

A feed design was quickly accomplished by modifying the existing RA-3 configuration. The modification involved the replacement of the linearly polarized dipole elements with circularly polarized turnstile elements consisting of two dipoles oriented 90 deg from each other and 45 deg from the balun slot on the outer conductor. In the design, circular polarization was achieved by the

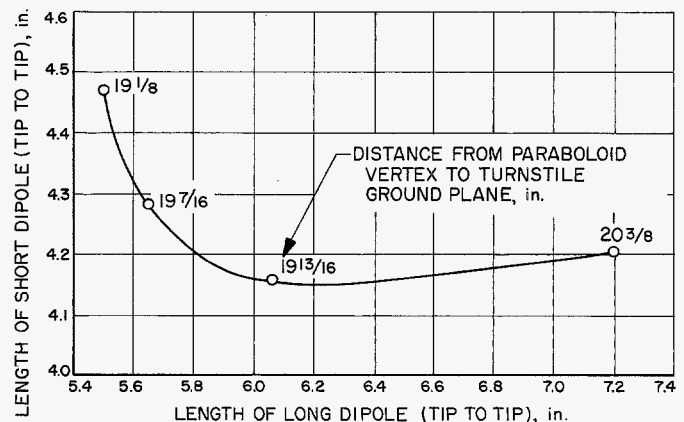


Fig. 120. Turnstile element lengths which produce circular polarization for various focal positions

phase quadrature of the essentially equal currents flowing in the crossed dipoles when one dipole is cut appropriately shorter than that required for resonance and the other appropriately longer than that required for resonance.

Several focal-length positions were examined in order to optimize the gain. At each position, the element lengths were adjusted to produce nearly circular polarization, meeting the criterion that the gain variation vs incident linear polarization angle was less than 0.2 db. Fig. 120 shows the element lengths that produced circular

polarization as defined above for various feed positions. Distances indicated are from the vertex of the paraboloid to the ground plane which is located a quarter wavelength past the plane of the turnstile. Fig. 121 gives the measured relative gain of the antenna for several focal positions. A ground plane position of 19-15/32 in. was chosen as optimum. This decreases the ground plane protrusion into the *Agna B* adapter diaphragm by 1 in. relative to the *RA-3* high-gain antenna.

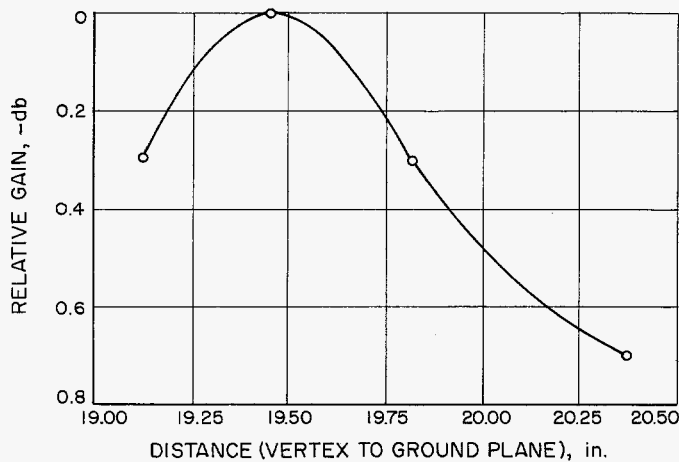


Fig. 121. Relative gain vs focal position

Type-approval, temperature-control, and flight-type models of the *Mariner R* high-gain antennas were delivered to JPL and underwent all required R-F and structural tests. Fig. 29 is the unpainted temperature control unit.

The voltage standing wave ratio of the TA unit as delivered was 1.96. A quarter wavelength transformer slug soldered to the center conductor lowered the VSWR to 1.01 on the TA unit and to 1.03 on the TC unit.

Linear-to-circular and circular-to-circular polarization radiation patterns were made of the TA unit. Fig. 122 shows a typical circular-to-circular polarization pattern. The 1- and 3-db beamwidths of the antenna are 10.3 and 16.5 deg, respectively. Absolute gain relative to right-hand circular polarization of the antenna was measured to be 20.0 ± 0.5 db. Gain variation of the antenna versus incident linear polarization angle (elliptically) was measured to be 0.33 db.

(5) *Rotary joint.* During environmental testing of the rotary joint, which was taken directly from the *Ranger I* design, it was found that elevated temperatures caused some cracking of the ceramic support spacers used in the joint. It was decided (because of the nature of the cracks, the type of bearing loads imposed on the ceramics, and

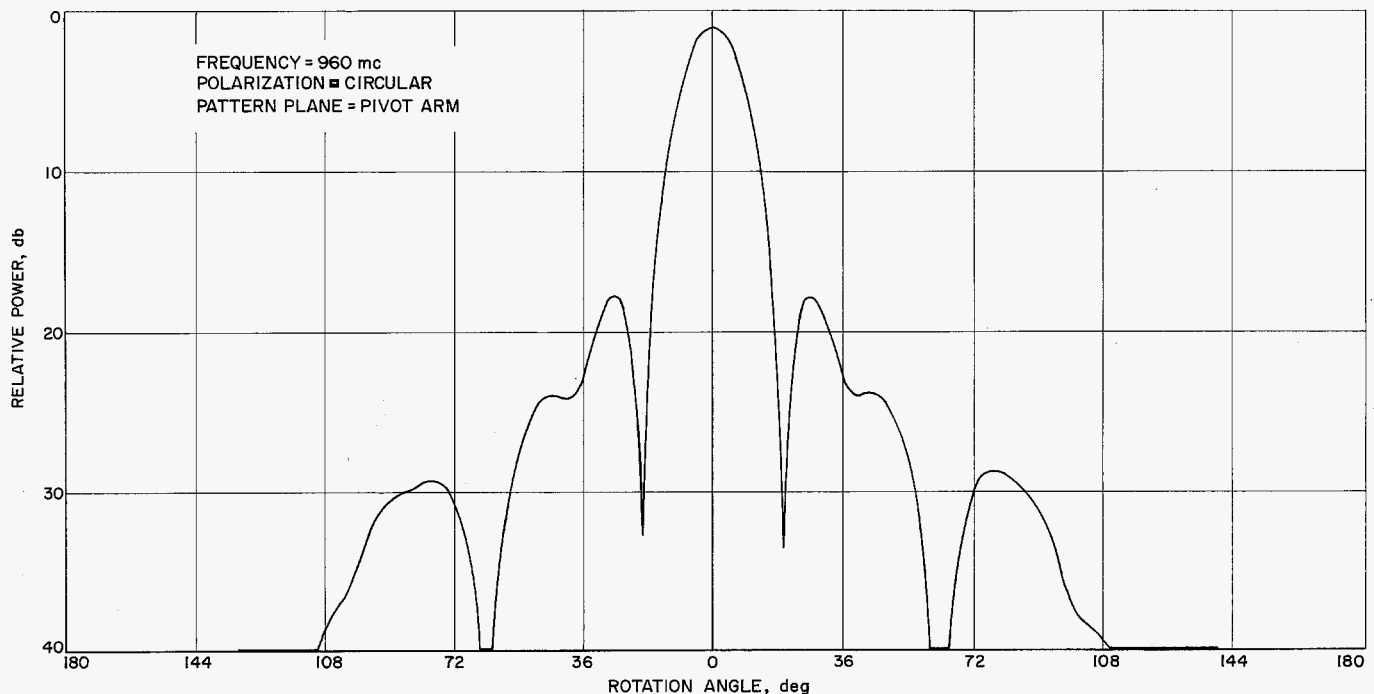


Fig. 122. High-gain antenna radiation pattern relative to right-hand circular polarization

the shortness of the mission) that the cracking presented no threat to *Ranger* mission reliability.

However, due to the longer mission time of the *Mariner R*, it was believed that this problem should be corrected. It was found that the cracking was due to differential expansion between the ceramics and the metal parts contained inside them. Since the ceramic and metal parts are glued together, the glue filled any possible differential expansion clearance. The joint was, therefore, modified so that the spacers that had previously cracked would have sufficient clearance to allow for differential expansion and are held in place by metal sleeves that bear lightly against the end of the ceramics. Tests at 200°F showed no ceramic cracking; this modification was incorporated in the *Ranger*-type joint used on *Mariner R*.

(6) *R-F couplers*. Following the philosophy of the *Ranger* Project, it was required that checkout of the spacecraft communications system through its radiating antennas be possible up to vehicle liftoff. Because of the similarities between the *Mariner* and *Ranger* spacecraft interfaces with the *Agna B*, it was decided to utilize as much of the *Ranger* coupling system as possible.

The basic differences between the *Mariner R* and the *Ranger I* and *II* spacecraft-*Agna B* R-F coupler interfaces are:

- (1) The *Mariner R* high-gain antenna is circularly polarized instead of linearly polarized
- (2) The *Mariner R* uses separate command antennas mounted on one of the solar panels instead of diplexing both 890 and 960 mc through the omni-antenna as in *Rangers I* and *II*

It was found during the initial R-F coupler test that these differences necessitated two essential yet minor changes to the *Agna* coupler system.

Because the *Mariner R* high-gain antenna feed is a turnstile, its four elements are oriented at 45 deg on either side of the dipole feed location on the RA-5 high-gain antenna. Thus, the *Agna-Ranger* coupler probe, which was lined up with the dipole elements, is at 45 deg to the *Mariner R* high-gain antenna feed elements. In this location, the probe is in a highly unstable and rapidly changing part of the field. The coupling loss in this position was 17 db. By moving the probe from its *Ranger I*-to-RA-5 position in the center of the screen in the *Agna* forward equipment rack antenna well, to the

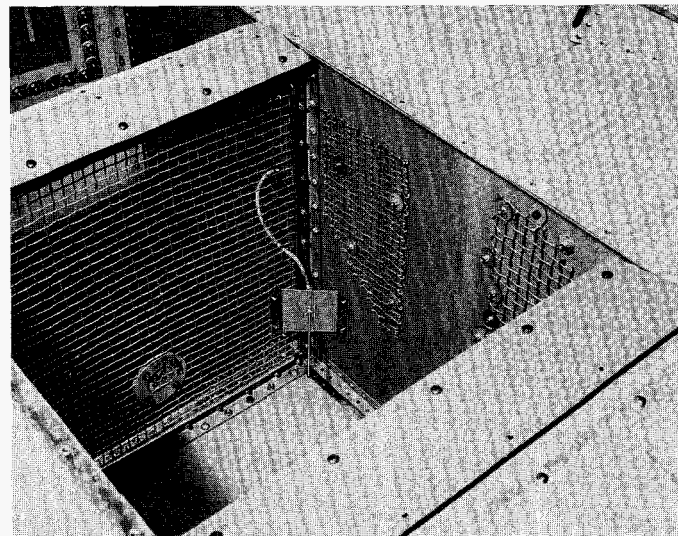


Fig. 123. High-gain antenna coupler probe

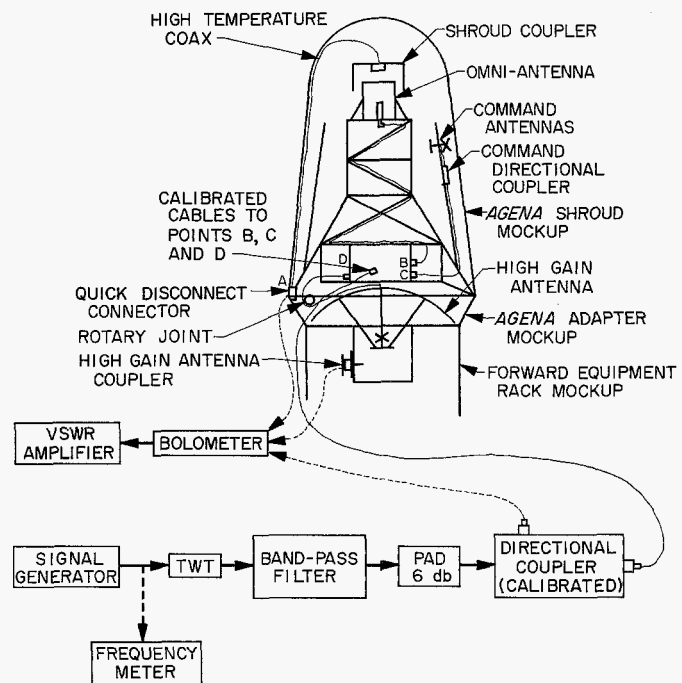


Fig. 124. *Mariner R* R-F coupler test setup details

corner of the well (Fig. 123), the probe can be brought parallel to one pair of turnstile elements and the coupling performance improved.

Lockheed was asked to make this change and, during the R-F coupler tests conducted at JPL in January 1962, a prototype model of this probe was installed in the *Agna* forward equipment rack and measured in the new location (The test setup is shown in Fig. 124 and 125).

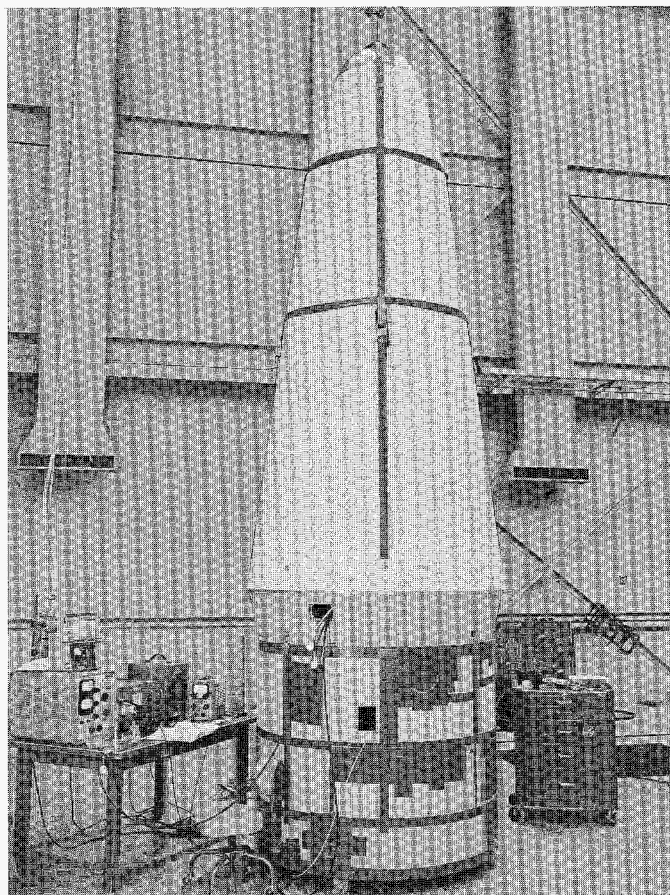


Fig. 125. Mariner R R-F coupler test setup

The coupling loss from the output of the communications pan, Point D, through two flight-type coaxial cables, the type-approval model of the rotary joint, the high-gain antenna, and to the output of the coupling probe (Point E), was 6.6 ± 0.5 db. This loss figure is satisfactory.

During the tests of the *Agena* shroud coupler, it became apparent that the absorber material, which comprises the lower half of the coupler cover, had a critical effect on the coupling between the command antennas and the coupler. The coupling loss varied between 25 and 40 db, depending on the position of the absorber panels. As a solution to this problem, the lower 3 in. of the absorber were trimmed off. Under these conditions, the command antenna-coupler loss became quite stable and the omni-antenna-coupler loss increased only a fraction of a db, compared to the *Ranger* configuration.

Match-mate and R-F coupler tests were conducted at the SAF in early April 1962, using the *MR-1* and *-2* spacecraft and their associated flight adapters and shrouds.

R-F coupling losses through the omni- and high-gain antenna systems, although higher than expected, were within specification limits and, therefore, considered acceptable. The omni-antenna system coupler losses at 960 mc were 12.3 db and 11.2 db for *MR-1* and *-2*, respectively, while the high-gain antenna coupler system losses at 960 mc measured 9.3 db for *MR-1* and 10.0 for *MR-2*.

Coupling losses at 890 mc through the command antenna omni-coupler system were excessive and highly unstable. This excessive loss, which was 10 to 20 db higher than expected, was frequency sensitive with the highest losses occurring within one megacycle of 890 mc. The losses decreased on either side of 890 mc, and were much more stable.

The cause of this excessive loss was isolated to be in the flight shroud configuration. It was determined that the installation of the high-temperature R-F cable in shrouds 6901 and 6901A was nonstandard.

On May 9 and 10, an additional match-mate test was performed between the *MR-1* spacecraft and the 6902 shroud and adapter. With the shroud R-F cable properly installed, the coupling loss from the communications pan through the command antenna omni-coupler system to the quick-disconnect at 890 mc was 29.3 db. It was apparent from the tests that the losses encountered during the *MR-1* and *-2* R-F match-mate tests at 890 mc were caused by the looped high-temperature cable.

F. Science

1. Introduction

The August 1961 shift in the *Mariner* design concept necessitated a different approach for the science experiments. The scientific package, instead of weighing 130 to 180 lb, could now weigh only 40 lb, in addition to corresponding power limitations. A complete redesign was not possible and the existing *Mariner A* instruments had to be used, as well as those which could be utilized from other programs. New instrumentation was to be kept to a minimum.

Four areas were considered for the newly defined *Mariner R* mission:

- (1) Photometry (Lyman-alpha)

- (2) Fields and particles
- (3) Radiometry (microwave and infrared)
- (4) Visual photography

Since a planetary horizontal platform was not feasible, any experiment which demanded a scan facility imposed a scan design problem. In addition, some attitude control ability for the spacecraft was considered mandatory. Without this capability, the mission was considered of little or no scientific value. As the design study for the mission proceeded, it soon became apparent that weight was available for only the following experiments.

a. Planet oriented

Microwave and infrared radiometer. The choice of wavelengths was 13.5 and 19 mm for the microwave radiometer, and 8 to 9 and 10 to 10.8 μ s for the infrared. These experiments were designed to acquire information on the surface temperature, phase effect, limb brightening or darkening, changes in emissivity over the surface, CO₂ and possibly H₂O atmospheric content, and fine detail of the cloud structure.

b. Near-planet and interplanetary-oriented

Solar plasma. To cover the proton energy range 240 to 8400 ev.

Magnetometer. In two ranges: (1) 0 to ± 64 γ ; and (2) 0 to ± 320 γ .

Ionization chamber. For proton energies greater than 10 Mev and for electrons greater than 0.5 Mev.

Geiger-Mueller counters. Two G-M counters to cover the range above 10 Mev for protons, and 0.5 Mev for electrons. One counter for the range above 0.5 Mev for protons, and 40 Kev for electrons.

Cosmic dust experiment. For particle momenta above approximately 1×10^{-4} dyne sec.

These experiments were all designed to obtain information on magnetic and particle flux, both the temporal and spatial distribution.

Considering all the various logistics of the problem, such as weight and power limitations, instrumentation that could be salvaged from the *Ranger* and *Mariner A* programs, and, above all, the time element, there was a finite chance of readying the scientific package for the 1962 firing window to Venus.

2. Microwave Radiometer (Fig. 46)

a. *Scientific goals.* For the *Mariner R* mission, it was obvious that, because of the restricting time schedule, it would be necessary to utilize as many components of the *Mariner A* microwave radiometer as possible. The four wavelengths originally planned were 4, 8.5, 13.5, and 19 mm, with each of the shorter wavelengths having its own dish and the two longer wavelengths, 13.5 and 19 mm, sharing the same dish. The new emission allowed only the choice of flying one of the shorter wavelengths or the dual system comprised of the longer wavelengths. It was decided that the dual wavelength combination had the most scientific merit.

Individually, measurements at the longer wavelengths might yield the following scientific information:

13.5 mm

- (1) If water vapor exists in the Venus atmosphere in constant mixing ratio with height of the order of 0.5% or more, the brightness temperature should be considerably cooler than indicated by the terrestrial 3- and 10-cm observations.
- (2) This wavelength gives a very marked limb brightening effect as predicted by the simple optically thick ionospheric or optically thinner radiating plasma striation models.
- (3) The temperature variations as the scan crosses the terminator should be large at this wavelength, and, coupled with the high geometrical resolution of the instrument, should produce valuable information for understanding the physics of the Cytherean atmosphere.
- (4) A standard, high-pressure atmosphere model or one containing a thin, highly microwave-absorbing cloud layer can be studied effectively at wavelengths lying in the apparent transition region from 4 or 8 mm to 3 cm. A wavelength of 13.5 mm is not far from the apparent center of this transition region.

19 mm

- (1) If the surface is hot, this wavelength would penetrate to, or very nearly to, the surface of the planet, allowing gross thermal features of the planet to be studied. The "pole-to-pole" variation (or rather variation normal to the ecliptic plane) in temperature over the planet can be obtained, as well as the longitudinal variations in tempera-

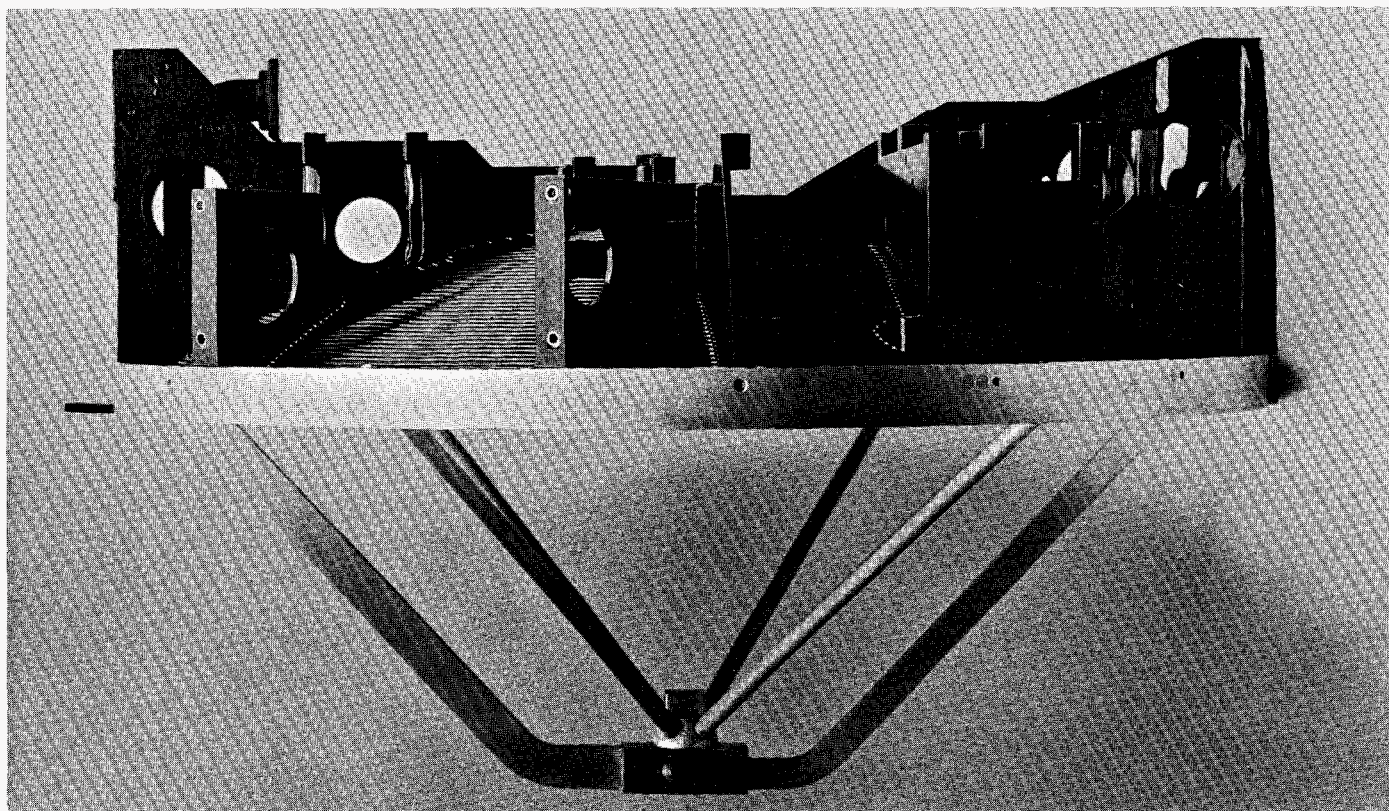


Fig. 126. Radiometer frame with antenna feed installed

ture. The subsolar and anti-subsolar temperatures can be obtained (these parameters only being estimated from the crude brightness temperature-vs-phase-angle measurements made from Earth, utilizing an assumed pole-to-pole temperature distribution, also unmeasurable from Earth).

- (2) A more precise determination of the temperature minimum and maximum with respect to the optical terminator can be obtained.
- (3) High-resolution thermal measurements will give some insight to the gross features of the planet's surface.

Of course, the comparative gross thermal variations obtained at the two wavelengths should yield important information regarding the transfer of heat, etc., around a slowly rotating planet.

b. Engineering of the instrument

(1) Development and design

Constraints. From the scientific point of view, it was desirable to utilize the two longer wavelength channels

(13.5 and 19 mm) of the four-channel radiometer already developed for the *Mariner A* program. The repackaging effort required for this system was more complex than that required for any one single channel, but much less so than for combining any two different channels. In fact, the probability of success in combining two channels other than 13.5 and 19 mm was considered marginal in view of the time scale, and to some extent, this consideration influenced the selection of the final wavelengths.

It was thus estimated that a finished dual-channel radiometer could be provided within the constraints of: (1) science requirements; (2) delivery in 4, 5, and 6 mo for the first, second, and third units, respectively; (3) maximum weight of 19 lb; (4) maximum power consumption of 9 w peak and 4 w average; and (5) environmental requirements.

In order to reduce engineering time, it was decided to limit the effort to mechanical layout redesign exclusively, using the *Mariner A* components as much as possible. The electronics were to be transferred without modifications onto the new frame. This approach, however, had to be abandoned about halfway through the project

when it was found that the performance of the electronics delivered was not satisfactory and had to be extensively modified.

Mechanical. Mechanically, the radiometer consists of a single parabolic dish antenna 19.1 in. in diameter, with heavy ribbing on the convex surface (Fig. 126). This frame is an integral unit for high strength and precision, and is machined from a solid block of aluminum. The feed structure is mounted on the front (concave) surface, while the waveguide components and the electronics packages with their interconnections are attached to the ribs in the back. In the finished instrument, a shield of polished aluminum sheet covers the back for temperature-control purposes.

The antenna is basically a *Mariner A* design, with the rib structure modified for the new layout on the back, for the different structural requirements, and for the special mounting of the instrument. At the bottom, the radiometer is free to pivot in a single ball-and-socket joint; at the top, it is held by an actuator designed to drive the instrument through a 120-deg scan angle. During the boost phases, the unit is latched to a neutral position by a steel pin that is later removed by an explosive squib.

The antenna features a stepped parabolic-surfaced construction. Small steps have been machined into the concave surface so that to very short wavelength radiation (infrared), the antenna will appear as a flat surface; whereas, at the longer wavelengths of interest, the steps have negligible effect and the antenna has its normal focusing properties. By this technique, damaging focusing of heat at the feed is avoided when the antenna is pointed at the Sun.

Special ribs are provided on the back of the antenna to allow the mounting of an infrared radiometer near the edge. Two reference horns, one for each channel, are mounted above the parabolic antenna, tilted at an angle of 60 deg with respect to the antenna axis. The two horns are connected by a box-like structure and form a single lightweight unit of extremely high rigidity. The assembly is made of thin aluminum, entirely dip-brazed. The feed assembly, with the two waveguides and four supporting legs, is also made of aluminum, and is similarly dip-brazed into a single rigid assembly.

Electrical. Each radiometer channel is of the crystal-video type, in a switched load or Dicke configuration.

The choice of this type of radiometer rather than that of another, such as the superheterodyne, was dictated at the start of the *Mariner A* program from considerations of simplicity, reliability, light weight, and low power consumption. The sensitivities achievable with this type of radiometer at the limit of the state of the art were then just adequate for a meaningful experiment. On the other hand, the other types of more sensitive radiometers were too complex, heavy, and wasteful of power for space applications, especially in a preferred multichannel configuration. The reasons for the choice of multichannel crystal-video radiometers were thus overwhelming.

The situation at present is somewhat changed, especially because of significant advances in the state of the art in local oscillators, mixers, and r-f amplifiers. These factors make superheterodyne and tuned r-f systems far more feasible for space use, and although crystal-video systems have also been improved, the choice now becomes increasingly difficult to make between various radiometer types.

A block diagram of the *Mariner R* dual-channel radiometer is shown in Fig. 127. In each channel, a ferrite switch alternates at an approximately 1000-cps rate between the r-f energy gathered by the parabolic antenna with its feed, and a reference horn. During normal measurement, the antenna looks at Venus, and the reference horn at deep space.

The output of the switch goes to a high-sensitivity crystal-video detector, where the r-f energy is demodulated into a sine-wave signal at the frequency of the ferrite switch. The audio-frequency signal is amplified in a tuned preamplifier-amplifier chain. The amplified signal, the amplitude of which is proportional to the difference in r-f noise power seen at the switch inputs, is then rectified by a phase-sensitive detector, and integrated. Since r-f power radiated by a hot body is proportional to its temperature, and since the reference horn points at cold space of very nearly 0°K, the output amplitude of the integrator is proportional to the source temperature seen by the antenna. The d-c voltage output of the integrator is the analog output of the instrument. A tuning-fork reference oscillator provides a signal for the ferrite switch drive-amplifier and the phase detector.

The circuitry is fully solid state, and silicon semiconductors are used to permit high-temperature operation. The preamplifier is of conventional LC tuned-circuit design, with a Fairchild 2N2049 low-noise input transistor; the following amplifier is also of conventional design,

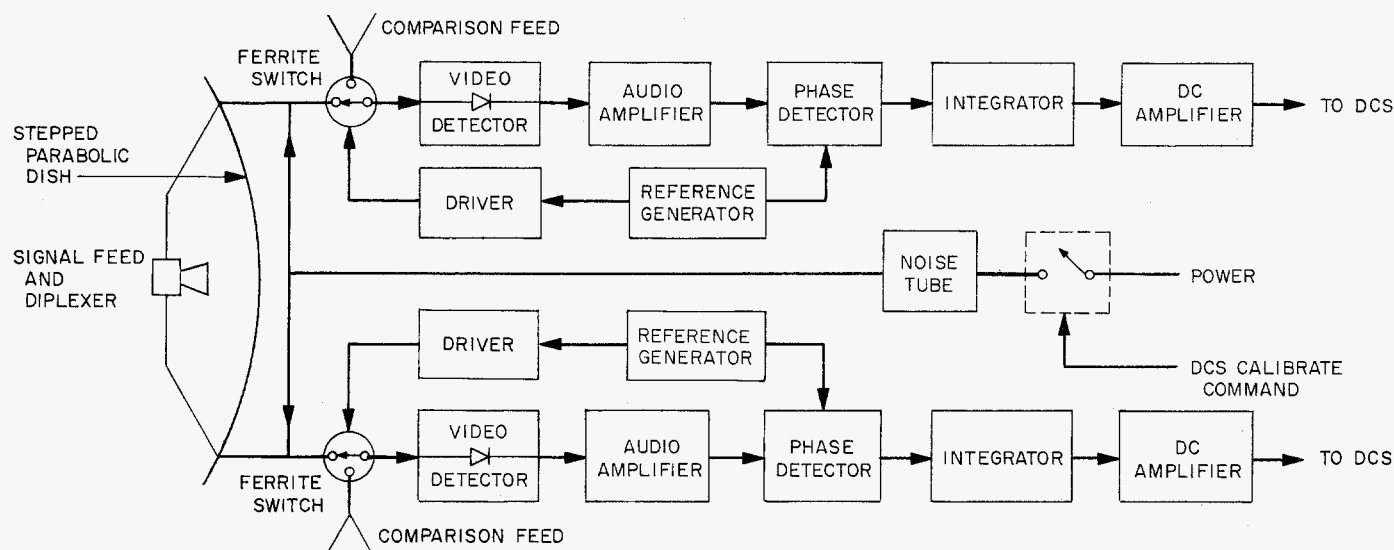


Fig. 127. Radiometer block diagram

but with a twin-tee feedback network. The bandwidth of both the amplifier and the preamplifier is approximately 20 cps. Demodulation is performed by a transistor driven at the base by the reference oscillator. The integrator consists of a d-c amplifier in a Miller configuration. The a-c chain has a voltage gain of approximately 120 db; the d-c gain is about 30 db.

The two channels are identical, except that the miniature tuning forks used for reference oscillators run at 950 cps, and 1050 cps for the 19-mm and 13.5-mm channels, respectively, to avoid crosstalk.

A feature of the system is a built-in calibration unit. It consists of a specially ruggedized 5000°K gas discharge tube coupled to both channels through directional couplers. When the gas tube is fired upon external command, a known signal of approximately 350°K is injected into the main signal path to provide system calibration.

The output voltages vary from 1 v dc for 0°K input temperature to 6 v dc for approximately 800°K input temperature. Each channel output is fed to the data conditioning system, where it is sampled every 20 sec for transmission by telemetry.

Problems encountered in design. Several problems were encountered during the development and testing of the radiometers. Most of the problems occurred in the electronics, from two sources: (1) the high over-all gain requirement in the system, and (2) the large temperature range (-10° to $+65^{\circ}\text{C}$) over which the equipment had to perform satisfactorily.

The high sensitivity and gain of the amplifier chain made it very sensitive to pickup, especially from the ferrite switches. The magnetic field of the switch coils and drive amplifiers is at the frequency to which the preamplifier and amplifier are tuned. Extensive magnetic and electrostatic shielding had to be used, as well as careful location and orientation of components to reduce the pickup to negligible levels. The pickup was most serious in the video-crystal detector and the preamplifier, where the signal level is the weakest.

A similar pickup and interference problem was encountered during explosive safe area tests at AMR. One or both channels of the radiometers showed large outputs when the spacecraft 960-mc transmitter was turned on. Investigation revealed that the pickup occurred at the video crystal directly and was dependent on the orientation of the source with respect to the radiometer. It was determined that, in flight configuration, the amount of interference was negligible and that no action was needed. However, additional shielding of the crystal detector was installed in one unit to demonstrate its effectiveness in reducing this problem should it have become serious.

Another area where spurious common-mode signals got into the channels was through the power supply. The only acceptable solution to the problem was to design a power supply with separate regulators and filters for each radiometer channel, with an a-c output impedance of about 0.01 ohm on each supply to achieve the needed isolation. The grounding of the instrument also had to be carefully handled to avoid ground loops and pickup problems.

Severe problems were encountered because of the temperature extremes to which the instrument was subjected. The temperature caused excessive gain variation and phase-shift between the reference oscillator frequency and the amplifier center frequencies, resulting in unacceptably large output shifts for a given input. The electronics from the *Mariner A* radiometers ceased to operate outside of a 40° range around ambient.

Extensive modifications were made in the circuitry, which included improved biasing and the addition of numerous temperature compensating elements. An extremely stable tuning-fork reference oscillator was substituted for the original twin-tee oscillator to help reduce the temperature effects to an acceptable level. The variations which still exist, although not desirable, do not degrade the value of the experiment because of the self-calibrating feature in the instrument.

Mechanically, problems were encountered in only one area during the environmental vibration tests. After vibrations equivalent to approximately three flight-acceptance tests in duration, the 13.5-mm waveguide exhibited cracks near the junction of the antenna feed. A high level of stress was apparently induced in that area by the antenna boresighting operations and the thin aluminum developed fatigue upon flexing under vibration. Application of Devcon compound around the weak area satisfactorily redistributed the stress and no evidence of further cracking was found on subsequent tests.

(2) *Final testing and evaluation.* The average characteristics of the two channels in the various flight radiometers are summarized in Table 10.

Table 10. Radiometer characteristics

Item	Channel 1	Channel 2	Unit
Center wavelength	19.0	13.5	mm
Center frequency	15.8	22.2	Gc
Predetection bandwidth	1.5	2.0	Gc
Sensitivity, peak-to-peak	30.0	30.0	°K
Sensitivity, rms	5.0	5.0	°K
Calibration signal	350.0	350.0	°K
Integration time	20.0	20.0	sec
Beamwidth	2.5	2.2	deg
Side lobes	-23.0	-23.0	db
Reference frequency	950.0	1050.0	cps
Total weight	22.0 lb		
Total raw power	4.0 w average 9.0 w peak		

Evaluation of the performance of the radiometer to a high degree of accuracy is a difficult task. Difficulties arise because the predetection bandwidth is so large and became the source at which the instrument will look during the measurements is much more extended than the beamwidth. The first problem involves widely varying antenna, feed, and detector efficiencies. An accurate direct calibration would involve an extremely large number of measurements. Black-body-type radiators like the Sun or gas discharge tubes can be used, but their temperatures are difficult to determine to much better than 5%. The second problem involves the appreciable contributions from the side lobes of the antenna which will be filled to varying degrees by the planet.

To obtain as precise a calibration as possible, a special test setup is used, in addition to standard hot and cold load, and noise-source injection techniques. The test involves aiming the radiometer at a disc 10 ft in diameter suspended 60 ft above the radiometer. The disc is lined with a microwave absorber and its temperature (ambient) can be measured to within a few degrees. In this configuration, all the side lobes look at cold sky, from which the contributions are small, and the effect on back lobes can easily be minimized. In addition, the test is performed at an elevation of 7500 ft above sea level to minimize sky temperature in the 13.5-mm water-vapor line region.

3. Infrared Radiometer

a. Introduction. The *Mariner R* two-channel infrared radiometer is designed to measure the effective temperature of small areas of Venus at 8.5 μ and 10.4 μ . The measurements obtained should complement the measurements of radiation temperature made by the microwave radiometer.

The radiation received by the infrared radiometer can come either from the planetary surface, clouds in the atmosphere, the atmosphere itself, or a combination of these. Earth-based measurements indicate that, around 3.8 μ and between 8 and 13 μ , the effective radiation temperature is close to 235°K. There is evidence of a short-term (daily) fluctuation in this temperature. One interpretation of the effective temperature is that the radiation comes partly from a cloud structure at a temperature less than 235°K, and partly from a hotter source or sources below the clouds. In such a model, the short-term variations could indicate either a real cloud cover

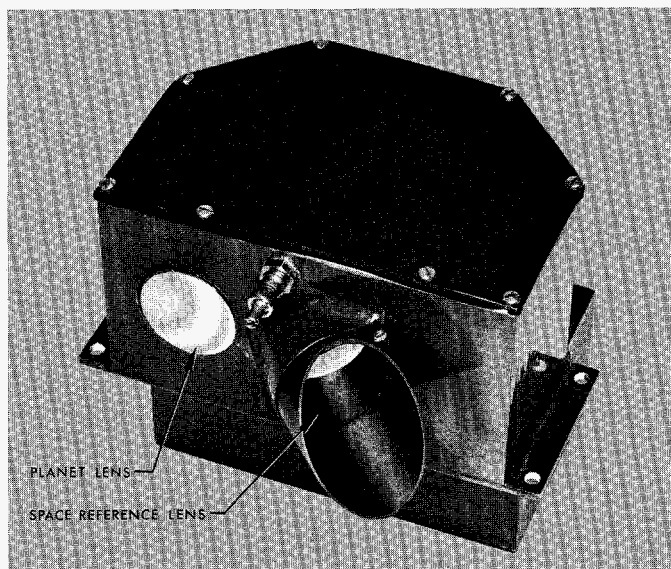


Fig. 128. Infrared radiometer in case

temperature change, or breaks in the clouds which let the radiation from below the clouds escape.

This experiment is designed to differentiate between these two situations, and either to map the temperature pattern of the cloud tops or to determine the effective extent of the breaks. In the former case, valuable information concerning the circulation of the atmosphere as a whole will be obtained, while a determination of the extent of the breaks, if they do exist, can be decisive in determining a correct model of the Cytherean atmosphere.

The 8- to 9- μ region of the infrared spectrum is, for the common gases, a transmission window at temperatures around 200 to 300°K, while an absorption band of CO₂ which has been detected on Venus is centered at 10.4 μ . Emission in the two wavelength intervals will be observed from essentially the same small region of Venus. In the case that the radiation comes from the cloud tops, the effective temperatures derived from the two channels should coincide after the small effect of the CO₂ above the clouds has been accounted for. Thus, in this case, the measurements derived from the two channels would give redundant temperature mapping of the cloud tops. If there are effective breaks in the clouds, a 1% break in a 235°K cloud cover over a 600°K source will change the energy in the 8- to 9- μ channel by a factor of two, while the CO₂ absorption will lead to a smaller energy change for the 10- to 10.8- μ channel. Thus, a comparison of the effective temperatures should lead to a differentiation between the two cases.

b. Description of the infrared radiometer. The infrared radiometer receives radiation in two spectral ranges: 8 to 9 μ , and 10 to 10.8 μ . A photograph of the instrument appears in Fig. 128. The two mounting flanges allow hard mounting to the microwave radiometer frame, and the alignment is such that the lens having its axis normal to the front face of the instrument is boresighted with the microwave radiometer beams. The other lens is used as a chopping reference and views dark space at an angle of 45 deg with respect to the first. After planetary acquisition, the radiometers scan the planet surface from limb to limb at a rate of 0.1 deg/sec.

Operational specifications

Chopper frequency	20 cps
Type of modulation	Amplitude modulation
Environmental capability:	
Operating temperature	-20 to +50°C
Survival temperature	-20 to +65°C
Lifetime	118 days
Vibration	10-15 g rms from 50 to 200 cps
Field of view	0.9 × 0.9 deg ±20% at half power points
Detector type	Uncooled thermistor bolometer immersed in germanium
Effective f/number	f/0.3
Weight	2.88 lb
Power	±12 v dc, 1% regulation, 0.5 w (obtained from microwave radiometer T-R unit) 26 v rms, 400 cps, single phase, 1.9 w

Performance

Planet temperature range	200 to 600°K
Dynamic range of input power	285
Sensitivity	Net = 1.5° at 200°K for signal equal to rms noise, 8.5 μ channel
Output format	Analog, logarithmically compressed, 1.0 to 6.0 v corresponding to planet temperature of 200°K and 600°K
Noise level at output	50 mv rms at 200°K

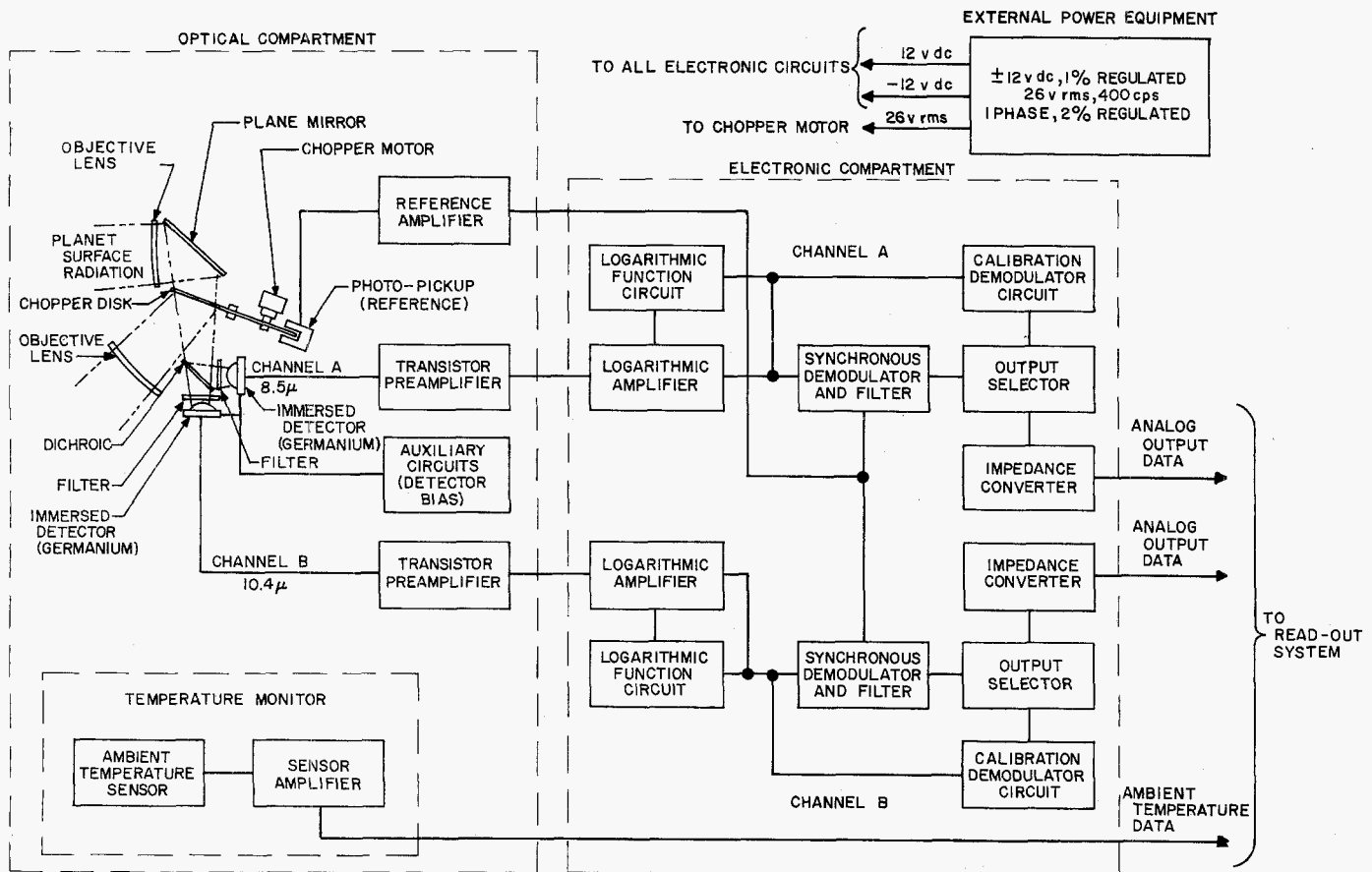


Fig. 129. Model Mariner R 2-channel infrared radiometer, block diagram

The block diagram of the instrument is shown in Fig. 129. The chopper disc is driven on its edge by a 400-cps synchronous motor and rotates at 600 rpm. It has alternate quadrants gold plated and cut out so that the radiation transmitter through the system comes alternately from one lens and then the other. The dichroic filter serves as a beam splitter; i.e., about 90% of the radiation having wavelengths longer than 9.5μ is transmitted, while 90% of the radiation of wavelengths shorter than 9.5μ is reflected.

Since the expected dynamic range of planet radiant energy is greater than that of the data system, it was necessary to provide compression of the data output. Accordingly, a logarithmic amplifier is employed so that one digitizing level of 23 mv corresponds to a temperature increment of about 1.0°C in the 200 to 250°K range; while at 600°K , the smallest resolvable temperature increment is 7°C .

A synchronous demodulator and low-pass filter were used as a relatively simple way to get narrow noise band-

width (0.1 cps) and still have the output voltage insensitive to fluctuations in chopper speed.

One of the firm requirements of the system was an in-flight calibration check. This was accomplished by mounting a small plate on the superstructure of the spacecraft in such a way that the space reference lens views the plate when the radiometer scan is near one end of its travel in the fast scan mode. The planet lens views space during this check.

Since the instrument is sensitive to the phase of the input radiation (one lens system compared to the other), the output voltage would be negative during calibration were it not for the output selector and calibration demodulator circuit. These circuits maintain a positive output voltage regardless of the sense of the input radiation. Emitter-followers are used at the output to obtain low output impedance.

c. Design and development. The time available for design, development, and fabrication of the instrument

was so short that neither a breadboard nor a prototype was attempted. The time from go-ahead to delivery of the first flight unit was about $3\frac{1}{2}$ mo. This time scale necessitated the use of many off-the-shelf components and stimulated short cuts in the design that later gave trouble.

(1) *Mechanical design.* There were two general problem areas; the first concerned the chopper drive system, and the second involved the hermetic sealing of the optical compartment.

Originally, the chopper was made from a standard gear with wedge-shaped quadrants cut out to pass the radiation from the planet lens. It was found, however, that these cut-out areas caused internal stresses to be relieved so that the gear became distorted and would not mate properly with the pinion. This problem was mitigated to some extent by cutting the holes and relieving the stresses before hobbing the teeth on the blank.

Hermetic sealing of the optics compartment is necessary since the chopper bearing contains lubricant which would otherwise evaporate in space. In practice, this was a significant problem, since the unit leaked through the porous magnesium casting as well as around the lenses. Hot epoxy resin was used to seal these leaks. It was applied to the exterior of the unit while a partial vacuum was maintained on the inside in order to force the resin into the pores of the casting. The cover is sealed in place by soft solder.

(2) *Optical design.* Germanium lenses and filter substrates are used throughout, and all have zinc-sulfide antireflection coatings. The detectors are uncooled, immersed bolometers. In this detector, the thermistor flake is mounted to the plane surface of a germanium hemisphere. While the detectivity can be increased by a factor of about 3.5 by this method, the temperature operating range is limited to about -20 to $+60^{\circ}\text{C}$ because of the difference in the expansion coefficients for the germanium lens and the selenium interface layer.

Several optical obscuration effects were observed on some of the units. These effects were caused by either unequal transmission in the two optical paths, or by one or the other fields of view being obscured partially by internal structure of the instrument. Obscuration of the field of view causes an offset in the output which is a strong function of instrument temperature. An illustrative example will give a feeling for the magnitudes involved: a 3% obscuration present in one field of view

and not in the other would cause an offset in the output equal to the signal when viewing a black body at 200°K .

In several of the units, the zinc-sulfide antireflection coating peeled away from the germanium objective lens and filters. The cause of this trouble is as yet unexplained, but a possible cause may be the adhesive (Silastic 891) used in the optics compartment, which gives off acetic-acid vapor during the curing process. Although it is a relatively weak acid, the fumes may tend to loosen the zinc sulfide coating so that, during shake tests, it comes off completely.

(3) *Electronic design.* The electronics design is, in general, straightforward. There were, however, several problem areas which necessitated some modification and rework of the flight units at JPL.

Due to ground loops around the preamplifiers, there was pickup of the demodulator driver signal at 20 cps. The third harmonic of the chopping frequency heterodyned with stray 60-cps fields in such a way as to cause low frequency (0.2 to 1 cps) bounce in the output. Much of the ground loop and pickup problem was eased by rearranging the grounds to the preamplifiers, and finally by insulating the instrument from the spacecraft and then tying chassis ground to circuit ground.

The output circuitry had to be modified to provide lower output impedance so that the data system would not load down the instrument. Also, several changes were made to improve the operation of the output selector and calibration demodulator.

d. *Testing and calibration.* Calibration of the instrument is performed by means of the setup shown in Fig. 130. Two black bodies are used: one at liquid nitrogen temperature for the space reference, and the other variable over the temperature range expected for the planet. Frost is prevented from forming on the black bodies by evacuating the entire system. Atmospheric absorption as well as convective air currents are eliminated by this technique also.

A close fitting shroud is provided which allows ethylene glycol solution to circulate so that the instrument can be calibrated over its operating range.

There are several inherent sources of error in the present calibration technique:

(1) *Differential heating of lenses.* Since the black bodies can be at widely separated temperatures, radi-

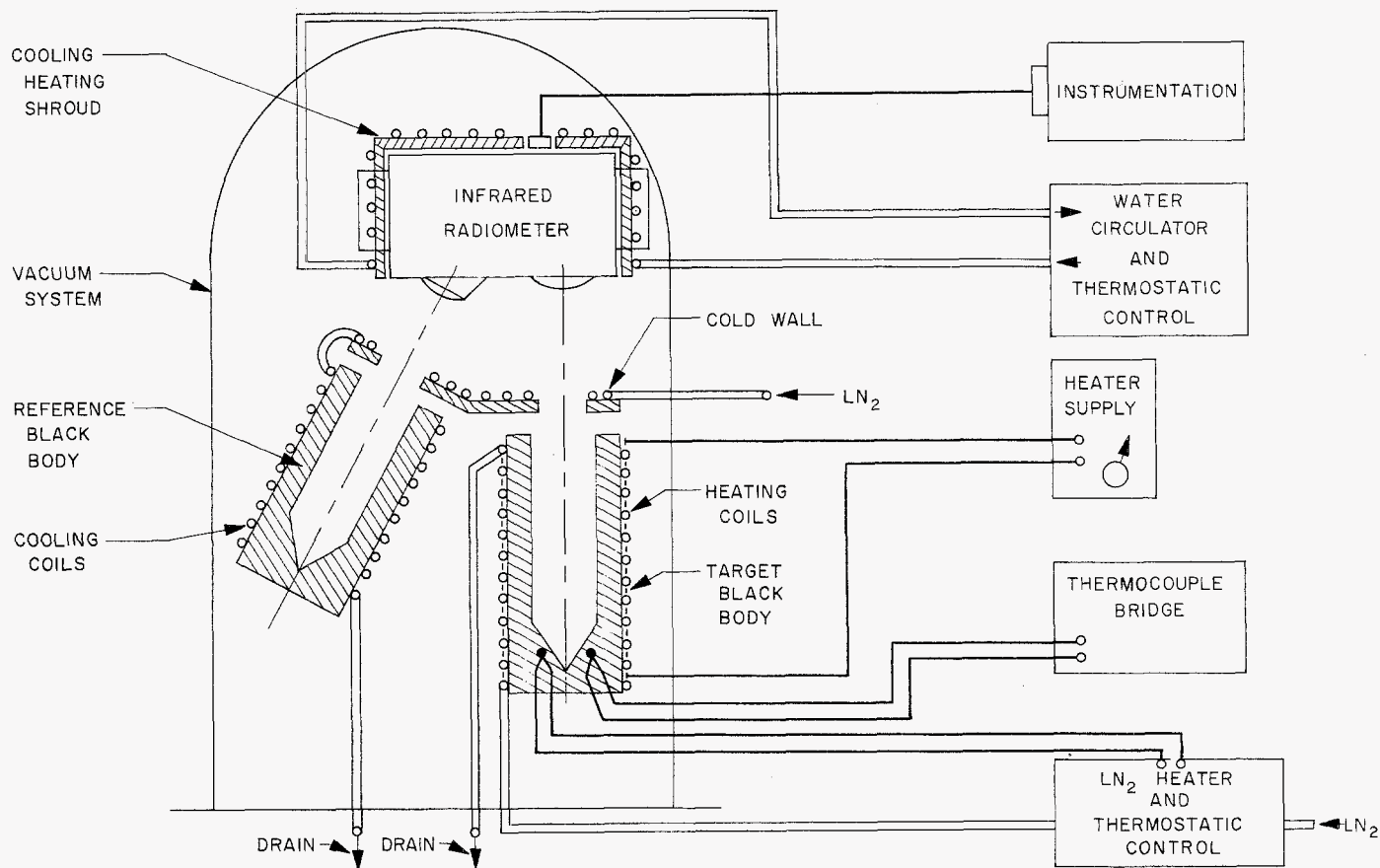


Fig. 130. Calibration setup

active coupling will cause a temperature differential between the lenses. Re-emission of energy into each optical path will cause an error proportional to the difference in temperature. For example, a 1°C difference in lens temperature will cause a 1° error in the reading when the radiometer is looking at a 200°K black body. The liquid-nitrogen cold wall was placed over the black bodies to prevent radiative exchange from areas other than the cavities. Results of recent tests show, however, that the gradient between the lenses is greater with the cold wall than without. A correction factor which accounts for this effect can be applied to the data taken in the laboratory, but it is doubtful that a factor can be found which will correct the data taken in space.

(2) *Spurious reflections.* Multiple reflections of energy from warm parts of the fixture may be a source of error. The cold wall and a liberal application of Sicon black paint to all parts of the system should reduce this effect.

(3) *Temperature gradients in the black bodies.* Unequal heating or cooling of the black bodies can cause

large temperature gradients to exist along the length of the cylinder, although the bodies are made of solid copper with 0.5-in.-thick walls. Larger than 10°C gradients from end to end are not uncommon. This effect was minimized by allowing the body to equilibrate after the heat was removed. Six thermocouples located along the cylinder were used to indicate equilibrium.

4. Fluxgate Magnetometer

a. Scientific objectives. The primary scientific objectives of the *Mariner R* magnetometer are to investigate the existence and nature of a planetary magnetic field. Experimental evidence concerning a magnetic field of Venus is practically nonexistent. Not enough information is available to predict theoretically whether or not a magnetic field exists.

It is, therefore, appropriate to attempt a direct magnetometer measurement in order to investigate the exist-

ence of a Cytherean magnetic field. The significance of such a measurement is related to various important physical properties, both interior and exterior to the surface of the planet. The most commonly accepted explanation for the origin of a planetary magnetic field involves fluid motion in a molten core. A determination of the magnitude of the Cytherean magnetic field will play an important part in hypotheses concerning the interior. Similarly, the properties and dynamics of the planetary atmosphere involving charged particles, magnetic storms, and aurorae depend on a knowledge of the planetary magnetic field.

The existence of a planetary magnetic field can be established by observing a transition region from interplanetary space to the region in the close vicinity of a planet. Generally accepted theories, which are supported by a few measurements of the geomagnetic field at tens of Earth radii, indicate that a characteristic transition region exists which is called the magnetopause. This region separates the planetary field from the ionized component of the interplanetary medium. Thus, a planetary magnetic field is confined to a cavity inside the interplanetary gas. Due to the effect of the so-called "solar wind," the planetary magnetic field may take the form of a teardrop with the tail pointing away from the Sun. The observation of a magnetic variation characteristic of such a boundary would constitute evidence for the existence of a planetary magnetic field. In addition, the magnitude of the planetary field near the magnetopause and the distance from the planet at which it is located, permit estimates of the magnetic field strength at the surface, assuming various origins of the field, such as dipole, quadrupole, etc.

The magnitude of the planetary field and the *Mariner R* trajectory may be such that measurements can be made at points well inside the magnetopause. Such measurements would establish the geographic dependence of the magnitude and direction of the essentially undisturbed planetary field. It should then be possible to establish the multipolarity of the source of the field and its orientation with respect to the planetary axis of rotation. If all of these results could be achieved, they would represent the ultimate information on the planetary field obtainable during a planetary encounter such as the *Mariner R* mission.

Another scientific objective of the magnetometer experiment is to make measurements of the interplanetary magnetic field during the trip to the planet. Some preliminary measurements were made by *Pioneer V*. These

results indicated that, approximately 20% of the time, magnetically quiet conditions prevailed with a steady interplanetary field of approximately 3 γ (1 γ = 10^{-5} oersted; approximately 1/50,000 of the Earth's magnetic field at the surface). During the remaining 80% of the transmission periods, the magnitude of the interplanetary field fluctuated irregularly, reaching magnitudes of approximately 50 γ just prior to a large geomagnetic storm.

The verification of the existence of the steady magnetic field components and an accurate measurement of its characteristics would represent an important contribution to an understanding of the gas dynamics of the inner solar system. However, it may be impossible to obtain a complete measurement of the steady-state interplanetary field, because the magnetic field associated with the *Mariner R* spacecraft may be substantially larger than the interplanetary field. If an absolute measurement of the interplanetary magnetic field is impossible, statistical data can still be obtained concerning the variations in the interplanetary field and the relative occurrence of magnetically quiet and magnetically disturbed periods during the declining part of the solar cycle.

It will also be possible to study long-period fluctuations in the interplanetary magnetic field. The experiment should establish both the direction and magnitude of such field variations. These data could lead to important information relative to solar disturbances, the existence of hydromagnetic waves or magnetized plasmas in interplanetary space, and estimates of the kinetic energy density of the interplanetary plasma.

b. Type of hardware selected. The short schedule required an instrument readily packaged with a minimum of development work. The Marshall Laboratories fluxgate was chosen because a working breadboard requiring little change existed from the *Mariner A* Project. The main modification consisted of eliminating the spectrum analyzer circuits. This change was dictated by weight and power limitations more severe than those for *Mariner A* and was permitted because elimination of fluctuating field measurements did not degrade the experiment too seriously.

Two other modifications of the *Mariner A* design were: (1) reduction of the number of ranges from 3 to 2; and (2) elimination of the probe-short mode in the in-flight calibrate sequence.

These changes were the result of trade-offs between weight, reliability, and experimental objectives.

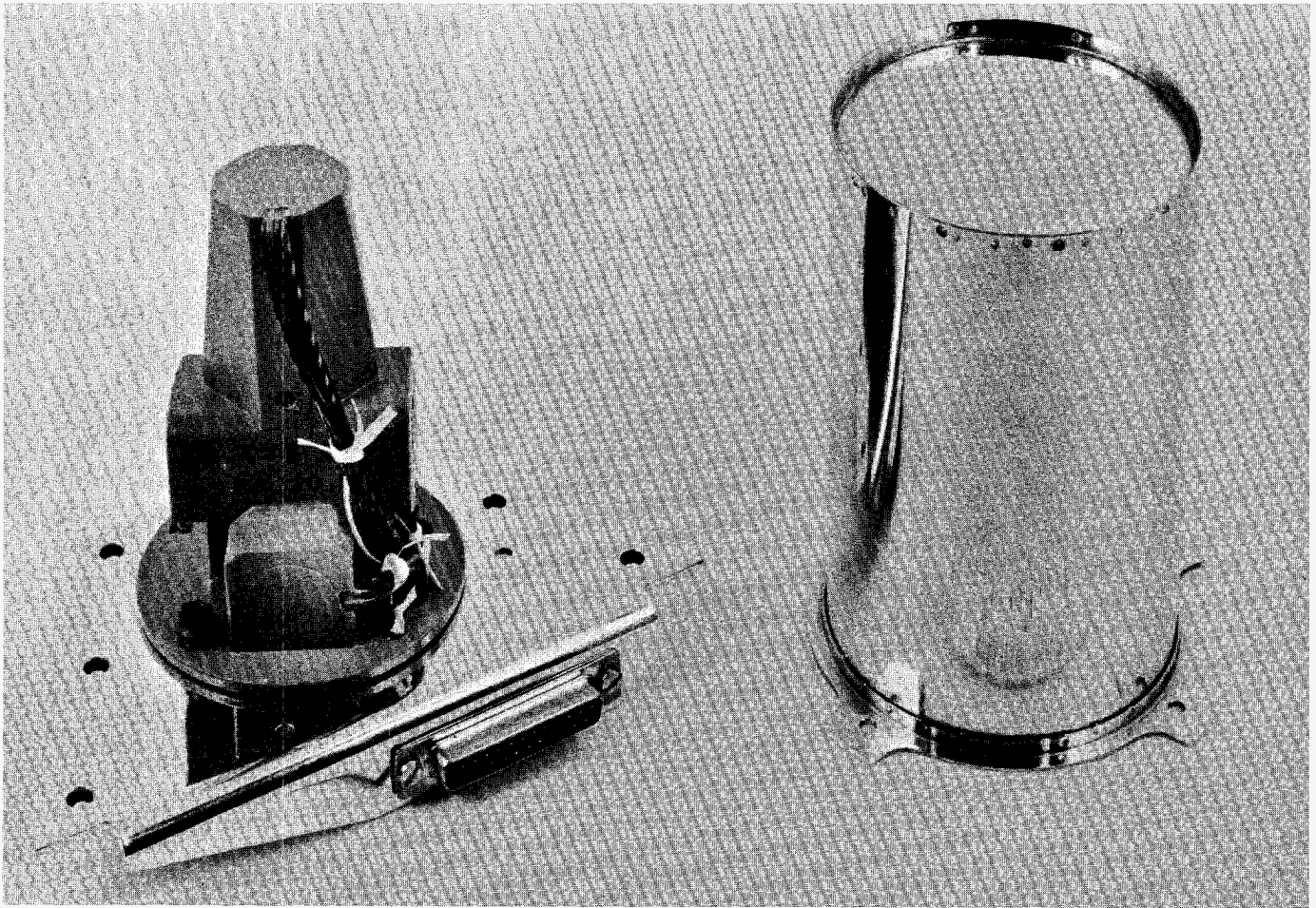


Fig. 131. Magnetometer sensor

c. Instrument development and design.

(1) *The sensor.* The sensor is designed and fabricated by Institut Dr. Förster in Reutlingen, Germany, and is shown in Fig. 131. The sensing element is a magnetic core containing a primary and a secondary winding. An alternating current of 20 kc is applied to the primary winding sufficient to saturate the core. In the presence of an ambient magnetic field with a component parallel to the core axis, a signal component is generated in the secondary which is proportional in amplitude to the magnitude of the field. Each triaxial sensor axis contains two cores and windings in parallel alignment, with the primary windings connected in series opposing and the secondaries in series aiding. The feature virtually eliminates the fundamental and odd harmonics in the secondary by a balancing effect and, thus, facilitates extraction of the second harmonic component. An auxiliary coil is wound on the combination for in-flight calibration and field biasing.

The sensor specifications are as follows:

- | | |
|--------------------------------------|---|
| (1) Sensitivity: | $10 \mu \text{ v}/\gamma$ |
| (2) Stability factor: | 0.25γ for ± 1 -oersted exposure |
| (3) Frequency: | 20 kc fundamental |
| (4) Power: | 100 mw/axis |
| (5) Crosstalk: | 1 part in 10^4 |
| (6) Auxiliary coil constant: | $0.5 \mu \text{ a}/\gamma$ |
| (7) Axis orientation accuracy: | 0.1 deg |
| (8) Total weight, including housing: | 0.67 lb |

(2) *The electronics.* A block diagram of the electronics is shown in Fig. 132 and the two subunits comprising the package in Fig. 133. The drive signal is derived from a

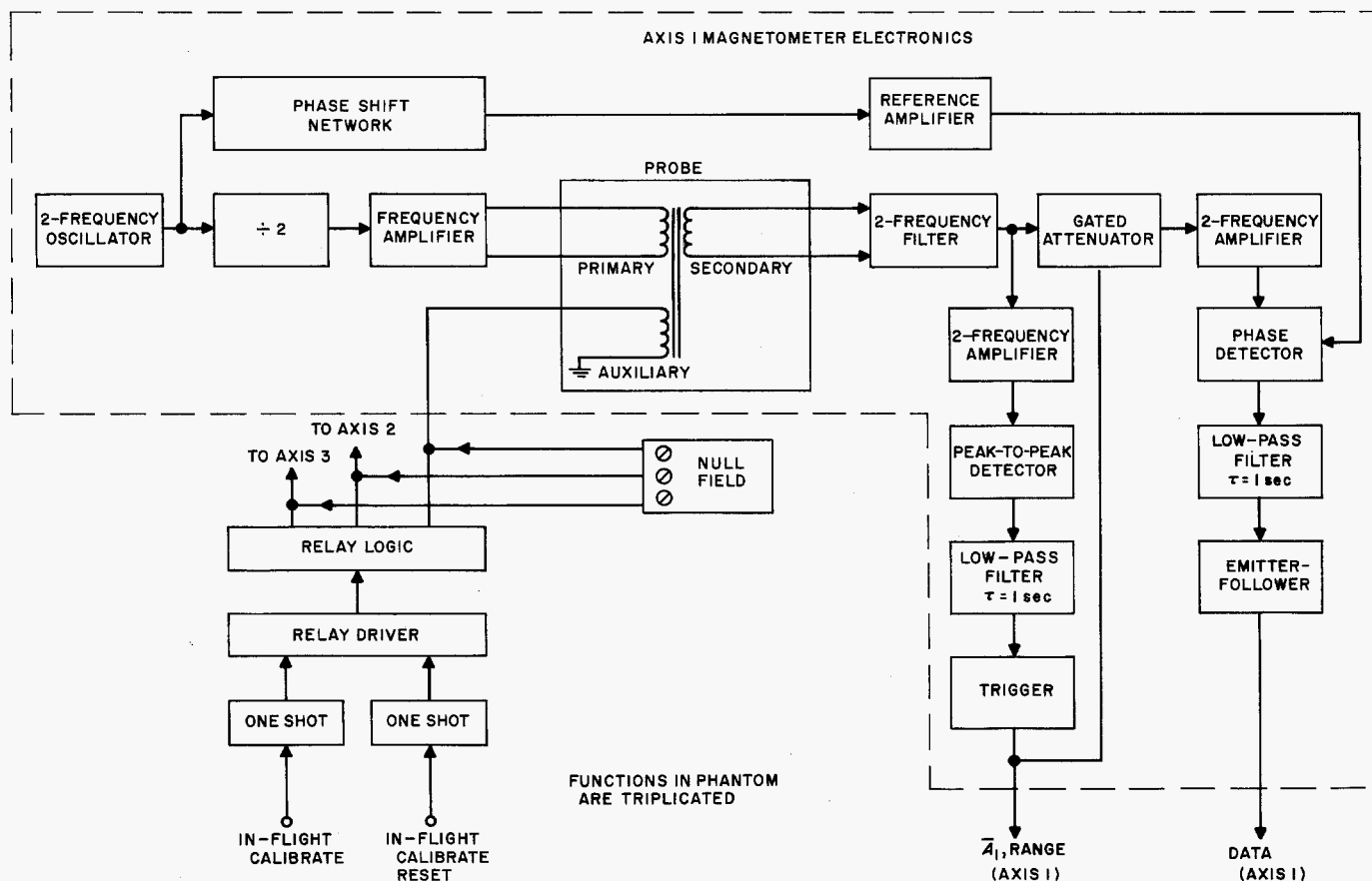


Fig. 132. Triaxial fluxgate magnetometer, block diagram

$2f_0$ oscillator (f_0 = fundamental drive frequency) after dividing by two, and is fed to the primaries through a tuned, push-pull Class B amplifier. The $2f_0$ reference for the synchronous detector is taken directly from the oscillator. This mode of operation reduces the effects of phase jitter as opposed to direct f_0 oscillator operation with frequency doubling for the detector. The secondary output is amplified, filtered, and fed into the detectors. The synchronous detector derives the analog signal output which passes through an emitter-follower, while a peak detector furnishes a voltage level which gates the attenuator for automatic scale switching. The triggering and gating circuitry also furnishes an output which indicates which scale is in operation.

The sensor is calibrated by passing a specific current derived from the regulated power supply through the auxiliary coil. The current is switched on and off in flight by pulses from the data conditioning system driving latching relays. Provision is made to apply a constant biasing current to auxiliaries to allow nulling out the effects of a possibly large field contributed by the spacecraft.

(3) Problems

(a) The probe-short made for in-flight calibration was removed from the sequence for reliability reasons. Although the output voltage reference for zero field is non-zero (3.5 v), the reference level was more reliable than the shorting circuit, which could get stuck in the short mode with consequent loss of further data.

(b) Enough crosstalk between circuits for the three axes was encountered to produce occasional beats and small offsets (≈ 1 or 2γ) in the outputs. The three axes were driven at frequencies mutually separated by 4 kc to reduce this problem, but harmonics of one axis could beat with those on another. Future fluxgates will be driven from the same oscillator to eliminate the beat problem, and a better circuit layout with shielding can eliminate offsets due to interchannel crosstalk.

(c) Offsets of the order of a few gammas were experienced due to pickup of quadrature voltage from the oscillator by the output amplifier. These offsets could be eliminated by exact adjustment of the phase relation between signal and reference in the detector, but adjust-

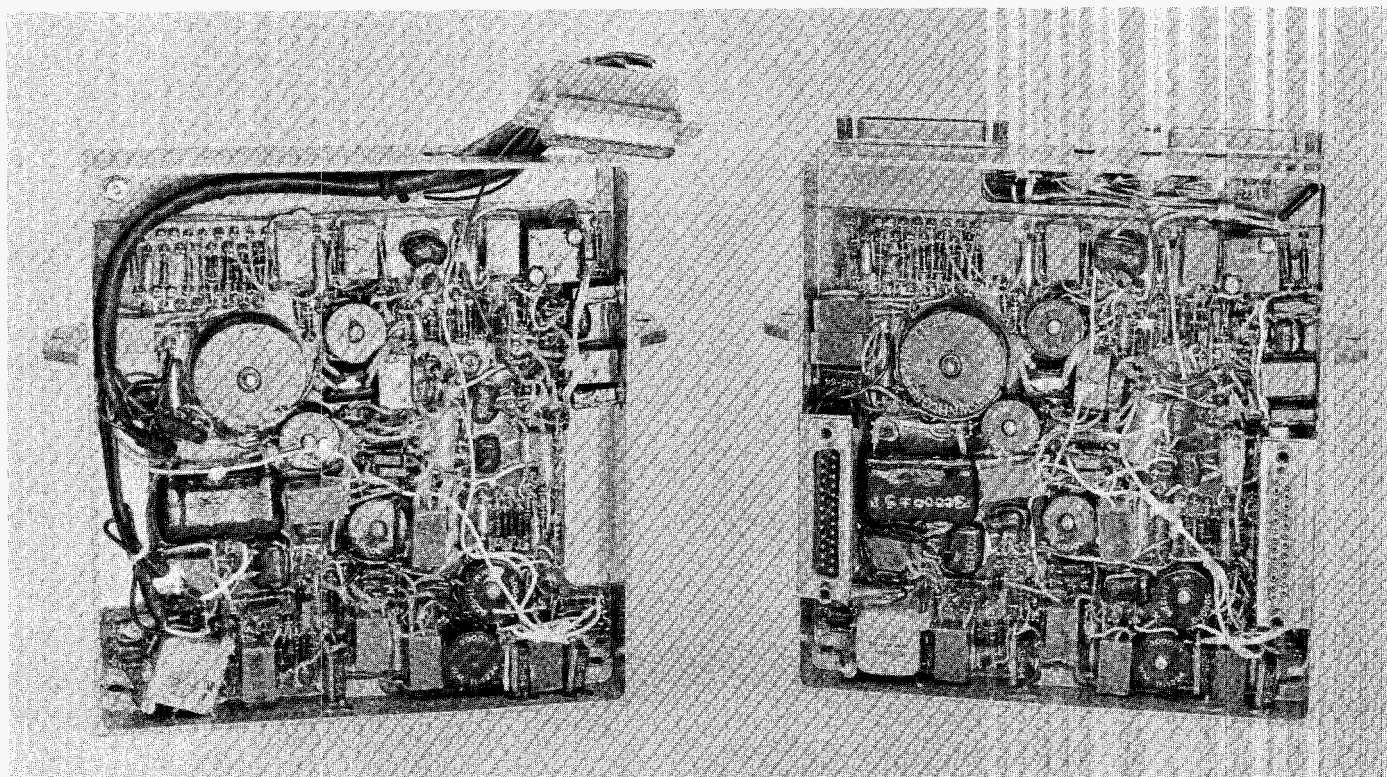


Fig. 133. Magnetometer electronics

able resistors in the phase shifter and slight changes in parameters of the sharply tuned amplifier circuits allowed phase changes to occur with vibration, heat cycling, etc. In one case, the phase change resulted in considerable loss of sensitivity, which was corrected by phase adjustment. Future remedies are: elimination of potentiometers from the design; better isolation between circuits; and servo, or field nulling operations, in which the output produces a current in the auxiliary to cancel the applied field.

(d) A variable offset was found to result from the presence of some second harmonic in the drive voltage, some of which coupled into the secondaries because of unbalance in the sensor cores and/or windings. Since the balance proved to be a function of drive amplitude and frequency, and the second harmonic a function of sensor cable capacity (the driver tank circuit contains the cable capacity), this problem seems solvable in the future. The offset was variable because of primary-to-secondary coupling dependence on the past magnetic history of the sensor. The immediate solution to this problem, plus offset due to core remanence, is to degauss the sensor immediately prior to flight. This is done by turning the sensor drive on and off a few times while the ambient field is nulled out by the auxiliaries from GSE. Sensor

exposure to the Earth's field in the nonoperating condition does not result in measurable offset.

(e) Some crosstalk between axes was traced to improper lead dress at the sensor. This was successfully eliminated by dressing the leads away from the sensor body at least $\frac{1}{2}$ in.

(f) The magnitude of the second harmonic in the drive waveform and the instrument calibration are somewhat dependent on temperature. Since the hex bay location of the package is temperature-controlled, the problem should not be severe. Sensitivity-vs-temperature calibrations were performed, and a thermistor sensor was placed in the package to allow corrections for unusual temperatures. Thermistor compensation was included in the push-pull driver amplifier to help assure full-wave symmetry. Servo schemes are being developed which promise greater stability regarding second harmonic distortion for future applications.

(g) Extensive testing showed that the automatic scale-switching points varied over a period of time. The solution lies in further circuit development for this function.

Much has been learned through testing of the *Mariner R* instrument. Some of the uncertainties have been re-

moved by probe degaussing and in-flight calibration, but an uncertainty of as much as 10% in the data from space can be experienced due to phase shift, crosstalk, and drive waveform distortion, depending on the stability of the various circuit parameters with time. Instrument sensitivity and resolution are within specification over long time periods, while total offset has varied enough to require occasional preflight adjustment. The *Mariner R* instrument is not considered to be pushing the fundamental limit of the fluxgate from a standpoint of absolute measurement near zero field. New sensor excitation and read-out concepts are being studied which promise considerable reduction of zero uncertainty and long-term instability.

It is planned to turn the magnetometer on before mid-course maneuver while the spacecraft rotates slowly about the roll axis. At this time, an accurate ambient field measurement will be obtained on the *X* and *Y* axes, and the total zero offset (including spacecraft field) will be determined for these axes. Good correlation between this measurement and preflight calibrations would increase confidence in the preflight calibrations for all axes.

d. Spacecraft field mapping. The contribution of the spacecraft to the measured field was determined before flight by a rotation technique. Since no field-free facility large enough to accept the spacecraft and the rotation jig was available, the measurement was made in the Earth's field. A number of assumptions are involved, some of which cannot be verified until a mapping in space (by spacecraft rotation) is possible.

The spacecraft was rotated on an oil table about two spacecraft axes with the magnetometer held fixed, which allowed separation of the spacecraft field component at the sensor from the large ambient or constant field. A considerable induced component due to interaction between spacecraft ferromagnetic materials and the large Earth's field existed, but this was eliminated mathematically from the data, using verified assumptions concerning the effective geometry of the field distorting body. In the absence of current in-space verification of the mapping technique, experiments using representative models under simulated launch and space conditions are being devised.

5. Cosmic Dust Detector

a. General. There has never been any direct measurement of the flux of dust particles in interplanetary space.

Our only knowledge of the dust content in space comes from observations of the zodiacal light. When the interplanetary dust flux derived from these observations is compared with the direct measurements made with rockets and satellites near the Earth, it is found that there may be an increase near the Earth as large as a factor of 10^3 . Thus, the main objective of any dust experiment on *Mariner R* is to obtain the first direct measurement of the interplanetary dust flux.

Two other important problem areas could also be explored with a dust experiment:

- (1) Some of the particles near the Earth may have been knocked off the lunar surface without enough energy to escape from the vicinity of the Earth. What fraction, if any, of the increased concentration near the Earth is due to this source is still unknown. Since Venus has no satellite, a comparison of the dust flux near Venus and near the Earth may indicate how important a role is played by the Moon.
- (2) It would also be interesting to study the properties of any meteor streams encountered. The dust experiment on *Vanguard III* observed many small particles associated with the Leonid meteor stream. However, there are some strong arguments to support the point of view that the particles may not have belonged to the incident stream, but instead, were produced when the Leonid stream hit the Moon.

For the reasons just enumerated, as well as for a more thorough demonstration of any potential hazard to manned flight due to dust particle bombardment, it is desirable to determine the flux of dust particles as a function of distance from the Sun, distance from the Earth and Venus, and time. An ultimate goal is to learn the mass, vector velocity, and composition of each incident dust particle.

b. The experiments. To determine flux as a function of time and position, it was decided to fly a large-area microphone experiment. The large sensitive area of the detector would be essential to obtain a statistically significant measurement if the interplanetary-dust flux should indeed be lower than the near-Earth flux by 10^{-3} . To meet the weight limitations, the individual particle analysis had to be restricted to a 2-channel pulse-height analysis of the microphone output. The pulse height is proportional to the impacting particle's momentum for low-

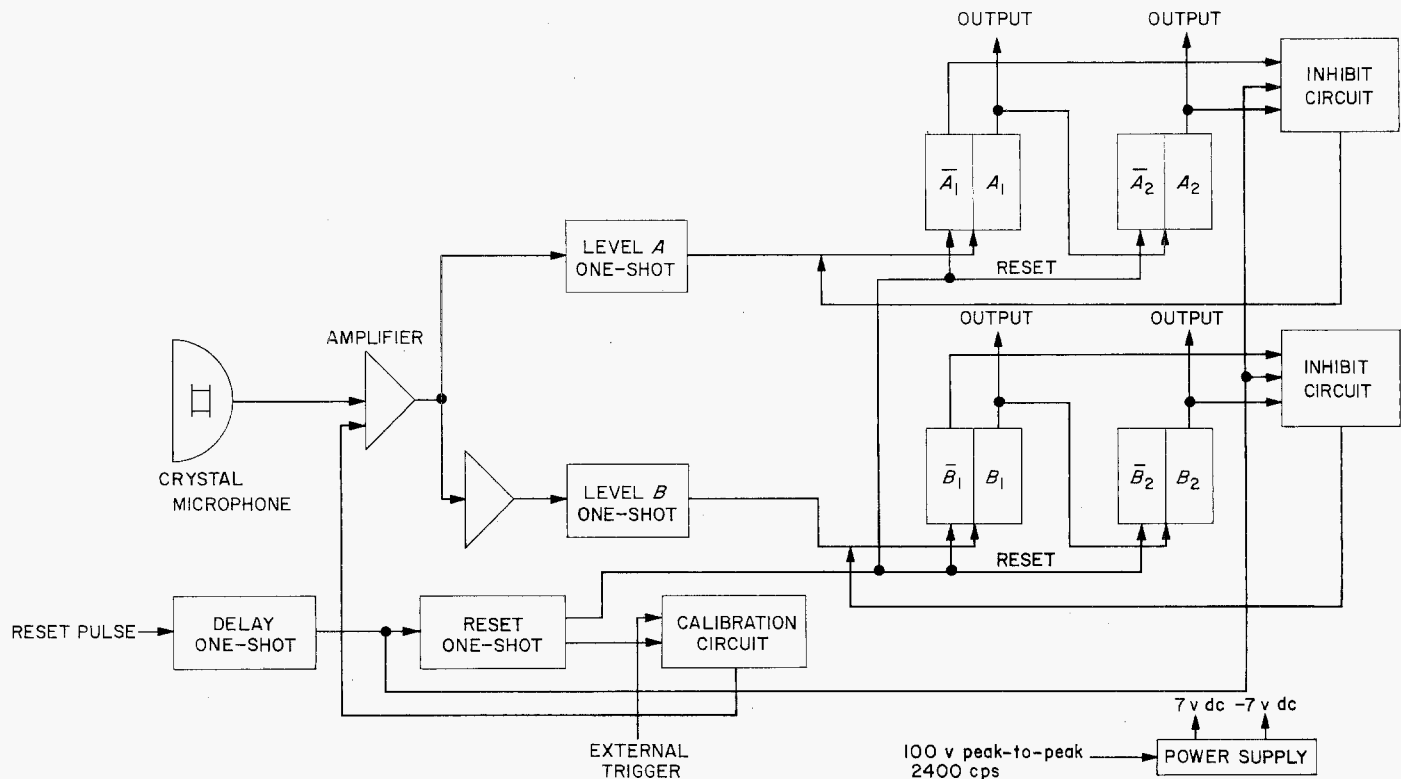


Fig. 134. Cosmic dust detector, block diagram

velocity particles; the two channel thresholds correspond to roughly 10^{-4} and 10^{-3} dyne-sec. At higher velocities, the response is more complex, but can be calibrated in the laboratory. Other, more sensitive experiments which were considered for inclusion were generally more complex, heavier, required more power, and/or had a smaller sensitive area. Thus, it was recommended to fly the microphone with a large rectangular (5.5×10 -in.) sounding board with two-channel pulse-height analysis proposed by W. M. Alexander of Goddard Space Flight Center. Since both the *Ranger I* and *II* and the *Mariner A* dust detectors provided by this same group contained microphones with two or more channels of pulse-height analysis, it was believed that the schedule and systems integration problems would be kept to a minimum.

Since the allowed time for fabrication would not permit development, the simplest approach was to use as much as possible the *Ranger I* microphone circuitry; indeed, some of the hardware was readily available. It was only necessary to repackage and make maximum use of the weight allowed. The transducer element, amplifiers, and logic circuitry are essentially identical to that portion of *Ranger I*. The block diagram is shown in Fig. 134.

The following modifications were applied for the *Mariner R* configuration:

- (1) Necessary addition, in any case, of a 2.4-kc square-wave power supply
- (2) Installation of inhibit circuitry to prevent the binary counters from recycling to zero impact count after saturation
- (3) Change in the calibration logic so that the read-out of its function would indicate zero count as a convenience of not having to subtract one count from the data for impact counts

It was desired to have an end weight of 1.5 lb and to use no more than 100 mw of power. The completed units weigh 1.8 lb and require 80 mw of power. The weight was increased slightly by the gold-plating requirements for passive temperature control of the sensor plate and associated brackets. Reducing the amount of circuitry would have reduced the over-all weight by only a few grams. Decreasing the area of the sensor plate to half would have saved about 0.2 lb, but it was believed that the larger impact surface area was well worth its weight.

Mr. Alexander of GSFC selected the same contractor, Labko Scientific, Inc., Stillwater, Okla., who fabricated the *Ranger I* experiment, to help speed delivery.

No problem was encountered in breadboarding and fabrication. Each flight unit (Fig. 135) was operated about 500 hr with no change in parameters prior to JPL delivery. Calibrations have been made several times since JPL delivery, with no changes detected.

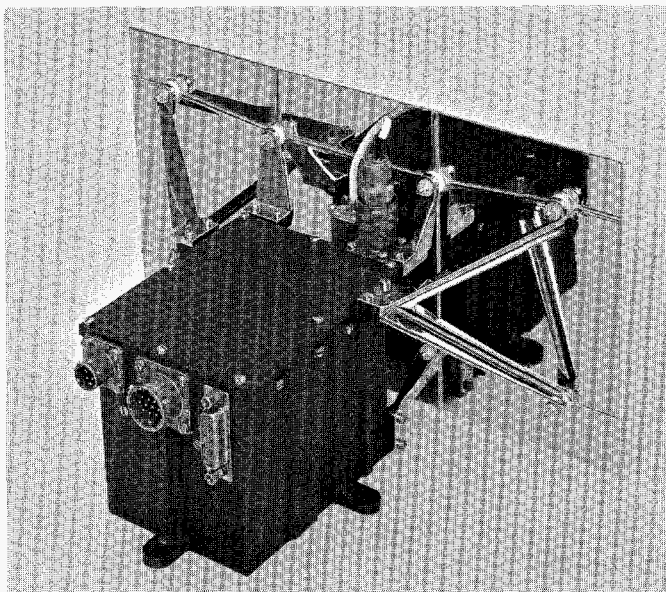


Fig. 135. Cosmic dust detector

6. Solar Plasma Analyzer

a. General. The solar plasma analyzer is designed to measure low-energy interplanetary positive ions that are emitted from the Sun in the energy range from 240 to 8400 ev. The system will measure the collection rate of the positive ions from 10^{-13} to 10^{-6} amp.

Because of the short development time available for *Mariner R*, it was decided to use the electronics from RA-1 and -2 solar corpuscular radiation experiments. Also, because of weight and power restrictions, only solar positive ions were to be measured.

The solar plasma analyzer (Fig. 136) consists of four basic elements: (1) the curved electrostatic deflection plates and associated collector; (2) the electrometer; (3) the programmer; and (4) the sweep amplifier. The curved analyzer plates, which electrostatically focus the charged particles onto an electrically isolated collector cup, consist of a boxlike structure with a 120-deg curvature. Voltages applied between the deflection plates create an electrostatic field transverse to the incoming particle velocity, which deflects incoming ions of the proper energy levels into the collector cup. The ion collection rate is measured as a current by the electrometer.

b. Electrometer. The electrometer consists of a stabilized, carrier-type operational amplifier with logarithmic feedback. The input modulator is a vibrating-reed capacitor, stabilized at its mechanical resonance by a

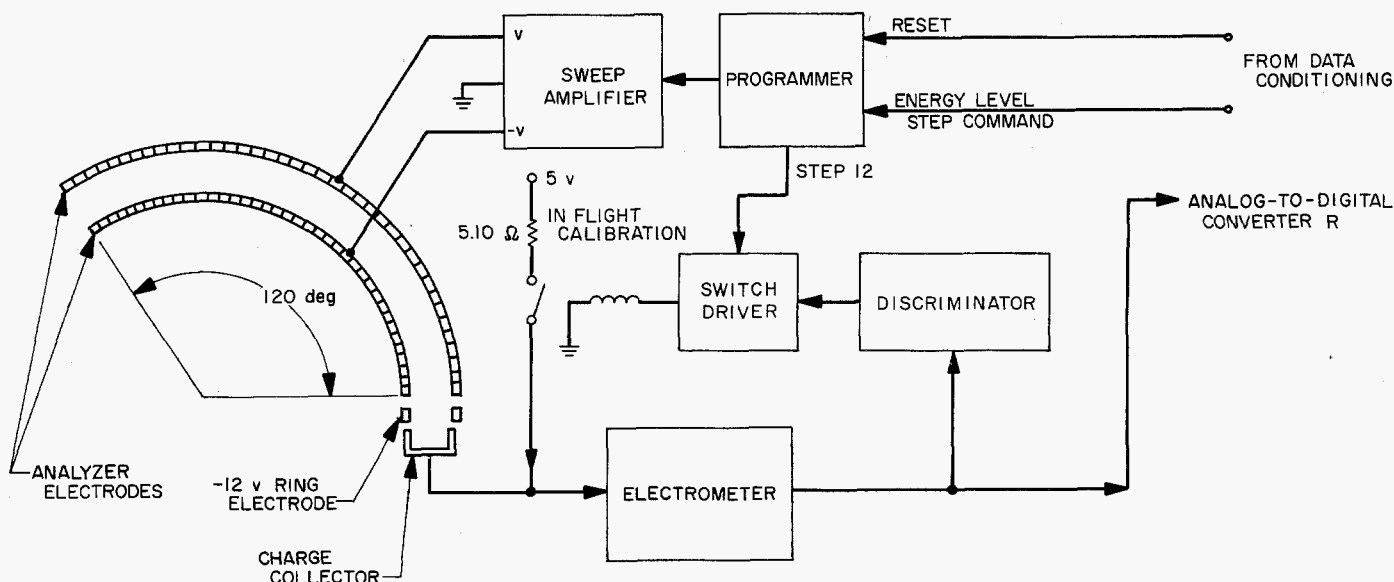


Fig. 136. Solar plasma analyzer, block diagram

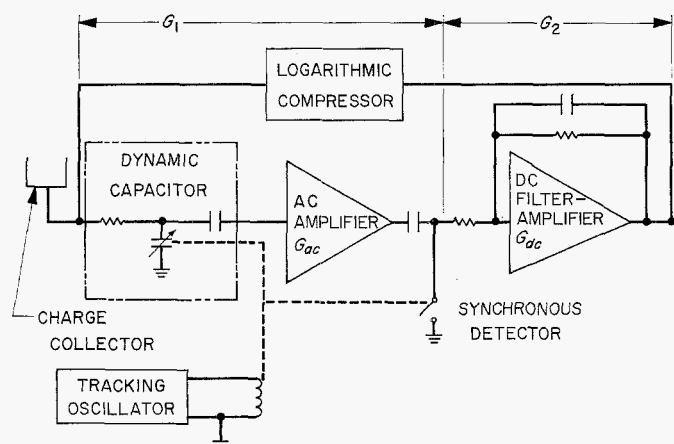


Fig. 137. Solar plasma electrometer

tracking oscillator. The oscillator also provides gain control in such a way as to maintain nearly constant modulation conversion efficiency over a substantial temperature range. As shown in Fig. 137, the remainder of the electrometer consists of an a-c amplifier, synchronous detector, and a d-c filter-amplifier. The logarithmic compressor is a 5886, pentode-connected as a diode that operates in the retarded field region. The resulting exponential characteristic of the feedback element produces voltage changes of 250 mv/current decade, thereby enabling the multidecade current measurement to be made within the dynamic range of the electrometer.

With no input current from the collector cup and with leakage currents that are of opposite polarity to the positive ion currents, the output of the electrometer tends to go to saturation. Since the principal cause of negative input leakage current is a modulator contact potential that produces a positive summing point voltage, a bias supply is used to adjust the summing point to a small negative voltage. Another precaution is to have a comparator at the output of the electrometer so that when the electrometer, in approaching saturation, goes above a certain voltage, a positive restorative current is connected to the input. The electrometer has an in-flight calibration accomplished by injecting a known current into the input. This current, which is generated by connecting a fixed resistor between the input and a fixed voltage, is the same current source used to restore the electrometer under saturating circumstances.

c. Sweep amplifier. The sweep amplifier, which generates the high voltages for the deflection plates, consists of a direct-coupled operational amplifier with resistive feedback, and input summing resistors which are switched to a regulated voltage. The amplifier output voltage is equal

to the ratio of the feedback resistor to the equivalent input resistor times the equivalent input voltage. The output stage generates the high voltage with a static inverter and a voltage quadrupler in the secondary of the static-inverter transformer. The voltage that is connected to the feedback resistor varies in 10 exponential steps from 30 to 1050 v. The voltage quadrupler is ground-referenced in such a way as to produce a voltage of equal magnitude and opposite polarity at its other output terminal. These outputs are connected to the deflection plates, with the positive voltage to the outer plate and the negative voltage to the inner plate, causing the electrostatic field to deflect positive ions into the cup. In sweep steps 11 and 12, the plates are driven, respectively, toward opposite polarity voltages but are clamped near ground by catching diodes. With this low voltage on the plates, there are no external ions reaching the collector cup so that the input is zero. In this way, the only current seen in step 12 is that which is produced by the calibration-current source.

d. Programmer. The programmer counts the number of input pulses which are received from the data conditioning system and switches in the appropriate voltage and resistance at the input of the sweep amplifier. When the pulse that puts the programmer in step 12 is received, it rejects further input pulses until it receives a reset pulse and then recycles through the 12 positions. The complete set of 12 steps takes 221.76 sec.

e. Instrument problems. Problems experienced during development, assembly, and testing of the system were:

- (1) Photoelectron current produced by ultraviolet light
- (2) Quadrature in the carrier signal as evidenced by a large demodulator waveform
- (3) Low gain in the a-c amplifier section
- (4) Low-frequency ripple on the electrometer output
- (5) A transistor (2N329A) that was incapable of withstanding the environmental requirements

It has been found that ultraviolet light striking the negatively charged suppressor grid of the electrostatic analyzers in a vacuum produces a significant photoelectron current. Although wavelengths of Lyman-alpha or shorter can cause this phenomenon, the shorter wavelengths are difficult to transmit. Since laboratory control of shorter wavelength ultraviolet is difficult, a more convenient simulation of the amount of harmful ultraviolet

that the experiment will use by looking at the Sun can be made by increasing the amount of Lyman-alpha by a factor of 10 over its normal proportion in the Sun's spectrum.

Two steps were taken to reduce the release of photoelectrons. First, the internal geometry of the analyzer was altered so that the suppressor is more concealed from the light source. It now takes a minimum of three reflections for the light to strike the suppressor. The second step was to blacken the reflecting surfaces with a conducting material. Gold, nickel, and platinum have been tried. Gold black was used on the *RA-1* and *-2* plasma experiments, but it has the disadvantages of being difficult to apply and of rubbing off on contact. Nickel black adheres well but is not nearly black enough. Platinum black is less reflective than gold black by a factor of two but the plating process is not compatible with the magnesium deflection plates. It was decided to use the gold black with a protective cover over the deflection plate opening to reduce the possibility of the blackening rubbing off.

Since unit 1 was the first built, it constituted an engineering model insofar as component layout and wire routing were concerned. Subsequent rerouting of the critical wires in the electrometer compartment either eliminated the quadrature or brought it well within acceptable limits.

The low gain between the modulator and demodulator was investigated thoroughly, although persistent efforts could not restore the gain to the levels obtained with identical circuits on *Ranger*. Drifts occurring in the d-c filtering-amplifier appear at the electrometer input reduced by the d-c gain, G_1 , preceding the filter-amplifier (Fig. 137). To preclude input drifts attributable to demodulator and filter-amplifier drifts, a minimum portion of the electrometer loop gain, which may be expressed as

$$K_{loop} = G_1 G_2$$

must be incorporated into the carrier section (G_1). The d-c carrier gain may be written as

$$G_1 = \eta_c G_{ac} \eta_D$$

where

$$\begin{aligned} \eta_c &= \text{modulation conversion efficiency} \\ G_{ac} &= \text{a-c amplifier gain} \\ \eta_D &= \text{demodulation efficiency} \end{aligned}$$

The carrier gain and electrometer loop gain were then measured over the instrument's specified temperature range (Table 11). Since the d-c filter-amplifier is highly

degenerated and as a result produces a gain G_2 that is quite stable, any variations in loop gain, therefore, reflect changes in the carrier gain G_1 . The test results, as shown in Table 11, reveal an acceptably stable, although somewhat low, loop gain. While working on unit 2, a minor layout change in the carrier amplifier raised the a-c amplifier gain to the desired level. This change was subsequently incorporated into all the units, with similar increases in a-c gain.

Table 11. MR-1 electrometer gains

Temperature °C	Loop gain $G_1 G_2$	Carrier gain G_1
-10	470	14.0
+25	600	17.7
+70	605	17.8

The major problem experienced on unit 1 was a low-frequency ripple on the electrometer output, the magnitude of which was high enough to give poor output resolution for input currents below 10^{-11} amp. In the worst case, the peak-to-peak magnitude of this signal was large enough to register in any of three adjacent quantization levels of the analog-to-digital converted in the DCS. This ripple was found to be the difference, or beat-frequency, produced when the power frequency and the carrier frequency were nearly equal. The 3-db bandwidth of the d-c amplifier is 0.5 cps and any beat-frequency signal of a few cps will be amplified and appear at the output. One solution to this problem was to have the carrier frequency lowered so that the difference frequency would be well out of the pass band of the d-c amplifier. Since the carrier frequency is fixed for any modulator by its mechanical resonance, the power frequency was varied and it was found that when the difference between carrier and power frequency was in excess of 30 cps, no beat-frequency ripple was observed at the electrometer output. Modulators with mechanical resonant frequencies 200 cps lower than that of the power frequency replaced those that were then on the instruments.

Unit 2 also had the problems of quadrature and low a-c gain, but the beat-frequency ripple did not exist because the carrier frequency was 30 cps lower than the power frequency. Quadrature was eliminated as in unit 1 by the rerouting of wires in the electrometer compartment. The a-c gain was raised to the desired level as before, by a layout change in the a-c amplifier. These changes were also made on units 3 and 4.

During subsystem testing of the solar plasma analyzer prior to the first system test at AMR, the GSE was unable to step the programmer on the *MR-1* spacecraft. Upon close examination, it was determined that the regulator transistor in the programmer module had failed. The transistor was later found to have a collector-to-emitter short. This type of failure is usually caused by excessive collector current or excessive collector-to-emitter voltage. Testing of the system produced no current or voltage spikes of sufficient magnitude to cause the regulator transistor to fail. The system was vibration-tested and the collector-to-emitter breakdown voltage of the replacement transistor was found to be substantially below its rated value.

The 2N329A transistor that had failed initially at AMR was analyzed further by the components evaluation group. The 2N329A transistors produced by one manufacturer were determined to be incapable of consistently surviving the environmental requirements. Transistors produced by two other manufacturers were recommended and the suspect units were replaced with the recommended transistors, which were environmentally tested prior to installation. For added protection, a current-limiting resistor and voltage-limiting zener diode were also installed in all units, which were temperature- and vacuum-tested before return to AMR.

f. Performance and accuracy. Each of the four instruments had electrometer output voltage drifts that were less than 100 mv over the 80°C temperature range. The room temperature output variations prior to, and during field operations were small: less than 10 mv. The uncertainty in the measurement of input currents due to these drifts would be 40% of a decade. With the in-flight calibrations and temperature measurements, this uncertainty is reduced to within 5% of a decade. The DCS quantization level, which is about 24 mv with an over-all temperature drift of less than 2 mv, represents an additional uncertainty of about 5% of a decade.

g. Environmental testing and calibration. The environmental tests performed on the instruments were temperature, vibration, and combined temperature-vacuum. The vibration test used the standard *Mariner R* flight-acceptance tape, whereas, the temperature and temperature-vacuum tests were modified versions of the flight-acceptance standard. The temperature extremes were extended to -10°C and +70°C from 0°C and 55°C, and an additional measurement was made at 23°C. The vacuum-temperature test, besides being a flight-acceptance test, also was used to calibrate the instrument

during environmental conditions of vacuum and temperature. A final vacuum calibration was made at AMR prior to the final systems test for both the *MR-1* and -2 flight units.

7. Ionization Chamber

a. Experimental objectives. The primary high-energy radiation-detecting device on *Mariner R* is the integrating ionization chamber. This type of instrument, which measures the total ionization produced per unit time in a unit volume of standard density air, is simple to operate, maintains a constant calibration for extended periods, and also may be accurately calibrated with respect to similar instruments to give an absolute value of the rate of ionization. Because of these characteristics, an ionization chamber measurement has the following properties:

- (1) Intensities measured at different times during a flight of this length may be compared with one another and with other quantities measured during the flight.
- (2) Intensities measured during the *Mariner R* flight may be reliably and absolutely compared with those measured by another spacecraft at a different time.
- (3) The ionization measured in space may be related to ionizations and particle fluxes measured in the Earth's atmosphere and at its surface. This is best accomplished by obtaining absolute values of the ionization in space at the same time measurements are made at Earth. Realization of this objective may increase greatly the scientific value of all cosmic-ray and related data already accumulated on Earth.

The ionization chamber was originally developed for the *Ranger* series. Its accuracy, stability, and proven reliability were the main considerations in its choice for *Mariner R*. Also appealing were the extremely low weight and power requirements of a chamber of this type.

b. Description of experiment. The ionization chamber consists of a spherical volume of argon gas contained by a thin stainless steel wall. The quantity actually measured is the ionization produced in the argon by all naturally occurring (i.e., primary) ionizing particles, and that produced by those secondary particles generated in the spacecraft which can penetrate the chamber wall,

plus the ionization caused by secondary particles generated in the chamber wall and the filling gas. The relationship between the rate of ionization in the argon and the flux of particles passing through the gas may be written

$$I = \sum_i \int_{4\pi} a \Omega(\hat{r}) \int_0^\infty dE J_i(E, \hat{r}) S_i(E) p$$

where I = ionization in ion pairs per cm^3 sec in gas of density p

p = gas density, g/cm^3

E = kinetic energy of particles, Mev

$J_i(E, \hat{r}) dE d\Omega$ = flux of type i particles, both primary and secondary, with energy between E and $E + dE$ arriving from solid angle $d\Omega$, units of particles per cm^2 sec

$S_i(E)$ = ion pairs per g/cm^2 produced by type i particles with energy E

It is assumed here that I does not depend upon location within the chamber. If I is location-dependent, the ionization chamber gives an average value of I in its filling gas

By a suitable calibration of the chamber, the ionization in the volume of argon can be reduced to the ionization in a unit volume of standard air. The effect of the wall can also be accounted for, since it is thin and has spherical symmetry. Because the effect of the secondary particles produced in the bulk of the spacecraft is difficult to calculate, the ion chamber was located as far from the spacecraft bulk as possible. Figure 138 shows the ionization chamber and its companion experiment, the particle flux detector, mounted on the *Mariner R* superstructure. The point of mounting is approximately 15 in. above the spacecraft proper.

Figure 139 shows the ionization chamber and its internal mechanism. The entire working mechanism is made of fused quartz, an excellent electrical insulator. The areas which are shown black in Fig. 139 are covered with a conducting coat of aquadag—a suspension of graphite. When no voltage is applied, the quartz fiber, which has a conducting coat, lies approximately 0.02 in. from the collector. When voltage is applied, the fiber is bent by electrostatic attraction and touches the collector. The fiber then moves back to its rest position away from the collector, since the fiber, collector, and shield can be all at the same potential.

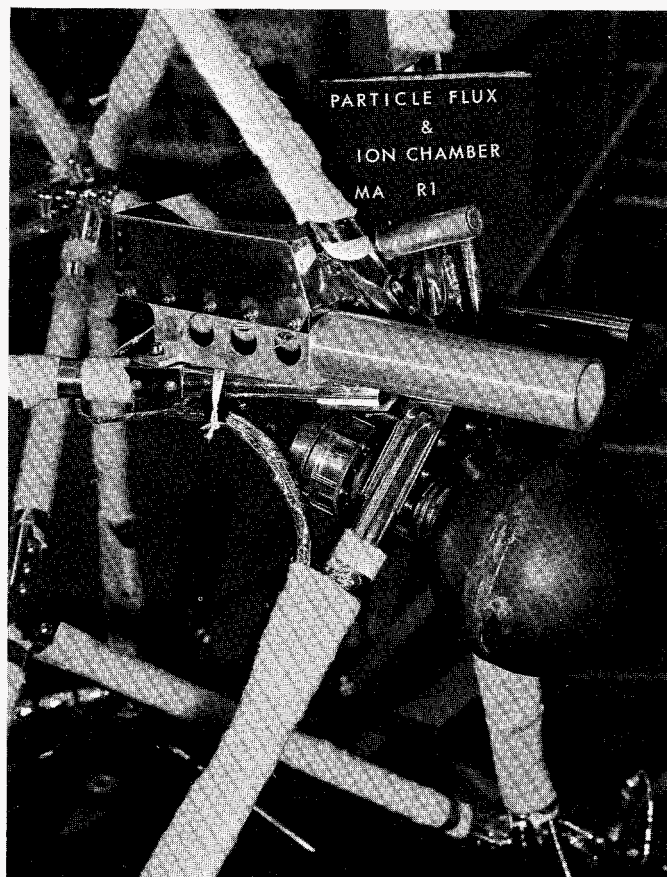


Fig. 138. Ionization chamber and particle flux detector mounted on spacecraft

The electric field between the collector and outer shell is more than adequate to collect all ions formed in the argon. The ionization current, thus formed, gradually discharges the collector until the fiber again touches and recharges it, simultaneously producing a voltage pulse across a load resistor. Hence, the time between pulses varies inversely with the rate of ionization in the argon. A pulse occurs after about 10^{-10} coulombs have been collected from the argon.

c. Instrument performance. The wall thickness determines the minimum energy particle which can reach the filling gas from the outside. The thickness was originally chosen to match that of a companion experiment—an unshielded triple-coincidence proportional counter telescope—flown on early *Rangers*. The performance of the chambers has been such that it was felt unnecessary to change for *Mariner R*. A new experiment—the particle flux detector—was developed for *Mariner* as a companion to the ionization chamber, and its energy thresholds have been matched to those of the ionization chamber.

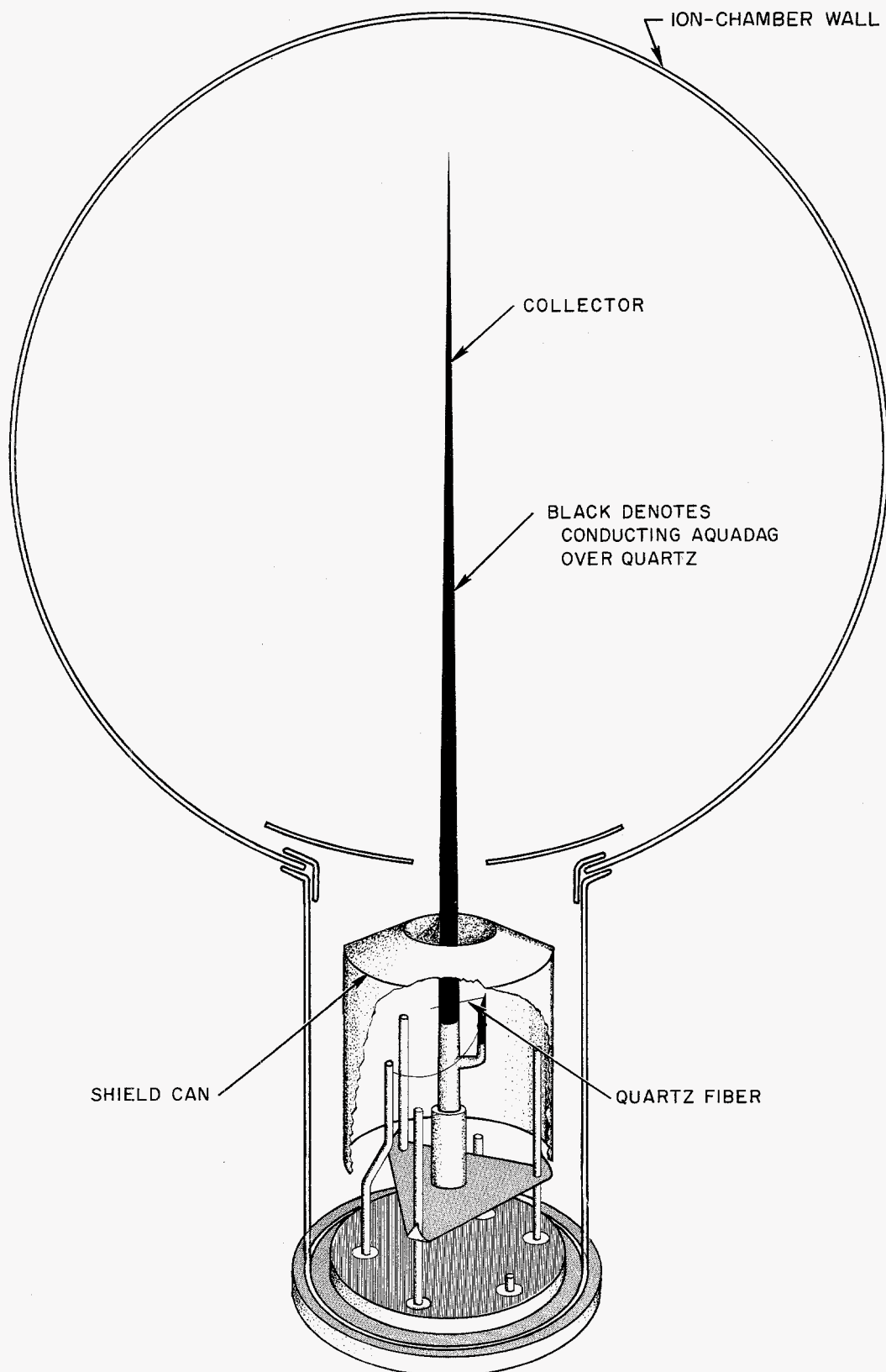


Fig. 139. Cross section of ionization chamber

Table 12. Pulse rate as a function of ionization

Pulse rate	Ionization	
	Ion pairs/cm ² sec atm of std air	Roentgen/hr
1/hr	106	1.8×10^{-4}
1/min	6400	0.011
1 sec	384,000	0.66
100/sec	3.8×10^7	66.4

This thickness is effectively 0.2 g/cm² of stainless steel. The minimum energy particle which can be detected by either these two instruments is 10 Mev for a proton, 40 Mev for an alpha particle, and 0.5 Mev for an electron.

Therefore, by combining the flux measured by the particle flux detector and the rate of ionization measured by the chamber, some information about the average total specific ionization $S(E)$ of the particles may be obtained. Since S is a function of energy, some information is also obtained about the energy of the particles present. The approximate relationship between pulse rate and rate of ionization is shown in Table 12.

As indicated in Table 12, the pulse rate varies linearly with ionization over a wide range. However, the maximum rate at which the chamber can operate is about 100 pulses per sec, and somewhere between 20 and 100 sec⁻¹ the response deviates significantly from linearity. Exact calibrations at high-ionization rates require techniques, the description of which are beyond the scope of this Report.

The ionization, due to galactic cosmic rays, probably lies between 100 and 1500 ion pairs/cm² sec atm. Ionization may rise to 400,000 ion pairs or more during a solar flare event. Corresponding values of interval (1/pulse rate) are 3600, 240, and 0.9 sec, respectively.

d. Fabrication, testing, and calibration. Most of the parts for the ionization chamber were procured locally. All assembly work was performed at JPL by Laboratory personnel. The chamber sphere is composed of two hemispheres, each spun to shape from flat stainless steel stock, and brazed together at their junction. The completed sphere is then brazed to a machined aluminum neck. The neck supports the internal workings of the chamber and also presents a precision outer surface by which the chamber assembly is attached to the spacecraft.

The quartz collector is drawn from commercial optical-grade quartz stock. A quartz rod is heated to the glow

point and then drawn until the rod assumes the proper diameter and taper. After cooling, the desired section of quartz is removed from the rod and immediately coated with aquadag. In this way, the collector is protected from accidental surface abrasions which would impair its mechanical properties. A stainless steel header is attached to the neck extremity, making the sphere and neck a pressure-tight vessel. The chamber capacity is one liter.

After the chamber is pressure-tested, it is baked out to remove impurities and filled with argon to a pressure of four atmospheres gage. Two additional operations are performed—one to the inside surface of the sphere, and one to the outside surface. The inside surface is copper plated (1) to provide a smooth surface free of possible machining marks, and (2) to act as a getter of any oxygen which might accompany the argon during the filling process and which, if present, would affect the ionization rate. The outer surface is dipped into a solution which forms a black oxide film. The resulting surface has the proper thermal characteristics so that the chamber temperature is kept within its operating limits of -50 to +125°C throughout the flight.

Several types of tests are performed on the ionization chamber during fabrication and later during evaluation. The chamber is pressure- and temperature-cycled prior to final assembly. After assembly, the unit is subjected to environmental tests to prove its flight worthiness. The chamber is also leak-checked to ensure that no more than 2×10^{-8} cc of argon are lost per second. With this, the maximum allowable leak rate, the chamber has a useful life of 10^7 pulses—about one pulse every 3 sec for a year.

Each chamber is calibrated using a standard fixture containing radioactive sources of known intensity. In this way, a history of each chamber is maintained so that minor deviations are immediately recognizable. Experience with similar chambers made both at JPL and at CIT over a period of years indicates that they may be calibrated to within $\pm 1\%$ absolutely and $\pm 0.5\%$ relative to one another, and that they may be expected to hold their calibration to within 0.5% for many months.

Only one failure of an ionization chamber occurred during the *Mariner R* program. Serial number 3 became dented, presumably in transit from JPL to AMR, and when examined, was found to be inoperative. A small piece of extraneous aquadag was found inside the sphere which, if lodged between the fiber and conductor, could have caused the failure. Rather than risk using the same

chamber after reassembly, a new chamber was fabricated and certified for flight.

8. Particle Flux Detector

a. Experimental objectives. The particle flux detector was designed to: (1) complement the ionization chamber experiment, the prime cosmic-ray monitor, and (2) detect and measure trapped corpuscular radiation in the vicinity of Venus. While two separate instruments would, under normal conditions, be employed to perform these functions, the shortage of time, weight, and power led to the consolidation of the two experiments.

The ionization chamber measures the total ionization rate per unit volume of gas produced by radiation able to reach the sensitive part of the instrument. This ionization is proportional to the rate of energy dissipation per unit volume of gas but does not depend upon the flux of ionizing radiation in a unique way. It was, therefore, believed useful to measure this flux with an instrument so matched to the ionization chamber that the two respond to particles of the same energies. The simplest device which can measure the required flux is a Geiger-Müller tube. The G-M tube produces a pulse of charge each time an ionizing particle produces one or more ion pairs within its sensitive volume of gas. The pulse rate is, therefore, proportional, within limits, to the omni-

directional flux of ionizing particles which traverse the sensitive volume. By surrounding the G-M tube with a material of the same type and thickness with which the ionization chamber was fabricated, the first objective was realized.

A G-M tube is also ideally suited for the detection and measurement of trapped radiation near Venus. However, for this purpose, the low-energy detection threshold must be considerably lower than that required to match the ionization chamber.

The ionization chamber, and necessarily any G-M tube designated to complement the chamber, responds to radioactive particles whose energies equal or exceed the following values: alpha particles, 40 Mev; protons, 10 Mev; electrons, 0.5 Mev. On the other hand, the G-M tube used to detect trapped radiation responds to radioactive particles with the following characteristics: protons, $E \geq 0.5$ Mev; electrons, $E \geq 40$ Kev.

Although requiring at least two separate G-M tubes, the experimental objectives could be met with a single instrument housing both tube types.

b. Instrumentation. The *Mariner R* particle flux detector is shown in Fig. 48. Except for the thermal shield, the instrument is complete as shown.

The choice of particular components for the particle flux detector evolved from considerations of scientific worth, available hardware, and program constraints. The instrument comprises three G-M tubes (two barrel-sensitive and one end-sensitive), an amplifier for each, and a high-voltage transformer-rectifier power supply. Figure 140 shows the particle flux detector in block diagram form.

The tubes are identical to others tested in conjunction with the *Mariner A* and *Ranger* programs. The high-voltage power supply was adapted from a similar supply developed for *Mariner A*. Each charge-sensitive amplifier presented to the data system a standard low-impedance (330-ohm) 6-v pulse for each ion pair formed in the G-M tube which preceded it. The pulses had rise and fall times of $0.75 \mu\text{sec}$ or less and varied in width from 2 to $30 \mu\text{sec}$. The data system sampled each output for a preset interval of time, from which the number of events per unit time or rate could be derived. Characteristics of the three G-M detectors are shown in Table 13.

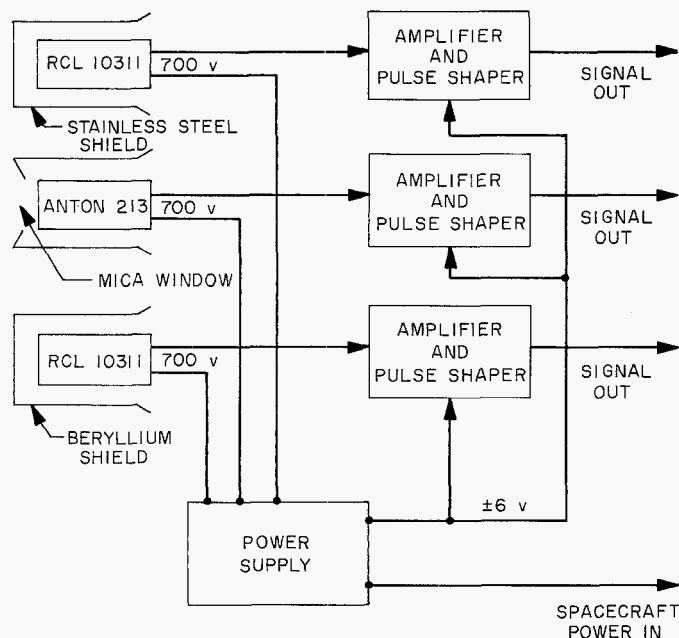


Fig. 140. Particle flux detector, block diagram

Table 13. Characteristics of Mariner R radiation detectors

Detector	Shielding	Corresponding energy for penetration	Geometric factors	Dynamic range of counting rates ^a
G-M tube I RCL 10311	0.03 g/cm ² glass plus 0.16 g/cm ² stainless steel	Protons: $E > 10$ Mev Electrons: $E > 0.5$ Mev	6.9 cm ² omnidirectional	15 to 45,000/sec
G-M tube II Anton 213	1.2 mg/cm ² mica window 0.55 g/cm ² aluminum	Protons: $E > 0.5$ Mev Electrons: $E > 40$ Kev Protons: $E > 20$ Mev Electrons: $E > 1$ Mev	0.1 cm ² sterad unidirectional 0.2 cm ² omnidirectional	0.1 to 30,000/sec
G-M tube III RCL 10311	0.03 g/cm ² glass plus 0.113 g/cm ² beryllium	Protons: $E > 10$ Mev Electrons: $E > 0.5$ Mev	6.9 cm ² omnidirectional	15 to 45,000/sec

^a Minimum rates are those expected from galactic cosmic rays; detector can count slower by a factor of 10^{-2} .
Maximum rates are determined by the instrument responses.

The chassis designed for this instrument served merely to act as a mounting fixture to which the known components were attached. The power supply, being the most massive component, was positioned in the center and the remaining components were arranged symmetrically about the center. The arrangement was not without purpose, of course. To cut the largest number of possible lines of force surrounding Venus, the barrel-sensitive tubes should lie in the planet's equatorial plane, which for this mission could be approximated by the ecliptic plane. This, of course, assumes a Cytherean magnetic field model similar to the Earth's. Additionally, the tube axes should parallel the Venus-probe line. The end-sensitive tube, on the other hand, should be located such that Venus passes through its field of view during encounter. Since the weight allotted for this experiment was only 2 lb, its over-all size and the material from which the chassis could be formed were restricted accordingly. It might be noted that the final flight weight averaged 1.82 lb (a figure originally thought unattainable).

A considerable effort was made to find a location on the spacecraft which afforded the maximum isolation from the main mass, with its attendant shielding and secondary emission problems. The location finally chosen was halfway up the support superstructure for the omni-antenna. This location was actually a compromise dictated by the effect of the spacecraft bulk on the G-M tubes, and the effect of the G-M tubes on the magnetometer, which rode higher in the support structure. These factors, plus those associated with the particular superstructure configuration at the chosen location, formed the set of parameters upon which the instrument configuration was based.

Figure 138 shows in detail the mounting of the particle flux detector to the *Mariner R* spacecraft superstructure.

c. Fabrication, testing, and calibration. All fabrication, testing, and calibration of the particle flux assemblies were performed at JPL. Assembly of each unit required approximately 2 man-wk after all the parts and components were selected for that unit. Component selection time varied according to the particular requirements. For example, since the rejection rate on commercially available G-M tubes was 80%, approximately 10 hr were spent screening tubes to obtain a single flight-quality item.

Each completed unit was environmentally tested to the appropriate specifications. During the tests, the instrument was monitored as required and records kept of all anomalies. Although several discrete failures were experienced, none could be attributed to a basic instrument discrepancy. In each case, the repairs were made on the test rerun to the satisfaction of the cognizant persons. In addition to environmental test, each instrument was calibrated repeatedly and each successive calibration compared against preceding ones. The precision with which these calibrations were repeated was such that variations of $\pm 1\%$ could be detected. In order to determine the response of the tubes to electron bremsstrahlung, the instrument was further calibrated at the State University of Iowa with the aid of Dr. J. A. Van Allen and his staff.

Four particle flux detector assemblies were fabricated for the *Mariner R* program. Ideally, the first completed unit would have been classed a type-approval model and subjected to extreme environmental tests. However, since

the time available for development was short, each unit was treated as a flight unit. After all four were complete and comparative test and calibration data was available, the three most flightworthy units were so classified and the fourth was reclassified as the type-approval unit. It subsequently underwent extensive environmental tests, often at levels far exceeding those recommended, without evidence of failure or even degradation.

9. Data Conditioning System

a. Introduction. The *Mariner R* data conditioning system² performs the functions of data compression, format conversion, pre-programmed instrument control, and adaptive instrument control. It serves as a buffer between CC&S and the scientific instruments to generate sampling subroutines designed to maximize the scientific value of the sampled data. Inherent in the design of the subroutines is the basic need to satisfy both the requirements of the scientific measurements and those of the transmission format of the spacecraft communications system. The 168-bit subframe word for the *Mariner R* science data is, in part, a consequence of this format-matching requirement.

The design of the DCS began with the microwave radiometer requirements, which included a 7-bit analog-to-digital conversion and parity. The data encoder format required a subframe word which was a multiple of 7 bits, the standard word length. In any given system, it is most economical in weight and power to make all words the same bit length. In addition to these considerations, it was desirable to time-share the communications channel between engineering and scientific data on approximately a 50-50 basis. The net effect of these requirements resulted in a 168-bit subframe for science data (21 8-bit words, 24 7-bit words) and a 140-bit interval for engineering data, alternating periodically.

Although the DCS contains approximately 3000 components, numerous steps were taken to ensure the reliable

operation of the device. Because previous experience indicated no catastrophic failures in 40 million component-hr of operation, the principal emphasis of the reliability work was on minimizing the probability of drift failures and primary DCS programmer perturbations by spacecraft noise. Each logic module was subjected to margin tests over the entire temperature range. Minimum acceptable margins were $\pm 12\%$. Approximately 15 million component-hr have been accumulated on a DCS undergoing a life test in the laboratory. No discernible shifts in the margins have been noted. The DCS on the spacecraft has operated for over 1000 hr without a single perturbation of the primary clock.

One problem which occurs early in any program is that of estimating capability and cost. Such an estimate was necessary in September 1961 for the *Mariner R* DCS. The estimated and actual values are listed below.

Item	September 1961 Estimate	September 1962 Actual
Weight	6 lb	6.45 lb
Power	2 w	2.014 w
Transistors	300	330
Components	2500	3000
Construction time	8 wk	9 wk, 1st unit; 8 wk, others
Testing time	4 wk	5 wk, 1st unit; 3 wk, others
Cost	\$178,000	\$176,400

b. DCS design. On the first design iteration, the DCS was planned to handle the microwave radiometer data only. This part of the system is shown enclosed by a dotted line in the DCS functional diagram, Fig. 141. The logical design centered about the 8-stage counter-shift register SR1 to SR8, which serves three purposes:

- (1) Operates as a counter to generate a staircase for the analog-to-digital conversion.
- (2) Provides buffer storage for the conversion until instructed by telemetry to shift the data out.
- (3) Utilizes a gated feedback to generate a PN sequence for data framing.

The principal reason for this type of design is to minimize the number of required components.

The logic outside the dotted line was added to accommodate the experiments other than the microwave

²The name of the device, it would seem, should be descriptive of the functions it performs. Since the *Mariner R* data device not only processes the data from the instruments, but also uses the data to control the instruments, it is, in a sense, an adaptive device. Hence, it would be more proper to call it a data automation system than a data conditioning system. However, the misnomer was placed on the system early in the program and, in the interest of preserving continuity for cross-reference purposes, the device will be called the data conditioning system or DCS in this discussion.

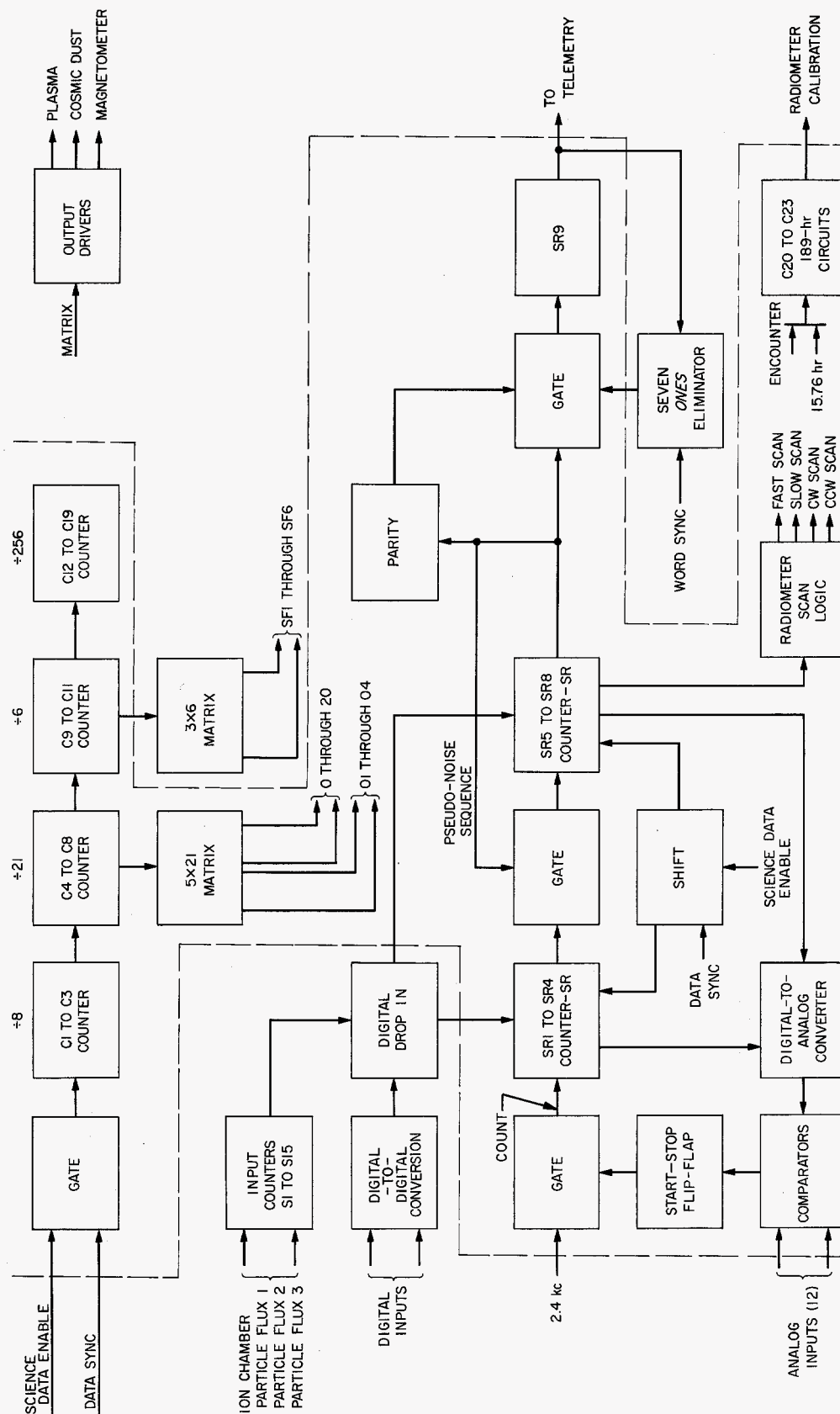


Fig. 141. DCS block diagram

radiometer. The plasma, infrared radiometer, and magnetometer used the microwave radiometer A/D converter on a time-shared basis. The particle and ion chamber experiments required a D/D converter. The over-all dynamic range of the D/D converter is from 1/1000 to 20,000 pulse/sec. For any given experiment, the range is about 10^5 . Again every effort was made to minimize the number of components. The D/D converter consisted of 7- and 8-bit scalers with gated event on clock inputs. The digital inputs operate on a time-shared basis and the D/D converter output operates in turn on a time-shared basis with the analog measurements.

The *seven-ones* eliminator was added as an aid to the data encoder. The data encoder sync word is seven consecutive ones between data encoder word sync markers. The DE designers desired to eliminate this condition from occurring in the science data because an ambiguous sync might have been generated.

The DCS programmer consists of 23 binary stages and two matrices, one for the main format and the other for subcommutated logical functions. Bit sync from the data encoder is used as the primary clock input. The bit sync is gated with an enable-signal, which only allows science data to be transmitted for 168 out of 308 bits. The remaining 140 bits consist of engineering data handled by the data encoder. The science data clock is only actuated during the science data transmission period.

The radiometer scan control was designed to locate Venus and then maintain a slow scan of the planet by using the microwave radiometer data. The digital form of the radiometer data is compared with fixed digital numbers. The outcome of the comparison switches the scan rate from 1 to 0.1 deg/sec when the voltage exceeds a preset value. If the radiometer then drops below a second threshold, the scan reverses direction. When the signal is lost for longer than about 160 sec, the scan reverts to the high rate. In the event the scan reaches its limit, switches actuate the scan reversal.

c. Design problems. The foremost problem of any science data-handling device is to perform a sampling or measurement which is as advantageous to the scientific mission as possible, within the weight, power, and telemetry constraints of the system. To be advantageous, the sampling and measurement accuracy or resolution, or both, must be compatible with the scientific sensor. Any design which reduces the measurement uncertainty increases the value of the scientific mission. Obviously, operational reliability is a strong factor, but no stronger

than the reduction of measurement uncertainty. For example, a measurement of 1% accuracy might be made with only a 0.8 reliability; whereas, it could also be made with a 10% accuracy and virtually a unity reliability. But the latter measurement may be absolutely worthless from a scientific point of view; therefore, the problem is to achieve a proper balance between operational reliability and a measurement of scientific significance.

The sampling and accuracy requirements of the experiments generally establish the data word lengths and spacings. The problem then becomes one of generating a format that satisfies the requirements of all the experiments, within the spacecraft design constraints. Some examples of these requirements for the *Mariner R* DCS follow:

- (1) 8-bit A/D conversion, magnetometer, plasma
- (2) Uniform intervals between samples, plasma
- (3) Magnetometer (X, Y, Z axis) samples as close together as possible
- (4) Infrared and temperature samples close together
- (5) A subframe marking sequence at the beginning of each subframe

The final format is as follows:

- (1) *Word 1 PN sequence.* Word 1 contains the first half of the PN sequence. The binary output is 00001110; octal output is 016.
- (2) *Word 2 PN sequence.* Word 2 contains the second half of the PN sequence plus parity bit. Binary output is 11001010; octal output is 145.
- (3) *Word 3 plasma analog-to-digital conversion.* The output code depends on the analog input applied. Representative codes are as follows:

Input	Binary	Octal
30 mv	00000001	001
1 v	00101011	053
3 v	01111111	177
5 v	11010101	325
6.1 v	00000000	000

Each voltage step is equivalent to 23.5 mv. An input of 6 v should result in a reading of 000.

- (4) *Word 4 ion chamber interval count.* If the ion chamber data input is grounded, the binary reading is 001010P (where P represents the parity digit); octal reading is 025 or 026, depending on phasing of word sync pulse. If pulses are applied to the ion chamber data input, a correspondingly lower reading applies.
- (5) *Word 5 subcommutated digital-to-digital conversion.* Word 5 consists of a read-out of the accumulated count in flip-flops S1 through S8. The count in this register depends on the subframe and main frame count, with the exception of SF1, which always reads out the first 8 bits of a PN sequence. SF2 through SF6 read out the accumulated counts of digital inputs particle flux I, II, III, and ion chamber.
- (6) *Word 6 particle flux I, II, III, ion chamber even count, digital-to-digital conversion.* Word 6 consists of a read-out of the accumulated count in flip-flops S9 through S15. The count in this register accumulates in SF2, SF4, and SF5 of the even main frame counts; the remainder of the time zeroes are read. SF1 always reads out the last 7 bits of the PN sequence, plus the parity bit. The last bit of word 6 is always a parity bit.
- (7) *Word 7 magnetometer X analog-to-digital conversion.* The output code depends on the analog input applied, and is equivalent to the readings described in word 3.
- (8) *Word 8 radiometer 1 analog-to-digital conversion.* The output code depends on the analog voltage applied to the input. The least significant digit of this number is a parity bit, which means that the following listing applies:
- | Input | Binary | Octal |
|--------|----------|-------|
| 30 mv | 0000000P | 000 |
| 1 v | 0010101P | 025 |
| 3.01 v | 0111111P | 077 |
| 5 v | 1101010P | 152 |
| 6.1 v | 0000000P | 000 |
- Each voltage step is equivalent to 47 mv where P is the parity digit.
- (9) *Word 9 magnetometer Y analog-to-digital conversion.* The output code depends on the voltage applied and is identical to that described in word 3.
- (10) *Word 10 infrared housing analog-to-digital conversion.* The output code is dependent on the input signal and is identical to that described in word 8.
- (11) *Word 11 magnetometer Z analog-to-digital conversion.* The output code is dependent on the input signal applied and is identical to that described in word 3.
- (12) *Word 12 radiometer scan position analog-to-digital conversion.* The output code is dependent on the input voltage and is identical to that described in word 8.
- (13) *Word 13 frame count digital-to-digital conversion.* Word 13 is the frame count and corresponds to the output of flip-flops C12 through C19. When power is applied for the first 6 subframes, word 13 consists of the octal read-out 000. For the next 6 subframes, the output consists of 001, etc.
- (14) *Word 14 power sensing, digital-to-digital conversion.* Only one power sensing input is applied to the DCS. The output is binary 0000001P and the octal notation is 001.
- (15) *Word 15 cosmic dust-magnetometer scale X, Y, Z digital-to-digital conversion.* Word 15 consists of a read-out of the magnetometer X, Y, Z, B2, A1, A2, and B1 scale factors, as well as the cosmic dust experiment.
- (16) *Word 16 magnetometer temperature analog-to-digital conversion.* Outputs are dependent on input voltage and are identical to those described in word 8.
- (17) *Word 17 infrared radiometer 1 analog-to-digital conversion.* Output is dependent on input voltage and is identical to that described in word 8.
- (18) *Word 18 radiometer 2 analog-to-digital conversion.* The output is dependent on input voltage and is identical to that described in word 8.
- (19) *Word 19 infrared radiometer 2 analog-to-digital conversion.* The output code is dependent on input voltage and is identical to that described in word 3.
- (20) *Word 20 infrared calibrate temperature analog-to-digital conversion.* The output code is a function of input voltage and is identical to that described in word 8.

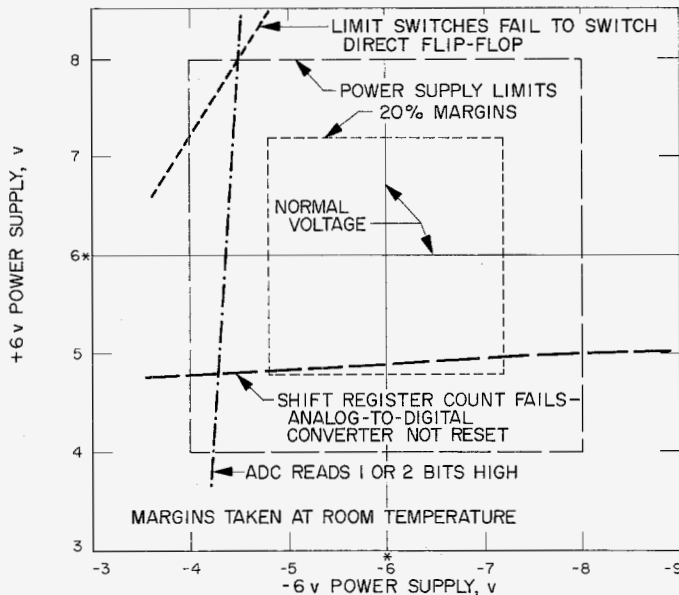


Fig. 142. Margin diagram

- (21) *Word 21 plasma analog-to-digital conversion.* The output code is a function of input voltage and is identical to that described in word 3.

All the words are 8 bits in length and every 16th bit is a single-error parity. Parity is added to indicate the presence of any single error in 15 bits of data which may occur at any point in the spacecraft-to-ground-computer communications link. During the cruise or interplanetary mode of operation, the parity check is less useful than it is at encounter because there are an abundance of data points available for comparison and nearly all errors could be found without parity. However, at the planet, the number of data points is relatively small; therefore, it is important to know whether or not each datum is valid.

Once the format was established, the designing of the A/D converter output buffer and DCS programmer was relatively straightforward. Emphasis was placed on long-term operational reliability and spacecraft noise protection. These problems are concerned with margin-power trade-offs. For example, the long-term reliability is a function of the margin available for the drift of any one component parameter or the accumulation of parameter drifts in any one logical element. A typical static margin diagram for the entire system is shown in Fig. 142. Nominally, the operational point is set as near the center of the operational area as possible. It is possible to increase the operational area by increasing the power consumed.

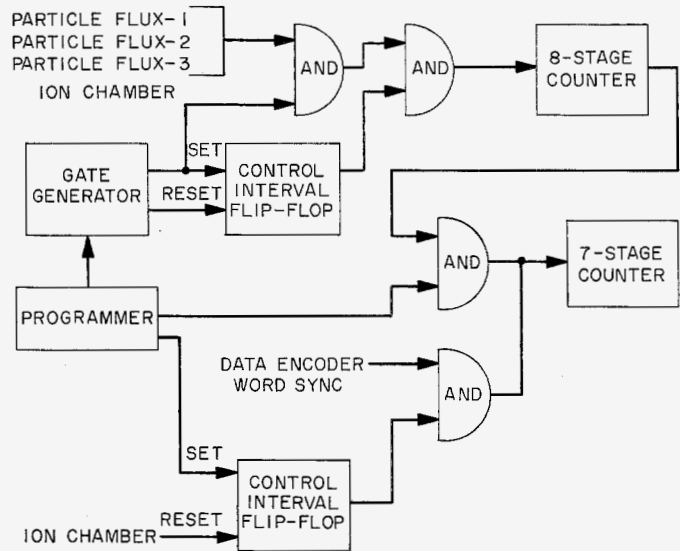


Fig. 143. Digital-to-digital converter

This trade-off is accepted for any logical element which must handle all the data.

Whereas the operational margins are called static margins, the noise margins are dynamic. The diode and transistor capacities, for example, do not affect the static margins, but play an important part in dynamic margins. Again, the increase in power consumption per logical element can increase the noise margins. This was done for the primary DCS programmer and 8-bit counter shift register. Many of the detailed circuit configurations of the DCS can be found in the DCS Manual.

The digital-to-digital converter presented one of the more difficult design problems. The objective of the design was to provide a minimum of 100 counts, events, or clock, for any event rate between 20,000 events/sec to one event per 1000 sec over a 1000-sec interval. It was also necessary to minimize the number of components required to perform the D/D conversion. The basic approach was to use a 7- and an 8-bit scaler, separately or in series, on a time-sharing basis and gate the incoming digital signals. A functional diagram of the converter is shown in Fig. 143. Particle flux sensors 1, 2, and 3 utilized 0.82- and 9.6-sec gates. Time between ion chamber events was measured for low-event rates, a 216-sec gate was used for intermediate rates, and a 0.82-sec gate for high rates. A plot of the number of counts available over a 1000-sec interval vs event rate is given in Fig. 144.

The scan control logic functions shown in Fig. 145 was designed to control the spatial scan rate and direction in

UNCLASSIFIED

JPL TECHNICAL REPORT NO. 32-353

accordance with the outcome of digital comparisons made with the radiometer data. Two problems occurred in this logic, one related to the choice of action at the decision levels, and the other concerning the high switching transients on the scan-limit switch lines. The two decision levels are octal 040 and 060, which correspond to 1.5 v and 2.25 v, respectively.

It was decided to go into slow scan when either radiometer output exceeded 1.5 v, and reverse scan when both radiometer outputs went below 1.5 v after either one had gone above 2.25 v. The reason for this choice was to virtually guarantee the scan system would go into slow scan if either radiometer operated normally and the

other failed in the below-1.5-v condition. It was fully realized that a base line shift in either radiometer to the above-1.5-v condition would result in slow scan throughout the encounter mode. This problem could have been completely circumvented with a base-line storage and reference system if there had been an additional pound of weight available.

The scan limit switches were the momentary-closure type and the wires connecting them to the DCS were unterminated at the switch end. Therefore, they acted as antennas and would pick up the noise transients, especially the fast-slow scan transient, thus affecting the control logic. This problem was corrected by adding line capacity isolation and transient filters.

A similar problem occurred in the 189-hr calibrate sequence counter. Originally, this counter was to be driven by the 16.7-hr signal from the CC&S. However, the CC&S signal consisted of a contact closure or opening. It appeared to be too difficult to isolate the noise in the contact-open condition. Therefore, the 15.6-hr signal generated within the DCS was used. In order to test the sequence in a reasonable length of time, GSE connections were made to the counter so that the 15.6-hr pulses could be injected at a higher rate. Although a final analysis of the problem is not complete, it is believed that this external connection is the main cause of the noise disturb-

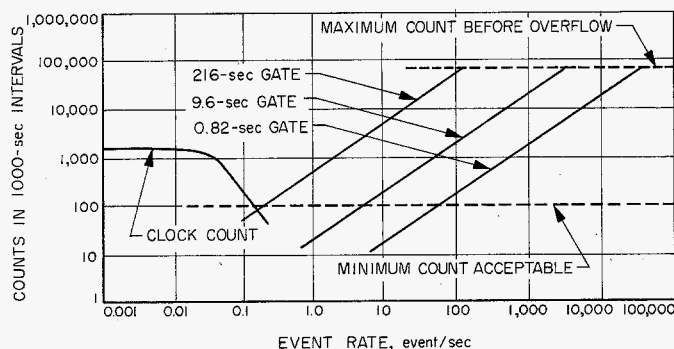


Fig. 144. Accumulated counts vs event rate, 1000-sec interval

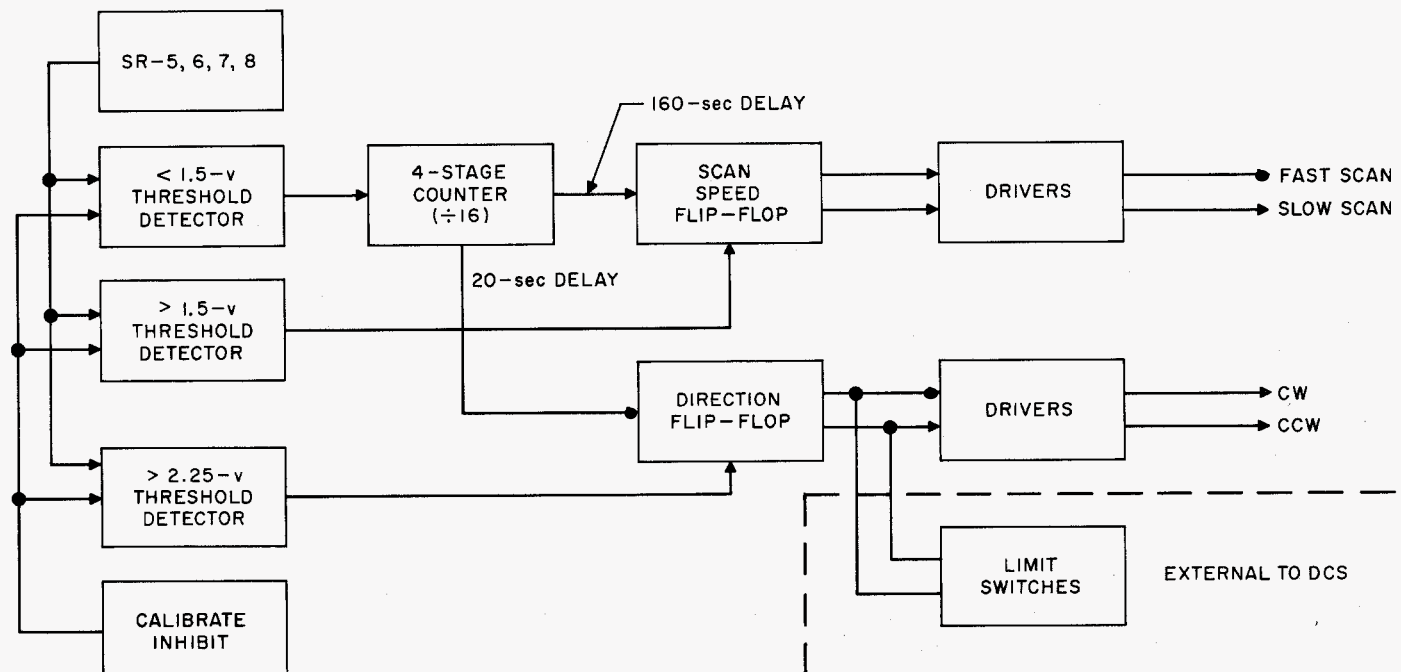


Fig. 145. Spatial scan control

UNCLASSIFIED

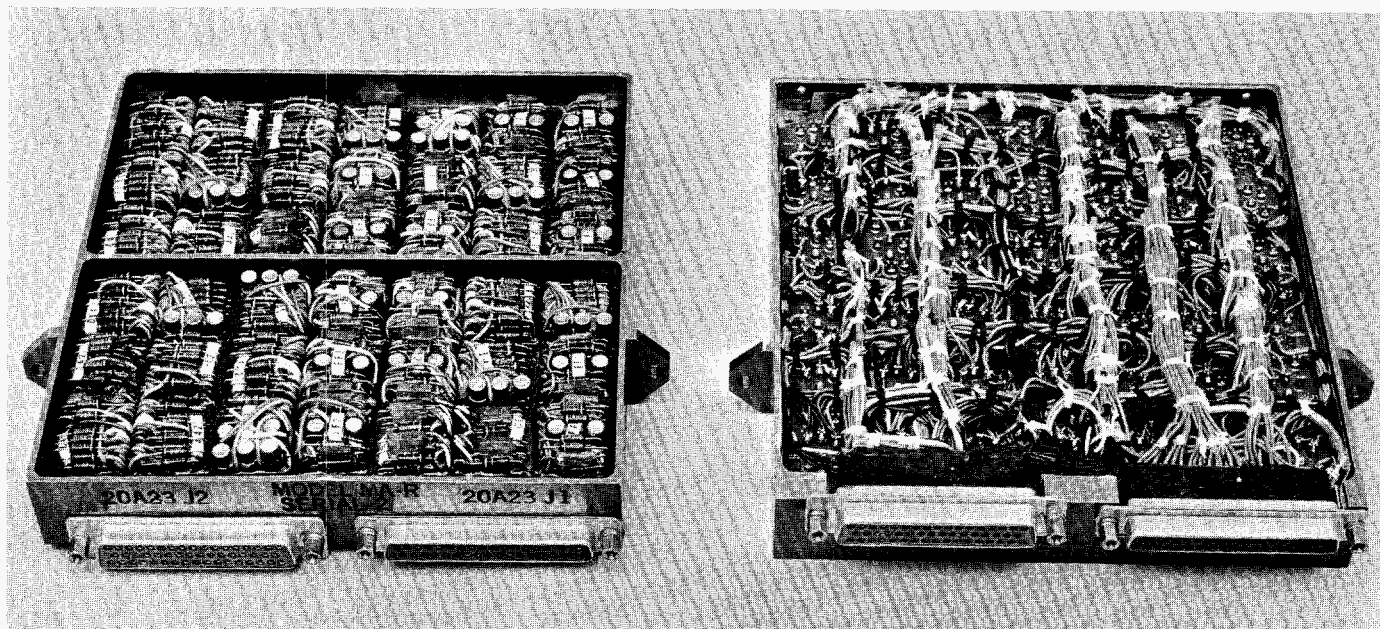


Fig. 146. Mariner R DCS casting assembly

ances in this counter during science-radiometer power switching.

d. Packaging design and problems. The general philosophy was to package the logical elements in modules, and leave the module interconnections as pigtails to reduce the number of soldered connections required. In mounting the modules on a standard 1- × 6- × 6-in. casting, the same amount of space was allocated for modules and interconnections. All modules were located on one side of the casting web and all interconnections on the other. The module pigtails were put through slots in the web. This type of packaging combined the best features of the RA-1 and -2 and the Mariner A designs. The interconnection wiring was readily accessible and logical changes to accommodate changes in the science subsystem could readily be made. A typical casting is shown in Fig. 146.

Some problems were experienced with the cable bundling and connector potting. In order to make full use of standard construction techniques, only three of four types of modules were used throughout the system. Consequently, there were numerous pigtails which were bundled in the cabling, but represented unused logic. Although the availability of this unused logic proved very helpful throughout the program, it also caused oversized cabling and congestion in some areas. Hopefully, this situation can be corrected in future designs.

The connector potting became a problem when a substitute compound was used which flowed into the female connectors and created a pin-retention problem. Actually, the floating section of the connector should not be potted or restricted in any manner. However, it is necessary to pot the soldered connections to achieve adequate connection reliability. As a result of these conflicting requirements, it may be necessary to develop a new type of connector.

The module package is a cordwood-type construction, but all component leads are connected to a single printed board. This choice resulted from the difficulties experienced with the RA-1 and -2 module where the components were inserted between two printed boards. It was found that elevated temperatures and vibration would cause strains in the diodes and result in malfunctions. This problem was circumvented in the Mariner R modules by bending the component leads in the shape of a U and connecting to the single printed circuit, as shown in Fig. 147. The average packing density of DCS components is 17 components per square inch. The DCS is shown in Fig. 148 packaged on four 1- × 6- × 6-in. castings and one 1- × 6- × 4-in. casting.

e. Summary. The Mariner R DCS was designed to handle the scientific data in a manner that would maximize the scientific value of the data, and implemented within the weight, power, schedule, and telemetry con-

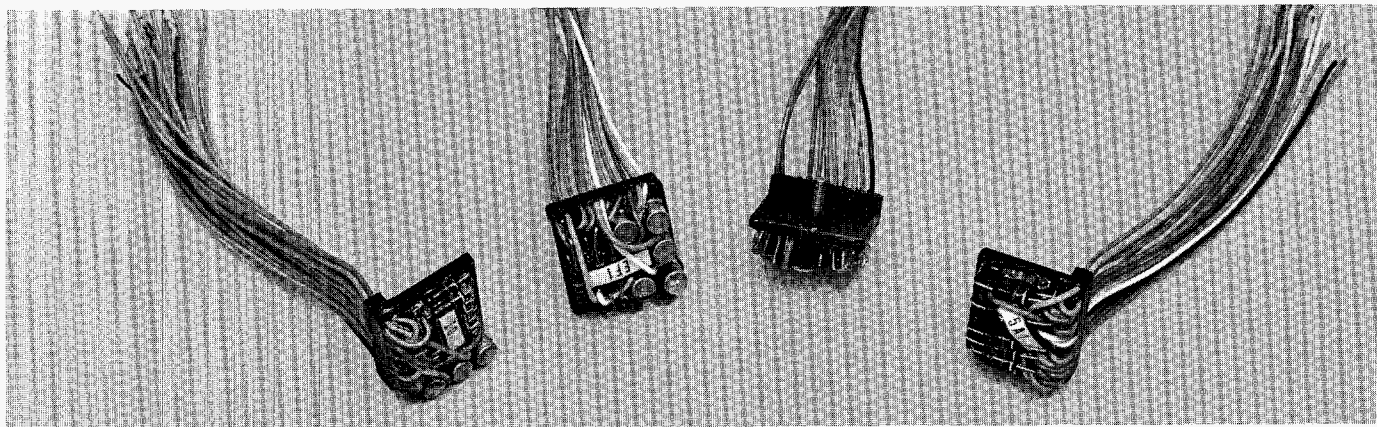


Fig. 147. Typical module assemblies

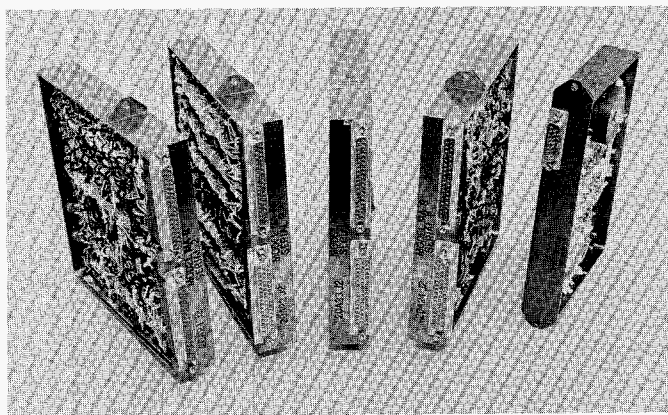


Fig. 148. Data-conditioning system

straints. The major DCS problems in chronological order were:

- (1) Format design
- (2) Minimizing logical function duplication
- (3) Large dynamic range digital-to-digital conversion design
- (4) Spacecraft noise protection
- (5) High-density component packaging
- (6) Accessibility for logical interconnection changes

Reliable long-term operation was achieved by maximizing the margin area within the power restriction and providing 1- to 2-v noise protection in all critical areas. In a laboratory life test currently in progress, the DCS has reached 4200 hr of operation with no failure or margin degradation. The flight unit has accumulated over 1000 hr of operation with no perturbations of the primary DCS programmer by spacecraft noise.

10. Ground Support Equipment

a. General. The ground support equipment for *Mariner R* scientific instrumentation, when operated in conjunction with appropriate stimuli applied to the instrument, provides an over-all check on instrument performance. Both visual monitoring of outputs and a hard-copy printed record of test results are provided. In addition, the GSE monitors and prints out on paper tape a record of all power supply voltages present in the scientific instrumentation subsystems.

The instrument stimuli are applied to the sensor inputs as nearly as possible in the same manner that stimuli are received during actual operation. However, for certain experiments, it is not feasible to generate controlled external fields or insert particles into the system. In this case, a downstream point as close as possible to the sensor has been utilized for test signal injections.

In general, the purpose of the GSE checkout procedure is to establish a *go, no-go* condition of the experiment rather than to check the absolute calibration of each experiment in terms of the physical units being measured, such as field or particle energy. Such absolute calibrations will have been performed by the individual scientific experiment groups prior to installation on the vehicle.

Physically, the GSE consists of three equipment racks (Fig. 149). Much of the test equipment in the racks is utilized for more than one experiment. The necessary flexibility of interconnection is obtained by use of interchangeable patchboards. Separate boards are inserted for each applicable experiment. The GSE largely utilizes commercial-type equipment.

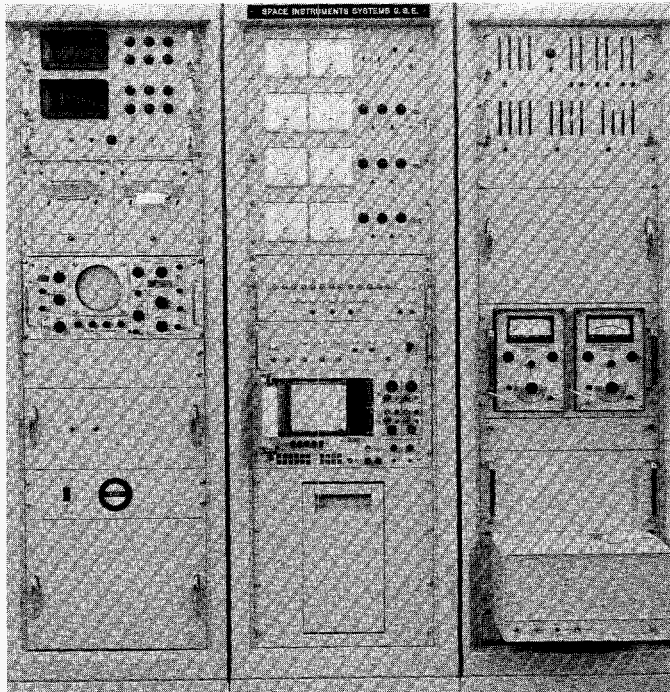


Fig. 149. Scientific ground support equipment

b. Stimulus and response. The following stimuli are applied to the various instruments, with responses as indicated:

(1) *Microwave radiometer*

Stimulus: An internal flight calibration signal, the microwave test bench, or a portable noise generator.

Read-out: Two analog voltages that are recorded on a Sanborn tape recorder located in rack 20A3; and/or scan mode is fast or slow.

(2) *Infrared radiometer*

Stimulus: A cold source located at the front of the sensor.

Read-out: A visual indication on rack 20A2 in the form of three analog voltages.

(3) *Particle flux and ion chamber experiments*

Stimulus: A cesium 137 source is placed on the spacecraft.

Read-out: A visual indication at a counter and a printed tape output of the counter readings is obtained from rack 20A4.

(4) *Solar plasma*

Stimulus: A special test box is fitted on top of the hex case. A current injection probe contacts the collector plate, which constitutes the electrometer

input. A stepping switch controls the current injection via a known voltage source into a precision divider network. Light indicators on rack 20A1 show the current step being injected.

Read-out: (1) the electrometer output appears on the digital voltmeter located in rack 20A2.

(2) The voltmeter output is printed out on the 20A2 printer.

(3) Both the demodulator and electrometer outputs can be displayed on the oscilloscope in rack 20A2.

(5) *Magnetometer*

Stimulus: (1) An in-flight calibrate command signal.

(2) Calibrated fields of 30 and 300 γ .

Read-out: (1) An analog indication on rack 20A3.

(6) *Micrometeorite*

Stimulus: Trigger and reset pulses from 20A3.

Read-out: A visual indication on 20A3.

c. Description of equipment. A block diagram showing the physical location of each of the components that make up the racks is shown in Fig. 150. The equipment was designed to be as simple as possible, with adequate performance of the necessary test functions. All the returns are floating at the GSE and are tied together at a common point at the spacecraft to prevent ground loop problems.

A brief description of the components in the scientific GSE follows:

(1) *Digital voltmeters (NLS model V34A).* The digital voltmeter provides a means of monitoring voltages from the spacecraft. These voltages may be either in the form of a signal or a B+ measurement from any individual instrument.

(2) *DVM print control and NLS printer (model 155).* These two units are used in conjunction with the NLS digital voltmeter. Any information presented to the digital voltmeter can be printed out on the printer. The DVM print control provides a means by which a print-out command is presented.

(3) *Oscilloscope (Tektronics model RM15).* The main function of this instrument is to monitor the demodulated output of the plasma experiment. However, any information presented to the GSE from the spacecraft can be patched in through the patch panel to the scope. It is an aid for troubleshooting.

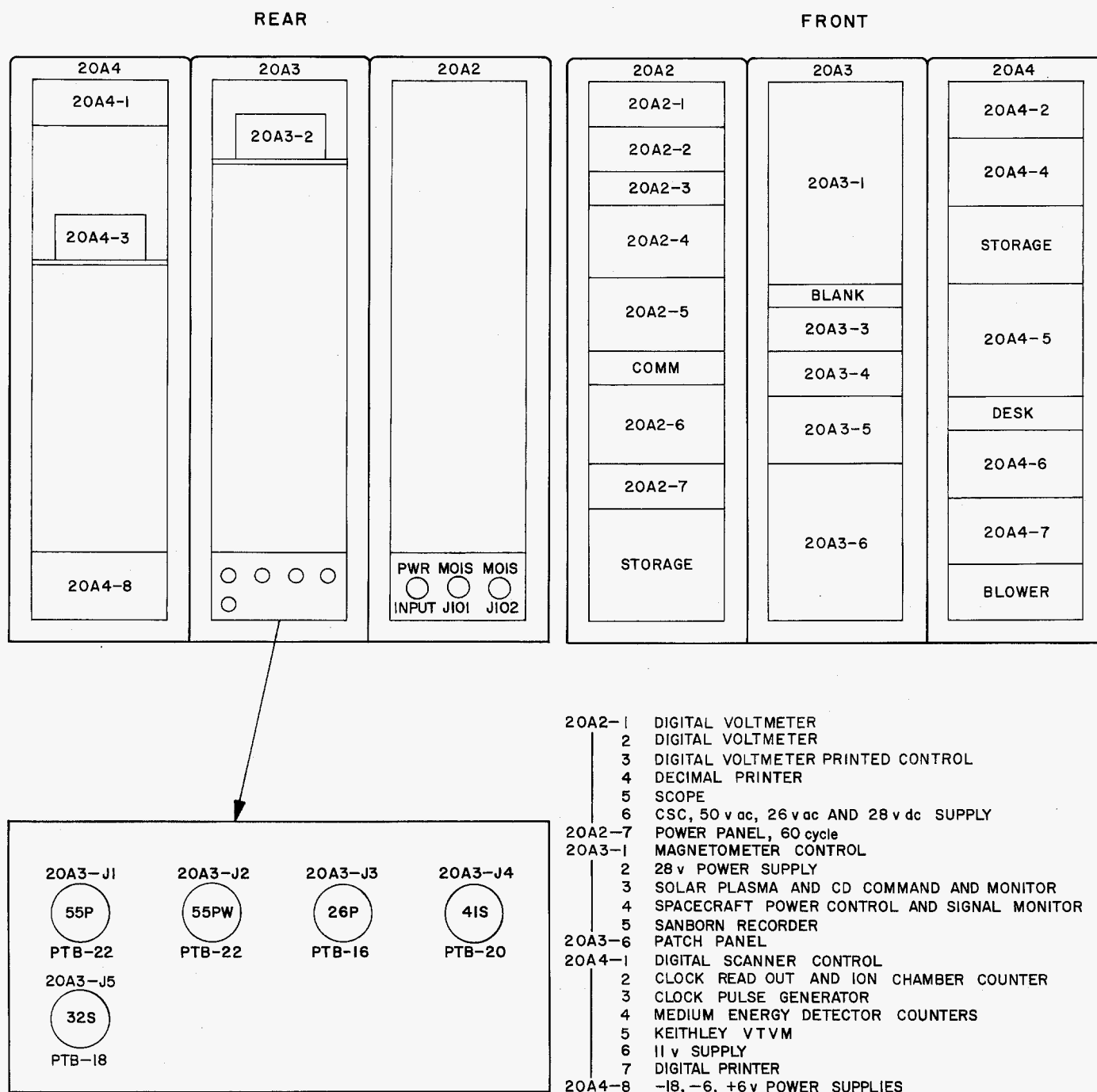


Fig. 150. Scientific GSE rack layout

- (4) *Power supply (Consolidated Systems Corp.).* This unit supplies 50-v a-c 2.4-kc square-wave power to the spacecraft and is only used during a sub-system test when the main spacecraft power is not available.
- (5) *Power panel.* This panel controls the 115-v a-c, 60-cps power to the GSE equipment.
- (6) *Magnetometer control (Marshall Laboratories).* The magnetometer control is used to check out the magnetometer in a *go, no-go* manner. The basic functions of the control unit are:
- (a) To generate known magnetic fields by passing stable currents through the magnetometer sensor auxiliary windings

- (b) To simulate command signals
 - (c) To monitor all pertinent output signals
 - (7) *28-v power supply (Dressen Barnes model 21-103)*. This 28-v supply furnishes power to the rotary stepping switch located in the solar plasma test fixture on the spacecraft.
 - (8) *Solar plasma and cosmic dust command and monitor (JPL)*. This chassis performs the following functions:
 - (a) Monitors the position of the plasma sweep amplifier.
 - (b) Gives an indication of the current being injected into the electrometer of the solar plasma.
 - (c) Provides the sweep amplifier stepping pulses and reset pulses.
 - (d) Monitors the binary outputs of the cosmic dust experiment.
 - (e) Provides the triggering and reset pulses to the cosmic dust experiment.
 - (9) *Spacecraft power control and signal monitor (JPL)*. This unit performs the following functions:
 - (a) Provides all the commands to the power switching unit in the spacecraft, which in turn may turn on power to the various instruments. This portion of the chassis is only used in a subsystem test when spacecraft commands, which normally come from other areas such as CC&S, are not available.
 - (b) All spacecraft voltages or signals are brought back to this chassis and tied to a rotary switch. By selecting the proper position of the switch, any signal or voltage is presented to the digital voltmeter.
 - (10) *Two-channel recorder (Sanborn model 297)*. The recorder provides a 2-channel recording of the analog voltage output from the microwave radiometer or the infrared radiometer.
 - (11) *Patch panel (Mac panel model 911)*. The patch panel is used to route all the command functions from the GSE and all the monitoring functions from the spacecraft. In this manner, any function that exists in the GSE or is presented to the GSE can be patched in to the digital voltmeter, the Sanborn recorder, or the oscilloscope. By changing wires on the patchboard, the test procedure for an experiment can be changed readily.
 - (12) *Clock read-out and ion chamber counter (Radiaphone Corp.)*. This chassis contains a clock, a counter, and timing circuits. The counter is used to count the ion chamber pulses and the timing circuits are used to shift or clear the counter of these pulses at some predetermined time.
 - (13) *Medium energy detector counter (Radiaphone Corp.)*. This chassis monitors the counts that return from the particle flux experiment. It consists of three counters.
 - (14) *Digital scanner control (Radiaphone Corp.)*. This chassis reads, stores, and commands print-out of the information that is in the ion chamber or the particle flux counters. The scanner is from the RA-1 design and is capable of handling 11 digital signals.
 - (15) *Clock pulse generator (Radiaphone Corp.)*. This chassis is a 2400-to-1 divider. It takes the 2.4 kc from the CSC power supply and divides it down to 1 pulse per sec. The 1 pps is used to run the clock and also is used as a time base in conjunction with the digital scanner control to read-out the information at the appropriate time.
 - (16) *VTVM (Keithley model 610A)*. This voltmeter is used to monitor the sweep voltages that exist on the solar plasma analyzer electrodes.
 - (17) *Power supply (Radiaphone Corp., Dressen Barnes model 22-213)*. This chassis supplies 11-v dc to the ion chamber counter and the medium energy detector counter.
 - (18) *Printer (Computer Measurement Co. model 400CT)*. This instrument prints out the digital information that exists in the ion chamber counter and the particle flux counters via the digital scanner.
 - (19) *Power supply (Radiaphone Corp., Dressen Barnes models 22-213, 20-6, 22-111)*. This chassis generates the -18, -6, and +6-v dc necessary to power the digital scanner control.
- d. Miscellaneous test equipment*
- Microwave radiometer test bench.* The radiometer test bench (Fig. 151) was built by Consolidated Systems Corporation, Monrovia, Calif., as a piece of test equipment to

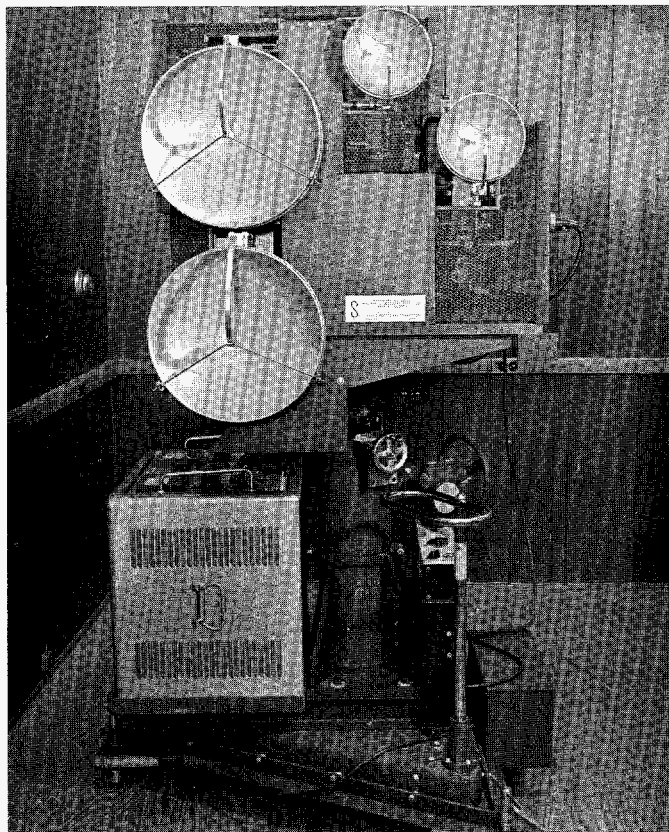


Fig. 151. Microwave radiometer test bench

check out the radiometer's mechanical and electrical alignment. Due to changing circumstances, the test bench is no longer required to mechanically align the radiometer; however, it is still used on the r-f range to check out the electrical characteristics of the radiometer.

The radiometer test bench, as applied to *Mariner R*, generates CW r-f energy at 15.8 and 22.2 kmc. By providing CW r-f energy at the two discrete frequencies and at a known power level, the radiometer is stimulated in the same manner as it would be in actual operation. Normally, both frequencies operate at a power level of -40 dbm down from the 1 mw, and the minimum distance between the test bench and the radiometer is 50 ft. The area between the instrument and the test bench is kept clear in order to prevent reflections. Figure 152 is a block diagram of the radiometer test bench.

(1) *Mechanical alignment-boresighting.* To obtain the optimum power transfer between the radiometer test bench and the radiometer antenna, it is necessary to align the axes of the antenna. This operation is accomplished by means of an optical telescope mounted on the test

bench and an alignment mirror pointed on the radiometer antenna. The optics of the telescope are oriented so that they are perpendicular to the electrical axis of the transmitting antenna. The mirror mounted on the radiometer antenna is also perpendicular to the electrical axis of the radiometer antenna. The result is that there is no parallax involved in boresighting. The dimension between the telescope and the 22.2-kmc antenna is the same as that between the alignment mirror center and the radiometer antenna, so that boresighting is accomplished by sighting through the telescope at the mirror and aligning the telescope crosshairs with the reflected image of the boresight telescope (Fig. 153).

(2) *Description of radiometer test bench.* R-F energy at a frequency of 15.8 kmc is generated by an X-12 Varian klystron. The X-12 is a micrometer-tuned reflex klystron with a frequency range of 12.4 to 18.0 kmc and is capable of an average power output of 150 mw. A semiprecision attenuator (FXR model X155A) is mounted on the klystron output and has a range of approximately 0 to 20 db. The frequency at which the klystron is oscillating is measured by the tunable cavity. When the tunable cavity is tuned to the frequency at which the klystron is operating, microwave energy is absorbed, thereby reducing the amount of energy passing into the crystal detector, and enabling a reading of frequency from the cavity by tuning for a dip on the 50 μ amp crystal current meter. The tunable short is a stub which is adjusted through the use of a micrometer. By tuning the device, the VSWR in the crossguide coupler may be optimized, thereby producing adequate crystal current.

The 10-db directional coupler is inserted in the waveguide so that a known energy level with respect to the energy in the main waveguide can be injected into the thermistor. The directional coupler delivers energy 10 db down to the thermistor. The FXR semiprecision attenuator is adjusted so that a power level of 0.1 mw is established at the thermistor. The thermistor unit contains two thermistor elements selected for matched characteristics. One thermistor is positioned in the r-f field such that its impedance will change proportionally to the amount of r-f power applied. The second thermistor is positioned adjacent to the r-f thermistor but outside the r-f field; this thermistor reacts to temperature changes only. Both thermistors are in a leg of a bridge which is part of the power meter (Fig. 154). Another leg of the temperature compensating bridge is contained in the thermistor mount and consists of a fixed resistor and an adjustable precision resistor. The setting of the adjust-

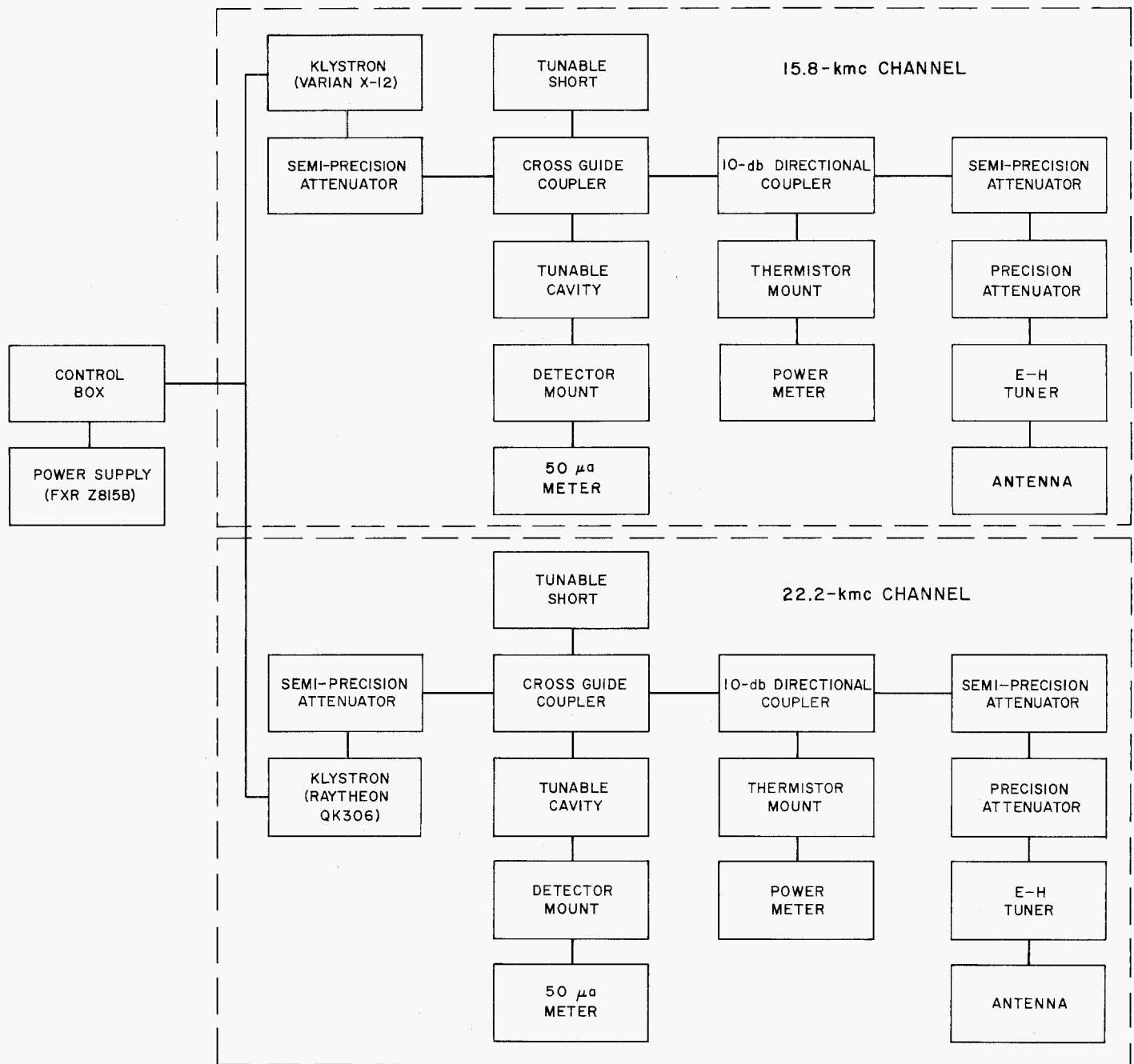


Fig. 152. Microwave radiometer test bench, block diagram

able resistor determines the operating condition of the two thermistor elements. The power meter provides excitation for both bridges, which are connected in series. When r-f power is applied, the r-f thermistor will decrease in resistance, thereby creating an error-voltage from the temperature compensating bridge. The error-voltage is directly proportional to the r-f power and is used to drive the error-detector amplifier whose output appears on the meter.

An additional semiprecision attenuator is mounted in the waveguide between the directional coupler and a precision attenuator. This unit is set at 20 db, which establishes an optimum level of energy at the precision attenuator. The precision attenuator is used to adjust the systems power output and has a range of 0 to 50 db with an accuracy of ± 1.15 db. Normally, the precision attenuator will be set to 20 db. Mounted at the antenna input is an E-H tuner, an impedance-matching device which

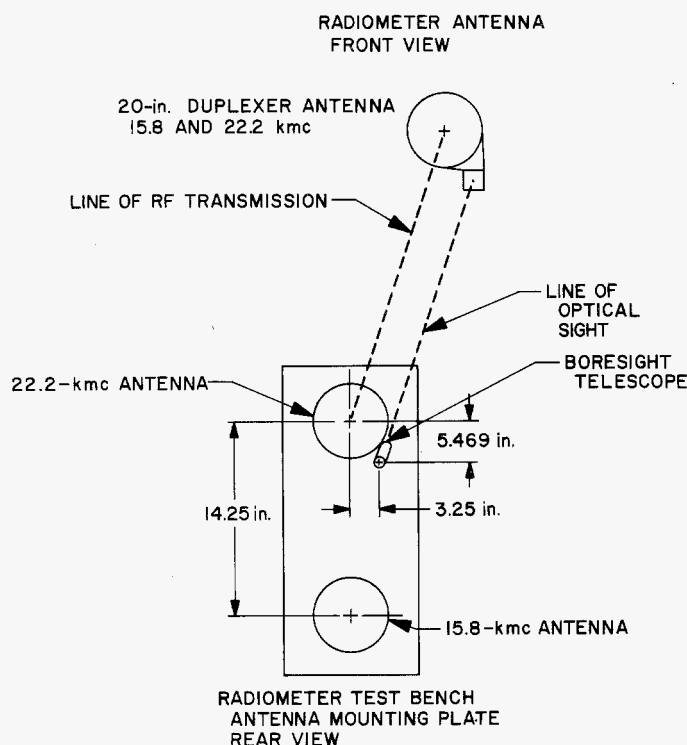


Fig. 153. Boresighting relationship

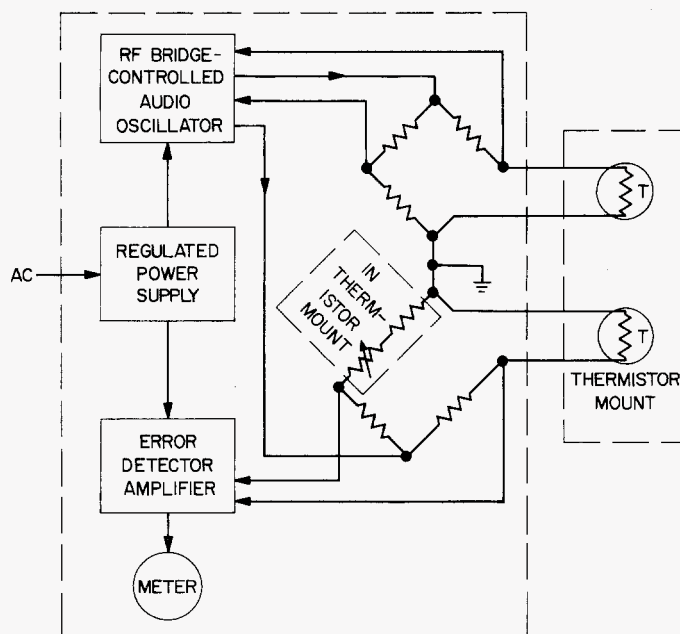


Fig. 154. Thermistor mount, power meter diagram

is used to establish a low VSWR at the antenna. The antenna is a 12-in. horn-fed parabola with a beam width of 4.6 deg and a gain of 1600. The first side lobe is at 7.3

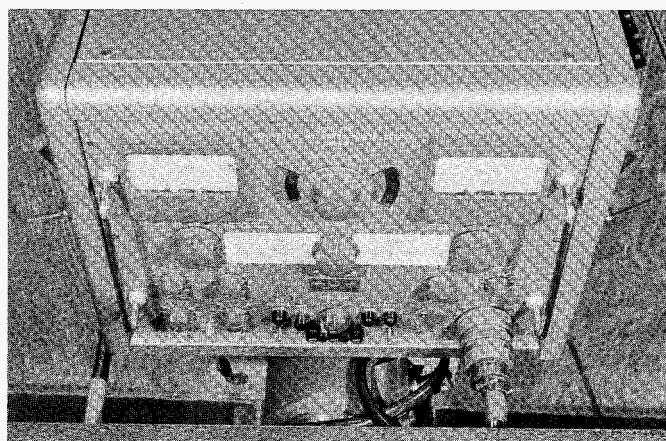


Fig. 155. FXR power supply

deg and the second at 11.2 deg, with both side lobes down by more than 15 db. With an input of 1 mw, approximately 25 μ W should be received by the radiometer.

The 22.2-kmc channel is the same as the 15.8-kmc channel, except that the r-f energy is generated by an RK 6253 Raytheon klystron, which is a micrometer-tuned reflex klystron with a frequency range of 18 to 22.3 kmc.

Power for the klystrons is derived from an FXR model Z815B power supply (Fig. 155). The beam voltage can be set between 200 and 2000 v in the low range and between 1800 and 3600 v in the high range. In either range, the required beam voltage can be preset to within $\pm 1\%$. The reflector voltage can be set between 0 and 1000 v negative with respect to the klystron beam voltage and preset to within $\pm 1\%$. The klystron used in the radiometer test bench requires negative grid voltages; therefore, the control grid polarity switch on the power supply has been modified so that only negative grid voltages can be generated. The grid voltage can be set between 0 and 300 v negative with respect to the klystron beam voltage.

The control box acts as a junction box for the filament reflector and grid voltages. The beam voltage is switched from one klystron to the other so that only one r-f channel can be activated. In order to prevent an excessive beam voltage from being applied to the 15.8-kmc klystron, a spark gap tube limits the voltage to 700 v.

Solar plasma current injector test fixture. The current injection box is mounted on top of the scientific case with the probe inserted through a hole in the case and into the collector of the solar plasma experiment. The circuitry provides a means by which current steps from

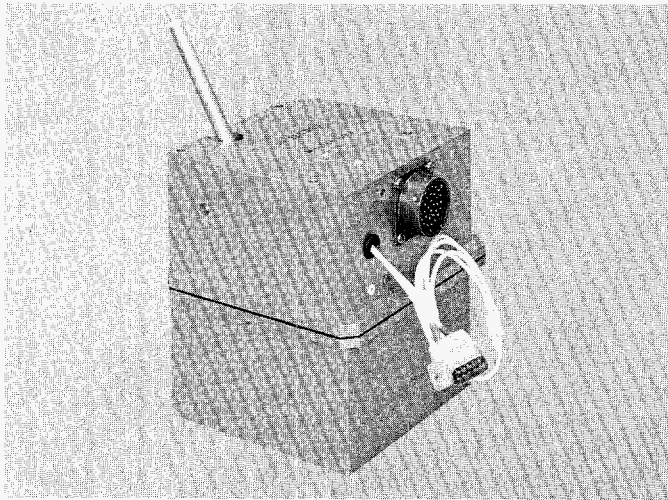


Fig. 156. Solar plasma current injection test fixture

10^{-6} to 10^{-13} amp can be injected into the collector. It also contains a voltage divider which is used to measure the sweep voltages of the electrostatic deflection plate. The high voltages on the plate are stepped down by a factor of 10 before presentation to the ground support equipment for monitoring purposes. The resistors in the divider are of such magnitude as to prevent loading of the plasma high voltage. The current steps are controlled by command from the GSE. Upon command, a rotary switch can be positioned such that the desired value of the injection current can be obtained. The desired currents are obtained by applying a fixed regulated voltage through high-value resistors. These currents are then injected into the collector cup through the probe. Figure 156 is a photograph of the current injection box, which was built at JPL.

Isolation box. Since the signals from some of the instruments located on the spacecraft had to travel through 60 ft of cable to reach the ground support equipment, line drivers had to be utilized. These signals, which come from the ion chamber and particle flux experiment, are pulses ranging from 4 to 40 μ sec in width. To prevent the cable capacitance from deteriorating these pulses, line drivers were developed and housed in the isolation box, which is located approximately 5 ft from the experiment.

e. Data conditioning system ground support equipment. The ground support equipment for the data conditioning system, when operated alone or in conjunction with the scientific GSE, can completely evaluate the electrical performance of the DCS. The output mech-

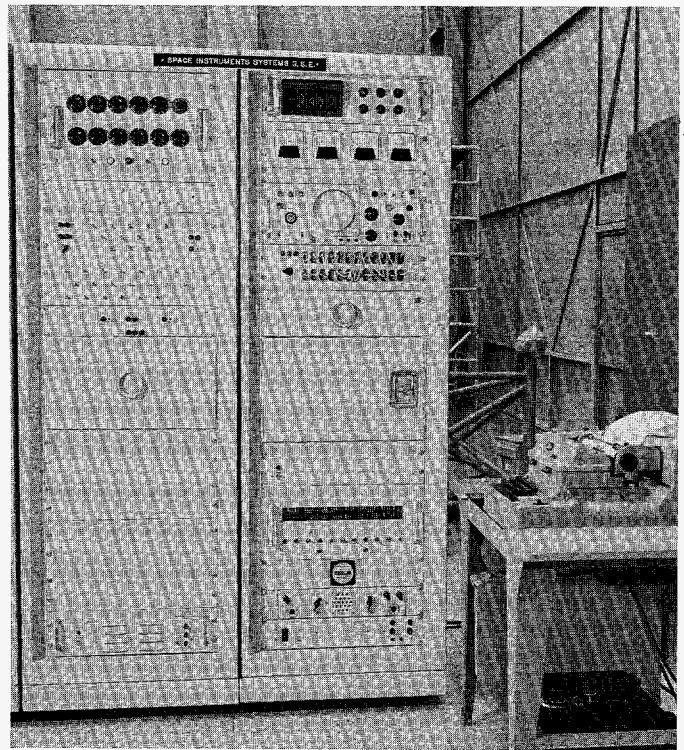


Fig. 157. Data-conditioning system ground support equipment

anism of the GSE provides hard-copy data which may be evaluated to establish a *go, no-go* condition; however, it is also capable of checking the absolute calibration of the analog-to-digital, digital, and pulse inputs, as well as the miscellaneous logic function and command of the DCS.

DCS test conditions. The GSE (Fig. 157) consists of two racks of equipment and a Friden Flexowriter. The equipment has the capability of testing the DCS under the following test conditions:

(1) All the experiment inputs are simulated and power is supplied by the GSE. In this case, data are obtained through a hard-line and printed out in octal notation by the Flexowriter. Logic levels of 0 and 6 v are applied to the DCS digital inputs to simulate power sensing, cosmic dust, magnetometer, particle flux, and the ion chamber. Analog inputs are applied to the DCS analog-to-digital converter to simulate the outputs from the radiometer, magnetometer, and solar plasma. The printed output is in octal form and is converted to binary or decimal form by the operator for immediate evaluation. This test configuration is used for the calibration and bench test of the DCS.

(2) All the experiments are connected to the DCS and the DCS GSE supplies bit sync and word sync. Power and stimuli for the experiment are supplied by the scientific GSE. The data from the DCS GSE are compared against the data from the scientific GSE and the readings should be the same.

(3) All the experiments are connected to the DCS and the spacecraft supplies power, bit sync, and word sync. The scientific GSE supplies only the stimuli to the experiment. As the experiments are stimulated, the printed output from the DCS GSE is compared to the monitored output of the scientific GSE and verified. This is the test configuration which is used for the evaluation of the spacecraft and the GSE. Figure 158 is a block diagram of the scientific system or subsystem intercabling.

Description of equipment. A block diagram showing the location of the components and the cabling of the GSE is shown in Fig. 159. A brief description of the components in the data condition system GSE follows:

- (1) *Current source (North Hills model CS-145).* This supply generates a precision current which is applied to a resistor on the analog input panel. This provides a precision voltage which is controlled by switches on the analog panel.
- (2) *Power switching indicator panel (JPL).* This monitoring panel is used for the power switching relays, which are located in the DCS isolation box. The relay contacts are brought to this panel and close the circuit to the appropriate light; thus, the position of the power switching relays is observed.
- (3) *Analog panel (JPL).* From this panel, either a precision voltage or a variable voltage of 0 to 6 v may be applied to the analog inputs of the DCS. Twelve SPDT switches, with a center off-position, allow complete flexibility as to the voltage that is applied to each input. In addition, two pairs of binding posts are available to monitor the bit sync and word sync.
- (4) *Digital input panel (JPL).* This panel simulates all the digital signals that would normally come from the CC&S, the radiometer scan limit switch, the particle flux, and the ion chamber. The digital signals are connected to the DCS through SPDT switches which allow all or any combination of inputs to be selected.

- (5) *Logic and timer chassis (JPL).* This chassis contains all the circuits required to generate bit sync, word sync, data and data bar (Fig. 160) as needed by either the DCS or the scientific data translator. This chassis also supplies the d-c voltages needed by the DCS isolation box simulated digital inputs and the variable voltage to the analog panel.
- (6) *Data display simulator panel (JPL).* This panel provides a means of monitoring the signals generated in the logic and timer chassis which simulates the data display console. These waveforms can be observed on an oscilloscope.
- (7) *Clock relay chassis (JPL).* This chassis contains a negative 15-v power supply, 20 emitter-followers, and 20 relays. Input logic levels indicating real time are obtained from the scientific GSE and drive the emitter-followers, which in turn actuate the relays. The relay contacts are connected to the SDT and are periodically sampled; the time is printed out on a Flexowriter.
- (8) *Power supply (Consolidated Systems Corp.).* This solid-state 50-v square-wave, 2.4-kc supply furnishes power to the DCS. This supply was modified in order to prevent the output voltage from exceeding 112 v peak-to-peak.
- (9) *Digital voltmeter (NLS model V-34A).* An NLS digital voltmeter is used to measure the output voltages of the transformer-rectifier unit and the precision voltages from the analog panel.
- (10) *Meter panel (JPL).* This panel is used as a supplement to the digital voltmeter as it provides quick-look T-R voltage information and also displays the radiometer scan position as a voltage between 0.5 to 6 v.
- (11) *Oscilloscope (Tektronics model RM503).* The oscilloscope is used to observe any of the waveforms that are present on the ground support equipment. The oscilloscope has a differential input which prevents any of the signals or waveforms from being tied back to chassis.
- (12) *Jack panel (JPL).* All of the monitored signals are brought to this panel and may be observed on the oscilloscope, read on the digital voltmeter, or patched into an oscillograph recorder. Also located on this panel is the digital voltmeter function switch, which permits the digital voltmeter

UNCLASSIFIED

UNCLASSIFIED

UNCLASSIFIED

JPL TECHNICAL REPORT NO. 32-353

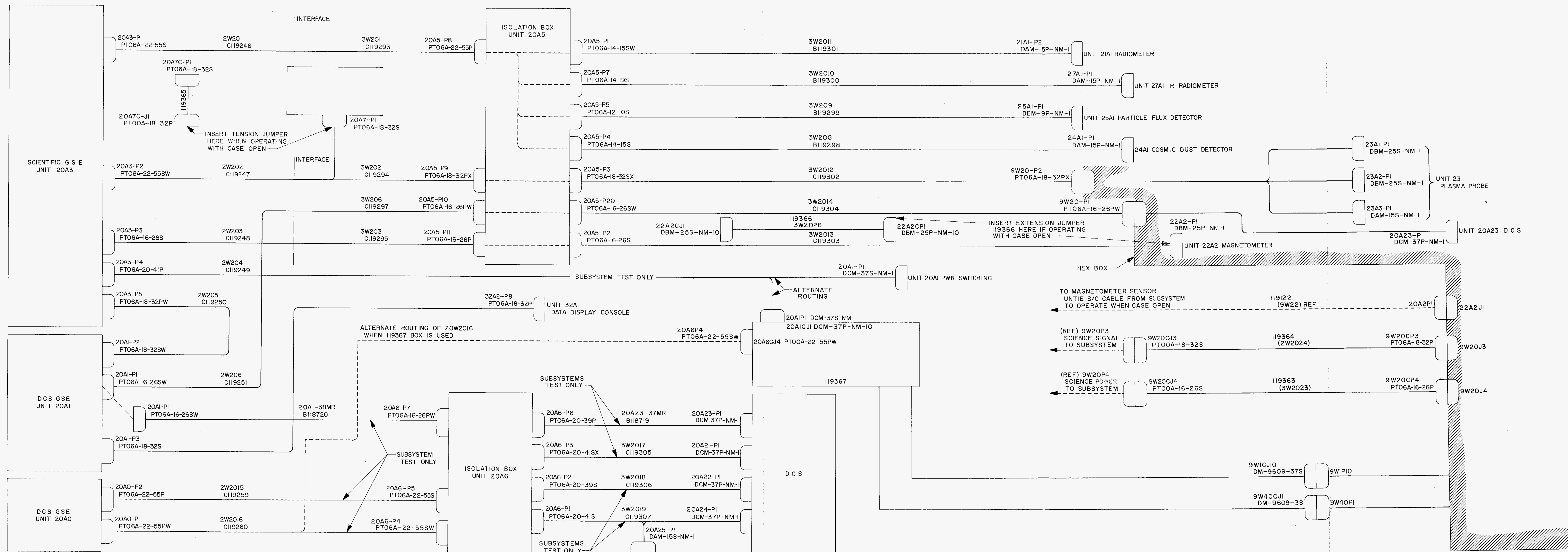


Fig. 158. DCS GSE system or subsystem intercabling

UNCLASSIFIED

UNCLASSIFIED

UNCLASSIFIED

UNCLASSIFIED

UNCLASSIFIED

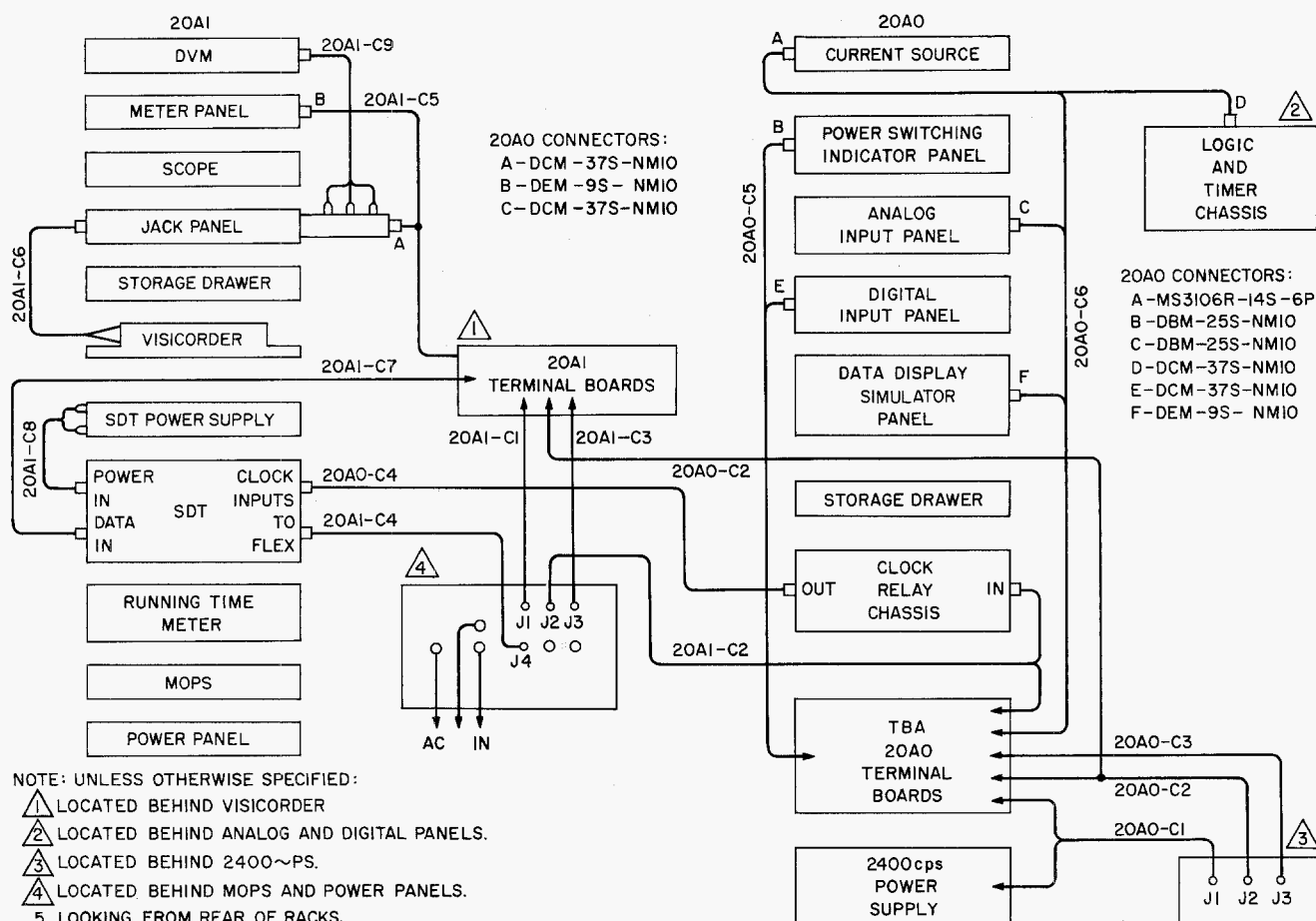


Fig. 159. DCS GSE inter-rack block diagram

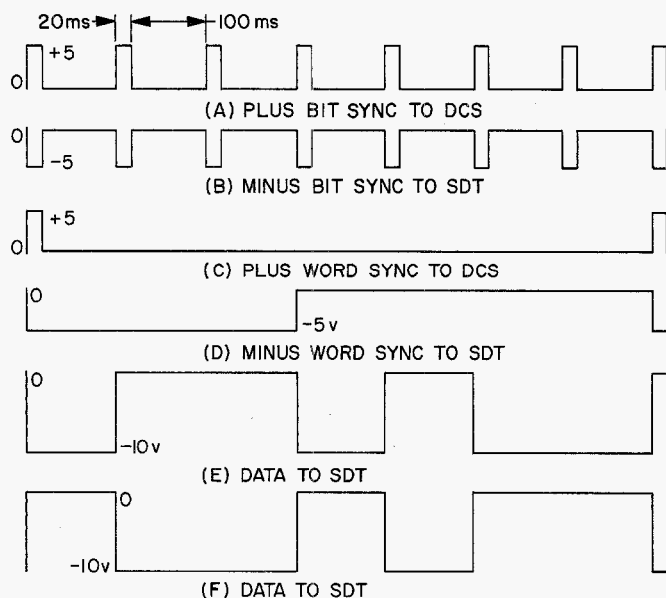


Fig. 160. DCS GSE logic and timer output waveforms

to be switched to any one of the DCS transformer-rectifier voltages, or to the monitoring terminals located above the switch. These terminals permit the digital voltmeter to be connected to any monitoring point on the GSE.

- (13) *Oscillograph recorder (Minneapolis-Honeywell model 906C)*. This recorder (Fig. 161), also known as a visicorder, is used to record all or any of the functions on the jack panel. This recorder uses light-beam galvanometers which have isolated inputs, thus allowing the polarity of the input signal to be reversed on the jack panel without causing a short circuit.

- (14) *A-C power panel (JPL)*. This panel controls the a-c power to the GSE. Also located on this panel is a plus and minus 10-v power supply, which is used to power the amplifiers in the DCS isolation box and the relays in the data display console.

- (15) *Science data translator and Friden Flexowriter.*
The science data translator, in conjunction with the Flexowriter, provides the means by which the

coded information from the DCS is decoded and printed-out in octal notation. A description of this equipment is contained in the next section.

Miscellaneous equipment.

Isolation box. The isolation box contains circuits which condition the DCS output signals so that they may be observed at the end of 60 ft of cable. These signal-conditioning circuits or line drivers are in the form of four emitter-followers. The pulse generating circuits used to simulate the particle flux and the ion chamber pulses, and the relays used to simulate the power switching unit are in this box, which is only used when the DCS is being checked out.

f. Scientific data translator

General description. The scientific data translator is an equipment complex designed to accept the coded signals from a spacecraft data conditioning system and convert this information into a form compatible with the transmission characteristics of a commercial teletype circuit and/or provide quick-look printed output suitable for operation evaluation.

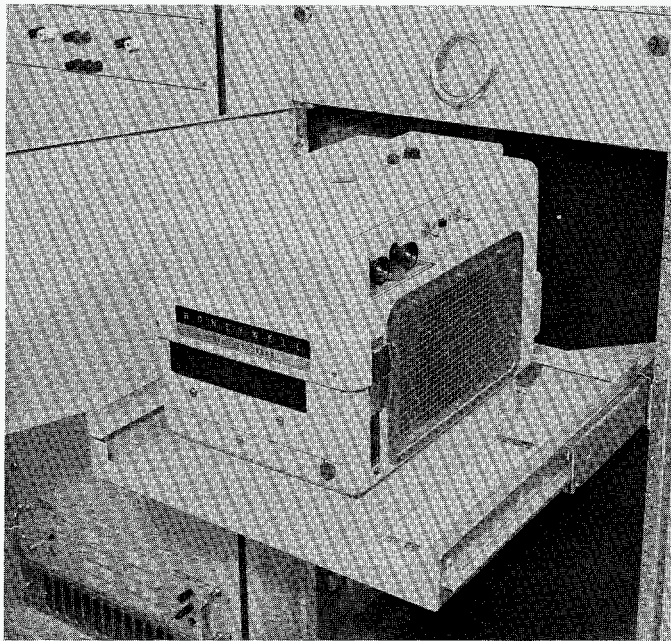


Fig. 161. DCS GSE oscillograph recorder

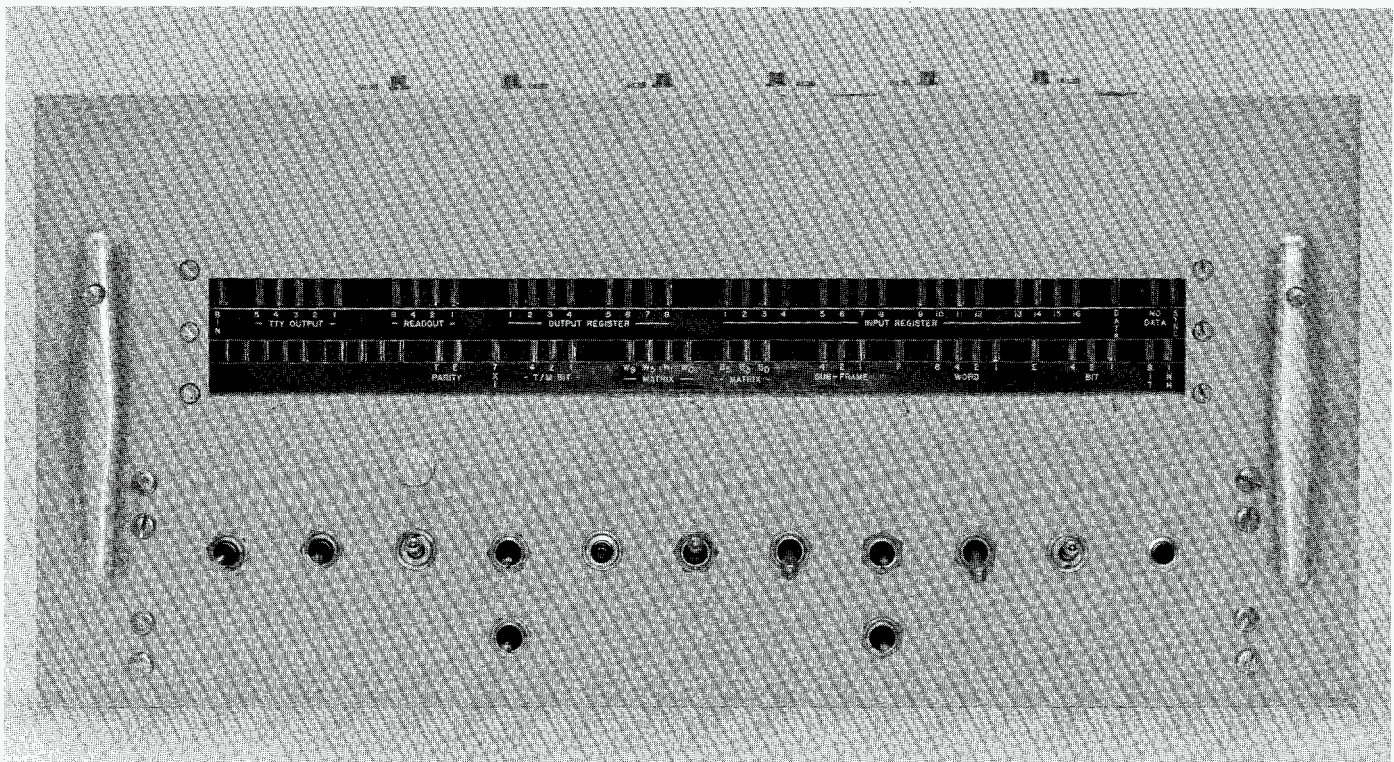


Fig. 162. SDT front panel layout

Design of this equipment, together with the format characteristics of the spacecraft DCS, is such as to make the SDT directly applicable to both the *Mariner R* and the *Ranger* follow-on programs. The SDT is suitable for use at DSIF tracking stations or as an integrated element of the ground support equipment associated with the spacecraft DCS.

Physical description. The SDT consists of three physically separate elements: (1) a logic drawer; (2) an output mechanism which may be, interchangeably, a Flexowriter or a paper-tape punch; and (3) a power supply. If installed at a DSIF site, the output mechanism would be the paper-tape punch. Under this condition, the entire equipment complement is physically interchangeable with the telemetry support equipment currently installed.

(1) *Logic drawer.* The logic drawer consists of a framework provided with a front panel, suitable for mounting three DEC type 1910 mounting panels, each capable of accepting 20 DEC logic modules or cards.

The drawer is designed for installation in a standard relay-rack-type equipment cabinet. It is provided with standard chassis track-type drawer slides having tilt mounts, permitting access to the equipment from the front of the equipment cabinet for maintenance.

Front-panel dimensions of the logic drawer are 19 in. wide by $8\frac{3}{4}$ in. high, both standard for the application and identical to the RA-1 and -2 equipment to facilitate interchangeability.

Mounted on the front panel of the SDT are the status display and all controls necessary for operation/maintenance of the equipment (Fig. 162). Connections to the logic drawer are made through several multicircuit connectors at the rear of the logic drawer.

(2) *Output mechanism.* Associated with the logic drawer is a mechanism capable of converting the electrical signals from the SDT logic into either teletype-format punched paper tape for subsequent transmission, or printed data for visual inspection, or both. This mechanism may be either a Flexowriter or a perforator.

(3) *Flexowriter.* Preparation of printed hard-copy, with or without associated punched tape, is accomplished by a Friden model FPC-5 recorder-reproducer, or Flexowriter.

The FPC-5 Flexowriter is a self-contained, heavy-duty electric typewriter combined with a punched paper tape reader and perforator. Both the tape-format and the keyboard layout of this machine conform to TTY standards.

Modifications have been incorporated into this machine to provide external electrical inputs to the code translator so that machine operation may be controlled by the output of the SDT. Normal machine functions have not been compromised by these modifications.

(4) *Perforator.* For applications of the SDT where no hard-copy requirements exist, typically at DSIF tracking sites, the output mechanism is a Tally Register Corporation model 420 tape perforator equipped with an integral model 1424 transistorized perforator drive package. This mechanism is completely self-contained and self-powered from the utility mains. The equipment is used as supplied, without modification.

(5) *Output format.* The electrical output of the SDT appears as an arrangement of *ones* and *zeroes*, in parallel, on five separate lines, together with the *start* signal on a sixth line. The *one/zero* combinations define the applicable alpha-numeric characters in a standard teletype code. They may be used either to prepare a punched paper tape, which may then be read through a tape reader for TTY transmission, or a typewritten record (hard-copy), with the option of simultaneously producing a by-product punched tape. Obviously, the punched tape will produce a hard-copy, when read into a page printer, identical to the typed record which may be the direct output of the SDT.

(6) *Format analysis.* Appearance of the hard-copy is shown in Fig. 163. The preamble is made up prior to a data run and its contents are a procedural matter. However, since SDT output includes only time in hours, minutes, and seconds, the preamble should include the day, station identification, and identification of the spacecraft from which the data was received. The data tape is thus completely unambiguous, regardless of any subsequent marking and/or filing systems. Supplemental information, such as pass number, etc., is optional, its inclusion being a simple matter of typing in the appropriate data.

Following the preamble, on the next line, are six decimal digits of time, spaced in pairs for hours, minutes, and seconds. The next two lines contain 19 octal digit triplets, corresponding to data words 3 through 21 of the

SCIENCE DATA FOLLOWS

MARINER R/STATION 2/DECEMBER 13, 1961

^a 22 59 02					
^b 377 ^d 177	^c 0016 ^e 145	377 # 177	377 # 177	377 # 177	
375 # 177	377 # 177	377 # 177	377 # 177	377	
22 59 39					
377 177	1377 177	377 177	377 177	377 177	
^g 375 177	377 177	377 177	377 177	377	
22 59 59					
377 177	2377 177	377 177	377 177	377 177	
375 177	377 177	377 177	377 177	377	
23 00 19					
377 177	3377 177	377 177	377 177	377 177	
375 177	377 177	377 177	377 177	377	
23 00 39					
³ 377 ⁴ 177	⁵ 4377 ⁶ 177	⁷ 377 ⁸ 177	⁹ 377 ¹⁰ 177	¹¹ 377 ¹² 177	{ DCS DATA WORD NUMBER
¹³ 375 ¹⁴ 177	¹⁵ 377 ¹⁶ 177	¹⁷ 377 ¹⁸ 177	¹⁹ 377 ²⁰ 177	²¹ 377	
23 00 59					
377 177	5377 177	377 177	377 177	377 177	
375 177	377 177	377 177	377 177	377	
23 01 19					
³ 377 ⁴ 177	⁵ 0016 ⁶ 145	377 177	377 177	377 177	
^g 376 177	377 177	377 177	377 177	377	
23 01 39					
377 177	1377 177	377 177	377 177	377 177	
376 177	377 177	377 177	377 177	377	
23 01 59					
377 177	2377 177	377 177	377 177	377 177	
376 177	377 177	377 177	377 177	377	

LEGEND

PREAMBLE — PUNCHED ON DATA TAPE TO INSURE PERMANENT IDENTIFICATION WITHOUT RECOURSE TO POST FACTO PENCIL MARKING OR SIMILAR HAPHAZARD AND AMBIGUOUS PROCEDURES.

^aSTATION TIME — HOURS, MINUTES, AND SECONDS. IDENTIFIES TIME OF RECEIPT OF FOLLOWING DATA FRAME.

^bFIRST SIGNIFICANT DATA WORD IN A DCS FRAME. SINCE WORDS 1 AND 2 CONTAIN PN SYN SEQUENCE, THIS IS DCS WORD 3. THE 377₈ NUMBER REPRESENTS THE MAXIMUM COUNT, OR ALL ONES, CONDITION IN THIS 8-BIT WORD.

^cSECOND SIGNIFICANT DATA WORD IN DCS FRAME, ACTUALLY, DCS WORD 4. SINCE THE WORDS ARE PAIRED IN A 16-BIT SEQUENCE BY THE DCS, AND THE 16TH BIT IS A PARITY BIT FOR THE ENTIRE SEQUENCE, THIS WORD IS ONLY 7 BITS LONG AND 177₈ REPRESENTS THE MAXIMUM INFORMATION POSSIBLE, THE ALL ONES CONDITION.

^dPARITY ERROR SYMBOL APPLICABLE, INDETERMINATELY, TO ONE OR THE OTHER, OR BOTH, OF THE WORDS BETWEEN WHICH IT IS LOCATED. A TOTAL OF NINE POSSIBILITIES EXISTS FOR THE OCCURRENCE OF THIS SYMBOL — ALL ARE INDICATED IN THIS FRAME.

^eREAD-OUT OF PN SEQUENCE WHICH APPEARS IN WORDS 5 AND 6 TO IDENTIFY A MASTER FRAME, MARKING THE POINT OF REFERENCE FOR A SEQUENCE OF SIX SUBFRAMES.

^fSUBFRAME COUNT — STARTS AT 0 AT MASTER FRAME AND INCREMENTS TO 5 IN THE SUBFRAME PRECEDING MASTER FRAME (SEE 23 00 59 AND 23 01 19).

^gFRAME COUNT, DCS WORD 13, WHICH INCREMENTS WITH EACH MASTER FRAME. NOTE NUMBER 375₈ THROUGH 23 00 59, SUBFRAME 5, CHANGING TO 376₈ AT 23 01 19, MASTER FRAME AND SUBFRAME COUNT 0.

^hDATA WORDS 5 AND 6, ONLY, ARE SUBCOMMUTATED SEQUENTIALLY THROUGH THE CYCLES OF SIX DCS FRAMES.

LEGEND

PREAMBLE — PUNCHED ON DATA TAPE TO INSURE PERMANENT IDENTIFICATION WITHOUT RECOURSE TO POST FACTO PENCIL MARKING OR SIMILAR HAPHAZARD AND AMBIGUOUS PROCEDURES.

^aSTATION TIME — HOURS, MINUTES, AND SECONDS. IDENTIFIES TIME OF RECEIPT OF FOLLOWING DATA FRAME.

^bFIRST SIGNIFICANT DATA WORD IN A DCS FRAME. SINCE WORDS 1 AND 2 CONTAIN PN SYNC SEQUENCE, THIS IS DCS WORD 3. THE 377^g NUMBER REPRESENTS THE MAXIMUM COUNT, OR ALL ONES, CONDITION IN THIS 8-BIT WORD.

^cSECOND SIGNIFICANT DATA WORD IN DCS FRAME, ACTUALLY, DCS WORD 4. SINCE THE WORDS ARE PAIRED IN A 16-BIT SEQUENCE BY THE DCS, AND THE 16TH BIT IS A PARITY BIT FOR THE ENTIRE SEQUENCE, THIS WORD IS ONLY 7 BITS LONG AND 177^g REPRESENTS THE MAXIMUM INFORMATION POSSIBLE, THE ALL ONES CONDITION.

^dPARITY ERROR SYMBOL APPLICABLE, INDETERMINATELY, TO ONE OR THE OTHER, OR BOTH, OF THE WORDS BETWEEN WHICH IT IS LOCATED. A TOTAL OF NINE POSSIBILITIES EXISTS FOR THE OCCURRENCE OF THIS SYMBOL — ALL ARE INDICATED IN THIS FRAME.

^eREAD-OUT OF PN SEQUENCE WHICH APPEARS IN WORDS 5 AND 6 TO IDENTIFY A MASTER FRAME, MARKING THE POINT OF REFERENCE FOR A SEQUENCE OF SIX SUBFRAMES.

^fSUBFRAME COUNT — STARTS AT 0 AT MASTER FRAME AND INCREMENTS TO 5 IN THE SUBFRAME PRECEDING MASTER FRAME (SEE 23 00 59 AND 23 01 19).

^gFRAME COUNT, DCS WORD 13, WHICH INCREMENTS WITH EACH MASTER FRAME. NOTE NUMBER 375^g THROUGH 23 00 59, SUBFRAME 5, CHANGING TO 376^g AT 23 01 19, MASTER FRAME AND SUBFRAME COUNT 0.

^hDATA WORDS 5 AND 6, ONLY, ARE SUBCOMMUTATED SEQUENTIALLY THROUGH THE CYCLE OF SIX DCS FRAMES.

Fig. 163. SDT annotated format

DCS serial format. These 19 words are arranged in two lines, 10 on the upper, or first line, and 9 on the lower, or second line.

Basically, the octal triplets are grouped in pairs, with a single space between the two triplets of one pair and a double space between pairs.

The first set of data in Fig. 163, at time 22 59 02, has the # symbol inserted in the single space between each of the two triplet numbers of a pair. This symbol is used to indicate existence of a parity error within the 16-bit transmission group containing the two octal triplets. The positions of the nine parity error symbols in these two lines represent all possible positions where a parity error indication may appear in the SDT output format.

Since the transmission format includes 15 data bits and a parity bit in each 16-bit group, and the 15 data bits comprise two data words, the allocation of word content is uneven with the first word of a group containing 8 bits and the second word 7 bits. The 377 177 notation appearing in most of the read-out position thus represents the largest possible octal number for the 8-bit first word and 7-bit second word of each 16-bit transmitted group.

The two lines, 19 triplets or words, correspond to one transmitted data subframe of 21 words. In transmission, however, the first two words of each subframe contain a PN sequence used to synchronize the SDT with DCS. Since this information is insignificant, it is not outputted by the SDT; rather, during the time when it is available for read-out, the SDT is reading out the time information from the station clock. Thus, the first entry in the data output of the SDT is transmitted word 3, the first significant data information. The first, left, pair of octal triplets on the first, upper line of data then becomes transmitted words 3 and 4, the second pair words 5 and 6, etc.

Note that, in contrast to the majority of data word octal triplet pairs, which are 377 177, the triplet pair representing transmitted words 5 and 6 in the first subframe of Fig. 163 contains 016 145, the zero preceding the first zero of the word-5 triplet not being part of the transmitted data. This 016 145 sequence is the octal representation of the 15-bit PN sequence transmitted as words 5 and 6 once every six data subframes. Its appearance identifies the particular subframe in which it occurs as a master frame, and the temporal significance of the subcommutation sequence is based upon recognition of the periodic appearance of a master frame. In conformity with this transmission scheme, the digit preceding the octal triplet of data word 5 indicates the sequential steps of the subcommutation process and identifies the information contained in octal triplets, or words 5 and 6. In the case of master frame, this digit will be 0 and progress through 5 before recurrence of master frame. This function may be observed by inspection of this digit position in sequential subframes of Fig. 163.

UNCLASSIFIED

JPL TECHNICAL REPORT NO. 32-353

The first word of the second line of a subframe of data corresponds to transmission word 13, which is the frame count associated with DCS transmission cycles. At time 22 59 02, in Fig. 163, this count is 375, and it remains thus through the sequence of six subframes, changing at the time of occurrence of the master frame identifier (016 145) at time 23 01 19. The combination of the frame-count number and the subframe count,

preceding word 5, thus uniquely defines all data information, including the content of subcommutated words 5 and 6.

Table 14 is used to convert the octal word data to analog voltages. This is done during system test to correlate the data between the DCS GSE and the scientific GSE.

Table 14. Mariner R SDT DCS analog input voltage vs SDT octal read-out

Use column A for truncated 8-bit words. Column B is SDT octal read-out. Use column C for complete 8-bit words.									
A	B	C	A	B	C	B	C	B	C
0.000	0	0.0000	3.008	100	1.5040	200	3.0080	300	4.5120
0.047	1	0.0235	3.055	101	1.5275	201	3.0315	301	4.5355
0.094	2	0.0470	3.102	102	1.5510	202	3.0550	302	4.5590
0.141	3	0.0705	3.149	103	1.5745	203	3.0785	303	4.5825
0.188	4	0.0904	3.196	104	1.5980	204	3.1020	304	4.6060
0.235	5	0.1175	3.243	105	1.6215	205	3.1255	305	4.6295
0.282	6	0.1410	3.290	106	1.6450	206	3.1490	306	4.6530
0.329	7	0.1645	3.337	107	1.6685	207	3.1725	307	4.6765
0.376	10	0.1880	3.384	110	1.6920	210	3.1960	310	4.7000
0.423	11	0.2115	3.431	111	1.7155	211	3.2195	311	4.7235
0.470	12	0.2350	3.478	112	1.7390	212	3.2430	312	4.7470
0.517	13	0.2585	3.525	113	1.7625	213	3.2665	313	4.7705
0.564	14	0.2820	3.572	114	1.7860	214	3.2900	314	4.7940
0.611	15	0.3055	3.619	115	1.8095	215	3.3135	315	4.8175
0.658	16	0.3290	3.666	116	1.8330	216	3.3370	316	4.8419
0.705	17	0.3525	3.713	117	1.8565	217	3.3605	317	4.8645
0.752	20	0.3760	3.760	120	1.8800	220	3.3840	320	4.8880
0.799	21	0.3995	3.807	121	1.9035	221	3.4075	321	4.9115
0.846	22	0.4230	3.854	122	1.9270	222	3.4310	322	4.9350
0.893	23	0.4465	3.901	123	1.9505	223	3.4545	323	4.9585
0.940	24	0.4700	3.948	124	1.9740	224	3.4780	324	4.9820
0.987	25	0.4935	3.995	125	1.9975	225	3.5015	325	5.0055
1.034	26	0.5170	4.042	126	2.0210	226	3.5250	326	5.0290
1.081	27	0.5405	4.089	127	2.0445	227	3.5485	327	5.0525
1.128	30	0.5640	4.136	130	2.0680	230	3.5720	330	5.0760
1.175	31	0.5875	4.183	131	2.0915	231	3.5955	331	5.0995
1.222	32	0.6110	4.230	132	2.1150	232	3.6190	332	5.1230
1.269	33	0.6345	4.277	133	2.1385	233	3.6425	333	5.1465
1.316	34	0.6580	4.324	134	2.1620	234	3.6660	334	5.1700
1.363	35	0.6815	4.371	135	2.1855	235	3.6895	335	5.1935
1.410	36	0.7050	4.418	136	2.2090	236	3.7130	336	5.2170
1.457	37	0.7285	4.465	137	2.2325	237	3.7365	337	5.2405
1.504	40	0.7520	4.512	140	2.2560	240	3.7600	340	5.2640
1.551	41	0.7755	4.559	141	2.2795	241	3.7835	341	5.2875
1.598	42	0.7990	4.606	142	2.3030	242	3.8070	342	5.3110
1.645	43	0.8225	4.653	143	2.3265	243	3.8305	343	5.3345
1.692	44	0.8460	4.700	144	2.3500	244	3.8540	344	5.3580
1.739	45	0.8695	4.747	145	2.3735	245	3.8775	345	5.3815
1.786	46	0.8930	4.794	146	2.3970	246	3.9010	346	5.4050
1.833	47	0.9165	4.841	147	2.4205	247	3.9245	347	5.4285
1.880	50	0.9400	4.888	150	2.4440	250	3.9480	350	5.4520
1.927	51	0.9635	4.935	151	2.4675	251	3.9715	351	5.4755
1.974	52	0.9870	4.982	152	2.4910	252	3.9950	352	5.4990
2.021	53	1.0105	5.029	153	2.5145	253	4.0185	353	5.5225
2.068	54	1.0340	5.076	154	2.5380	254	4.0420	354	5.5460

UNCLASSIFIED

Table 14. (cont'd)

A	B	C	A	B	C	B	C	B	C
2.115	55	1.0575	5.123	155	2.5615	255	4.0655	355	5.5695
2.162	56	1.0810	5.170	156	2.5850	256	4.0890	356	5.5930
2.209	57	1.1045	5.217	157	2.6085	257	4.1125	357	5.6165
2.256	60	1.1280	5.264	160	2.6320	260	4.1360	360	5.6400
2.303	61	1.1515	5.311	161	2.6555	261	4.1595	361	5.6635
2.350	62	1.1750	5.358	162	2.6790	262	4.1830	362	5.6870
2.397	63	1.1985	5.405	163	2.7025	263	4.2065	363	5.7105
2.444	64	1.2220	5.452	164	2.7260	264	4.2300	364	5.7340
2.491	65	1.2455	5.499	165	2.7495	265	4.2535	365	5.7575
2.538	66	1.2690	5.546	166	2.7730	266	4.2770	366	5.7810
2.585	67	1.2925	5.593	167	2.7965	267	4.3005	367	5.8045
2.632	70	1.3160	5.640	170	2.8200	270	4.3240	370	5.8280
2.679	71	1.3395	5.687	171	2.8435	271	4.3475	371	5.8515
2.726	72	1.3630	5.734	172	2.8670	272	4.3710	372	5.8750
2.773	73	1.3865	5.781	173	2.8905	273	4.3945	373	5.8985
2.820	74	1.4100	5.828	174	2.9140	274	4.4180	374	5.9220
2.867	75	1.4335	5.875	175	2.9375	275	4.4415	375	5.9455
2.914	76	1.4570	5.922	176	2.9610	276	4.4650	376	5.9690
2.961	77	1.4805	5.969	177	2.9845	277	4.4885	377	5.9925

G. Cabling

1. Introduction

The *Mariner R* spacecraft wiring design differed from previous programs. The change was necessitated by design restraints, power requirements, and a new type of subassembly that was not used on earlier *Ranger* equipment. Furthermore, the midcourse motor had to be installed from the bottom of the spacecraft with free access provided to its final position in the center of the spacecraft. This and the power requirements had a direct effect on the ring harness structure. The new subassembly design affected all of the spacecraft wiring. The main hex bays are shown in Fig. 164 through 169, with callouts for the interface wiring. Each interface will be described separately.

The ring harness structure was designed so it could be suspended and fastened by gussets to the underside of the lower main hex as shown in Fig. 170, a cross section of one of the bays. The configuration of the structure was determined by the accessibility of the various connectors, the segregation of the 2400-cps power from the signal wiring, and the size required to support the main groups of ring harness wiring. A modified S-design was selected and is shown in Fig. 170.

Because assemblies have to be flight-accepted as a unit and for ease of disassembly, brackets had to be added to the top of the ring harness structure to hold connectors. One bracket was installed for the power switch and logic case harness, two for the power case harness, one for the antenna hinge assemblies, and one for the GSE power monitoring. Connectors on the ring harness were arranged as in Fig. 171, which shows the ring harness wiring installed in the ring structure.

To make the ring harness structure a workable design, it was necessary to have access from the ring harness main wiring to the ring harness connectors. Holes were cut in the ring harness structure to reduce the over-all weight and to provide access from the main ring harness wiring to the ring harness connectors. Fig. 172 is a view from the bottom showing a small section of the ring harness with wire routed from the ring harness to the connectors.

2. Power System Wiring

The 2400-cps square-wave power wiring attached to the ring harness structure was made an independent harness to prevent cross-talk effects on signal functions. The design allowed this harness to be moved without disturbing the other wires of the ring harness.

The power system design required a terminal board and a d-c power return bus attached to the ring harness structure. The terminal board had four resistors soldered

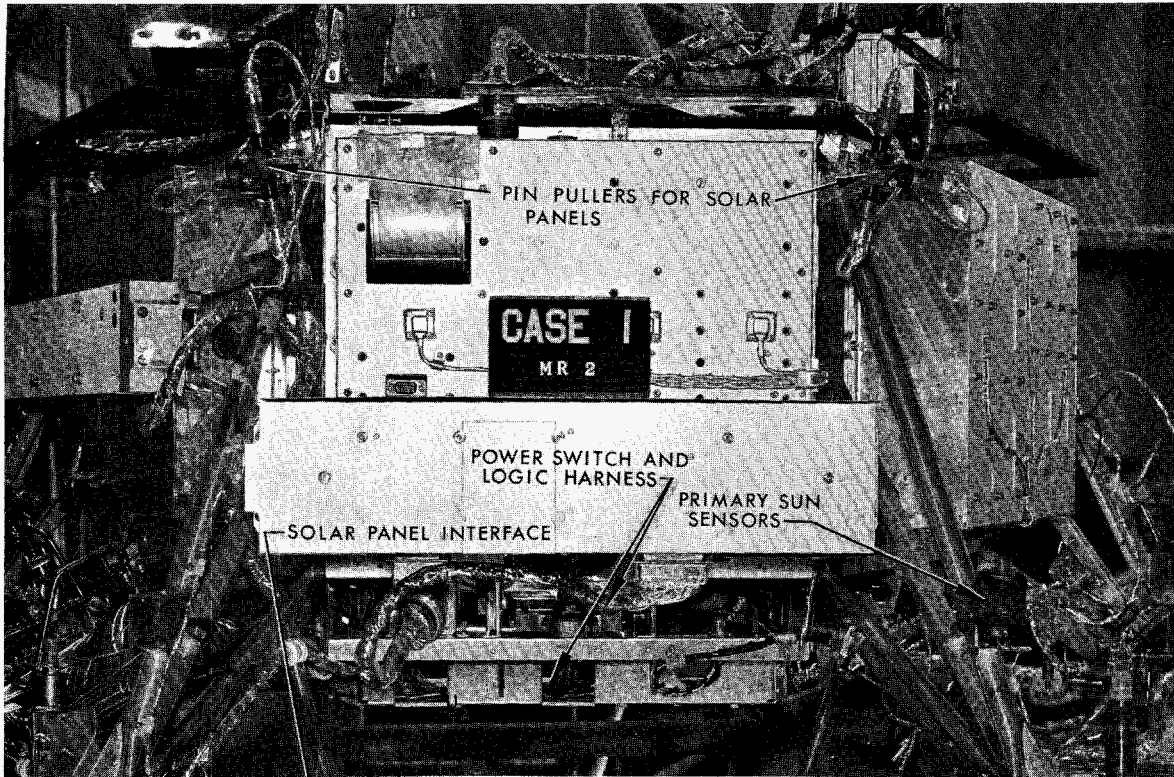


Fig. 164. Main hex bay cabling, showing Case I

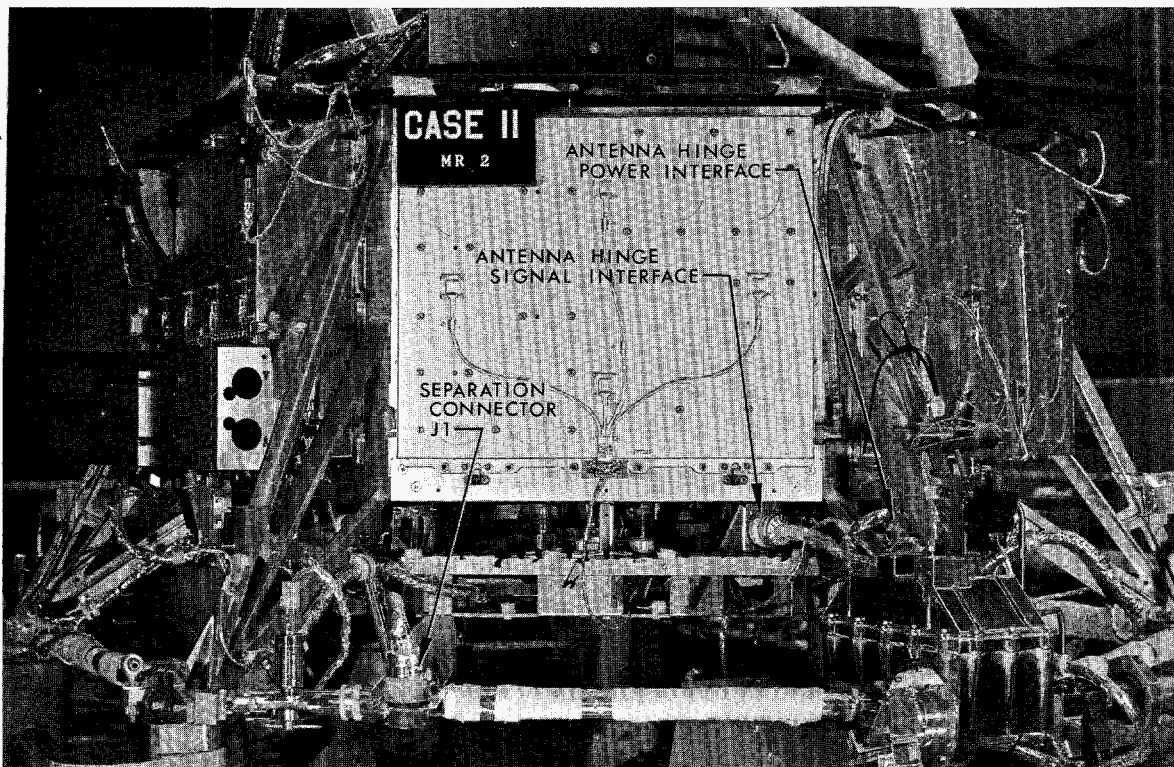


Fig. 165. Main hex bay cabling, showing Case II

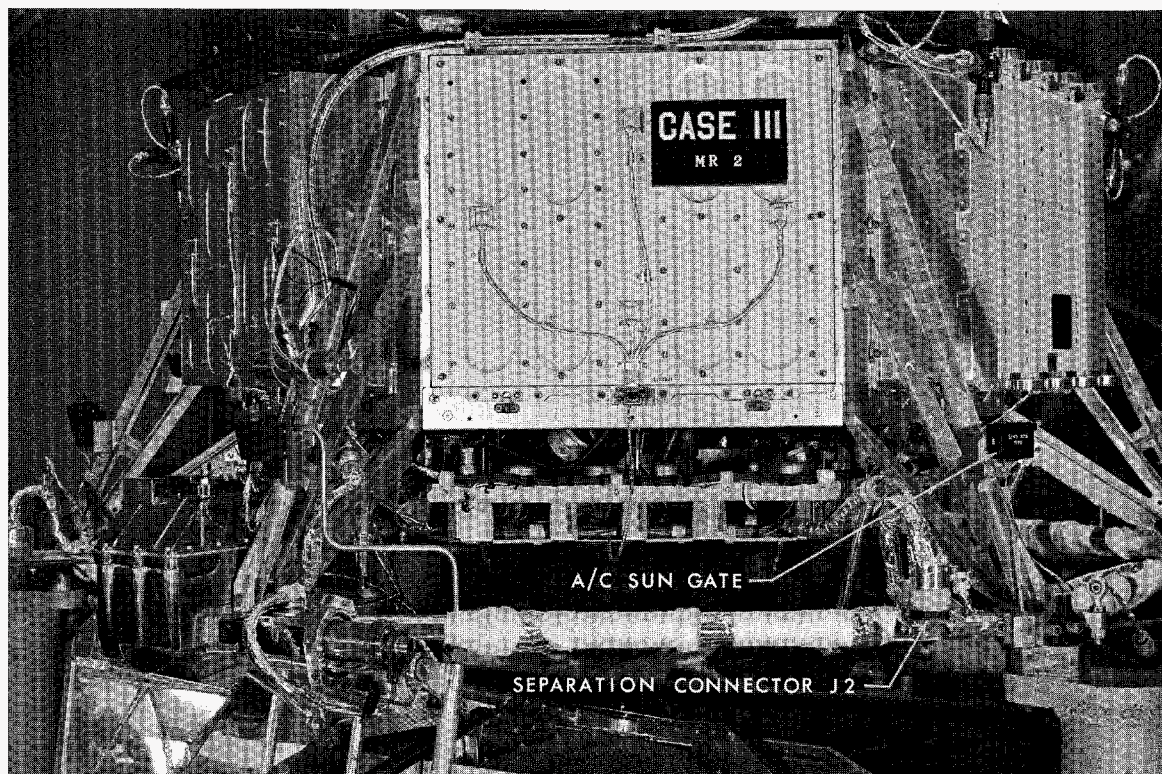


Fig. 166. Main hex bay cabling, showing Case III

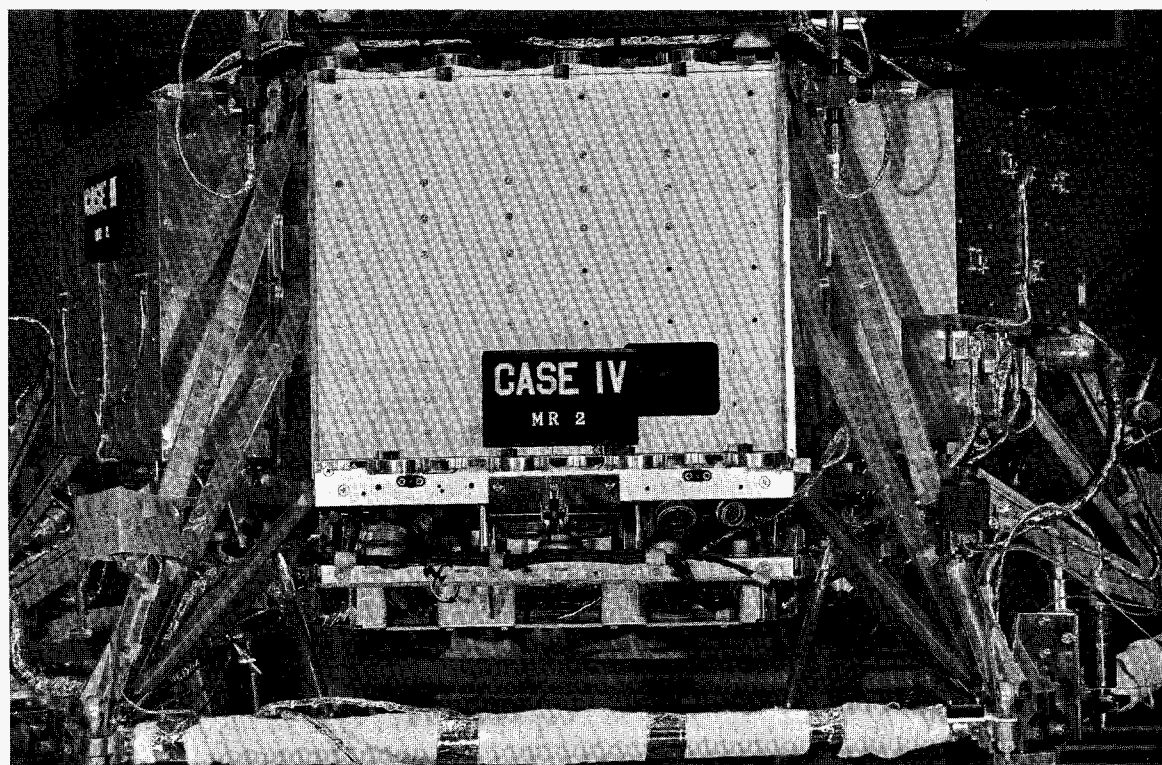


Fig. 167. Main hex bay cabling, showing Case IV



Fig. 168. Main hex bay cabling, showing Case V

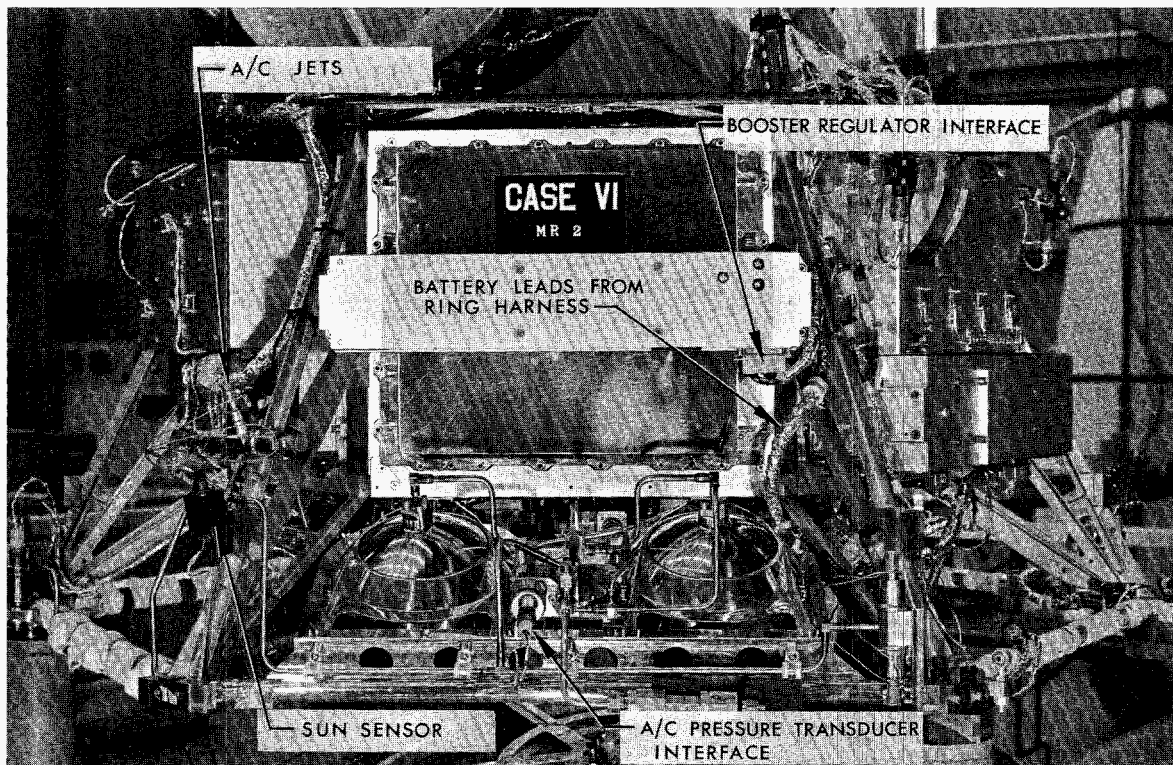


Fig. 169. Main hex bay cabling, showing Case VI

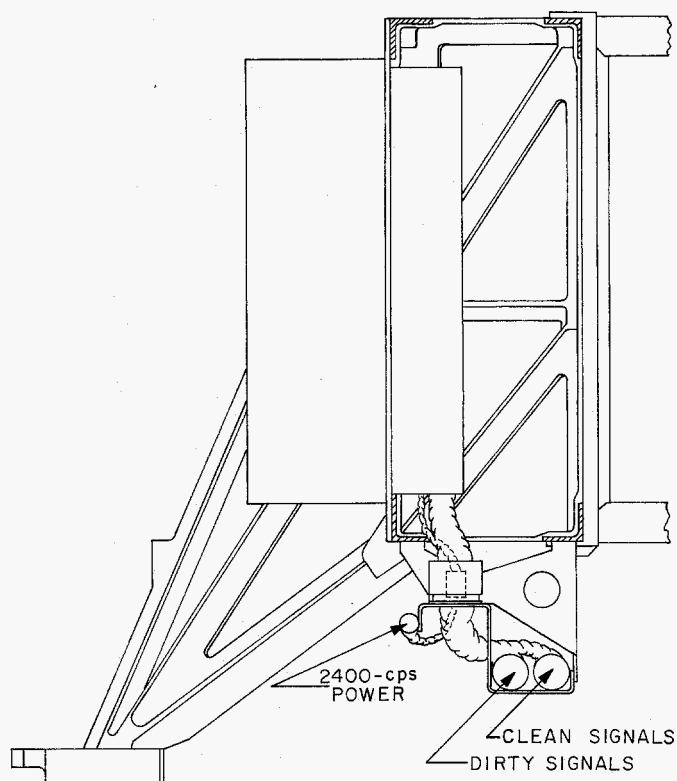


Fig. 170. Ring harness structure

to it (two as dropping resistors and two as a voltage-divided network), so the GSE could monitor the 2400-cps power. The d-c power return bus utilized a connector with the upper half of its pins bonded together with solder, which was sealed with potting compound. All of the power return wires were connected to the bottom half of the connector, providing a common point for all of the power returns. One wire from the bottom half of the connector was returned to spacecraft ground to ensure that the d-c power return would maintain the same potential as spacecraft ground. The access to this connector located on the ring harness structure was very poor. If it were disconnected and not reconnected, damage to the spacecraft could occur. However, this connector (Fig. 171) was accessible when the battery in Bay VI was removed.

The power switch and logic wiring shown in Fig. 164 was a separate harness because of the unique method in which this unit was packaged. Booster regulator and battery wiring were pigtailed from the ring harness. This wiring, shown in Fig. 169, was pigtailed because the case could not be hinged out from the structure. The power case wiring (Fig. 168) was a separate harness due to packaging techniques. This harness connected to the pyrotechnic control, 400-cps and 2400-cps power ampli-

fiers, battery charger, and the power sync. Two connectors were used to interface with this harness. The reason for the separate 2400-cps connector was so 2400-cps power could be maintained as an independent harness.

3. Electrical Design of the Ring Harness

This design was based on the categorizing of various signals into different groups of wire bundles in the ring harness and requiring all return lines to be independent of one another. These signals were divided into: (1) 2.4-kc power harness; (2) high-amplitude signals and relay closures; and (3) low-amplitude signals and digital pulses.

The 2.4-kc power harness has been discussed with the power system wiring. The high-amplitude signals and relay closures were grouped together and these were labeled as the "dirty" signals. The low-amplitude signals and digital pulses were grouped together and were referred to as the "clean" signals. This grouping was maintained throughout the ring harness and is shown in Fig. 170.

To maintain the philosophy of return lines previously mentioned, independent splices were used in the ring harness for signal and shield returns. Due to the number of return leads for both the signal return and the shield return, approximately three to four splices were used for each lead. Each of the return circuits was maintained independent of the others and one lead from each was returned to spacecraft ground.

4. Case Harness Wiring

Case harnesses were originally fabricated on a mock-up jig. These jigs were built as close to the actual dimensions of the flight case as possible. Figure 173 shows a CC&S case harness and its mock-up jig. Note that the two connectors at the bottom of the photograph interface into the ring harness. The smaller of the two connectors is the connector interface to the 2400-cps squarewave harness and is independent until it interfaces into the CC&S T-R unit. This procedure was adopted in all of the case harnesses. Figures 174 through 176 and Fig. 38 show the case harnesses assembled to the flight units.

5. Midcourse Motor Harnesses

The midcourse motor wiring was comprised of three separate harnesses: a squib harness, a telemetry harness,

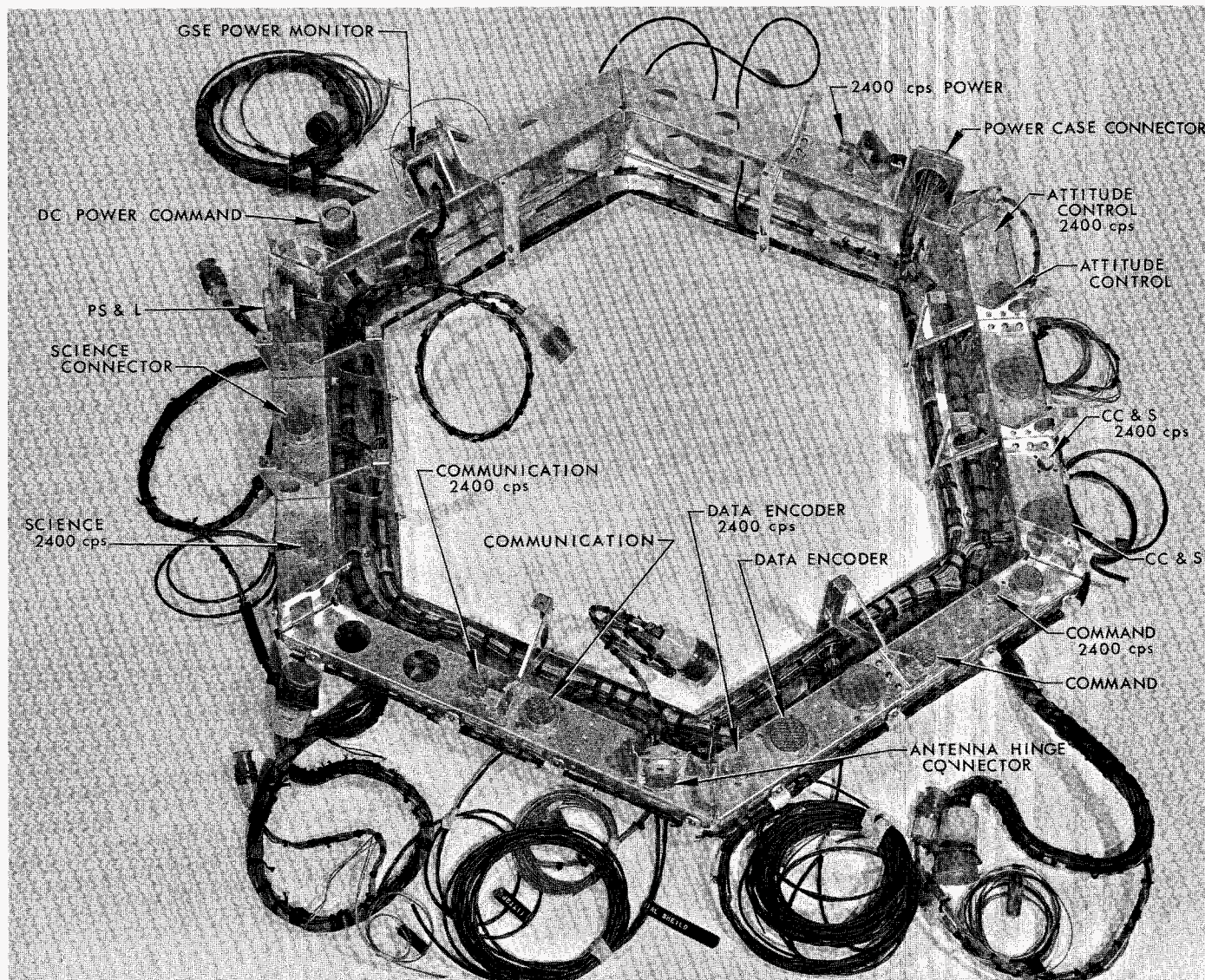


Fig. 171. Ring harness wiring installed in ring structure

and an actuator harness. The telemetry and the actuator harness interfaced into the ring harness. The signals were transmitted from the attitude control system and were routed to the data encoder system (whose case harnesses interfaced into the ring). The squib harness interfaced into the main pyrotechnic harness.

6. Pyrotechnic Harnesses

The main pyrotechnic harness is shown in Fig. 168. It originated in a Bendix connector and was routed below Case V interfaces into the squib harness of the midcourse motor. The portion that goes up the leg interfaces into the pin pullers for the radiometer and the solar panels.

The cylindrical-shaped part just to the right of the yaw jet in the lower left portion of the photograph is an arming switch. Another arming switch is placed 180 deg opposite on the other side of the spacecraft. One side of this switch is connected to the power switch and logic assembly (where battery current is monitored upon squib activation). The other side is connected to the pyrotechnic control. This wiring was routed through the ring harness since it was supplying battery voltage.

7. Attitude Control Wiring

The attitude control functions, such as the attitude control jets, primary Sun sensors, and Sun gate were

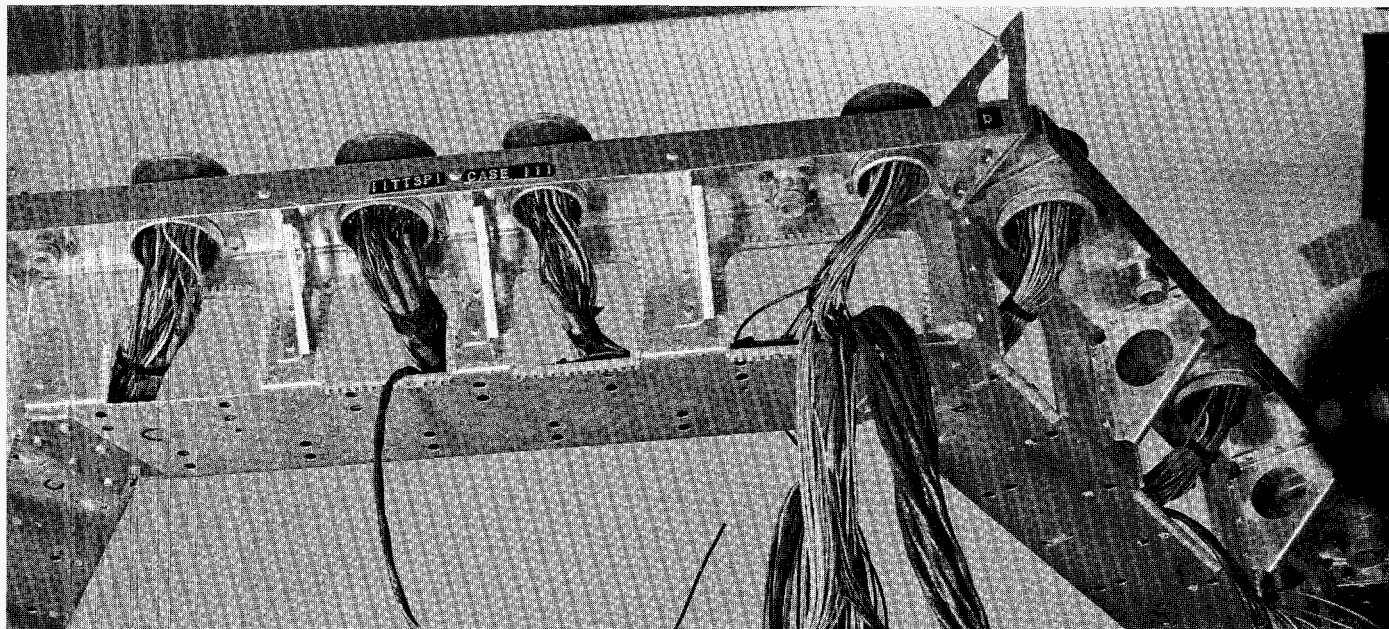


Fig. 172. Wire routed from ring harness to connectors

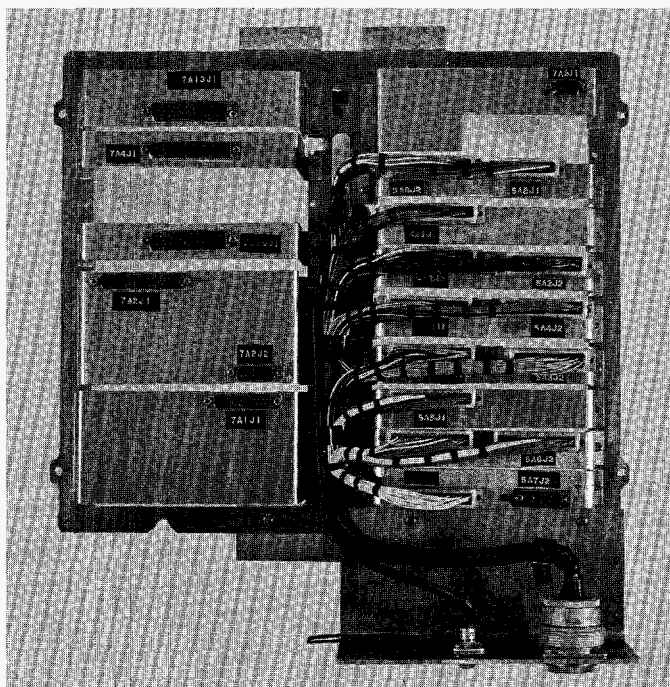


Fig. 173. CC&S case harness and mock-up jig

soldered at the respective component and wired directly to the interface with the ring harness. The pressure transducer on the nitrogen regulator was an exception, since it has a connector interface. The attitude control secondary Sun sensors were also an exception, since they were

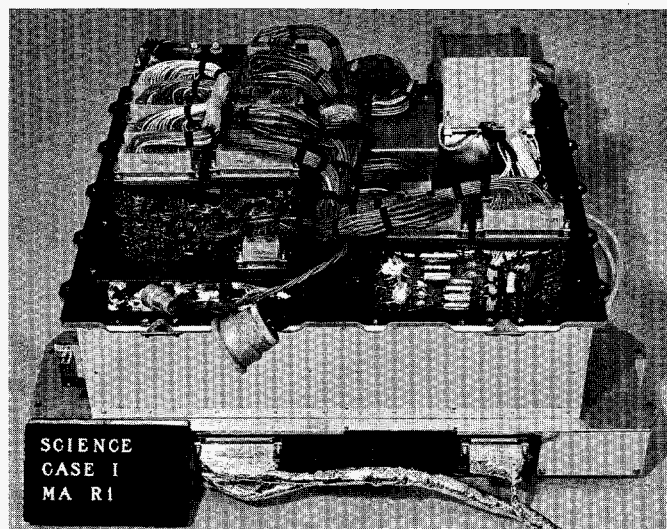


Fig. 174. Case harness assembled to Case I

located on the tips of the solar panels. The interface problem of the secondary Sun sensors is discussed below.

8. Solar Panel Interfaces

The solar panel interfaces consisted of the two connectors on each solar panel (one for power and one for attitude control plus telemetry functions). The power leads are routed from the solar panel to the power switch and



Fig. 175. Case harness assembled to Case IV

logic assembly by way of the ring harness. The attitude control and telemetry functions leads are routed to their respective case harness interfaces with the ring harness through the ring harness.

9. Motion Sensor Harness

The motion sensor harness carries the functions from the solar panel and radiometer pin puller (located on the upper structure) to permit blockhouse monitoring of pin-puller actuation. An interface was mandatory in this harness because the leads from the motion sensor terminate in the J1 separation connector. Without this interface, the upper structure could not be removed.

10. Separation Connectors

The separation connectors consisted of two Bendix connectors designated 9W1J1 (the "dirty" functions connector) and 9W1J2 (the "clean" functions). Both connectors were fabricated as a pigtail of the ring harness. The separation connectors carry the leads to and from the spacecraft to permit monitoring and operation while the vehicle is on the pad. The separation connector, 9W1J1, is shown in the lower left corner of Fig. 165.

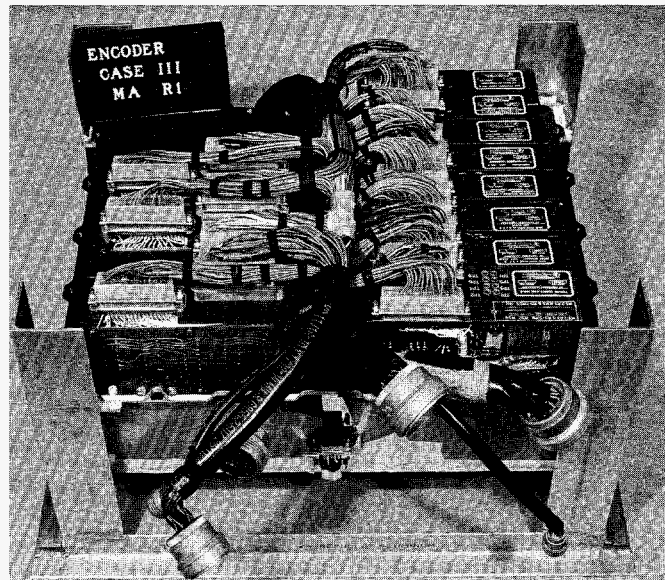


Fig. 176. Case harness assembled to Case III

11. Antenna Hinge Harness

This harness was designed with five connectors: (1) one connector interfaced into the ring; (2) one interfaced with the 2400-cps square-wave power harness; (3) one to the antenna yoke temperature; (4) one for the antenna actuator; and (5) one for the Earth sensor. A separate connector to the 2400-cps power maintained an independent harness and minimized coupling effects into the sensitive signals transmitted from the long-range Earth sensor.

12. Temperature Transducer Wiring for Electronics Cases

Temperature transducer wiring for the electronics cases on the main hex were pigtails from the ring harness, utilizing a 9-pin Cannon D connector as interface with the transducers on the case, with the exception of Case IV, which had a louver on it and required a 15-pin connector. A typical electronics case temperature transducer wiring configuration is shown in Fig. 168.

13. Upper Structure Wiring

This wiring consisted primarily of the scientific experiment harnesses and the main pyrotechnic harness previously discussed. An independent harness connected the fluxgate magnetometer with the magnetometer electronics. The other scientific experiments, such as the par-

ticle flux, cosmic dust, and radiometer, were connected with the scientific circuitry in Case I by a power harness and a signal harness.

14. Miscellaneous

All temperature transducer wiring was twisted-pair, shielded, and jacketed, since the signals were in the range 0-100 mv, and the wiring was then compatible with that furnished with the transducer.

All 2400-cps square-wave power harnesses were fabricated with shielded, jacketed, single-conductor cable, with power and return cables twisted together. This mechanization was derived from tests to determine minimal coupling effects on the square-wave power. The results of such testing showed that this fabrication technique reduced the coupling by a ratio of 5 to 1 (compared to twisted-pair, shielded, and jacketed wire).

15. Deutsch-to-Bendix Conversion

In the original *Mariner R* design, the interface between the ring harness and the assemblies were Deutsch connectors but, due to poor pin retention that caused an intermittent in one of the Deutsch connectors, it was believed that a change should be made. The Deutsch was replaced with the Bendix Pygmy series connector because of its better properties of pin retention as compared to the Deutsch. This conversion was performed on all three *Mariner R* spacecraft.

H. Propulsion

1. Introduction

The function of the *Mariner R* midcourse propulsion system is to remove or reduce *Agna B* injection dispersion errors so that a Venus flyby with sufficiently small miss distance can be reasonably assured. This function is performed during the single spacecraft midcourse maneuver (executed approximately 8 days after launch) when the spacecraft is directed to turn to a prescribed position in space and to impart a corrective impulse through the midcourse propulsion system.

During the initial design phase, it was decided to utilize the *Ranger* midcourse propulsion system design with a minimum of modification for the *Mariner R* mission. Initial design requirements called for a single-start 45 m/sec velocity increment capability to cover the expected 2.5σ launch vehicle dispersions. This velocity increment requirement was increased to the CC&S maximum capability of 61 m/sec at the time of *MR-1* midcourse propulsion system fueling at AMR.

Due to thermal control requirements, a permanent, multilayer, aluminized mylar radiation shield covering the upper portion of the basic hex structure was incorporated into the *Mariner R* spacecraft design. The inclusion of this shield resulted in a requirement for loading the propulsion system through the bottom of the hex instead of through the top, as in *Ranger*. The requirement for bottom loading, along with a requirement for an additional 1/2-in. propulsion system adjustment capability in the -Y direction, comprised the primary operational and interface changes over the *Ranger* midcourse propulsion system.

Ranger flight propulsion systems 5 and 5-spare were diverted from the *Ranger* program for modification and designation as *MR-1* and *MR-2* flight systems. The *MR-3* system was procured as an additional system in the *Ranger* follow-on program.

2. System Description

The *Mariner R* midcourse propulsion system comprises essentially the same 50-lb-thrust monopropellant hydrazine propulsion system developed for the RA-3, -4, and -5 spacecraft. Primary variations to the *Ranger* system consisted of the utilization of nitrogen instead of helium as the pressurizing medium to accommodate better the nominal 8-day launch-to-midcourse maneuver storage requirement; painting and surface finish changes consistent with *Mariner R* thermal control requirements; rerouting of the oxidizer-start tube to accommodate propulsion system loading through the bottom of the spacecraft; enlargement of the thrust plate mounting and adjustment slots to allow an additional 1/2-in. adjustment capability in the -Y direction; and the inclusion of dual-bridgewire, hermetically sealed squibs in place of the single-bridgewire *Ranger* squibs.

A schematic diagram of the propulsion system is shown in Fig. 177. Figure 178 depicts a flight system. The system utilizes a liquid monopropellant, anhydrous hydrazine as

COMPONENTS

- 1 ROCKET ENGINE
- 2 IGNITION CARTRIDGE GN_2 FILL VALVE
- 3 IGNITION CARTRIDGE GN_2 RESERVOIR
- 4 IGNITION CARTRIDGE ACTUATION VALVE
- 5 IGNITION CARTRIDGE OXIDIZER RESERVOIR
- 6 IGNITION CARTRIDGE BURST DIAPHRAGM
- 7 SHUTOFF PROPELLANT VALVE
- 8 START PROPELLANT VALVE
- 9 PROPELLANT TANK FILL VALVE
- 10 PROPELLANT TANK
- 11 PROPELLANT TANK BLADDER
- 12 PROPELLANT TANK PRESSURIZATION VALVE
- 13 HELIUM PRESSURE REGULATOR
- 14 HELIUM FILTER
- 15 HELIUM START VALVE
- 16 HELIUM TANK FILL VALVE
- 17 HELIUM TANK
- 18 VISUAL PRESSURE GAGE, 0-4000 psi
- 19 VISUAL PRESSURE GAGE, 0-500 psi
- 20 PROPELLANT FILL BLEED
- 21 HELIUM SHUTOFF VALVE

INSTRUMENTATION

PRESSURE

- (P₁) NITROGEN TANK
(P₂) PROPELLANT TAN






PRESSURE MONITORING GAGES





- (G₁) NITROGEN TANK
- (G₂) PROPELLANT TANK
- (G₃) IGNITION CARTRIDGE RESERVOIR

TEMPERATURE

- (T₁) PROPELLANT TANK
- (T₂) NITROGEN TANK

SYMBOLS

-  TWO-WAY VALVE, EXPLOSIVELY OPERATED
 ANGLE VALVE, MANUALLY OPERATED
 BURST DIAPHRAGM
 FILTER
 PRESET REGULATOR

- | | |
|---|-------------------------|
|  | VISUAL PRESSURE GAGE |
|  | COMPONENT NUMBERS |
|  | INSTRUMENTATION NUMBERS |
|  | CAPPED TUBE END |

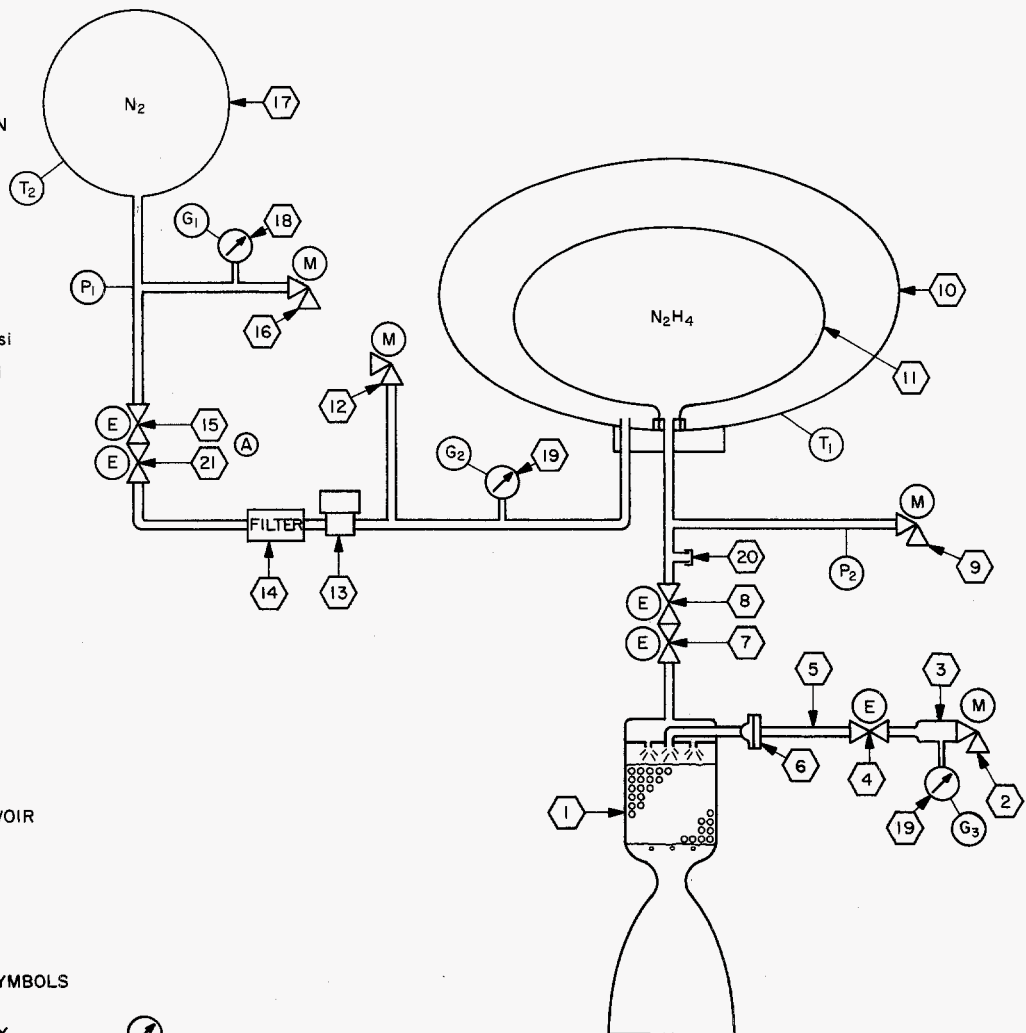


Fig. 177. Mariner R midcourse propulsion system, schematic diagram

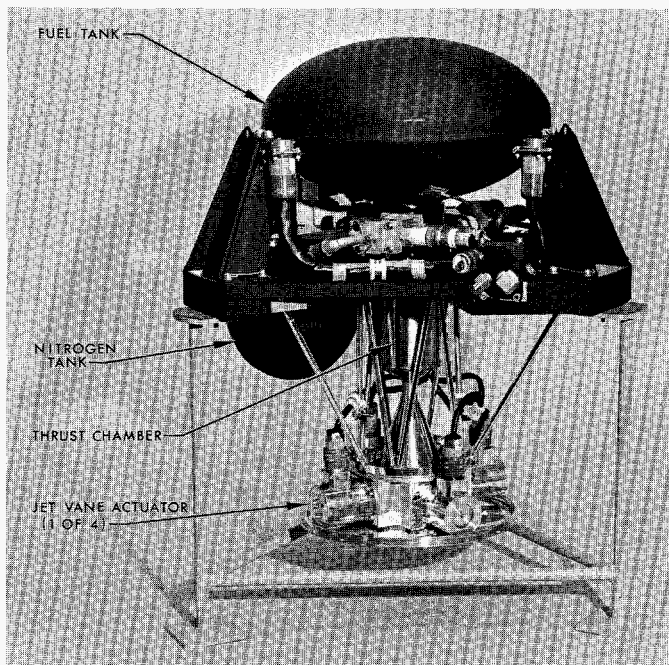


Fig. 178. Mariner R flight propulsion system

the propellant. It is functionally a regulated gas pressure-fed, constant-thrust rocket. Principal system components consist of a high-pressure gas reservoir, a gas-pressure regulator, a propellant tank, and a rocket engine. The rocket engine contains a quantity of catalyst to accelerate the decomposition of hydrazine. The engine nominally develops a vacuum thrust of 50 lb and a vacuum specific impulse of 235 lb-sec/lb (without jet vanes).

Explosively actuated valves are used throughout the system. Normally closed, explosively actuated valves are fired to initiate nitrogen pressurization of the propellant tank, to initiate propellant flow to the rocket engine, and to release nitrogen tetroxide from the engine ignition cartridge. Normally open, explosively actuated valves are fired to terminate nitrogen pressurization of the propellant tank and propellant flow to the rocket engine.

The design and operational philosophy of the system represented in Fig. 177 are directed toward maximizing system reliability and reproducibility, minimizing preflight handling and spacecraft interactions, minimization of inflight electrical signals, and minimization of the number of system components. In order to avoid electrical or mechanical sequencing, the propellant tank is prepressurized with nitrogen during the preflight operation so that engine ignition and regulated nitrogen pressurization of the propellant tank can occur simultaneously through one signal from CC&S. Similarly, only one signal

is necessary for thrust termination; therefore, only two signals are required by the midcourse propulsion system for impulse initiation and termination.

The propulsion system can be fueled and pressurized several weeks prior to launch and emplacement within the spacecraft. The system in the pressurized and fueled condition is safe for personnel to work around over the temperature extremes of 35 to 165°F. No spacecraft umbilicals or hard-lines are required to maintain the propulsion system in the ready condition.

The system is installed in the spacecraft through the bottom of the basic hex structure by hand, and mounts on three pads which are slotted to allow relative movement between the mounting bolts and propulsion system thrust plate for location of the thrust vector. The propulsion system, i.e., thrust vector, can be adjusted ± 1 in. in the X direction and $+1$, -1.5 in. in the Y direction about the spacecraft roll axis.

The firing of the midcourse propulsion system is controlled by the CC&S. For midcourse maneuver, the CC&S receives the time, direction, and magnitude of the midcourse firing through the ground-to-spacecraft communications link. After the spacecraft has assumed the correct firing attitude, the midcourse propulsion system is ignited (at the prescribed time) through an electrical signal from the CC&S. Inasmuch as the propellant tank is prepressurized, the rocket engine ignition can occur concomitantly with the release of the high-pressure nitrogen to the regulator without allowing time for the propellant tank pressure to build up to the normal operating level. Thrust termination is controlled from the CC&S by an electrical signal once the specified velocity increment has been realized, as computed by the spacecraft integrating accelerometer. During the rocket engine firing, spacecraft attitude is maintained by the autopilot-controlled jet vane actuators.

The specific sequence of events for the propulsion system subsequent to spacecraft orientation and up to thrust termination is as follows:

- (1) At the command signal from the CC&S to ignite the rocket, normally closed explosive valves $\textcircled{15}$ ³, $\textcircled{8}$, and $\textcircled{4}$ are fired, allowing regulated nitrogen pressurization of the propellant tank, propellant flow to the rocket engine, and injection of a small quantity of nitrogen tetroxide to the rocket engine.

³ Refer to Fig. 177.

- (2) Hypergolic ignition occurs, followed by continuous catalytic monopropellant decomposition of the anhydrous hydrazine.
- (3) At the command signal from the CC&S to terminate rocket thrust, normally open, explosively actuated valves (7) and (21) are fired, terminating propellant flow to the rocket engine and positively isolating the remaining pressure in the nitrogen sphere from the propellant tank.

3. Performance Capabilities

The *Mariner R* midcourse propulsion system develops, nominally, 50 lb of vacuum thrust and a vacuum specific impulse (without jet vanes) of 235 lb_r-sec/lb_m. Table 15 summarizes the major engine performance characteristics of the monopropellant engine and jet vane system, and Table 16 represents a weight breakdown of the propulsion system.

A relatively important consideration in the determination of the velocity increment capability of the propulsion

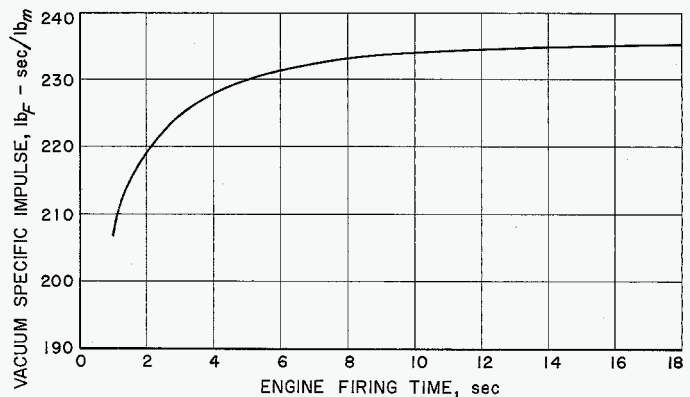


Fig. 179. Vacuum specific impulse engine vs engine firing time

system is the fact that the engine requires, roughly, 30 sec to achieve nominal steady-state operation and temperature. The specific impulse degradation during the start transient should, therefore, be considered when computing the maximum capabilities of the system. Figure 179 depicts a nominal start transient for the 50-lb-thrust engine.

The specific impulse degradation during the start transient can be accounted for in a number of ways; however, for ease of velocity increment or propellant load computations, it appears that a comparable steady-state propellant load value to compensate for the below-normal impulse propellant burning during the start transient can be used to ease the computation. Evaluation of the propellant needed to compensate for the start transient impulse degradation results in a value of approximately 0.09 lb. Therefore, in order to determine the propellant needed to propel the spacecraft with a specific velocity increment, 0.09 lb of propellant was added to the value obtained from the momentum exchange relationship. Also, an additional 0.16 lb of propellant has been added

Table 15. Nominal performance summary

Parameter	Value
Vacuum specific impulse, $I_{s_{vac}}$ (without jet vanes) ^a	235.05 $\frac{\text{lb}_r - \text{sec}}{\text{lb}_m}$
Vacuum specific impulse, $I_{s_{vac}}$ (jet vanes (4) deflected 10 deg) ^b	231.71 $\frac{\text{lb}_r - \text{sec}}{\text{lb}_m}$
Vacuum thrust, F_{vac} (without jet vanes) ^a	50.71 lb _r
Vacuum thrust, F_{vac} (jet vanes (4) deflected 10 deg) ^b	50.00 lb _r
Vacuum thrust coefficient, $C_{F_{vac}}$ ^c (without jet vanes) ^a	1.7558
Characteristics velocity, c^* ^c	4306 fps
Flow rate, \dot{w}_p	0.21574 lb _m /sec
Throat area (ambient) A_t	0.15 in. ²
Stagnation chamber pressure, p_c ^c	189.1 psia
Expansion ratio, e	44:1
Specific heat ratio, γ	1.28
Maximum thrust vector deflection capability (jet vanes (2) deflected 25 deg)	± 5.5 deg

^aJet vane drag in null position is negligible; therefore, null position engine data and engine data without jet vanes are essentially equal.

^bJet vane maximum deflection capability equals 25 deg, but expected *Mariner R* maximum steady-state deflection is on the order of 8 to 10 deg.

^cBased on actual steady-state hot throat area (1.82% larger than ambient cold throat area).

Table 16. Propulsion system weight breakdown

Item	Weight, lb
Dry unserviced propulsion system weight	21.07
Nominal ^a propellant load N ₂ H ₄ (including reserves)	12.22
Nitrogen (including N ₂ in the following: N ₂ tank, propellant tank, and start cartridge)	0.85
Oxidizer, N ₂ O ₄	0.04
Cabling	1.51
Jet vane actuators (4)	2.01
Pyrotechnics	0.41
Total propulsion system weight	38.11

^aBased on 61 m/sec velocity increment requirement and 446-lb spacecraft.

to the calculated propellant to allow for reserves and propellant holdup in the expulsion bladder and lines; therefore, the propellant load value of 12.22 lb shown in Table 16 includes 0.25 lb for start transient compensation, holdup, and reserves.

Data from 10 midcourse engine firings were analyzed to determine the magnitude of the impulse imparted to the spacecraft subsequent to the engine shutoff command from the accelerometer. These tests were conducted in a near-vacuum environment at the facility of the Sundstrand Corporation in Pacoima, California. In order to understand better and predict the magnitude of the tail-off, the total tailoff impulse I_T can be divided into two parts, as shown in Fig. 180. Part of the impulse I_1 is caused by delays in the circuit which fires the fuel shutoff valve, while the remainder of the tailoff impulse I_2 is due to propellant, trapped between the fuel shutoff valve and the engine, being expelled after engine shutoff has occurred. The magnitude of each contributing factor and the total tailoff impulse are summarized below:

$$I_1 = 0.43 \pm 0.23 \text{ lb-sec}$$

$$I_2 = 6.79 \pm 2.4 \text{ lb-sec}$$

$$I_T = 7.22 \pm 2.63 \text{ lb-sec}$$

For a 450-lb spacecraft, this tailoff impulse corresponds to a velocity increment of $0.158 \pm 0.057 \text{ m/sec}$.

The components contributing to the delays in the fuel shutoff valve firing circuit and their errors are as follows:

- (1) Delay in the CC&S: $3 \text{ msec} \pm 2 \text{ msec}$
- (2) Delay in the pyrotechnic control box: $1.3 \text{ msec} \pm 0.2 \text{ msec}$
- (3) Delay in the squib firing: $4.2 \text{ msec} \pm 2.3 \text{ msec}$.

Summing up the delays and arithmetically summing the errors gives a tailoff impulse due to the circuit delays in firing the fuel shutoff valve of $0.43 \pm 0.23 \text{ lb-sec}$.

The tailoff impulse due to the trapped propellant being expelled after engine shutoff was determined from the engine vacuum tests by numerically integrating the area under the engine stagnation chamber pressure versus engine firing time curve from the start of chamber pressure decay to 0 psia. A typical test curve is shown in Fig. 180. Upon multiplying this area by the engine thrust

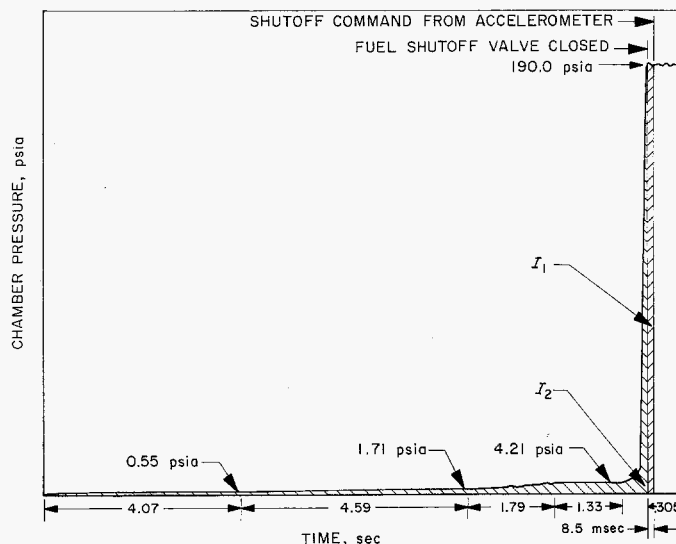


Fig. 180. Chamber pressure decay vs time

coefficient and throat area, the tailoff impulse is obtained since

$$I_2 = \int_0^t F dt = C_F A_t \int_0^t p_c dt$$

where

I_2 = tailoff impulse, lb-sec

F = engine thrust, lb

C_F = engine thrust coefficient

A_t = engine throat area, in.²

p_c = engine stagnation chamber pressure, psia

t = time, sec

Reduction of data from 10 tests gave an average tailoff impulse subsequent to engine shutoff of 6.79 lb-sec. The average time over which the tailoff occurred was 12.1 sec. Note, however, that the initial decay is exponential and occurs rapidly, while the remainder of the decay occurs at a low pressure over a relatively long period of time. The pressure transducer measuring chamber pressure is accurate to $\pm 0.75 \text{ psi}$. Thus, the reduced data should be accurate to $\pm 2.4 \text{ lb-sec}$.

The maximum velocity increment capability of the midcourse propulsion system, as limited by the propellant tank capacity (13.5 lb), for a 450-lb spacecraft is 66.7 m/sec. Since the CC&S velocity increment capability

is limited to 61 m/sec, the *MR-1* and -2 propulsion systems were fueled consistent with the 61 m/sec requirement. The minimum velocity increment capability of the propulsion system is limited by the firing delays (in this case, shutoff delays) and the propulsion system tailoff. The minimum velocity increment resolution capability of the CC&S is 0.03 m/sec, and this velocity increment must be added to the system shutoff delays and thrust decay velocity increment. This addition results in a total minimum velocity increment capability (450-lb spacecraft) of 0.19 m/sec.

4. Development Program

Most of the development work on the *Mariner R* mid-course propulsion system was conducted during the *Ranger* program and has been reported in Ref. 1 and 2.

In addition to that work, a flight-weight propulsion system with solenoid valves in place of the explosive valves was thoroughly tested at ambient test cell conditions over the *Mariner R* design limits. Figure 181 depicts the test cell setup. A 4:1 flight-weight engine in lieu of a 44:1 flight engine was used for the ambient tests. Ten hot firings were conducted with propellant tank pre-pressurization levels ranging from 0 to 550 psig, oxidizer-start cartridge pressures ranging from 327 to 415 psig, and oxidizer (N_2O_4) injection quantities of 18 cc and 12 cc. Successful ignitions and steady-state operation were realized for all 10 firings. It is interesting to note that successful engine ignitions with simultaneous actuation of all valves (no sequencing) can be accommodated with propellant tank pre-pressurization levels as low as 0 psig and as high as 550 psig, and with injected oxidizer quantities of 12 cc and 18 cc. It appears that the bi-propellant ignition scheme for the *Mariner R* engine is not critically affected by N_2H_4 injection pressure, N_2O_4 injection pressure, and quantity of injected N_2O_4 . System operation with the nitrogen pressurizing medium was wholly satisfactory during the course of system testing.

Ranger propulsion systems RA-5 and RA-5-Spare were diverted from the *Ranger* program and modified for use on the *MR-1* and -2 spacecraft. In addition, a third system was fabricated in conjunction with the *Ranger* follow-on program to be used as a spare system for *Mariner*, and the flight-weight test system was modified consistent with *Mariner R* temperature-control requirements for use in the temperature control model spacecraft. All flight thermal control features (surface finishes, etc.) were duplicated on the test unit, and 9 lb of water

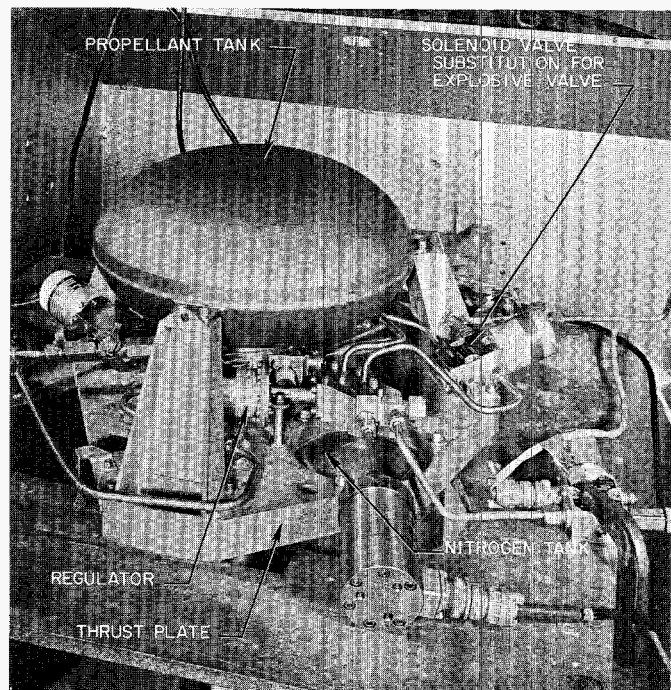


Fig. 181. Flight-weight system test-cell setup

were placed in the fuel tank to simulate the propellant thermal load during the course of the TCM tests.

During engine qualification testing utilizing the new dual-bridgewire squibs in the engine-start and shutoff explosive valves, local yielding and in some cases rupturing of the normally closed explosive valve trigger assembly were witnessed. In the cases where rupturing occurred, the normally closed valves failed to operate. These failures were attributed to the different pressure-time characteristic of the dual-bridgewire squib compared with the single-bridgewire squib originally designed for the system. It should be mentioned, however, that the trigger assembly would probably not have ruptured had the assembly been torqued properly at installation. With correct torquing, the units appeared only to yield. In order to relieve this problem, it was decided to thicken the walls of the trigger assembly to withstand better the over-pressure condition and assure successful valve actuation. The new assemblies, with additional wall thickness in the pressure vessel cavity of the trigger assembly, solved the problem and no further valve failures were noted during the course of the development program.

Because of the relatively long period between *Mariner R* launch and midcourse correction (approximately 8 days) during which the propulsion system will see a hard vacuum, it was decided to replace the original *MR-1*

and -2 regulators, which were lubricated upon assembly with Hercules lubricant No. 2031, with regulators utilizing essentially no lubricant. Satisfactory regulation was achieved during testing with regulators whose moving and critical surfaces were silver plated and utilized no additional lubrication. It was expected that the dry regulators and their regulation characteristics would be relatively unaffected by the 8-day hard-vacuum storage from launch to midcourse correction; whereas, the original lubricated regulators would undergo friction changes, and therefore, regulation changes, due to lubrication boiloff. Dry regulators were then successfully flight-acceptance tested and retro-fitted on the *MR-1* and -2 flight propulsion systems.

The three flight systems were delivered to the Spacecraft Assembly Facility following final jet vane alignment operations, and installed in their respective spacecraft. Propulsion system transducer and telemetry calibrations were conducted during the spacecraft testing at JPL. The three flight propulsion systems were leak-tested prior to shipment to AMR; they were shipped in June, 1962, installed in the spacecraft.

5. AMR and In-flight Operations

Upon arrival at AMR, the midcourse propulsion systems were subjected to a leak-test of all fittings. The two flight propulsion systems successfully passed the test. Several leaks were noted in the *MR-3* nitrogen tank fitting, to which is attached the nitrogen tank, nitrogen tank pressure transducer, and the nitrogen tank explosive valves. The high-pressure circuit was disassembled and the fittings were examined in detail. Several scratches were noted on the faces of fittings against which O-rings must seal. The fittings were polished and the propulsion system was reassembled. Another leak-check of the system revealed no leakage, and it was considered flight-worthy. It should be noted that the high-pressure gas circuits were leak-checked with helium and "Snoop Leak Detector," thereby representing a stringent leak check and assuring a leak-tight circuit suitable for nitrogen service.

During the course of the AMR spacecraft systems, pre-countdown, JFACT and other testing, the propulsion system telemetry measurements were monitored and checked out. The propellant tanks were pressurized (both sides of the bladder) to 150 psig and the nitrogen tanks were pressurized to 1000 psig for most of these tests to provide a finite binary read-out on the propulsion telem-

etry channels. During the *MR-3* spacecraft systems test, it was noted that the propellant tank pressure telemetry channel was reading a zero binary count. Subsequent investigation revealed that the pressure transducer was faulty and it was replaced. Other than the *MR-3* propellant tank transducer failure, no further discrepancies were noted on the three propulsion systems during the tests.

The *MR-1* propulsion system was fueled and pressurized on July 12, 1962. The *MR-1* unit was fueled with 12.24 lb of hydrazine to provide a 61 m/sec velocity increment capability to the 446.6-lb spacecraft and pressurized to 2990 psig in the nitrogen tank, 300 psig in the fuel tank, and 350 psig in the oxidizer-start cartridge. These pressures remained constant up to and through launch on July 21, 1962. Note that, based on telemetry data, the *MR-1* propulsion system remained leak-tight and apparently suffered no damage during the boost phase up to the time of vehicle destruct by range safety.

The *MR-2* propulsion system was fueled and pressurized on June 6, 1962. The system was fueled with 12.28 lb of hydrazine to provide a 61 m/sec velocity increment capability to the 447.7-lb spacecraft and pressurized to 3000 psig in the nitrogen tank, 275 psig in the fuel tank, and 350 psig in the oxidizer start cartridge. The pressures remained constant up to the time the propulsion system was installed in the spacecraft on July 14, 1962. The *MR-2* spacecraft remained in a flight-steady backup condition through the *MR-1* launch; however, no telemetry data were taken during this period and, consequently, no pressure data were available.

When the propulsion system was removed from the *MR-2* spacecraft on July 23, 1962, it was noted that the fuel tank pressure had dropped to 0 psig. Subsequent leak checks and evaluation indicated that the beryllium copper diaphragm in the nitrogen regulator was leaking and had allowed the propellant tank to vent down. The regulator was replaced and the tank again pressurized to 285 psig. It is interesting to note that the original regulator, with a bad diaphragm, functioned within tolerance when tested under flow conditions and that, based on previous system-test work, the *Mariner R* propulsion system will undergo satisfactory ignition and steady-state operation with an initial tank pressure of 0 psig. It is, therefore, concluded that the *MR-2* propulsion system would have successfully accomplished a mid-course engine firing had it been flown with the apparent failure. Inspection of the beryllium copper diaphragm

[REDACTED]

UNCLASSIFIED

JPL TECHNICAL REPORT NO. 32-353

revealed a tear at the diaphragm convolution where the diaphragm flexes during normal operation, and some discoloring due to N_2H_4 vapor attack. As a result of the vapor attack and the nature of the diaphragm failure, a 17-7 PH diaphragm with an aluminum gasket (both materials are compatible with N_2H_4) was installed on a regulator and flight-acceptance tested. This regulator, with the stronger and compatible diaphragm, was then shipped to AMR and installed on the MR-3 propulsion system. As a result of a propellant-tank pressure rise which started to occur roughly 1 mo after the MR-2 unit was initially fueled, and the fact that the MR-3 propulsion system was equipped with an improved regulator, the MR-3 propulsion system was fueled and pressurized on August 11, 1962, for utilization in the MR-2 spacecraft.

The MR-3 propulsion system was fueled with 12.28 lb of hydrazine to provide a 61 m/sec velocity increment capability to the 447.7-lb spacecraft, and pressurized to 3020 psig in the nitrogen tank, 285 psig in the fuel tank, and 365 psig in the oxidizer-start cartridge. The pro-

pulsion system pressures remained constant during the succeeding 3-day monitoring period, and the propulsion system was installed in the spacecraft on August 13, 1962. After installation, and during the 13-day period up to MR-2 launch, a fuel tank pressure rise of roughly 3 psig per day was witnessed and recorded by telemetry. It was believed that the pressure rise was not excessive, would not jeopardize the engine operation at mid-course, and would possibly level out with time; a decision was therefore made to fly the system with an elevated propellant tank pressure.

With reference to the propellant tank pressure rise noted in both the MR-2 and -3 propulsion systems, it is believed that an incompatibility exists between the N_2H_4 and the particular butyl compound employed in the propellant bladder. The possible incompatibility is being investigated further and tests are being conducted to determine what incompatible constituents are present in the butyl compound used in the propellant bladders. Early results indicate that there is a wide batch-to-batch variation in compatibility with hydrazine.

[REDACTED]

UNCLASSIFIED

UNCLASSIFIED

03/10/2018

UNCLASSIFIED

03/10/2018

1/1

UNCLASSIFIED

JPL TECHNICAL REPORT NO. 32-353

VI. Spacecraft Assembly and Launch Operations

1. Introduction

Prior to launching, the *Mariner R* spacecraft were subjected to a number of preflight operations at JPL-Pasadena, and at the Atlantic Missile Range. This section reviews the test philosophy and preflight preparations involved in the *Mariner R* (1962) Project.

2. Supporting Personnel

One Test Direction Team was assigned to each of the two flight spacecraft (*MR-1* and *-2*). Each team consisted of JPL system representatives for each of the major spacecraft subsystems, and included a Test Director, Guidance and Control, Telecommunications, Mechanical, and Science representatives, in addition to a system test engineer and a technician. The divisions supplying spacecraft components or subassemblies such as space science experiments, propulsion components, superstructure, etc., also supported the operations. Some divisions employed

contractor personnel who worked with the JPL test teams and cognizant engineers; other divisions supplied JPL personnel. In keeping with the requirement that JPL maintain control of all operations, the system representatives on the test direction teams were all JPL personnel.

A strict personnel discipline was enforced during the *Mariner R* operations. Only designated persons were permitted to work with the spacecraft. All operations on the spacecraft were performed with detailed procedures and by qualified persons responsible for the spacecraft flight components. Discipline was enforced to ensure that spacecraft integrity was not jeopardized by personnel error, and to further guarantee fulfillment of the spacecraft mission.

3. Test Philosophy

The intent of the spacecraft operations was to reach the respective launch periods with two spacecraft in

UNCLASSIFIED

UNCLASSIFIED

flight-ready condition. The limited *Mariner* development time prohibited a proof-test model program, so the pre-launch operations were also required to verify adequacy of spacecraft system design, as well as flight readiness.

The absence of a PTM also required careful observation and reporting of any deviations or abnormalities in spacecraft functional checkout. At all times, problems had to be recognized, resolved, and corrected to produce flightworthy spacecraft. Test procedures were diligently followed to preclude damage to the spacecraft. All subsystem testing not requiring the spacecraft system environment were performed isolated from the spacecraft.

All calibrations, implementation of Engineering Change Requests, inspections, and special tests were to be completed before shipment from Pasadena. The only exceptions were the solar panel extension hardware change and a few scientific instrument calibrations that had to be scheduled for AMR. At the completion of the JPL final system test, the spacecraft were considered flightworthy by all cognizant personnel and were shipped to AMR on schedule.

Both spacecraft, after arriving at AMR, were again system-tested. If these test results had been the same as at JPL, the spacecraft would have been put in storage until the on-pad checkouts. The *MR-1* spacecraft did not pass the first system test, however, and had to complete four such tests before it was approved for flight. The *MR-2* spacecraft was sent to the ESA for early storage after successfully completing its first system test at AMR. A total of 50 failure reports were issued at AMR, indicating that the equipment prevented these test objectives from being completely met.

4. Test Data Reduction

The *Mariner R* Project used a new concept in test data reduction. Rather than only one printer in the System Test Complex for all subsystem and system test data, several printers were used. They were located throughout the test complexes and made a complete real-time evaluation of spacecraft performance possible. The subsystem personnel were also requested to evaluate all system-test data thoroughly. In some cases, however, it was later discovered that the data from various JPL tests had not been studied carefully enough and certain important read-outs had been overlooked.

A computer data processing system was developed during prelaunch test operations to achieve two advantages:

- (1) To present the test data in a better format to allow a more thorough and quicker evaluation.
- (2) To verify the computer program for flight-time operation.

The first potential advantage was not fully realized. The computer process was useful, but did not read back in time for immediate evaluation. Recommendations have been made to overcome this difficulty. The second benefit of the computer program was achieved.

Reviews of the test data indicate that some of the problems occurring late in the program had existed throughout the operations. These problems would indicate that the procedures and test plans should be reviewed and modified. As an example, the dummy-run test was not carried out far enough into the spacecraft flight operations to indicate a potential r-f interference problem. The interference was discovered during ESA spacecraft flight preparations.

5. Assembly and Test Operations (JPL)

The preflight operations performed at JPL-Pasadena are specified in this Section. See Fig. 16 for operations schedules, beginning with the system test.

a. Spacecraft hardware delivery. Most of the flight hardware was delivered to the SAF on schedule. Difficulty was encountered with hardware delivered on time, but which, due to failures, had to be returned to the responsible division for repair. Such delays sometimes jeopardized the established operations schedules and had to be compensated for by rescheduling of tests. Examples of these delays were:

- (1) Connector changes were required in the main cable harness for reliability considerations.
- (2) All temperature transducers were also replaced twice when the first two sets supplied were found to be unreliable.

b. Quality control operations. All hardware delivered to SAF was inspected by the Quality Control Group. Mechanical inspection and microscopic examinations were performed. Accurate records of all inspections were kept by quality control personnel. All failures and all modifications were recorded. A failure report system

UNCLASSIFIED

unique with *Mariner R* spacecraft was used. The failure reports were used to simply indicate any items requiring attention, whether the item was a discrete equipment failure or an observation of some electrical phenomenon observed during a test. A total of 231 such failure reports were issued during *MR-1*, -2 and -3 operations at JPL and AMR. Table 17 presents a compilation of these reports. See Section VIII of this Report for a more complete discussion of the quality control program.

c. Spacecraft assembly. Assembly operations were performed in the SAF at Pasadena, beginning in January 1962. The mechanical assembly was supervised by the Mechanical Design representatives of the JPL Test Direction Team. Support was also given by the Mechanical Design Division representatives. The *MR-3* spacecraft was assembled just before shipment of *MR-1* and -2 to AMR. This spacecraft consisted of flightworthy spares assembled to provide a test-evaluation vehicle.

d. Ground integrity checks and initial power turn-on. A System Test Complex, consisting of the GSE, the GSE spacecraft handling fixture, and cabling was assembled for the subsystems and system tests on *MR-1* and -2. Each spacecraft was assigned a separate test complex. Upon completion of complex setup, ground and wiring integrity checks were performed on the GSE and spacecraft to eliminate all ground loops that might exist and cause false indications. These checks were made prior to initial power application to the spacecraft to avoid the needless noise problem investigations that generally occur in a new system.

The first power turn-on was accomplished by a step-by-step procedure to avoid possible damage to the spacecraft, which was mounted on the system test fixture to verify proper interconnecting circuitry. The power output of the GSE was measured at the input to the spacecraft power subsystem. The connectors on the spacecraft ring harness were checked to see that the power supply and spacecraft harness provided the required voltages and currents before connecting the representative subsystems.

e. Subsystem tests. After the power system verification, specific and comprehensive testing of all spacecraft subsystems was undertaken. The spacecraft configuration was maintained as for the initial power turn-on, except that the spacecraft cable harness assemblies were connected to form a complete electrical system. The spacecraft electrical system was connected to the test equipment in the SAF System Test Complex. During subsystem

Table 17. Failure report summary, *MR-1*, -2, and -3^a

System	Number of failure reports		
	MR-1	MR-2	MR-3
Science	29	19	7
Communications	8	9	4
Command	3	4	1
Data encoder	18	8	0
CC&S	4	12	4
Attitude control	15	10	5
Power	8	7	4
Battery	3	1	0
Spacecraft wiring	25	12	1
Mechanical	7	2	1
Total failure reports by system			
Science	55		
Communications	21		
Command	8		
Data encoder	26		
CC&S	20		
Attitude control	30		
Power	19		
Battery	4		
Spacecraft wiring	38		
Mechanical	10		
Total	231 for MR-1, -2, -3		

^aThe table includes failures beginning with spacecraft assembly; it does not include failures occurring during flight-approval and type-approval testing, etc.

testing, a complete evaluation of the subsystems performance and associated read-outs of end instruments and transducers was conducted. The compatibility of the various subsystems, as well as the freedom from r-f interference caused by capacitive or inductive coupling, was established. Special tests were run to evaluate the operation of circuits under foreseeable contingencies.

f. Calibrations interface and system tests. At the conclusion of subsystem testing, interface tests were conducted to verify the operating characteristics between the subsystems. Calibrations were performed to verify the accuracy of the telemetry subsystem with the various subsystem transducers.

A system test followed the subsystem testing. The system test is intended to verify that a spacecraft does in fact perform properly during a typical flight sequence. The test was designed to discover any subsystem interactions that might occur during the spacecraft mission. The spacecraft configurations were maintained as nearly in flight condition for the system test as possible.

During the system test, the spacecraft was commanded through a complete operational sequence, from launch countdown preparation through fulfillment of the spacecraft mission. Monitoring the test was accomplished through direct-access cables mated to the subsystem GSE and the telemetry read-outs. The test data were evaluated during the test by the subsystem representative and cognizant engineers to determine the flight-worthiness of the spacecraft subsystems. Both MR-1 and -2 spacecraft were subjected to many system tests and various problems were uncovered. An additional test was performed on each spacecraft to verify correction of these problems.

g. Environmental tests. The spacecraft were also subjected to environmental tests to reveal any problems associated with prelaunch, launch, boost, and space environments.

R-F radiation tests. R-F tests were conducted to demonstrate that whatever radiation environment was produced either by the spacecraft or from ground-based sources did not influence spacecraft operations. Two types of r-f tests were conducted: (1) a test to determine the susceptibility of all on-board spacecraft subsystems; and (2) a test to determine the power absorbed by each squib of the total squib-firing assembly subsystem, and the power absorbed by the squib-firing power supply.

Space simulator tests. Space chamber tests simulated as closely as possible the conditions the spacecraft might encounter in flight, and sought to verify that the spacecraft functional systems would operate satisfactorily in the space environment. The tests also verified spacecraft temperature-control design. The operability of the spacecraft in each environment was verified by performing complete system tests after each environmental condition was simulated at the spacecraft temperatures predicted for various phases of the flight. The thermal design verification consisted of operation at power modes of long duration to assure that the spacecraft temperatures were within the expected range. The same kind of verification was also performed during spacecraft operation at short-duration power modes.

Some significant failures were discovered during the space simulator tests on both MR-1 and -2 spacecraft. Some of these failures would not have been apparent elsewhere and perhaps not even discovered in a normal test environment. The environmental tests also generated confidence in temperature control. Local pad heaters were used to bring localized spacecraft temperatures to

expected flight temperatures. A number of power profiles were made during environmental testing to indicate to temperature-control cognizant engineers where and how much power was being dissipated.

Vibration tests. Vibration tests verified that the spacecraft was not adversely affected by vibration resulting from the spacecraft boost environment. The vibration tests were programmed as sequences of band-limited Gaussian noise, harmonic sweeps, and combined noise with sinusoidal sweeps performed along the spacecraft roll axis and along the pitch and yaw axes. Resonant frequencies of the spacecraft were not emphasized. The vibration test indicated that test data from the dynamic test model was correct and accurate.

h. Dummy run. Both the MR-1 and -2 spacecraft were subjected to a dummy-run test, which simulated real-time operations to be performed during the preflight countdown. The following objectives were achieved:

- (1) Simulation of the launch equipment
- (2) Evaluation of the spacecraft in a simulated launch complex situation, including r-f environments
- (3) Evaluation of the operation and compatibility of the blockhouse and launch complex equipment with the spacecraft
- (4) Evaluation of test techniques, including hardware and telemetering methods that are utilized during launch operations at AMR
- (5) Verification of the countdown procedures
- (6) Familiarization of operating personnel with simulated field conditions and procedures
- (7) Verification of the operability of spacecraft pyrotechnics and ability of the spacecraft to withstand shocks resulting from the firing of pyrotechnics

Both MR-1 and -2 spacecraft performed successfully during the dummy-run tests.

i. Joint closed-loop operations test. The MR-1 spacecraft was used in the joint closed-loop operations test, which involved the spacecraft, Communications Center, Central Computing Facility, and other equipment and personnel normally utilized for evaluating spacecraft performance; or controlling, commanding, or otherwise communicating with the spacecraft. The test did not involve AMR, or any of the DSIF; however, elements of the Systems Test Complex GSE were used to simulate por-

UNCLASSIFIED

JPL TECHNICAL REPORT NO. 32-353

tions of a DSIF station. The test achieved the following objectives:

- (1) Checkout of the adequacy and compatibility of all possible spacecraft system equipment
- (2) Verification of flight procedures and operational plans to the extent possible
- (3) Familiarization of the control center and space flight operations personnel with space flight operations, and evaluation of their performance
- (4) Checkout computer programs and data processing directly with the spacecraft and communication system in a real-time mode of operations

j. Match-mate and r-f coupler tests. Match-mate and r-f coupler tests of the assembled *Agena B* stage and the spacecraft checked the mechanical and r-f compatibility between the booster vehicle and the spacecraft. The major objectives accomplished by these tests were:

- (1) Demonstration that the mechanical mating of the spacecraft adapter bracket assembly, shroud, latches, O-rings, ejection devices, and accessory hardware was proper
- (2) Determination of the operating signal levels of the antenna systems through the *Agena* antenna couplers

k. Spacecraft magnetic field mapping. Mapping of the spacecraft permanent magnetic field for the magnetometer experiment was accomplished in the SAF building. The magnetic field of the spacecraft was measured so that the flight magnetometer could be calibrated to compensate for this field.

l. Weight and cg measurements. Both *MR-1* and *-2* spacecraft were measured for weight and cg. The total weight of the spacecraft and the location of the cg with respect to the reference coordinates were measured. Following the cg measurement, the midcourse motor was aligned so that the thrust axis intersected the cg of the spacecraft.

m. Final electrical clean-up and system test. Prior to shipping the spacecraft to AMR, the flight configuration was finalized. Conditionally accepted items were replaced or modified to flight acceptance. Instruments or assemblies that required laboratory calibration were released for the final calibrations. The temperature-control paint patterns were completed. The final inspection was performed using microscopes to view the cable connections

and electronic modules. The spacecraft were then reassembled and wiring ground-loop checks performed. A final button-up procedure took place prior to the system tests. The intent was that, following system test, the spacecraft would be in a flight-ready condition.

A final system test was then run and the data were analyzed by all systems and subsystems cognizant personnel. The spacecraft were considered flight-ready and *MR-1* and *-2* were shipped to AMR, along with all associated GSE. Most of the problems discovered during system test were resolved before shipment. The separation connectors on the spacecraft were changed from the male to the female type. All outstanding failure reports originating prior to shipment were carefully investigated. When the spacecraft left JPL for AMR, they were considered to be in an optimum condition for flight.

n. Shipping procedure. Extensive shipping preparations were made for the spacecraft. Specialized equipment for hauling electronic units was contracted to transport the spacecraft and supporting gear to AMR. The spacecraft were shipped in separate vans with only a few parts removed. The flight solar panels were packaged in special containers designed to protect them from shock and moisture contamination.

6. Test Operations (AMR)

The operations reviewed in this section are those conducted at AMR prior to launch. Operations on the *MR-3* spacecraft were limited to those conducted in the spacecraft checkout facility. The spacecraft was used primarily to verify flight spacecraft spares. The testing philosophy at AMR was the same as that at JPL-Pasadena. Testing was conducted until it was certain that all subsystems were functioning properly. Informational-type testing was stopped when necessary to maintain test schedules. It should again be emphasized that the real purpose in testing at JPL was to produce two spacecraft that were in a flight-ready condition upon arrival at AMR. The intent was, if possible, to cut AMR test time, although sufficient time was scheduled to allow for unforeseeable contingencies. Figures 18 and 19 are schedules of AMR operations.

a. Initial spacecraft and GSE setup. The spacecraft and GSE arrived at AMR in good condition. Some minor damage was discovered, but it was not definitely attributed to shipment. After visual inspection, the spacecraft and system test equipment were set up for the system test operations in the spacecraft checkout facility.

UNCLASSIFIED

UNCLASSIFIED

JPL TECHNICAL REPORT NO. 32-353

b. System tests. A system test was conducted on both spacecraft after build-up at AMR, to again verify proper spacecraft operation and to determine which subsystems, if any, required further testing. The *MR-1* spacecraft experienced certain difficulties during the first system test and required additional testing. During its first system test, *MR-2* was found to function properly.

After the system tests proved that the spacecraft were in proper operating condition, both spacecraft were prepared for launch complex tests. Preparation consisted of general clean-up, attitude control leak-checks, equipment "button-up," a temperature-control clean-up, and finally, a cover was installed over the spacecraft and loaded on the adapter and transport dolly for moving the spacecraft to the explosive safe area. While being transported, the spacecraft were continually purged under the shroud with dry nitrogen.

c. Explosive Safe Area operations. The preparations carried out in the ESA were a continuation of those begun in the spacecraft checkout facility. The ESA operations included initial power application, r-f coupler tests, and evaluation of the spacecraft in the launch complex configuration. Both spacecraft were purged under their shrouds with dry nitrogen while en route from the ESA to the launch complex.

d. Launch complex checkouts and tests. Prior to combined launch complex tests with the spacecraft and booster vehicle, the launch complex itself was checked out. A spacecraft simulator was used to establish that blockhouse controls and monitors were properly installed and operational. All interconnecting cables between the AMR operational stations were checked. Spacecraft on-pad functional tests were conducted with the spacecraft on the pad to establish the integrity of all spacecraft systems in the launch complex.

Dummy-run tests. Following the above tests, a dummy-run was accomplished on *MR-1*. On completion of its complex checks, the *MR-2* spacecraft was returned to the ESA for flight-ready storage and back-up to the *MR-1* launch. The *MR-2* spacecraft on-pad checks were conducted just before the *MR-1* operations. The dummy-run tests performed on both spacecraft before launch fulfilled the following objectives:

- (1) Evaluation of the spacecraft in the launch complex environment, including r-f interference
- (2) Evaluation of the test procedures and personnel, including spacecraft components and telemetering methods

- (3) Verification of countdown procedures and familiarization of all operating personnel with these procedures

Joint flight-acceptance composite test. The joint flight-acceptance composite test (JFACT) was the primary test establishing vehicle-spacecraft launch readiness and ensuring that all systems continued to operate correctly from umbilical release through postlaunch flight simulation. All agencies at AMR participated in the JFACT test and provided data necessary to establish that complete coordination between all ground support activities was effectively accomplished. The *MR-1* JFACT test was conducted immediately after its dummy-run test.

e. Final flight preparations. Prior to launch, the spacecraft was removed to the spacecraft checkout facility and the ESA for final flight preparations.

SCF preparations. Following JFACT testing, the *MR-1* spacecraft was returned to the SCF for final flight preparations and a final system test. During final flight preparations, calibrations were verified. The spacecraft permanent magnetic field was mapped for the magnetometer experiment calibration, temperature-control painting was completed, and all final mechanical assembly and clean-up operations were performed.

A final system test verified that the spacecraft was ready for flight and that no damage was sustained during the launch complex tests. The final system test was the last test performed when all functions on the spacecraft were exercised.

ESA preparations. Following the final SCF operations, the spacecraft was transported to the ESA, where the midcourse motor was fueled and pressurized. Live pyrotechnics and flight battery were also installed. Shroud-off and shroud-on electrical tests were performed. With all preflight testing and preparations completed, the spacecraft was moved to Launch Complex No. 12.

The *MR-2* spacecraft prelaunch operations were identical to those for *MR-1*, with the exception that the spacecraft was run through ESA flight preparations and stored in a flight-ready condition as a back-up during *MR-1* launch operations. After launch of *MR-1*, the *MR-2* spacecraft was removed from storage and an identical dummy-run test and JFACT test, plus the other preflight operations in the SCF and ESA, were performed.

UNCLASSIFIED

7. Launch Countdowns

Both MR-1 and -2 spacecraft went into the launch countdowns with approximately 600 hr of accumulated testing time. The first attempt to launch was cancelled to permit further investigation of the range safety command system. On July 22, 1962, MR-1 was launched, but a deviation in the initial flight path from the standard forced the flight to be aborted.

The first launch countdown for MR-2 was started on August 25, 1962. This attempt was scrubbed. The spacecraft was then successfully launched on August 27, 1962. The launch was nominal.

8. Philosophy of Dual Spacecraft Mission Support

The *Mariner R* Project has clearly indicated advantages and disadvantages related to the concept of two flight spacecraft completely supporting a mission through launch. Some of the apparent advantages are the following:

- (1) Two concurrent preflight spacecraft operations yielded data that could be compared and verified; i.e., a standard was automatically established. At AMR, data comparison was further enforced by the introduction of MR-3 spacecraft test data.

- (2) The parallel operations provided protection against temporary manpower shortages during illness or other emergencies.
- (3) The existence of two test teams made the generation of test procedures a cooperative operation between the two engineers responsible for a particular area. This cooperation reduced the time required for any one engineer to devote to writing procedures.
- (4) Two flight-ready spacecraft provided a launch back-up capability that better ensured a successful launch within the established firing period.

The disadvantages relating to multiple spacecraft preparation are the following:

- (1) More checkout facilities are required, including the test equipment and buildings to house the operations.
- (2) When two spacecraft are launched within a short time, there is insufficient opportunity for the flight-test data from the first spacecraft to be evaluated and applied to the spacecraft awaiting launch, except for minor modifications. The 1962 Venus mission launch period was relatively short, so the two spacecraft were by necessity launched within approximately 1 mo of each other.

UNCLASSIFIED

UNCLASSIFIED

VII. Spacecraft Ground Support Equipment and Facilities

A. Introduction

The planning and development of the spacecraft ground support equipment and facilities had been in progress under conditions imposed by the *Mariner A* Project requirements when that project was replaced by *Mariner R*.

One of the new requirements was to restrict modifications peculiar to the *Mariner R* Project to a minimum. However, some changes were mandatory because of major changes in the system, such as the use of the *Atlas-Agena B* launch vehicle in place of the *Atlas-Centaur*, which in turn necessitated the use of Launch Pad 12 instead of Launch Pad 36. The implementation of pad modifications, including changes in hardware design, was to be accomplished so as to minimize down-time during the change-over from the *Ranger* program to the *Mariner R* and back again to *Ranger*.

B. Facilities

Each of the facilities discussed in this Section was used for *Mariner R* operations. The physical properties and the types of operations performed in each facility are described.

1. JPL-Pasadena Facilities

a. Spacecraft Assembly Facility building. The spacecraft are assembled, tested, calibrated, and prepared for shipment to AMR in the high-bay area of the SAF building (Fig. 182). The test and calibration operations conducted in this facility consist of the subsystem and system tests, dummy-run test, weight and cg measurements, and magnetometer mapping.

The high-bay operations area has an overhead crane and a 20-ft-deep pit for operations requiring the space-

UNCLASSIFIED

JPL TECHNICAL REPORT NO. 32-353

craft attitude control and propulsion units to be pressurized. The building also includes personnel offices, laboratories, a stock room, potting shop, machine shop,

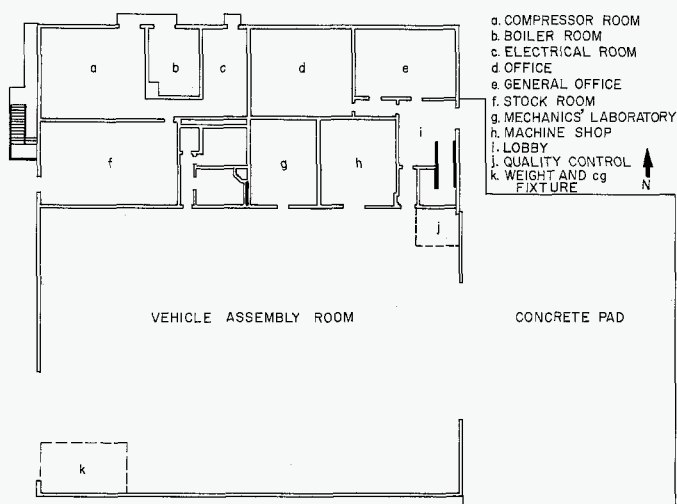


Fig. 182. Spacecraft assembly facility

cabling shop, and a quality-control area for incoming subsystem inspection.

b. Environmental Laboratories. Spacecraft vibration tests are conducted in the Vibration Laboratory (Fig. 183). This facility contains equipment capable of subjecting the complete spacecraft to the conditions of vibration it will experience in flight. A large electrodynamic shaker is used to produce random vibration frequencies. The frequency cycles are programmed on tape and fed into the shaker from a remote control console. The space simulator tests are conducted in a stainless steel vacuum chamber approximately 6 ft in diameter and 7 ft high. The simulator can produce a vacuum of 5×10^{-5} mm Hg. It can also simulate solar radiation with a 0.6 solar constant intensity. For the *Mariner R* program, however, no solar simulation was used.

On completion of JPL-Pasadena operations, the spacecraft are taken to AMR, where additional assembly and test operations are performed prior to launch.

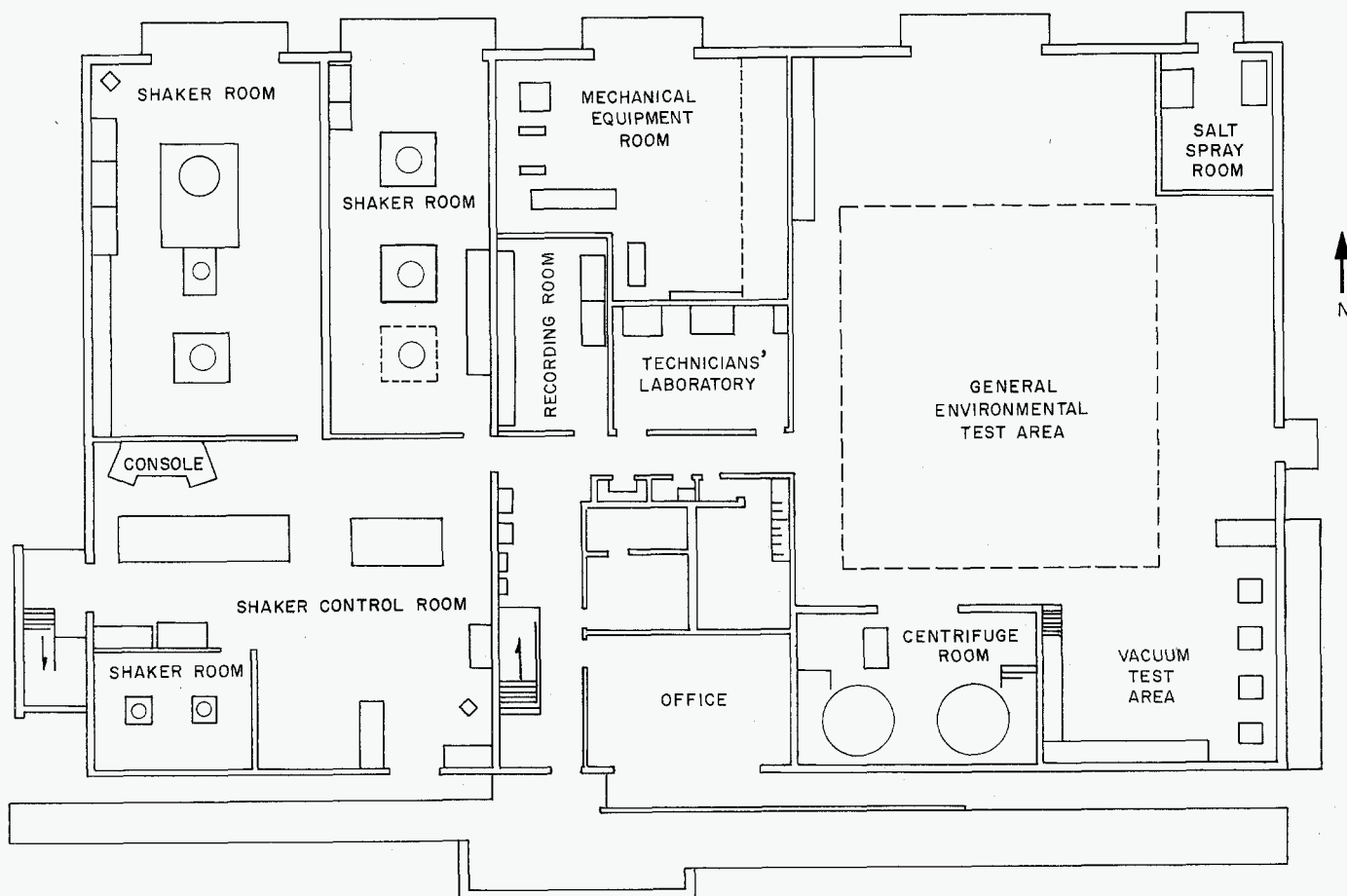


Fig. 183. Environmental Laboratory

UNCLASSIFIED

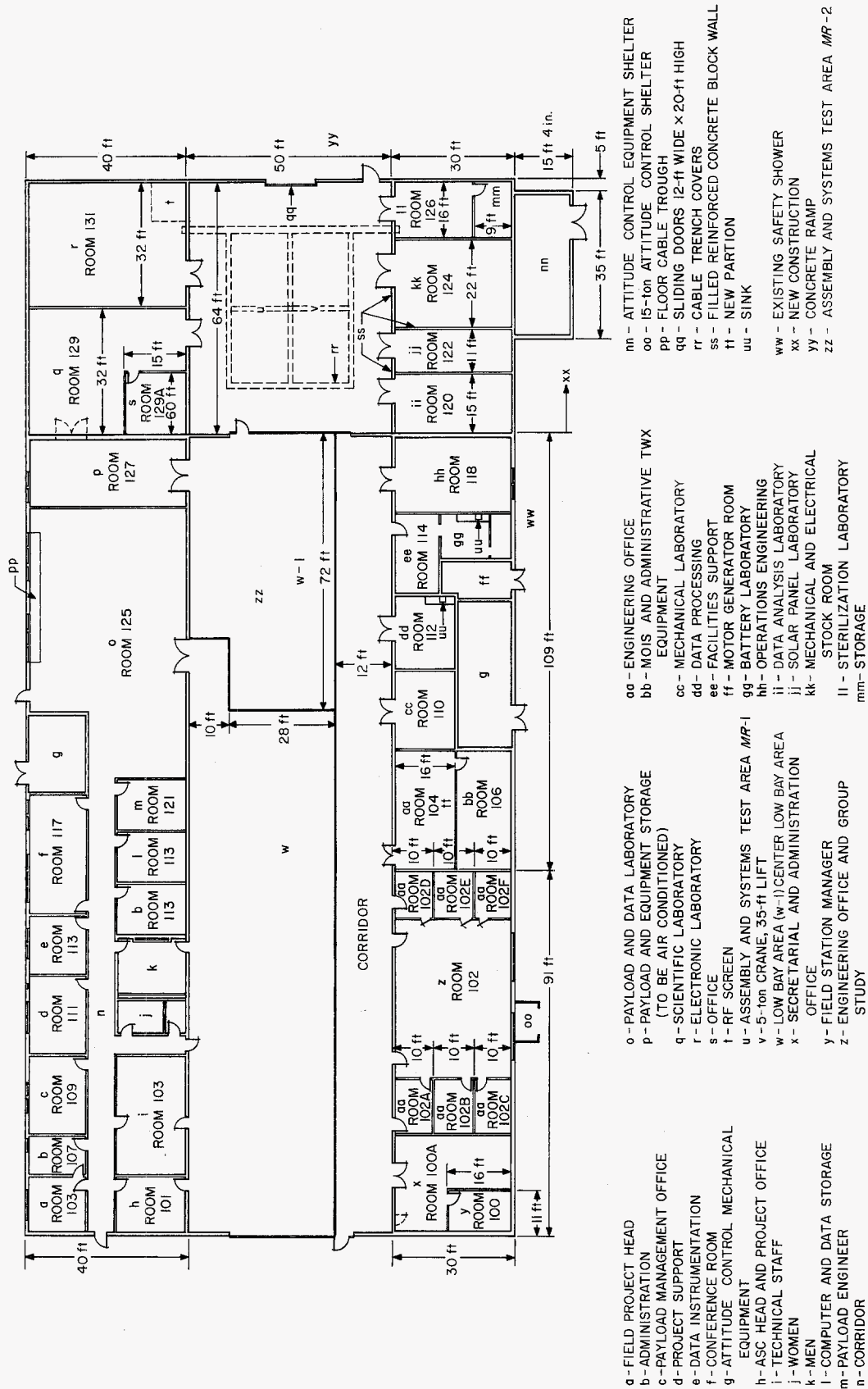


Fig. 184. Spacecraft checkout facility

2. AMR Spacecraft Operation Facilities

a. Hangar AE. The hangar (spacecraft checkout facility) contains a high-bay area and center low-bay area (Fig. 184) for spacecraft assembly and test operations. Each area has a traveling overhead crane to facilitate spacecraft handling. In addition to the assembly and test operations areas, the facility contains the JPL Operations Center, Communications Center, administrative and engineering offices, and supporting laboratories. The laboratories are the Electronic Laboratory, Scientific Laboratory, Sterilization Laboratory, and the Solar Panel Laboratory.

During those operations involving both the blockhouse and the spacecraft checkout facility, the direction and coordination of all mission operations between JPL and other participating agencies are concentrated in the Operations Center. Conference tables and consoles for the Mission Director, the Operations Center Coordinator, the Status Coordinator, and their assistants are located in the center of the room. The Center also contains three status boards. One board indicates condition of the

tracking and communications equipment at the various stations supporting the mission; the other two boards indicate the real-time events during flight.

The JPL Communications Center houses the operation teletype and MOIS equipment. It is the tie-point for JPL communications lines between AMR and JPL-Pasadena.

b. Explosive Safe Area. Final preparation of the completed spacecraft and installation of fueled propulsion systems and pyrotechnic devices are accomplished in the ESA (Fig. 185). The area includes a Sterilization and Assembly Laboratory, Propulsion Laboratory, Capsule Laboratory, and a quonset-type hut for storage purposes. Several trailers are also used in the ESA to supplement the permanent facilities.

The Sterilization and Assembly Laboratory is approximately 20×40 ft. The building has a 2-ton traveling crane and a stationary 2-ton hoist. In this facility, the midcourse propulsion unit is installed in the spacecraft bus, the spacecraft is weighed, and the shroud is installed.

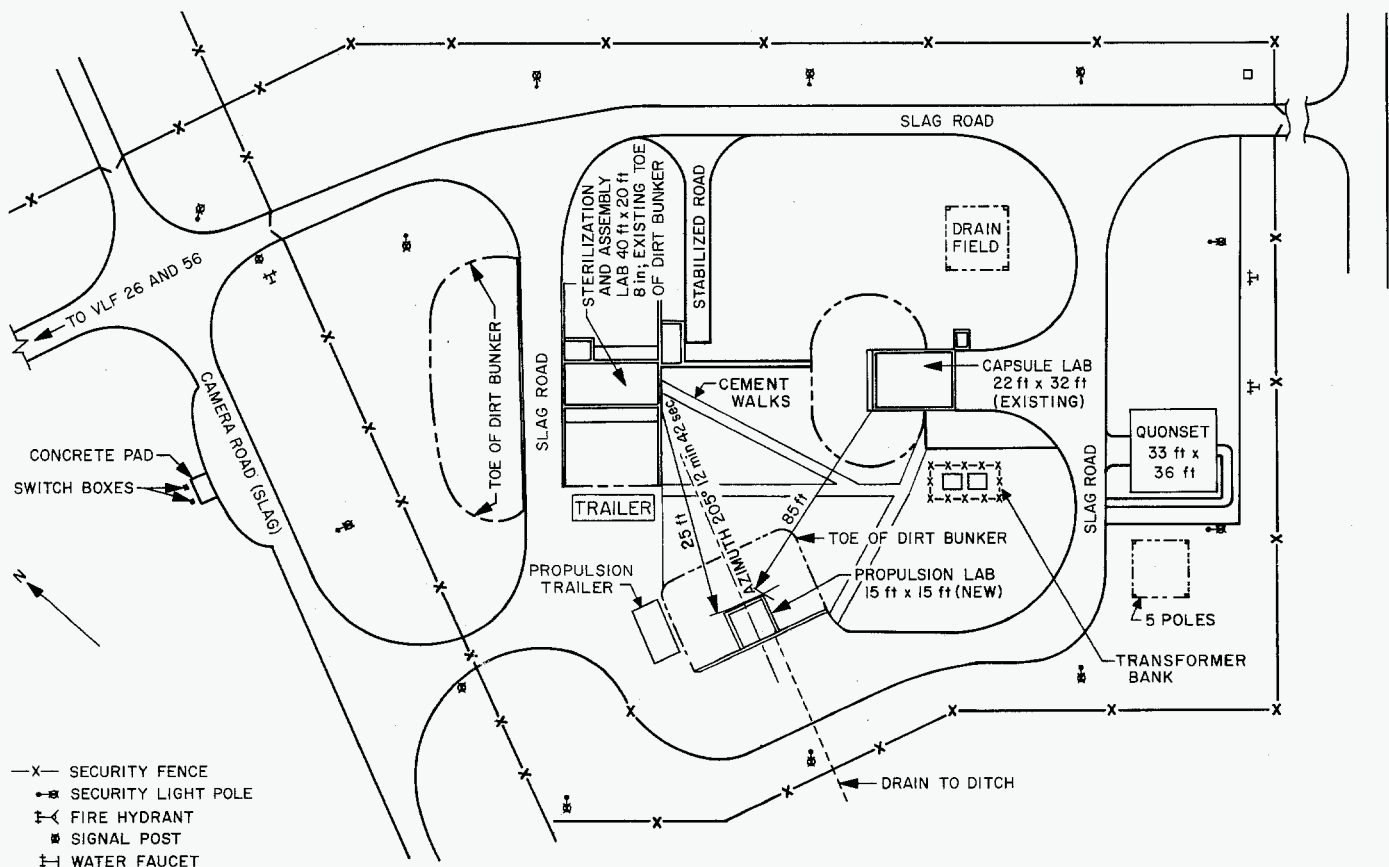


Fig. 185. Explosive Safe Area

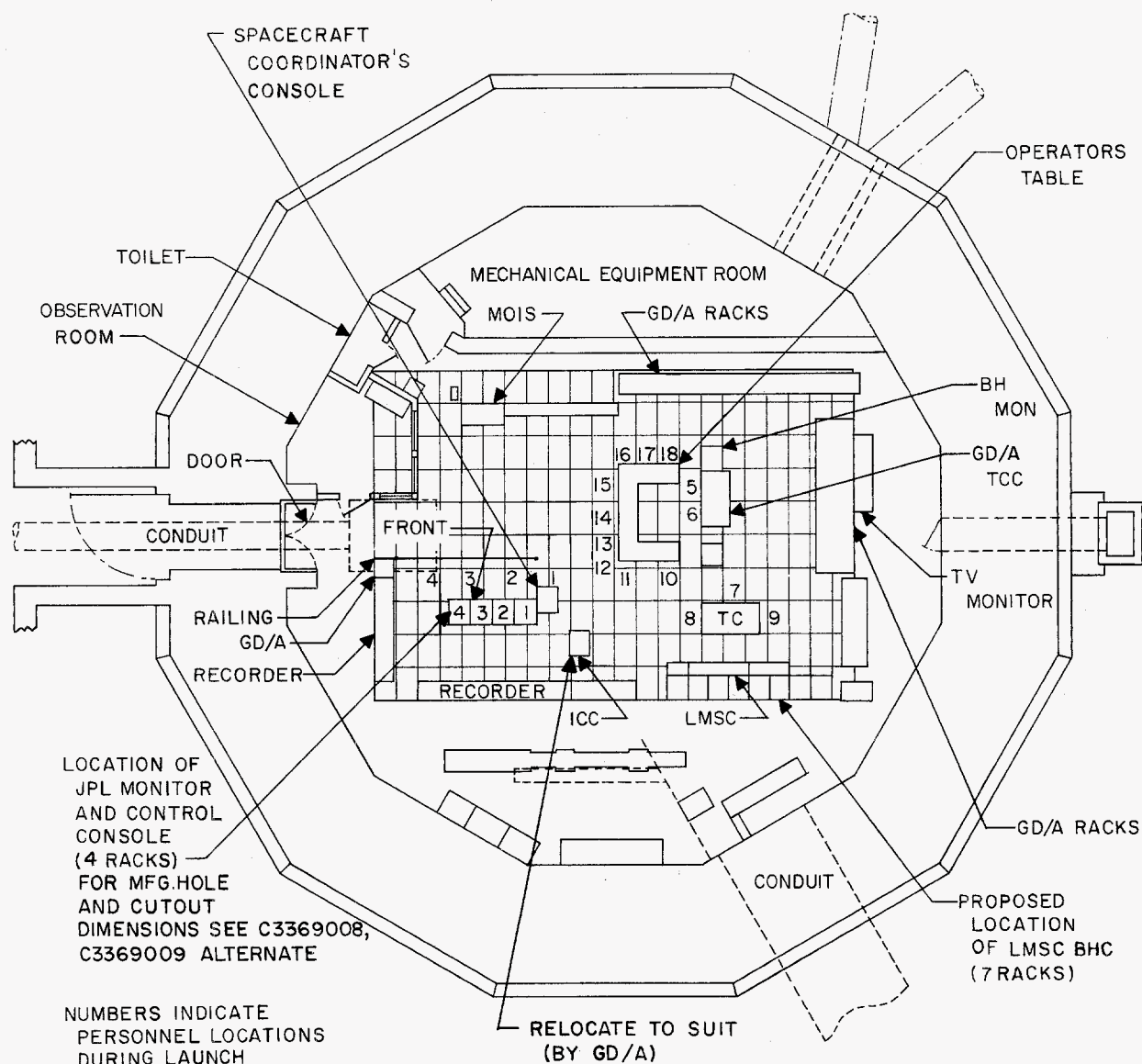


Fig. 186. Blockhouse plan view

The Propulsion Laboratory is used for checking, assembling, fueling, and pressurizing the spacecraft midcourse propulsion unit. The checkout and pressure-testing of the inert, storable, liquid rocket motor is accomplished in a trailer parked adjacent to the laboratory. The laboratory is approximately 15 ft square, with a ceiling height of 12 ft and a "blowout" roof. Equipment includes an overhead, deluge-type sprinkler system, revetments on three sides of the laboratory, and other safety features required for handling liquid propellants. Shed-type fuel and oxidizer shelters are located in those revetments on opposite sides of the building.

The Capsule Laboratory is primarily used for the *Ranger* program. During *Mariner R* operations, the MR-2

spacecraft was made flight-ready and placed in the Capsule Laboratory as a stand-by spacecraft. The laboratory is approximately 24 × 32 ft.

c. Launch Complex No. 12. Launch Complex No. 12 comprises the blockhouse, launch control shelter, umbilical tower, launch complex equipment, spacecraft simulator, launch stand, and gantry.

The blockhouse (Fig. 186) is a steel-reinforced, concrete structure located approximately 1200 ft from the launch pad. The blockhouse is the center of operations for hard-line command and monitoring of the spacecraft, and for the launch vehicle during prelaunch and launch operations. The blockhouse contains consoles with equip-

ment for transmitting the necessary commands to the *Atlas-Agena B-Mariner* vehicle, and for verifying proper operational modes and circuitry.

The launch control shelter is a 20- by 36-ft prefabricated metal building with a usable height of approximately 10 ft. It houses power equipment which must be in close proximity to the spacecraft. The building contains racks housing power supplies and other equipment that can be remote-controlled from the blockhouse.

The umbilical tower provides a transition point from the spacecraft catenary cable to the long-line cables. A junction box is located on the tower, close to the point at which the cables enter the catenary. The junction box contains three modules consisting of a line amplifier for mixed modulation signals, a 7-channel isolation amplifier for the data encoder circuitry, and a signal conditioning unit for 400-cps and 2.4-kc power monitoring.

The spacecraft simulator is a unit designed to ensure electrical compatibility of the launch complex with the spacecraft. This is accomplished by simulating, or actually duplicating, the appropriate spacecraft circuitry and conducting a checkout of the unit with blockhouse GSE according to a formal procedure.

d. AMR Launch Station and Instrumentation Complex (DSIF Zero). DSIF Zero contains the r-f trailer and the telemetry trailer. The primary purpose of the r-f trailer is to provide an r-f link from the spacecraft to the telemetry nad doppler data read-out equipment. Basically, the RFT consists of a radio system, a command checkout system, and various types of commercial test equipment.

The telemetry trailer makes permanent records, in the form of magnetic tapes, of all flight data received by the r-f trailer. The TT equipment includes direct-write oscillograph recorders, Ampex magnetic tape recorders, a time-code generator, a digital printer, and the necessary discriminators. During preflight operations, the telemetry trailer demodulates telemetry signals received by the RFT from the spacecraft. The demodulated telemetry signals are then relayed to Hangar AE.

C. System Test Complex

The System Test Complex (Fig. 187) is the basic test equipment used for performing the system test, which

has as its objective the verification that the spacecraft is performing properly in a simulated flight sequence.

The System Test Complex consists of a system test fixture, which has the capability of orienting the spacecraft in pitch, yaw, and roll, and an arrangement of test consoles designed to support the testing of the individual subsystems and the spacecraft as a whole. The STC also provides external power to the spacecraft.

The System Test Complex has the following capabilities:

- (1) Operation of the entire spacecraft in a manner simulating the countdown and flight sequence.
- (2) Monitoring of spacecraft system functions, as well as subsystem inputs and outputs for quantitative evaluation of spacecraft performance.
- (3) Exercising of all elements of the spacecraft through their entire dynamic ranges for the purpose of evaluating their performance under influences produced by the presence of the complete spacecraft.
- (4) The STC was designed with verification features (self-test) to minimize the time required for isolation of trouble.

The Complex equipment was designed to operate under the applicable conditions stipulated in the JPL Environmental Specification. However, since all the equipment remained in the southern half of Continental United States, both in transit and in use, these requirements were modified so as to make them less stringent.

In order to optimize the STC layout, the elements composing it were arranged with particular attention to the following considerations:

- (1) Test cable length was kept to a minimum, and insofar as practicable, the cable length from each test position to the spacecraft was equal. Complete uniformity of the interconnect cables, connectors, J-boxes, etc., was maintained in the three STC layouts. Furthermore, slack in any of the cables was not taken up by coiling; instead, it was distributed in a random manner over as wide an area as feasible.
- (2) Sufficient clearances were provided around the spacecraft and system test fixture to permit articulation of booms, solar panels, antennas, etc., and also to allow repositioning of the spacecraft in roll, pitch, and yaw.

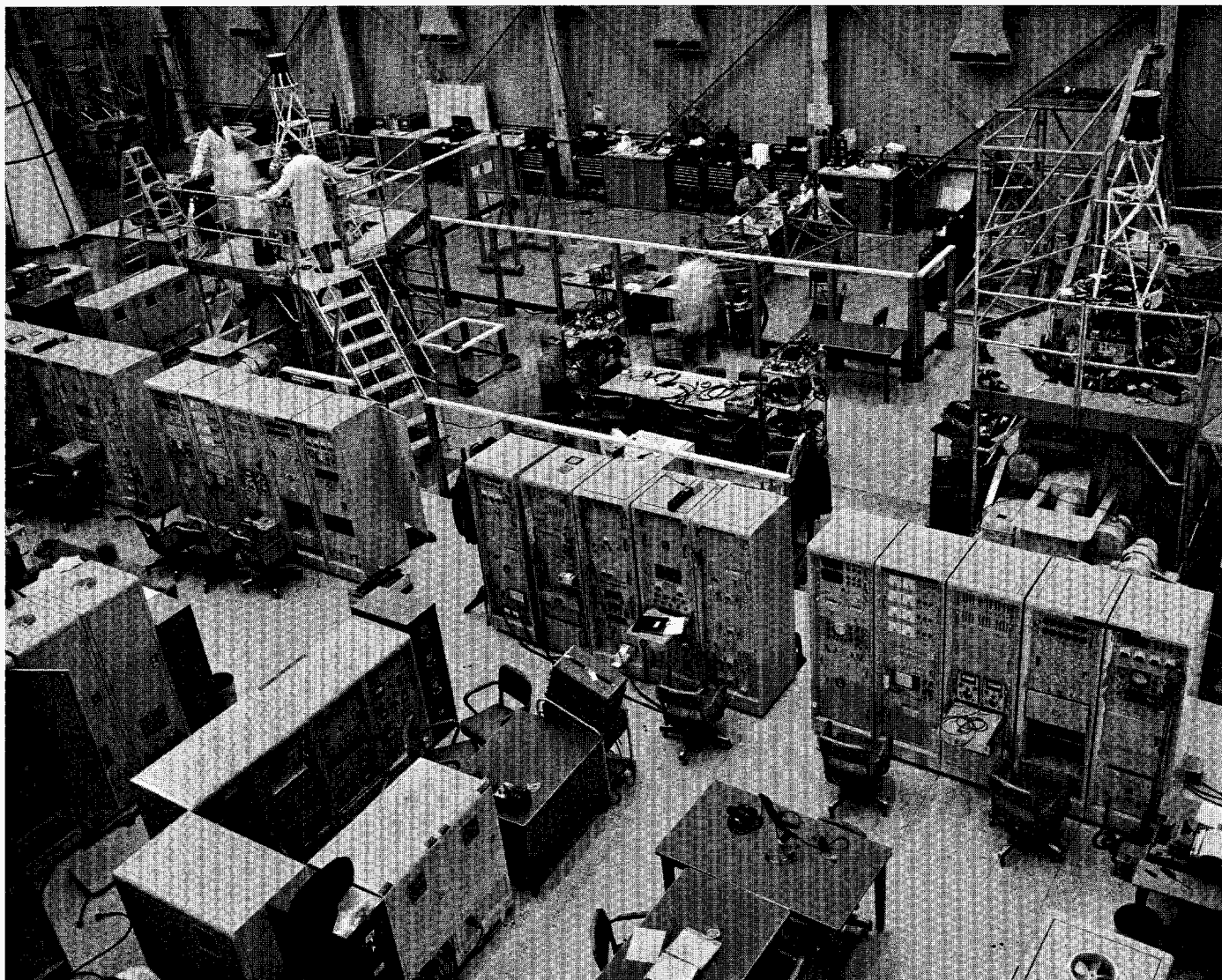


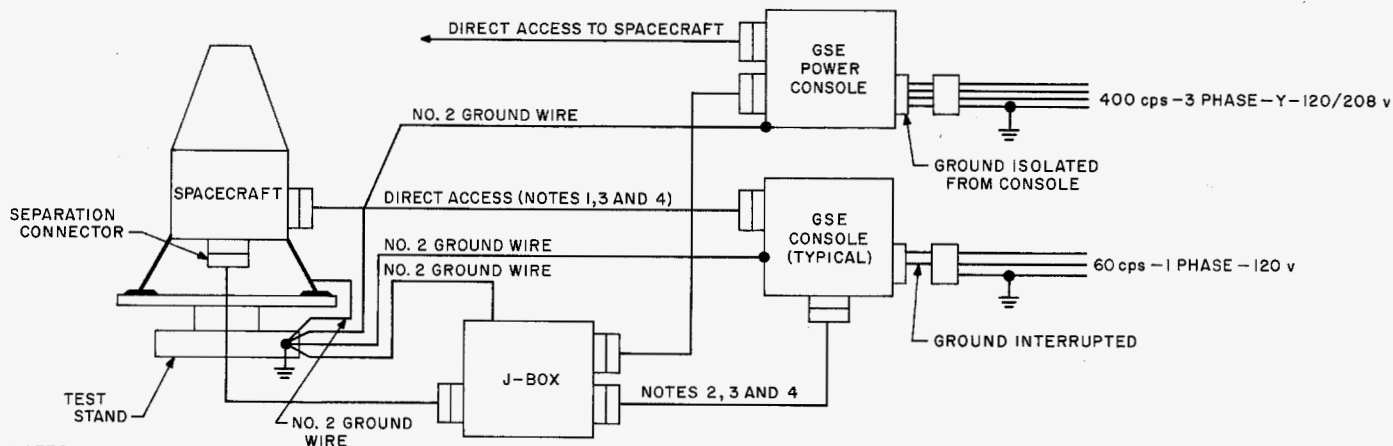
Fig. 187. System Test Complex

- (3) All cables from the various test positions to the spacecraft through the separation connector only were routed through a junction box in the proximity of the spacecraft.
- (4) The consoles constituting the STC were mounted on a raised platform. The space between the platform and the building floor was utilized for the routing of cables.
- (5) A tape recorder was provided as part of the STC for recording the mixed telemetry signal.
- (6) A spacecraft-GSE interface connector panel simulated space chamber feed-through ports for all of the direct-access cables. The panel was located as close to the spacecraft as practicable. During

space environment testing, the space chamber feed-through ports were used.

All elements of the System Test Complex operated normally from a power source of 105-125 v, 60 cps, single-phase; and 120-208 v., 400-cps, 3-phase, 4-wire power. The system test fixture, however, used a 3-phase source for the motor drives. Each rack, or group of racks, had an appropriate overload protective device.

The system test equipment had the capability of providing power to individual subsystems in the spacecraft at times when basic spacecraft power was not available because the spacecraft power supply or ring harness were inoperative, and during certain types of trouble



NOTES:

1. ALL SHIELDED TEST LEADS SHALL HAVE THEIR SHIELDS COMMON AT THE SPACECRAFT END ONLY, AND SHALL BE CONNECTED TO SPACECRAFT STRUCTURE.
2. A SHIELD POTENTIAL LEAD MUST BE CARRIED THROUGH ALL CABLES GOING THROUGH THE JUNCTION BOX SO THAT SHIELDING WILL NOT BE LOST AT THIS POINT. ALL CABLING SHALL BE GROUNDED BY CONNECTING ITS SHIELDS TO THIS COMMON EQUIPOTENTIAL LEAD AT THE CABLE END CLOSEST TO THE SPACECRAFT.
3. EXTRA CARE MUST BE TAKEN WHEN USING COAXIAL CONNECTOR SHELLS TO PREVENT GROUND LOOPS DEVELOPING.
4. SHIELDING MUST NOT BE GROUNDED BY CONNECTION TO A JUNCTION BOX, CHASSIS OR CONSOLE STRUCTURE.

Fig. 188. Typical test equipment setup

shooting or noise isolation. It was a requirement that each subsystem test position be equipped so as to be capable of providing this independent operation through a special cable plugged directly into the appropriate spacecraft subsystem. The input power required for this operation had the same characteristics as that normally supplied from the spacecraft power supply. The leads carrying this power were not incorporated into the direct-access test cable since this condition poses a potential hazard to the rest of the spacecraft by allowing power supplied to test equipment possibly to get into other subsystems through spacecraft wiring. It also could result in a power source paralleled with the spacecraft-furnished 2400-cps or 400-cps supplies, if main spacecraft power were turned on simultaneously. A special self-power adapter cable was used, having a connector which can be plugged into the subsystem only when the ring harness power input plug is disconnected from the system.

The following techniques for grounding were adhered to both in design and fabrication of system test equipment and associated cabling, to eliminate, as far as possible, all potential ground-loop and polarity problems between test equipment and the corresponding subsystem. Figure 188 illustrates a typical grounding scheme. All System Test Complex consoles and the spacecraft were tied together at a common point with braid or wire,

No. 2 AWG or larger, and, in general, followed the same route as the direct-access cables. The common tie point was at the spacecraft system test fixture. A hole for a $\frac{3}{8}$ -in. copper stud was provided at each rack and at the system test fixture. The standard three-wire power cables were plugged into the racks through a special short adapter in which the ground wire had been omitted. This adapter was painted red, so that a quick visual check during system test will verify that power cabling is correctly connected, and also to help ensure that the adapters will not be mistakenly used elsewhere.

As a precautionary measure, dummy loads were used in place of the actual subsystem cases during the initial turn-on operations following spacecraft assembly. A dummy-load box was required for each subsystem assembly. These boxes simulated the load each case would normally draw from the spacecraft main harness. Break-in boxes or in-line cable adapters, which allow access to all leads at a connector interface, were permitted during spacecraft testing except during system test. Line amplifiers were used to counteract the interference and attenuating effects of long cables on low-level signals. In the use of these amplifiers, consideration was given to the following requirements:

- (1) The line amplifiers used in the STC junction box were identical to those used in the launch-complex junction box.

- (2) The direct-access cable line amplifiers were placed as close to the spacecraft as practicable.

A number of restraints were imposed on the spacecraft by the System Test Complex. It was a test requirement that subsystem functions, as well as selected subsystem inputs and outputs, be monitored for quantitative evaluation of spacecraft performance. To meet this requirement, direct-access test connectors were provided as a part of the spacecraft configuration. It was also required that sufficient isolation be incorporated at the spacecraft end of each monitoring circuit to prevent harm to the subsystem being monitored in case of an inadvertent short or voltage across the leads somewhere in the cabling or test equipment. In addition, the isolation was such that the monitoring of any of the spacecraft functions should not affect the performance of the spacecraft in any manner. In some instances, the introduction of isolation consisting exclusively of passive circuit elements degraded the measurement so that it became meaningless; in these instances, an equitable compromise was established to reconcile these conflicting circumstances through the use of an absolute minimum of active circuit elements required to accomplish essential monitoring and control.

D. Launch Complex

1. Launch Complex Equipment

The facilities in Launch Complex 12 at AMR were used for the *MR-1* and *-2* launchings. The principal elements of this facility were the blockhouse, umbilical tower, launch control shelter, gantry, and launch complex equipment.

The LCE comprised certain equipment in the blockhouse, umbilical tower, and launch control shelter; it included the launch complex cabling and the spacecraft simulator (Fig. 189).

The launch complex equipment was designed to perform several over-all functions, one of which was to monitor prelaunch operations from the blockhouse in order to verify proper operation of the spacecraft. These prelaunch operations included measuring power and sending commands to the spacecraft; measuring signal levels; and verifying proper responses, conditions, and positions of the spacecraft equipment. The telemetry

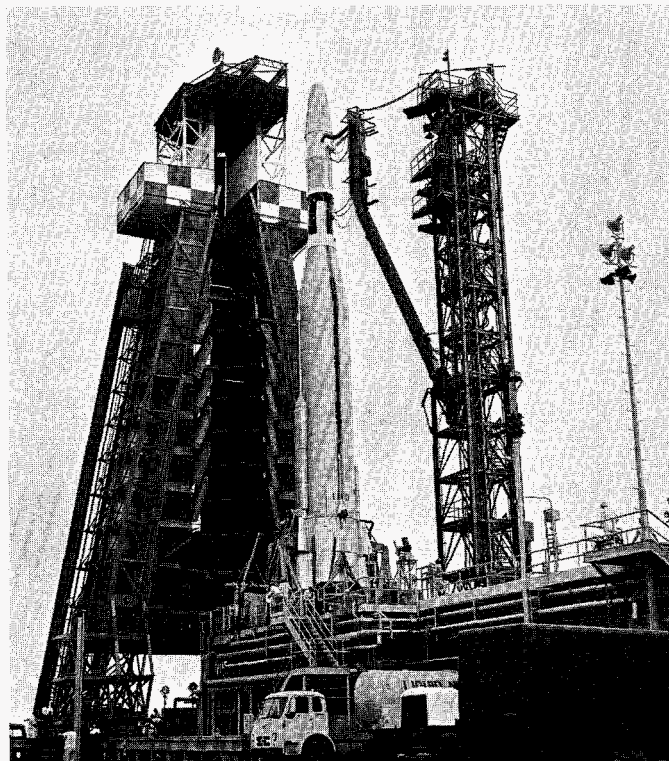


Fig. 189. Launch Complex No. 12, Atlantic Missile Range

mode within the spacecraft could be selected and certain telemetry levels could be measured. The number of these measurements was limited in order to simplify operations at the launch site.

2. Blockhouse

The blockhouse contained several JPL-furnished consoles. Equipment for verifying proper operation and for transmitting commands to the spacecraft was located in the blockhouse (Fig. 186).

Normally, in the *Ranger* program, certain consoles furnished by JPL are part of the fixed-station equipment and are bolted to the blockhouse floor. Only the chassis and the intercabling are changed to meet the different mission requirements. For *Mariner R*, it was decided to provide a new set of racks which had been completely installed and tested at JPL. The five *Ranger* racks were removed and replaced by four pieces of *Mariner* equipment. This change reduced the blockhouse down-time and minimized the equipment verification time.

A monitor and control junction box for the routing, distribution, and termination of cables between the blockhouse and the spacecraft was installed in one of the

UNCLASSIFIED

JPL console racks. A power distribution panel, containing circuit breakers for the a-c power sources, was located in the same rack.

Guidance and control panels were established in a second rack in the JPL console to control and monitor prelaunch operations of the spacecraft. These panels controlled the operation of the power supplies, and monitored the central computer sequences, the gyro-controlled servo loops for attitude control, the pyrotechnic control reset condition, and the antenna transfer coaxial switch position. Controls for an intercommunications set were also installed in the guidance and control rack.

Equipment to control the commutator and to read the individual channels on visual and digital printer read-out was mounted in the third and fourth racks of the JPL blockhouse console. These racks contained the necessary power supplies for the equipment and a line amplifier which fed the mixed signal to the data encoder consoles in the spacecraft checkout facility and in the launch checkout telemetry trailer.

The spacecraft coordinator's console was located in its normal position adjacent to the JPL consoles described above. Equipment at this console included a countdown clock, an intercom which linked all of the JPL stations at the launch complex, a LMSC spacecraft condition panel, and a General Dynamics/Astronautics spacecraft ready-hold panel.

3. Launch Control Shelter

The launch control shelter had contained one rack for the *Ranger* operations. One additional rack was installed in order to satisfy the increased number of chassis required for *Mariner R*—essentially the power supplies. The ground power supply required a 400-cps power input. This power supply had been designed for the *Mariner A* high-power requirements and included design features which reduced the size of the transformer-rectifier units, filters, and other components. Independent 400-cps power generators were provided as sources for the *Mariner R* power supplies in order to eliminate power-sharing interferences.

The building contained other equipment, in addition to the power supplies, which could be controlled from the blockhouse. A J-box which had been mounted in one of the racks provided the capability of handling the land-lines of other equipment in the shelter.

4. Umbilical Tower

The umbilical tower (Fig. 189) contained a new JPL-supplied J-box, a spacecraft umbilical plug and catenary conforming to JPL requirements, which were furnished by LMSC, and a 400-cps power outlet to provide power to the spacecraft simulator. The simulator is used at the top of the umbilical tower and is connected to the umbilical plug. Some 400-cps power functions were also necessary in order to perform tests on the *Mariner R* launch equipment.

The new umbilical tower J-box was required because umbilical signals and signal functions for the spacecraft were significantly different from those of the *Ranger* systems. Advantage was taken of this opportunity in order to improve the J-box design so that it would more reliably resist corrosion, fungus, and moisture. The fact that the new box was fabricated at JPL allowed the J-box to be used during the Pasadena checkout before shipment.

The umbilical tower J-box was used in the normal manner as an interconnection between the umbilical (catenary) cable and the tower cables. In addition to its use for cabling, the J-box served as a housing for the following three modules:

- (1) A line amplifier for the mixed modulation signal
- (2) A seven-channel isolation amplifier for the data encoder circuitry
- (3) A signal-conditioning unit for 400-cps and 2.4-kc power monitoring

5. Ground Support Cabling

All of the cabling for ground support equipment at the launch complex interconnects the separate J-boxes which are located at the following sites:

- (1) The monitor and control console
- (2) The launch control shelter
- (3) The umbilical tower

Ground cables, classified generally as being hard-line trunk cables, interconnecting cables, or video-pair cables, were changed slightly because of changes in the ground equipment.

Hard-line trunk cables, i.e., those cables connecting the top of the umbilical tower to the blockhouse, included

UNCLASSIFIED

UNCLASSIFIED

JPL TECHNICAL REPORT NO. 32-353

additional twisted-pairs and power cables which were necessary because of changes in the ground support equipment.

Interconnecting cables between the panels and racks in the JPL consoles were modified to accommodate changes in the control equipment.

The use of pseudo-noise techniques for spacecraft mixed modulation signals required wider bandwidths and higher-quality data transmission cables. A new video-cable was installed from the umbilical tower J-box to the blockhouse.

6. Ground Handling Equipment

A spacecraft protective cover was developed for the purpose of protecting the spacecraft from the environment during AMR operations. The *Ranger* spacecraft were normally encapsulated for sterilization purposes. The *Ranger* spacecraft adapter included a diaphragm which sealed the shroud bottom structure. This diaphragm was eliminated for *Mariner R* in order to increase the payload capability. The *Agena* forward equipment rack was sealed to prevent spacecraft contamination during flight. This, however, did not seal the spacecraft during operations prior to the mating with the *Agena*. A special fiberglass protective cover was developed and installed on the spacecraft supporting ring. This cover sealed the shroud and remained with it until the mating of the spacecraft with the *Agena*.

7. Dummy Run Trailer

To house the launch complex equipment during dummy-run tests at JPL-Pasadena, a ground support equipment trailer was provided. Blockhouse and launch control shelter equipment was installed and interfaced to the spacecraft through simulated pad cables. During AMR tests, the trailer was used at the explosive safe area during the spacecraft operations and was capable of providing a spare set of launch complex equipment if necessary.

8. Launch Checkout Station

The launch checkout station which was used for RA-4, consisting of the telemetry trailer and the L-band launch checkout trailer, was modified slightly for use in the *Mariner R* Project.

E. Engineering Support Facilities

1. Introduction

Spacecraft development and flight programs require a number of supporting engineering activities and facilities. This Section is devoted to a summary of the use of the following such facilities in the *Mariner R* Project:

- (1) Environmental test laboratories
- (2) Instrumentation support
- (3) Computer applications and data systems

2. Environmental Test Laboratories

The achievement of the high reliability and long life necessary for interplanetary spacecraft demands well-planned testing programs and adequate environmental test facilities. The size and lightweight construction of the *Mariner R* spacecraft required refined vibration testing techniques with emphasis on low-frequency vibration testing due to the low resonant frequencies of the spacecraft structure in bending and torsion. New techniques were developed in space environment simulation and vacuum-temperature testing. Since spacecraft equipment must operate also in the Earth environment, there was a continuing need for climatic testing.

a. Vibration testing. The testing of a complete *Mariner R* spacecraft required vibration testing facilities capable of handling large-sized packages and fixtures-plus-spacecraft weights up to 2000 lb. To accommodate such tests, a Ling L-249, 30,000-lb vector-force-rating vibration exciter and a Ling 175-kva power supply and control console were used. This system has the capability of testing spacecraft and fixture combinations at levels in excess of 5 g (rms). The low-frequency (1-80 cps) vibration testing was performed with a new Vard Electrohydraulic Exciter, which was installed in December 1961. This machine is capable of generating 25,000 lb of force and of producing displacements of 6 in. double amplitude. The test program required vibration of the spacecraft along three orthogonal axes. This was done with a special granite oil table and horizontal test fixture (Fig. 190) with a hole in the center of both to allow clearance for the high-gain antenna feed.

In vibration-testing the spacecraft in the thrust axis, an 800-lb cast conical fixture was used. Figure 191 shows the spacecraft and this test fixture mounted on the L-249 vibration exciter.

UNCLASSIFIED

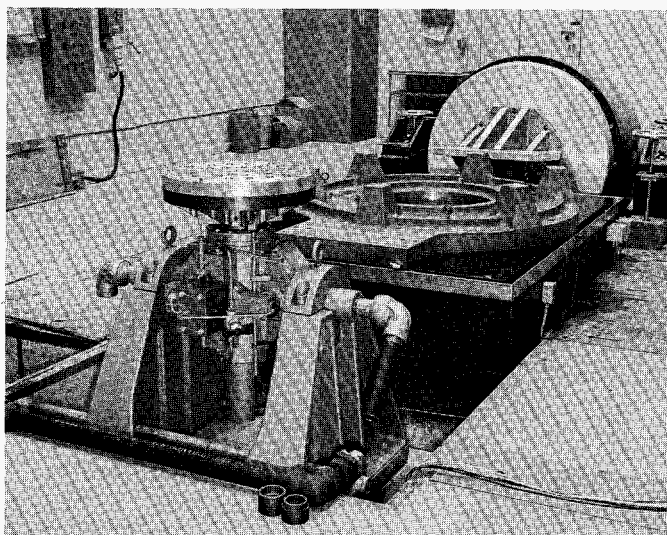


Fig. 190. Granite oil table and slider plate

To accommodate the spacecraft component and assembly testing work load, a smaller granite block and oil slider plate test fixture was used (Fig. 192). Under normal operating conditions, one of the vibration exciters is kept in a vertical orientation, while the other remains horizontal. Consequently, changing of the axis of vibration can be accomplished by running vertical axis tests on one vibration exciter and the two transverse axes on the second exciter. The use of these fixtures resulted in improved quality and control of the vibration tests and helped to speed up the testing program.

b. Vacuum-temperature testing. The vacuum-temperature testing capabilities of the Environmental Test Laboratory were expanded and improved to handle the requirements of *Mariner R*. Tests were carried out in six vacuum chambers, all equipped with JPL-built automatic temperature-control systems. Two of these are 30- × 50-in. metal horizontal chamber high-vacuum systems such as shown in Fig. 193, and four are 18- × 30-in. glass bell-jar, high-vacuum systems, as shown in Fig. 194. These systems are capable of an ultimate chamber pressure of 10^{-7} mm Hg when using their automatically filled, liquid-nitrogen, chevron-baffle cold traps.

Automatic temperature-control devices were installed on each of these vacuum systems, making use of liquid or gaseous nitrogen from the 1300-gal Dewar near Building 144. These devices are used to control the temperature of components inside the vacuum chambers either by direct conduction from heat exchangers connected to the components, or by radiation to cold-wall shrouds. The systems are capable of controlling the temperature

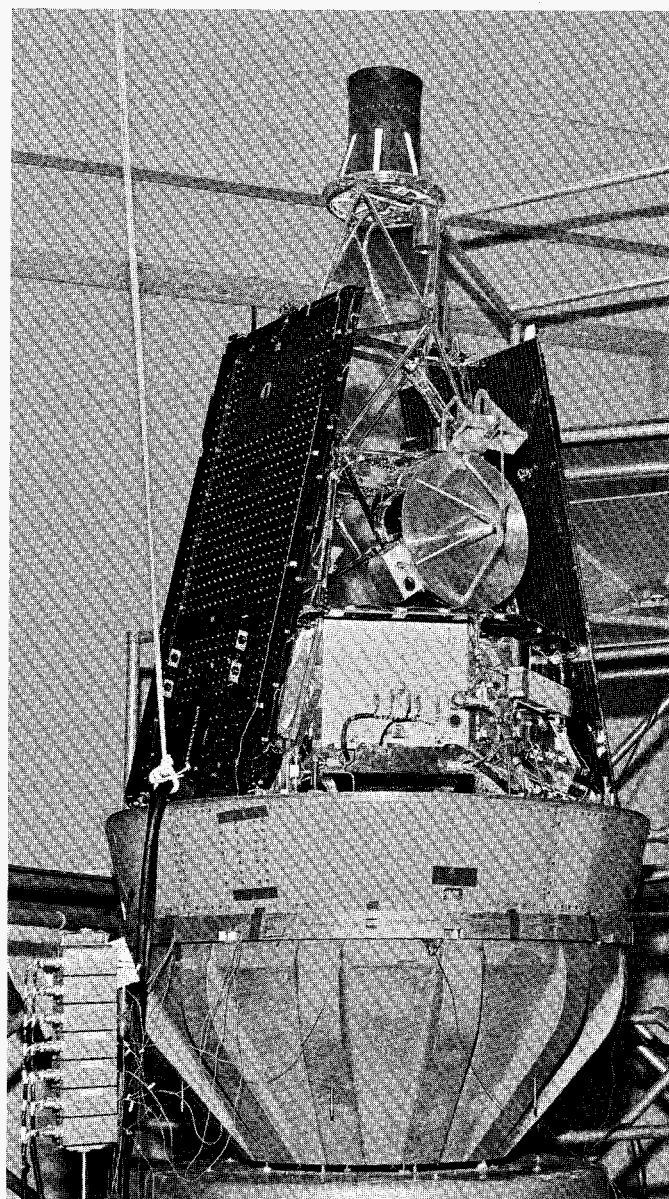


Fig. 191. *Mariner R* vibration test

in the range between -320°F (-195°C) and $+300^{\circ}\text{F}$ (149°C). The temperature is controlled and continuously recorded by Leeds and Northrup Model R recorders.

c. Space environment simulation

(1) *6-ft space simulator.* The MR-1 and -2 flight spacecraft were tested in a vacuum-temperature environment in the 6-ft space simulator (Fig. 195). The environment during steady-state conditions was: vacuum, 5×10^{-6} mm Hg, shroud temperature, -300°F . The spacecraft temperature was controlled by resistance heaters mounted on the spacecraft structure. Test objectives were design verification at predicted flight temperatures in a vacuum-

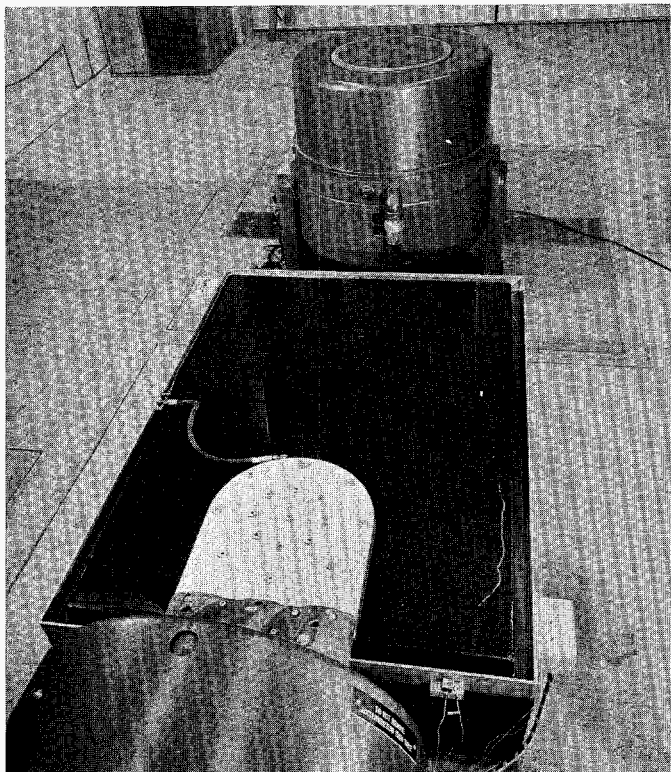


Fig. 192. Vibration exciter and electrodynamic shakers

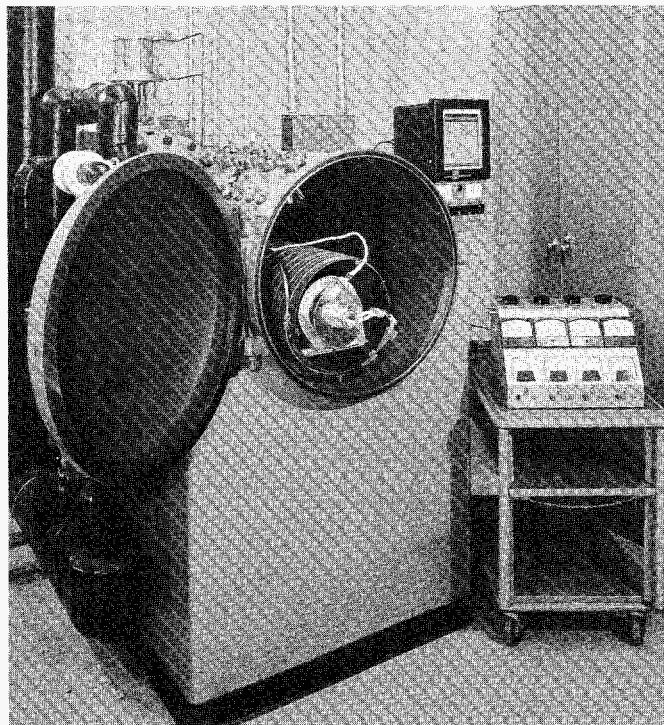


Fig. 193. Vacuum-temperature test setup, showing horizontal chamber and temperature-control shroud

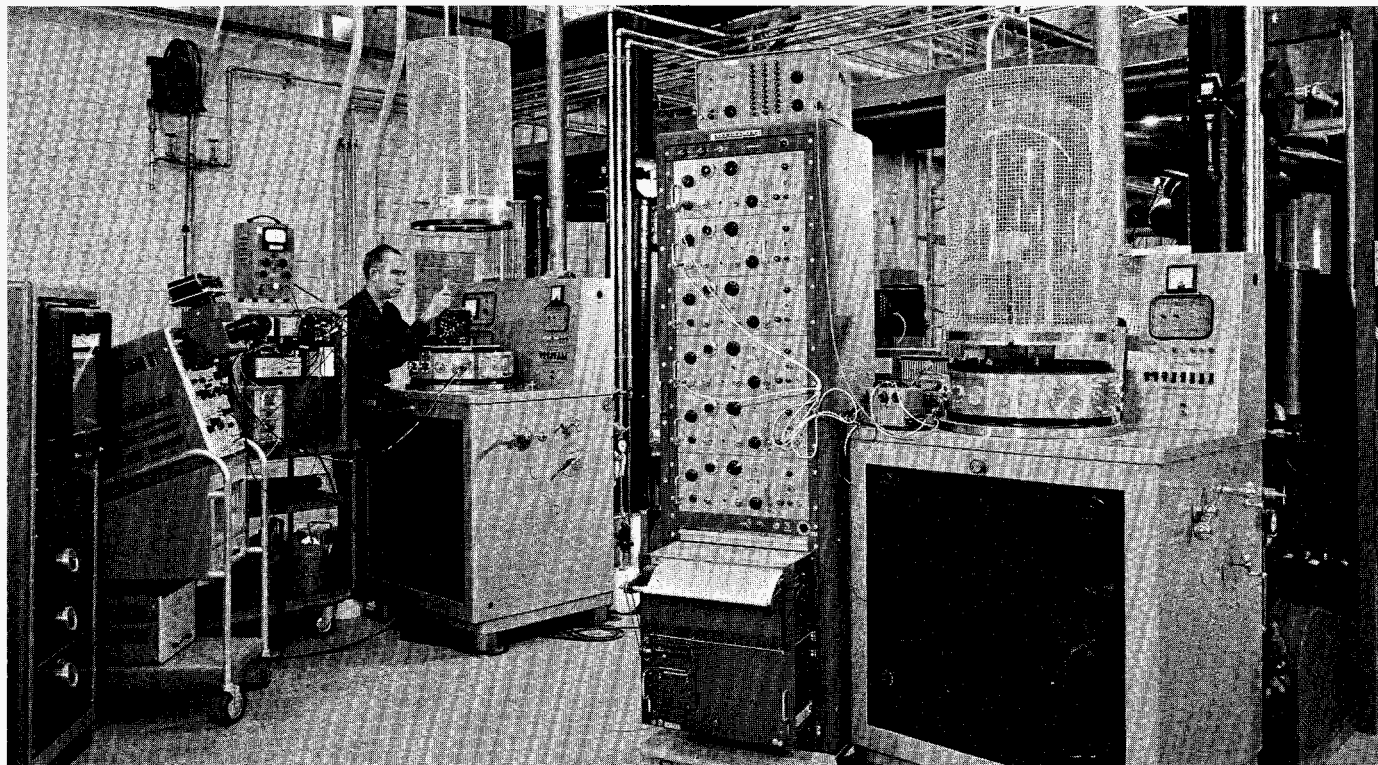


Fig. 194. 18 × 30-in. bell-jar vacuum system

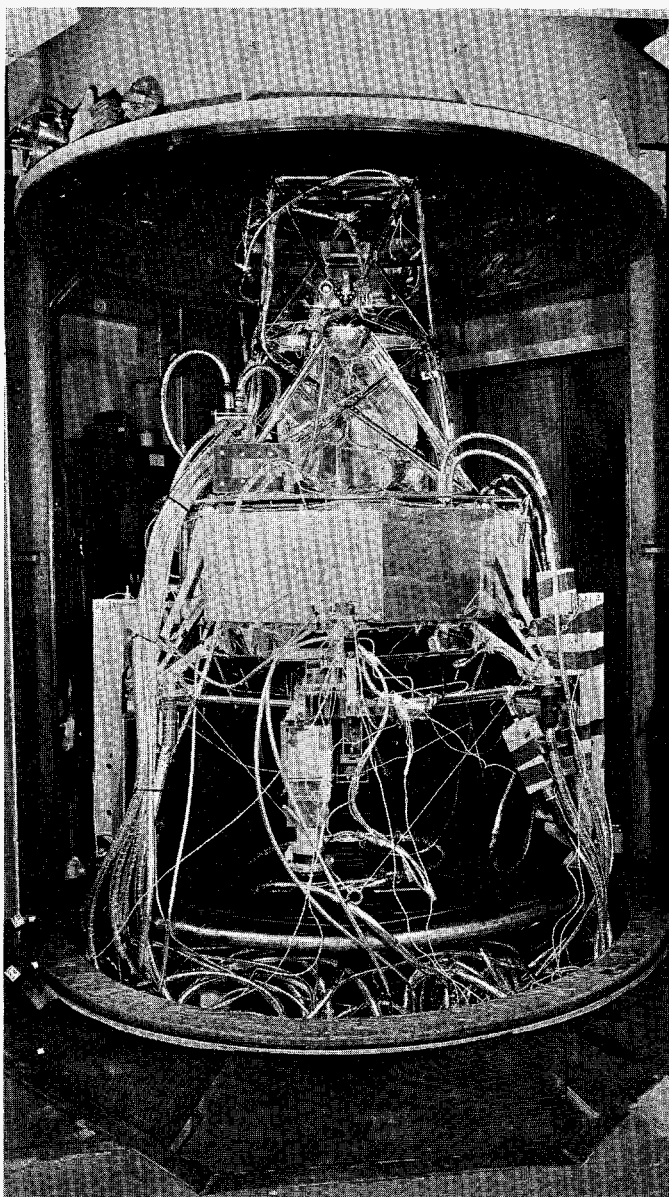


Fig. 195. *Mariner R* in 6-ft space simulator

temperature environment, and calibration of the spacecraft telemetry as a complete system at different temperatures while in a vacuum-temperature environment. The *Mariner R* temperature-control model was also tested in the 6-ft space simulator.

(2) *25-ft space simulator*. A major addition to the environmental test facilities is the new 25-ft space simulator (Fig. 196). This facility is an environmental test chamber combining vacuum, a cold-wall heat sink, and a source of collimated radiant energy simulating the solar energy spectrum. In addition to the test chamber itself, the facility includes a 10,000 sq ft building housing equip-

ment, and an operations area encompassing both the facility control center and a setup area for the user's test racks and instrumentation. The simulator provides a test volume 25 ft in diameter and 25 ft high, within a stainless-steel vacuum chamber of slightly larger diameter but with an over-all height of nearly 50 ft. Access is through a 15- × 25-ft door in the side of the chamber, or alternatively through a personnel door contained within the larger access door.

Chamber pump-down is accomplished in three phases. The first utilizes, as a matter of convenience, the nearby JPL wind tunnel compressor plant. This is followed by a period of pumping using conventional mechanical vacuum pumps and blowers, and finally the ultimate vacuum (about 10^{-6} mm Hg) is produced by the use of 10 32-in. oil-diffusion pumps. The whole evacuation process requires several hours, the exact time depending on the previous conditioning of the chamber and the nature of the test item. The heat sink of space is simulated in the chamber by means of liquid-nitrogen-cooled panels which blanket the interior walls of the chamber. These have a dull black finish and are maintained at a temperature of approximately 100°K. Thus, a negligible amount of energy is reflected or radiated by them to the test article.

The energy sources for the solar simulation features, together with important elements of the optical system, are contained within a 25-ft-diam., 25-ft-high housing on top of the vacuum vessel. Energy from 131 2.5-kw mercury-xenon compact arc lamps is collected and directed downward into the vacuum vessel through a 3-ft-diam. quartz transfer lens. Inside the chamber, this beam is reflected upward to fill a parabolic mirror, which then directs the energy downward in a collimated beam. It is intended that radiation intensity be variable from that corresponding to the orbit of Mars to that of the orbit of Venus. Unfortunately, however, the Venus range could not be simulated for *Mariner R*.

The *Mariner R* temperature-control model was the first spacecraft tested in the 25-ft space simulator (Fig. 197). The tests included four pump-downs during the period from late February to mid-April 1962. The purposes of the tests were to verify the passive temperature control design and freedom from large thermal gradients, and to estimate thermal time constants. Due to construction schedule slippages, the facility was not completed at the time of these tests and it was used under a loan agree-

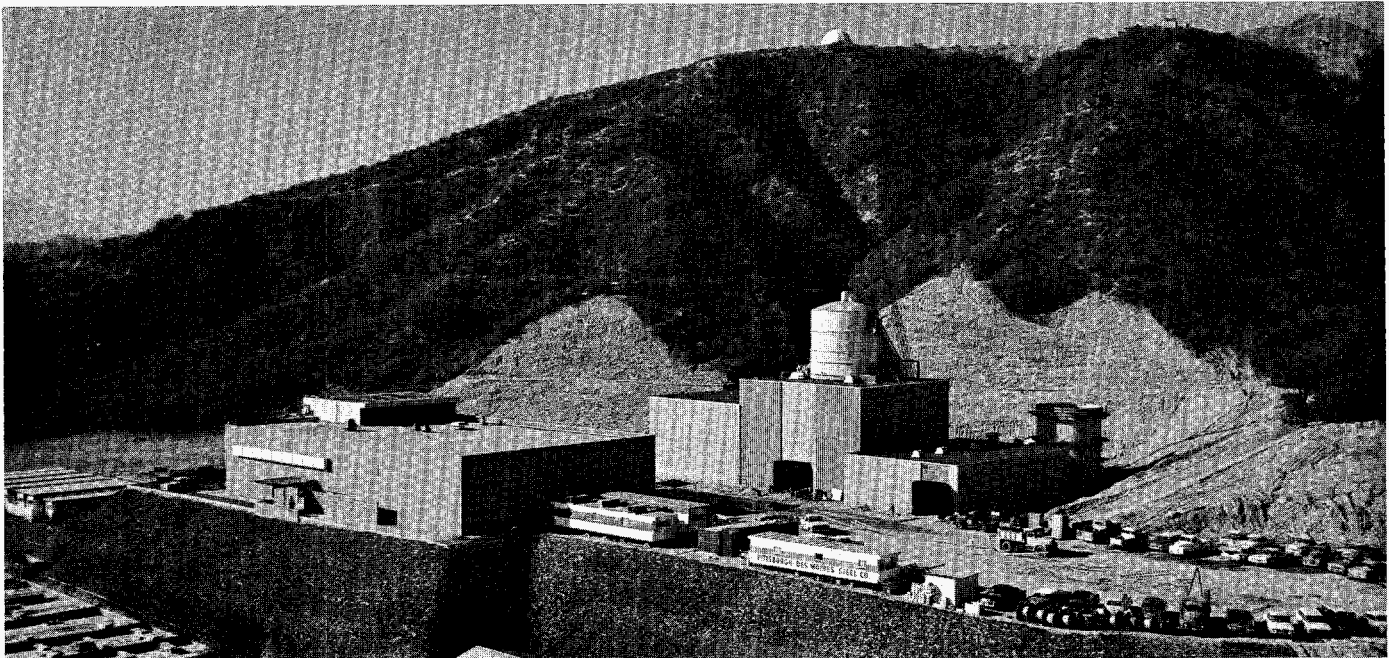


Fig. 196. Environmental facilities building (25-ft space simulator on right)

ment with the contractor. The test conditions attainable were as follows:

Vacuum: Pressures were in the low 10^{-5} mm Hg range.

Cryogenics: The liquid-nitrogen shroud furnished by the contractor was not yet operable; therefore, a special shroud was built by JPL for the test. This shroud provided a sufficiently complete and cold background; its smaller diameter did not permit the use of full-size solar panels on the spacecraft.

Solar simulation: The facility's solar simulation system was not complete and could not be used for testing; therefore, it was necessary to simulate solar heating with heating pads mounted on the spacecraft.

In spite of the limitations imposed by the incomplete state of construction, it was believed that useful data were obtained.

d. Summary of environmental testing required by MR-1 and -2. Mariner R environmental testing began during September 1961, and 975 tests were run between that date and August 1962. The heaviest test load occurred during January and February, when flight-

acceptance testing deadlines were in effect. A tabulation of the tests follows:

Vibration	493
Vibration, low-frequency	45
Centrifuge	33
Shock	30
Vacuum	46
Vacuum-temperature	236
Space simulation	18
Temperature	47
Humidity	19
Salt fog	2
Explosive atmosphere	4
Off-Lab testing (arranged by ETL):	
Vibration	1
Explosive atmosphere	1
Total	<u>975</u>

Breakdown of these tests by types was: (1) experimental, 169; (2) type-approval, 238; and (3) flight-acceptance, 568.

2. Instrumentation Support

a. Vibration testing. In order to support the large number of type-approval and flight-acceptance vibration tests for the Mariner program, an enlarged instrumentation system was devised. Included in this system were

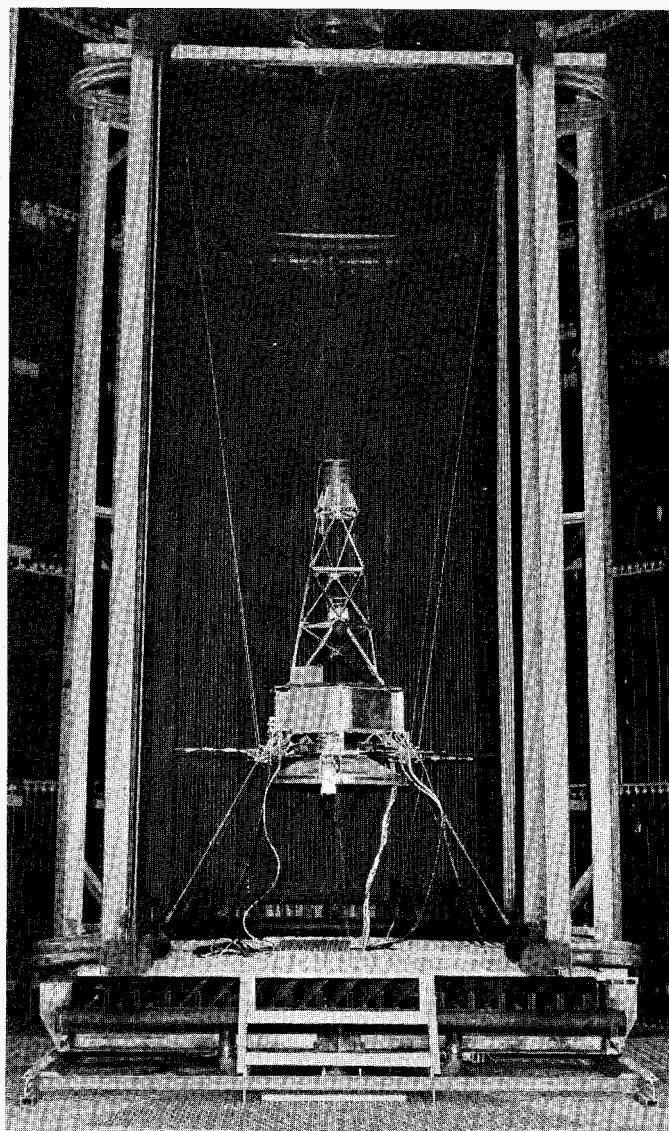


Fig. 197. Mariner R TCM in 25-ft space simulator

accelerometers of high- and low-frequency response, amplifiers, direct-write oscillograph recorders, and magnetic tape recorders. This equipment was mounted in racks that could be readily moved to various test locations and could be expanded to handle large assignments. The maximum signal-handling capacity was 30 oscillograph channels and 25 magnetic tape channels.

In June 1962, most of the original instrumentation equipment was installed in the centrally located recording room of the new Environmental Laboratory building (Fig. 198). Instrumentation support was provided for tests on a large variety of spacecraft components, including the solar panels, high-gain antenna, component cases, magnetometer boom, and midcourse propulsion system.

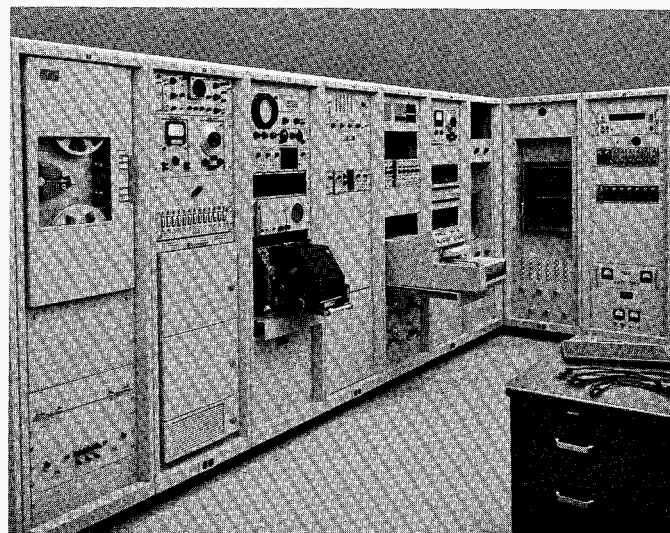


Fig. 198. Environmental Laboratory recording equipment room

In addition, many composite-structure tests were supported, using a maximum instrumentation capacity.

b. Static structural and thermal testing. Increased capabilities were procured for recording force, strain, deflection, and temperature data by automatic means. Two Giannini-Datex 50-channel data loggers (extendable to 192-channel units) are used to measure spacecraft temperature distribution during tests in the 6-ft and 25-ft simulators (Fig. 199). The use of voltage-to-frequency conversion techniques and an adjustable gate length counter provides for read-out of all data in engineering units. Chromel-constantan thermocouple signals in the ranges -325 to $+300^{\circ}\text{F}$ and 200 to 1800°F are linearized and presented in $^{\circ}\text{F}$. Output consists of a 4-digit plus sign data display, point number, and time, with tabulation of data available by use of either a Flexowriter (with or without paper-tape punch) or an integral digital printer. The time to scan a channel varies from 0.7 to 1.4 sec, depending on whether the Flexowriter is used.

c. Pyrotechnic tests. The design and evaluation of squib-actuated devices used in the spacecraft required a test program for which special transducers were designed and instrumentation equipment provided and operated. Several "bombs" were designed to measure pressure characteristics of the squibs fired, at high and low temperatures and in vacuum. Several hundred tests were made in this squib-firing program.

d. System tests. Performance evaluation of the ground support equipment for each spacecraft required a central recorder which recorded up to 36 signals during the sys-

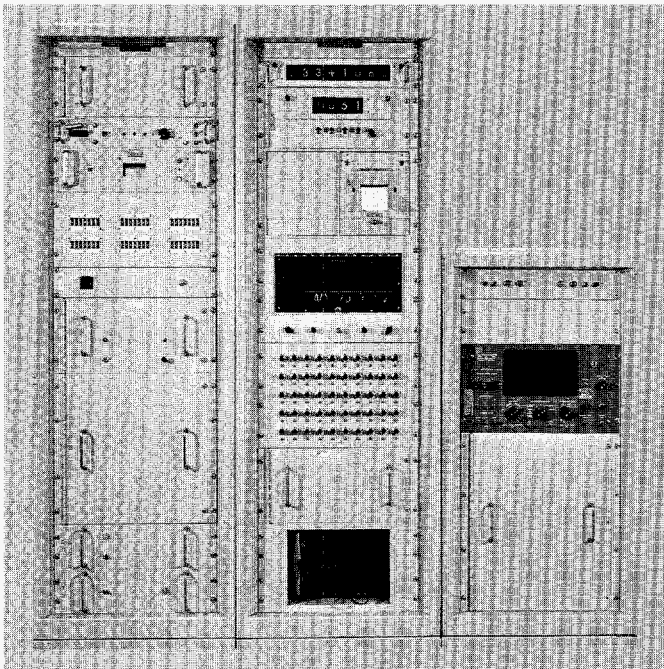


Fig. 199. Data loggers providing engineering units tape read-out

tem test operations. This recorder was a direct-write oscillograph operating at various speeds and bandwidths to suit the test requirements. As a part of the System Test Complex, it was moved to various test locations at JPL and to AMR. Two such recorders and operators constituted the instrumentation support for the *Mariner* operations.

e. Propulsion system vacuum tests. Instrumentation was provided for a series of tests conducted to determine the performance of the *Mariner R* 50-lb-thrust midcourse motor in a near-vacuum environment. These tests were run at the facility of the Sunstrand Corporation at Pacoima, California, where the instrumented propulsion system was operated in a vacuum tank capable of simulating an altitude of 107,000 ft during the firings.

Performance characteristics determined from this testing program were engine thrust coefficient, specific impulse, characteristic velocity, starting transients, thrust tailoff at shutoff, starting ability in vacuum environment, and the reproducibility of all these characteristics. Measurements required to meet the test objectives were thrust, five pressures, two fuel flow rates, seven temperatures, two valve positions, and four valve operation events.

(1) *Thrust stand.* A thrust stand was designed to measure the axial component of thrust with an over-all accuracy of 0.25%. The fixture to which the propulsion

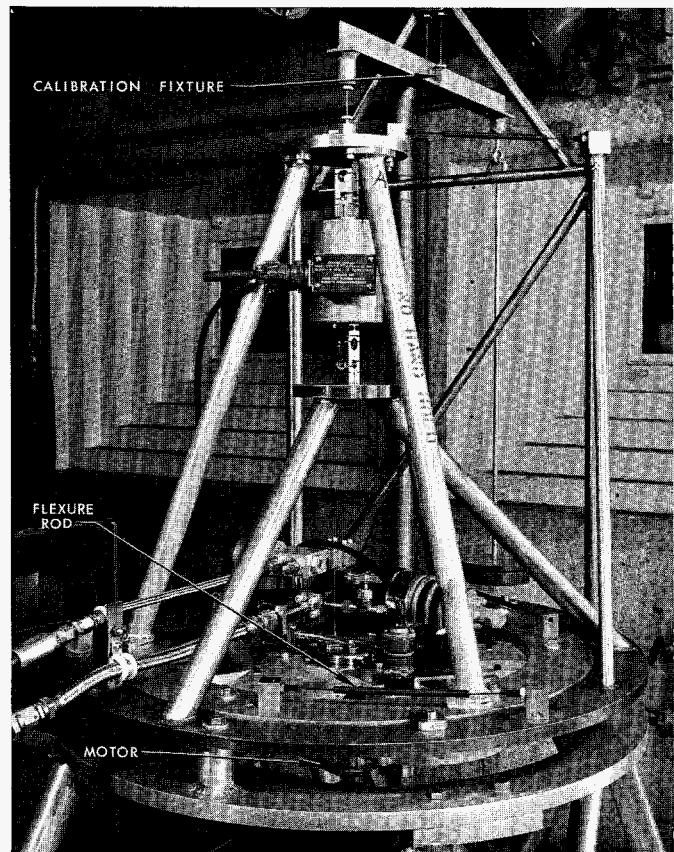


Fig. 200. Thrust stand for 50-lb motor

assembly was attached was supported at six points in such a manner that all moments and forces were restrained except in the direction of axial force, where high compliance was attained through the use of flexure rods (Fig. 200). The force transducer was then coupled to the structure by universal flexures. This nonredundant design minimized the effects of temperature and vibration on the thrust measurement. The force transducer was a conventional strain-gage, bridge-type with its case vented to eliminate the force error due to differential pressure under vacuum environment. To minimize temperature effects, the transducer and all cables were wrapped with aluminum-backed tape. In-place calibration of the thrust stand was made with dead weights and a wire-supported lever.

(2) *Recording trailer.* All signal lines were connected to a termination panel in the vacuum tank, and one multiple-conductor cable routed the signals through a sealed fitting to a nearby JPL trailer. Power and control lines were handled similarly by separate cabling. The trailer, which served as a recording and control center for the firings, contained a 36-channel oscillograph, three precision pen recorders, transducer excitation power sup-

plies, pulse converters for flow-rate signals, d-c amplifiers, and a thermocouple calibrator. A control panel and valve-operation power supply were also provided.

f. Magnetic field mapping and calibration. All spacecraft materials, structures, and components were tested for magnetic field magnitude and direction to ensure minimum interference with the magnetometer experiment. A single-axis magnetometer was used for field mapping and for determining maximum and minimum field strength in three orthogonal planes for all spacecraft components. In the latter stages of spacecraft assembly, the single-axis magnetometer, a triaxial magnetometer, and a 3-channel recorder were used in the SAF to map the field strength of the completed spacecraft.

The acceptance tests and calibration of the flight magnetometer were performed at the Malibu Magnetic Facility of STL. JPL triaxial and single-axis magnetometers and recording equipment were used in conjunction with the STL coil system to provide zero field and known reduced fields for flight-equipment checkout.

JPL magnetometers were used at AMR for final spacecraft mapping and for component rechecking when modifications or substitutions of components were made. The most noteworthy operation of this kind was the mapping performed following the substitution of a new midcourse propulsion system.

3. Computer Applications and Data Systems

a. Introduction. The Central Computing Facility has devoted a major effort in the 1961-1962 period to space

flight operations. The facility has expanded and purchased additional equipment and data systems for supporting both lunar and interplanetary flight programs. Improvements were made to existing computer programs and new ones were added to process data from the *Mariner R* data system. More emphasis was placed on computer flight programs becoming operational long before launch to provide computing services for preflight testing and checkout.

Services provided by the Central Computing Facility to the *Mariner R* project were data-processing systems design, implementation, and operation; digital computer applications; analog computer applications; preflight data processing; and flight data processing.

b. Data systems. The following data systems and associated equipment have been implemented during the period of this Report.

(1) *IBM 7090-1401 computing system.* In addition to the existing IBM 7090-1401 system (Fig. 201 and 202) (Space Flight Operations Station C), a second duplicate system (Fig. 203) was added (Space Flight Operations Station D) to handle the increase in computing and processing requirements for new projects such as *Mariner R*. The additional system was used in meeting the need for a back-up system during the operations.

(2) *Digital Equipment Corporation PDP-1 computer* (Fig. 204). This small, fast, general-purpose computer was designed specifically for data processing. It was installed in early 1962 to process quick-look telemetry data, providing meaningful spacecraft data in real time



Fig. 201. IBM 7090-1401 computing system, Space Flight Operations Station C

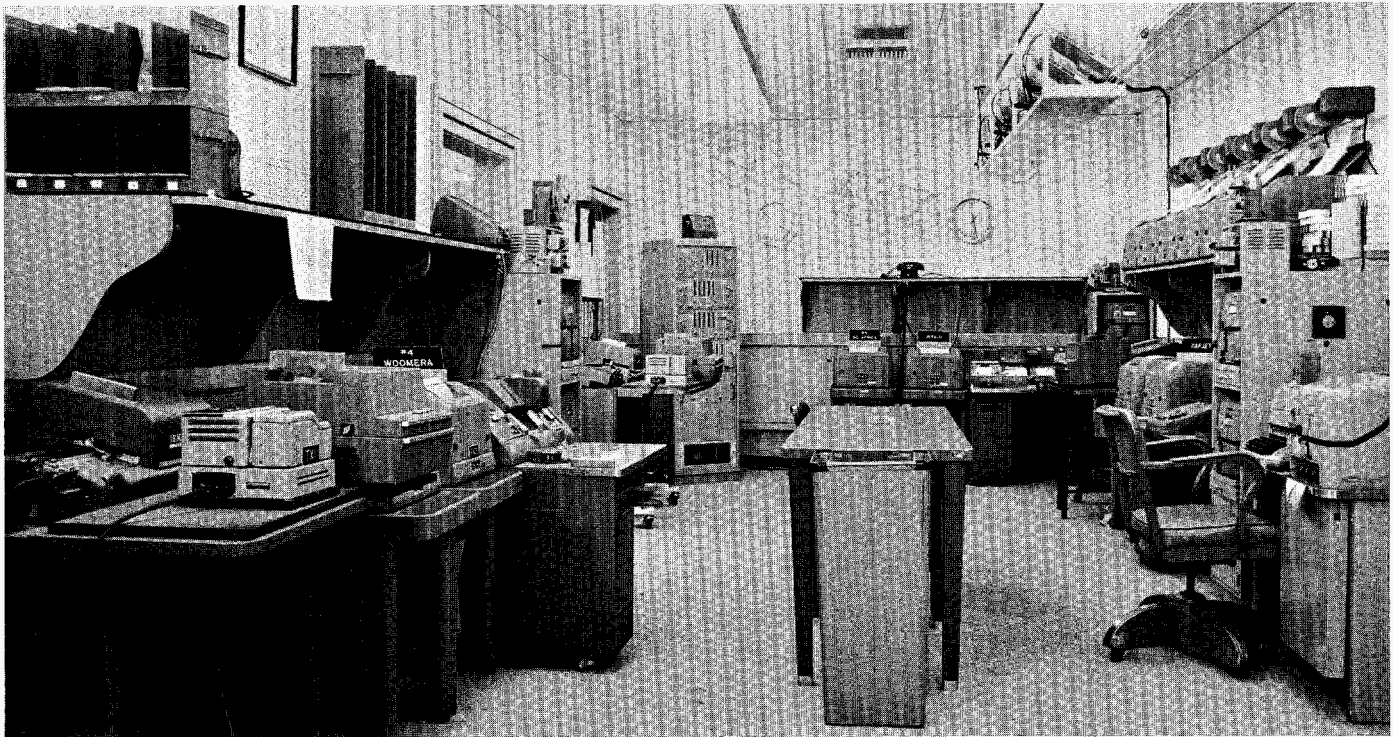


Fig. 202. Teletype data and communications center, Space Flight Operations Station C

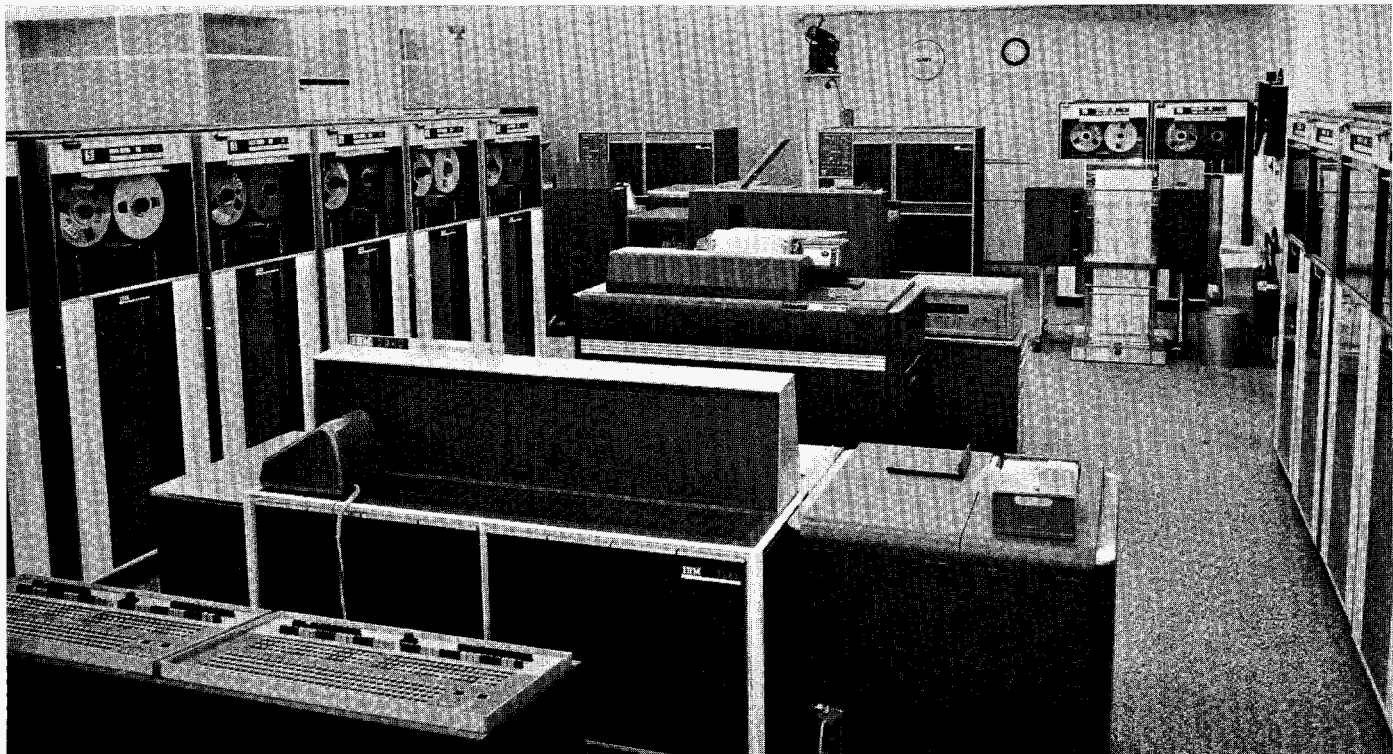


Fig. 203. IBM 7090-1401 computing system, Space Flight Operations Station D

UNCLASSIFIED

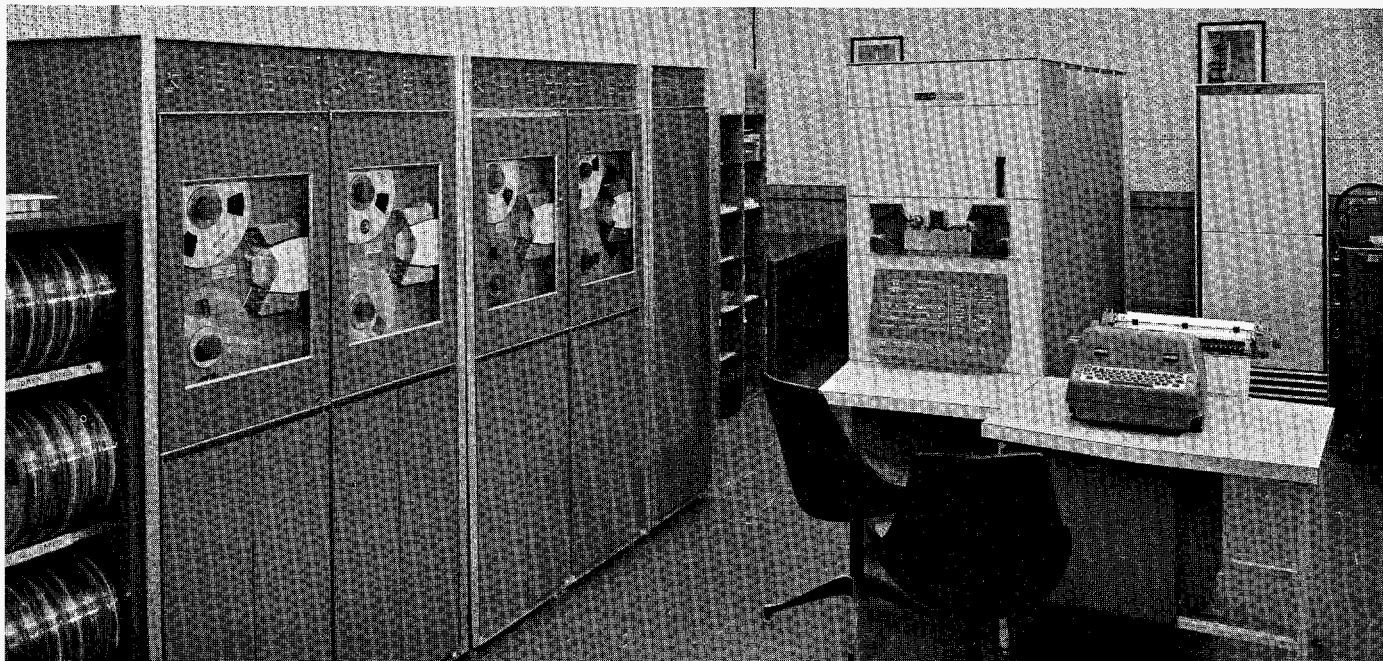


Fig. 204. Digital Equipment Corporation PDP-1 computer

to responsible engineers and scientists during flight. The computer accepts raw telemetry data directly from teletype lines from the overseas DSIF sites, and from a high-speed data line from Goldstone. The equipment used to format data from these lines to the PDP was designed and built by the Data Systems Group at JPL. During periods when the IBM 7090 was being used for real-time orbit determination, the PDP was used as the primary processor for telemetry data. The use of the PDP-1 as an on-line processor replaces special-purpose hardware such as decommutators. While this is the first application of this type in the lunar and planetary projects, future plans will be based upon increased use of on-line data processors.

(3) *Stromberg Carlson 4020*. The SC 4020 is a high-speed printer-plotter (Fig. 205) which uses magnetic tapes generated by the IBM 7090 for input. This machine was purchased in winter 1961, primarily to generate engineering-type plots (paper or microfilm) for spacecraft performance analysis. During the *Mariner R* operation, the 4020 was used to generate microfilm engineering plots at the rate of 3 plots per sec. One of the primary advantages of the equipment over more conventional strip-chart or X-Y plotters is the capability to provide complete annotation and digital output with the analog plot. Multiple plots and cross plots are also readily available.

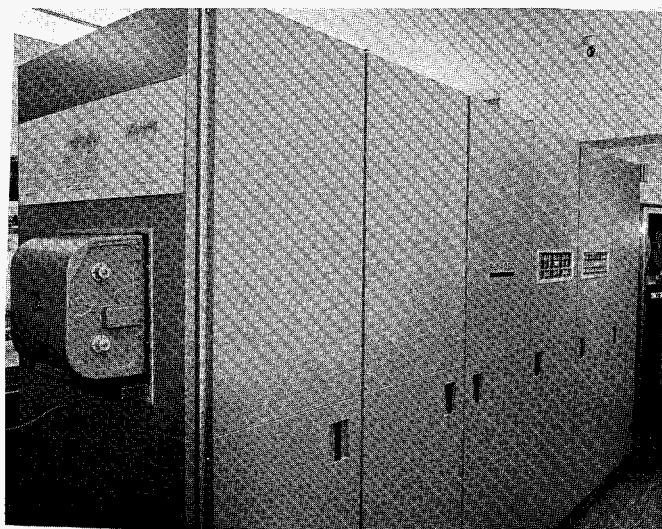


Fig. 205. Stromberg Carlson 4020 printer-plotter

(4) *Telemetry processing station* (Fig. 206). In the past year, the Central Computing Facility accepted the responsibility for processing telemetry magnetic tapes received from the DSIF stations. During the first 6 mo of 1962, the *Mariner R* telemetry processing station was designed, purchased, and brought into operational status.

In the design phase, it was recognized that processing magnetic tapes at the same speed at which they were

UNCLASSIFIED

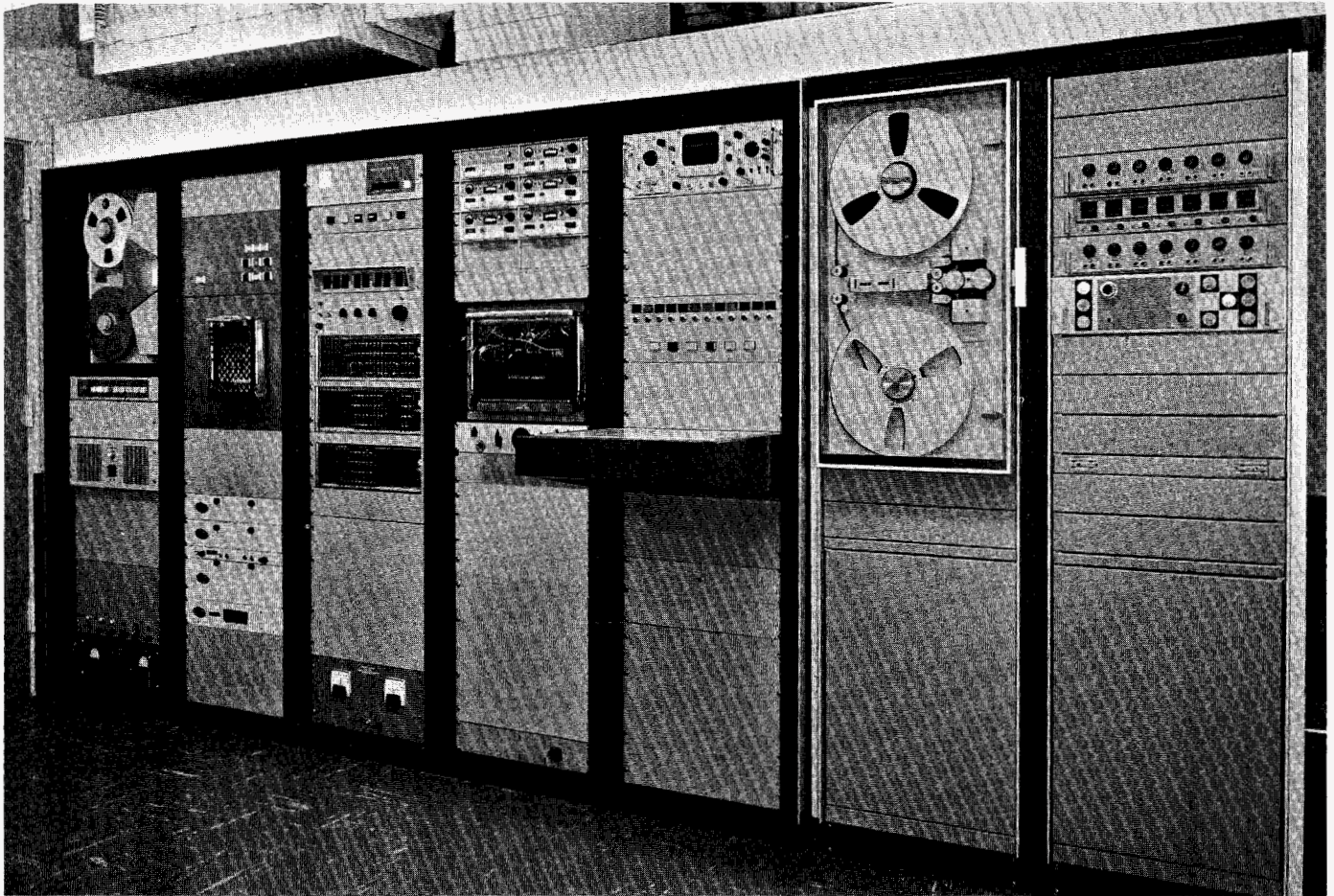


Fig. 206. *Mariner R* telemetry processing station

recorded would entail many man-hours of play-back operation. In order to reduce the time for play-back and processing, the telemetry station was built to process magnetic tape eight times faster than the speed at which the tapes were recorded.

The following equipment was installed to process *Mariner R* telemetry data for computer entry:

- (1) Magnetic tape reproduce-record unit with associated electronics (FR 600 Ampex Corp.)
- (2) NASA time-code translator (Astrodata, Inc.)
- (3) Telemetry discriminators (Data Control Systems, Inc.)
- (4) Analog-to-digital converter (Packard-Bell)
- (5) Magnetic tape translator (JPL)

The primary function of the telemetry-processing station is to accept analog magnetic tapes recorded at the

DSIF stations and translate them into acceptable IBM format tape for computer processing. In the *Mariner R* application, all decommutation and engineering units conversions are carried out in the PDP-1 or IBM 7090.

c. Digital computer applications

(1) *Spacecraft design.* Computer programs were written to support the initial design and development of the *Mariner R* spacecraft early in the program. Structural analysis programs were developed for the design and analysis of the spacecraft bus, midcourse motor, and interconnecting members. In the area of heat transfer, a system of programs was written for solving the transient and steady-state heat equations used in calculating the radiosity between bodies.

Other smaller programs were produced to aid engineers in the areas of communications analysis and environmental testing.

(2) *Flight-path determination and analysis.* Computer programs for flight-path determination and analysis fall into three categories: tracking data editing, space trajectories, and orbit determination.

Tracking data editing. The specialized tracking data editing program edits all information received from the DSIF and deletes such nontracking data as administrative messages, teletype headers, partial messages, "blunder points," and data out of range. It also discriminates between missions, compresses data, supplies weight codes, makes refraction corrections, makes pass identification, and sets up frequencies of the orbit-determination program. The output of this program is an IBM-format magnetic tape with edited and formatted data for use by the ODP.

Space trajectories. At launch time, the trajectory program determines the powered-flight phase parameters from launch to injection and produces nominal trajectory values for preliminary analysis. Later, during the flight phase, the trajectory program computes transformations from one coordinate system to another and determines view periods for the DSIF. For the *Mariner R* program, additional refinements were added to allow for the effects of solar radiation as a polynomial in time and the disturbance of an uncoupled pitch gas ejection from the spacecraft which was anticipated prior to launch. From this program, public information data were generated. The various outputs from the trajectory program were selectable, using a program-control tape.

Orbit determination. The orbit-determination program accepts tracking data from the tracking data editing program, fits a trajectory to the data using least-squares methods, computes statistics, i.e., gives an estimate of the confidence level of the orbit, and plots residuals, which are the difference between calculated and observed quantities.

Due to requirements for improved accuracy and for the ability to solve for selected astronomical constants, the orbit-determination program was completely reworked for *Mariner R*. This new program will become the primary orbit-determination operation for planetary and lunar flights in the future. Significant new capabilities include: the ability to solve for the position and velocity of the spacecraft at any given epoch and to consider the effect of certain astronomical constants such as solar radiation pressure; the astronomical unit; radius of the Earth; gravitational constant of the Earth or Moon; the masses of Venus, Mars, and Jupiter; the speed of

light; and the second, third, and fourth harmonics of the Earth's field of gravity. Also, the *Mariner* orbit program generated view periods and prediction angles for the DSIF.

(3) *Midcourse-maneuver determination.* The intricate midcourse maneuver and command program is capable of determining a variety of information. The fundamental purpose is to compute the three-axis positioning of the spacecraft along with the correct velocity increment to be added by the midcourse motor at the proper time. Commands to the spacecraft for this maneuver are then generated by the program to correct for any launch errors that would give an undesirable trajectory. Additional capabilities of the midcourse program are to compute the "fly-by fine print," generate a capability ellipse, and plot, in polar coordinates, certain information in the vicinity of Venus.

The fly-by fine print computes information about the encounter phase, such as DSIF station loss and gain, the radiometer first-view time of Venus, antenna hinge and swivel angles, and the illumination from Venus. The capability ellipse generator gives information about what is possible with the midcourse motor, and other pertinent information such as the angular diameter of Venus that will be seen by the spacecraft.

Telemetry. Telemetry computer programs fall into three broad categories: quick-look, general processing, and data analysis.

Quick-look computer programs were used by the PDP-1 computer for processing on-line telemetry data without further formal processing by the IBM 7090 computer. These programs provided engineers and scientists with quick, usable telemetry data.

On-line PDP-1 programs include:

- (1) Complete engineering decommutation, data editing, and data identification
- (2) Science decommutation and editing
- (3) Preliminary science alarm
- (4) Quick-look output

The outputs from the PDP include the quick-look prints, the on-line science alarm, a 7090-format tape of all telemetry data, and an up-dated master data tape, which is a complete file of all *Mariner R* telemetry data in a convenient format for retrieval and processing.

General processing programs were written for the IBM 7090 to process raw telemetry data into tabulated data and engineering plots for preliminary analysis and formal reports. Analysis programs operated on processed engineering and science data to give "alarms" when data fell out of prescribed tolerances. In addition, these programs provided JPL engineers and scientists with data in a form that fulfilled their specific needs for rapid analysis.

To facilitate the ease of operation of the telemetry programs, a master program tape was generated from which all or any one of the following telemetry programs could be run on the IBM 7090 without additional setup:

Program	Output
Engineering decommutation and processing	Tabulated listings
Engineering plotting	Plots
Engineering analysis	Tabulated listings and plots
Engineering alarm	Tabulated listings
Science decommutation and processing	Tabulated listings
Science analysis	Tabulated listings and plots
Science alarm	Tabulated listings

d. *Analog computer applications.* The Analog Computer Facility (Fig. 207) has been used extensively in preliminary design and advanced studies leading to the

Mariner program. By fall 1960, simulations oriented specifically to the *Mariner* program were initiated.

The nature of this support is best described with reference to the divisions and groups to which the support was rendered. Over 60% of this support went directly to the Guidance and Control Division. Forty percent of the computer load was utilized by the Analytical Design Group of the Guidance and Control Analysis Section of this division. These studies were initially simplified single-axis investigations dealing primarily with the attitude control system. The fuel consumption to disturbing torque ratio, including effects of solar torques, were studied by analog simulations. These simulations grew rapidly in detail and were extended to three-axis simulations. By March 1961, the emphasis was placed on the simulation of the midcourse autopilot. These initial simulations were single-axis studies of behavior about the pitch, roll, and yaw axes. However, by September 1961, the simulation had been extended to three-axis simulation. The effects of the elastically coupled structural members were included.

By February 1962, a highly systematized general block diagram of the spacecraft was submitted by the Analytical Design Group. The description of the spacecraft was in the form of a block diagram of matrices and was titled "Six Channel Autopilot with Elastically Coupled Structural Members." This description has resulted in a very systematic manner of specifying spacecraft design

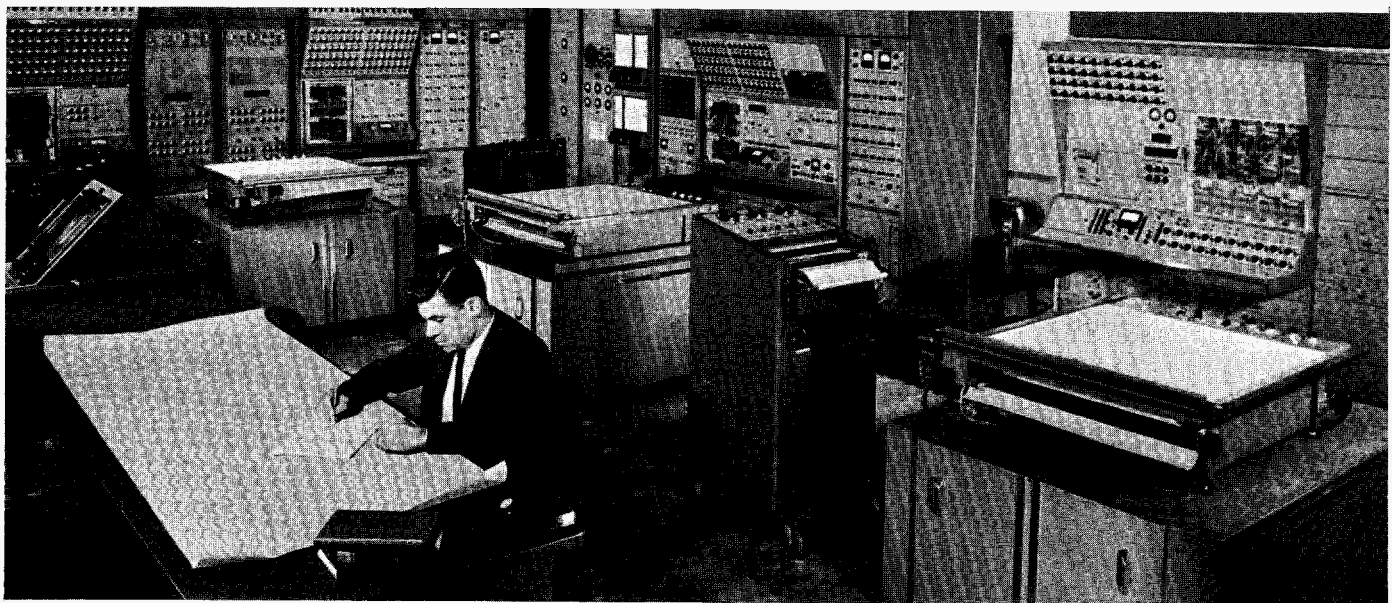


Fig. 207. Analog Computer Facility

changes to be studied. The size of the computer program can be quickly modified to meet the needs of the study at hand. This program served an important role in final preflight evaluation of the effects of late spacecraft modifications, and observations of the spacecraft performance. At that time, the study was so detailed that the resulting simulation was the largest ever executed at the JPL Analog Computing Facility. This simulation utilized four computing consoles with over 250 amplifiers.

Twenty percent of the *Mariner* analog computer support went to the Control Systems Group of the Spacecraft Control Section. Much of this simulation was directed toward studying the detailed design and behavior of components of the spacecraft control systems and their effect on over-all performance. The Earth-sensor and Sun-sensor nonlinearities were studied in detail. Extensive detail studies of the gyro loop were made. There

were several direct simulations using flight hardware such as the gyros and jet vanes with their actuators. The results of these studies were incorporated into the overall analog simulations.

Over 30% of the *Mariner* support was given to miscellaneous groups. Several of the problems were simulations of the temperature distribution on the spacecraft in various attitudes and throughout the various possible maneuvers. R-F acquisition was simulated with DSIF r-f equipment for the Telecommunications Division.

e. Preflight operations

(1) *On-Lab support.* Early in 1962, an accelerated effort was made to bring the telemetry programs and computing support up to operational status as soon as possible to support the *Mariner R* tests being performed at JPL.

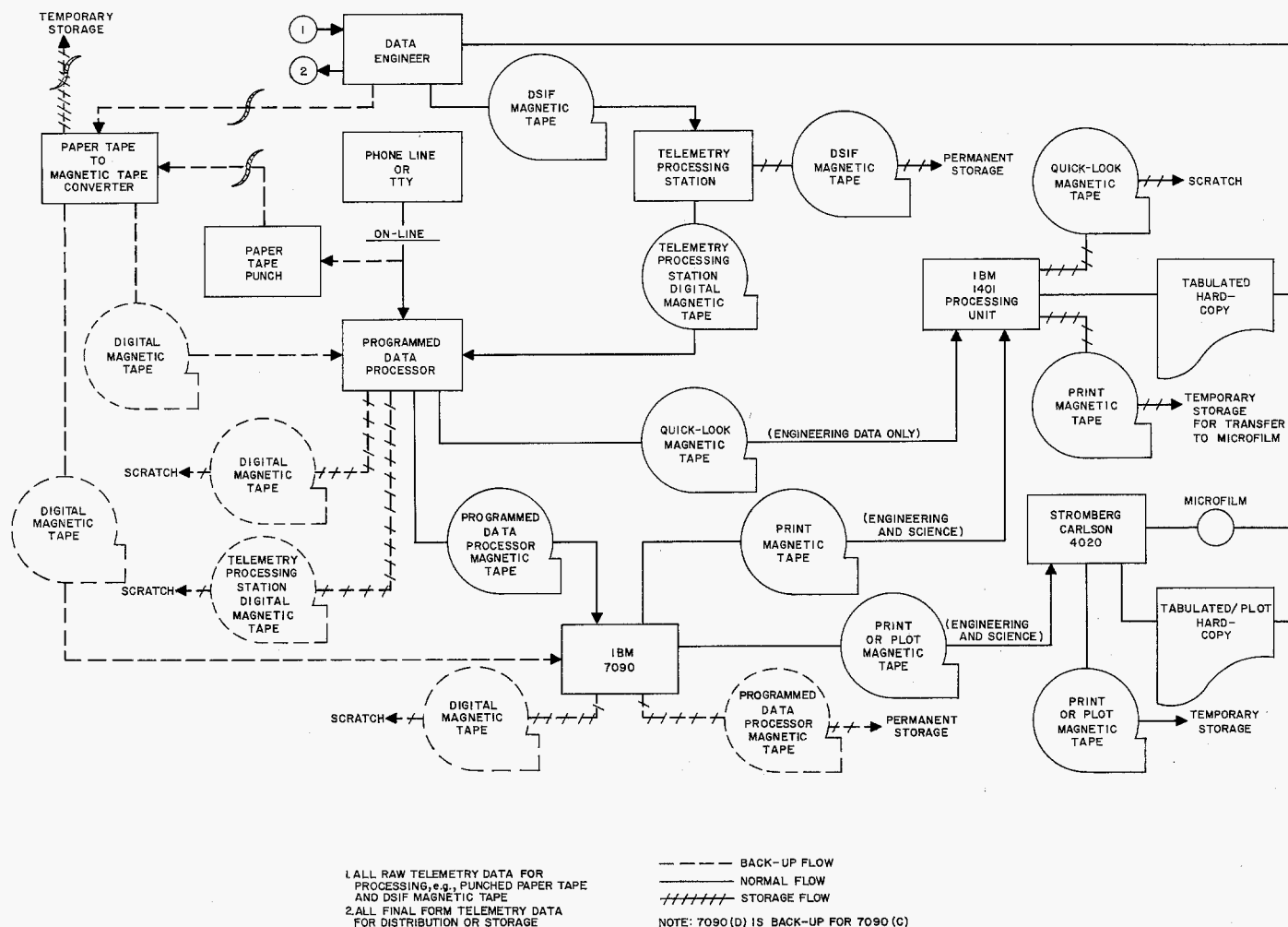


Fig. 208. Mariner R telemetering data flow

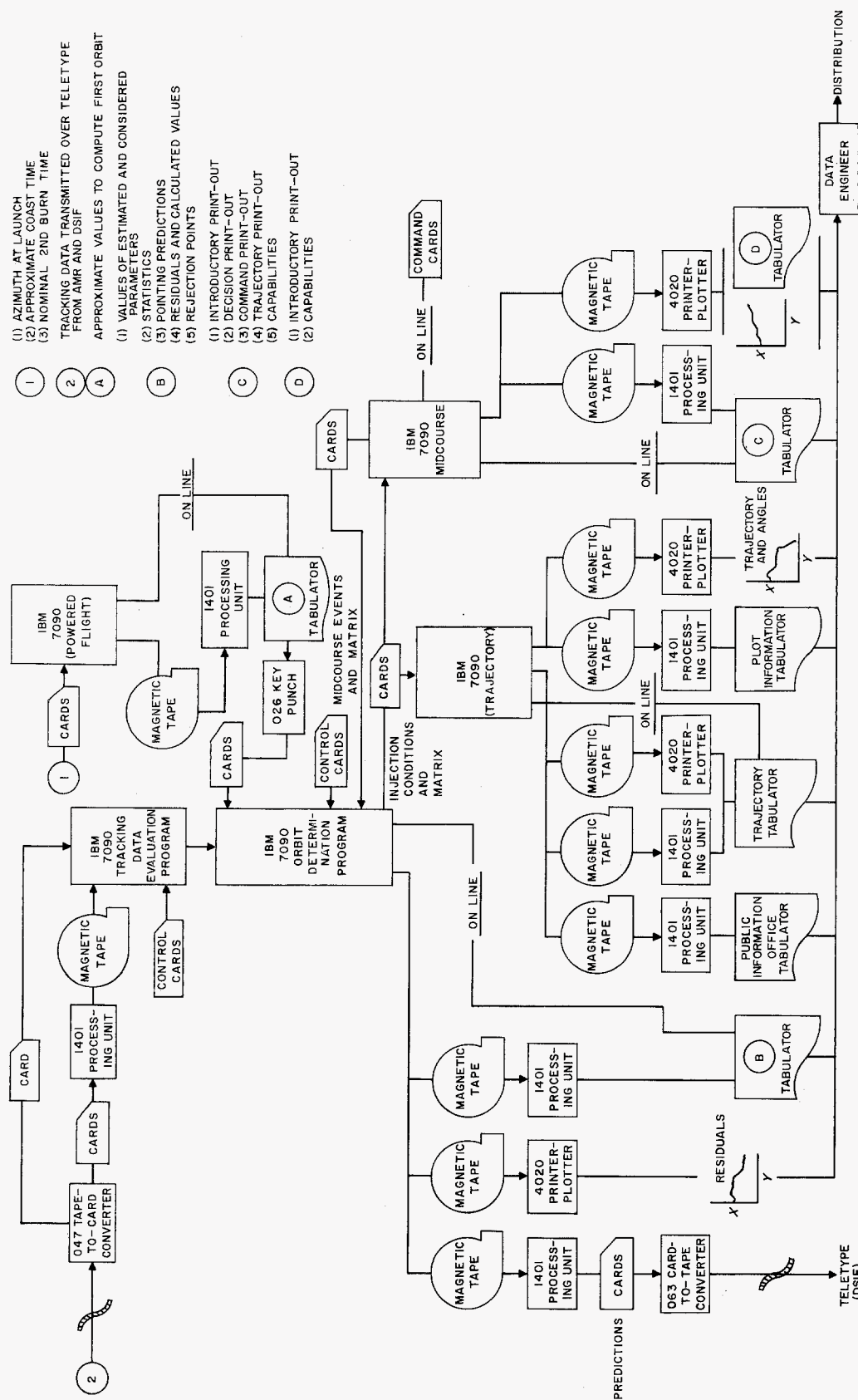


Fig. 209. Mariner R tracking data flow

UNCLASSIFIED

JPL TECHNICAL REPORT NO. 32-353

In April, the final configuration of the telemetry teletype encoder, which was to be used at the DSIF stations, was built and installed in the SAF building to transmit data by hard-line to the Central Computing Facility for operational checkout and test support. As a result, the Spacecraft Data Analysis Team was able to familiarize themselves with data formats and content as the spacecraft underwent flight simulation tests. This early approach to integrated spacecraft-data processing operations contributed significantly to flight operational readiness.

(2) *Atlantic Missile Range support.* With support by the Central Computing Facility, teletype communications for data transmittal were set up for tests conducted prior to launch and during the launch operation. This procedure enabled JPL operational personnel to act in a more

realistic environment. In some tests conducted at AMR, data were received, processed in real time, disseminated to JPL flight analysis teams, and flown back to AMR for final analysis within 24 hr.

f. Flight operations. In order to support the flight program, the CCF had to consider not only the requirements of manpower and machines for the initial and critical phases of the flight, but also for the long, extended period of the total flight time. This involved detailed scheduling of computer time and personnel to support the operation; nominal data-processing procedures had to be developed along with cases of abnormal techniques. Fig. 208 and 209 show the planned flow of data within the Central Computing Facility.

UNCLASSIFIED

[REDACTED] UNCLASSIFIED

JPL TECHNICAL REPORT NO. 32-353

VIII. Quality Control

A. Quality Control Requirements

1. Project Requirements

The *Mariner R* Project requirements pertaining to quality assurance are documented as follows:

a. Quality assurance requirements. Each division was responsible for accomplishing all quality assurance functions during the development, fabrication, and checkout of *Mariner R* equipment. The basic project requirements for specific quality assurance activities were for visual workmanship inspection and use-hardware certification on delivery to the Spacecraft Assembly Facility. The meeting of these requirements and the establishment and maintenance of an over-all project quality assurance program demanded the following additional project requirements.

b. Quality assurance procedures. The *Mariner R* Project Office set the following quality assurance requirements:

- (1) Inspection as required by the Project Office was a redundant operation performed by other than the fabrication and checkout personnel, if possible. Consequently, the inspection personnel of the Systems Division were expected to provide inspection service support to all divisions. All divisions were required by the Project to utilize such inspection support, unless waived by the Systems Division.
- (2) The inspection personnel were required to establish the technical requirements for all inspection prior to its being carried out, by discussion and

[REDACTED] UNCLASSIFIED

agreement with the concerned division. The concerned division's opinions in regard to appropriate requirements were accepted as satisfactory.

- (3) The inspection personnel were responsible for inspecting hardware and accepting or rejecting it, depending on its meeting the agreed-upon technical requirements. If the hardware were rejected, it could only be utilized as a result of a Project-required Materials Review Board action. The MRB consisted of the inspector, the equipment cognizant engineer, and a senior technical representative of the concerned division, or their alternate representatives.
- (4) The Systems Division was required to establish and maintain documentation and recording systems for all inspection reporting and MRB actions. Furthermore, the division was required to collect and appraise all inspection reports and MRB action documents and to prepare a Project Quality Assurance Results Manual.
- (5) All divisions were required to certify all hardware prior to its acceptance at the SAF for system use. Certification consisted of the following minimum requirements:
 - (a) Written acknowledgment that the flight-acceptance testing was satisfactorily accomplished.
 - (b) Written acknowledgment that the hardware had passed inspection or had been accepted through MRB action.
 - (c) Certification that all engineering change orders of record were implemented on the hardware being delivered.
 - (d) Certification that certain special technical requirements, as defined by each cognizant division, had been satisfied.

The Systems Division was required by the Project to establish, maintain, and operate facilities and a documentation system for such certification of hardware at the SAF. The Systems Division also determined that the actual certified equipment was so marked.

2. Quality Assurance Activities Actually Performed

Quality assurance requirements were established and implemented at the beginning of the *Mariner R* Project

through a close coordination with the cognizant engineer of each division to determine the specifications and requirements necessary to achieve the quality objectives of the program.

An inspector from each division was assigned to assist the cognizant personnel in establishing and performing stage inspections for in-process hardware. The inspector also assisted and advised outside contractors when necessary. He provided the contractors with JPL-acquired knowledge, interpreted JPL workmanship requirements, audited their quality control systems, and performed in-process and final inspections of the hardware. He assured the cognizant JPL groups that the contractor was indeed capable of providing a level of quality compatible with JPL requirements. All inspections at JPL and at the source were documented.

In many instances, it was necessary for inspection personnel to assist in the delivery of electronic modules and components where a critical schedule problem existed. Microscopes were often hand-carried by JPL inspection personnel to perform inspections at the source.

Vendor surveys were performed at the request of cognizant JPL personnel. This procedure proved beneficial, although not all contractors building hardware for this program were surveyed.

Many inspections were performed at the source, at the request of the cognizant engineers. All pertinent information, such as status of hardware, problem areas, etc., was relayed to the JPL cognizant engineers. In addition, quality assurance personnel performed all electrical tests on harnesses and cabling to JPL specifications. All cables and harnesses were inspected microscopically; a traveler tag was attached, and a history card maintained. A quality assurance stamp control system was established for the control of harnesses, cabling, and connectors.

The Materials Review Board was installed on this program for the disposition of nonconforming materials. Toward the end of the program, a traveler-tag system was expanded to include all hardware entering the SAF area. A tag was attached giving a history of the hardware as well as spelling out the sequence of operations, such as inspections performed.

A failure-reporting system was put into effect during this program. This method was used to document all failures, malfunctions, and items to be investigated and analyzed. Corrective action and follow-up were accomplished on the failure report form.

The spacecraft inspector played an important role in this program. The inspector was assigned to MR-1 to -3 and had the prime responsibility of receiving and inspecting all electronic hardware for the *Mariner* spacecraft. Quality assurance was instrumental in designing a method for handling and controlling all flight and spare hardware entering the SAF area. A certification of hardware for initial delivery at SAF was set up. This certification was called "Quality Control Requirement Report." A criterion was established to assure that all flight hardware was certified upon delivery to SAF as to its having passed flight-acceptance testing, weight limits, incorporation of all engineering change orders, etc. All hardware had to be identified as to its being flight-acceptable. A flight certification stamp was affixed to the hardware to preclude the possibility of flying nonflight hardware. A method of materials control was initiated in the form of history control cards and SAF removal slips. A Spacecraft and Equipment Configuration Status Log was designed so that a current status of the spacecraft and associated hardware could be maintained. A rigid control of the stock room was maintained to assure accountability and control of the hardware.

All QCRR's were screened by the spacecraft inspector to ensure compliance. A current ECR Log, Spacecraft Log, and Spare Hardware Status Log were maintained. A history control card was attached to each piece of hardware, listing all transactions affecting a given unit. The Test Director was informed of the status of the spacecraft and a weekly status sheet was distributed to the Project office. Distribution of a Hardware Delinquent List prior to shipment to AMR proved effective. A close liaison with cognizant engineers, the Test Director, project engineer, Project Manager, and spacecraft personnel was established throughout the program.

Prior to shipment to AMR, the spacecraft was subjected to a final tear-down inspection so that all electronic hardware and spares could be given a final inspection at SAF. The results of this inspection were distributed in the form of a status log compiled by the spacecraft inspector.

The spacecraft inspector assured the cognizant JPL groups that all flight spares were packaged, handled, stored, and identified in the best manner possible. He witnessed the packaging of the hardware prior to shipment to AMR.

The spacecraft inspector then proceeded to AMR to receive the hardware. Initial receiving of ground support

equipment was also included. Quality assurance responsibilities at AMR were primarily the same as at the SAF. Upon receipt of the spacecraft and spare hardware, an inspection was performed to assure that no damage was incurred during the transportation period. A laboratory was acquired at AMR for the purpose of carrying out quality assurance functions. All flight hardware was stored in this laboratory, assuring an absolute control of material.

The spacecraft inspector witnessed the final button-up of the spacecraft, mechanically and electrically, and the installation of the flight squibs. After the spacecraft had been launched, the spacecraft inspector inspected packing of all spare hardware for return to JPL.

The records maintained by quality assurance during this program are now proving most helpful in compiling the *Mariner R* Results Manual.

B. Environmental Requirements

1. Introduction

This Section covers the type-approval tests, flight-acceptance tests, spacecraft environmental tests, and special tests (usually environmental) performed during the *Mariner R* Project, and also covers the failures which occurred during spacecraft assembly and operations.

Environmental-type tests are included for obvious reasons. System failures are included in this Report because it is thought that they may indicate the adequacy of the environmental testing. Whenever possible, the relationship between a system failure and an environmental test is pointed out.

The *Mariner R* 1962 program was a unique experience at JPL, in that it was the first project to require a formalized test program. This program started with project-required specifications and test reports, and ended with a project-required test results manual. Since it was a first attempt, many weaknesses in the test program were uncovered. The outstanding deficiency was the reporting of assembly-level tests. Only one type-approval test was

UNCLASSIFIED

reported, although many were performed. Of the flight-acceptance test reports, most were candid and informative, but a few were rubber-stamp reports.

2. Summary of Flight-Acceptance Tests

a. General information. The environmental tests performed in a spacecraft program are of two general kinds, performing two different functions. Type-approval tests are intended to verify designs. They are intentionally severe, in order to compensate for material and fabrication variations in flight hardware. In short, it is believed that if a prototype passes T-A testing, any flight hardware which is built to the same design as the prototype is capable of performing the mission, fabrication discrepancies notwithstanding.

Flight-acceptance tests are intended to be quality control tools; these tests are given to all flight equipment. The T-A test is to have verified that the design is adequate for its intended use; it now remains to show that the flight item is truly like the proof-tested prototype. It is thought that if a flight unit passes an environmental test (the test environment being conservatively that encountered in the mission), then it is near enough to the prototype to complete its mission (i.e., there are no fabrication discrepancies). Recounting, T-A tests verify a design; F-A tests establish that the flight item was fabricated such as to be basically equivalent to that prototype, and adequate for the mission.

For the *Mariner R* program, flight-acceptance testing of all flight assemblies was a project requirement, but due to the short time schedule between program start and launch, type-approval testing was not a requirement. Because there would be little T-A testing, the philosophy on F-A tests was modified slightly; failures during F-A testing required careful examination to determine if they were only quality control discrepancies or whether there was a design weakness.

Environmental specifications were released by Systems Division (JPL Specifications 30250 and 30251 for type-approval testing and flight-acceptance testing, respectively), which specified precisely the procedure for establishing the test environment. These specifications were inadequate by themselves, however. First, they could not possibly specify the functional tests necessary to determine whether an item passed or not. Furthermore, with a large, complex spacecraft, it is difficult to write an environmental specification which is applicable in its entirety to all items on that spacecraft.

For these reasons, the hardware cognizant engineers each wrote a test specification for his own equipment, including all functional tests, pass-fail criteria, and deviations from the environmental specification, or special tests in addition to it. These test specifications were reviewed prior to release by the Environmental Requirements Group to be certain that the environmental test program specified was appropriate to the particular piece of hardware.

b. Review of test procedures

Vibration. The vibration levels prescribed for this test were based on experience gained in connection with various other JPL missile and space programs, in addition to flight data from *Atlas* and *Atlas-Agena* vehicles.

The number of actual flight vibration measurements that these test levels were based on was small, and only the low-frequency spectrum (i.e., the spectrum well below the local resonance frequencies, say 50 cps) could be predicted with any reasonable degree of confidence. Such low-frequency measurements are representative of actual vehicle motion in the payload area and were considered as inputs to the spacecraft rather than local responses. By multiplying this input by the upper bound of an envelope of transfer functions developed from laboratory tests of similar spacecraft, the maximum low-frequency assembly response was predicted and the specification level was designed to simulate this value. This method does not predict the effect of acoustic excitation on assemblies; however, the amount of acoustic energy at these frequencies is comparatively small. The transfer functions were determined from *Ranger* spacecraft vibration tests, since no *Mariner* data were available at the time.

The high-frequency spectrum has been measured in the payload area on several *Atlas-Agena* vehicles. The measurements were made on what appears to be fairly rigid structures that could be expected to respond to the acoustic and mechanical environments in a manner similar to that of a spacecraft-type assembly. The measurements were considered as assembly responses rather than spacecraft inputs and the test levels were generated directly from them.

The test levels were designed to apply to the majority of spacecraft assemblies, typically those enclosed in the hex structure. The science experiments on the *Mariner*

UNCLASSIFIED

tower structure were subject to a more severe environment than that typified by the specification and required a special vibration test.

Thermal. One of the most significant features of space is the lack of heat transfer through the gas. This feature is one, therefore, to be closely simulated in temperature testing as it can influence test results. At a pressure of 10^{-5} mm Hg, it is reasonable to assume that all heat transfer is by radiation and structural conduction, and none by gaseous conduction.

In flight, the temperature of an item is controlled by some radiating surface, either the surface of that item or another surface in thermal contact. The test is intended to include all thermal paths by being applied at the radiating surface. For example, the radiating surface on a moderate-power dissipation assembly is held at an established set high temperature; if the thermal path is not good, then the interior will be at an even higher temperature and the faulty thermal path is thus revealed. Although the temperature levels (0° and 55°C for flight-acceptance) do include a safety margin on each side of the predicted flight temperature range, they were actually arrived at by a consideration of what electronics should be capable of withstanding and are probably far in excess of flight temperatures. The test is mechanized in one of two ways: a circulating-fluid manifold is attached to the radiating surface, or the radiative environment is regulated by cold walls and heat lamps to adjust the temperature of the radiating surface (all tests are conducted in vacuum chambers).

Electrical discharge. An insulation test to check for potential electrical discharge was included as a quality control check on potting and insulation. The test was believed worthwhile in view of problems encountered during RA-1 composite tests. It should be recognized that the test presented was for the purpose of weakness detection, and did not simulate an expected environment. These tests were applicable only to circuits experiencing greater than 250 v. This test was commonly deleted in test specifications because the spacecraft is predominantly a low-voltage device.

Another similar test was performed as part of the vacuum-temperature tests on all circuits, regardless of voltage. To simulate corona conditions which occur during ascent, the equipment is left operating while the vacuum chamber is being opened. Only circuits known to be inoperative during launch could waive this step.

c. Special tests and deviations. In a large, complex spacecraft, it would be difficult (or even impossible) to write one specification applicable in its entirety to all parts of the spacecraft; special tests and deviations from the environmental specification, incorporated into the test specifications, take care of this problem. As an example, it was learned that units mounted in the superstructure were subject to excessive vibration levels during shake tests. For these units, a special high-level sine test was incorporated as a part of their test program. The mid-course propulsion unit has a low-temperature limit of 35°F , at which point the propellant freezes. It makes no sense to attempt a standard test because it is known that it will fail. The Earth sensor and battery had similar problems. Also, there were two tests in the environmental specification which were intended for only a few special items: the electrical discharge tests for high-voltage circuits and the midcourse motor vibration test for units that operate only during midcourse maneuver. These were all clear-cut examples of special tests and deviations from the environmental specification which were properly included in the test specifications. Other deviations were those where scheduling or complexity made it necessary to test by subassembly. These deviations were approved only if the subassembly were to be tested as a part of a dummy assembly which was thermally and dynamically similar to the assembly in which the subassembly would fly. In all instances, the Environmental Requirements Group acted as an agent of the Project Manager in approving special tests and deviations.

The following special tests or deviations were contained in the test specifications:

- (1) High-level vibration test for superstructure-mounted equipment.
- (2) Propulsion system not tested environmentally as a system, but all components are flight-acceptance tested separately.
- (3) Battery waived thermal test.
- (4) Infrared radiometer combined temperature calibration and vacuum-temperature flight-acceptance test.
- (5) Magnetometer waived shake on probe No. 3 because of perming on units 1 and 2. Previous units had satisfactorily passed standard flight-acceptance test and special high-level shake.
- (6) Attitude control tested by subassembly due to difficulty of checking closed loops in a system configuration.

(7) Earth sensor had upper limit of 104°F.

(8) Microwave radiometer was to have an RFI test.

d. Summary of flight-acceptance test deviations from test specifications. The following unapproved deviations and special tests were not included in the test specifications:

Data encoder: preacceptance test at 70°C performed on serial 1.

Omni-antenna: waived Y shake on serial 1, 2, 5.

Directional antenna: waived Y shake on serial 7, 5, 8.

Command antenna and coupler: waived humidity.

Power subsystem: vibration not indicated but probably performed.

Power switching and logic: vibration not indicated, but probably performed.

Boost regulator: vibration not indicated, but probably performed.

Gyros: waived midcourse motor test.

Gyro electronics: waived midcourse motor test.

Celestial relay and power: waived midcourse motor test.

CC&S: appears to have waived midcourse motor test.

Earth sensor: serial 4 waived special heat test (4.3.4.4 of Specification 30835).

Attitude control gas system: waived one plane of shake.

Midcourse motor pressure regulator: waived one plane of shake.

Science power switch: on serial 2, 5 g sine sweep 20-100 cps, X-axis; 3 g, 20-100 cps, Y-Z axes.

Solar plasma: waived electrical discharge, all serials.

Microwave radiometer: waived RFI, all serials; no other test information available.

Particle flux detector and cosmic ray ion chamber: over-voltage waived by PFD serial 1 and 4.3 in whole waived by rest.

Antenna actuators: did midcourse motor tests.

Solar panel actuation: no reports.

e. Summary of failures during flight-acceptance test

(1) Circulator (originally on transponder serial 13) failed during shake; apparently due to water in connector.

(2) Command (originally for MR-2) failed; apparently due to accidental short on T-R output.

(3) High-gain antenna, serial 7, failed during shake; metal chip found in feed.

(4) 400-cps power amplifier, serial 003, had relay failure during vibration; later analyzed as a design deficiency and relay type was changed.

(5) Power switching and logic, serial 002, failed during shake. Collector-to-emitter short in a 2N1015C.

(6) Battery, serial 14, found to have ruptured cell after shake; time of occurrence unknown; not thought to be a vibration failure.

(7) Gyro electronics, serial 004, failed during high-temperature test; 2N1650 was sensitive to mechanical stress; changed to type 2N1050.

(8) Accelerometer, serial 013-JR332, failed at 135°F during temperature calibration; trigistor Q10 failed; no explanation.

(9) CC&S, serial 002, failed in shake due to wrong value of component. Transfluxor core had low switching output and transistor S4373 had low beta during low-temperature F-A test.

(10) CC&S, serial 003, passed F-A test. Two transistors, S4373, one transfluxor core and one capacitor failed during preacceptance testing.

(11) Magnetometer electronics, serial 2, had cordwood module failure at high-temperature F-A test.

(12) Solar plasma experiment, serial 1, had failure of capacitor, C22, during low-temperature F-A test.

(13) Solar plasma experiment, serial 3, had failure of Q3 (2N329A) during high-temperature F-A test. Later, shown to be a design deficiency and all 2N329A transistors replaced.

(14) Infrared radiometer, serial 1, failed during shake; loose motor. Also failed at low temperature; gear binding.

(15) Infrared radiometer calibrator, serial 2, had spot weld fail during shake.

- (16) Particle flux detector (originally on *MR-1*) failed during vibration; hermetic seal on RCL 10311, center electrode fractured.
- (17) Particle flux detector, serial 3, failed at low temperature; two transistors shorted.
- (18) Particle flux detector, serial 4, changed calibration during F-A and sensors were replaced; upon re-shaking, glass Geiger tube broke.
- (19) Pyrotechnics control, serial 005, had a capacitor (C6) failure during high-temperature F-A test; capacitor later determined to have been a pre-acceptance test reject.

f. Analysis of appropriateness of flight-acceptance tests. Although *Mariner R* was the initial attempt at JPL to channel all test information to one central point for a program, it must be remembered that much test information is missed. Based on what was submitted, the following conclusions can be stated:

- (1) Failures Nos. 3, 4, and 13, above, recurred later in the program, indicating that the F-A tests are conservative enough to detect some design deficiency.
- (2) In a later Section, it will be shown that three of the four failures which occurred during the vibration test of the complete spacecraft would not have been found on the assembly level: structural failure of solar panel mounts (SFR X203), a central clock drift (later determined to result from the power subsystem), and an unexplained component failure in DCS (SFR X221). The fourth failure, in science power switching (SFR X201), and follow-up action did not indicate that the F-A vibration test adequately accounted for a structural resonance at 47 cps. No failures during F-A assembly level thermal tests recurred during space simulator tests.

g. Summary of type-approval tests. Because of the short time schedule, type-approval testing was not a project requirement, although the desirability of performing such tests if time and manpower permitted was heavily emphasized by the Project Manager. A type-approval environmental specification was released for *Mariner R* and some type-approval testing was performed to it. Additionally, since many of the *Mariner R* components were repackaged *Ranger* or *Mariner A* equipment, they were thus type-approval tested to the specifications for those programs.

3. Space Simulator Tests

a. Introduction. A space simulator test has two objectives: a checkout of the thermal control subsystem, and a checkout of spacecraft operation in the space environment. Although the second objective was realized, the first was not.

The space simulator tests for *MR-1* and -2 were performed in a rather artificial manner. Due to unavailability of an adequate space simulator, these tests were performed in a less-than-optimum facility, using heaters instead of solar simulation. Furthermore, the heaters did not approximate the solar input; they were only controlled to obtain the desired temperature. (It is possible to simulate solar input with heaters, and such was done on the temperature control model, but, due to a misunderstanding, it was not done on the flight units.)

b. MR-1 test results. The *MR-1* spacecraft was subjected to a space simulation test during the period April 4 to April 12, 1962. Testing was conducted in accordance with JPL Specification 30256 and Test Procedure P37M/38M 317.001.

During the test period, the spacecraft was tested at three temperature levels and a mean vacuum of 7.7×10^{-6} mm of Hg. The temperature levels were established by applying heat to solar-dependent areas with locally controlled contact heating pads. Cold vacuum chamber walls operating at -300 to -100°F provided a heat sink to dissipate spacecraft thermal energy. Total operating time for the test was 176.4 hr.

The following are brief descriptions of notable failures which occurred during this test.

Command decoder. The VCO frequency drifted about 2 cps high. The cause was not known, but since further testing on spare units showed that the effect was a characteristic of all the detectors, it was compensated for by a biased frequency adjustment. The subsystem was not type-approval tested, so this long-term vacuum effect was not found until late in the schedule.

Power. One leg of the 400-cps, 3-phase power dropped during routine operations. This appears to have been the first occurrence of a malfunction which recurred several more times during field operations and eventually led to design change. The malfunction was evidenced by the fusing of a contact on the relay which furnishes the gyro motor power. The relay type was changed in a field modification at AMR.

c. **MR-2 test results.** The MR-2 spacecraft was subjected to a space environmental simulation test in accordance with JPL Specification 30259 and test procedure P37M/38M 317.001, starting April 27 and ending May 5, 1962.

During the test period, the spacecraft was held at a mean vacuum of 4×10^{-6} mm of Hg. The cold walls of the chamber were held at -300 to -100°F , in accordance with the spacecraft temperature desired. The spacecraft was maintained at three levels of temperature by independently controlled contact heaters. Total operating time for the test was 156 hr.

The one significant failure during this test was the inability to obtain an Earth gate at the time in the test when command AC6B was set. Vacuum was broken and problem investigation revealed that the booster regulator went into oscillation, creating excessive noise which prevented the Earth gate from operating. Booster regulator S/N2 was replaced with S/N5 and operations were normal for the remainder of the test. This malfunction resulted in the necessity to match booster regulators and power switching and logic subassemblies to prevent this phenomenon.

4. MR-1 and -2 Flight-Acceptance Vibration Tests

a. **Summary.** The flight-acceptance vibration tests of the MR-1 and -2 spacecraft, performed in accordance with JPL Specification 30259 (for MR-1, the test procedure was revised to minimize cross-coupling), were completed on April 27 and 21, respectively. Four failures were detected during or immediately after these tests;

one was found on MR-1 (Failure Report 221) and three on MR-2 (Failure Reports 201, 203, and 210). Discussion of these failures follows in Section B5.

Acceleration data for all axes of shake on both spacecraft were recorded on magnetic tape. Frequency spectrum analyses were performed on the noise burst portion of the test data and transfer functions were computed between an input point on the spacecraft separation plane (bus foot A) and the other accelerometer locations. Representative transfer functions are given in Fig. 210, 211, and 212.

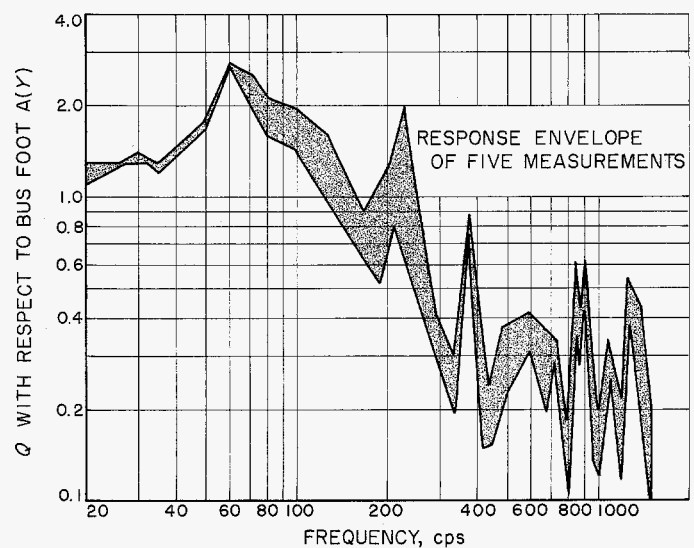


Fig. 211. MR-1 and -2 bus structure (Y) Y shake

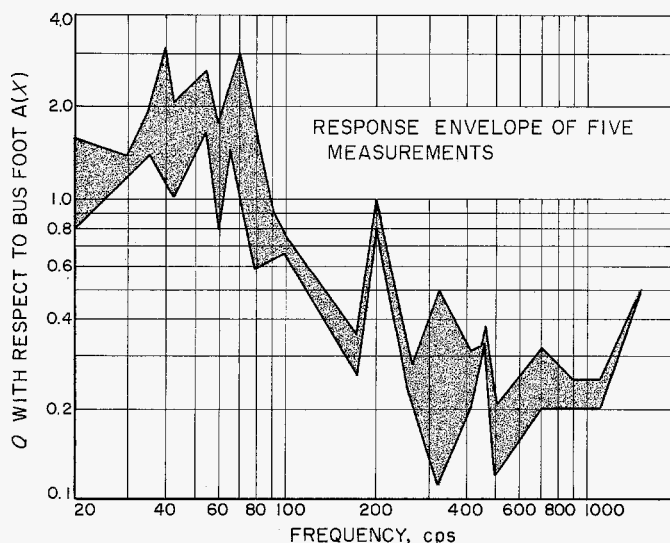


Fig. 210. MR-1 and -2 bus structure (X) X shake

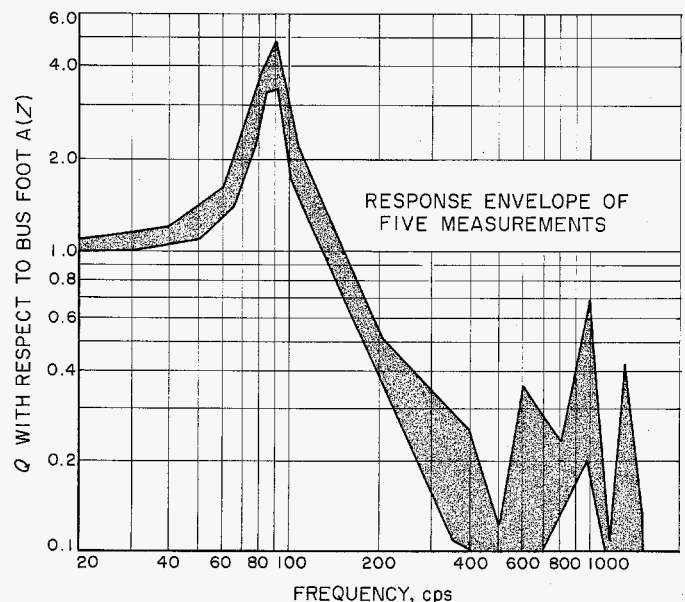


Fig. 212. MR-1 and -2 bus structure (Z) Z shake

b. Discussion of shake tests. In performing the shake tests, several problems were encountered and deserve comment.

A problem that is most apparent in reducing the accelerometer data is the presence of a large 60-cps component in the random noise due, apparently, to the use of 60-cps power in the tube heater elements of the random noise generator. The presence of this 60-cps spike is mainly objectionable from the standpoint of data reduction, where it produces inaccuracies in the 55 to 65-cps region. It is also possible that such a spike could cause physical damage to a test specimen under certain resonant conditions. It should be eliminated by changing to a d-c power supply.

Another item is the cross-coupling that occurred during the pitch and yaw test of the first spacecraft tested (MR-2). It was not too pronounced during the noise portion of the test, but became quite evident in the 40 to 50-cps region of the combined sinusoid and noise. This phenomenon appeared to result from the dynamic unbalance of the spacecraft-adapter-fixture combination in the pitch and yaw axes; it was not noticeable in the axial direction. Reduction of the problem was facilitated during the test of the second (MR-1) spacecraft by monitoring the cross-axis acceleration and controlling the shaker output to the rms sum of this acceleration and the on-axis acceleration. This control procedure was applied up to 60 cps, beyond which the normal control procedure was used. A permanent system for restraining the low-frequency cross-coupling of the pitch and yaw fixture by use of high-pressure oil bearings is being installed by the Environmental Facilities Group.

The use of the *Agna* adapter as a shake fixture for the spacecraft provided a problem in controlling the test levels at the spacecraft separation plane. The first resonance of the spacecraft on the adapter occurred at about 40 cps in the pitch and yaw axes, and at a slightly higher frequency in the axial direction. Above these resonances, acceleration levels measured in the direction of shake on the two instrumented bus feet, A and D, varied considerably; also, excessive cross-coupling was measured on bus foot A. Good equalization was nearly impossible to obtain because of resonances of the bus feet on the adapter structure. Had it been possible to hard-mount the spacecraft to the fixture, a relatively flat response would have been obtained up to about 300 cps, as opposed to the 40 cps obtained.

c. Derived transfer functions. Note that these transfer functions were derived for the spacecraft on the *Agna* adapter, which is effectively a much softer mounting than the usual shake fixture. Bus foot A was arbitrarily chosen as the separation plane input reference; all data have been normalized to this input. Because of adapter resonances, this foot does not represent a true spacecraft input—the true input is the sum of the accelerations of all six bus feet.

Figures 210 to 212 illustrate the composite response of the bus structure normalized to the reference point. The maximum gain would appear to be about three in the pitch and yaw, and five in the axial directions. Beyond 70 cps, the response rolls off and remains below 0.5 beyond about 300 cps. This illustrates the difficulty involved in producing high-frequency acceleration levels in bus equipment during a shake of the entire spacecraft. Flight vibration that is mechanically transmitted to the spacecraft will also be attenuated to a similar degree. However, acoustically produced flight vibration may not be adequately simulated by this type of test.

Transfer functions for the Earth sensor (three axes) and for the solar panel support plate (pitch and yaw) were also obtained.

d. Conclusions. The transfer functions given in Fig. 210, 211, and 212 may be considered as a good representation of the bus structure response, since the envelopes contain a minimum of five measurements. There are, however, no other data with which to correlate these measurements. The transfer functions for the solar panel support plate and solar panel corner (not shown) should not be considered reliable, since they represent only one measurement and do not correlate with similar measurements on the dynamic mock-up spacecraft.

The cross-coupling functions (not shown) were derived only to indicate the extent of cross-coupling that might be expected in a similar test setup—a setup that hopefully will not need to be repeated. The use of the adapter for vibration tests at any frequency except those well below any adapter resonance should be discouraged. Cross-coupling due to dynamic unbalance of the test configuration can be reduced by either of the methods referred to above.

The principal objective of the flight-acceptance vibration test was to subject the spacecraft to an environment similar to that which may be encountered during launch vehicle motor burning. This objective was accomplished

and the spacecraft survived with the exception of the four failures mentioned.

e. Spacecraft transfer functions. The frequency spectrum analyses from which the transfer functions were generated had the following characteristics:

portion of the test when the sinusoid sweep was at about 48 cps.

In an effort to duplicate the failure, the switching unit was removed from the spacecraft after system checkout

Spacecraft	Frequency interval	Sample length	Filter bandwidth	Degrees of freedom	90 % confidence limits	
					Lower limit	Upper limit
MR-1	20-100 cps	4 sec	2 cps	16	0.6	2.1
	100-1500	4 sec	10 cps	80	0.8	1.3
MR-2	20-100 cps	3 sec	2 cps	12	0.5	2.4
	100-1500	3 sec	10 cps	60	0.8	1.4

5. Summary of Failures

Four failures occurred during the flight-acceptance vibration tests of spacecraft MR-1 and -2: On MR-1, Failure Report 221; on MR-2, Failure Reports 201, 203, and 210.

a. Failure Report 221, transistor in DCS. Increase in voltage at output indicated that the series regulator circuit was not operating correctly. Check of unit in laboratory showed Q-1 (series regulator transistor) in 12-v regulator circuit had no voltage drop from collector to emitter. Voltage at output was up to 13.15 v. Diagnosis by JPL and the vendor indicated that base of Q-1 was open. All solder points looked good.

The unit was returned to the vendor and the transistor was changed. Check of the unit then showed correct operation. The removed transistor was checked on a Simpson Beta tester and found to be in good condition, indicating that the trouble could have been a bad solder joint. Failed unit was retested for flight acceptance. This failure is considered random and is still on open report.

b. Failure Report 201, science power switch. During the flight-acceptance composite vibration test of MR-2, the science power switching unit (module 2) turned on the power to the science experiments four times under the following conditions:

- (1) Axial (z) vibration test, during equalization or test.
- (2) Pitch (x) vibration test, during equalization and test.
- (3) Yaw (y) vibration test, during test. The unit turned on power during the noise plus sinusoid

and placed in a dummy-loaded case. The case was then tested with the sinusoid portion of the flight-acceptance assembly vibration test in the Y and Z axes and no failure occurred. The unit was then placed in the flight case (dummy-loaded) with flight cable harnesses and given the complete assembly flight-acceptance test in the X spacecraft axis. As in the composite spacecraft test, a failure occurred during the noise plus sinusoid portion of the assembly test, again when the swept sinusoid was at about 48 cps. As a result of the measurements then made on the module, the location of the failure was determined to be most probably in one of two relays. The identical vibration test was again applied to determine if the failure would repeat; it did not. Testing of this unit was then discontinued since one failure had occurred and it was not desired to put an undue amount of vibration time on a unit that possibly could be repaired and made flightworthy.

The type-approval module was then tested to determine if the failure was of a module design or a component quality control nature. The unit was mounted in a dummy-loaded case and shaken to the following sinusoidal levels in the spacecraft axis:

5 g rms	20 to 100 cps
10 g rms	30 to 100 cps
18.5 g rms	35 to 100 cps

No failure occurred during the test and the unit checked out upon completion of each shake.

c. Conclusion. The follow-up testing of the flight unit indicated that it cannot reliably pass the flight-acceptance

assembly vibration test. The fact that the T-A unit survived the high-level sinusoid test indicates that the failure was most likely one of quality control of component parts; i.e., relays, rather than one of module design. This failure was random and is considered closed.

d. Failure Report 203, rubber bushings. A rubber bushing in the solar panel actuator cracked during shake. The purpose of this bushing is to lower the resonant frequency of the extended panels. Although it is believed that the failed bushings will still achieve their intended purpose, a mechanical stop was added to prevent recurrence. This is a design-corrected failure and is considered closed.

e. Failure Report 210, plasma experiment. During shake, a piece of loose solder caused a short. This personnel-caused failure is considered closed.

f. Conclusions. Failure 201 could have been detected by a more severe assembly-level vibration test. This condition has been covered in the *Mariner R* (1964) environmental specifications.

Failure Report 203 is a typical example of the class of failures which only can be detected when a complete, flight-configuration spacecraft is tested. This failure could not have been found at the assembly level.

Failure Report 210 is a good illustration of the danger of performing rework after assembly-level flight-acceptance and inspection.

6. Mariner R Pyrotechnic Shock Test

a. Synopsis: The environment produced by the actuation of on-board and separation pyrotechnic devices was measured at various spacecraft locations during the *MR-1* and -2 dummy runs. The performance of the launch mode operating systems was monitored during the actuation to observe possible deleterious transients. A system test was performed at the conclusion of the run to determine any residual damage.

In addition to the normal dummy-run squib firings, a special pyrotechnic test was performed on *MR-1*. This test consisted of the simultaneous firing of double pin pullers at each spacecraft location. It had been anticipated that such a test would produce higher shock levels than the normal single firing.

In essence, the results of the pyrotechnic tests were as follows:

(1) No degradation in spacecraft performance was observed during or after the tests. The only transient observed was considered negligible: a slight jerk at a guidance gyro during the doubled firing of the radiometer and solar panel latches on *MR-1*.

(2) The structural responses recorded conformed to past measurements in both amplitude and frequency. The amplitude of the low-frequency components of the responses were well below the levels used in type-approval shock testing. The high-frequency components that were observed cannot be simulated by existing shock machines.

(3) The anticipated higher shock levels from the doubled pin pullers did not clearly materialize. In terms of total measured structural response, the doubled pin pullers produced only 87% of the excitation levels of the single pin pullers. Whether this was due to a peculiarity of measurement locations or non-simultaneous squib ignition, is not resolved.

Test setup. The *Mariner* spacecraft were mated to the *Agna* adapter, which was hard-mounted to the transporter. Past experience has shown that such hardmounting causes no significant changes in the spacecraft shock response.

The shock generated by the pyrotechnic-actuated gas valves on the midcourse propulsion unit of *MR-2* was simulated by firing the squibs on an identical set of valves clamped to the flight valves. The flight valves were not fired because of the difficulties involved in replacing them after the test. Similarly, appended valves were fired on *MR-1*; however, no attempt was made to hard-mount them to the flight valves for shock evaluation purposes.

After the normal pin pullers had been fired on *MR-1*, doubled pin pullers were installed at the solar panel and radiometer latches and connected to external firing circuitry. The doubled pin pullers were constructed by bolting a *Mariner* and *Ranger* pin puller together in special latch brackets. Except that they lack a telemetry plug, the *Ranger* pin pullers are identical to the *Mariner* pin pullers.

MR-1 and -2 used 13 and 10 Endevco accelerometers, respectively. Data was recorded on a tape recorder at 60 ips. A visual record was obtained by playing the tape

back at 3 ips and re-recording on an oscillograph. The over-all frequency response of the recording system was flat from 10 cps to 10 kc.

The mechanical frequency response of the accelerometer and mounting block combination is difficult to estimate. The use of lightweight accelerometers (Endevco No. 2221) and small magnesium blocks should have resulted in a combination significantly stiffer than the spacecraft structure to which they were attached. The transfer function between the accelerometer and the attachment point on the structure should have been near unity for frequency spectrums of interest. The transfer function between the Earth sensor and the attached triaxial accelerometer is more questionable. Due to the construction of the Earth sensor, there was no possibility of bolting the accelerometer to it. Gluing with Eastman 910 was ruled out because of possible damage to the sensor when performing the necessarily violent removal of the accelerometer. The only alternative left was to use double-backed tape. The frequency response of such an accelerometer taped to a solid block is reasonably flat to about 8 kc at acceleration levels less than 1 g. The response to shocks such as were recorded in this test is not resolved.

b. Procedure

(1) *MR-1*. The LMSC pin pullers were installed in the adapter and fired from external circuitry. The normal spacecraft pin pullers were then fired by spacecraft power on command from the sequencer. The firing order for the spacecraft pin pullers was first the radiometer and one solar panel (A-B), and then about 4 sec later, the other solar panel (D-E). The doubled pin pullers were then installed and fired by external circuitry in the same order as the normal pin pullers.

(2) *MR-2*. The LMSC and spacecraft pin pullers were fired in the same manner as for *MR-1*. An error by the tape recorder operator prevented data from being taken on the spacecraft pin puller firing. The pyrotechnic-actuated gas valves that had been clamped to the spacecraft system were then fired by spacecraft power.

All spacecraft systems that operate during the launch mode were monitored for possible deleterious transients and a system test was performed afterward to detect any permanent damage.

c. Results. The measured shock responses are tabulated in Fig. 213. The amplitude is quoted in peak g; the frequency given is the principal forced frequency apparent in the oscillograph playback. A low-frequency ring-out was apparent on very few channels; where such ring-out

appeared, its frequency has been given along with the forced frequency. In all cases, the frequency components below 2 kc were well below the levels used in type-approval testing for equipment contained within the bus structure.

The anticipated higher shock levels from the doubled pin pullers did not clearly develop. The summation of the accelerations produced by the doubled pin pullers was about 87% of the summation of the singles. However, of the 20 individual responses recorded during the double and single firing, the majority (12) were higher during the double firing.

No shock response was apparent due to the firing of the *MR-2* midcourse valve pyrotechnics. Hence, any excitation produced by the valves must have resulted in a response at the monitored locations of less than 10 g—the system noise level. Because of this low level, the test was not repeated on *MR-1*.

d. Conclusions. The results indicate that the measured response levels, below 2 kc, are adequately simulated by present shock-testing procedures; the response above 2 kc cannot be simulated by existing shock machines. The only simulation presently possible is the actual firing of the spacecraft and separation pin pullers, which has three disadvantages: (1) This is not an assembly level test; it cannot be performed until the whole, or a large part, of the spacecraft is assembled. (2) No reliable method of producing a type-approval (higher than normal) shock is presently available. The experience with the doubled pin pullers indicates that this is a doubtful method of producing an above-average shock. (3) The shock wave is shaped into fairly discrete frequencies by the mass of structure between the equipment and the pin puller. A good shock test should excite all frequencies of interest (say 2 to 10 kc).

There would seem to be a definite need for a pyrotechnic simulator that could reliably produce normal and above-normal shocks at the assembly test level. Until more adequate methods are available, the combination of the low-frequency assembly level shock test and the complete pyrotechnic firing during the dummy run gives confidence in the ability of the spacecraft to withstand pyrotechnic shocks.

7. Radio-Frequency Interference Tests of MR-1 and -2

Both *MR-1* and -2 were subjected to an r-f environment simulating a condition calculated to exist during the

ACCELEROMETER LOCATIONS	ACCELEROMETER ORIENTATION	MR-1 EVENTS												MR-2 EVENTS		
		CHANNEL	SEPARATION		SOLAR PANEL / RADIOMETER		SOLAR PANEL		SOLAR PANEL / RADIOMETER (DOUBLED)		SOLAR PANEL (DOUBLED)		CHANNEL	SEPARATION		
			AMPLITUDE peak g	FREQUENCY kc	AMPLITUDE peak g	FREQUENCY kc	AMPLITUDE peak g	FREQUENCY kc	AMPLITUDE peak g	FREQUENCY kc	AMPLITUDE peak g	FREQUENCY kc		AMPLITUDE peak g	FREQUENCY kc	
CASE V TOP OF CASE ABOVE LEG F	AXIAL (Z)	1	70	4.5	740	8	*	—	440	8/2.5	25	5	6	80	13	
	NORMAL	2	50	7	880	6.5	24	—	290	6.5	40	~2	5	145	3	
	LATERAL	3	130	11	480	8	~20	—	840	8.5	90	5	4	55	3.3	
CASE V BOTTOM OF CASE ABOVE LEG E	AXIAL (Z)	5	200	11	190	8	46	2.5/12	130	12	70	11/2	—			
	NORMAL	6	140	8	110	10	28	~4	74	6/2.4	60	4	—			
	LATERAL	4	130	8	120	10	28	9	96	6.5	86	4	—			
CASE III TOP OF CASE ABOVE LEG C	AXIAL (Z)	7	250	8	30	6	16	9	36	6	20	—	3	260	9	
	NORMAL	9	310	7	40	~5	20	2.5	46	3	32	3	2	250	8/1.1	
	LATERAL	8	180	7	~25	0.9	20	—	~24	~4	16	0.8	1	135	6.3	
EARTH SENSOR	Z	11	20	5/0.9	32	—	*	—	*	—	*	—	8	*	—	
	X	12	32	0.8	*	—	*	—	*	—	*	—	9	*	—	
	Y	10	24	0.9	*	—	*	—	*	—	*	—	7	20	1	
SOLAR PANEL TOP OF DIRECTIONAL COUPLER	Z	13	30	0.7	36	2/0.6	*	—	74	2.8	*	—	10	*	—	

X, Y, AND Z ARE SPACECRAFT AXES
 ~ VALUE APPROXIMATE
 * VALUE BELOW NOISE LEVEL
 — VALUE UNDETERMINED

Fig. 213. Pyrotechnic shock test

launch of a spacecraft at AMR. The environment was provided during dummy-run tests in the SAF. No effects were noted attributable to the r-f environment in either test with the shroud on or removed. The "on-board" vehicle r-f sources and selected high-power AMR sources that were simulated for the test are listed below, together with the created power densities in the spacecraft vicinity. These simulated densities are 3 db greater in magnitude than values calculated to exist at a height above the launch area devoid of ground effects.

On-board sources

Source	Power density
Atlas telemetry	0.5 mw/M ²
Atlas beacon	0.024 mw/M ²
Atlas guidance rate beacon	0.22 mw/M ²
Atlas guidance pulse beacon	0.5 mw/M ²
Agenda telemetry	1800.0 mw/M ²
Agenda beacon	48.8 mw/M ²

Off-board sources

Mod II radars	13.7 mw/M ²
Mod IV radar	23.0 mw/M ²
FPS — 8 radar	9.4 mw/M ²
FPS — 16 radar	548.0 mw/M ²
Command transmitter	3.9 mw/M ²

To determine spacecraft safety, the r-f power present at each readily accessible electro-explosive device harness connector was measured while the spacecraft was in the simulated environment with the shroud removed. The measured power values included only the absorbed energy from the simulated sources because the spacecraft transponder signal was not connected to a spacecraft antenna. The measuring device was a standard microwave power meter and a thermistor mount with an adapter to connect to the squib leads. The power measured by the device could only be treated as an order of magnitude indication since the adapter and thermistor mount do not simulate the electrical characteristics at the diverse r-f frequencies. A safety margin of at least 20 db was calculated at a pin-puller squib with the maximum power measured.

8. Summary of MR-1 and -2 Random Failures

Of the 198 malfunction/failure reports which were written for MR-1 and -2, 33 are considered to be random failures⁴. (Tables 18 and 19).

⁴Random failure is a failure whose probability of occurrence depends on normal, expected stresses, or a failure which is repaired or replaced without changing the probability of recurrence.

Malfunctions are events which cause the spacecraft system or a part of it not to operate within prescribed limits. Failures are a subset of malfunctions.

UNCLASSIFIED

JPL TECHNICAL REPORT NO. 32-353

Table 18. MR-1 random failures

Failure report No.	Unit name	Unit No.	Description of failure	Action taken
13	Plasma	23A1, 2, 3	Signal return ground	Replaced wiring.
93	Data-conditioning system	20A21 through 20A25	During "radiometer calibrate" an improper sequence occurred.	Circuitry examined but no failed components detected. Careful observation for this phenomenon will be instituted.
219	Plasma	23A1, 2, 3	Contaminated plates caused reset and noise.	Deflection plates kept clean.
221	Data-conditioning system	20A25 Serial 3	After Z-axis shake test, increase in voltage at output regulator transistor) had no voltage drop from collector to emitter. Diagnosis indicated base of Q-1 was open. Transistor removed, checked out and found good. With new transistor, operation correct.	
57	Transponder	Serial 14	Receiver threshold degraded 3 db.	Subsystem module replaced (X 42).
222 and 251	Telecommunications system	2A4 Serial 4	Transient in L-band T-R.	2A4 Serial 4 replaced.
98	Data encoder	6A1-6TR1	Antenna reference potentiometer (Ch. 13) and antenna position potentiometer show 7-deg discrepancy.	T.M. channels recalibrated.
14	Attitude control gyro package	Serial 3	Large roll offset noted at GSE. Unit returned to lab and checked out normal then reinstalled on spacecraft. However, and abnormal indications again obtained. when spare gyros installed, normal indications obtained. Antenna hinge moves approximately half speed going compared to coming in.	Unit not considered flightworthy and was replaced with new gyro.
30	Antenna servo electronics	7A13	Gas system leaked.	Defective component SCRG10 was replaced.
234	Attitude control gas system		When counter stopped, T/M blip did not function properly due to defective tantalum capacitor and diode.	System replaced with spare. Leak repaired.
5	End counter (CC&S)	5A3	C-phase voltage remained out of tolerance for long period.	Defective components replaced.
83	400-cps power amplifier	4A8	Failure in PS&L module causing erratic reading of T/M read-out for battery drain.	Unit replaced with spare. Original unit subjected to various tests without success in inducing same failure. Circuit under examination by Westinghouse.
225	Power, PS&L	4A1	Starting register in oscillator circuit of telemetry damaged.	Unit repaired.
229	PS&L	4A1 Serial 3	Limit switch suspected of failure due to malfunction of DCS.	Resistor replaced and sent to components group for analysis.
60	Radiometer scan actuator	21A2		Unit inspected, no damage to unit.

UNCLASSIFIED

Table 19. MR-2 random failures

Failure report No.	Unit name	Unit No.	Description of failure	Action taken
69	Data-conditioning system	20A21 through 20A24	Relay drive gave improper action.	Defective cable replaced.
201	Science power switching	20A1 Serial 2	Science improperly came ON and OFF during shake. One relay, either K2A or K2B, failed to operate properly. Cause was severe welding of contacts. Probably caused in turn by high current surges associated with microwave radiometer turn-on prior to installation of current limiters.	New relays (K2A and K2B) installed in unit 20A1 Serial 2 and unit passed F-A tests. An ECR (4736) submitted, proposing change in wiring which would reduce switched power per relay by approximately 20%. Change necessary because of other possible source, besides the radiometers, of current surges that may cause contact welding.
254	Science subsystem		Radiometer calibrate sequence came on at wrong times during system test. Condition caused by science power switching transients.	Condition tolerated. Operation of calibrate sequence to be monitored.
X280	Microwave radiometer	21A1 Serial 3	Calibrate signal size decreased by approximately 25% over period of month in 13.5 mm channel. Tests showed 6-cps shift in narrow-band amplifier system set to narrower bandwidths than other systems. Calibration gas tube intermittent under vibration.	Gas tube changed; intermittent tube to be failure-mode analyzed. Narrow-band amplifier returned. 13.5-mm channel electronics package replaced by spare.
X285	Microwave radiometer	21A1 Serial 3	Narrow-band amplifier could be set into self-sustaining oscillations by random transients, saturating 13-mm channel output. Difficulty due to slightly narrower bandwidth than normal in amplifier and shift in center frequency, making phasing of phase-sensitive loop marginal with possibility of transients completely unbalancing it, causing oscillations.	Narrow-band amplifier returned and broadened. 13-mm electronics removed and replaced by spare 7/20/62.
61	Transponder	Serial 13	Transponder had low threshold.	X42 module replaced.
76	Transponder		Transponder threshold showed degradation.	Investigation in lab did not duplicate problem. Unit continuously tested on spacecraft with no degradation observed. FR still open.
228	Transponder	2A1-2A2	X16 multiplier (varactor) failed.	450 varactor diode replaced. Multiplier module returned to JPL and retuned. Motorola performing analysis of component and re-examining Hi-rel testing program for varactor diodes.
241	Junction box in transponder subsystem	2A5 Serial 2	Open between pin 35 and 36. From 9WIP20 pin Y to S C. A and B also open.	Cause unknown.
X279	Transponder	2A1-2A2 X/N 15	Transponder threshold out of acceptable limits.	Motorola returned 3 modules, bringing transponder within 2 acceptable limits. Unit being tested.
X301	Antenna drive actuator	7A11	Leak between gear box and cover. Test indicated faulty gasket seal between gear box cover and box.	Gear box inspected; action to be taken to ensure acceptable leak rate.

UNCLASSIFIED

JPL TECHNICAL REPORT NO. 32-353

Table 19. (cont'd)

Failure report No.	Unit name	Unit No.	Description of failure	Action taken
32	400-cps power supply	4A8	Incorrect resistance reading observed on pins of module, caused by shorted 1N645 diode.	Diode replaced and design reviewed. Diode application appeared correct and it was demonstrated that an instantaneous polarity reversal could cause diode failure.
82	400-cps power supply	4A8	C-phase power supply out of specification.	Defective transistor replaced and investigation by manufacturer to determine cause of failure.
39	Attitude control wire harness	9W7	Waveform change observed on one pin of connector by tapping or wiggling 7A13P1.	Cable examined and tested but no reason for failure detected. C-cable considered unflightworthy.
59	Case harness	9W24	Intermittent open between two connectors.	New 9W24 harness fabricated and used to replace old harness.
X291	Midcourse motor pressure transducer	10PT1 Serial 8549	Defective pressure transducer.	Replaced.
X300	Midcourse motor		Leak in propellant tank pressure regulator.	Unit replaced.

UNCLASSIFIED

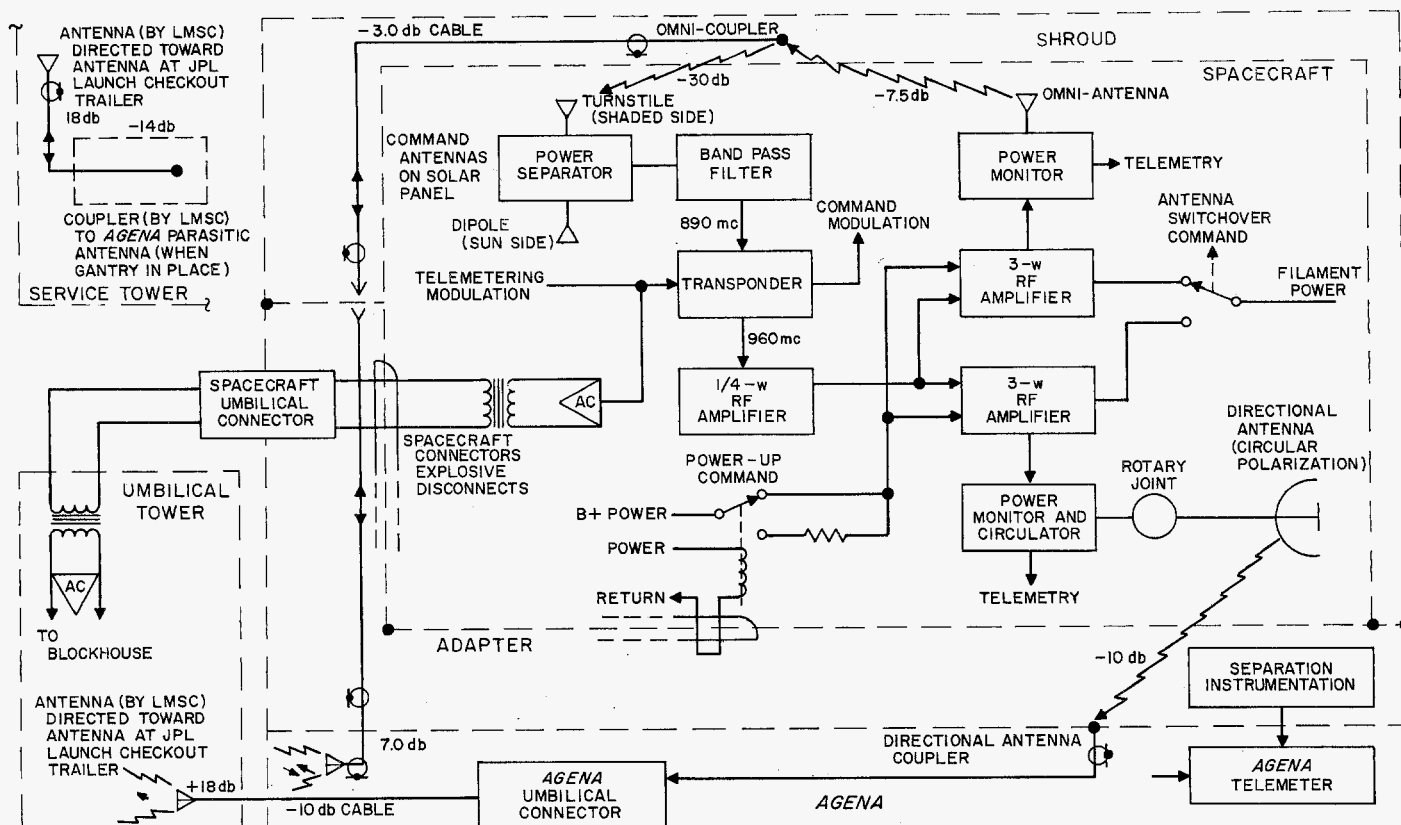


Fig. 216. Mariner R communications system

Interface planning resulted in a clear definition of the required scope of effort. In brief, LMSC modified the fifth *Ranger* vehicle and planned a second vehicle to satisfy the requirements of the *Mariner R* program.

Because of the short launch period for the 1962 Venus mission, a study was made of the means by which the pad turn-around time could be shortened to 3 wk. This 21-day plan was extended to 24 days by the Flight Test Working Group to allow for days off. Actually, the required time was 36 days due to extensive *Atlas* 179-D servo problems.

2. Retrothrust by Propellant Vent System

A new retro system was designed for the *Agena*, based on the following considerations:

- (1) The solid retromotor, as utilized for the *Ranger* program, provided an impulse far in excess of that needed to give the *Mariner* program *Agena* vehicles an acceptable planet-miss probability.
- (2) Since weight was of primary importance, elimination of this excess capability was desirable.

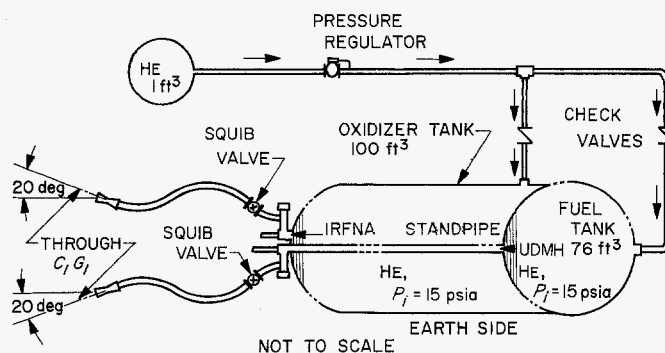


Fig. 217. Retro-thrust propellant vent scheme

- (3) It was decided not to utilize a biased trajectory in order to effect an *Agena* planet miss.

Studies were made of a propellant-vent system which would provide sufficient impulse to result in an acceptable planet miss. The system decided upon provided an adequate *Agena* velocity decrement by over-board discharge of residual propellants and gases. A relatively simple system for accomplishing this purpose was evolved (Fig. 217).

Tests and studies were made by JPL and LMSC to determine the possibility of contamination of the spacecraft, the behavior of the propellant when vented in space, and the possibility of hypergolic ignition of the vented propellants. *Agena* planet-miss probability studies were also made for varying conditions.

It was decided that a 400-ft distance between the spacecraft and the *Agena* at the start of propellant venting, in conjunction with a change in the yaw turn maneuver from 180 to 140 deg, would minimize the possibility of spacecraft contamination. This system provided the desired *Agena* planet-impact probability throughout the launch period. Figure 218 shows the miss probability for the final design configuration.

3. Shroud-Adapter Decision

At an Interface Panel Meeting, it was decided that three sets of shrouds and adapters would be provided for the *Mariner R* program. This number was agreed upon in order to provide a spare shroud and adapter for the second launch.

4. Spacecraft Environmental Sealing

A new and more stringent requirement for isolation of the payload compartment from the *Agena* ground air-cooling system was required by JPL because of possible Earth-sensor contamination. A differential pressure existed on the pad between the LMSC and the JPL systems, and was sufficient to cause air leakage into the nitrogen atmosphere maintained inside the nose shroud. A pressure increase in the JPL system was not feasible because of shroud limitations; therefore, sealing of the *Agena* forward rack and/or the spacecraft adapter was indicated. LMSC studied the problem of accomplishing an effective seal. Silicone, mylar (polyester), and vinyl tapes were tested, with or without silicone coatings and silicone rubber fillers.

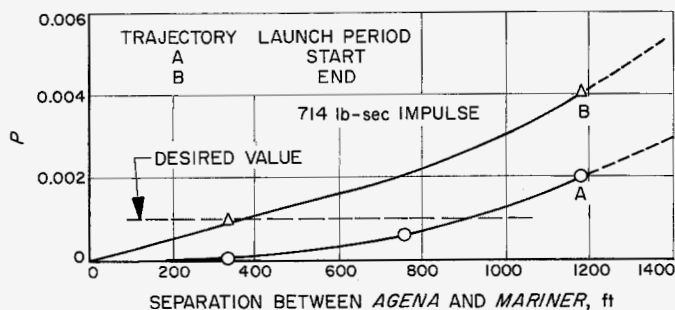


Fig. 218. Probability of *Agena* Venus target area impact

Sealing methods for the *Agena* forward midbody were evaluated in tests at JPL and found to be adequate. The sealing with mylar tapes and silicone coatings effectively prevented contamination of the spacecraft envelope by the air from the *Agena* air-conditioning system during pad operations.

5. Development Testing

Combined vibration testing was completed at JPL, utilizing an adapter and shroud in combination with a spacecraft mock-up. Tests of antenna performance were conducted at JPL and LMSC in order to investigate the performance of the antenna-coupler systems. A separate coupler was not provided for the command receiver antenna on the tip of the spacecraft solar panel. These tests were run with mock-up equipment at LMSC, and with the vibration test shroud and adapter at JPL. Antenna performance was also evaluated during design verification testing at JPL. Two mock-up *Agena* forward equipment racks were provided by LMSC for these tests.

6. Spacecraft-Agena Electrical Connection

As a result of RA-4, it was realized that the two halves of the spacecraft-Agena electrical disconnect should be reversed so that the male portion of the connection would be on the *Agena* side of the interface and the female portion on the spacecraft side. Tests of the explosive disconnect were made at Lockheed's Burbank (Calif.) facility, and it was apparent that there was a remote possibility of a bounce of the *Agena* half of the connection sufficient to overcome the spring restraint and to strike a portion of the connection to the spacecraft. Male pins on the spacecraft half could be shorted unintentionally at spacecraft separation in such a case. Change of the spacecraft half to a female connection eliminated this possibility.

7. Design Verification Tests

Design verification tests of the compatibility between the spacecraft adapter, shroud, and the MR-1 spacecraft were accomplished at JPL during March 1962. The LMSC components were similarly tested with the MR-2 spacecraft in April 1962. A third adapter and shroud were made available at AMR as back-up flight equipment during the *Mariner* launch period.

8. Separation Tests

Spacecraft separation testing started at the LMSC Burbank facility in November 1961. Differences in payload and sterilization requirements called for structural

A mean-time between-failure⁵ analysis was performed periodically on *Mariner R*. On a statistical analysis which gives MTBF at a specific confidence level, the MTBF is never much greater than the duration of the test, even for a failureless unit. Therefore, since the testing time is only a small fraction of the flight duration (and as mentioned earlier, these times are poorly known) it is misleading to publish a report which gives MTBF's that are of mathematical necessity shorter than the mission. The only value of these reports is the trend of the MTBF's over a period of time.

9. Other Failures and Rejections

A complete summary of all spacecraft failures by subsystems appears in Table 20. Table 21 totals all failures by classification. Rejection occurrences by types are shown in Table 22.

10. Special Tests

a. Compatibility shake. The *Mariner R* combined unit vibration test was completed on January 26, 1962. The testing procedure (JPL Specification 30908A) was intended to verify clearance between the dynamic envelopes of the shroud and the spacecraft, under extreme steady-state flight vibration environments as they are presently known. The dynamic deflections of the critical interface locations were successfully measured and found to remain well within the prescribed dynamic envelope of the spacecraft. The scheduled date of completion of the testing program was satisfied, and no major delays or problems were encountered.

This clearance was again checked following a spacecraft structural change. It was verified on the modified structural test model by means of a strobe light and scale that the spacecraft dynamic envelope was still well within the shroud dynamic envelope.

b. Structural model shake and reshake. The analysis of the spacecraft as a complete unit was conceived as a result of the need for a detailed dynamic analysis of the hex structure. Using a structural prototype model of the spacecraft, a series of tests was performed to qualify the vehicle as a flightworthy structure. From experience gained during the *Ranger* program and the results of analysis, it was determined that a static test of the entire spacecraft would be unnecessary.

⁵The mean-life parameter or mean-time-between-failures is the expected time between *random* failures. From this parameter, probability statements are made such as probability of survival and one-sided confidence intervals.

Table 20. Spacecraft failures by subsystems

Subsystem	Number of failures				
	Flight acceptance ^a	MR-1		MR-2	
		SAF	Field	SAF	Field
Science	8	18	7	9	9
Communications	2	13	1	7	2
Command	1	2	1	3	
Data encoder		10		4	1
Attitude control	2	9	3	6	2
CC&S	2	3	1	7	3
Power	3	10	1	6	3
Cabling		24	1	10	1
Mechanical	1	13		3	2
Propulsion					2
Complete spacecraft		1		3	
Totals	19	103	15	58	25

^aFlight-acceptance data incomplete

Table 21. Spacecraft failures by classifications

Subsystem	Classification of failures ^a					No. of Failures
	D	R	P	G	X	
MR-1						
Science	9	4	8	1	4	
Communications	2	2	4	1	2	
Command	1		2			
Data encoder	3	1	2	2	2	
Attitude control	4	3	5			
CC&S		1	1	1	1	
Power	4	1		1	1	
Cabling	16		7	2		
Mechanical	8	1	3	1		
Propulsion						
Spacecraft	2					
Totals	49	13	32	9	10	113
MR-2						
Science	3	6	3	2	5	
Communications	2	5	1	1		
Command	1		1	1		
Data encoder		1	2	1	1	
Attitude control	4	1	2		1	
CC&S	2		3	4	2	
Power	3	2	3		1	
Cabling		2	4	3	1	
Mechanical	1		3		1	
Propulsion		2				
Spacecraft						
Totals	16	19	22	12	12	81

^a

D = design-corrected failure

R = random failure

P = personnel

G = GSE (these malfunctions not included in any statistical analysis)

X = malfunction on which no corrective action taken

Table 22. Spacecraft rejection occurrences by types

Type	Number of rejection occurrences
Soldering errors	626
Wiring errors	644
Hardware errors	188
Potting errors	147
Identification errors	74
Damaged components	145
Contamination	209
Accepted	478
Materials Review Board	36
Total	2547

A dynamic test program was undertaken to determine whether or not the spacecraft was structurally capable of withstanding the dynamic loads, as defined in JPL Specification 30254. The test program was basically divided into two parts:

- (1) Modal survey testing
- (2) Structural type-approval testing

See Section VI-A of this Report for a full coverage of these test programs.

c. Purging tests. The Earth sensor was sensitive to any foreign matter, since scattered light from that matter would degrade the sensor threshold in the presence of the bright Venus albedo. Because LMSC does not have any cleanliness requirements on the cooling air for the *Agna* forward equipment rack, it was important that the forward bulkhead on the *Agna* not leak air into the spacecraft area. Tests with an *Agna* forward equipment rack were carried out and it was concluded that, although taping was not satisfactory, a carefully applied silastic caulking compound, together with vinyl tape, adequately sealed the bulkhead. The forward equipment rack was pressurized to 20 in. H₂O (the normal pad condition) and held the head for 2 hr with no measurable leak rate.

d. Retro-maneuver contamination tests. Degradation of the spacecraft by propellants vented from the *Agna B* is possible should liquid or solid particles leave deposits on the mirror associated with the long-range Earth sensor. The Earth sensor could conceivably be confused by light scattering off any deposits of fuel or oxidizer on the mirror and Earth lock in the vicinity of Venus could be lost. The UDMH in the liquid state tends to wet the surface of the mirror and spread out, leaving a

deposit which resembles an oil slick. Impurities in the IRFNA are left on the mirror in the form of nitrate salts. Contamination of thermal control surfaces by the vented propellants is not considered to be a problem.

The question of whether liquid and/or solid particles could be expected to be present in the vicinity of the spacecraft at the time the maneuver was performed had been approached analytically. LMSC made the assumption that all liquid and solid particles ejected from the venting nozzles would be evaporated before they reached the spacecraft. This assumption was challenged by JPL, and LMSC had intended to perform tests which would verify that any liquid or solid particles will evaporate before reaching the spacecraft (LMSC apparently did not carry out this work).

The tests conducted at LMSC, witnessed by JPL representatives, verified their initial assumption that contamination by vapor impinging on the spacecraft would not be a problem. However, it was concluded that for a spacecraft-*Agna* separation distance of 400 ft, liquid-propellant droplets may impact the spacecraft and that solid droplets will strike it. At 5000 ft, no liquid droplets would be expected to reach the spacecraft, but solid particles would probably impact the vehicle.

This question of spacecraft degradation was never settled analytically or experimentally because it became apparent that an involved and lengthy effort was required. Instead, the *Agna* retro-maneuver was modified in such a way that the chances of propellants hitting the spacecraft were negligible and the planetary impact probability was still adequately small.

e. Noise box. A sample of the cloth solar sail material to be used on the solar ballast successfully passed a test in a progressive wave acoustic test chamber. The sail material, being light in weight, was subjected to high-frequency acoustic excitation during the boost phase. Although the test was not a duplication of the actual use conditions, it was thought that there was sufficient conservatism to provide confidence that passing this test would assure no use-failures. If the test had resulted in a failure, more exact simulation or a more complete analysis would have been necessary.

A 10- × 11½-in. sample of sail material was held crossways in the test segment of the 1-ft-square progressive wave tube. The material was restrained by rods slipped through stitched hems at the two 10-in. sides.

The test consisted of 20 min of a random noise sound field. A wide-band sound pressure level in excess of 140 db (re. 0.002 μ bar) was obtained. The bulk of the energy was contained between 300 and 1500 cps. Upon completion of the test, no damage whatever was apparent to the material.

f. GSE radio-frequency interference. Interference tests were performed on the MR-1 System Test Complex on February 6-8, 1962. The tests consisted of measuring the noise put out through power lines on each item of GSE in the Complex. The tests were conducted to JPL Specification 30236A and covered the frequency range of 150 kc to 1 kmc. The test was performed because of RFI troubles experienced with the Complex by operations personnel on earlier projects. Because no interference was found during this test, the MR-2 System Test Complex was not checked.

g. Earth-sensor shake. During type-approval vibration testing of the spacecraft, excessive *g* levels were noticed in the region of the antenna yoke and the Earth sensor. These levels were estimated at 45 *g*, zero to peak, an unacceptable level for Earth-sensor survival.

A series of vibration tests was run on various pieces of hardware in an attempt to reduce the Earth-sensor *g* levels. The final solution selected for flight involved stiffening of all antenna support feet by changing the rubber pads to rubber-covered aluminum, addition of torsion struts to the gear case lid, and the installation of concentric tube greased dampers on the Earth-sensor yoke plate. This fix reduced lateral vibration levels by a factor of at least 7 and reduced vertical vibration levels by a factor of more than 11, while shifting the predominant resonant frequency from 24 to 45 cps.

~~SECRET~~ UNCLASSIFIED

UNCLASSIFIED

~~SECRET~~

~~SECRET~~

IX. The Launch Vehicle

A. Atlas-Agena System

1. Preliminary Studies

During summer 1961, preliminary studies were made of the performance and the possible weight reduction of hardware for the *Atlas-Agena* launch vehicle system. As a result, the spacecraft weight and general configuration were established. JPL Specification 30881, released on September 28, 1961, defined the technical requirements and constraints which the *Mariner R* spacecraft imposed upon the *Atlas-Agena* vehicle and upon the associated ground support equipment.

A family of five interface planning schedules was established in order to ensure that each phase of the coordinated effort would be completed in its proper sequence and at the proper time. The five schedules were:

a. Interface plan. The interface plan for spacecraft support equipment included the time requirements for the release of specifications and drawings; delivery dates

for hardware; completion of the match-mate, mechanical, electrical, and vibration tests; and final design verification tests.

b. Trajectory schedule. The trajectory schedule for *MR-1* and *-2* included the dates for transmittal, approval, publishing, and distribution of information concerning trajectories, range safety, and firing tables.

c. Documentation schedule. Dates for the transmittal and publishing of information were placed in a documentation schedule. The status was indicated of the Project Development Plan, the Program Requirements Document, and the Booster Requirements Document, as well as the scheduled due-dates for other documentation requirements.

d. Pad loading, modification, and checkout. A schedule was provided for the installation, modification, and checkout of spacecraft monitoring and control equipment at the launch site.

e. Milestone schedule—pad operations. A schedule of operations on the launch pad was established to indicate the sequence and timing requirements for mating, erecting, and checkout of all phases of the prelaunch operation.

The shroud, adapter, and other spacecraft support equipment design was critically evaluated during this time in order to determine whether or not it would meet the *Mariner* spacecraft requirements. It was determined that weight reduction would present the major problem within the system and that certain other changes were necessary because of modifications in spacecraft sterilization, environmental control, and launch pad requirements.

2. Weight Reduction

Studies were made of the means by which weight reduction could be achieved in the *Agena* vehicle for the *Mariner R* program. The following list shows the areas where weight reduction was accomplished:

- (1) Titanium was used in the heat shield.
- (2) The helium sphere was made smaller.
- (3) A new electrical system was installed featuring lighter-weight components.
- (4) The Type I telemetry was changed to a new 7-channel FM/FM system.
- (5) Certain peculiarities and the retrorocket, used in the *Ranger* design, were eliminated.

3. 100-n mi vs 85-n mi parking orbit

Initially, consideration was given to utilizing an 85-n mi parking orbit for the *Mariner R* missions to gain additional performance. However, it was a project decision that, from over-all system considerations, the advantages of a 100-n mi parking orbit just as *Ranger* was using would more than compensate for the attendant reduction in allowable spacecraft weight or the launch period equivalent. It was necessary to cut the spacecraft weight from 460 to 446 lb, based on a reduction in the estimated weight, primarily of the spacecraft battery.

4. Launch Complex Modifications

Efforts were made to keep to a minimum those launch complex modifications which might have been desirable but not mandatory for *Mariner R* (e.g., long cable runs and umbilicals were not changed). Pad modifications which were actually made because of *Mariner R* requirements were:

- (1) New J-boxes were installed at the top of the umbilical tower.
- (2) An additional rack was provided in the launch control shelter.
- (3) A video pair was installed from the transfer room to the J-boxes on the umbilical tower.
- (4) An independent spacecraft power source was installed under the pad ramp.

5. System Launch Constraints

General Dynamics-Astronautics and Lockheed Missiles and Space Company defined the constraints which would be imposed upon the system by the *Atlas* and *Agena*, respectively. Efforts were made by both GD/A and LMSC to broaden the limits of constraints when permissible. For example:

- (1) GD/A conducted studies and tests which resulted in an extension of the permissible time that *Atlas* LOX topping could take place.
- (2) LMSC conducted studies which resulted in the extension of the guidance system validation time for the *Agena*.

See Section XI for a more comprehensive treatment of launch restraints.

6. AMR Activities

During the period prior to the launch of *MR-I*, information was gathered from the following sources relating to launch constraints:

- (1) GD/A (constraints pertaining to the *Atlas* vehicle).
- (2) LMSC (constraints pertaining to the *Agena* vehicle).
- (3) DSIF (constraints pertaining to spacecraft tracking and telemetry).
- (4) AMR (telemetry and tracking constraints from launch to injection).
- (5) JPL (constraints pertaining to the spacecraft).
- (6) Range Safety (constraints regarding permissible flight azimuths).

The above constraints were evaluated and depicted in summary form on the chart shown in Fig. 214. This chart was maintained continuously throughout the *Mariner R* launch operations.

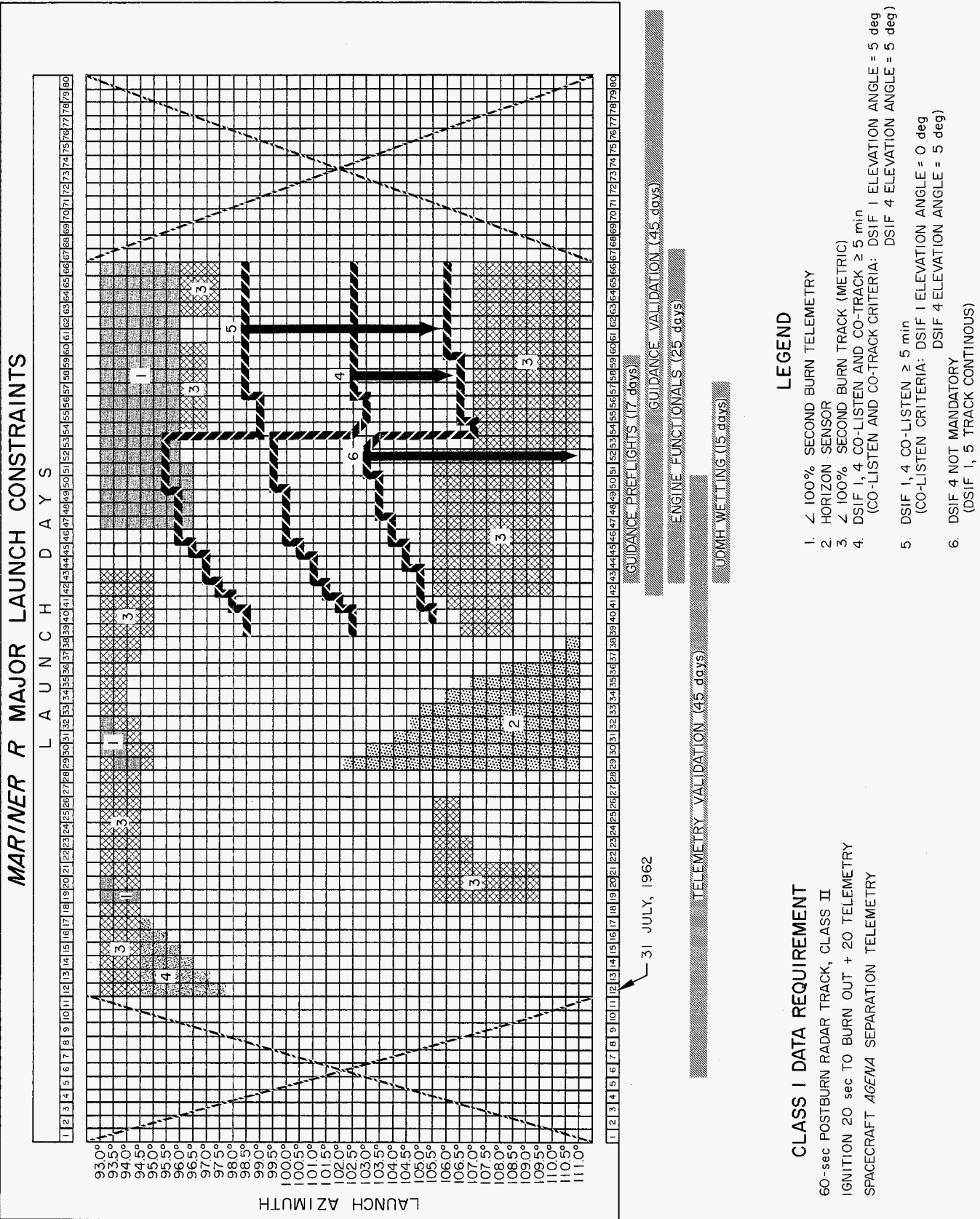


Fig. 214. Chart of launch restraints

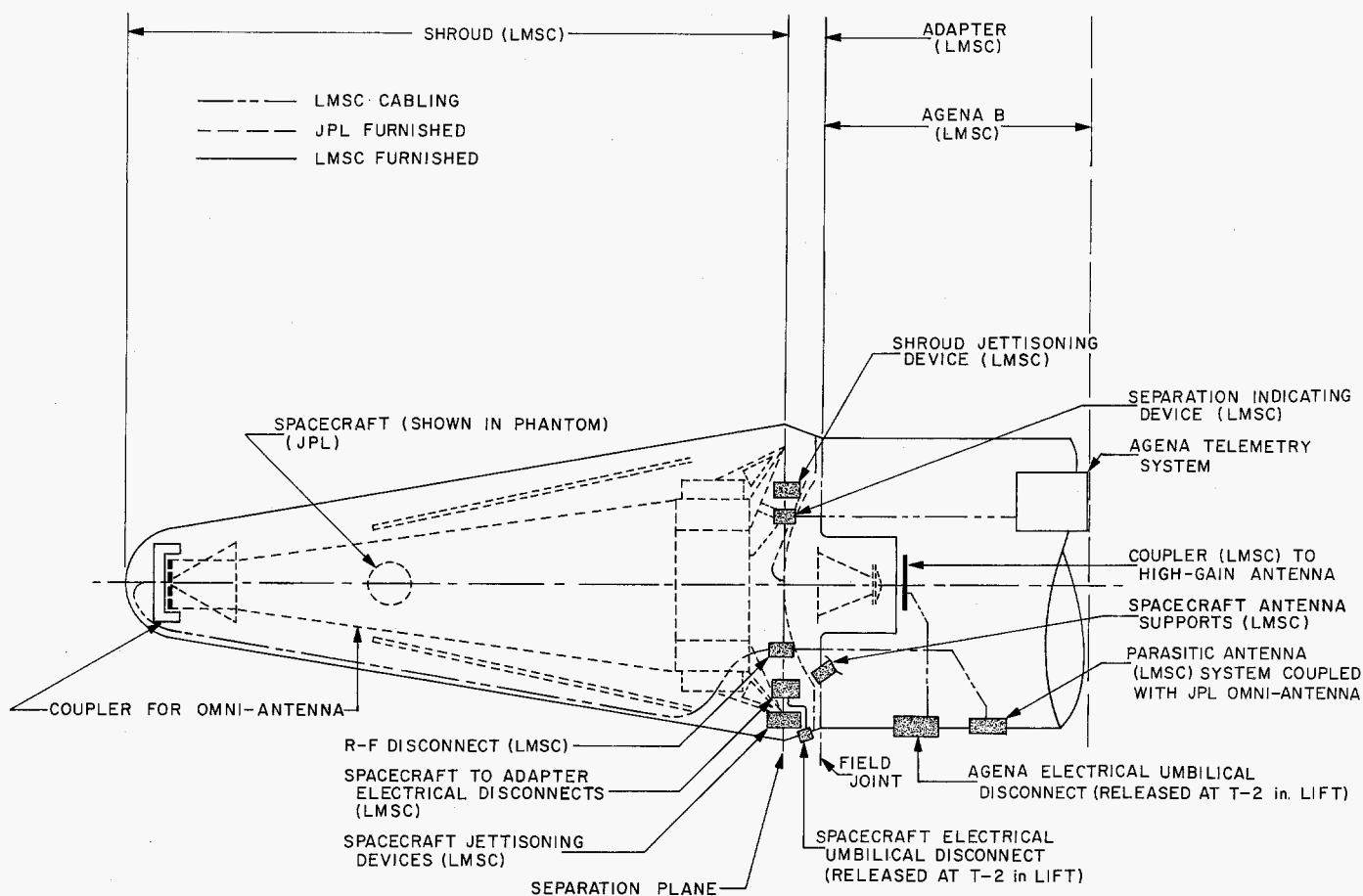


Fig. 215. Spacecraft configuration

Large-range maps were used in the JPL Launch Control Room for launch operations. The launch corridor, major vehicle events, range tracking, and telemetry coverage were plotted to give an immediate picture of overlapping range restrictions and to permit immediate evaluation in the event of equipment malfunction.

Launch vehicle integration personnel participated extensively in liaison activities between the various agencies involved in the launch operations.

B. Vehicle Integration

1. Integration Design Criteria

During the preliminary study period, the definition of interface demarcation was agreed upon by JPL, MSFC, and LMSC. These agreements are shown in Fig. 215.

In view of the short time schedule necessary to meet the requirements of the *Mariner R* launch period, it was decided that the interface design would be as nearly like *Ranger* as possible. The following decisions were made:

- (1) The shroud design remained essentially unchanged.
- (2) In view of the fact that *Mariner R* had no sterilization requirements, and in order to effect a weight saving, the sterilization diaphragm was removed from the spacecraft-Agena adapter.
- (3) In order to provide spacecraft environmental control, the forward equipment rack of the *Agena* was sealed to prevent the influx of *Agena* cooling air into the spacecraft cavity. This change also permitted the use of nitrogen in the spacecraft cavity to provide a controlled environment.
- (4) Routing of spacecraft telemetry signals was modified so that the spacecraft telemetry signal was not presented to the *Agena* telemetry system (Fig. 216).

 **UNCLASSIFIED**

JPL TECHNICAL REPORT NO. 32-353

analyses, modification of the *Ranger* spacecraft adapter, evaluation of moments involved in spacecraft separation (*Mariner R* had less mass), and redesign and manufacture of a new spacecraft adapter and a new forward midbody for structural tests.

LMSC was directed to perform additional *Mariner* spacecraft separation tests in March 1962. These tests were started, but were delayed by the urgency of similar

Ranger tests. The *Mariner* tests checked the effects of Earth-sensor vibration damping provisions on the spacecraft. Earlier vibration tests indicated the need for Earth-sensor damping. The compression block damping method exerts a force in a direction that is offset with respect to the spacecraft center of gravity. The additional tests evaluated the upsetting moment and enabled JPL and LMSC to develop adequate balance by means of suitably placed compression blocks and spring loadings (Ref. 3).

 **UNCLASSIFIED**

~~CONFIDENTIAL~~ **UNCLASSIFIED**

~~CONFIDENTIAL~~ **UNCLASSIFIED**



X. Trajectories and Systems Analysis

A. Introduction

This Section describes the systems analysis activities for the *Mariner R* program. Section B is concerned with trajectory design. Postinjection trajectories, preinjection trajectories, and related subjects, such as range safety and tracking coverage, are discussed in that order.

Section C covers guidance analysis. The error analysis of the boost vehicle injection guidance system is described, followed by the analysis of the single-impulse radio command midcourse guidance system in the spacecraft. The ground operations necessary for the midcourse maneuver are also covered.

Section D briefly describes the orbit determination operations, as planned for the 1962 *Mariner R* missions, including the evolution of the tracking data editing program and the orbit determination program from their *Ranger* counterparts, and the tracking analysis accuracy studies in support of the *Mariner R* missions.

B. Trajectories

1. Postinjection Trajectories

a. Introduction. The *Mariner* trajectories were designed and selected to satisfy strict objectives and constraints. Parametric studies of the relationship between flight time, launch date, energy, etc., were first conducted to reveal the acceptable launch intervals and the characteristics of the various ballistic trajectories. After considering all physical limitations or constraints that were to be placed upon the flight path, the *Mariner* trajectories were then selected and computed precisely on the IBM 7090 computer, using a multiple-body program.

b. Parametric study of Venus 1962 trajectories. Approximately every 19 mo, the energy⁵ required to effect

⁵The term "energy" as used here corresponds to the *vis viva* energy C_3 that the boost vehicle delivers to the spacecraft at injection into the geocentric escape trajectory.

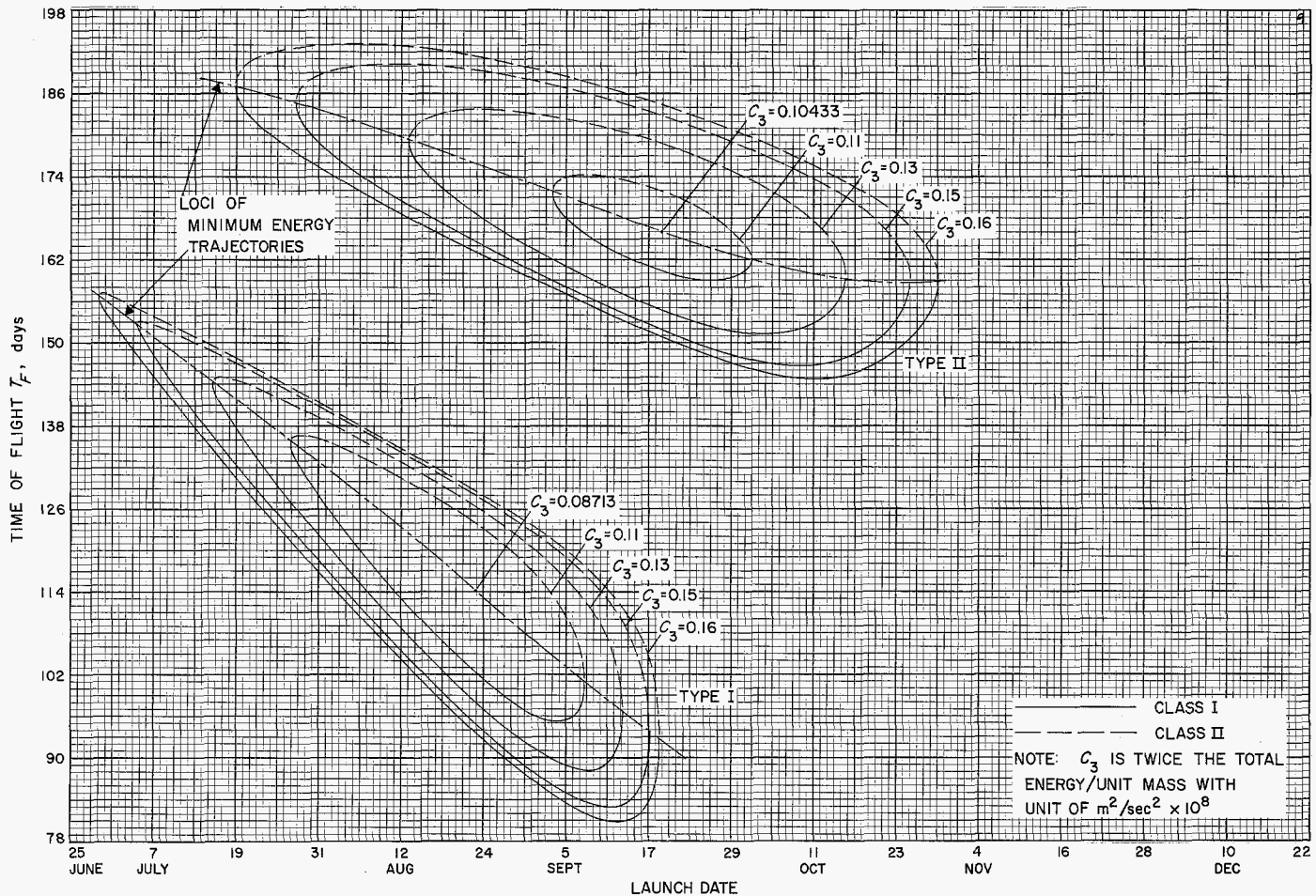


Fig. 219. Time of flight vs launch date

a ballistic transfer from Earth to Venus becomes a minimum. To obtain the largest possible payload weight from the *Atlas-Agena* booster, it was, therefore, necessary to launch near this date in 1962. Parametric studies of the relationship between flight time, launch date, and energy reveal the acceptable launch intervals.

Results of these studies are illustrated in Fig. 219 and 220. Two sets of closed contours denoted Type I and II are presented. Type I trajectories are characterized by the fact that the probe transits a heliocentric central angle of less than 180 deg from launch to encounter; whereas, for Type II trajectories, the total transfer angle lies between 180 and 360 deg. It is worthwhile to note several important properties of these trajectories:

- (1) Type II trajectories have longer flight times and communications distances at encounter than Type I.

- (2) For a given injection energy C_3 and launch date, up to four different trajectories can be used.
- (3) For both Type I and II, there are minimum-energy transfers for each launch date, with absolute minimums occurring on August 23 for Type I (flight time of 114 days and C_3 of $8.7 \text{ km}^2/\text{sec}^2$) and on September 19 (flight time of 166 days and C_3 of $10.4 \text{ km}^2/\text{sec}^2$) for Type II.
- (4) For a given fixed energy above the absolute minimum, there is a corresponding launch interval or permissible firing period.

A more detailed description of the parametric study is given in Ref. 4.

c. Major trajectory constraints. Before precise trajectories could be selected and designed for the *Mariner* Venus mission, a list of design constraints and objectives first had to be established. Four of the major constraints

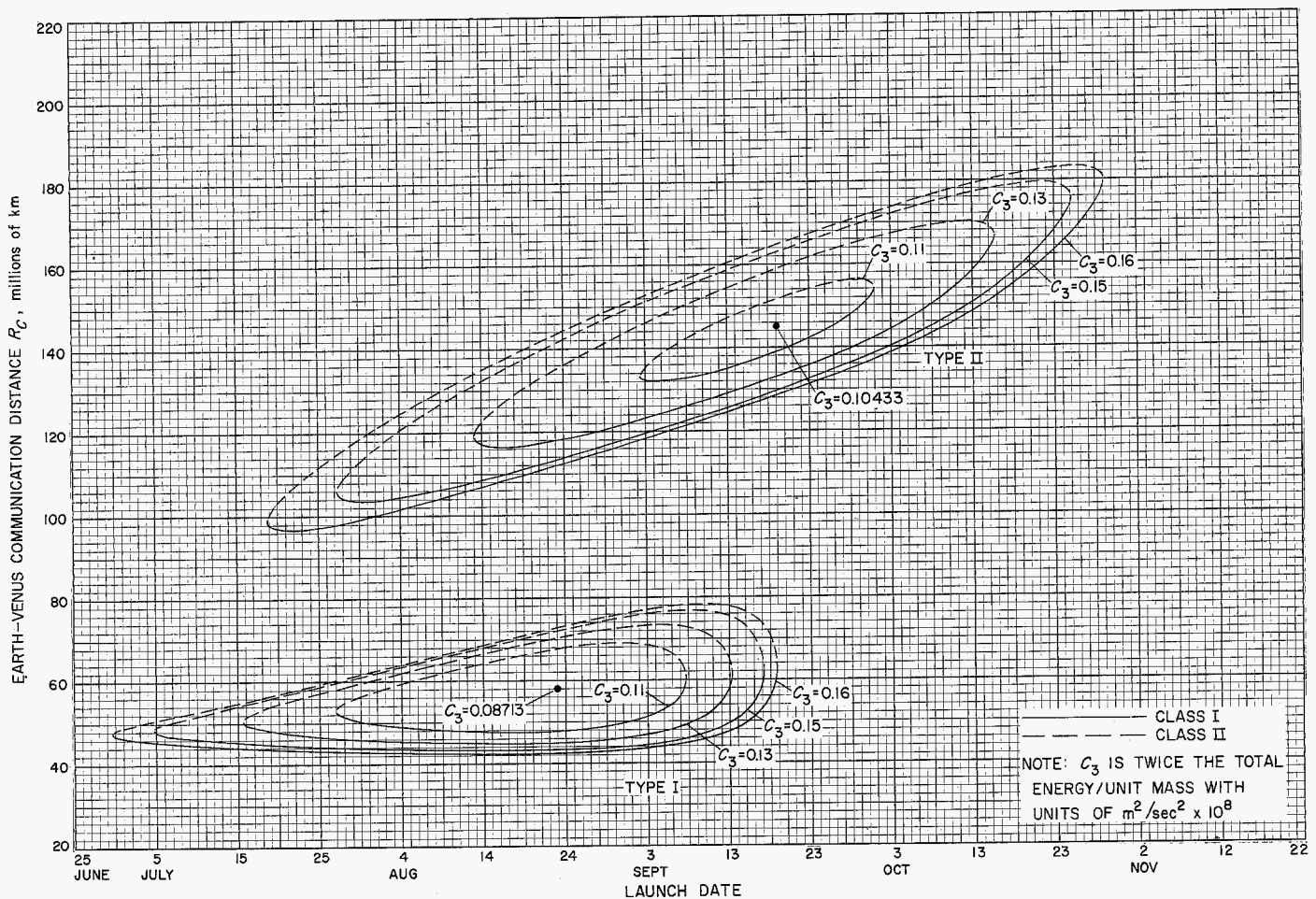


Fig. 220. Earth-Venus communications distance vs launch date

which proved decisive in selecting the launch day and arrival day trajectories were:

- (1) The maximum distance between Earth and spacecraft at which communications might still be achieved was approximated to be 100,000,000 km.
- (2) Two spacecraft were to be launched at Venus, with the use of a single launch pad, requiring a substantial firing period.
- (3) Each spacecraft had to encounter the planet near the middle of a Goldstone tracking day.
- (4) A two-day separation in arrival dates for each spacecraft was mandatory to prevent simultaneous reception of planet-encounter data at Goldstone.

d. Over-all trajectory design

Rejection of Type II transfers. For the Mariner mission, Type II trajectories were immediately discarded as

the choice of ballistic transfers because of their long flight times and communications distances.

Selection of Type I minimum-energy transfers. By deduction, Type I transfers with their relatively low flight times and distances at encounter were selected for the task. Upon closely observing and checking all Type I transfers, the decision was to use a trajectory near minimum energy for each launch date. Such transfers satisfied all constraints mentioned previously and at the same time: (1) assured that a maximum firing period would ultimately be available once the spacecraft was built and the maximum injection energy attainable by the Atlas-Agena-spacecraft was calculated; and (2) produced hyperbolic excess speeds at Venus which were almost a minimum, thereby maximizing the time which the spacecraft would spend in the near vicinity of Venus.

Firing period. Since there was a direct relationship between injection energy achievable from the booster

and the weight of the spacecraft, a tradeoff between firing period and spacecraft weight was evident. A design goal for the spacecraft of 450 lb was finally established, allowing an approximate 55-day firing period for the two launchings. A decision was made that if the weight of the spacecraft after construction should be greater or less than the nominal 450 lb, the firing period would then be altered accordingly. Changes in the performance of the *Atlas-Agena* boost vehicle would also reflect upon the firing period. In order to include all feasible launch days, a firing period of 69 days was utilized in the trajectory design. This firing period extended from July 10 to September 15, 1962. Subsequent to spacecraft completion, however, the scheduled launch date of *MR-1* was established as July 21, 1962. The nominal launch date for *MR-2* was then to be 21 days after *MR-1* was launched.

Arrival date selections. The arrival dates of the minimum-energy trajectories which were selected for the *Mariner* missions varied with the day of launch. Close examination of Table 23 and Fig. 219 reveals that the trajectories essentially followed the minimum-energy loci of the Type I trajectories. For these trajectories, the Earth-Venus communications distance at encounter varied from 51.7 to 58.9 million km, which was safely less than the 100,000,000 km maximum distance permitted by communications system constraints. The time of closest approach to Venus for each selected arrival date was chosen to correspond to the middle of the Goldstone viewing interval. Figure 221 shows the typical flight path of *Mariner* from launch to Venus encounter.

Aiming point selection. Concurrent with the selection of trajectories based upon the major constraints listed previously, targeting studies were conducted of the near-Venus trajectories to choose the aiming point. Essentially, the aiming point is the location of closest approach to Venus. Again, the selection of the aiming point was governed by a number of constraints, such as:

- (1) The probability of impacting Venus should be less than one part in a thousand.
- (2) When the spacecraft crosses the planet terminator, the planet must subtend an angle between 10 and 45 deg for magnetometer and radiometer considerations.
- (3) The angle measured at the spacecraft from the Earth-probe-Sun plane, normal to the probe-Sun direction, to the far edge of Venus, must not exceed 55 deg because of radiometer limitations.

Table 23. Launch date — arrival date schedule

Launch 1962	Flight time, days	Arrival time 1962
July 10–July 17	149–142	Dec. 6, 18 hr 14 min
July 18–July 27	143–134	Dec. 8, 18 hr 8 min
July 28–Aug. 6	135–126	Dec. 10, 18 hr 3 min
Aug. 7–Aug. 16	127–118	Dec. 12, 17 hr 57 min
Aug. 17–Aug. 31	119–105	Dec. 14, 17 hr 55 min
Sep. 1–Sep. 15	106– 92	Dec. 16, 17 hr 53 min

- (4) Venus must not occult the Sun from the spacecraft because of attitude control and power considerations.
- (5) The Earth-probe-near-limb of Venus angle must remain greater than 60 deg until the radiometer scan goes off the planet because of limitations of the Earth sensor.

Subject to these constraints, a design aiming point on the trailing edge of Venus was selected within the permissible area shown in Fig. 222. The plane of the coordinate system in Fig. 222 is normal to the incoming asymptote. Vector **T** is a unit vector parallel to the ecliptic plane and **R** is normal to **T**. Vector **B** is the perpendicular from the center of Venus to the incoming asymptote. The nominal aiming point has components $\mathbf{B} \cdot \mathbf{T} = -29,545$ km and $\mathbf{B} \cdot \mathbf{R} = +5,210$ km. The magnitude of the closest approach distance from the center of Venus is 20,000 km for this aiming point.

e. Precision trajectories and documents. After considering all constraints in much detail, final precision trajectories were calculated and a final trajectory document was published, up-dating the preliminary trajectory report. A targeting criteria specification was also prepared for the boost-vehicle contractor's use in generating firing tables. These tables (Ref. 5) were prepared by Space Technology Laboratories, Inc., under subcontract to the Lockheed Missile and Space Company. Their preparation required detail simulation of the *Atlas-Agena* boost trajectory as constrained by the guidance equations, and the free-flight trajectory from injection to target under the influence of Earth, Moon, Sun, Venus, Jupiter, and solar radiation pressure. The tables were computed for a 93- to 111-deg launch azimuth interval, as prescribed by range safety and instrumentation coverage constraints. The daily firing window was about 2 hr; injection locations were confined to a region of about 6 deg in latitude and 35 deg in longitude in the South Atlantic Ocean off the coast of Africa. A more detailed explanation of the preinjection trajectories follows.

UNCLASSIFIED

JPL TECHNICAL REPORT NO. 32-353

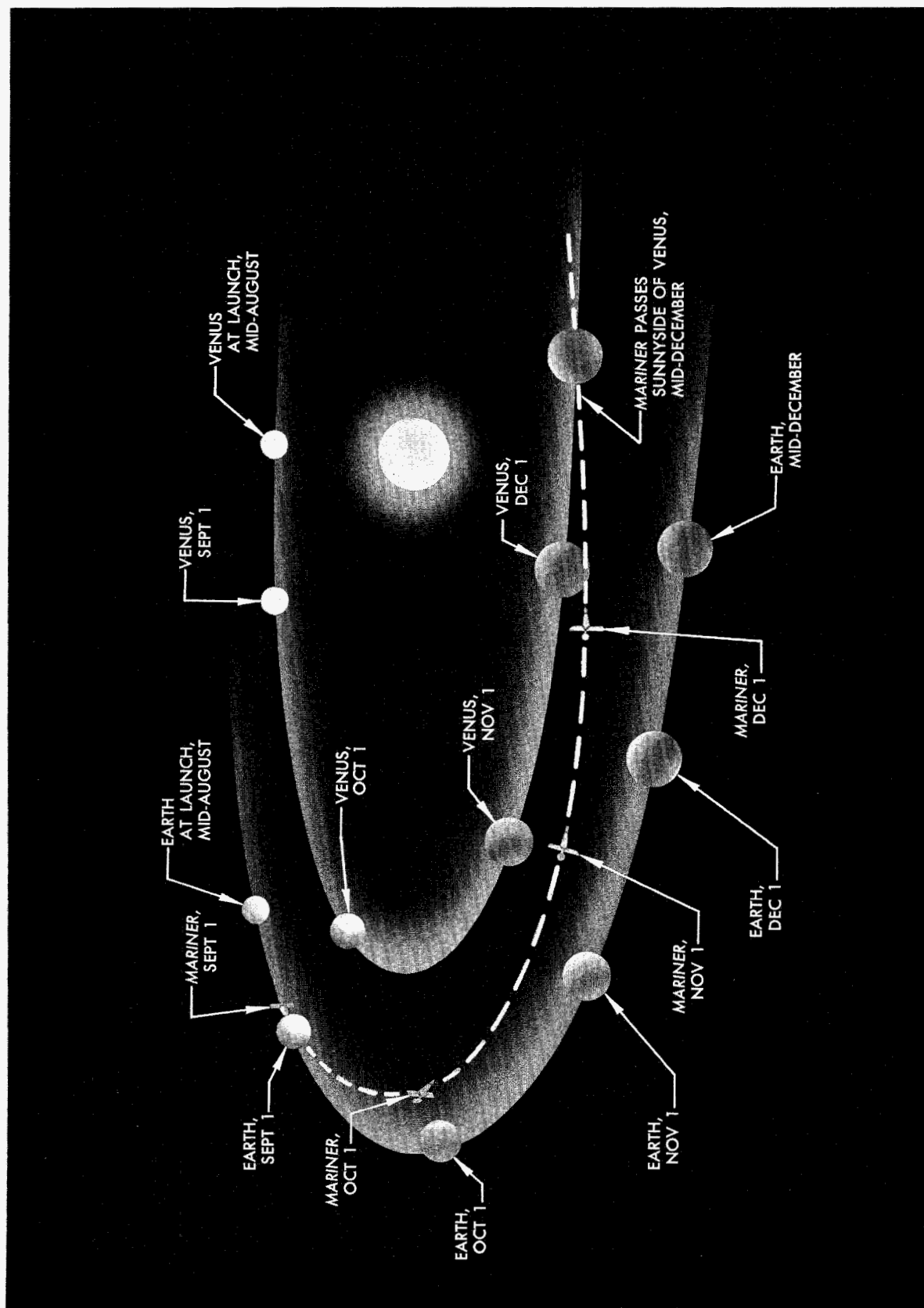


Fig. 221. Typical Mariner 2 trajectory

UNCLASSIFIED

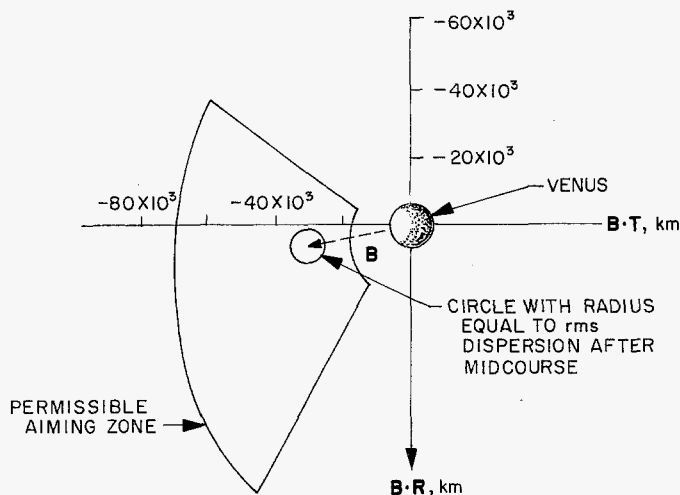


Fig. 222. Permissible aiming zone region

2. Preinjection Trajectories

The *Mariner* preinjection trajectories are similar to those used for *Ranger*. The *Atlas-Agena* launch sequence proceeds as follows:

The launch vehicle-spacecraft system lifts off vertically from the launch pad. Since the Earth is rotating, the direction in which the *Atlas* should fly constantly changes. Therefore, the *Atlas* rolls to the proper bearing from its initial bearing of 105 deg east of north shortly after liftoff. The *Atlas* is then pitched from the vertical in the desired flight direction, 15 sec after liftoff. Approximately 140 sec after liftoff, the booster engine shuts down and the engines are jettisoned. The *Atlas* sustainer engine continues to burn until the vehicle has reached the proper altitude with the desired velocity. The sustainer engine then shuts down and the vernier engines provide the final trim in velocity and altitude.

At this point, the *Agenda* and *Atlas* separate, and the *Agenda*/spacecraft are on the desired coast ellipse to the parking orbit. Prior to apogee, the *Agenda* engine ignites for the first time to provide the additional velocity increment needed to obtain orbital velocity at the parking orbit altitude of 100 n. mi. When this velocity increment has been attained, the *Agenda* engine shuts down and the *Agenda*/spacecraft are in the parking orbit. The vehicle remains in the parking orbit until it reaches the point at which the *Agenda* engine is re-ignited to provide the second velocity increment necessary to inject the vehicle into the desired ballistic transfer orbit to Venus.

The new orbit attained after end of the second burn is an Earth-centered hyperbola which will allow the space-

craft to escape the Earth-Moon system. Shortly after injection into the escape orbit, the *Agenda*/spacecraft separate and the *Agenda* performs a retro-maneuver to avoid impacting Venus, and to change its orbit from that of the spacecraft.

Two concepts have been mentioned which warrant further discussion. One is the concept of a launch azimuth which changes with time. The second is the principle of the parking orbit.

The positions of the Earth and Venus constantly change with respect to each other and the Sun. Thus, one expects that the position over the Earth's surface at which the spacecraft will be injected to Venus will change. The changes which, in fact, do occur are discussed in the previous section.

A second factor is, however, of immediate interest. This is the rotation of the Earth on its axis. This rotation once every 24 hr causes the desired injection location to move in a westerly direction roughly parallel to the equator so that it returns to about the same point 24 hr later. Thus, the direction in which the launch must be made from AMR continually changes. However, consideration of safety to populated land masses in the event the *Atlas* or *Agenda* malfunctions prevents a launch from occurring at any azimuth except a narrow band between 93 and 111 deg. Thus, a "launch window" has been created; that is, a period during the day during which the launch can take place.

The principle of the parking orbit is easy to understand if one realizes that the Earth-Venus-Sun geometry is constantly changing, and yet the launch site is fixed. Thus, the parking orbit simply moves the launch site above the Earth's surface to 100 n mi and to any desired position around the world, within the limits of range safety.

Figure 223 is a sketch of the ascent trajectory from liftoff through the *Agenda* retro-maneuver. The location of the second ignition point will vary from day to day. Figure 224 is a map of the Earth tracks of the spacecraft on the most northerly and most southerly injection loci.

3. Related Activities

The discussion of trajectories, both preinjection and postinjection, cannot be divorced from several other

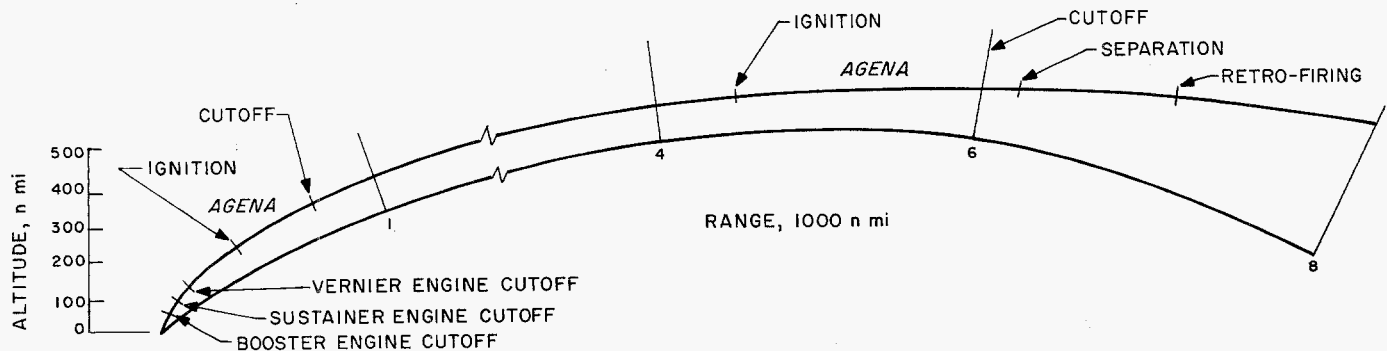


Fig. 223. Typical Mariner R flight profile

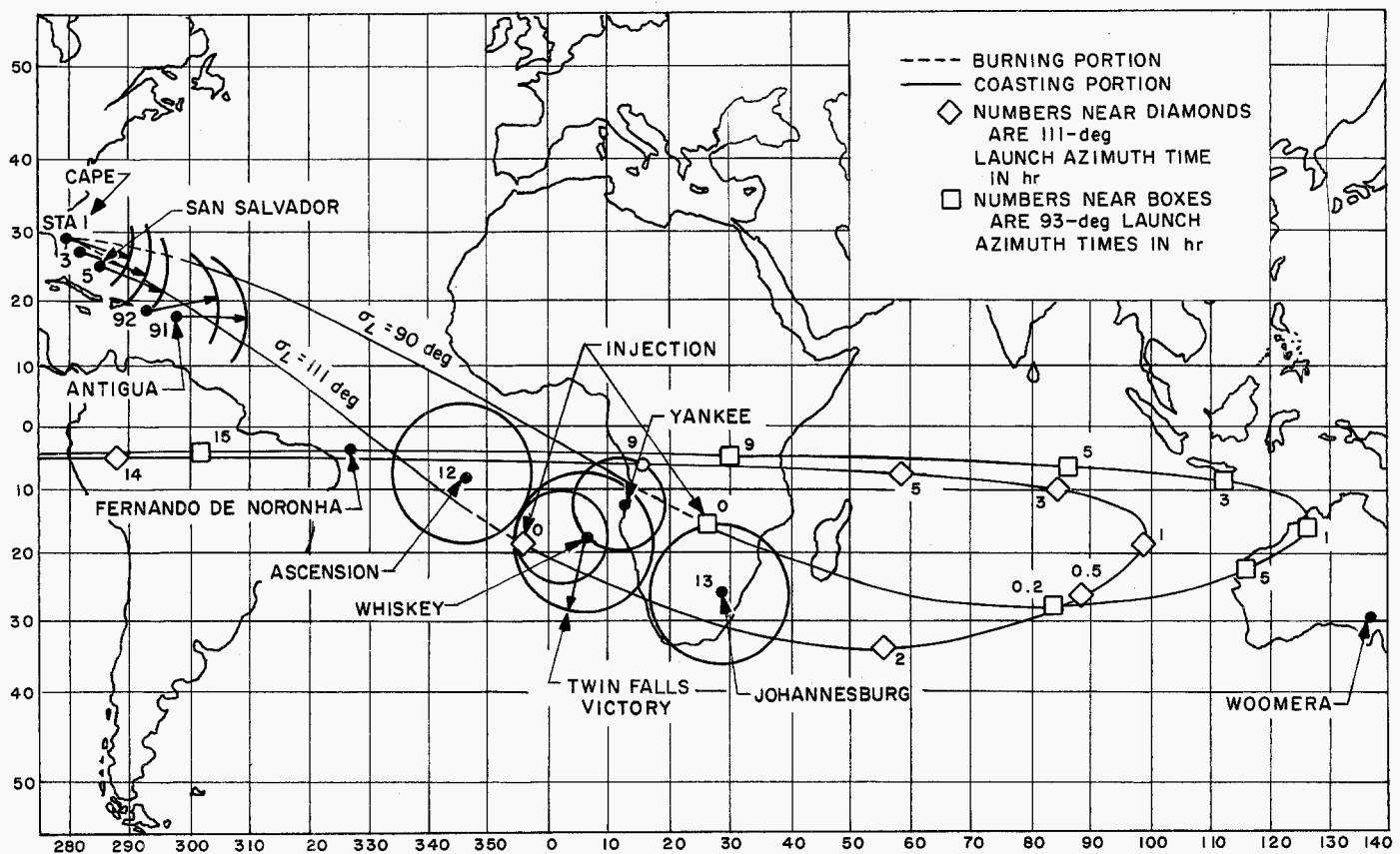


Fig. 224. Typical Mariner R Earth track

topics because of the important influence the trajectories have on these other areas. A brief discussion of these interfaces is presented in an attempt to tie together these areas which are discussed elsewhere in this report in detail.

a. Spacecraft design. The design of the spacecraft is interrelated with the design of the postinjection trajectory. The interface is covered elsewhere.

b. Tracking and telemetry coverage

Atlantic Missile Range. AMR provides four functions to the Mariner Project: (1) the launch operation; (2) telemetry coverage; (3) tracking coverage; and (4) range safety. The launch operations are discussed in Section VI.

(1) **Telemetry coverage.** AMR coverage of launch vehicle and spacecraft telemetry is requested in the Program Requirements Document 3300 (Ref. 6). This

coverage is provided by the range with telemetry stations at various AMR sites. The coverage of the launch vehicle telemetry is provided by the stations listed in Table 24. Equipment is provided by JPL to the range to record spacecraft telemetry at the sites which are indicated in Table 24. These sites and the approximate coverage of the trajectory are shown below.

(2) *Tracking coverage.* AMR tracking is provided by the stations listed in Table 24. This information is used by AMR to calculate the elements of the parking orbit and the elements of the escape orbit. These calculations are made on the IBM 7090 range safety computer. The range also uses these data to generate DSIF acquisition information, which is sent to JPL for relay to the DSIF.

(3) *Range safety.* The launch of the spacecraft entails certain risks to inhabited land masses in the area. The function of range safety is to ensure that these risks are kept acceptably low. The satisfactory execution of the range safety mission involves the calculation of the vehicle position as a function of time and determining, in real time, the point at which the vehicle will impact if thrust were suddenly terminated. The range tracking stations and the 7090 computer are used to accomplish this mission.

DSIF. The DSIF assumes responsibility for the tracking and telemetry coverage after the vehicle is in an escape orbit. There is, of course, an overlap of coverage capability between AMR and the DSIF in the near-Earth realm. The variation of the trajectory on a minute-by-minute and day-by-day basis poses severe problems to the tracking stations. These problems are most severe during the launch-to-injection 4-hr time span. During these periods, initial spacecraft appearance may occur at almost any point on the station's horizon. Tracking rates are usually very high and continuous tracking is difficult under the best of conditions.

A number of aids are provided to assist the stations in their attempts to track successfully during this critical period. In-flight prediction messages based on AMR tracking are provided to correctly position the antenna. Preflight predictions are provided for each launch day in the form of graphs of station quantities. Figure 225 is an example of the plot of the station elevation angle-vs-time for the Mobile Tracking Station at Johannesburg, South Africa. Other parameters plotted include station pointing angles, spacecraft telemetering frequencies, signal strengths, and signal attenuation.

Table 24. Atlantic Missile Range tracking stations

Station	Name	Equipment
1	Cape Canaveral	FPS 16, 2 TLM 18
3	Grand Bahama Island	FPS 16
5	San Salvador	FPS 16
92	East Island, P. R.	FPS 16
91	Antigua	MPS 26, TLM 18
12	Ascension	FPS 16, TLM 18
13	Pretoria	FPS 16, TLM 18
Twin Falls Victory (Ship)	ORV Uniform (Ship)	FPS 16, TLM 18
	ORV Whiskey (Ship)	TLM 18
	ORV Yankee (Ship)	TLM 18

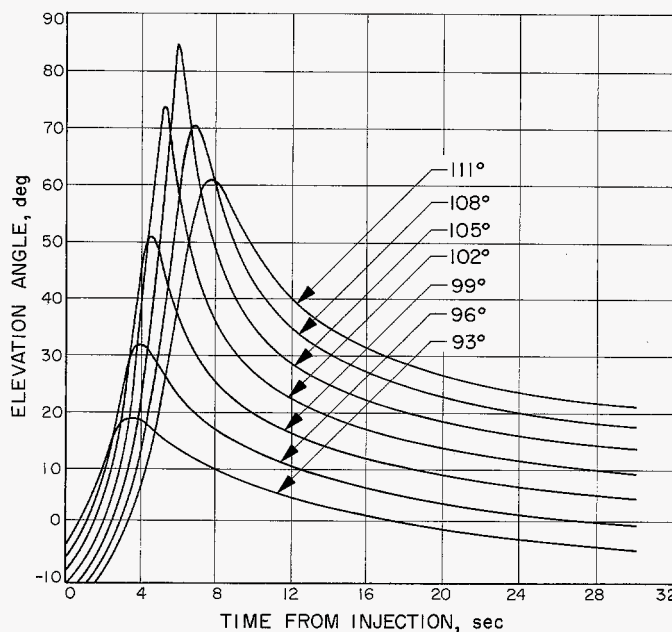


Fig. 225. Elevation angle at Johannesburg

Launch vehicles. A strong interface exists between the trajectory and the launch vehicle. In many instances, the launch vehicle directly determines the design of the trajectory. (Thus, the ascent trajectory from launch to injection into the parking orbit is shaped to extract the maximum performance from the launch vehicle.)

The design of the trajectory must also consider the constraints imposed by the launch vehicle. For example, *Mariner R* utilizes a second stage (*Agena*) which cannot be ground-controlled after the first and second stages have separated. The particular characteristics of the launch vehicle are discussed in Section IX.

Space flight operations. The final major interface with trajectories which exists in the calculations is the area of launch and space flight operations. These areas are discussed in Sections VI and XII.

C. Guidance

1. Injection Guidance

A statistical description of the coordinate deviations at injection is necessary to determine the midcourse correction capability needed to assure arrival at the desired aiming point at Venus. An analysis of the *Atlas-Agena* injection guidance system was made to determine this information for the *Mariner* trajectories.

The analysis was performed as follows:

- (1) The $1\text{-}\sigma$ value of each independent component error source and the sensitivity of injection coordinates to these errors were obtained from Lockheed Missiles and Space Company.
- (2) The $1\text{-}\sigma$ injection coordinate deviations were then obtained.
- (3) This information was used to form a noise moment matrix (6×6 covariance matrix Δ^I) of injection coordinate deviations.
- (4) This matrix, Δ^I , was used to calculate the target miss components in the absence of midcourse guidance.
- (5) The Δ^I matrix was also used to compute the rms midcourse velocity capability need for the *Mariner* flight.
- (6) A units-of-variance analysis was performed to obtain the relative effect of each component error on the midcourse maneuver.

a. Determination of injection errors. The following sequence of events occurs prior to the spacecraft injection:

- (1) The *Atlas* burning interval puts the spacecraft on a coast ellipse with a prespecified energy and eccentricity.

- (2) After a short coast, the *Agna* ignites and injects the spacecraft into a circular parking orbit.
- (3) The *Agna* is reignited at the proper time to obtain the desired injection position, attitude, and velocity.

When the spacecraft is actually launched, it will not, in general, be injected precisely into the desired, or standard, trajectory because of small errors in the guidance components. Nonstandard *Mariner* trajectories have two important characteristics:

- (1) The trajectory errors are caused by component errors which are random quantities with zero mean and distributed approximately according to the Gaussian Law (Ref. 7).
- (2) The trajectories which are in error differ only slightly from the standard, so that linear perturbation theory may be used to calculate deviations.

Let the column matrix δE be the values of the independent component random errors δe_j

$$\delta E = \begin{bmatrix} \delta e_1 \\ \delta e_2 \\ \vdots \\ \delta e_n \end{bmatrix}$$

The first-order sensitivity of the six injection coordinates X , R , V , Γ , W , and \dot{W} (Fig. 226) with respect to the

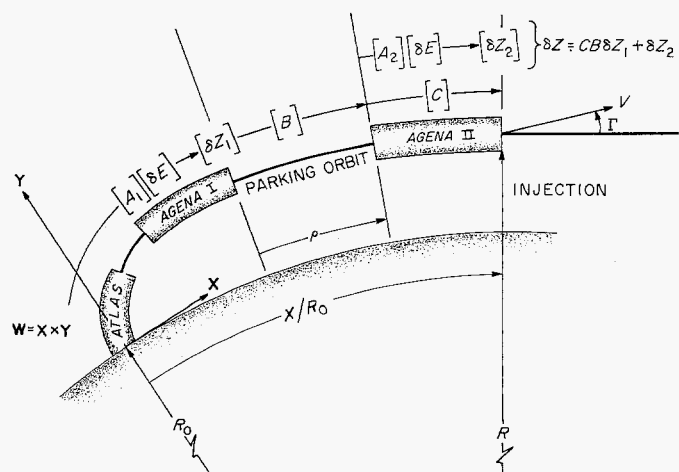


Fig. 226. Launch to injection

errors δe_j may be written in matrix form as

$$A = \begin{bmatrix} \frac{\partial X}{\partial e_1} & \frac{\partial X}{\partial e_2} & \dots & \frac{\partial X}{\partial e_n} \\ \frac{\partial R}{\partial e_1} & \frac{\partial R}{\partial e_2} & \dots & \frac{\partial R}{\partial e_n} \\ \dots & \dots & \dots & \dots \\ \frac{\partial \dot{W}}{\partial e_1} & \frac{\partial \dot{W}}{\partial e_2} & \dots & \frac{\partial \dot{W}}{\partial e_n} \end{bmatrix}$$

The δE -matrix and the A -matrix were obtained from Lockheed Missiles and Space Company. The first-order coordinate deviations at injection into the parking orbit (noted by subscript 1) are

$$\delta Z_1 = \begin{bmatrix} \delta X \\ \delta R \\ \delta V \\ \delta \Gamma \\ \delta \dot{W} \\ \delta \ddot{W} \end{bmatrix}_1 = A_1 \delta E$$

The injection coordinate errors due to the *Agena* second burn (noted by subscript 2) are assumed to be independent of the preceding errors and of the parking orbit duration; thus,

$$\delta Z_2 = A_2 \delta E$$

By mapping the errors at entry into the parking orbit through the parking orbit by the B -matrix

$$B = \begin{bmatrix} 1 & \frac{R_0}{R_1} (2 \sin \rho - 3 \rho) & \frac{R_0}{V_1} (4 \sin \rho - 3 \rho) & -2R_0 (1 - \cos \rho) & 0 & 0 \\ 0 & 2 - \cos \rho & \frac{2R_1}{V_1} (1 - \cos \rho) & R_1 \sin \rho & 0 & 0 \\ 0 & \frac{-V_1}{R_1} (1 - \cos \rho) & 2 \cos \rho - 1 & -V_1 \sin \rho & 0 & 0 \\ 0 & \frac{\sin \rho}{R_1} & \frac{2 \sin \rho}{V_1} & \cos \rho & 0 & 0 \\ 0 & 0 & 0 & 0 & \cos \rho & \frac{R_1}{V_1} \sin \rho \\ 0 & 0 & 0 & 0 & \frac{-V_1}{R_1} \sin \rho & \cos \rho \end{bmatrix}$$

and through the last burn by C ,

$$C = \begin{bmatrix} \frac{\partial X_2}{\partial X} & \frac{\partial X_2}{\partial R} & \frac{\partial X_2}{\partial V} & \frac{\partial X_2}{\partial \Gamma} & 0 & 0 \\ 0 & \frac{\partial R_2}{\partial R} & \frac{\partial R_2}{\partial V} & \frac{\partial R_2}{\partial \Gamma} & 0 & 0 \\ 0 & \frac{\partial V_2}{\partial R} & \frac{\partial V_2}{\partial V} & \frac{\partial V_2}{\partial \Gamma} & 0 & 0 \\ 0 & \frac{\partial \Gamma_2}{\partial R} & \frac{\partial \Gamma_2}{\partial V} & \frac{\partial \Gamma_2}{\partial \Gamma} & 0 & 0 \\ 0 & 0 & 0 & 0 & \frac{\partial \dot{W}_2}{\partial \dot{W}} & \frac{\partial \dot{W}_2}{\partial \ddot{W}} \\ 0 & 0 & 0 & 0 & \frac{\partial \ddot{W}_2}{\partial \dot{W}} & \frac{\partial \ddot{W}_2}{\partial \ddot{W}} \end{bmatrix}$$

the total injection coordinate deviations are obtained

$$\delta Z = (CBA_1 + A_2) \delta E$$

b. Statistical description of injection errors. Having obtained a set of injection deviations corresponding to the N different component random errors, one can form a covariance matrix of injection coordinates which statistically describes the injection errors. To do this, form the product

$$\delta Z \delta Z^T = (CBA_1 + A_2) \delta E \delta E^T (CBA_1 + A_2)^T$$

where δZ^T is the transpose of δZ . The ensemble average is now taken of all terms in the matrices.

$$\overline{\delta Z \delta Z^T} = (CBA_1 + A_2) \overline{\delta E \delta E^T} (CBA_1 + A_2)^T$$

or

$$\Lambda^I = (CBA_1 + A_2) \Lambda^E (CBA_1 + A_2)^T$$

when the $(n \times n)$ symmetric matrix $\overline{\delta E \delta E^T} (= \Lambda^E)$ is the covariance matrix of the independent error sources

$$\Lambda^E = \begin{bmatrix} \sigma_{e_1}^2 & 0 & 0 & 0 & \cdots \\ & \sigma_{e_2}^2 & 0 & 0 & \cdots \\ & & \sigma_{e_3}^2 & 0 & \cdots \\ & & \vdots & & \\ & & \cdots & \sigma_{e_{n-1}}^2 & 0 \\ & & & 0 & \sigma_{e_n}^2 \end{bmatrix}$$

and the covariance matrix of injection coordinate errors, Λ^I , is of the form

$$\Lambda^I = \begin{bmatrix} \sigma_X^2 & \rho_{XR}\sigma_X\sigma_R & \rho_{XY}\sigma_X\sigma_Y & \rho_{XT}\sigma_X\sigma_T & 0 & 0 \\ & \sigma_R^2 & \rho_{RY}\sigma_R\sigma_Y & \rho_{RT}\sigma_R\sigma_T & 0 & 0 \\ & & \sigma_Y^2 & \rho_{YT}\sigma_Y\sigma_T & 0 & 0 \\ & & & \sigma_T^2 & 0 & 0 \\ \text{(Symmetric)} & & & & \sigma_W^2 & \rho_{W\dot{W}}\sigma_W\sigma_{\dot{W}} \\ & & & & & \sigma_{\dot{W}}^2 \end{bmatrix}$$

c. Uncorrected miss components at Venus. A convenient system for expressing miss distances at Venus resulting from injection coordinate deviations is one which defines two components of a miss parameter \mathbf{B} and time of flight. \mathbf{B} is computed by integrating the trajectory to closest approach to the target and then finding, from the conditions at closest approach, the target centered conic on which the spacecraft would travel under only the influence of the target. \mathbf{B} is the position vector, in the plane of the conic, originating at the center of the target and directed perpendicularly to the incoming asymptote of the conic (Fig. 227). If \mathbf{S} is a unit vector in the direction of the incoming asymptote of the conic, \mathbf{T} a unit vector normal to \mathbf{S} , and $\mathbf{R} = \mathbf{S} \times \mathbf{T}$; then $\mathbf{B} \cdot \mathbf{T}$, $\mathbf{B} \cdot \mathbf{R}$, and flight time t_F define the three coordinates of miss.

A U -matrix is now defined, having elements which are first-order differential corrections of each of the miss components with respect to each of the coordinate dispersions at injection.

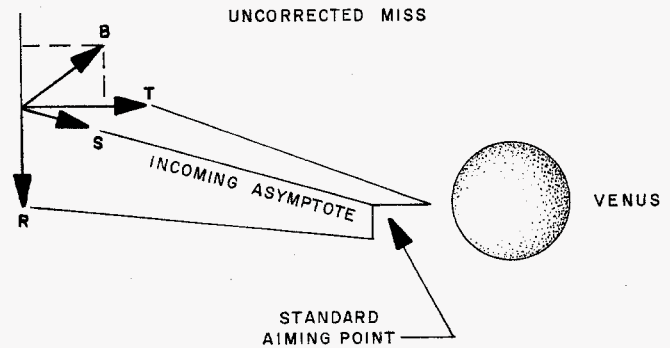


Fig. 227. Venus approach coordinates

$$U = \begin{bmatrix} \frac{\partial \mathbf{B} \cdot \mathbf{R}}{\partial X} & \frac{\partial \mathbf{B} \cdot \mathbf{R}}{\partial R} & \cdots & \frac{\partial \mathbf{B} \cdot \mathbf{R}}{\partial W} \\ \frac{\partial \mathbf{B} \cdot \mathbf{T}}{\partial X} & \frac{\partial \mathbf{B} \cdot \mathbf{T}}{\partial R} & \cdots & \frac{\partial \mathbf{B} \cdot \mathbf{T}}{\partial W} \\ \frac{\partial t_F}{\partial X} & \frac{\partial t_F}{\partial R} & \cdots & \frac{\partial t_F}{\partial W} \end{bmatrix}$$

When the covariance matrix Λ^I is multiplied by U and the transpose of U , a 3×3 covariance matrix of the uncorrected miss is obtained.

$$\Lambda^M = U \Lambda^I U^T = \begin{bmatrix} \sigma_R^2 & \rho_{RT}\sigma_R\sigma_T & \rho_{RT}\sigma_R\sigma_t \\ & \sigma_T^2 & \rho_{Tt}\sigma_T\sigma_t \\ \text{(Symmetric)} & & \sigma_t^2 \end{bmatrix}$$

Associated with covariance matrices are contours of constant probability density. For a two-dimensional covariance matrix, the contours are ellipses in the plane of the two coordinates. The semimajor and semiminor axes in the \mathbf{R} - \mathbf{T} plane are given by

$$\lambda_1, \lambda_2 = \left\{ \frac{\sigma_R^2 + \sigma_T^2}{2} \pm \left[\left(\frac{\sigma_R^2 - \sigma_T^2}{2} \right)^2 + \rho_{RT}^2 \sigma_R^2 \sigma_T^2 \right]^{1/2} \right\}^{1/2}$$

the probability of being within such an ellipse is 40%. Representative values for the axes of the 40% probability ellipses are given in Table 25.

d. Units of variance analysis for the midcourse maneuver. From the data given in Table 25, it is apparent that the accuracy of the *Atlas-Agena B* is such that a midcourse correction is needed to satisfy mission requirements. Hence, it is not realistic to specify the accuracy of the injection system in terms of the uncertainties in

Table 25. Representative 1- σ target miss for Mariner trajectories

Launch date	Parameter	Representative value
July 10, 1962	Semimajor axis	0.255×10^6 km
	Semiminor axis	0.345×10^5 km
	Time of flight	0.376×10^5 sec
September 15, 1962	Semimajor axis	0.851×10^5 km
	Semiminor axis	0.382×10^5 km
	Time of flight	0.183×10^5 sec

the individual injection coordinates. The injection accuracy must be specified in terms of the variance of the midcourse maneuver, because there are many combinations of injection errors that will map into the same magnitude of the midcourse correction.

The statistically averaged magnitude of the midcourse maneuver can be found once the covariance matrix of injection coordinate deviations, the time of the maneuver, and the sensitivity of target miss components with the maneuver are known. A units-of-variance analysis may then be performed to determine the relationship between the variance of the magnitude of the maneuver and the variances of the individual component errors.

A K-matrix is defined having elements which are first-order differential coefficients of each of the miss components with respect to mutually orthogonal midcourse velocity components, V_1 , V_2 and V_3 .

$$K = \begin{bmatrix} \frac{\partial \mathbf{B} \cdot \mathbf{R}}{\partial V_1} & \frac{\partial \mathbf{B} \cdot \mathbf{R}}{\partial V_2} & \frac{\partial \mathbf{B} \cdot \mathbf{R}}{\partial V_3} \\ \frac{\partial \mathbf{B} \cdot \mathbf{T}}{\partial V_1} & \frac{\partial \mathbf{B} \cdot \mathbf{T}}{\partial V_2} & \frac{\partial \mathbf{B} \cdot \mathbf{T}}{\partial V_3} \\ \frac{\partial t_F}{\partial V_1} & \frac{\partial t_F}{\partial V_2} & \frac{\partial t_F}{\partial V_3} \end{bmatrix}$$

The sensitivity coefficients of velocity components with the individual injection errors follow as

$$K^{-1}U(CBA_1 + A_2) = \begin{bmatrix} \frac{\partial V_1}{\partial e_1} & \frac{\partial V_1}{\partial e_2} & \dots & \frac{\partial V_1}{\partial e_n} \\ \frac{\partial V_2}{\partial e_1} & \frac{\partial V_2}{\partial e_2} & \dots & \frac{\partial V_2}{\partial e_n} \\ \frac{\partial V_3}{\partial e_1} & \frac{\partial V_3}{\partial e_2} & \dots & \frac{\partial V_3}{\partial e_n} \end{bmatrix}$$

from which the first-order sensitivity coefficients of the total velocity increment, P_j , can be found.

$$P_j = \left[\left(\frac{\partial V_1}{\partial e_j} \right)^2 + \left(\frac{\partial V_2}{\partial e_j} \right)^2 + \left(\frac{\partial V_3}{\partial e_j} \right)^2 \right]^{1/2}$$

Since the individual component errors are uncorrelated, the variance of the midcourse maneuver may be written as

$$\sigma_v^2 = \sum_{j=1}^N P_j^2 \sigma_{e_j}^2 \quad j = 1, 2, \dots, N$$

The number of units of variance of each component error UOV_j is defined as the percentage of the figure of merit FOM contributed by each component error, where the figure of merit can be thought of as a "design standard deviation."

$$UOV_j = \frac{100}{(FOM)^2} P_j^2 \sigma_{e_j}^2$$

An acceptable injection guidance system is one where

$$\sum_{j=1}^N UOV_j \leq 100$$

Representative values for the units of variance due to individual component errors were computed for the *Atlas-Agena*. The total units of variance figure was 80.40, based on a figure of merit of 15 m/sec.

2. Midcourse Guidance Analysis

Analysis of the maneuver. In designing the midcourse guidance system, it is assumed that the injection guidance system is accurate enough so that linear perturbation theory may be used with the preflight standard trajectory as the reference trajectory. This approximation is sufficiently accurate for engineering design of the system. In computing the maneuver during an actual flight, iterative schemes are used to refine the linear approximation.

The following terminal coordinates are used

$$(m_1, m_2, m_3) = (\Delta \mathbf{B} \cdot \mathbf{T}, \Delta \mathbf{B} \cdot \mathbf{R}, \Delta t_F)$$

where $\mathbf{B} \cdot \mathbf{T}$ and $\mathbf{B} \cdot \mathbf{R}$ are defined in the section on trajectories, t_F is flight time and Δ denotes the change from the desired value. Let $m^* = (m_1, m_2, m_3)$ be the estimate of the terminal errors from radio tracking data. Let $m^T = (m_1, m_2, m_3)$ be the perturbation in terminal coordi-

nates due to an impulse of thrust applied to the spacecraft. It is required that

$$m^* + m = 0$$

Two midcourse maneuver options are distinguished:

- (1) All three miss components, m_1^* , m_2^* , and m_3^* are nulled.
- (2) Only m_1^* and m_2^* are nulled, but the magnitude of the correcting velocity v is minimized.

Actually, it is desired to use option (1), but if the injection errors were abnormally large, it might be necessary to use option (2).

Let $v^T = (v_1, v_2, v_3)$ be a matrix of the three correcting velocity components.

Then

$$m = K_1 v$$

where K_1 is a (3×3) matrix with elements $\frac{\partial m_i}{\partial v_j}$. Thus, for option (1), the correcting velocity is given by

$$v = -K_1^{-1} m^*$$

For option (2), the correcting velocity is given by

$$v = -K_2^{-1} m^*$$

where $m^{*T} = (m_1^*, m_2^*, 0)$. The elements in the first two rows of K_2 are the same as those in K_1 . The elements in the third row of K_2 are obtained by taking the cross product of the first two rows. For a more detailed analysis, see Ref. 7.

Let Λ^M be the covariance matrix of injection errors mapped to the target. That is

$$\Lambda^M = \overline{mm^T}$$

For option (1) (neglecting small errors in orbit determination) the covariance matrix of correcting velocity components is

$$\overline{vv^T} = K_1^{-1} \Lambda^M (K_1^{-1})^T$$

Similarly, for option (2)

$$\overline{vv^T} = K_2^{-1} \Lambda^M (K_2^{-1})^T$$

The mean squared maneuver $\overline{v^2}$ is given by the trace of $\overline{vv^T}$

Table 26 lists four typical *Mariner R* trajectories and their dispersions, assuming no midcourse correction. The semimajor and semiminor axis of the 40% probability ellipse are obtained by taking the square root of the eigenvalues of the (2×2) partition of Λ^M which involves m_1 and m_2 . The rms time of flight error $(\Delta t_F^2)^{1/2}$ is the square root of the element in the third row and third column of Λ^M . The Λ^M matrix was obtained from an error analysis of the injection guidance system. Figure 228 shows the 99% dispersion ellipses and the desired aiming zone.

Table 27 shows the rms midcourse correction for both options. The nominal midcourse time is 7 days 18 hr after launch. This time was determined by two constraints: (1) the maneuver cannot occur until after Earth acquisition; and (2) the maneuver should occur as soon after Earth acquisition as possible in order to obtain strong telemetry signals during the maneuver.

Note from the results for trajectory I that the rms maneuver increases only slightly with application time. In fact, the rms maneuver varies approximately inversely as the time-to-go and thus is quite flat in this region. Note also from Table 27 that the maneuver requirements are roughly the same over the whole firing period, which is convenient from a design viewpoint. For the results shown here, the elements of the K matrix were determined by running perturbed trajectories on a digital computer.

It can be shown that, in order to correct for at least 99% of all possible injection errors, a correction capability V of 2.6 times the rms maneuver is required. Thus, a capability of about 40 m/sec is required for *Mariner R*. Actually, to be conservative, the midcourse propellant

Table 26. Trajectory characteristics and dispersions due to injection errors

Trajectory	Launch date	Time of flight, days	Semimajor axis km	Semiminor axis km	Days
I	July 10, 1962	149	0.2552×10^6	0.3458×10^5	0.436
II	August 1, 1962	131	0.2044×10^6	0.3843×10^5	0.364
III	August 28, 1962	108	0.1122×10^6	0.3252×10^5	0.273
IV	September 15, 1962	92	0.8514×10^5	0.3826×10^5	0.212

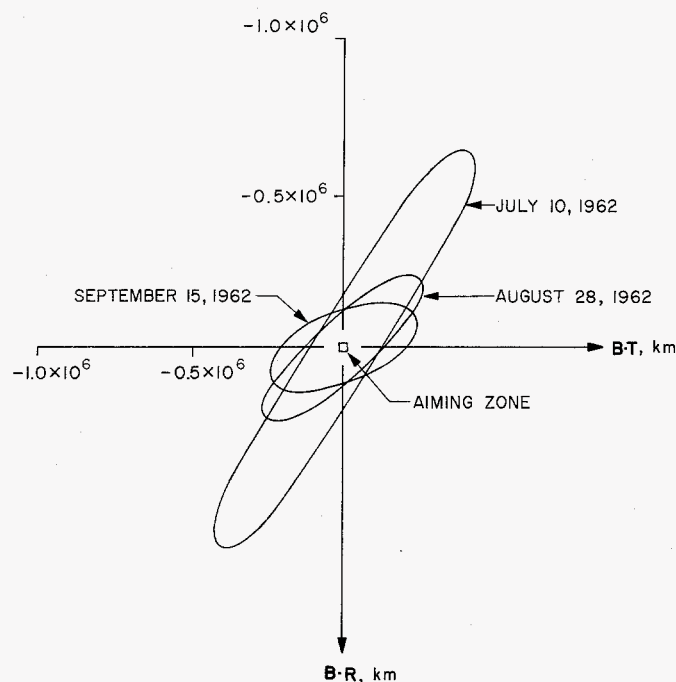


Fig. 228. 99% dispersion ellipses before midcourse

tanks are loaded to a capability of 61 m/sec, which is the maximum range of the counter for the digital accelerometer. Thus,

$$\frac{V}{g_{sp}} \times 100\% = \frac{61 \times 100}{9.8 \times 230} \% = 2.7\%$$

of spacecraft weight is required for midcourse fuel.

Given the correction capability V available in the spacecraft, it is useful to know the range of terminal errors which can be correction. For option (1)

$$v^T v = m^T (K^{-1})^T (K^{-1}) m$$

Setting $v^T v = V$, the equation defines a capability ellipsoid in m space. Figure 229 shows the capability ellipses for $V = 61$ m/sec and for the case in which flight time is not corrected. If the ellipse is centered at the actual aiming point, it will contain all coordinates which can be reached with the midcourse maneuver.

f. Error analysis

Four types of error exist in a midcourse guidance system:

- (1) In the execution of the commanded maneuver.
- (2) In the radio observations.

Table 27. Magnitude of the midcourse maneuver

Trajectory No.	Application time	RMS maneuver, m/sec	
		Option 1	Option 2
I	6 days 18 hr	12.6	14.0
I	7 days 18 hr	12.2	13.7
I	8 days 18 hr	12.3	13.8
II	7 days 18 hr	12.7	13.8
III	7 days 18 hr	11.3	12.1
IV	7 days 18 hr	13.8	15.4

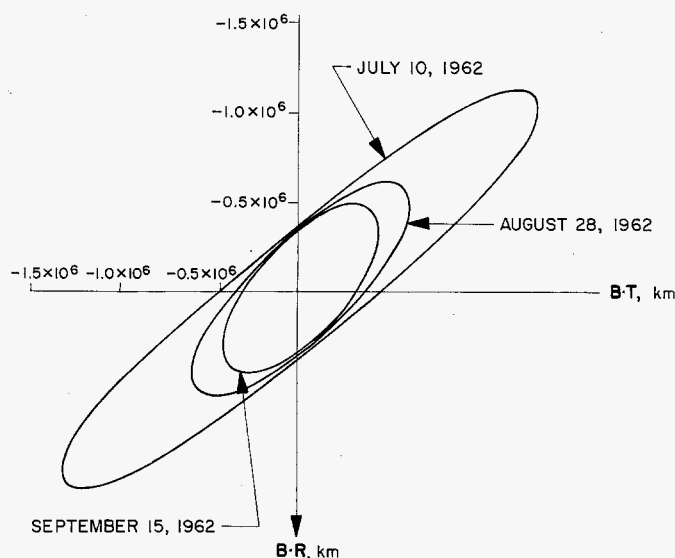


Fig. 229. Capability ellipses for $V = 61$ m/sec

- (3) Imperfections in the mathematical model used for trajectory computation.
- (4) Unpredictable disturbances occurring after the maneuver.

First, consider type 1 errors, which are called execution errors. Figure 230 shows the desired midcourse velocity increment v . Vector δw , extending from the tip of v , is the velocity error in executing v . The components of δw are δw_1 , δw_2 , δw_3 , where δw_3 is measured along v ; δw_2 is normal to v and parallel to the v_1, v_2 plane and δw_1 completes the orthogonal system. The δw vector depends on component errors in the midcourse system. For *Mariner R*, the main source of execution error is the pointing error, so that

$$\delta w^T = (\delta w_1, \delta w_2, \delta w_3) = (\alpha v, \beta v, 0)$$

where α and β are the pointing errors in radians. They result from gyro and attitude sensor errors.

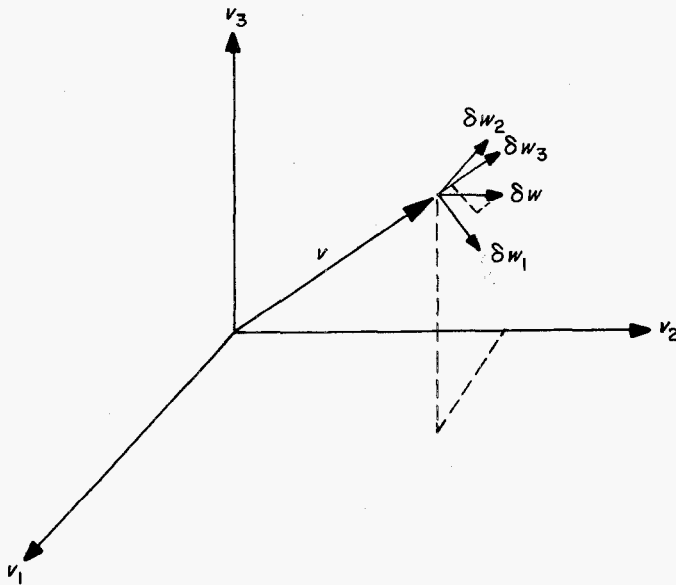


Fig. 230. Execution error components

The δw vector is transformed into the v system by means of the orthogonal transformation H :

$$\delta v = H \delta w$$

where $\delta v^T = (\delta v_1, \delta v_2, \delta v_3)$ are the transformed execution errors. The covariance matrix of execution errors is

$$\overline{\delta v \delta v^T} = \overline{H \delta w \delta w^T H^T}$$

Assuming that $\alpha^2 = \beta^2$ and that α and β are independent of each other and of v ; it can be shown that

$$\overline{\delta v \delta v^T} = \alpha^2 (\overline{v^2} I - \overline{v v^T})$$

where I is a (3×3) unit matrix. The covariance matrix of miss components due to execution errors is given by

$$\Lambda = K_1 \overline{\delta v \delta v^T} K_1^T$$

If option (2) is used, the maneuver itself causes a perturbation in the time of flight. The total error in time of flight is

$$\Delta t_F = m_3 - L m^*$$

where L is obtained by premultiplying K_2^{-1} by the third row of K_1 . The mean-squared time of flight error is

$$\overline{\Delta t_F^2} = \overline{m_3^2} - 2L \overline{m_3 m} + L \Lambda^M L^T$$

Table 28 shows the results of the execution error analysis. The pointing error is $(\alpha^2)^{1/2} = 24$ mrad. The column labeled rms miss is the square root of the trace of the partition of Λ which involves m_1 and m_2 only. For option (1), the rms flight time error is the square root of the

element in the third row and third column of Λ . For option (2), the rms flight time error is obtained from the above equation for Δt_F^2 .

Type 2 errors are caused by random noise in the radio tracking observations. This noise produces an error in the estimate of miss components m^* , which in turn causes an error in the computed maneuver. For *Mariner R*, two-way doppler and angles are measured by the DSIF, but the two-way doppler data have overwhelming power in determining the orbit. The random noise in the doppler data is about 0.05 m/sec and is uncorrelated at the sample rates employed. Using this noise magnitude and statistical estimation theory, one may compute the rms error in predicting the miss after 7 days of tracking. The results are strongly dependent on the amount of tracking data obtained near injection. A typical figure for the rms miss is 700 km.

Type 3 errors arise from uncertainties in physical constants such as: astronomical unit, gravitation constant of the Earth, tracking station locations, speed of light, etc. They also arise from uncertainties about the spacecraft such as: the area and reflectivity for computing the solar pressure effect, the translational acceleration caused by attitude control jets, etc. The total rms miss due to type 3 errors is estimated to be 1500 km.

An example of a type 4 error is the miss caused by corpuscular pressure if a solar storm should occur after the maneuver. Type 4 errors are assumed to be negligible.

Combining the three error sources, the total rms miss after the maneuver is about 8200 km.

g. Related analysis

Probability of obtaining radiometer data without a midcourse maneuver. It is possible that some failure may occur during the flight which would preclude the execution of a midcourse maneuver. Thus, it is useful to

Table 28. Midcourse execution errors

Trajectory	Application time	RMS miss km	RMS time of flight error, days	
			Option 1	Option 2
I	7 days 18 hr	7,960	0.0128	0.0345
II	7 days 18 hr	6,630	0.0119	0.0480
III	7 days 18 hr	4,230	0.0100	0.0560
IV	7 days 18 hr	3,820	0.0105	0.1060

determine the probability of obtaining radiometer data if there is no maneuver. In order to obtain radiometer data, two events must occur: (1) the spacecraft must pass through the desired aiming zone; and (2) the radiometer must be turned on.

The desired aiming zone is the circular sector defined in the section on trajectories. In order to conserve attitude control gas, the radiometer is activated 10 hr before the nominal encounter time by stored command from the CC&S. The second column in Table 29 shows the probability of passing through the desired aiming zone when there is no maneuver. This probability is computed by integrating the distribution of m_1 , m_2 (with covariance Λ^M) over the desired area. The third column shows the mean value of the time-of-flight error given that the spacecraft passes through the desired zone. The fourth column shows the standard deviation about the mean flight time.

From Table 29, it is evident that the probability of passing through the desired area and not having the radiometer on is negligible. Thus, the probability of obtaining radiometer measurements without utilizing a midcourse maneuver is approximately the same as the second column. It is also evident that a maneuver is required to ensure reasonable probability of success.

Agena retro-maneuver. In order to prevent biological contamination of Venus, it is desired that the probability of either the spacecraft or the *Agena* impacting the planet be less than 0.001. In order to ensure that the spacecraft does not hit Venus, it is necessary to choose an aiming point which is sufficiently far away from the planet. Assuming an rms miss of 8000 km after midcourse, it can be shown that, for the nominal aiming point ($B = 30,000$ km), the probability of impact is quite small (typically 0.0002). Thus, assuming that the maneuver is fairly reliable, the impact probability requirement is satisfied for the spacecraft.

Table 29. Probability of obtaining radiometer data without a midcourse maneuver

Trajectory	Probability of arriving in desired sector percent	Mean time of flight error hr	Standard deviation in time of flight error hr
I	5.3	0.83	0.99
II	6.1	0.80	1.2
III	12.3	0.91	1.3
IV	14.0	0.85	2.1

The probability of *Agena* impact may be computed assuming that m_1 and m_2 are normal with covariance matrix Λ^M . It is found that the impact probability varies from 0.007 at the beginning of the firing period to 0.020 at the end of the period. Thus, it is necessary to move the *Agena* aiming point farther away from the target. This can be accomplished in either of two ways:

- (1) Bias the injection conditions and correct the spacecraft trajectory by means of a standard midcourse maneuver.
- (2) Apply a retro-thrust to the *Agena* after spacecraft separation.

Method 1 was rejected because it reduced the probability of success if the midcourse maneuver could not be performed due to some failure. Method 2 had the additional advantage that it reduced the possibility that the Earth sensor might lock onto the *Agena*.

Statistical analyses show that the *Agena* aiming point must be moved about 200,000 km away from the planet in order to achieve the desired probability level. From linear perturbation analysis, it is determined that a retro-impulse of about 5 m/sec is adequate. The *Ranger* spacecraft uses solid retro-rockets, but *Mariner* uses a different scheme, in order to save weight. After injection, the leftover oxidizer and propellant is vented through separate nozzles to provide the required impulse. The thrust curve due to venting is supplied by Lockheed Missiles and Space Company and is used in the JPL powered-flight trajectory program to compute the change in miss. With this retro-maneuver, the probability of impact is 0.0005 at the beginning of the firing period and 0.001 at the end.

For fear of contaminating the spacecraft with vented propellant and oxidizer, the yaw angle for the retro-maneuver has been changed from 180 to 140 deg, causing the probability of *Agena* impacting the planet to increase to 0.0006 at the beginning of the firing period and 0.004 at the end. In between these periods, the probability is quite low, because there is a larger amount of fuel left over.

3. Midcourse Guidance Operations

a. Description of operations program. The primary function of the midcourse maneuver operations program is to formulate the three stored commands and one real-time command required to achieve standard operation

with the midcourse maneuver. The three stored commands, when transmitted to the spacecraft, are stored in the memory of the CC&S prior to performance of the maneuver. The one real-time command initiates the maneuver sequence.

If optimum utilization of spacecraft resources for this function will not permit achievement of standard operation, the program has the capability to determine the feasibility of certain nonstandard modes of operation. In this event, decisions as to which mode shall be adopted will be made and executed by the Space Flight Test Director during flight, subject to the approval of the Project Manager.

b. Sequence of guidance operations. The sequence of events in computing and executing the midcourse maneuver is as follows:

- (1) The spacecraft is tracked from launch. On about the seventh day of flight, a definitive orbit determination is made.
- (2) The midcourse velocity impulse required to modify the trajectory of the spacecraft so that it flies by Venus in an acceptable way at a favorable time is computed. Certain constraints must be satisfied:
 - (a) The velocity impulse delivered cannot exceed the maximum value set by the amount of propellant available.
 - (b) The terminal phase must occur in view of a DSIF station with the capability for recovering the scientific data during the encounter sequence.

If a maneuver which modifies the best-fit orbit so that it passes through the optimum aiming point with an acceptable time of flight cannot be found, a failure situation exists. If the spacecraft is operating properly and is following a trajectory which takes it sufficiently close to Venus, an attempt will be made to determine a midcourse maneuver which places the spacecraft on the most advantageous trajectory available. The trajectory evaluation features of the guidance operations program enable the operations personnel to choose a revised aiming point intelligently. Once a suitable aiming point has been chosen, the midcourse maneuver is computed.

- (3) The vector impulse is converted to the appropriate coordinates: roll-turn angle, pitch-turn angle, and

magnitude of impulse. The two angles and magnitude are then converted to the binary-coded form acceptable to the spacecraft.

- (4) The three stored commands (ROLL SC-1, PITCH SC-2, MAGNITUDE SC-3) are transmitted, properly coded, to the appropriate DSIF station (nominally Goldstone), where the command operator checks them and sends them to the spacecraft, using the Read-Write-Verify system. The spacecraft stores the commands in registers in the CC&S.
- (5) RTC-6, the real-time EXECUTE MIDCOURSE MANEUVER command, is transmitted.
- (6) The roll and pitch turns are executed by the spacecraft.
- (7) The midcourse motor is ignited and burns until the required velocity impulse is measured by the accelerometer and integrator. Digital output from the integrator counts down the register containing SC-3 each time an increment of 0.03 m/sec in the velocity is sensed.
- (8) After completing the maneuver, the spacecraft returns to the cruise mode, orienting itself by means of Sun and Earth sensors.

c. Considerations determining the optimum midcourse maneuver. A large number of constraints and experimental requirements affect the choice of an optimum trajectory for a particular operational situation. The nominal aiming point was, of course, chosen to satisfy all the constraints in an optimum way. The various requirements will be listed only briefly.

Experimental requirements. Three experiments impose special requirements on the trajectory.

- (1) *Radiometer experiment.* The radiometer experiment imposes the following restrictions:

- (a) When the spacecraft passes through the plane (hereafter called the Venus terminator plane) which contains the center of Venus and is normal to the Venus-Sun line, the planet must subtend an angle which is greater than 10 deg, else the spacecraft may be too far from the planet to obtain useful radiometer data.
- (b) When the spacecraft passes through the Venus terminator plane, the planet must subtend an angle which is less than 45 deg, else a complete scan cycle of the planet may not be completed.

- (c) When the spacecraft passes through the Venus terminator plane, the angle subtended at the spacecraft between a line parallel to the Earth-probe-Sun plane and the far limb of Venus must not exceed 60 deg. This is an absolute constraint imposed by mechanical limitations on the radiometer scan device.
- (2) *Infrared experiment.* The infrared experiment imposes the same constraints as the radiometer experiment.
- (3) *Magnetometer experiment.* The magnetometer experiment imposes no absolute constraints; however, it is desired to approach as close to the planet as possible.

Engineering subsystem requirements. Several hardware constraints are imposed by the various subsystems:

- (1) *Attitude control.* The following restrictions are imposed by the attitude control system:

- (a) The angular separation between the limbs of Venus and the Earth should be greater than 30 deg until after the completion of the encounter sequence.
- (b) The angular separation between the limbs of Venus and the Sun should be greater than 6 deg until the completion of the Venus encounter sequence.

- (2) *Communications.* The following restrictions are imposed by the communications requirements:

- (a) The orientation of the spacecraft during the midcourse maneuver should permit the transmission of telemetry over the low-gain antenna, if at all possible.
- (b) The high-gain antenna must be pointed at the Earth during the encounter sequence while the data-taking is in progress.
- (c) The midcourse maneuver must be performed while the spacecraft is over a DSIF station with command capability.
- (d) The encounter sequence must take place during a Goldstone view period.

- (3) *Propulsion.* The midcourse impulse cannot exceed the maximum provided. The satisfaction of all these constraints is guaranteed if the spacecraft passes near the nominal aiming point. If it is not possible to reach the nominal aiming point, a revised aiming point must be chosen during the operation, once the operational situation is understood.

Inputs. The input to the operations program has been divided into three classifications:

- (1) *Input from tracking program.* The basic inputs from the tracking program are the best estimates of the six injection coordinates and the injection time.

- (2) *Prelaunch input.* The prelaunch input consists in general of items which can be considered constants of the spacecraft system and thus not subject to variation during changing or unexpected operating conditions.

- (3) *Postlaunch input.* Items in the postlaunch input fall into two classifications: (a) items which are subject to change during changing or unexpected operating conditions; and (b) control commands for the program.

During the operation, the tracking program input will be entered on-line, the prelaunch input will be entered off-line, and the postlaunch input will be entered on-line. The capability to change one or more prelaunch input items on-line has been provided.

d. Functional blocks. Figure 231 is a functional block diagram of the *Mariner R* maneuver operations program. There are seven independent blocks, all of which utilize the JPL lunar and interplanetary trajectory program.

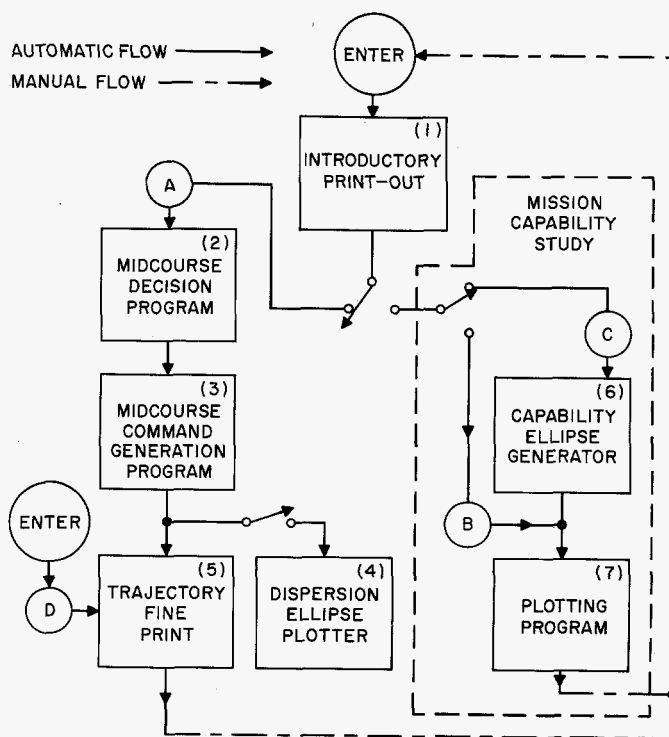


Fig. 231. Maneuver operation program, functional block diagram

Functional blocks 1, 2, 3, and 5 are required for both standard operation (i.e., it is possible to put the spacecraft on a trajectory which passes near the nominal aiming point at a satisfactory time), and nonstandard operation (i.e., it is *not* possible to put the spacecraft on a trajectory which passes near the nominal aiming point at a satisfactory time). Functional blocks 4, 6, and 7 have been designed to assist in making operational decisions during nonstandard operating conditions.

Midcourse maneuver program introductory printout. The information required on the introductory printout describes the quality of the orbit determination and gives an initial estimate of the quality of the orbit obtained. All input quantities from the orbit determination program will be included in the introductory printout. The trajectory program will be utilized to obtain an initial estimate of the miss distance and time-of-flight error that exist between the best-fit trajectory and the nominal aiming point.

Midcourse decision program. The purpose of the midcourse decision program is to calculate the midcourse maneuver subject to various constraints. The constraints which are evaluated are: (1) the propulsion constraint; (2) the time-of-flight constraint; and (3) the omnidirectional antenna constraint (if one exists). The propulsion constraint and the time-of-flight constraint are absolute. If it is not possible to reach the $B \cdot R$, $B \cdot T$ location requested without violating an absolute constraint, then the midcourse decision program will print a simple statement to this effect and wait for an on-line instruction to proceed with the mission capability study. If it is possible to reach the location requested without violating an absolute constraint, the output of the midcourse decision program will be fed directly to the midcourse command generation program. If the midcourse maneuver violates an omni-antenna constraint, some of the telemetry data during the midcourse maneuver will be lost.

The output from the midcourse decision program falls into three groups. The first group specifies the trajectory conditions (i.e., position, velocity, and time) at which the midcourse rocket motor ignites. The second group consists of a set of brief statements which will be printed-out if called for by the decision sequence which formulates the midcourse maneuver. The third group contains detailed numerical information related to the test for the antenna constraint, if one exists and has been violated.

Midcourse command generation program. The command generation program converts the velocity vector correction determined in the midcourse decision program into a roll turn, a pitch turn, and a velocity magnitude, expressed in binary form and adjusted to a form which is usable by the CC&S. The commands will be punched out on cards on command for input to the card-to-teletype tape machine. The midcourse command generation program will also calculate a noise moment matrix of midcourse injection errors and do a complete trajectory error analysis. The midcourse command generation program is followed by the flyby fine-print program and the dispersion ellipse plotter.

Maneuver dispersion ellipses. A set of dispersion ellipses will be computed from the covariance matrix of errors in the orbit and the execution of the maneuver mapped to the target. These ellipses will be plotted to the same scale that is used in the plots of the general constraints.

Fly-by trajectory fine-print program. The purpose of the flyby fine-print program is to obtain a special print-out on individual trajectories which will provide the capability to choose a trajectory intelligently in both standard and non-standard situations. The print-out is obtained by running the trajectory program from the midcourse point past closest approach. Many additional calculations are performed that are not now provided for in the trajectory program.

Capability ellipse generator. The capability ellipse generator will generate the maximum capability ellipse in the R, T plane, assuming that maximum maneuvers are applied in the critical plane. This is the first of two programs that will be used in a mission capability study during the flight.

Plotting program. The plotting program aids in the evaluation of various spacecraft and trajectory constraints as they pertain to various areas of interest in the R, T plane. This program has been developed primarily as an aid in selecting new aiming points in nonstandard situations.

e. Operational use of the program. The various functional blocks described above are combined to form four operational options, as follows:

- (1) Operational Option A: midcourse maneuver program.
- (2) Operational Option B: mission capability study.

UNCLASSIFIED

- (3) Operational Option C: spacecraft and trajectory constraint evaluation.
- (4) Operational Option D: flyby fine-print.

In general, all operational options will be used before the midcourse maneuver to select the midcourse maneuver. Operational Option D will be used after the midcourse maneuver to monitor the trajectory obtained.

All four operational options require access to the pre-launch input, and the input from the tracking program. Each option requires the trajectory program.

In Fig. 231, the functional block diagram of the maneuver operations program, the dashed lines in the diagram represent manual flow, and the solid lines indicate programmed connection of the functional blocks that are used in the various operational options. The starting points for the various operational options are indicated.

Operational Option A, the midcourse maneuver program, is the only option that has the capability of computing a maneuver. The postlaunch input provides a considerable amount of flexibility. The following alternatives are provided:

- (1) Specify the aiming point in **B • R, B • T** coordinates and time to closest approach or in rectangular coordinates in the Venus terminator plane and time to closest approach.
- (2) Proceed with the mission capability study, if necessary, or do not proceed with the mission capability study.
- (3) Attitude control normal or Earth-finder locked on the Moon, Venus, or Jupiter.
- (4) Punch-out command cards or do not punch-out command cards.
- (5) Plot or do not plot dispersion ellipses.
- (6) Continue or do not continue with the flyby fine-print program.

Operational Option B, the mission capability study, will be used to evaluate the effects of the various spacecraft and trajectory constraints on trajectories which are within the propulsion capability of the system. The output from the capability ellipse generator is fed directly

into the plotting program. These two programs constitute the mission capability study section of the operations program being requested.

Operational Option C, spacecraft and trajectory constraint evaluation, is used to evaluate the suitability of various areas in the *R, T* plane as potential aiming points.

Operational Option D, the flyby fine-print, will aid in the final decision on the midcourse maneuver and will be used to monitor the trajectory obtained following the midcourse maneuver.

D. Orbit Determination

1. Orbit Determination Operations

The *Mariner R* orbit determination operations center around two digital programs, the tracking data editing program, and the orbit determination program. The relationship of these two programs with respect to each other and to their inputs and outputs is depicted schematically in Fig. 232.

The TDEP functions as a service program to the ODP. Its principal function is to speed up the ODP. In line with this objective, the TDEP:

- (1) Removes blunder points from tracking data.
- (2) Uses data compression methods to reduce the amount of data the ODP must process.
- (3) Reduces tracking data from different sources to a uniform format for the ODP.
- (4) Compiles auxiliary data which the ODP needs to utilize the tracking data.

The TDEP can be pictured as an elaborate bookkeeping program. It accepts as inputs the tracking data, portions of the station reports, and control cards which allow the operator certain options on how the data are to be handled. Aside from the use of the control cards, the editing of the TDEP is currently limited to automatically removing blunder points caused by such things as tele-

UNCLASSIFIED

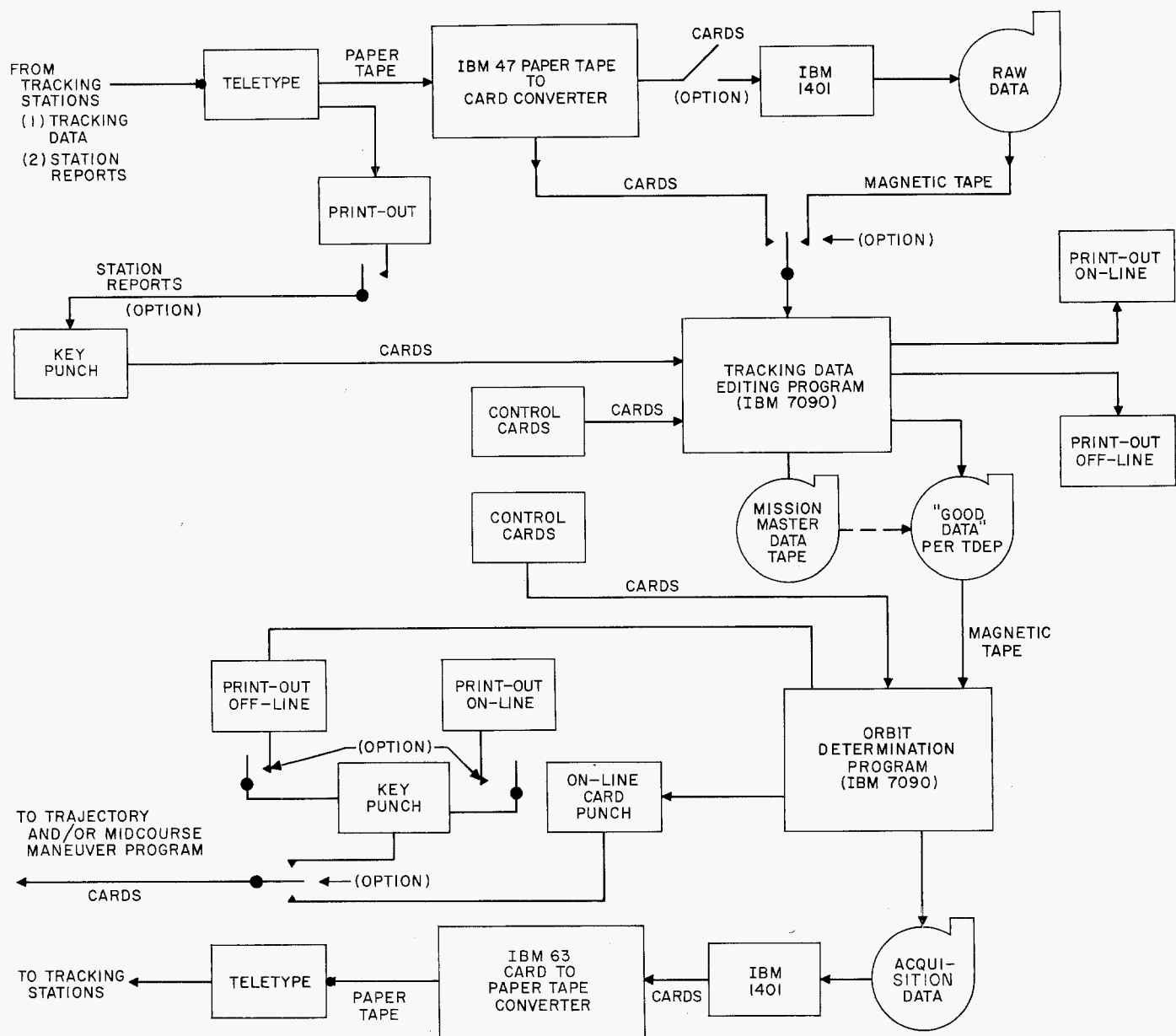


Fig. 232. Orbit determination, operations schematic diagram

type transmission errors when unrecognizable characters occur or certain quantities exceed physical limits. This editing is most important during the early phase of the mission due to the relatively small amount of data available. At this stage, such gross blunders will have a strong effect on the least-squares solution to the orbit as determined by the ODP.

A significant difference between the *RA-4* and *Mariner R* TDEP's is the addition of data compression schemes. The quantity of data gathered between epochs for *Mariner R* will be an order of magnitude greater than for

Ranger missions. This would translate into about 3 hr per iteration near the end of an epoch without data compression. With data compression, plus the fact that the *Mariner* ODP runs three times faster than the *Ranger* ODP for large quantities of data, hopefully, iteration times can be kept under 30 min.

All tracking data must be converted into a data type which the ODP is equipped to handle. As an example, the ODP assumes that all counted doppler is labeled with the time at the center of the count interval. This means that all DSIF counted doppler data which are tagged with

UNCLASSIFIED

JPL TECHNICAL REPORT NO. 32-353

the time at the end of the count must be "re-time tagged" by the TDEP. In addition, the ODP needs to know such things as the sample time, count time, which station is transmitting, and what the transmitter frequency is. The TDEP compiles all this information from the tracking data messages, station messages, and/or control card inputs and either labels the appropriate tracking data or passes on this information to the ODP in tabular form.

The TDEP provides both on-line and off-line print-out for a visual record of what the state of the data is, how much was discarded and why, and what systems the operator selected. In addition, it compiles a mission master data tape which includes all tracking data that may contain useful data. That is, this master data tape includes certain data which currently is considered "bad" but which the operation may still want to use on option. A separate data tape (which contains a subset of the data from the mission master tape) is prepared as an input tape to the ODP. This data tape contains only "good" data which the operator has selected to determine the orbit.

The ODP accepts this data tape from the TDEP and proceeds to determine the orbit using the trajectory program (DBH07) in subroutine form as a model for a least-squares solution. A $3\text{-}\sigma$ rejection scheme, as an option, allows the ODP to statistically edit the input tape from the TDEP and to construct its own "good data" records for future use.

The output of the ODP includes acquisition data for the tracking stations which is sent out via teletype, cards punched on-line which are used as inputs to the mid-course maneuver program, and print-out (off- and on-line) which describes the characteristics of the predicted spacecraft trajectory.

2. Evolution of the Mariner R TDEP

The *Mariner R* tracking data editing program contains the basic features of the *Ranger* TDEP, and the items mentioned in the preceding section. The more significant of the additional capabilities include the ability to handle continuous count doppler and two new data types.

Continuous count (i.e., non-destruct cycle count) doppler has two advantages over destruct count doppler:

- (1) It is well suited to data compression schemes which can result in a significant reduction in computer running time.

- (2) The round-off error, which is inversely proportional to count time, can be reduced. This is particularly true for the Mobile Tracking Station, which can only use a 1-sec count time for destruct cycle count doppler.

The two new data types are constructed by differencing already existing doppler data types. This differencing technique is designed to reduce the effect of error sources common to the primary data types. The two differenced doppler data types constructed by the *Mariner R* TDEP are:

- (1) *Differenced one way*: One-way doppler from one receiver is subtracted from that simultaneously received at another receiver.
- (2) *Differenced two way*: This data type is presently only obtainable from the Goldstone complex. It is constructed by subtracting coherent two-way doppler received at DSIF 3 from the pseudo-coherent two-way doppler simultaneously received at DSIF 2. (Note: For both primary data types, DSIF 3 is the transmitter.)

During the evolution from the *Ranger* TDEP to the *Mariner R* concept, the general philosophy was to make the TDEP as automatic as possible, but at the same time, provide a manual override at every conceivable point in the program where the operator can improve the situation, based on knowledge not available to the program. By option, the on-line print-out can contain sufficient information to define nonstandard conditions for the operator. However, an attempt has been made to anticipate logical inconsistencies that may confront the TDEP. In each case where practical, the TDEP is provided with a course of action which allows it to continue. Each inconsistency is documented by the off-line print-out (on-line by option) and these comments are complete to the extent that a running time history is available for post-flight analysis.

3. Evolution of the Mariner R ODP

The development of the *Mariner R* orbit determination program has proceeded as a modification of the existing orbit determination program for *Ranger*. In the area of numerical computation, the advantages inherent in the current JPL trajectory program (DBH07) have significantly influenced the organization of the orbit determination program. However, a description of these numerical modifications is discussed elsewhere in this report and only the theoretical aspects of the program are considered here.

UNCLASSIFIED

Three areas of study have resulted in new formulas for the computer program:

- (1) An examination of the statistical estimation formula for a set of orbital parameters.
- (2) The development of error expressions that provide a reasonably realistic error description.
- (3) Construction of a data-weighting scheme.

In the first area, certain physical constants that influence both the trajectory and the data have been included as additional parameters, and the dimension of the parameter space has increased from six, the number representing the six initial conditions for the equations of motion, to some number representing the total number of orbital parameters and physical constants. Also, the estimation formula has been modified to include *a priori* information which makes it possible to process the data in discrete blocks. In other words, in estimating parameters from one block of data, the estimate of the parameters from all preceding blocks is used to influence the new estimate of the orbit. An error description of the *a priori* estimate is required to properly weight the old estimate of the orbital parameters and physical constants. In fact, it is this requirement that has motivated the second area of study.

The error descriptions for the *Mariner* program differ from *Ranger* in that the effect of physical constants are included as error sources. Thus, a recognition of the overly optimistic results obtained from simply using the inverse of the normal matrix in the least-squares procedure is accepted, and the error matrix is degraded by including the errors introduced by physical constants that are not estimated along with the orbital parameters. Also, the capability of mapping these error matrices to other points in the trajectory is included, with a consideration of the integrated effect of physical constants on the position and velocity coordinate description. This capability is required for two reasons. First, there is a general interest in the knowledge of the position and velocity of the probe at various points in its orbit. For example, at a point where a midcourse maneuver is performed, the knowledge of the orbit influences the maneuver (see Section XC on midcourse maneuver).

Second, for numerical reasons, the reference point for the trajectory (i.e., the epoch) should be located near the data under consideration. In a long trajectory such as *Mariner* flies, this involves periodically forwarding the

epoch and, as mentioned earlier, if previous information about the orbit is used in solving for the parameters from the new data, then the error matrix on those parameters is required. In addition to the physical constant degradation in this error matrix, formulas for including unknown systematic errors are included so that, for example, one can examine the contribution to the total parameter error matrix from an unknown bias in one data type from a station.

The third area of study was performed because the estimate of the parameters can be heavily affected by the weighting of the data. Because of the large amount of data, the estimation procedure is limited to a weighted least-squares. Correlations in the data are known and can be represented mathematically. Thus, an estimator other than that of weighted least-squares (a minimum variance estimator) would theoretically yield a better estimate. However, the program as constructed makes use of the known correlations by adjusting the data weights in such a way that the estimate and its error matrix either agree quite well with the minimum variance estimator, or else give a more pessimistic description of the error. Therefore, information about the orbit tends to be conservative instead of overly optimistic as, for example, in the application of uniform weighting.

It was the recognition that the *Ranger* program would yield highly unrealistic statistical results about an orbit of the *Mariner* type that led to the development of the present program. In addition, numerical problems that would cause considerable concern in the *Mariner* mission have been removed, and the capability of perhaps obtaining information about constants of the solar system has been added.

4. Tracking Analysis Accuracy Studies

The quality of the estimate of the premaneuver orbit estimate is judged by the miss at Venus caused by the covariance of the estimate. That is, the net effect is a product of two factors, the covariance of the estimate of the near-Earth orbital parameters, and the subsequent mapping of these parameters into miss coordinates at the planet. These two factors are *separable*:

- (1) *Earth-centered orbit estimate.* It has been found that all information known about an Earth-centered orbit, for purposes of estimating its effects at Venus, can be described by a covariance

UNCLASSIFIED

JPL TECHNICAL REPORT NO. 32-353

matrix of the velocity-at-infinity vector, described for example by its magnitude, right ascension, and declination. Thus, a six- or greater dimensional problem for mission purposes can be reduced to a three-dimensional problem. Even such factors as Earth's mass and station location covariances can be incorporated in the three-dimensional estimate.

- (2) *Mapping of estimate.* It was found for the *Mariner* mission that the mapping of perturbations in the Earth-centered velocity-at-infinity vector depended heavily on the launch day. Time-of-flight and target-approach geometry produced a 6-to-1 variation in effects at the target from mid-July to mid-September.

UNCLASSIFIED

XI. Launch Restraints

A. Introduction

In March 1962, a study was begun of the many effects influencing the utilization of the available launch period and launch window for the *Mariner R* missions. This study sought to identify those items which had direct bearing on the attempt to launch two spacecraft to Venus in summer 1962, and to provide information to the Project Manager which would assist him in making decisions relative to the utilization of the launch period and committing the entire system to launch. It was desirable that this information also be of such nature as to provide high confidence of no loopholes existing in the coordinated plans and capabilities of the many operations necessary for a successful launching.

Many factors involved in the *Mariner R* launches had never been encountered before in any of the AMR programs. Since Venus is in a favorable position only briefly each 19 mo, long delays in launching the spacecraft after the period opened could not be tolerated. This fact was

further complicated by the desire to launch two spacecraft to Venus in 1962. The launch period (the number of days on which a launch is possible) and the launch window (the number of minutes a day when a launch is possible) limit the attempts to launch a spacecraft. Efficient use of these days and minutes was a necessity realized by all the agencies involved. This Section summarizes those items which might influence the capability to launch the two spacecraft within the required time intervals.

In many respects, this information was limited in those areas where JPL has only superficial knowledge of the details of the many systems involved with the launch. The information was obtained from various sources: letters, reports from Flight Test Working Group meetings, project status meetings, program requirements documents, program support documents, and personal contacts. Those areas directly involving the spacecraft were explored in most detail, and, consequently, more of those items are included in this summary.

UNCLASSIFIED

JPL TECHNICAL REPORT NO. 32-353

B. Atlas Booster Vehicle

The Jet Propulsion Laboratory was concerned that many time-consuming tests might have to be performed on the *Atlas* booster should the launch be delayed for some time after the initial date for which the final booster flight-acceptance composite tests were completed. It was reported by General Dynamics/Astronautics that, following the final acceptance of the booster prior to the first launch day, the *Atlas* could support a launch on any day of the launch period, assuming that malfunctions which caused cancellation of any previous launch attempt were not attributable to the *Atlas*. Although no further testing would necessarily be required on the *Atlas* which would cause loss of days in the period, an additional period of flight-acceptance testing would be desirable if other causes make it necessary to recycle the countdown for a long period of time. This procedure would essentially buy more insurance in the *Atlas* at the expense of some other systems.

To get maximum use of the launch period, it is desirable to attempt a launch every day until a countdown is successfully completed, although such an operation also carries with it the implication of a decreasing confidence of getting high reliability in the launch attempt. The *Atlas* crews must conduct extensive countdowns prior to the time when the spacecraft picks up the count and, in the case of a "scrub," much work is required to get the vehicle in a condition suitable for resuming the count the next day. The Air Force claims the fatigue of the crew has a direct bearing on the reliability of the launch and recommends that after every scrub a day of rest be provided for the crew. This procedure would put a handicap on the total utilization of the launch period, and, realizing that the crews had conducted countdowns on successive days for the lunar launch attempts, it was thought that such arrangements could probably be made again if the situation warranted.

All available minutes of the launch window should be usable and not be limited by equipment capabilities. *Ranger* shots have had a limitation on them because of the *Atlas*, and it was feared that this restriction would prevent the *Mariner* from fully utilizing the launch window. The constraint was the supply of liquid oxygen available for LOX topping to replace that LOX boiled off after the tank was almost full, just before liftoff. Continued holds required usage of the LOX-topping supply. *Ranger* launch windows were limited to about 85 min because of this problem.

Further investigation and tests were conducted to determine more accurately how long LOX-topping could continue to support a launch window of about 2 hr. Results of this analysis showed that LOX-topping could be maintained for at least 150 min, indicating that the LOX-topping supply should not be a problem to *Mariner R* launch attempts.

One significant event exists in the *Atlas* countdown procedure which could cause a cancellation for the day: the progression of the countdown beyond T-4 sec. After that time, the vernier engine will have ignited and cannot be prepared for another ignition in time to support another launch attempt that day.

Certain *Atlas* subsystem checks are performed regularly and batteries must be replaced periodically if no launch occurs. These checks do not require periods in excess of several hours and can be performed on a noninterference basis with launch attempts.

C. Agena B Second Stage

Various features of the *Agena B* design affect the utilization of the launch period and, in some cases, even the launch window. Requirements for performance of revalidation tests exist which necessitate that the *Agena* be demated from the *Atlas* and returned to the missile assembly building for a period of days. As with the *Atlas*, there are some checks and parts replacements which can be performed while the *Agena* is in the gantry.

The three major revalidation tests which must be performed involve the telemetry system, the propulsion system, and the guidance and flight control system. Different intervals of validation time are involved with each of these tests, necessitating the choice of a launch date much in advance so the various tests may be performed at a time which essentially maximizes the number of possible launch attempt possibilities prior to the expiration of the validation period. The requirement for these tests has a vast potential effect on the utilization of the launch period.

The *Agena* telemetry system must be revalidated every 45 days. Operationally, it is desirable to perform this test early and then have the 45th day occur near the last possible day of launch. A complete engine functional test

UNCLASSIFIED

must be performed no more than 25 days following the previous test, and 15 days after the propellant loading occurs. This test is normally performed 5 or 6 days prior to the initial launch date. Guidance and flight control system checks are performed at the time the engine functional tests are performed. These checks are valid for 17 days and consist of exercising of the hydraulic actuators and pneumatic control valves to verify the integrity of the *Agena* to control the thrust vector in flight.

It is evident that once a date for the initial launch attempt is chosen, the propulsion system and control system tests can be scheduled. Then, the last day a launch should safely be attempted can be ascertained. This date of the final launch attempt prior to repeating the validation test is negotiable at the time and therefore, any decisions made in advance of that time are subject to change. At any rate, assuming the above date and the expiration of the flight and control system validation period as firm, the time for the telemetry subsystem calibration and validation checks can be established.

Other tests are required also, but some can be performed on a schedule dictated by the above revalidation requirements and some while the *Agena* is mated to the *Atlas*, on a noninterference basis with the countdown on any particular day. Examples of this type are checks of the propellant relief valves on the helium pressurization package, which must be checked every 3 days after fueling, and the propellant umbilical couplings, which must be performed every 6 days after fueling.

One troublesome feature since the early *Ranger* missions has been the *Agena* horizon sensor. Pitch and roll control are derived from the device. The geometry of some trajectories that were planned for *Mariner* caused the portside horizon-sensor head to view the Sun during the first burn and the parking orbit, which would cause that head to be inhibited. The *Agena* would then use the roll gyro for control about that axis and accept a lesser signal into the pitch channel. Initial estimates of the error involved in this situation indicated that significant mid-course maneuver corrections would be required just from this error source. However, later analyses showed that, in order to correct the error from this mode of operation, a velocity increment of about 2 ft/sec at midcourse would have to be applied. Although this situation could not be classified as a major contributor to the injection errors, the risk of having this inhibit circuitry not function properly was avoided by electing not to launch MR-2 on those days when this problem was possible. As it turned out, there were only 10 consecutive days in August 1962

when this was a problem. Entire days would not have been lost because this phenomenon occurred only over the larger launch azimuths.

D. Mariner R Spacecraft

The *Mariner R* spacecraft presents no actual restraints on the launch period or the launch window, other than the fact that its weight could not be propelled to the necessary velocity by the vehicle on all days of the launch period. Because a minimum geocentric energy was required from the booster to launch a spacecraft to Venus, bounds were placed on the number of days on which a launch could be accomplished. This subject is discussed in more detail in Section X.

It was the philosophy of the *Mariner R* Project that two spacecraft be ready for launch in July—one to go to the launch complex and one to remain in ready-storage, capable of being launched the next day if some failure in the first spacecraft caused it to be removed from the launch complex. This technique would cause only one day to be lost due to the spacecraft.

Certain launch and hold criteria must be satisfied before the spacecraft is considered ready for launch. All subsystems must pass the final system test prior to the delivery of the spacecraft to the launch complex. On the launch complex, it must be certified that the spacecraft is in a launch-ready condition. Not all subsystems are monitored in detail after the spacecraft is on the vehicle; only those which must necessarily be functioning at launch. Spacecraft monitoring in the launch configuration is accomplished through the normal spacecraft telemetry and direct-access, umbilical connections to the blockhouse, in addition to the r-f link between the spacecraft and the launch telemetry trailer radio communications subsystem.

In general, hard-line connections to the blockhouse concern only those functions which are not monitored on the spacecraft and must necessarily be monitored to assure that the spacecraft is in a launch-ready condition. This requirement places a heavy reliance on the spacecraft telemetry for certifying the launch-ready state.

UNCLASSIFIED

JPL TECHNICAL REPORT NO. 32-353

One consideration in the launch-ready decision is whether the minimum requirements for information from the direct-access functions and the telemetry measurements have been met. The minimum requirements vary widely; e.g., where in the launch period is the launch being attempted, how many days remain before the validation period expires, or what is the risk factor. These variables are evaluated by the Project Office and appropriate decisions are made.

Table 30 summarizes the spacecraft telemetry measurements. A similar Table, which was not included here, was prepared for the launch complex direct-access monitors. These Tables list in one place the reasons for these measurements and monitors, and the relative importance of the measurements in accomplishing the mission objectives.

Table 30 indicates the requirements for operational engineering telemetry measurements at launch upon which in-flight decisions can be made and achievement of the mission objectives can be attained. Priorities have been assigned to the telemetry measurements according to their value in providing required information for spacecraft operation. Three levels of priority were designated: mandatory, highly desirable, and desirable.

Accessibility to the spacecraft during the countdown is primarily through telemetry. Hard-line accessibility is restricted to monitor and control functions that are necessary to assure that the spacecraft is in a launch-ready condition. Consequently, there are few expendable direct-access functions during the countdown. The functions carried in the long-lines between the spacecraft and the blockhouse were listed for launch decision.

UNCLASSIFIED

Table 30. Mariner R spacecraft launch and hold criteria — telemetered functions

Measurement	Deck position No.	Purpose of measurement	On-pad monitor	Priority ^a		Effect on mission objectives		Comments
				Function being measured	Measure-ment via telemetry	Loss of function being measured	Loss of measurement	
Sync word	A0	Allows automatic data reduction.	Observed via r-f and hard-line. No addresses on data	M	M	No automatic data processing	—	Review decks, C, D, E, F, below
Deck C signals	A1	Allows commutation of Deck C, D, E, and F data.	Observed via r-f and hard-line. No commutation of Decks C, D, E, F.	M	M	Risky to commit to midcourse, turn on cruise science or expect two-way doppler at planet.		
Battery voltage	A2	Indicates battery voltage from which battery condition may be inferred. Aids in determining existence of power load-sharing mode by comparison with solar panel voltage.	Observed via telemetry and hard-line. On internal power, observable on primary system voltage meter in Launch Complex GSE. On external power, reads approximate external supply voltage	M	D	Launch impossible without functioning battery	Less performance analysis	A2 or A6 highly desirable
Yaw control gyro	A3	Gives coarse data on separation rates and combined with position error signals provides acquisition data.	Observed via telemetry and hard-line. Functional failure most rapidly observed in Launch Complex GSE. Instrumentation failure or bias discernible by comparing Launch Complex GSE and telemetry readings.	M	D	Sun acquisition highly improbable	Less performance analysis. Lose information pertinent to RTC9 decision	A3 or A4 and A5 mandatory for launch

^aPriorities

M—Mandatory, HD—Highly Desirable, D—Desirable

UNCLASSIFIED

JPL TECHNICAL REPORT NO. 32-353

Table 30. (Cont'd)

Measurement	Deck position No.	Purpose of measurement	On-pad monitor	Priority ^a		Effect on mission objectives		Comments
				Function being measured	Measurement via telemetry	Loss of function being measured	Loss of measurement	
Pitch control gyro	A4	Gives coarse data on separation rates, maneuver rates, and combined with position error signals provides acquisition data.	Same as A3	M	HD	Sun acquisition highly improbable	Risk involved in attempting midcourse. Lose information pertinent to RTC9 decision.	A3 or A4 and A5 mandatory for launch
Roll control gyro	A5	Same as A4	Same as A3	M	M	Earth acquisition highly improbable	Risk involved in attempting midcourse. Lose information pertinent to RTC9 decision.	A3 or A4 and A5 mandatory for launch
Battery drain current	A6	Indicates battery loads.	On internal power, reads battery drain. On external power, reads ground d-c supply current.	M	D	Battery necessary to launch	Less performance analysis	A2 or A6 highly desirable; very handy tool for determining spacecraft operation.
Pitch Sun sensor position error	A7	Helps verify and maintain Sun acquisition. Provides information on acquisition maneuvers and limit cycle operation. Necessary to establish inertial attitude accurately for computing midcourse maneuver.	Telemetry should read mid-band on pad. No other means of checking while on pad.	M	HD	Maintenance of Sun orientation impossible.	Increases risk of performing midcourse maneuver because orientation relative to Sun is not known accurately.	Inertial attitude may be inferred from A8 and whether gyros are on, the condition which exists when spacecraft is not pointing within 2 deg of Sun. A7 or A8 and A9 mandatory for midcourse maneuver.
Yaw Sun sensor position error	A8	Helps verify and maintain Sun acquisition. Provides information on acquisition maneuvers and limit cycle operation. Necessary to establish inertial attitude accurately for computing midcourse maneuver.	Same as A7	M	D	Same as A7	Same as A7	Inertial attitude may be inferred from A7 and whether gyros are on, the condition which exists when spacecraft is not pointing within 2 deg of Sun. A7 or A8 and A9 mandatory for midcourse maneuver.

^aPriorities

M—Mandatory, HD—Highly Desirable, D—Desirable

UNCLASSIFIED

Table 30. (Cont'd)

Measurement	Deck position No.	Purpose of measurement	On-pad monitor	Priority ^a		Effect on mission objectives		Comments
				Function being measured	Measurement via telemetry	Loss of function being measured	Loss of measurement	
Earth sensor roll position error	A9	Helps verify and maintain Earth acquisition. Provides information on acquisition maneuvers and limit cycle operation. Necessary to establish inertial attitude accurately for computing midcourse maneuver.	Same as A7	M	M	Maintenance of Earth orientation impossible; midcourse maneuver impossible.	Increases risk of performing midcourse maneuver because orientation relative to Earth is not known accurately.	Inertial attitude may be inferred from gyro condition after 167 hrs; gyros are off if Earth is acquired.
Event sequencer	B0	Indicates occurrence of various spacecraft events by sampling 4 binary counters sequentially.	Event Counters 3 and 4 are activated and then cleared prior to launch. Counters 1 and 2 are not activated prior to launch.	—	HD	—	Valuable information for quick spacecraft analysis and RTC9 decision lost.	This measurement is an extremely handy one to have; however, the mission can be performed without it. Inference of this information requires A3 or A4 and A5, A7 or A8 and A9, B7 or B9, D2 or D7.
Command detector monitor	B1	Indicates state of out-of-lock signal and VCO frequency of spacecraft command detector.	Telemetry is only indication on pad.	M	M	Command system would be inoperative if out-of-lock signal within detector failed.	Much risk to expect to get commands into spacecraft.	This is valuable operational tool in sending commands to the spacecraft.
Earth brightness	B2	Indicates viewing of some bright object.	No checkout on pad.	M	D	Mission not affected.	Mission not affected. Helps verify Earth acquisition.	Of interest in failure analysis. Do not hold for it. Does not give accurate indication of roll position error.
Antenna reference hinge angle	B3	Indicates angle to which antenna will go when Earth acquisition is initiated or lost; updated every 16.7 hr.	Observed by telemetry and hardline. Value can be adjusted on pad and verified.	M	HD	Initial acquisition requires it. Automatic reacquisition of Earth is very uncertain.	Lose important operational data.	B3 or B4 mandatory

^a Priorities

M—Mandatory, HD—Highly Desirable, D—Desirable

Table 30. (Cont'd)

Measurement	Deck position No.	Purpose of measurement	On-pad monitor	Priority ^a		Effect on mission objectives		Comments
				Function being measured	Measurement via telemetry	Loss of function being measured	Loss of measurement	
Antenna hinge position	B4	Indicates antenna position.	Should read zero deg on pad.	M	HD	Maintenance of Earth acquisition not possible.	Loss important operational data.	B3 or B4 mandatory
L-band AGC (coarse)	B5	Indicates in-lock condition of receiver. Serves as measure of received signal strength. Good indicator of transponder performance.	Telemetry is only indication on pad. Variation can be forced from RFT.	M	M	Prevents signal reception over large range of communication distances.	Loss indication of receivers capability to receive signals.	Necessary for prelaunch verification of transponder performance.
L-band phase error (coarse)	B6	Facilitates acquiring two-way lock. Useful in attaining receiver threshold. Provides valuable operational information for sending ground commands.	Telemetry is only indication on pad. Variation can be forced from RFT.	M	HD	Prevents receiver from locking on ground signal.	Loss valuable information which assists DSIF in getting commands to the spacecraft.	B6 or C4 mandatory C4 is preferred to maximize command capability and establishment of two-way doppler at planet.
Propellant tank pressure	B7	Indicates pressure in midcourse motor propellant tank.	Telemetry is only indication on pad.	HD	HD	Slight risk in performing midcourse if pressure < 100 psia at time of midcourse maneuver.	Must depend on extrapolation to indicate pressure at time of midcourse.	B7 not essential for launch if some pressure history has been obtained.
Battery charger current	B8	Indicates amount of battery charging. Provides information to ascertain load-sharing mode.	Reads zero except when charging from flight source, i.e., when operating on external power at sufficiently high voltage.	M	M	Loss battery charge capability. Completion of planet encounter uncertain. Turn on of cruise science doubtful.	Loss information on battery charging and one means of verifying a load-sharing condition.	This measurement gives best information on battery charging, load-sharing condition, and the condition of the battery.

^a Priorities

M—Mandatory, HD—Highly Desirable, D—Desirable

Table 30. (Cont'd)

Measurement	Deck position No.	Purpose of measurement	On-pad monitor	Priority*		Effect on mission objectives		Comments
				Function being measured	Measure-ment via telemetry	Loss of function being measured	Loss of measurement	
Midcourse motor N ₂ pressure	B9	Indicates pressure in midcourse motor nitrogen reservoir.	Telemetry is only indication on pad.	M	HD	No possibility of midcourse maneuver without N ₂ pressure.	Lose positive assurance of motor capability to perform midcourse.	If sufficient data exists to assure N ₂ pressurization at midcourse, there is no need for hold.
Sync word	C0	Allows automatic data reduction.	Observed via r-f and hard-line. No addresses on data from Decks C, D, E, F.	M	M	No automatic data processing or commit to midcourse.		
Deck D signals	C1	Allows commutation of Deck D.	Observed via r-f and hard-line. No commutation of Deck D.	M	M	Risky to turn on cruise science or commit to midcourse.		Review deck D below.
Deck E signals	C2	Allows commutation of Deck E.	Observed via r-f and hard-line. No commutation of Deck E.	M	M	Lose data for thermal control analysis.		Review deck E below. Questionable to commit to midcourse without C2 or C3.
Deck F signals	C3	Allows commutation of Deck F.	Observed via r-f and hard-line. No commutation of Deck F.	M	M	Lose data for thermal control analysis.		Review deck F below. Questionable to commit to midcourse without C2 or C3.
L-band phase error (fine)	C4	Facilitates acquiring two-way lock, particularly at planet distance. Useful in attaining receiver threshold. Provides valuable operational information for sending ground commands.	Telemetry is only indication on pad. Variation can be forced from RFT.	M	HD	Prevents receiver from locking on ground signal.	Lose valuable information which assists DSIF in getting commands to the spacecraft. Risky to expect command capability or two-way doppler at planet.	B6 or C4 mandatory C4 is preferred to maximize command capability establishment of two-way doppler at planet.

*Priorities

M—Mandatory, HD—Highly Desirable, D—Desirable

UNCLASSIFIED

JPL TECHNICAL REPORT NO. 32-353

Table 30. (Cont'd)

Measurement	Deck position No.	Purpose of measurement	On-pad monitor	Priority ^a		Effect on mission objectives		Comments
				Function being measured	Measurement via telemetry	Loss of function being measured	Loss of measurement	
L-band direct power	C5	To measure r-f power output of power amplifier to directional antenna.	Observed via telemetry and inferred from RFT measurements. However telemetry measurement gives desired accuracy to measure of radiated power.	M	HD	No rf from spacecraft via high gain antenna.	No accurate measure of radiated power from directional antenna on pad. Lose data for engineering analysis of system.	Not essential to perform the basic mission. Needed for r-f certification on pad. Operational aid.
Louver position	C6	Indicates position of louvers on Electronics Assembly IV.	Telemetry is only indication on pad. Should give no reading on pad.	M	D	Improper thermal control of Electronics Assembly IV.	Lose data as to when the louvers opened enroute to the planet.	The measurement is not essential to mission success.
Spares	C7, 8, 9							
Sync word	D0	Allows automatic data reduction of Decks D, E, F.	Observed via r-f and hard-line. No addresses on data from Decks D, E, F.	M	M	No automatic data processing for decks D, E, F.		
Low reference	D1	Combined with D9 provides method of adjusting raw data to compensate for shifts in the data encoder analog-to-digital converter.	Observed via telemetry only.	HD	HD	Lose ability to compensate raw data to allow utilization of calibration curves.		D1 and D9 highly desirable. Erratic measurements indicate defective analog-to-digital converter and hold is necessary if data is desired.
Solar panel 4A11 voltage	D2	Indicates voltage developed by solar panels.	No solar panel checkout is possible under the shroud. The measurement can be checked by comparison with Launch Complex GSE primary system voltage. They read the same.	M	HD	No voltage from this panel will abort the mission.	Lose engineering data for determining spacecraft performance and load sharing mode. Cruise science turn-on is jeopardized.	D2 or D7 mandatory

^a Priorities

M—Mandatory, HD—Highly Desirable, D—Desirable

UNCLASSIFIED

Table 30. (Cont'd)

Measurement	Deck position No.	Purpose of measurement	On-pad monitor	Priority ^a		Effect on mission objectives		Comments
				Function being measured	Measure-ment via telemetry	Loss of function being measured	Loss of measurement	
L-band omni power	D3	To measure r-f power output of power amplifier to omni-antenna.	Observed via telemetry and inferred from RFT. Accuracy of measurement from RFT is satisfactory for checkout.	M	D	The r-f link from the spacecraft during the time before Earth acquisition is questionable. Intermittent signals from directional antenna could be expected.	Lose data for checking assumptions used in radio system performance estimates.	Not essential to perform basic mission. Operational aid.
Attitude control N ₂ pressure	D4	Indicates amount of gas in attitude control nitrogen tanks.	Telemetry is only indication on pad.	M	M	N ₂ gas required to remove separation rates, to orient spacecraft for Sun acquisition and Earth acquisition, and to orient the spacecraft for the midcourse maneuver.	Lose assurance of gas system integrity at liftoff and the condition of gas supply prior to decision to perform the mid-course maneuver.	This measurement gives best indication of the attitude control gas supply.
Solar panel 4A11 current	D5	Indicates load supplied by this solar panel.	No checkout on pad. Zero current should be read on pad.	M	HD	This panel current is required to provide sufficient power for the mission.	Lose engineering data required for determining spacecraft performance and load-sharing mode. Cruise science turn-on is jeopardized.	D5 or D8 mandatory
Spare	D6							

^a Priorities

M—Mandatory, HD—Highly Desirable, D—Desirable

Table 30. (Cont'd)

Measurement	Deck position No.	Purpose of measurement	On-pad monitor	Priority ^a		Effect on mission objectives		Comments
				Function being measured	Measure-ment via telemetry	Loss of function being measured	Loss of measurement	
Solar panel 4A12 voltage	D7	Same as D2	Same as D2	M	HD	Same as D2	Same as D2	D2 or D7 mandatory
Solar panel 4A12 current	D8	Same as D5	Same as D5	M	HD	Same as D5	Same as D5	D5 or D8 mandatory
High reference	D9	Combined with D1 provides method of adjusting raw data to compensate for shifts in the data encoder.	Observed via telemetry only.			Same as D1		D1 and D9 highly desirable. Same as D1.
Reference temperature	E0	Indicates voltage across precision 500-ohm resistor to show bias in temperature measurements.	Telemetry is only check on pad. All temperature measurements would be lost if a transducer shorted to ground or the bridge circuit power supply failed.	HD	HD	Loss ability to compensate raw temperature data if variation in temperature bridge supply voltage occurs.	Accuracy of temperature measurements would be in doubt.	Not mandatory in order to perform basic mission. Loss of all temperature measurements makes mid-course maneuver risky and sacrifices critical data on spacecraft operation and thermal design.
Booster regulator temperature	E1	Measure internal temperature of 4A4 on front of Electronics Assembly VI.	Same as E0	D	D	Loss of information contained in that measurement. Short to ground eliminates all temperature measurements.	Loss of information contained in that measurement.	Same as E0
Midcourse motor N ₂ tank temperature	E2	Measure skin temperature of nitrogen tank.	Same as E0	D	D	Same as E1	Same as E1	Same as E0
Midcourse motor propellant tank temperature	E3	Measure skin temperature of propellant tank.	Same as E0. E3 is good average of all case temperature measurements	HD	HD	Same as E1	Same as E1	Same as E0. Propellant freezes at 32°F.

^aPriorities

M—Mandatory, HD—Highly Desirable, D—Desirable

UNCLASSIFIED

JPL TECHNICAL REPORT NO. 32-353

Table 30. (Cont'd)

Measurement	Deck position No.	Purpose of measurement	On-pad monitor	Priority ^a		Effect on mission objectives	Comments
				Function being measured	Measurement via telemetry		
Earth sensor temperature	E4	Earth sensor.	Same as E0. Should read temperature similar to F8 on pad.	HD	HD	Same as E1. Useful failure analysis.	Same as E0. Photomultiplier tube performance seriously degraded above 100°F.
Battery temperature	E5	Measure internal temperature of battery.	Same as E0. Monitored via hard-line.	D	HD	Same as E1	Same as E0. Battery lifetime is function of temperature.
Attitude control nitrogen temperature	E6	Measure skin temperature of N ₂ gas bottle.	Same as E0	HD	HD	Same as E1. Combined with D4 indicates quantity of gas remaining in bottles more accurately than by D4 alone.	Same as E0. Accurate knowledge of gas supply may affect RTC8 and RTC7 decision.
Solar panel 4A11 front temperature	E7	Measures temperature on front of solar panel 4A11.	Same as E0	D	D	Same as E1. Lose one means of identifying which solar panel the system is operating on.	Same as E0. The current, voltage measurements can be plotted in order to correlate the solar panel performance characteristics with test data. E7, 8, or 9 highly desirable.
Solar panel 4A12 front temperature	E8	Measures temperature on front of solar panel 4A12.	Same as E0	D	D	Same as E1	Same as E7, E7, 8, or 9 highly desirable.
Solar panel 4A11 back temperature	E9	Measures temperature on back of solar panel 4A11.	Same as E0	D	D	Same as E1	Same as E7, E7, 8, or 9 highly desirable.
Electronics Assembly I temperature	F0	Measures average temperature of front of Case I.	Same as E0	D	D	Same as E1	Same as E0
Electronics Assembly II temperature	F1	Measures average temperature of front of Case II.	Same as E0	D	D	Same as E1	Same as E0. If two-way lock cannot be achieved, this temperature can be indicative of oscillator frequency.

^a Priorities
M—Mandatory, HD—Highly Desirable, D—Desirable

UNCLASSIFIED

UNCLASSIFIED

Table 30. (Cont'd)

Measurement	Deck position No.	Purpose of measurement	On-pad monitor	Function being measured	Priority ^a	Effect on mission objectives		Comments
						Loss of function being measured	Loss of measurement	
Electronics Assembly III temperature	F2	Measures average temperature of front of Case III.	Same as E0	D	D	Same as E1	Same as E1	Same as E0
	F3	Measures average temperature of front of Case IV.	Same as E0	HD	HD	Same as E1	Same as E1.	Same as E0. Gyro drift rate is a function of this temperature could result in a more accurate midcourse maneuver computation.
Electronics Assembly IV temperature	F4	Measures average temperature of front of Case V.	Same as E0	D	D	Same as E1	Same as E1	Same as E0
	F5	Measures average temperature of lower thermal shield temperature	Same as E0	D	D	Same as E1	Same as E1	Same as E0
Upper thermal shield temperature	F6	Measures average temperature of upper thermal shield.	Same as E0	D	D	Same as E1	Same as E1	Same as E0
	F7	Measures temperature of electrometer probe to establish calibration curve.	Same as E0	HD	HD	Same as E1	Same as E1	Temperature can be inferred from other measurements taken in science equipment.
Plasma electrometer temperature	F8	Measures temperature on antenna yoke.	Same as E0. Should read temperature similar to E4 on pad.	D	D	Same as E1	Same as E1	Same as E0
	F9							
^a Priorities M—Mandatory, HD—Highly Desirable, D—Desirable								

UNCLASSIFIED

UNCLASSIFIED

JPL TECHNICAL REPORT NO. 32-353

E. Range Safety

In order to provide a large number of minutes on any one day when a launch might be attempted, JPL requested that AMR Range Safety permit the *Mariner* launches to utilize the launch azimuth sector of 90 to 114 deg east of north. Range Safety granted permission to launch over the sector of 93 to 111 deg. The 3 deg subtracted from both sides of the desired sector greatly reduced the probability of an errant rocket or one of its components landing on an inhabited land mass.

On the basis of this sector, the launch window on any day was approximately 2 hr in duration. It was hoped that this was sufficient time to launch the vehicle. Statistically, a 2-hr window results in a high probability of completing the countdown before the window closes. Or, if troubles are going to develop within the complex launch vehicle system, they will probably be evidenced early in the window, and, if no significant difficulty develops in the system, the liftoff will have occurred prior to the expiration of the 2-hr limit.

F. Tracking and Telemetry Coverage

Tracking and telemetry coverage up to that time when the DSIF can lock-on to the spacecraft is important to the definition of the launch restraints. The time span involved is encompassed primarily by the preinjection trajectories. Since the preinjection trajectory projections at the time of the second burn, injection, separation, and the retro-maneuver cover a large sector of the Atlantic Ocean, tracking ships are employed in addition to the land-based tracking stations to obtain critical telemetry and tracking data at the time of the second *Agena* burn and immediately thereafter. The Atlantic Missile Range provides three ships in addition to tracking stations on Ascension Island and at Pretoria on the African continent. Two of the three ships record only telemetry and do not provide tracking data. Much information is gained from

data received at the time of significant events in the vehicle's flight sequence.

The coverage of the many possible trajectories by the AMR tracking and telemetry stations was known to be less than 100% and, with this in mind, it was necessary to decrease the number of possible trajectories on a particular day because much valuable data would be lost if the actual flight trajectory were not covered. In effect, the launch window on some days was decreased in length because the trajectories eliminated were a function of launch azimuth and the required azimuth did, indeed, have to change with time.

The capability of the DSIF stations in Africa and in Australia to provide sufficient tracking data after injection was also a consideration in choosing the usable launch azimuths for a given day. In some instances, the spacecraft would pass over the African stations so rapidly that the chances of getting two-way doppler immediately after injection were quite small. More detailed information on this problem is given in Section VII.

G. Space Flight Operations

Space flight operations also affect the decision to launch a spacecraft. This aspect of the mission is responsible for the spacecraft after liftoff and, in order to perform this function fully, the facilities for receiving, transmitting, and displaying the data must be operating satisfactorily. Possible failure of an important link in the chain of information flow from ground receiver to JPL-Pasadena must be weighed, along with the many additional factors influencing the mission, in order to judge whether a hold condition exists which should delay the mission until the deficiency is corrected.

Certain criteria were established which allowed quick judgment to be made on the advisability of launch in particular circumstances. Those pertaining to the tracking and telemetry coverage, both from AMR and the DSIF, are discussed in Section XII.

UNCLASSIFIED

UNCLASSIFIED

UNCLASSIFIED

UNCLASSIFIED

JPL TECHNICAL REPORT NO. 32-353

XII. Space Flight Operations

A. Purpose and Organization

Space flight operations are defined as those operations necessary to obtain and process spacecraft information and commands required by JPL during the portion of flight from launch to the accomplishment of the mission.

This Section describes the organizational structure established to ensure successful execution of the launch and space flight operations of the *Mariner* P-37 and -38 missions. The brief statement of responsibilities is supplemented by an organization chart (Fig. 233).

1. Project Manager

The Project Manager has the responsibility and authority for the execution to completion of the develop-

ment and operation of the *Mariner* R P-37 and -38 missions.

2. Space Flight Test Director

The Space Flight Test Director is responsible for:

- (1) Interpreting the space flight operations plan and placing requirements consistent with the SFOP on the various operating groups.
- (2) Resolving any ambiguities directly associated with the SFOP arising during its execution.
- (3) Making appropriate decisions requiring emergency action to assure success of the mission if the Project Manager cannot be contacted.

The Space Flight Test Director is accountable to the Project Manager and is delegated the authority of the

UNCLASSIFIED

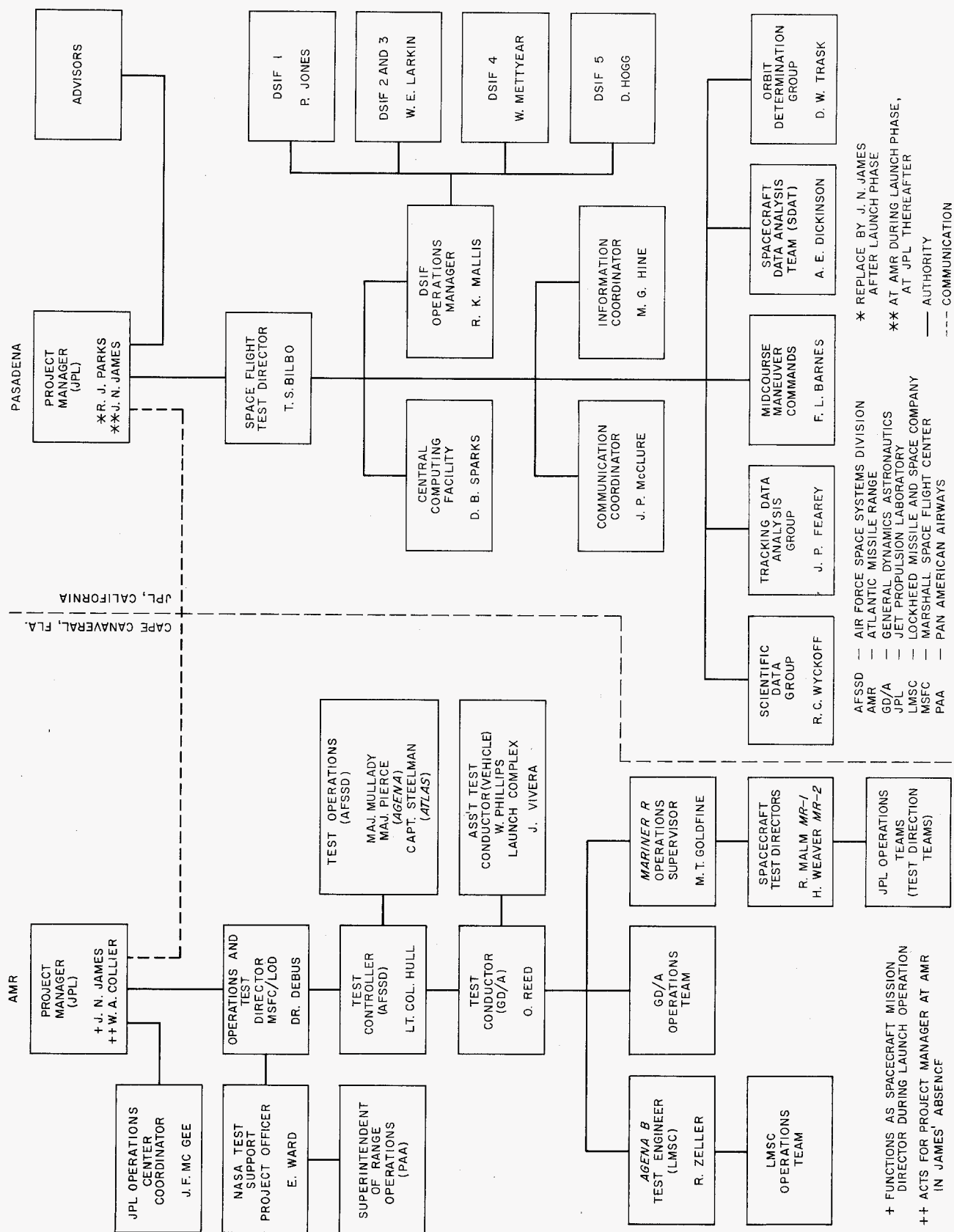


Fig. 233. Mariner R organization


UNCLASSIFIED

JPL TECHNICAL REPORT NO. 32-353

Project Manager for placement of requirements on operating groups, in accordance with the SFOP.

3. JPL/AMR Operation Center Coordinator

The JPL/AMR Operation Center Coordinator is responsible for systematically conducting all activity of the Operation Center during countdown and immediately after launch. He supervises the communications control system at AMR and provides coordinated use of cross-country leased voice circuits.

4. Advisors

The advisors must be aware of the performance of the spacecraft system, instrumentation subsystems, and DSIF during flight, and supply judgment to the Project Manager as to possible future courses of action in the event of nonstandard behavior of the spacecraft.

5. DSIF Operations Manager

The DSIF Operations Manager directs the operation of the Deep Space Instrumentation Facility, including the transmission of data and commands between the spacecraft and the Central Computing Facility, so as to meet the requirements placed by the Space Flight Test Director in accordance with the SFOP.

6. Central Computing Facility

The Central Computing Facility personnel program and operate the computers and peripheral equipment used in connection with space flight operations.

7. Scientific Data Group

This group is responsible for controlling the flow of and mathematical operations on the data related to scientific experiments during the interval between its receipt from the DSIF and its transmission to the appropriate scientists. Any analysis or in-flight evaluation of the scientific data is supplied by this group.

8. Tracking Data Analysis Group

This group evaluates the tracking data to be utilized in the orbit determination process and evaluates the operation of the DSIF equipment used to generate that data.

9. Spacecraft Data Analysis Team

It is the responsibility of this group to evaluate spacecraft performance, to recommend to the Test Director that commands be transmitted to the spacecraft as required, and to inform the Test Director of the results of these transmissions.

10. Orbit Determination Group

This group is responsible for using the tracking and pertinent telemetry data to obtain the best estimate of the actual trajectory of the spacecraft. Acquisition and prediction information are supplied to the DSIF by this group.

11. Midcourse Maneuver Commands

The commands required for the midcourse maneuver will be generated in accordance with the approved procedure.

12. Communications Coordinator

The Communications Coordinator establishes such operational voice and teletype circuits between JPL, AMR, and the DSIF stations as may be necessary to conduct the operations and maintain the operational communications networks used to coordinate the activities of the Space Flight Operations Complex at JPL.

13. Information Coordinator

The Information Coordinator obtains status information from all elements of the Space Flight Operations Complex on a timely basis, maintains the status boards in the Operations Center, and prepares status reports for the Test Director and Project Manager.

B. Operational Facilities

1. Atlantic Missile Range Support

The support for the *Mariner R* missions required from AMR is fully described in the AMR Program Requirements Document No. 3300 (Ref. 6). The facilities used by AMR to support the missions are detailed in the AMR Program Support Plan No. 3300.


UNCLASSIFIED

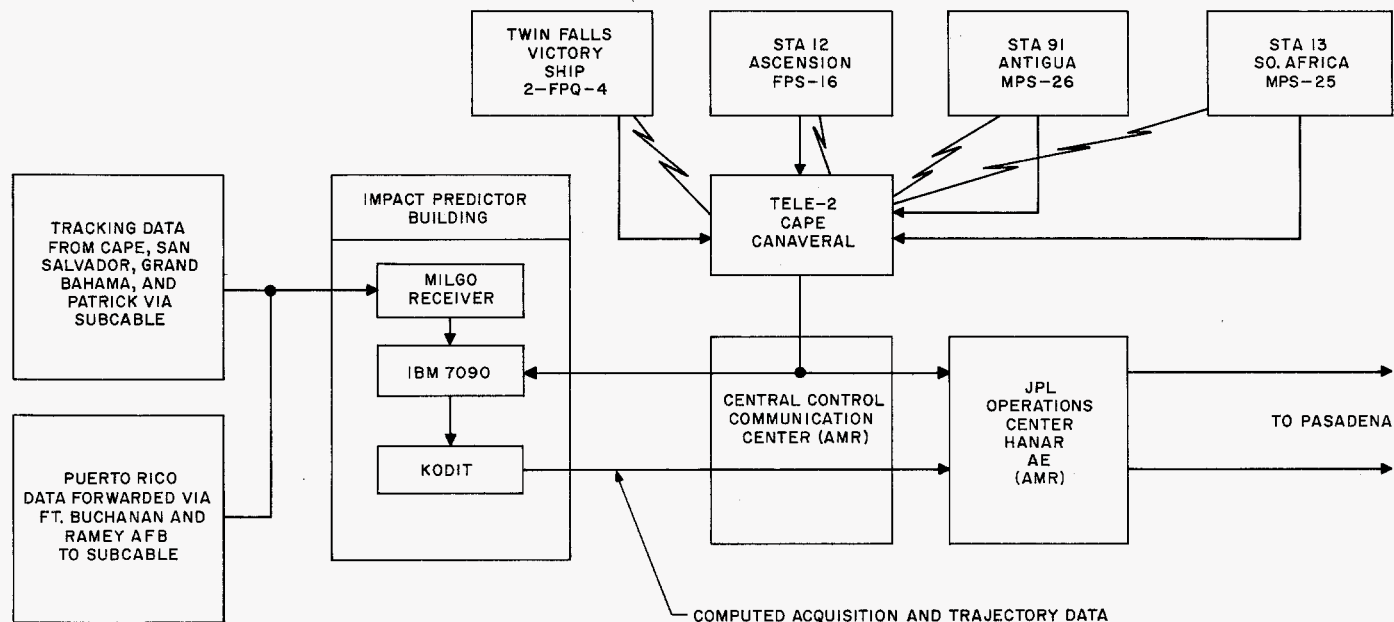


Fig. 234. *Mariner R* tracking facilities support at AMR

After launch, extensive use of the tracking and telemetry facilities at AMR was made in support of *Mariner R*. Tracking and pertinent telemetry data from AMR facilities (shown in Fig. 234) were forwarded in real time to the JPL Operations Center at AMR for relay to the Central Computing Facility in Pasadena. Detailed countdown information was forwarded to JPL from Hangar AE during the prelaunch countdown.

The ground station schedule for the preinjection period of a typical trajectory is illustrated in Fig. 235.

2. Central Computing Facility

The Central Computing Facility is located at JPL-Pasadena. The CCF is composed of three stations:

- (1) The primary computing facility, Station C, located in Building 125 (Fig. 236).
- (2) The secondary computing facility, Station D, located in Building 202 (Fig. 237).
- (3) The telemetry-processing station, located in Building 125 (Fig. 238).

It is the function of the CCF to reduce the tracking data and telemetry data so that the required orbital calculations and command decisions can be made. After the magnetic tapes of telemetry data recorded by the

DSIF have been received at JPL, the CCF processes the raw data into the form required by the user. All real-time data processing and normal non-real-time data processing are performed in the CCF.

3. Deep Space Instrumentation Facility

a. General. The DSIF obtains angular position, doppler, and telemetry data from the spacecraft during the postinjection phase of the trajectory. Additionally, the DSIF sends ground-computed commands to the spacecraft to execute corrective in-flight maneuvers.

b. DSIF stations. The DSIF consists of four permanent stations and one Mobile Tracking Station. For *Mariner R*, these stations had the following capabilities (Table 31 summarizes this area):

Mobile Tracking Station, DSIF 1. The Mobile Tracking Station was used primarily to obtain data at or near the spacecraft injection point. The station has a 10-ft parabolic antenna reflector that is capable of tracking 10 deg/sec. A circular polarized tracking antenna feed is mounted at the receiving equipment; a 25-w, 890-mc transmitter is diplexed on the antenna for obtaining two-way doppler data. Angle and doppler data are transmitted to JPL by teletype in real time. Real-time engineering telemetry data required for station operation are available at the station.

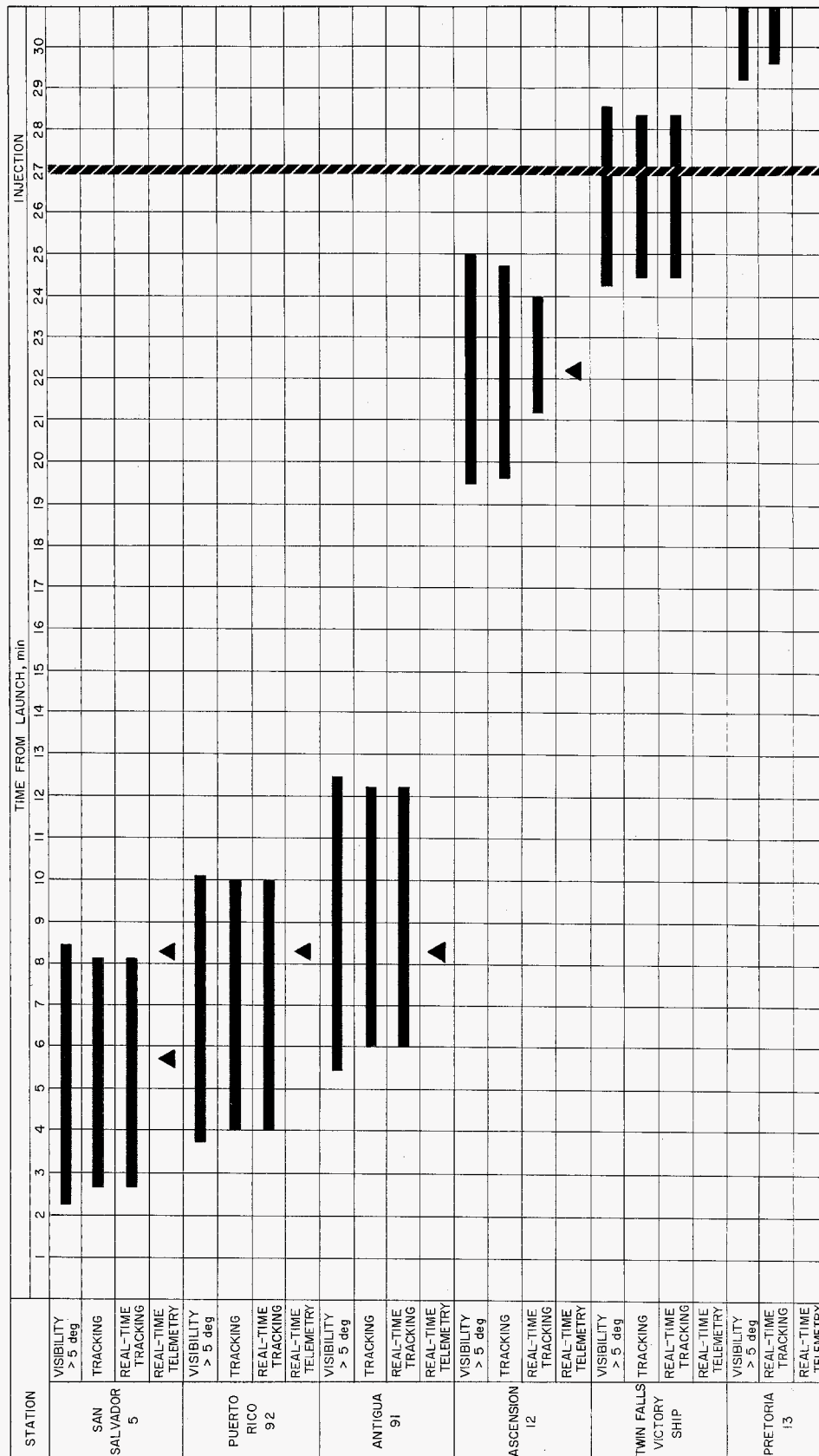


Fig. 235. Preinjection ground station schedule

UNCLASSIFIED

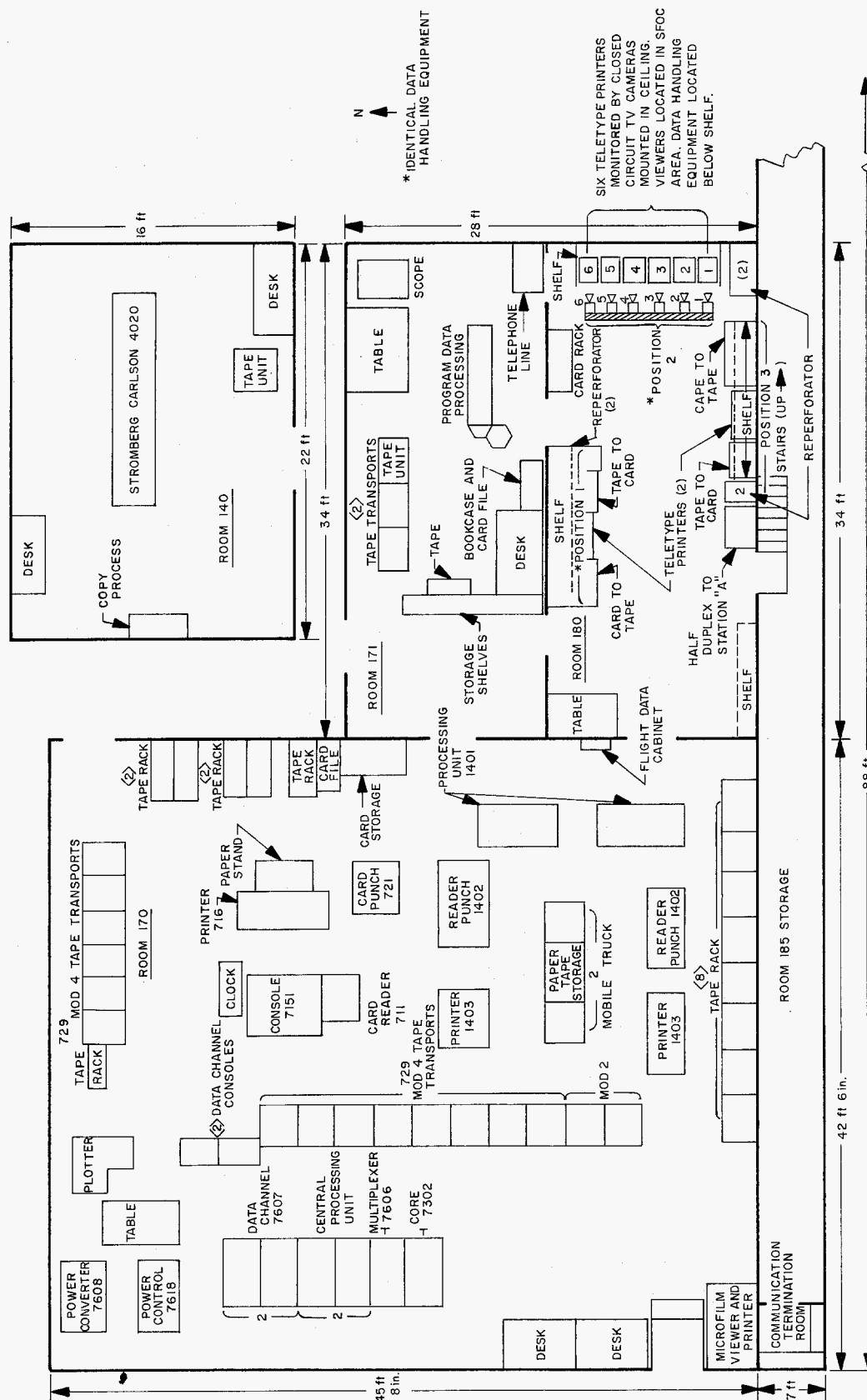


Fig. 236. Primary computing facility, Station C, JPL

UNCLASSIFIED

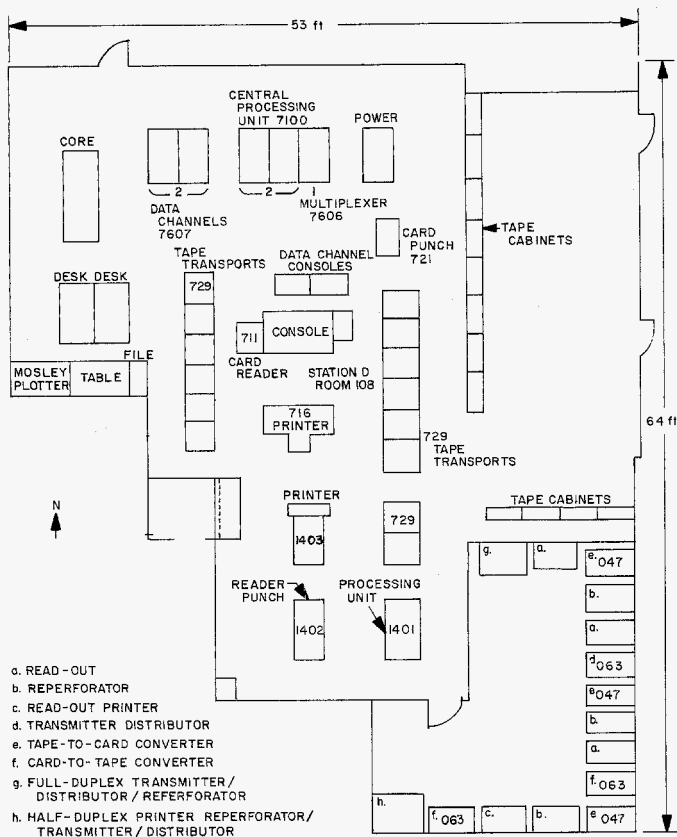


Fig. 237. Secondary computing facility, Station D, JPL

Goldstone Pioneer Station, DSIF 2. The Pioneer Station was used as a primary low-noise receiving station for the mission. The station has a standard, phase-locked, 960-mc receiver. A maser amplifier and a parametric amplifier are used in conjunction with a Cassegrain feed to increase the receiver sensitivity and reduce the system noise temperature. This station provided the precision doppler and also served as the primary telemetry station. A wide-band telephone circuit was utilized to transmit the high bit-rate telemetry to JPL in real time.

Goldstone Echo Station, DSIF 3. The Echo Station was used as the primary Goldstone transmitting station. The station has a 10-kw, 890-mc transmitter to provide both precision two-way doppler and spacecraft command capability.

A Read-Write-Verify unit is incorporated in the command system and allows readback and confirmation of transmitted commands. The primary function of this station during the mission was to command the spacecraft and to provide the transmitted signal for obtaining precision doppler data.

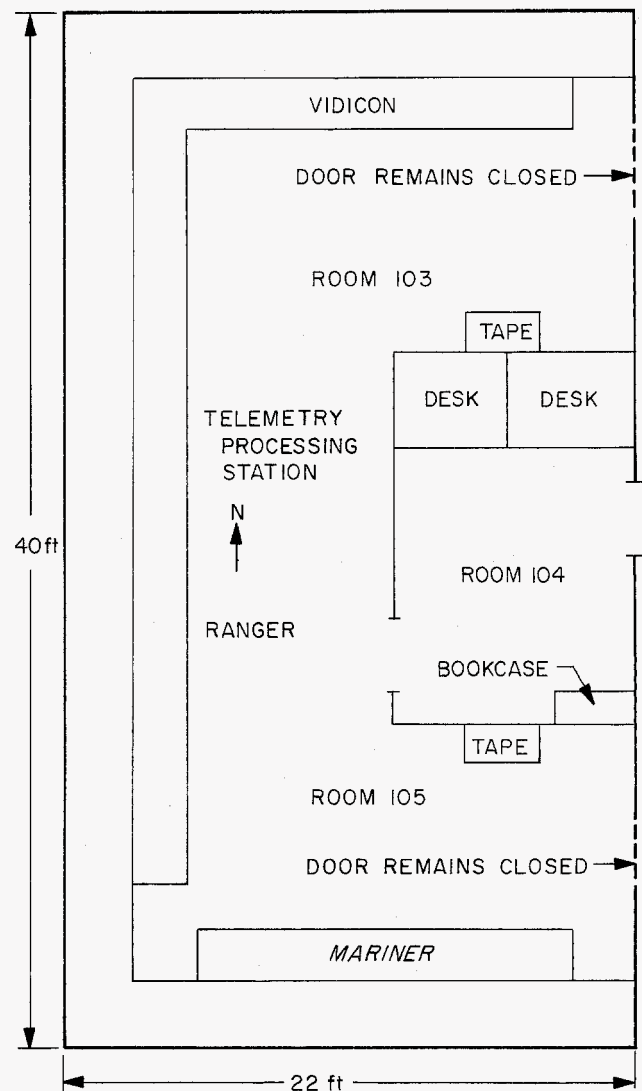


Fig. 238. Telemetry processing station, JPL

Woomera Station, DSIF 4. The Woomera (Australia) Station utilizes an 85-ft, polar-mounted, antenna reflector with a maximum tracking capability of 0.7 deg/sec. The station is equipped with a circular polarized antenna tracking feed and has a circular polarized listening feed. A parametric 960-mc preamplifier, diplexed with a 50-w, 890-mc transmitter, is used in conjunction with the 960-mc receiver. The station provides angle and two-way doppler data read-outs for real-time data transmission to JPL by teletype.

Johannesburg Station, DSIF 5. The Johannesburg (South Africa) Station utilizes an 85-ft, polar-mounted, antenna reflector with maximum rate capabilities in both

Table 31. DSIF capabilities for Mariner R

Item	DSIF 1 Mobile Tracking Station	DSIF 2 Goldstone Pioneer Station	DSIF 3 Goldstone Echo Station	DSIF 4 Woomera Station	DSIF 5 South Africa Station
Antenna size	10-ft azimuth elevation	85-ft hour-angle declination	85-ft hour-angle declination	85-ft hour-angle declination	85-ft hour-angle declination
Maximum angular rate	10 deg/sec	0.7 deg/sec in both axes	0.7 deg/sec in both axes	0.7 deg/sec in both axes	0.7 deg/sec in both axes
Antenna gain: (960 mc/s) track and listen	22.2 db —	43.5 db 45.5 db	43.5 db 46.0 db	43.5 db 46.0 db	43.5 db 46.0 db
Receiver noise figure	6.3 db	0.6 db	N/A	1.8 db	1.8 db
Transmitter power	25 w	—	200 w/10 kw	50 w	200 w/10 kw
Command capability	No	No	Yes	No	Yes
Data transmission					
a. Angles-doppler	Real time	Doppler only Real time	Not applicable	Real time	Real time
b. Telemetry	None	Real time	Not applicable	Near-real time	Near-real time
Recorded telemetry	Yes	Yes	Yes	Yes	Yes
Air mail time to JPL	7 days	1 day	1 day	7 days	7 days

axes of 0.7 deg/sec. Two configurations of apex-mounted antenna feeds are available:

- (1) Circular-polarized 890/960-mc diplexed tracking antenna feed
- (2) Circular-polarized 890/960-mc transmitting/listening antenna horn

A 10-kw transmitter is installed for obtaining two-way doppler and transmitting commands to the spacecraft. Two modes of operation are available: (1) 10-kw transmit; (2) 200-w diplexed (transmit/receive). Mode 2 will utilize the tracking antenna feed, while Mode 1 uses the circular-polarized 890-mc transmitting horn. A 10-kw diplexer is used with reduced transmitting power output in place of Mode 2 in conjunction with the 960-mc receiver. A parametric preamplifier is used in conjunction with the 960-mc receiver. The station provides angle and doppler data read-outs for real-time transmission to JPL by teletype. The telemetry demodulator output is encoded in a suitable teletype format and the data are transmitted to JPL in near-real time.

c. DSIF modes of operation. The eight modes of operation of the DSIF are identified as Ground Modes and are defined as follows:

- (1) *GM-1.* Tracking the transponder signal in the two-way mode, obtaining angles, telemetry, and two-way doppler (C_2). This mode is possible at DSIF 1, 4, and 5.
- (2) *GM-2.* Listening to the transponder signal in the two-way mode, obtaining telemetry and two-way doppler (C_2). This mode is possible at DSIF 4 and 5.
- (3) *GM-3.* Tracking the transponder signal in the one-way mode, obtaining angles, telemetry, and one-way doppler (C_1). This mode is possible at DSIF 1, 4, and 5.
- (4) *GM-4.* Listening to the transponder signal in the one-way mode, obtaining telemetry and one-way doppler (C_1). This mode is possible at DSIF 2, 4, and 5.
- (5) *GM-5.* Tracking the transponder signal in the pseudo two-way mode, obtaining angles, telemetry, and pseudo two-way doppler (C_3). This mode is possible at DSIF 1, 4, and 5.
- (6) *GM-6.* Listening to the transponder signal in the pseudo two-way mode, obtaining telemetry and

pseudo two-way doppler (C_3). This mode is possible at DSIF 2, 4, and 5.

- (7) *GM-7.* Listening to the transponder signal in the coherent pseudo two-way mode, obtaining telemetry and coherent pseudo two-way doppler (C_3). This mode is possible only with the combination of DSIF 3 transmitting and DSIF 2 receiving.
- (8) *GM-8.* Transmitting only to the spacecraft transponder. This mode is possible at DSIF 3 and 5.

d. DSIF operating procedures. Operating procedures for the DSIF specified coverage of the *Mariner R* mission as follows: The DSIF will provide a total of 24-hr-per-day coverage from launch through midcourse maneuver + 2 days, or a maximum of 10 days for each mission. The DSIF will provide a total of 10-hr-per-day coverage for both missions from midcourse maneuver + 2 days or L + 10 days, whichever occurs earlier, to E - 24 hr. From E - 24 hr to E + 24 hr, 24-hr-per-day coverage will be provided. During the period, midcourse maneuver + 2 days to E - 24 hr, DSIF 2 and 3 will track for one 10-hr period every 4 to 10 days, averaging one period every 7 days. The DSIF will provide 24-hr-per-day coverage, on 6- to 12-hr notice, during scientific and engineering alarms, as required. Conflicting requirements between P-37, P-38, and *Ranger 5* will be resolved during the mission.

4. JPL Communications Center

The JPL Communications Center (Fig. 239) is located in Building 190. The Center is the terminus for all communications associated with the mission, and controls all communications circuits providing data flow to or from any DSIF station and the Space Flight Operations Complex at Pasadena, except for the high-speed data line between Goldstone and Station C.

The following circuits were available for the *Mariner R* missions:

a. Data transmission circuits

- (1) *Goldstone.* The Communications Center normally has four half-duplex teletype circuits available for data transmission to or from either Goldstone site. These circuits are available for full-time usage as required. Data transmission is restricted on any one circuit to one direction only.

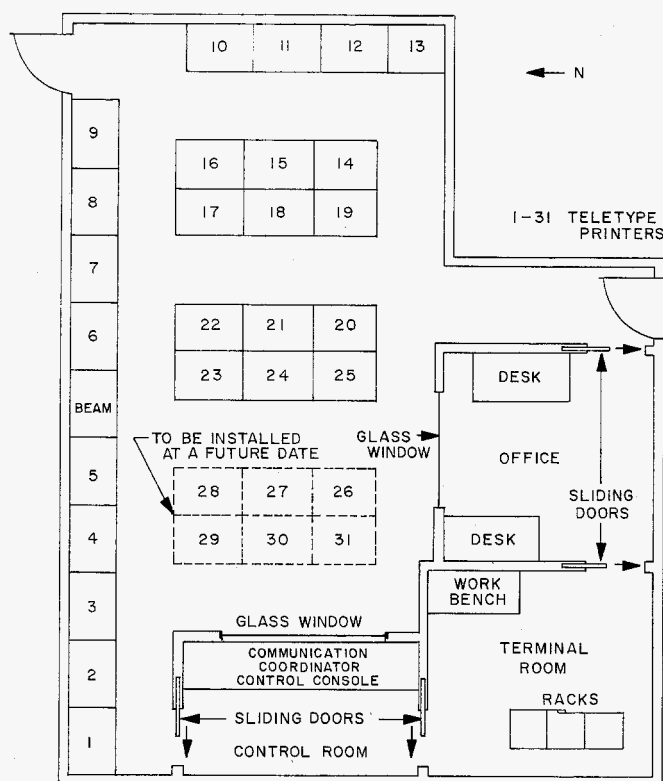


Fig. 239. JPL Communications Center

- (2) *Woomera and South Africa.* One full-duplex circuit is available to each of the overseas stations on a full-time basis. A second circuit is available to each site on a limited basis during critical periods, or when the primary circuit fails. Due to the use of radio teletype over a major portion of the transmission path, both circuits are subject to failure during periods of poor high-frequency radio propagation. The primary and secondary circuits have been routed over different paths to minimize this effect as much as possible. Data transmission over these circuits can take place simultaneously in both directions.
- (3) *Mobile Tracking Station.* The Mobile Tracking Station utilizes the same teletype circuits as the South Africa station.
- (4) *AMR.* Two half-duplex circuits are available to AMR on a full-time basis. These circuits were used for data flow between the launch complex and the JPL Communications Center.
- (5) *JPL Space Flight Operations Complex.* Control of the connections to the external lines is exercised by the Communications Controller in the JPL Communications Center. The lines to Building

125 terminate in page printers and/or re-perforators in the Sub-Communications Center, the DSIF Control Room, SDAT Room, SDAT Support Room, and in the Standby Room. The lines to Building 202 terminate in page printers and/or re-perforators in the Sub-Communications Center. The line to Building 111 terminates in a page printer.

b. Voice circuits

- (1) *Goldstone.* Two voice circuits are available to Goldstone. These are 4-wire telephone circuits capable of being conferenced at the JPL Communications Center with other voice circuits used as part of the DSIF operations.
- (2) *South Africa.* A long-distance toll call is placed to South Africa prior to each launch operation. This circuit is used as required for the first day after launch and is not available on a full-time basis.
- (3) *Woomera.* The Mercury voice circuit (SCAMA) is normally used for communications to Woomera during the launch operations and for the first day after launch. A toll call is placed if this circuit is not available.
- (4) *Mobile Tracking Station.* The MTS shared the voice circuit with the South Africa station.
- (5) *AMR.* Two voice circuits are available during the launch period for communications with the launch complex. One circuit is used for coordination between the launch complex and the SFOC; the other is used for dissemination of status information.
- (6) *JPL Space Flight Operations Complex.* Extensive voice communications exist within the Operations Complex at JPL. Both operational telephone and intercommunications systems are supplemented by the normal JPL telephone system where necessary. Speakers in the various stations of the complex, conference rooms at JPL, and at facilities external to JPL are normally utilized to disseminate prelaunch and postlaunch information to interested persons.

5. Space Flight Operations Center

The Space Flight Operations Center at JPL-Pasadena, shown in Fig. 240, is utilized as the focal point for the coordination of all activities associated with the space

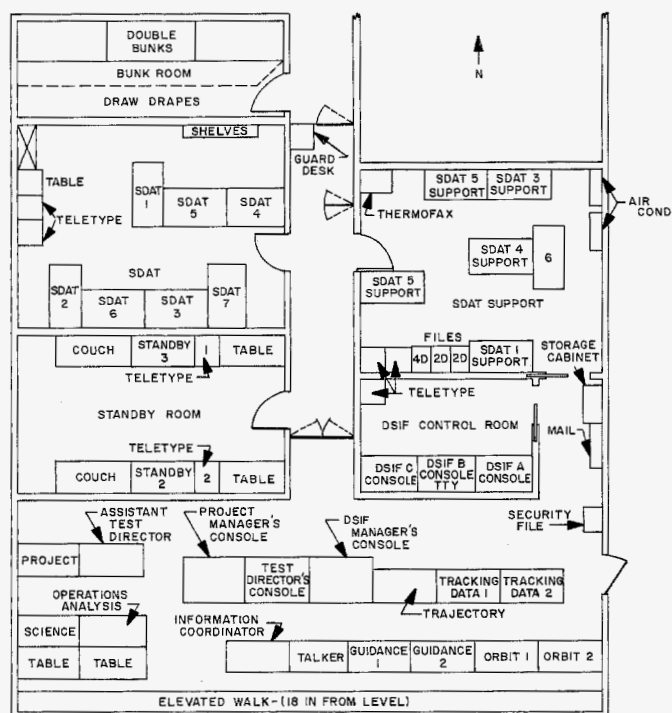


Fig. 240. JPL Space Flight Operations Center

flight operation by the Project Manager, the Space Flight Test Director, and the DSIF Operations Manager. Information relative to the performance and trajectory of the spacecraft is analyzed in the SFOC by the Spacecraft Data Analysis Team, the Scientific Data Group, and the Orbit Determination Group. All ground-generated spacecraft commands originate in the SFOC. Over-all status of the operation is kept current on the status boards in the SFOC by the Information Coordinator, and all status reports to outside persons or agencies are compiled at this point.

The SFOC contains an Operations Room, a DSIF Control Room, an SDAT Room, and an SDAT Support Room used for data handling and filing, and in conjunction with a spacecraft model, is used to visualize the spacecraft configuration. A standby room is provided for additional conference space, and a relaxation area and sleeping facilities are available for operating personnel.

Coordination of all activities associated with the operation is attained by utilization of the voice and teletype communications, and by means of closed-circuit television.

Television monitors are available in the following consoles: Project Manager, Test Director, DSIF Operations Manager, and DSIF Operations A and C. Six fixed cameras, each viewing a teletype page printer in the Sub-

Communications Center, may be selected and controlled in pan, tilt, and zoom functions by the Project Manager, Test Director, and DSIF Operations Manager and are located in the following areas:

- (1) Communications Center, Building 190
- (2) CCF, Building 125 (2 cameras)
- (3) CCF Back-up, Building 202
- (4) Sub-Communications Center, Building 125

Additionally, a full-duplex, direct-writing system is employed between the DSIF Control Room and the Communications Center to forward outgoing messages for relay to the DSIF stations, and for notification of accomplishment of routine procedures.

C. Data Flow and Processing

1. General

This section describes the flow of operational data and information to, from, and within the Space Flight Operations Complex. The complex consists of facilities at the Space Flight Operations Center, the Atlantic Missile Range, the DSIF, and the Space Flight Operations Document Control. The data are generated and processed through the data handling facilities described in Section XII-B. The nature of the space flight operations is such that data flow in real time is of prime concern. This Section indicates the different paths of flow that real-time and non-real-time data will follow.

2. Data Flow to the JPL Operations Complex

The two prime sources of data-flow into the complex are AMR and the DSIF. The AMR data includes the period from launch to injection. It is handled in real time to provide the vital information required for DSIF initial acquisition and for early trajectory computation. The DSIF data is required in real time to provide further acquisition information, assessment of tracking facilities, detailed trajectory and orbit determination, and estimations of spacecraft performance. Tracking and telemetry data utilized for these purposes are recorded on punched paper tape and magnetic tape, respectively, and are transmitted in real time and non-real time as indicated in Fig. 241 and 242.

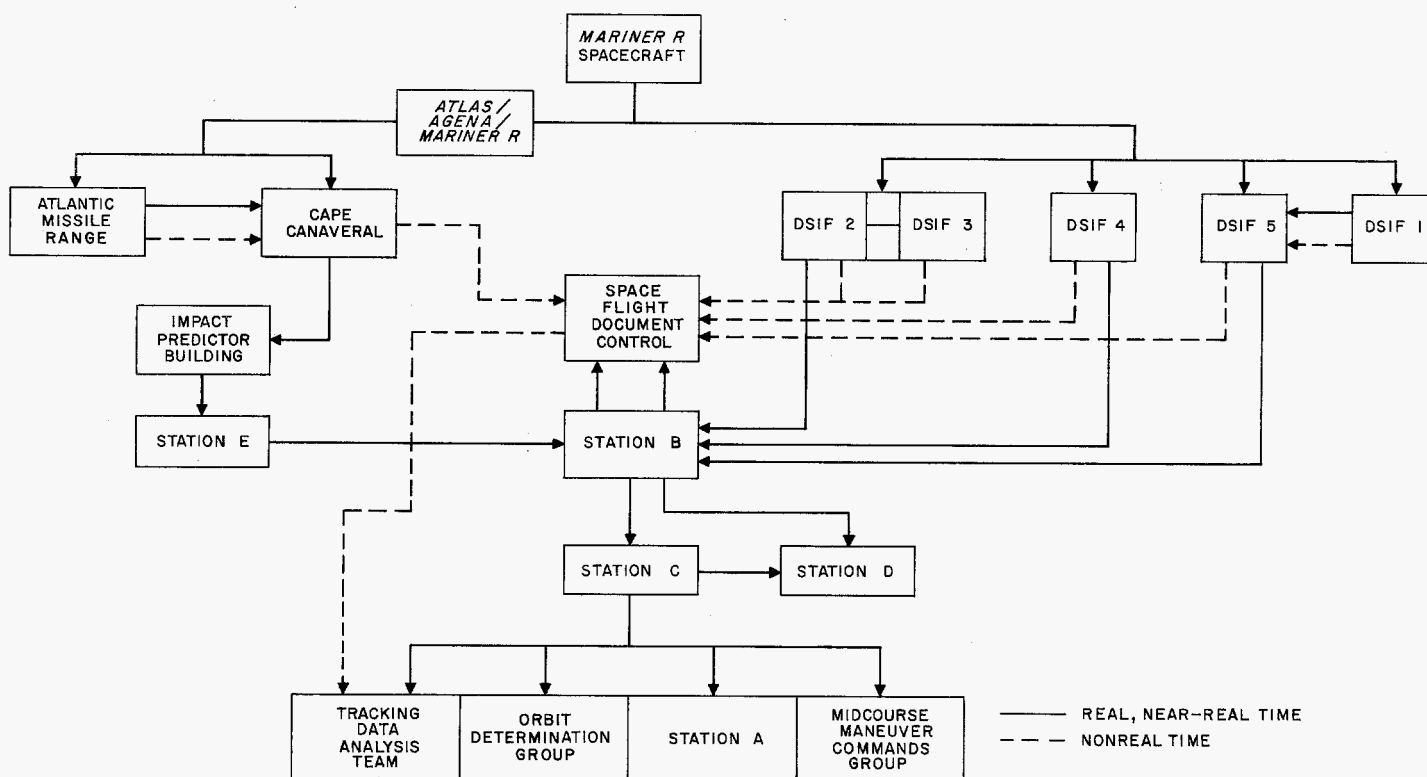


Fig. 241. Tracking data flow

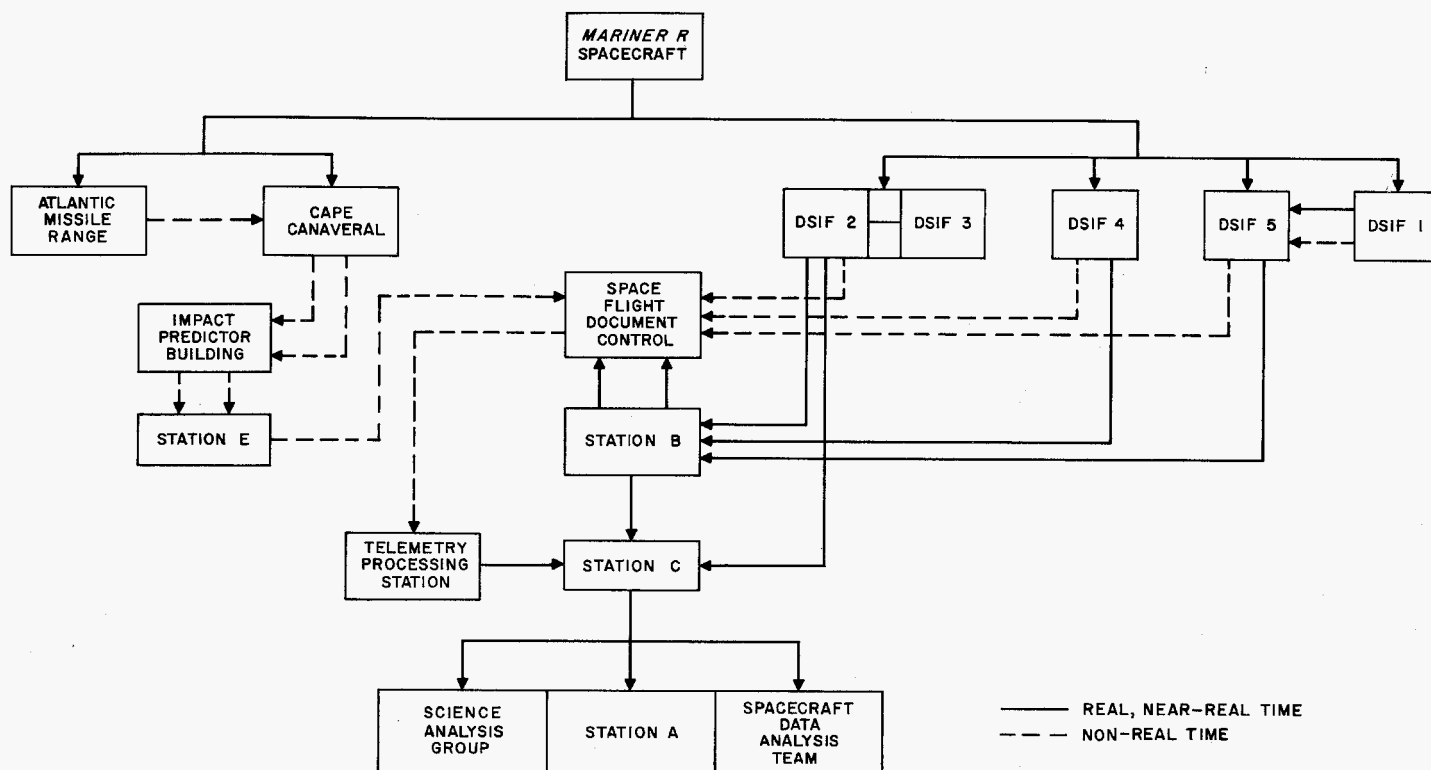


Fig. 242. Telemetry data flow

UNCLASSIFIED

JPL TECHNICAL REPORT NO. 32-353

lished on June 18, July 9, July 19, August 7, and August 15, 1962. The many revisions were made in order to keep the document up to date, utilizing the latest information possible, much of which was obtained during the operational tests.

Operational checkout of various areas of the Space Flight Operations Complex began in early May. These checks consisted initially of processing by the Central Computing Facility of data obtained during system testing on the spacecraft. A joint closed-loop operational test was performed on May 10, 1962, using the *MR-1* spacecraft as the test vehicle. Considered a qualified success due to obvious limitations in simulating space environment and controlled spacecraft stimuli, the test established initial compatibility between the SFO Complex and the spacecraft, and familiarized operations personnel with their duties.

In the interval between the JCLOT and the start of a series of complex integration tests, the reception, processing, and analysis of data taken during extensive AMR operations continued as a parallel effort with AMR spacecraft checkout teams. Equipment installation and facility modifications proceeded as scheduled.

Approximately 3 wk before the established launch date in July 1962, testing of communications, computational processing, analysis, and modes of operation began. Three in-house tests were conducted, utilizing the Cen-

tral Computing Facility, Communications Centers, and the Space Flight Operations Center. On July 16 and July 19, 1962, net integration tests were conducted with the DSIF and AMR personnel participating. For the 2 wk preceding these tests, the DSIF stations had been undergoing extensive internal checkout through r-f boresight and angle-tracking jitter and star-track calibration testing. Data obtained were analyzed and results were used to assist in establishing DSIF tracking accuracies for the flights.

Integration test phasing and duration allowed evaluation of the completed operation systems and procedures to be made and a state of operational readiness was declared for the launch of P-37 (*MR-1*).

The launch date of P-38 was established shortly thereafter and operations testing resumed on August 11, with processing and analysis of data received from AMR tests on *MR-2*. Four space flight operations complex tests were conducted, two of which exercised only the Communications Centers, Computing Facilities, and SFO Center; and two net integration tests, involving the coordinated efforts of the entire complex, were held.

Due to the lack of coordination in the final scheduled integration test, an unscheduled checkout was performed to ensure performance quality and reliability, and the Space Flight Operations Complex was determined to be in a ready condition on August 17, 1962.

UNCLASSIFIED

Appendix A

Mariner R

Project Policy and Requirements

September 29, 1961

1. Purpose of the Document

The purpose of this document is to state program policies and requirements for the *Mariner R* Project. This shall be the controlling policy and requirements document for the *Mariner R* Project. Mission objective, systems definitions, project requirements, milestones, and schedules are established.

2. Project Description

a. Mission objective

The primary objective of the *Mariner R* Project is to develop and launch two spacecraft to the near vicinity of the planet Venus in 1962, to receive communications from the spacecraft while in the vicinity of Venus, and to perform a radiometric temperature measurement of the planet. A secondary objective is to make interplanetary field and/or particle measurements on the way to Venus and in the vicinity of Venus.

b. Systems configuration

(1) Spacecraft system

The *Mariner R* spacecraft will be of a hybrid design utilizing assemblies which have been developed for both the *Ranger* and *Mariner A* Projects. Two flight-ready spacecraft and one set of spares will be delivered to AMR for two launchings occurring in sequence.

Systems Test Complex. The Systems Test Complex will be the basic test equipment unit used in tests and operations to verify the adequacy of the spacecraft design, fabrication, assembly, and flight readiness. The STC will have the capability to power, command, and monitor the performance of the spacecraft down to the assembly level. Two STC's and one set of spare units will be required for *Mariner R* Project.

Launch Complex Equipment. Launch Complex Equipment will be used to power, command, and monitor the spacecraft during all pad operations. Detailed perform-

ance monitoring of the spacecraft during pad operation will be performed through the telemetry system. Hence, only gross performance parameters will be monitored by the LCE. The *Mariner R* LCE must be compatible with all hardware in the blockhouse, transfer room, and other fixed hardware at AMR Complex 12 as it is expected to exist at the completion of the *Ranger 4* launch to the maximum extent possible for the purpose of making the transfer between *Ranger 4* and 5 to *Mariner R* as simple as possible. Two sets of LCE will be required for the *Mariner R* Project.

Launch Check-Out Station. The L-Band Launch Check-Out Trailer and Telemetry Trailer utilized in the *Ranger 4* operation to establish r-f communication and telemetry contact with spacecraft will be modified to a minimum extent and utilized in the *Mariner R* Project. These two trailers combined constitute the Launch Check-Out Station.

Additional Ground Support Equipment. Additional ground support equipment will include dummy loads, and in-line cable adapters.

(2) Launch vehicle

Two launch vehicles of the *Atlas-Agena B* configuration as modified for the *Ranger 1* through 5 launchings will be utilized for the *Mariner R* Project. Minimum further modification to these vehicles will be permitted as required to accomplish the project mission.

(3) Deep space instrumentation facility

The Deep Space Instrumentation Facility will be utilized to communicate with the *Ranger R* spacecraft during space flight operations.

c. Relationship to other JPL projects

The objectives of the *Mariner R* Project and the characteristics of its mission are such that it is inappropriate to require that either hardware or its creation have any prescribed relationship to those of other projects. Since it will be essential in carrying out the project to utilize

UNCLASSIFIED

both previously established hardware and methods, there will be incidental relationship. This incidental relationship should not be confused with any requirement for such. All efforts in the *Mariner R* Project should be directed toward accomplishment of the project within the framework of the requirements presented here and good engineering practice.

3. Spacecraft Requirements

a. Performance requirements

The general spacecraft performance requirements, including the system integration requirements needed to establish a total workable spacecraft compatible with the launch vehicle, and the subsystem interface requirements needed to permit the definition of areas of technical responsibilities for the participating JPL divisions shall be established during a Preliminary Design effort. The Preliminary Design for *Mariner R* shall be accomplished under the direction of the Systems Division with the active participation of all divisions. The detailed results of this work will appear in several documents such as "Spacecraft Design Specification-*Mariner R*," and "Vehicle Systems Integration Requirements & Restraints for *Mariner R*."

b. Hardware development, fabrication, and delivery requirements

It is appropriate that the Project Office delegate authority in various areas to the Systems Division to assist in the management of the project. In exercising this authority, it is required that the Systems Division obtain Project concurrence, and keep Project informed of status on all requirement placed upon the divisions of a significant work level. An appeal channel exists to Project when any case exists where requirements placed by Project or Systems are endangering the meeting of the mission objectives stated in Section 2a.

The development, fabrication, and delivery of hardware which meets the performance requirements of Section 3a should be accomplished within the framework of the following requirements. To carry out the *Mariner R* Project, it has been concluded that the meeting of these minimum requirements is essential to a satisfactory technical job and that verification must be made by the Project Office that they are accomplished in an appropriate manner. Since this document contains the minimum project level requirements, it is expected that all divisions will impose within their areas of responsibility additional

requirements which are consistent with policies and requirements established here. Any conflicts between this document and divisional requirements should be brought to the attention of the Project Office immediately.

(1) General requirements

Functional specifications. The Spacecraft Design Specification will contain a section on Mission Objectives issued by the Project Office, a section on Design Objectives and Constraints issued by the Systems Division, and the particular functional specifications issued by the cognizant division.

Based on the results of the Preliminary Design effort for *Mariner R*, each hardware-contributing division will be charged with the responsibility of providing certain spacecraft and GSE hardware. The basic performance requirements for each subsystem shall be described in sufficient detail in the form of a Functional Specification which must include the lists of necessary spacecraft layout and envelope drawings. The Functional Specifications are an integral part of the above mentioned Spacecraft Design Specification. The satisfactory completion of these documents by each division shall be a Project Requirement. In order to maintain the integrity of the total spacecraft system design and the Spacecraft Design Specification as implied in Section 3a, the Systems Division shall be responsible for, and is given the authority to review and sign off, all individual Functional Specifications to verify their technical adequacy and compatibility with the total spacecraft system and all subsystems. This review and sign-off by the Systems Division of all Functional Specifications shall be a Project Requirement. Project Office will approve the Spacecraft Development Specification for *Mariner R*. Project Office approval will be required of any changes in the Spacecraft Design Specification that affect the *Mariner R* mission objective.

Flow plans and schedules. In order to carry out the development, fabrication, and delivery of the resulting subsystem hardware, each division will be required to prepare a plan of technical activities, including scheduled times. In order to demonstrate that interdivisional agreements have been reached and to allow the Program Office to verify the adequacy and compatibility of these plans, Flow Plans shall be a Project Requirement.

Flow Plans shall consist of a series of blocks representing basic technical events related by arrows and lines to illustrate their logical informational and time relationships. Flow Plans will be developed for division hardware delivered to SAF. Flow Plans will be prepared down to

UNCLASSIFIED

UNCLASSIFIED

the "assembly" level of detail wherein each equipment portion is under one division's cognizance. The events included shall cover the period starting with the completion of Preliminary Design and ending with the delivery of hardware to the SAF and shall include:

- (a) Project requirements and milestones
- (b) Significant interdivisional relationships
- (c) Development, fabrication, and check-out activities determined to be important by the particular division concerned

All events on the Flow Plans must be amenable to scheduling and established with a scheduled date. All Flow Plans should be consistent with the project milestones, including Design Freeze and change control established and Use-Hardware Delivery and Certification at SAF complete described below:

These Flow Plans shall represent the commitment by each division to other divisions and to the Project Office of the basis for carrying out its hardware development, fabrication, and delivery responsibilities and shall be a Project Requirement. The maintenance of all Flow Plans as representative of the true situation and the periodic reporting to the Program Office of the division's performance in relation to their Flow Plan shall also be a Project Requirement.

Critical drawings and specifications. Detailed design documentation shall be limited to those critical drawings and specifications required to carry out the *Mariner R* Project. No Project Requirements will be established within the area of responsibility of a given division.

Critical drawings and specifications will be necessary to define interfaces between the spacecraft, the GSE, and the launch vehicle. Also, to accomplish design compatibility and provide assembly and system test and operations, certain critical drawings and specifications are a Project Requirement. As a minimum, the following critical drawings are required:

- (a) Spacecraft envelope drawings
- (b) Spacecraft launch vehicle interface control drawings
- (c) Complete spacecraft signal drawing
- (d) Complete GSE signal drawing
- (e) System test layout
- (f) Launch complex layout

- (g) Schematics for each module, GSE, and cabling at certification of equipment to SAF

It shall be a Project Requirement for the Systems Division to modify the list of critical drawings for satisfaction of mission objectives and for all divisions to support and assist in this area.

Complete drawings and specifications for *Mariner R* will be a Project Requirement. This project requirement is not to contradict the aforementioned requirements. A complete set of drawings and specifications are required and must be completed by the launch date. The quality of drawings and specifications must be such that duplication of the mission is possible in 1964. The time-phasing of this requirement shall not interfere with the accomplishment of *Mariner R* Program milestones.

Testing. Throughout the development, fabrication, and check-out of all subsystem hardware, many tests will be carried out in support of good engineering practice. Of these many tests, Environmental Flight Acceptance tests shall be a Project Requirement. The associated project requirements to establish and maintain an over-all project test program are described in Subsection 3b (2), Test Requirements. All other significant subsystem test requirements will be division-imposed requirements and should appear on the Flow Plans.

Quality assurance. Through the development, fabrication, and check-out of subsystems hardware, many activities which are accomplished can be classed as quality assurance efforts. Of these many activities, Visual Workmanship Inspection and Use-Hardware Certification on delivery to the SAF shall be Project Requirements. The associated project requirements required to establish and maintain an over-all project Quality Assurance program are described below in the section on Quality Assurance Requirements. All other subsystem quality assurance efforts will be division imposed requirements and should appear on the Flow Plans.

Design freeze and change control. As all activities within the project approach the critical mission dates, it is necessary that design and hardware change control be established for the over-all system. The Systems Division shall, as a Project Requirement, be responsible for, and given the authority to coordinate, establish and document appropriate subsystem design-freeze technical requirements and scheduled dates. All divisions shall, as a Project Requirement, be expected to meet the resulting Design-Freeze Requirement.

UNCLASSIFIED

UNCLASSIFIED

Further, the Systems Division shall, as a Project Requirement, be responsible for and given the authority to establish, maintain and control an Engineering Change Request system to establish a basis for authorization and control of all design and hardware changes. In emergency situations ECR changes may be made concurrent with Systems Division authorization. All divisions shall, as a Project Requirement, be expected to operate within the ECR system and carry out all changes and related documentation in a controlled fashion consistent with ECR system objectives.

For the *Mariner R* Project, an Engineering Change Request system will be established to cover the following interface areas:

- (1) SDS functional specification
- (2) Telemeter channel assignments
- (3) Power requirements
- (4) CC&S output requirements
- (5) Midcourse guidance accuracy requirement
- (6) Attitude control output electrical requirement
- (7) Flight harness and GSE electrical requirements and mechanical requirements
- (8) Envelope of each module including mechanical locations
- (9) Packaging of each module
- (10) Number of pyrotechnic measurements and functions
- (11) Weight and cg for each module
- (12) Heat-dissipation profile at module level

A complete hardware freeze will be instituted. At that time all engineering changes will be subject to the ECR system. Dates of Design Freeze and ECR are shown in Appendix B.

(2) *Testing requirements*

Each division shall be responsible for accomplishing all testing of equipment at the assembly level and below. The only Project Requirement for specific testing shall be for Environmental Flight Acceptance testing at the assembly level. The meeting of this requirement and the establishment and maintenance of an over-all project testing program demand the following additional Project Requirements.

General environmental requirements. The Systems Division shall, as a Project Requirement, be responsible for establishing the general environmental requirements in the form of General Specifications for Type Approval, and Flight Acceptance and Pre-Acceptance testing. All divisions shall, as a Project Requirement, be expected to perform all testing so that it is consistent with the intent of these general Environmental Specifications as appropriate to each piece of hardware.

Test specifications. All divisions shall, as a Project Requirement, be responsible for establishing and documenting environmental Flight Acceptance tests in the form of Test Specifications. Divisions are encouraged to document all environmental tests that are performed. The Test Specifications shall identify the subject assembly, listing the portions of the various subsystems included in that assembly for test purposes, state the environmental Type Approval (if applicable) and Flight Acceptance tests consistent with the intent of the General Environmental Specifications (as appropriate to each piece of hardware) to which the assembly is to be subjected, and indicate performance criteria by which the acceptance or rejection of the assembly is to be determined.

To implement this Test Specification Requirement, the Systems Division shall be responsible for reviewing all test specifications prior to publication. It is permissible for this review and approval action to occur concurrent with environmental test by the cognizant hardware division.

All divisions shall be required, as a Project Requirement, to prepare Final Test Reports for each assembly on the completion of all environmental testing described in the applicable Test Specifications. This report must include:

- (a) Test carried out
- (b) Date of completion
- (c) Results which clearly describe pertinent information on all failures, including failure analysis and corrective action taken.

To meet this requirement it is acceptable for cognizant hardware divisions to submit to Systems Division duplicates of cognizant division test reports, providing the aforementioned requirements are satisfied. The Systems Division shall be required, as a Project Requirement, to collect and appraise these reports, monitor the testing progress and prepare for submission to the Program

UNCLASSIFIED

Office a Project Test Results Manual based on this information.

The certification by all divisions at the time of delivery of use-hardware to the SAF that the Flight Acceptance testing requirements have been accomplished shall be a Project Requirement. The certification will be accomplished between the hardware contributing division and the Systems Division at the SAF as described in the Section on Quality Assurance Requirements following.

(3) *Quality assurance requirements*

Each division shall be responsible for accomplishing all Quality Assurance functions during the development, fabrication, and checkout of equipment. The basic Project Requirements for specific Quality Assurance activities shall be for Visual Workmanship Inspection and Use-Hardware Certification on delivery to the SAF. The meeting of these requirements and the establishment and maintenance of an over-all project Quality Assurance program demand the following additional Project Requirements.

Quality assurance requirements and procedures. Inspection as required by the Program Office shall be a redundant operation performed by other than the fabrication and checkout personnel, if possible. Consequently, the inspection personnel of the Systems Division and the Administrative portion of the Laboratory will be expected to provide inspection service support to all divisions. All divisions shall, as a Project Requirement, utilize such inspection support, unless waived by Systems Division. The inspection personnel shall, as a Project Requirement, establish the technical requirements for all inspection, by discussion and agreement with the concerned division, prior to its being carried out. The concerned division's opinions in regard to appropriate requirements shall be accepted as satisfactory.

The inspection personnel shall, as a Project Requirement, be responsible for inspecting hardware and accepting or rejecting it, depending upon its meeting the agreed-upon technical requirements. If the hardware is rejected, it can only be utilized as a result of a Materials Review Board action. This MRB action shall be a Project Requirement. The MRB shall consist of the inspector, the equipment cognizant engineer, and a senior technical representative of the concerned division, or their alternate representatives.

The Systems Division shall, as a Project Requirement, establish and maintain documentation and recording

systems for all inspection reporting and MRB actions. Further, they shall, as a Project Requirement, collect and appraise all inspection reports and MRB action documents and prepare a Project Quality Assurance Results Manual.

Hardware certification at SAF. All divisions shall, as a Project Requirement, certify all hardware prior to its acceptance at the SAF for system use. Certification shall consist of the following minimum Project Requirements.

- (a) Written acknowledgment that the Flight Acceptance testing was satisfactorily accomplished.
- (b) Written acknowledgment that the hardware has passed inspection or has been accepted through MRB action.
- (c) All ECR's of record were implemented on the hardware being delivered.
- (d) Certain special technical requirements, as defined by each cognizant division, have been satisfied.

The Systems Division shall, as a Project Requirement, establish, maintain and operate facilities and a documentation system for such certification of hardware at the SAF. The Systems Division will see that the actual certified equipment is so marked.

c. Spacecraft system operations requirements

All hardware-contributing divisions shall, as a Project Requirement, support the spacecraft system operations in terms of hardware, documentation and procedures, and operations and technical support personnel. The Systems Division shall, as a Project Requirement, be responsible for and given the authority for the coordination, planning and direction of all such activities.

In exercising this authority, it is required that Systems Division obtain Project Office concurrence and keep Project informed of the status of all requirements of a significant work level placed upon the Divisions. The term operations, as used here, includes all spacecraft-system activities starting with the spacecraft and GSE assembly and ending with spacecraft launching and certain related activities through injection of the spacecraft into an appropriate trajectory.

Within this broad responsibility, the Systems Division shall, as a Project Requirement, be responsible for establishing, maintaining, and implementing the following, the

UNCLASSIFIED

JPL TECHNICAL REPORT NO. 32-353

first issue and subsequent major revisions of which are to be approved by the Project Manager:

- (1) Assembly and Operations Plan, including a Flight Preparation Schedule
- (2) System Flow Plan and Schedule to SAF
- (3) Detailed over-all spacecraft and GSE operational procedures and instructions, including subsystem and system checkout, environmental and compatibility testing procedures
- (4) Spacecraft Environmental Test Specifications
- (5) Quality Assurance Requirements and Procedures
- (6) Appropriate documentation, recording and reporting system covering all activities, including a Spacecraft Operation Log
- (7) Shipping and storage requirements and procedures
- (8) Space Flight Operations Plan
- (9) Range documentation
- (10) Standard Trajectories and Criteria

The Systems Division shall, as a Project Requirement, and as a function of their charter, establish, maintain and control the technical interfaces in the following areas and prepare and maintain a schedule in each of the following areas for Project Manager approval:

- (1) Spacecraft Development Flight Preparation
- (2) Spacecraft/Vehicle Integration
- (3) Spaceflight Operation Complex
- (4) Ground Support Equipment and Support Facilities
- (5) Assembly and Operations

4. Project Milestones

Project requirements which are amenable to definitive scheduling and necessary to effective project management shall be established as Project Milestones. Although other technical events may occur between or within the Project Milestones and must be accomplished, they are not included since they are not amenable to scheduling. The following Project Milestones are established as Project Requirements and should appear on all Flow Plans. The following information includes a definition of the mile-

stone, its scope, and the organization responsibility relating to it.

a. Spacecraft Design Specifications complete

Spacecraft Design Functional Specifications will be established under the direction of the Systems Division and distributed and upgraded by means of a Design Specification Manual. All divisions will participate in the creation of functional specifications, with the Systems Division establishing technical requirements and constraints as appropriate. The functional specifications will define system interfaces, interactions and transfer functions, including drawings and defining assembly locations.

b. Hardware Flow Plans and schedules established

All divisions will develop equipment Flow Plans in accordance with equipment flow plan format developed by the Systems Division. Systems Division will develop a system flow plan utilizing Division inputs. It is required that divisions organize and report progress based on Division Flow Charts.

c. Critical drawings and specifications complete and listed

All divisions will assess the degree of completeness of drawings and specifications based on the following criterion: "Critical drawings that have system interactions will be completed so that analysis of the spacecraft vehicle may be accomplished in an expeditious and efficient manner." Released drawings are preferred, but sketches will be satisfactory. A schematic of every module is necessary. All other drawings and specifications are to be completed, but can be accomplished in the time discretion of the divisions within final date requirements. Systems Division will maintain a list and a complete set of the critical drawings for SAF integration.

d. Test specifications

Test specifications shall be prepared by all technical divisions to establish the tests intended to verify the environmental integrity of each assembly. The test specifications shall identify the subject assembly, (listing the portions of the various subsystems included in that assembly for test purposes), state other environmental Type Approval (as applicable) and Flight Acceptance tests, consistent with General Specification No. 30250 and 30251, to which the assembly is to be subjected, and indicate performance criteria by which the acceptance or rejection of the assembly is to be determined.

UNCLASSIFIED

e. Design freeze and changes

A design freeze will be imposed on all divisions at the milestone date. Engineering changes after design-freeze dates will be controlled by an ECR system.

f. Use-hardware delivery and certification at SAF complete

All use-hardware, including spares, will be complete and certified by all cognizant divisions. GSE is considered as use-hardware. It will be the responsibility of each division to provide hardware to the System activities at this milestone. Technical divisions will coordinate any delay in this milestone with Systems Division prior to the milestone date. Procedures and check sheets necessary for SAF operations will be provided.

g. Spacecraft system JPL operations initiated

The following five milestones are concerned with the assembly, test, and shipment of the spacecraft further defined in the *Mariner R* AOP. These milestones are the responsibility of the Systems Division.

- (1) *Assembly Complete.* The system is ready for testing.
- (2) *Subsystem and System Performance Tests.* The system has been tested and its performance is satisfactory.
- (3) *Spacecraft Environmental Tests Complete.* Vibration, radio interference, and space simulation environmental tests have been conducted and the spacecraft performance is satisfactory.

- (4) *Dummy Run and Compatibility Tests Complete.* The spacecraft is electrically and mechanically compatible with the *Agena B* adapter and shroud and other spacecraft adapter equipment. The spacecraft is compatible with the flight launch complex.

- (5) *Shipment to AMR Complete.* The system has been received at AMR.

h. Spacecraft system AMR operations initiated

Spacecraft system has arrived at AMR and preparations for launch, including system test and JFACT test are being performed. System Division.

i. Spacecraft launching accomplished

Spacecraft is launched from AMR.

j. Space flight operations initiated

The spacecraft has been injected into a suitable trajectory and tracking, data collection and processing, utilizing the DSIF and SFOF, shall be in process. Further definition of these activities shall be defined in the *Mariner R* SFOP.

k. All drawings and specifications complete and listed

Drawings and specifications completed in released form. From these documents, a *Mariner R* spacecraft could be duplicated.

l. All test reports completed

All reports covering environmental and system tests completed.

Appendix B

Mariner R Change Freeze Requiring ECR Action

Items frozen for Mariner R

Reference document	Reference No.	Freeze date 1961	Document engineer
SDS Functional Specifications (Systems)	MR-4-110	October 16	D. Alcorn
	MR-4-120	October 16	D. Alcorn
	MR-4-130	October 16	D. Alcorn
	MR-4-140	October 16	D. Alcorn
	MR-4-150	October 16	D. Alcorn
(Space Science)	MR-4-210	October 16	D. Alcorn
	MR-4-220	October 16	D. Alcorn
	MR-4-230	October 16	D. Alcorn
(Telecommunications)	MR-4-310	October 23	D. Alcorn
	MR-4-320	October 23	D. Alcorn
	MR-4-321A	October 16	D. Alcorn
	MR-4-322	October 23	D. Alcorn
(Guidance and Control)	MR-4-410	October 16	D. Alcorn
	MR-4-420	October 16	D. Alcorn
	MR-4-430	October 16	D. Alcorn
	MR-4-450	October 16	D. Alcorn
	MR-4-460	October 23	D. Alcorn
(Engineering Mechanics)	MR-4-510	October 16	D. Alcorn
	MR-4-520	October 16	D. Alcorn
	MR-4-521	October 16	D. Alcorn
	MR-4-530	October 16	D. Alcorn
	MR-4-540	October 16	D. Alcorn
(Propulsion)	MR-4-610	October 16	D. Alcorn
Interface control drawing	J-4100300	October 16	J. Wilson
Configuration drawing	J-4100305	October 16	J. Wilson
Packaging layout	J-4900501B	October 16	J. Wilson
Circuit data sheets, interface	2-12001 to 2-120081	October 16	D. Alcorn
Circuit data sheets, direct access	2-120101 to 2-120120	October 23	D. Alcorn
Circuit data sheets, composite	-----	October 23	D. Alcorn
Flight Acceptance environmental specification	30251	October 16	J. MacLay
Engineering (ring) harness 9W1MR	119101	October 30	W. Gill
L-band harness 9W2MR	119102	November 1	W. Gill
Command harness 9W3MR	119103	November 13	W. Gill
Power switch and logic 9W4MR	119104	November 8	W. Gill
CC&S 9W5MR	119105	October 30	W. Gill
Data encoder 9W6MR	119106	November 13	W. Gill
Attitude control 9W7MR	119107	November 8	W. Gill
Main pyrotechnic 9W8MR	119108	October 30	W. Gill
Power 9W9MR	119109	November 8	W. Gill
MCM pyrotechnic 9W10MR	119110	October 30	W. Gill
MCM instrument 9W11MR	119111	October 30	W. Gill
MCM control 9W12MR	119112	October 30	W. Gill
Antenna hinge 9W13MR	119113	November 8	W. Gill
A-C power 9W14MR	119114	November 8	W. Gill
Science electronics assembly 9W20MR	119120	November 8	W. Gill
Science signal 9W21MR	119121	November 8	W. Gill

UNCLASSIFIED

JPL TECHNICAL REPORT NO. 32-353

Items frozen for Mariner R (Cont'd)

Reference document	Reference No.	Freeze date 1961	Document engineer
Magnetometer 9W22MR	119122	November 8	W. Gill
Science power 9W23MR	119123	November 8	W. Gill
DCS case assembly 9W24MR	119124	November 8	W. Gill
Particle flux detector 9W25MR	119125	November 8	W. Gill
50V-2400 power 9W40MR	119115	November 8	W. Gill
SDS Functional Specification (Telecommunications)	MR-4-330	November 16	T. Sorensen
	MR-4-331	November 16	T. Sorensen
	MR-4-332	December 6	A. Burke
	MR-4-333	December 5	A. Burke
	MR-4-334	December 5	A. Burke
	MR-4-335	December 5	A. Burke
GSE CC&S cable drawing		November 20	W. Gill
GSE attitude control cable drawing		November 20	W. Gill
GSE power and cable drawing		November 20	W. Gill
GSE L-band cable drawing		November 20	W. Gill
GSE scientific cable drawing		November 20	W. Gill
GSE data encoder cable drawing		November 20	W. Gill
GSE command cable drawing		November 20	W. Gill
GSE propulsion cable drawing		November 20	W. Gill
Mariner R General System Test Specification		November 25	W. Woods
400-cps power requirements for Launch Complex AMR	IOM	December 8	M. Piroumian
Block diagram Launch Complex	8900826	December 15	T. Meyer
Drawing outline umbilical J-box	8900833	December 15	T. Meyer
Monitor control J-box	8900839	December 15	T. Meyer
Block diagram, systems test	J-119200	December 1	W. Gill
Systems Test Complex layout	C-119201	December 15	W. Gill
Launch Control Shelter J-box drawing	8900838	December 22	W. Gill
Catenary and long-line cable drawing	(all)	December 15	W. Gill
Panel layout of monitor and control console (LOD)	8900831		T. Meyer
Panel layout of Launch Control Shelter (LBP)	8900832		T. Meyer

UNCLASSIFIED

UNCLASSIFIED

JPL TECHNICAL REPORT NO. 32-353

Appendix C

Mariner R P List

(Problems considered to be jeopardizing the mission)

July 20, 1962

Mariner R P list

No.	System	Problem description	Primary responsibility for re-solving problem assigned to:	Special design assistants	Date assigned 1961
P-14	Spacecraft	IR Radiometer Spare Unit #4 will be shipped to AMR 2/27. Unit #1 was overheated in oven tests and apparently damaged. The exact damage is not yet known. It will not be possible to predict a delivery date to AMR yet.	Division 32: J. Martin W. Fawcett	Division 32: S. Chase	May 24
P-34	GSE	Command System RWV Phase Reversals W. Natzic and R. Lowe have already checked out Goldstone and AMR. Natzic will proceed to JoBurg and will make those tests by 7/19.	Division 33: J. Bryden W. Apel R. Mallis (DSIF)	Division 33: W. Natzic	June 20
P-38		Transponder — Serial #15 Progressive degradation of sensitivity. Returned to JPL for rework. This is the only unit exhibiting this characteristic. Retuning has been performed, and qualification tests are under way. This is MR-2 spare and will be returned to AMR as soon as Div. 33 considers this unit flight worthy. Delivery to AMR 7/26-7/27.	Division 33: W. Apel	Division 33: D. Hughes	July 13
P-40	Spacecraft	Microwave Radiometer, Serial #3, MR-3 Serial #3 is exhibiting the same symptoms of degradation of sensitivity that previously occurred on P-40, MR-2, 7/10. The investigation is to be conducted at AMR. There is a defective gas (noise) tube which is used for calibration. This is being replaced and further tests will be run.	Division 32: W. Fawcett J. Martin		July 10
P-42	Spacecraft	A/C (Gyro Package) Overvoltage During set up for investigation of the P-41 above (at AMR), an inadvertent overvoltage was applied to the SC A/C resulting in damage to Gyro Package and gyro electronics package Serial #6. The gyro unit was repaired at AMR and the electronics unit was returned to JPL for rework. The calibrated unit will be at AMR on 7/21. This will then be removed from the list.	Division 34: D. Runkle		July 11
P-43	Spacecraft	DCS, Serial #4, MR-3, FR 298 The Particle Flux readout is abnormal. A broken wire is suspected. This unit is to be at JPL on 7/18 for repair. During the trouble shooting, the problem disappeared and has not reoccurred except when a solder joint (suspected to have been cold) was broken. This will be returned to AMR 7/20. This will then be removed from the list.	Division 32: W. Fawcett J. Martin		July 17
P-44	Spacecraft	Command Decoder, Serial #7, MR-3, FR 297 There is an error in the most significant bit in the command detector monitor measurement. This unit is to be at the Lab on 7/18. The specific problem has not yet been found, tests are continuing. Div. 33 does not recommend holding the flight for this one.	Division 33: W. Apel J. Bryden		July 18
P-45	Spacecraft	Gas Bottle Bracket, MR-3, FR 295 A broken weld was discovered. Repair at AMR.	Division 34: D. Runkle		July 18

UNCLASSIFIED

UNCLASSIFIED

JPL TECHNICAL REPORT NO. 32-353

References

1. Lee, D. H., *Development of the Midcourse Trajectory Correction Propulsion System for the Ranger Spacecraft*, Technical Report No. 32-335, Jet Propulsion Laboratory, Pasadena (in preparation).
2. *The Ranger Project: Annual Report for 1961*, Technical Report No. 32-241, Jet Propulsion Laboratory, Pasadena, June 15, 1962.
3. *Spacecraft Separation Test*, Report No. 15689, Lockheed Aircraft Corporation, Burbank, Calif., May 9, 1962.
4. Clarke, V. C., Jr., *Summary of the Characteristics of Ballistic Interplanetary Trajectories, 1962-1977*, Technical Report No. 32-209, Jet Propulsion Laboratory, Pasadena, January 15, 1962.
5. *Firing Tables and Trajectory Data of Mariner R-1 and R-2*, Vol. I, Space Technology Laboratories, Los Angeles, June 1, 1962.
6. *Program Requirements Document No. 3300 (Mariner R) (C)*, Air Force Missile Test Center, Florida, March 15, 1962.
7. Noton, A. R. M., Cutting E., and Barnes, F. L., *Analysis of Radio Command Midcourse Guidance*, Technical Report No. 32-28, Jet Propulsion Laboratory, Pasadena, September 8, 1960.

UNCLASSIFIED